Mediators of Inflammation

Cytokines and Chemokines: Disease Models, Mechanisms, and Therapies

Guest Editors: Salahuddin Ahmed, Charles J. Malemud, Alisa E. Koch, Mohammad Athar, and Dennis D. Taub

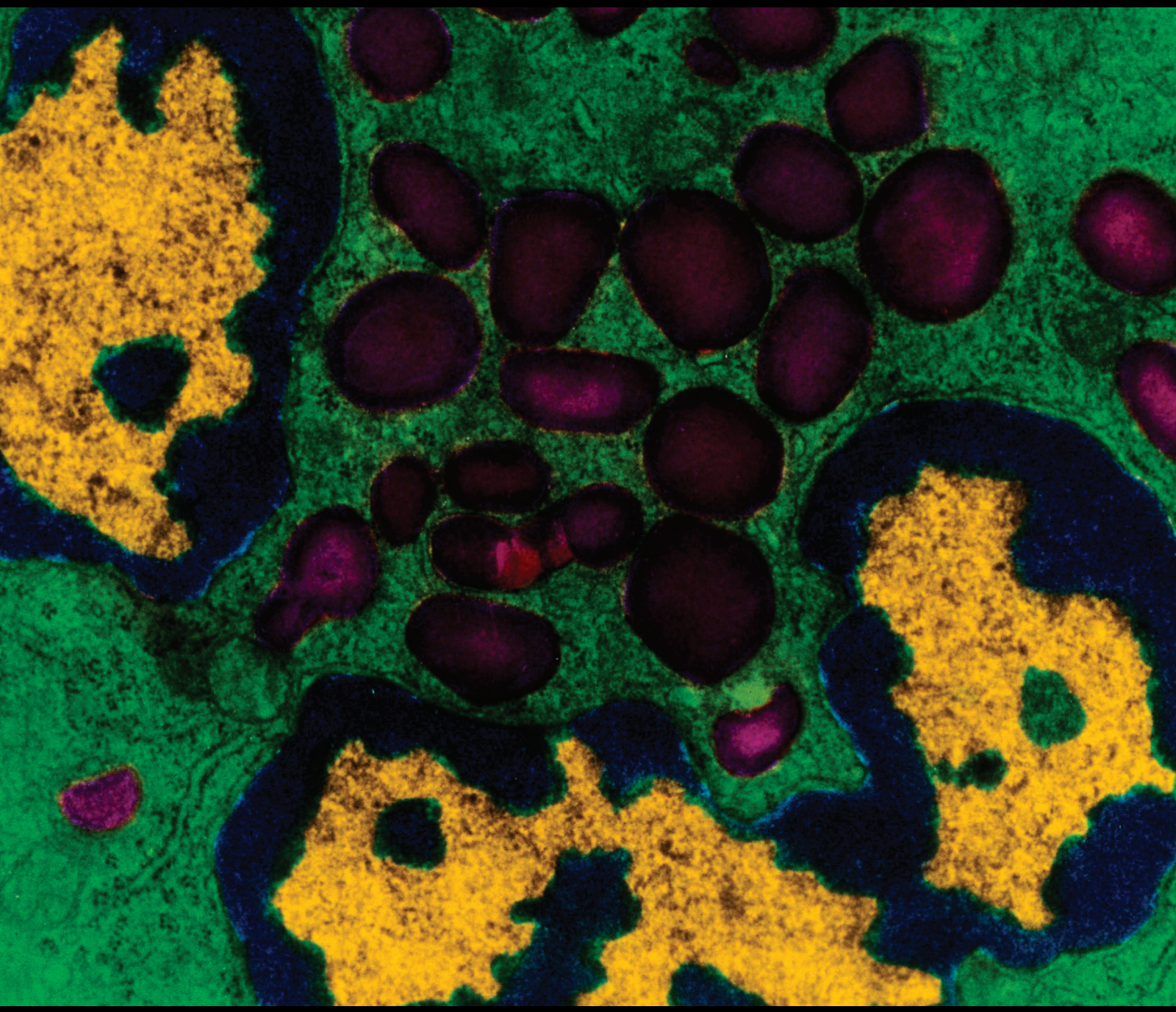

Cytokines and Chemokines: Disease Models, Mechanisms, and Therapies

Mediators of Inflammation

Cytokines and Chemokines: Disease Models, Mechanisms, and Therapies

Guest Editors: Salahuddin Ahmed, Charles J. Malemud, Alisa E. Koch, Mohammad Athar, and Dennis D. Taub

Editorial Board

Contents

Cytokines and Chemokines: Disease Models, Mechanisms, and Therapies, Salahuddin Ahmed, Charles J. Malemud, Alisa E. Koch, Mohammad Athar, and Dennis D. Taub
Volume 2014, Article ID 296356, 5 pages

Erratum to "Palmitic Acid Induces Production of Proinflammatory Cytokines Interleukin-6, Interleukin-1β, and Tumor Necrosis Factor-α via a NF-κB-Dependent Mechanism in HaCaT Keratinocytes", Bing-rong Zhou, Jia-an Zhang, Qian Zhang, Felicia Permatasari, Yang Xu, Di Wu, Zhi-qiang Yin, and Dan Luo
Volume 2014, Article ID 513027, 2 pages

The Pathology of Orthopedic Implant Failure Is Mediated by Innate Immune System Cytokines, Stefan Landgraeber, Marcus Jäger, Joshua J. Jacobs, and Nadim James Hallab
Volume 2014, Article ID 185150, 9 pages

Effect of Tumor Necrosis Factor Family Member LIGHT (TNFSF14) on the Activation of Basophils and Eosinophils Interacting with Bronchial Epithelial Cells, Huai Na Qiu, Chun Kwok Wong, Jie Dong, Christopher Wai-Kei Lam, and Zhe Cai
Volume 2014, Article ID 136463, 14 pages

Monocyte Subsets in Schistosomiasis Patients with Periportal Fibrosis, Jamille Souza Fernandes, Maria Ilma Araujo, Diego Mota Lopes, Robson da Paixão de Souza, Edgar M. Carvalho, and Luciana Santos Cardoso
Volume 2014, Article ID 703653, 12 pages

The Proinflammatory Cytokine High-Mobility Group Box-1 Mediates Retinal Neuropathy Induced by Diabetes, Ahmed M. Abu El-Asrar, Mohammad Mairaj Siddiquei, Mohd Imtiaz Nawaz, Karel Geboes, and Ghulam Mohammad
Volume 2014, Article ID 746415, 10 pages

Interactions between Neutrophils, Th17 Cells, and Chemokines during the Initiation of Experimental Model of Multiple Sclerosis, Dagmara Weronika Wojkowska, Piotr Szpakowski, Dominika Ksiazek-Winiarek, Marcin Leszczynski, and Andrzej Glabinski
Volume 2014, Article ID 590409, 8 pages

Regulation of Chemokine CCL5 Synthesis in Human Peritoneal Fibroblasts: A Key Role of IFN-γ, Edyta Kawka, Janusz Witowski, Nina Fouqet, Hironori Tayama, Thorsten O. Bender, Rusan Catar, Duska Dragun, and Achim Jörres
Volume 2014, Article ID 590654, 9 pages

Chemokines and Chemokine Receptors in Multiple Sclerosis, Wenjing Cheng and Guangjie Chen
Volume 2014, Article ID 659206, 8 pages

The Inflammatory Chemokine CCL5 and Cancer Progression, Donatella Aldinucci and Alfonso Colombatti
Volume 2014, Article ID 292376, 12 pages

CD38 Ligation in Peripheral Blood Mononuclear Cells of Myeloma Patients Induces Release of Protumorigenic IL-6 and Impaired Secretion of IFNγ Cytokines and Proliferation, Giorgio Fedele, Marco Di Girolamo, Umberto Recine, Raffaella Palazzo, Francesca Urbani, Alberto L. Horenstein, Fabio Malavasi, and Clara Maria Ausiello
Volume 2013, Article ID 564687, 7 pages

Differential Influence of Inositol Hexaphosphate on the Expression of Genes Encoding TGF-β Isoforms and Their Receptors in Intestinal Epithelial Cells Stimulated with Proinflammatory Agents, MaThlgorzata Kapral, Joanna Wawszczyk, StanisThlaw Sośnicki, and LudmiThla Węglarz
Volume 2013, Article ID 436894, 10 pages

Enhanced Inflammatory Activity of Endometriotic Lesions from the Rectovaginal Septum, Dominic Bertschi, Brett D. McKinnon, Jakob Evers, Nick A. Bersinger, and Michael D. Mueller
Volume 2013, Article ID 450950, 7 pages

The Role of T Cell Immunoglobulin Mucin Domains 1 and 4 in a Herpes Simplex Virus-Induced Behçet's Disease Mouse Model, Ju A. Shim, Eun-So Lee, Bunsoon Choi, and Seonghyang Sohn
Volume 2013, Article ID 903948, 13 pages

IRF5 Is a Specific Marker of Inflammatory Macrophages *In Vivo*, Miriam Weiss, Katrina Blazek, Adam J. Byrne, Dany P. Perocheau, and Irina A. Udalova
Volume 2013, Article ID 245804, 9 pages

Modulation of Conjunctival Goblet Cell Function by Inflammatory Cytokines, L. Contreras-Ruiz, A. Ghosh-Mitra, M. A. Shatos, D. A. Dartt, and S. Masli
Volume 2013, Article ID 636812, 11 pages

Induction of Tumor Necrosis Factor (TNF) Release from Subtypes of T Cells by Agonists of Proteinase Activated Receptors, Haiwei Yang, Tao Li, Jifu Wei, Huiyun Zhang, and Shaoheng He
Volume 2013, Article ID 165453, 10 pages

The Mechanism of Sevoflurane Preconditioning-Induced Protections against Small Intestinal Ischemia Reperfusion Injury Is Independent of Mast Cell in Rats, Xiaoliang Gan, Guangjie Su, Weicheng Zhao, Pinjie Huang, Gangjian Luo, and Ziqing Hei
Volume 2013, Article ID 378703, 12 pages

Progression of Luminal Breast Tumors Is Promoted by Ménage à Trois between the Inflammatory Cytokine TNFα and the Hormonal and Growth-Supporting Arms of the Tumor Microenvironment, Polina Weitzenfeld, Nurit Meron, Tal Leibovich-Rivkin, Tsipi Meshel, and Adit Ben-Baruch
Volume 2013, Article ID 720536, 19 pages

Haplotype Analysis of Interleukin-8 Gene Polymorphisms in Chronic and Aggressive Periodontitis, Petra Borilova Linhartova, Jan Vokurka, Hana Poskerova, Antonin Fassmann, and Lydie Izakovicova Holla
Volume 2013, Article ID 342351, 8 pages

Intricacies for Posttranslational Tumor-Targeted Cytokine Gene Therapy, Jeffry Cutrera, Denada Dibra, Arun Satelli, Xuexing Xia, and Shulin Li
Volume 2013, Article ID 378971, 9 pages

A Possible Role for CD8+ T Lymphocytes in the Cell-Mediated Pathogenesis of Pemphigus Vulgaris, Federica Giurdanella, Luca Fania, Maria Gnarra, Paola Toto, Daniela Di Rollo, Daniel N. Sauder, and Claudio Feliciani
Volume 2013, Article ID 764290, 5 pages

Hyperoxia Exacerbates Postnatal Inflammation-Induced Lung Injury in Neonatal BRP-39 Null Mutant Mice Promoting the M1 Macrophage Phenotype, Mansoor A. Syed and Vineet Bhandari
Volume 2013, Article ID 457189, 12 pages

Contents

Chemokines and Neurodegeneration in the Early Stage of Experimental Ischemic Stroke, Pawel Wolinski and Andrzej Glabinski
Volume 2013, Article ID 727189, 9 pages

Cytokines and Chemokines as Regulators of Skeletal Muscle Inflammation: Presenting the Case of Duchenne Muscular Dystrophy, Boel De Paepe and Jan L. De Bleecker
Volume 2013, Article ID 540370, 10 pages

Strength Training and Testosterone Treatment Have Opposing Effects on Migration Inhibitor Factor Levels in Ageing Men, D. Glintborg, L. L. Christensen, T. Kvorning, R. Larsen, K. Brixen, D. M. Hougaard, B. Richelsen, J. M. Bruun, and M. Andersen
Volume 2013, Article ID 539156, 7 pages

Palmitic Acid Induces Production of Proinflammatory Cytokines Interleukin-6, Interleukin-1β, and Tumor Necrosis Factor-α via a NF-κB-Dependent Mechanism in HaCaT Keratinocytes, Bing-rong Zhou, Jia-an Zhang, Qian Zhang, Felicia Permatasari, Yang Xu, Di Wu, Zhi-qiang Yin, and Dan Luo
Volume 2013, Article ID 530429, 11 pages

Hindawi Publishing Corporation
Mediators of Inflammation
Volume 2014, Article ID 296356, 5 pages
http://dx.doi.org/10.1155/2014/296356

Editorial

Cytokines and Chemokines: Disease Models, Mechanisms, and Therapies

Salahuddin Ahmed,[1] Charles J. Malemud,[2] Alisa E. Koch,[3] Mohammad Athar,[4] and Dennis D. Taub[5]

[1] *Department of Pharmaceutical Sciences, Washington State University College of Pharmacy, 412 E. Spokane Falls Boulevard, Spokane, WA 99204, USA*
[2] *Department of Medicine/Rheumatology, Case Western Reserve University, Cleveland, OH 44106, USA*
[3] *Veteran's Administration, Ann Arbor, MI and Department of Internal Medicine/Rheumatology, University of Michigan, Ann Arbor, MI 48109, USA*
[4] *Department of Dermatology, University of Alabama at Birmingham, Birmingham, AL 35294, USA*
[5] *Department of Veterans Affairs, VA Medical Center, Washington, DC 20422, USA*

Correspondence should be addressed to Salahuddin Ahmed; salah.ahmed@wsu.edu

Received 2 July 2014; Accepted 2 July 2014; Published 24 July 2014

The mechanistic insights gained through research into cytokine and chemokine pathways have progressed to the point where it has made possible the successful targeting of these factors in order to limit their role in orchestrating a variety of rheumatic, skin, vascular, and infectious diseases. While this has set the stage for a new generation of biological therapies, significant gaps still remain in our understanding of how these cytokines and chemokines actually work at the cellular and molecular level. This gap in knowledge demands that research continue to explore for novel insights into the existing mechanisms of established inflammatory mediators and for the discovery of the possible role of silent or new participants in the processes of acute or chronic inflammation. This special issue invited contributors to submit original research articles or reviews in order to further strengthen the efforts to understand the cellular and molecular mechanisms of cytokine- and chemokine-mediated inflammation in disease pathogenesis. We were particularly interested in papers that provide novel understanding of the role of cytokines, chemokines, or their receptors in disease pathogenesis and testing of therapeutic strategies in cell/tissue culture systems, in animal models, or in the clinical evaluation of inflammatory diseases. We received overwhelming response to the call for papers that went beyond our expectation in terms of not only submission numbers, but also the variety of research that were accepted in this special issue. We would like to thank all the authors for their outstanding contributions and responsiveness to the reviewer's concerns. Our editorial board would also like to thank and warmly acknowledge the reviewers for their service in reviewing these interesting papers.

This special issue is comprised of 26 papers that cover the spectrum of novel findings in this area of research ranging from the basic molecular biology of cytokines and chemokines to some related clinical findings and therapeutic applications. More interesting to the readers will be the breadth of diseases covered in terms of these inflammatory mediators including those relevant to rheumatic diseases, atherosclerosis, multiple sclerosis, pulmonary fibrosis, diabetic retinopathy, kidney diseases, carcinogenesis, inflammatory bowel disease, periodontitis, stroke, and aging.

In the paper entitled "*The pathology of orthopedic implant failure is mediated by innate immune system cytokines*," S. Landgraeber et al. provide a comprehensive review and update on clinical and basic science studies that are needed to address progressive pathological bone loss or "aseptic loosening" of orthopedic implants and the implications this has as a potentially life-threatening condition especially in

the elderly. Based on their summary, the authors presented their viewpoint which discussed the underlying mechanisms for how failed orthopedic implants might contribute to activation of the innate and adaptive immune responses. They also highlighted the role that different components of innate immunity such as cytokines, toll-like receptors, apoptosis, bone catabolism, and hypoxic responses play in the failure of orthopedic implants.

In the paper entitled "*Effect of tumor necrosis factor family member LIGHT (TNFSF14) on the activation of basophils and eosinophils interacting with bronchial epithelial cells*," H. N. Qiu et al. investigated the underlying mechanisms of the activity of LIGHT in cocultures of human basophils/eosinophils and BAES-2B epithelial cells. Using well-validated techniques, the authors found that LIGHT could significantly promote intercellular adhesion and extracellular matrix (ECM) remodeling in basophil/eosinophil/BAES-2B cell cocultures through the enhanced expression of intercellular adhesion molecule-1 (ICAM-1) as well as via the enhanced synthesis of interleukin-6 (IL-6), CXCL8, and matrix metalloproteinase-9 (MMP-9). An evaluation of the signal transduction mechanisms suggested that LIGHT mediates these negative effects by activating ERK, p38-MAPK, and NF-κB pathways. Overall, these findings provided a firmer understanding of the immunopathological role of LIGHT relevant to allergic asthma and proposed LIGHT as a potential therapeutic target for this disease.

The paper by J. S. Fernandes et al. addressed the mechanism and role of monocyte subsets in the development of periportal fibrosis induced by egg antigens that leads to *Schistosoma mansoni* infection. Using extensive flow cytometric analysis, the authors discovered that the level of the classical subset of monocytes (i.e., $CD14^{++}CD16^{-}$) was elevated in the *S. mansoni* patient population and in addition primarily showed higher expression of HLA-DR, IL-6, tumor necrosis factor- (TNF-) α and transforming growth factor- (TGF-) β, which correlated with moderate to severe fibrosis as compared to the other patient groups. This study differentiated the presence and abundance of different monocyte subsets in the individuals with varying degrees of periportal fibrosis secondary to schistosomiasis. In addition, this analysis also provided an impetus to target the $CD14^{++}CD16^{-}$ monocyte subset which should further provide an understanding of their role in the pathogenesis of schistosomiasis and potentially target these cells in the treatment of periportal fibrosis associated with this parasitic infection.

In the research article entitled "*The proinflammatory cytokine high-mobility group box-1 mediates retinal neuropathy induced by diabetes*," A. M. Abu El-Asrar et al. tested the hypothesis that the increased expression of the proinflammatory cytokine, high-mobility group box 1 (HMGB1), in epiretinal membranes and vitreous fluid from patients with diabetic retinopathy plays an important pathogenic role in rats with diabetes-induced retinal neuropathy. Their data showed that HMGB1 was upregulated early in the development of diabetes in these rodents, which also correlated with the enhanced activation of ERK1/2, active caspase-3 and glutamate levels. Furthermore, their analysis also found a marked downregulation of synaptophysin, tyrosine hydroxylase, glutamine synthetase, and glyoxalase 1. The treatment of these diabetic rats with glycyrrhizin significantly attenuated diabetes-induced HMGB1 upregulation without affecting their metabolic status. These findings suggested that HMGB1 could be an important mediator in the early events that lead to diabetic retinal neuropathy. Thus, HMGB1 could be a potential therapeutic target for the amelioration of diabetic neuropathy.

In the study entitled "*Interactions between neutrophils, Th17 cells, and chemokines during the initiation of experimental model of multiple sclerosis*," D. W. Wojkowska et al. analyzed the expression of CC and CXC chemokine receptors, Th17 cell activation, and neutrophil migration to the brain in an experimental model of multiple sclerosis (MS). MS is a demyelinating disease affecting the central nervous system (CNS) in which activated T cells and their interaction with neutrophils lead to chronic pathological CNS deterioration. However, the immunopathogenesis of MS and the progression of CNS damage in a validated experimental model of MS, namely, experimental autoimmune encephalomyelitis (EAE), remain unclear despite many decades of active research. Thus, the authors provide evidence for the role of Th17 in upregulating CCR6, CXCR2, and CXCR6 expression which allowed neutrophil accumulation and neuronal damage. This study also provided evidence that anti-IL-23R and anti-CXCR2 antibodies were effective in amelioration of EAE by decreasing the intracerebral accumulation of Th17 cells.

In the paper entitled "*Regulation of chemokine CCL5 synthesis in human peritoneal fibroblasts: a key role of IFN-γ*," E. Kawka et al. studied the potential of IFN-γ to synergistically exacerbate IL-1β or TNF-α responsiveness of stimulated human peritoneal fibroblasts (HPFB) to produce CCL5, a potent chemokine for mononuclear leukocytes. They further showed that interferon-γ (IFN-γ) induced the expression of CD40 receptor in HPFB cells which led to an enhanced response to CD40L and consequently CCL5 synthesis. The results of this study suggested that HPFB synthesize CCL5 in response to inflammatory mediators, which may contribute significantly to the recruitment of mononuclear leukocytes in peritonitis.

In the article entitled "*Chemokines and chemokine receptors in multiple sclerosis*" by W. Cheng and G. Chen. The authors compiled results from recent studies that provided novel evidence for the role of chemokines and chemokine receptors in multiple sclerosis (MS) pathogenesis. These authors systematically detailed the 4 distinct patterns of human MS, relapsing-remitting, primary progressive, secondary progressive, and primary-relapsing. In light of current results, the authors also discussed how migration of T cells and macrophages from peripheral blood to the CNS and the destruction of blood brain barrier were two of the key pathogenic events where the chemokine/chemokine receptor duality may have pathologic relevance. Based on this contention they suggested that the chemokine network may be a potential therapeutic target for intervention in human MS.

In the review article entitled "*The inflammatory chemokine CCL5 and cancer progression*," D. Aldinucci

and A. Colombatti discussed the importance of chemokines as the "gate keepers" of immunity and inflammation. However, the activity of chemokines is flipped in the tumor microenvironment wherein cancer cells start subverting chemokine networks to their advantage in such a way that these chemokines now exert tumor-promoting effects relevant to carcinogenesis. The authors focused their review on CCL5/CCR5 duo and highlighted newer therapeutic strategies which are aimed at inhibiting the binding of CCL5 to CCR5, thus inhibiting CCL5 secretion or alternatively using this strategy to inhibit interactions between tumor cells and their microenvironment leading to decreased CCL5 secretion.

In the research paper entitled "*CD38 ligation in peripheral blood mononuclear cells of myeloma patients induces release of protumorigenic IL-6 and impaired secretion of IFNγ cytokines and proliferation*," G. Fedele et al. studied the role of CD38 in impairing T cell immune responses in multiple myeloma (MM) peripheral blood mononuclear cells (PBMCs). The authors employed a monoclonal antibody ligation method to detect the differences in response to DC38 stimulation. The results of this study found that PBMCs from MM patients failed to proliferate and secrete IFNγ induced by CD38 ligation while retaining their response to TCR/CD3. It was concluded from their findings that CD38 may be functionally involved in the progression of MM via secretion of high levels of IL-6 that protects neoplastic cells from apoptosis.

In the paper entitled "*Differential influence of inositol hexaphosphate on the expression of genes encoding TGF-β isoforms and their receptors in intestinal epithelial cells stimulated with proinflammatory agents*," M. Kapral et al. studied the effect of inositol hexaphosphate (IP6), a naturally found phytochemical, on lipopolysaccharide- (LPS-) induced TGF-β and TGF-β receptor expression in intestinal cells. Using qRT-PCR, they found that IP6 inhibited TGF-β1, whereas IP6 induced LPS- or IL-1β-induced TGF-β2 and -β3 expression in Caco2 cells. Based on these novel findings, M. Kapral et al. concluded that IP6 elicits immunoregulatory and chemopreventive activity by differentially modulating the expression of TGF-βs and their receptor genes.

The paper entitled "*Enhanced inflammatory activity of endometriotic lesions from the rectovaginal septum*" by D. Bertschi et al. is a clinical study which was aimed at understanding the role of chemokines and cytokines in causing inflammation in ectopic and eutopic lesions from the rectovaginal septum. Their study found that the gene expression of chemokines ENA-78 and RANTES and the cytokines IL-6 and TNF-α was higher in endometriotic lesions compared to a nonlesion ectopic tissue. The results of this study should provide the impetus for further clinical and/or experimental studies designed to validate these findings and to test whether the inhibition of these cytokines and/or chemokines may be beneficial to the reduction of inflammation in the endometriotic lesions of the rectovaginal septum.

In the paper entitled "*The role of T cell immunoglobulin mucin domains 1 and 4 in a herpes simplex virus-induced Behçet's Disease mouse model*," J. A. Shim et al. provided novel understanding of the regulatory role of T cell immunoglobulin-1 (TIM-1) and TIM-4 in a mouse model of Behçet's disease. The results of this study showed that siRNA targeting TIM-1 attenuated the symptoms typical of Behçet's disease while also decreasing the severity of the disease. In a parallel study J. A. Shim et al. also found that knockdown of TIM-4 also elicited a beneficial effect. These findings underlined the importance of TIM-1 or TIM-4 as potential therapeutic targets for intervention in Behçet's Disease.

In the paper entitled "*IRF5 is a specific marker of inflammatory macrophages in vivo*," M. Weiss et al. validated the transcription factor, IRF5, to be a biomarker specific for inflammatory macrophage subset, M1. The study provided evidence that IRF5 regulates the expression of proinflammatory genes such as IL-12β and IL-23α whilst repressing anti-inflammatory genes such as IL-10. Mouse bone marrow derived macrophage (BMDM) that differentiates into macrophages under granulocyte-macrophage colony-stimulating factor (GM-CSF) stimulation produced high levels of IRF5 mRNA and IRF5 protein while also displaying MHC II expression (a marker of the M1 type), but these cells lacked M2-marker CD206 expression. These findings were further validated in an antigen-induced arthritis model which emphasized the relevance of the *in vitro* studies to physiological conditions. The results of this study established the species-invariant role of IRF5 in controlling the inflammatory phenotype which in the future may have clinical application.

In the study paper "*Modulation of conjunctival goblet cell function by inflammatory cytokines*," L. Contreras-Ruiz et al. explored a possible role for proinflammatory cytokines in regulating inflammation at ocular surfaces that are associated with mucin secreting goblet cells. In Sjögren's syndrome, primary cultures of mouse goblet cells from conjunctival tissue were developed to determine their responsiveness to cytokines. They found that TNF-α and IFN-γ induced goblet cell apoptosis as well as inhibiting mucin secretion in response to cholinergic stimulation. Surprisingly, IL-6 enhanced the secretion of mucin, whereas IL-13 and IL-17 had no modulating effect on mucin secretion. These findings identified key proinflammatory cytokines that directly disrupt conjunctival goblet cell functions and contribute to damage at the ocular surface. The further testing of these changes is likely to facilitate our understanding of the underlying mechanism responsible for ocular damage in Sjögren's syndrome.

The paper entitled "*Induction of tumor necrosis factor release from subtypes of T cells by agonists of proteinase activated receptors*" evaluated the role of protein activated receptors (PARs) in mediating TNF-α secretion from highly purified T cells obtained from human peripheral blood. The results of this study showed that PAR-1 antagonist, but not PAR-2 antagonist, completely inhibited trypsin- or thrombin-induced TNF-α secretion. This analysis study also showed that ERK1/2 and PI3K/Akt pathways were involved in trypsin- or thrombin-induced TNF-α release from T cells. Importantly, TNF-α section was observed only in $CD4^+$, IL-4^+, or $CD25^+$ T cells, but not in IFN^+ or IL-17^+ T cells, which underscores the role that PAR-1 plays in the induction of TNF-α release from IL-4^+ and $CD25^+$ T cells. Thus, regulating PAR-1-mediated TNF-α release may be beneficial

in limiting its role in immunological responses and chronic inflammation.

The paper entitled "*The mechanism of sevoflurane preconditioning-induced protections against small intestinal ischemia reperfusion injury is independent of mast cell in rats*" by X. Gan et al. focused on investigating the efficacy of a novel inhaled anesthetic, sevoflurane, in ischemic reperfusion injury (IR) in rats induced by artery occlusion method. The findings of this study suggested that preconditioning with sevoflurane inhibited IR injury primarily by inhibiting the synthesis of $p47^{phox}$ and $gp91^{phox}$, ICAM-1, malondialdehyde, and IL-6. Moreover, mast cells were not involved in this attenuation process.

In the paper entitled "*Progression of luminal breast tumors is promoted by Ménage à Trois between the inflammatory cytokine TNFα and the hormonal and growth-supporting arms of the tumor microenvironment*," P. Weitzenfeld et al. showed that TNF-α may have strong tumor-promoting actions in luminal breast cancer cells when combined with estrogen and EGF, but not when TNF-α acts alone. Interestingly, the presence of TNF-α along with the other two growth promoting agents was sufficient to convert nonmetastatic tumor cells into a highly aggressive and metastatic phenotype. This novel finding highlights the strong prometastatic ability of TNF-α which may warrant testing of the clinically approved inhibitors of TNF-α employed for the treatment of rheumatoid arthritis and Crohn's disease to breast cancer.

The paper which is entitled "*Haplotype analysis of interleukin-8 gene polymorphisms in chronic and aggressive periodontitis*" is a clinical study. P. B. Linhartova et al. examined the role of IL-8 gene polymorphisms in chronic and aggressive periodontitis and how these polymorphisms may influence specific pathogen-mediated connective tissue loss and alveolar bone destruction. Thus, an evaluation of the genomic DNA isolated from chronic periodontitis and aggressive periodontitis, and control human subjects identified the rs4073, rs2227307, rs2227306, and rs2227532 gene polymorphisms and showed that the A(−251)/T(+396)/T(+781) and T(−251)/G(+396)/C(+781) haplotypes were significantly less frequent in patients with chronic periodontitis. Thus, the results of this study provide evidence that some of the IL-8 haplotypes could be protective against chronic periodontitis in the affected population.

Although immunotherapies are one of the most promising treatment strategies for cancer, systemic tumor-targeted delivery of these agents has proven to be the biggest obstacle to their clinical success. In the research article entitled "*Intricacies for posttranslational tumor-targeted cytokine gene therapy,*" J. Cutrera et al., using multiple syngeneic murine tumor models, examined the potential impact of the location of the targeting peptide, choice of targeting peptide, tumor histotype, and cytokine utilization on clinical efficacy. Using IL-12 gene therapy as a model system, the authors found that, within the same tumor model, the location of targeting peptide was very critical in achieving a good clinical response.

In the paper entitled "*A possible role of $CD8^+$ T lymphocytes in the cell-mediated pathogenesis of Pemphigus vulgaris*," F. Giurdanella et al. examined the role of $CD8^+$ T cells in CD8 deficient mice by evaluating the development of acantholysis with passive transfer of pemphigus vulgaris (PV) autoantibodies. The results showed a lower incidence of PV in the CD8 deficient mice compared to their wild-type counterpart. These findings also pointed to the possible role of Fas/FasL death receptor complex and ligand duo in mediating $CD8^+$ T cell immune response.

Bronchopulmonary dysplasia (BPD) is a chronic lung disease in neonates primarily caused by inflammation and epithelial cell death from mechanical ventilation and excess oxygen exposure otherwise known as hyperoxia. In the study entitled "*Hyperoxia exacerbates postnatal inflammation-induced lung injury in neonatal BRP-39 null mutant mice promoting the M1 macrophage phenotype*," M. A. Syed and V. Bhandari studied O_2-induced macrophage polarization and the anti-inflammatory role of breast regression protein-39 (BRP-39) as causative in neonatal lung injury. The results of their study showed that hyperoxia enhanced LPS-induced M1 polarization while inhibiting the IL-4-induced M2 phenotype. The absence of BRP-39 further enhanced LPS-mediated M1 phenotype macrophage polarization. Furthermore, BRP-$39^{-/-}$ mice also showed a higher sensitivity towards hyperoxia-induced lung injury and higher mortality compared to wild-type mice. Thus, the results of this study highlighted the protective role of BRP-39 in reducing neonatal lung injury by deactivating M1 macrophage-induced inflammatory responses.

In the study entitled "*Chemokines and neurodegeneration in the early stage of experimental ischemic stroke*," P. Wolinski and A. Glabinski analyzed the expression of several inflammatory biomarkers and correlated these biomarkers with the development of neurodegenerative symptoms in the early phase of experimental stroke. Using endothelin-1- (ET-1-) induced ischemic stroke model, they found that the early phase of experimentally induced stroke was characterized by migration of inflammatory lymphocytes and macrophages to the brain. However, the study did not find any conclusive evidence to correlate this migration with neurodegeneration. These findings suggest that chemokines may be a potential therapeutic target for regulating inflammatory cell accumulation in the early stage of experimentally induced stroke which might minimize ischemic neurodegeneration.

In the study entitled "*Cytokines and chemokines as regulators of skeletal muscle inflammation: presenting the case of Duchenne muscular dystrophy*," B. D. Paepe and J. L. D. Bleecker reviewed the growing accumulation of evidence for the role of cytokines and chemokines in the pathophysiology in a case of Duchenne muscular dystrophy. For obvious reasons, these findings in this individual case require further validation in animal models of Duchenne muscular dystrophy to justify for future therapeutic development.

The benefits of testosterone replacement therapy (TRT) are still debated due to significant untoward changes that are triggered in the body by TRT including changes in body composition and lipid metabolism, along with decreased high density lipoprotein (HDL), adiponectin, and osteoprotegerin levels. In the study entitled "*Strength training and testosterone treatment have opposing effects on migration inhibitor factor*

levels in ageing men," D. Glintborg et al. studied the clinical effect of TRT gels on strength training (ST) in aged men and the possible role that chemokines play in the process. The results of a double-blinded, placebo-controlled study of six-month TRT therapy showed a decrease in MIF levels in the ST placebo group, compared to increased MIF levels with TRT therapy. Thus, a consistent increase in MIF levels during TRT therapy suggests its possible association with increased inflammatory activity.

In the paper entitled "*Palmitic acid induces production of proinflammatory cytokines interleukin-6, interleukin-1β, and tumor necrosis factor-α via a NF-κB-dependent mechanism in HaCaT keratinocytes*," B. Zhou et al. studied the effect of palmitic acid on keratinocytes. This study found that palmitic acid treatment induced production of IL-6, TNF-α, and IL-1β via activation of the NF-κB pathway in human keratinocytes. They also found that palmitic acid upregulated peroxisome proliferator-activated receptor- (PPAR-) α activation and the phosphorylation of signal transducers and activators of transcription-3 protein by keratinocytes *in vitro*. These findings provided evidence that blockade of IL-6 via NF-κB pathway was a very effective in regulating palmitic acid-induced inflammation and hyperproliferation in keratinocytes.

We sincerely hope that the present special issue may provide useful information to help understand the mechanisms of inflammation mediated by cytokines or chemokines and potential new therapeutic targets. We hope that the reader will find some novel input for future research.

Salahuddin Ahmed
Charles J. Malemud
Alisa E. Koch
Mohammad Athar
Dennis D. Taub

Hindawi Publishing Corporation
Mediators of Inflammation
Volume 2014, Article ID 513027, 2 pages
http://dx.doi.org/10.1155/2014/513027

Erratum

Erratum to "Palmitic Acid Induces Production of Proinflammatory Cytokines Interleukin-6, Interleukin-1β, and Tumor Necrosis Factor-α via a NF-κB-Dependent Mechanism in HaCaT Keratinocytes"

Bing-rong Zhou, Jia-an Zhang, Qian Zhang, Felicia Permatasari, Yang Xu, Di Wu, Zhi-qiang Yin, and Dan Luo

Department of Dermatology, The First Affiliated Hospital of Nanjing Medical University, Nanjing 210029, China

Correspondence should be addressed to Dan Luo; daniluo2013@njmu.edu.cn

Received 15 March 2014; Accepted 27 April 2014; Published 21 May 2014

In the paper, the 3 bottom photos in Figure 2(a) were the same as the 3 bottom photos in Figure 2(b), and here we provide the right form of Figure 2(a). We apologize for this oversight and for any confusion that it has caused.

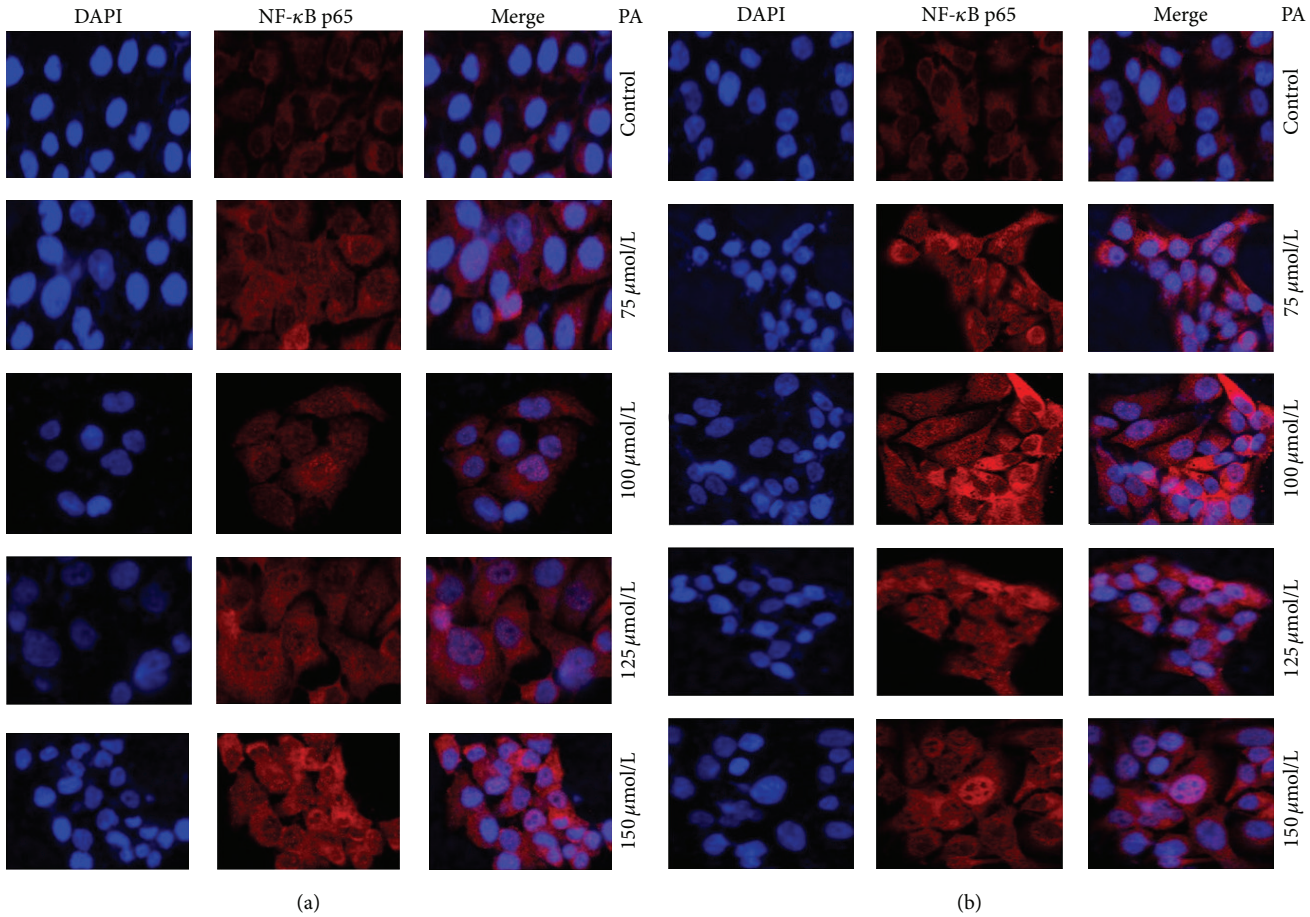

Figure 2: PA-induced nuclear translocation of NF-κB p65 subunit in HaCaT cells immediately after the treatment and 24 hours after the PA depletion. Keratinocytes were untreated or treated with PA (75, 100, 125, and 150 μmol/L) for 24 hours under serum-free conditions. Immunostaining was performed with specific mouse anti-p65 antibody followed by Cy3-conjugated mouse anti-rabbit immunoglobulins (red) immediately after the treatment (a) and 24 hours after the PA depletion (b). Images are representative of three independent experiments.

Hindawi Publishing Corporation
Mediators of Inflammation
Volume 2014, Article ID 185150, 9 pages
http://dx.doi.org/10.1155/2014/185150

Review Article

The Pathology of Orthopedic Implant Failure Is Mediated by Innate Immune System Cytokines

Stefan Landgraeber,[1,2] Marcus Jäger,[1] Joshua J. Jacobs,[2] and Nadim James Hallab[2]

[1] *Department of Orthopaedics, University Hospital Essen, University of Duisburg-Essen, Hufelandstraße 55, 45122 Essen, Germany*
[2] *Department of Orthopedics, Rush University Medical Center, 1735 W Harrison MC107, Chicago, IL 60612, USA*

Correspondence should be addressed to Nadim James Hallab; nhallab@rush.edu

Received 11 September 2013; Revised 25 March 2014; Accepted 8 April 2014; Published 7 May 2014

Academic Editor: Charles J. Malemud

All of the over 1 million total joint replacements implanted in the US each year are expected to eventually fail after 15–25 years of use, due to slow progressive subtle inflammation at the bone implant interface. This inflammatory disease state is caused by implant debris acting, primarily, on innate immune cells, that is, macrophages. This slow progressive pathological bone loss or "aseptic loosening" is a potentially life-threatening condition due to the serious complications in older people (>75 yrs) of total joint replacement revision surgery. In some people implant debris (particles and ions from metals) can influence the adaptive immune system as well, giving rise to the concept of metal sensitivity. However, a consensus of studies agrees that the dominant form of this response is due to innate reactivity by macrophages to implant debris where both danger (DAMP) and pathogen (PAMP) signalling elicit cytokine-based inflammatory responses. This paper discusses implant debris induced release of the cytokines and chemokines due to activation of the innate (and the adaptive) immune system and the subsequent formation of osteolysis. Different mechanisms of implant-debris reactivity related to the innate immune system are detailed, for example, danger signalling (e.g., IL-1β, IL-18, IL-33, etc.), toll-like receptor activation (e.g., IL-6, TNF-α, etc.), apoptosis (e.g., caspases 3–9), bone catabolism (e.g., TRAP5b), and hypoxia responses (Hif1-α). Cytokine-based clinical and basic science studies are in progress to provide diagnosis and therapeutic intervention strategies.

1. Introduction

Total hip and knee replacements are examples of successful surgical interventions with overall success rates of >90% at ten years after surgery [1]. However, increasing time after surgery correlates with greater incidence of loosened/failing hip and knee arthroplasties, where survival rates at 15–20 years after operation are very low <50%. Currently, 40,000 hip arthroplasties have to be revised each year in the US because of painful implant loosening and it is expected that the rates of revision will increase by 137% for total hip and 601% for total knee revisions over the next 25 years [2]. Painful loosening is a serious long-term complication because of the high clinical/surgical risks of revision surgery and the associated high health-care costs. The number of revisions is accompanied by diminishing bone stock and the need for even larger implants, which increases the risk profile. Improvements in surgical techniques, materials, and implant designs have reduced the problem over the years by reducing particle production but the underlying problem remains. Thus diagnosing and stopping debris induced osteolysis are particular problems that have not been solved and are needed to improve the long term performance of joint replacement implants.

Aseptic loosening (no infection) is the main cause for revision surgery over the mid- and long-term and is responsible for >70% of hip revisions and >44% of knee revisions [3, 4]. Various biomechanical factors like micromotion may play a role in the induction of aseptic loosening directly but also indirectly through the formation of additional wear particles. The various implant debris induced biological reactions have been well established as the central causal problem [5–7].

This local bone loss (or peri-implant osteolysis) is initiated by aseptic inflammatory responses to phagocytosis of small implant wear particles (generally <10 microns in diameter) resulting in increased proliferation and differentiation of osteoclast precursors into mature osteoclasts [8–10]. Various cytokines and chemokines are involved in this inflammatory activation of osteoclasts. This paper will discuss implant debris (e.g., wear particle) induced release of cytokines and chemokines due to activation of the innate and the adaptive immune system and the subsequent formation of osteolysis and how this knowledge is currently used for diagnosis and therapy.

2. Innate Immune System Response to Wear Debris Particles

2.1. Macrophages. Inflammatory responses to implant debris over time have been attributed to macrophage reactivity and have been the primary focus of investigation over the past 40 years. Recent studies demonstrate a predominance of M1 macrophages in response to implant debris challenge (released metal ions and particles), which produce primarily proinflammatory mediators that affect other local cell around implants (Figure 1) [11]. Thus, given that wear particles are biologically active and influence the innate immune pathway, the amount, appearance, rate of production, time of exposure, and antigenicity of the wear particulates are important [12, 13]. It has been shown that macrophages release a host of M1 associated cytokines after contact with wear debris. These include IL-1α, IL-1β, IL-6, IL-10, IL-11, IL-15, tumor necrosis factor α (TNF-α), transforming growth factor α (TGF-α), granulocyte-macrophage colony stimulating factor (GM-CSF), macrophage colony stimulating factor (M-CSF), platelet-derived growth factor, and epidermal growth factor (Figure 1) [14]. It is likely that more subtle, less studied cytokines and tissue responses are involved in this reactivity as well. The interaction of all these cytokines is very complex and not fully understood yet. While M-CSF and others activate the formation of osteoclasts directly, IL-1, TNFα, and IL-6 can affect osteoblasts and other cells which in turn activate osteoclasts and increase cytokine release by macrophages [14]. GM-CSF is responsible for formation of multinucleate giant cells (MNGCs), which act very similar to osteoclasts.

Chemokine expression by macrophages, fibroblasts, and osteoblasts exposed to implant debris is also a central innate immune effector reaction to implant debris [15–19]. The chemokines, particular to implant aseptic loosening pathology, include IL-8, MCP-1 MIP-1α, CCL17/TARC, and CCL22/MDC [20]. IL-8, a CXC chemokine, is upregulated by macrophages and MSCs in periprosthetic tissues by different types of wear particles like titanium, CoCr, and UMHWPE [21, 22]. This migration of macrophages and osteoclasts to the sites around implants leads to accelerated osteolysis [20].

Increased expression of MCP-1, MIP1 (CCL-2), and MIP 1α (CCL3) was observed in periprosthetic tissues from failed arthroplasties and also in macrophages analyzed cell culture after exposure to different types of wear particles [16]. In contrast to MIP1α, an increased release of MCP-1 was also observed from fibroblasts after exposure to titanium and PMMA particles [17]. Reactions in vivo to UHMWPE and PMMA particle challenge were judged responsible for recruitment of macrophages [23, 24] given systemic migration of macrophages in a mice model decreased when deficient in the CCR2 receptor [23] or after blocking CCR2 receptor [24]. Blocking CCR1 or CCR2 eliminated the migration of MSCs in vitro and blocking CCL17/TARC and CCL22/MDC in osteoclasts and hFOB and their cognate receptor CCR4 in osteoclasts precursors decreased recruitment of osteoclast precursors to the bone-implant interface [25] and are currently potential targets of future interventions [24, 26].

2.2. Bone Responses

2.2.1. Osteoclasts. The role of osteoclasts is central to osteolysis, as they are the primary bone resorbing cells. RANK(L) signalling is central for the activation of osteoclasts and activates a variety of downstream signalling pathways required for osteoclast development, but crosstalk with other signalling pathways also fine-tunes bone homeostasis both in normal physiology and disease [27, 28]. The degree to which other cells with the potential to resorb bone (e.g., macrophages) can participate directly in debris induced osteolysis is not known. The role of released cytokines such as TNF-α is also important, but their contribution to osteoclast formation is currently unclear.

Kadoya et al. showed that MNGCs express some markers which are also expressed by osteoclasts, like tartrate-resistant acid phosphatase (TRAP) and vitronectin receptor (VNR) [29]. This applied to MNGCs located on the bone side of the soft-interfacial-tissue (located between implants and bone) but not to those on the implant side. Additionally, in vitro studies have shown that macrophages, exposed to wear debris particles, are capable of a type of low-grade bone resorption [30]. But although if the bone resorbing activity of macrophages is very reasonable, given their abundance and close ontogenic relationship with osteoclasts, it is far from certain that macrophages participate in bone destruction and further studies will be necessary to clarify their role in this context.

Osteoclasts in turn are also capable of phagocytosing a wide size range of ceramic, polymeric, and metallic wear particles. After particle phagocytosis, they remain fully functional, hormone responsive, bone resorbing cells [31, 32], thus showing that at least in vitro there is substantial plasticity between these key cell types involved in implant associated osteolysis that derive from the same precursor cells in bone marrow. Even participation of the early forms of macrophages and osteoclasts, mesenchymal stem cells, have been implicated in aseptic loosening [21], where the endocytosis of wear particles reduced proliferation and osteogenic differentiation and induces an increased production of IL-8 [21]. The association between MNGC and osteoclast formation does not reflect some sort of transdifferentiation or plasticity, but rather than that all macrophage populations include immature macrophages that form both osteoclasts and mature

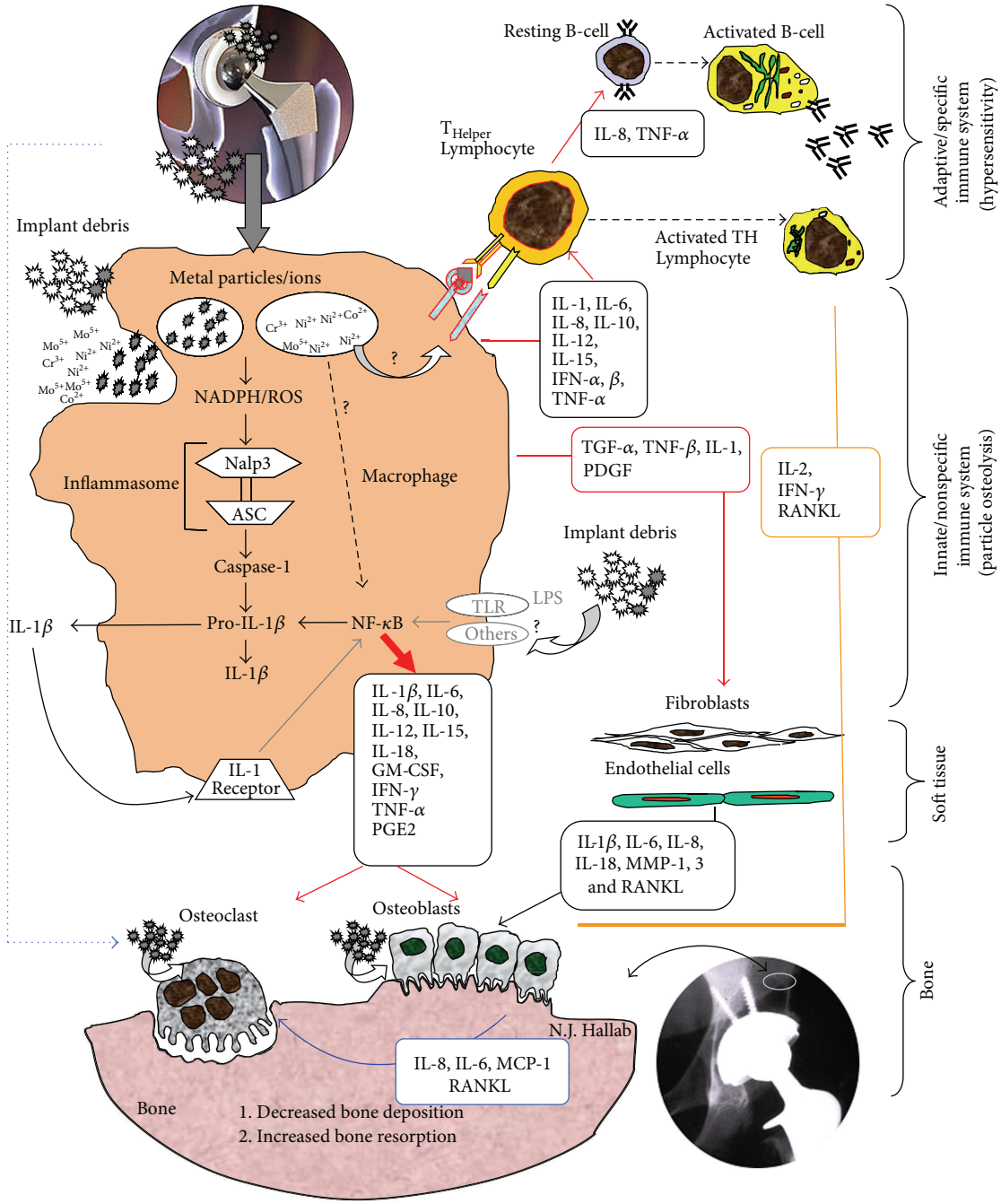

FIGURE 1: Schematic of how the inflammasome pathway is centrally involved in the pathology of implant debris-induced local cytokine responses (courtesy of Bioengineering Solutions Inc.).

macrophages. This makes it difficult to distinguish MNGC from osteoclasts in histological sections unless they are opposed to the bone surface.

2.2.2. Osteoblasts. Osteoblasts are stimulated by wear particles to produce the osteoclastogenesis factors RANKL and M-CSF [33] and cytokines such as IL-6 and IL-8 [34]. The same study also reports a slightly increased expression of VEGF induced by all particle entities and decreased de novo synthesis of type 1 collagen as well as increased expression of matrix metalloproteinase (MMP)-1.

2.3. Soft Tissue Responses

2.3.1. Fibroblasts. Soft tissue cells such as fibroblasts are also actively involved in osteoclastogenesis and bone resorption [35]. The most prominent upregulated genes and proteins secreted by fibroblasts in response to wear debris were matrix metalloproteinase 1 (MMP-1), monocyte chemotactic

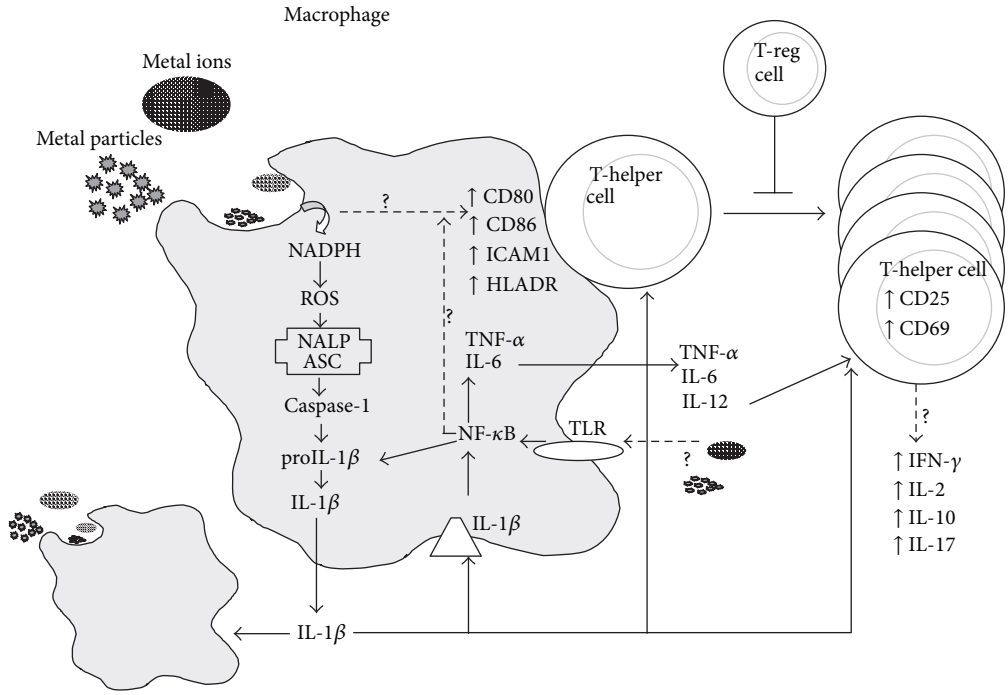

Figure 2: Innate immune system (i.e., macrophage) interactions with implant debris produce danger signalling (inflammasome) and pathogen (NF-κB) associated cytokines such as IL-1β and TNFα and increased expression of costimulatory molecules such as CD80/86, ICAM1, and HLADR. These innate responses can trigger adaptive immune responses where destructive TH1 type cytokine profiles require T-regulatory cells (e.g., IL-10) to control this response (courtesy of Bioengineering Solutions Inc.).

protein-1 (MCP-1), IL-1β, IL-6, IL-8, cyclooxygenase 1 (cox-1), cox-2, leukemia inhibitory factor, transforming growth factor beta 1 (TGFβ1), and TGFβ receptor type I. Stimulated fibroblasts express RANKL and osteoprotegerin.

2.4. Adaptive Immune Responses

2.4.1. Lymphocytes. Lymphocytes can play a crucial role in the peri-implant "debris-reactivity" environment as well. It is well recognized that T and B lymphocytes are present in peri-implant tissues [36, 37]. The subtypes of T cells that dominate implant debris associated responses are T-helper (TH) and not T cytotoxic/suppressor (TC/S) which have been found at an in vivo ratio of 7.2 : 1 [38]. Of the T-helper cells present, TH1 cells predominate as characterized by production of IFN-γ and IL-2 and to a lesser degree IL-17, fractalkine, and CD40, which indicate the possibility of TH17 activity (versus nonobserved TH2 cell mediated IL-10 responses) [39, 40]. The involvement of specific lymphocyte responses TH1 cells that can also recruit and activate macrophages, with relatively very few participating local cells, suggests that the role of adaptive immune response may be overlooked and falsely (in some cases) attributed to innate macrophage innate nonspecific immune responses, Figure 2. It has been difficult to readily identify these responses in peri-implant tissues, by such signature cytokines as IL-2, interferon-γ, TNF-α, and IL-2 receptors [41]. But some studies using mRNA detection instead of tissue immunohistochemistry (IL-2) have shown the increased expression of these TH1 cytokines [42, 43]. Furthermore, macrophages and lymphocytes seem to interact with each other via lesser reported coreceptors and cytokines such as IL-15 and its related IL15 receptor (IL-15Rα) on the macrophages, respectively, IL2 receptor (IL-2Rβ) on the lymphocytes [44]. These TH responses have been characterized as type IV delayed type hypersensitivity. DTH response to metal implant debris is an adaptive slow cell mediated type of response. Metal-antigen sensitized and activated DTH T-cells release various cytokines which recruit and activate macrophages, Figure 2 [38], such as IL-3 and GM-CSF (promotes hematopoiesis of granulocytes); monocyte chemotactic activating factor (MCAF) (promotes chemotaxis of monocytes toward areas of DTH activation); IFN-γ and TNF-β (produce a number of effects on local endothelial cells facilitating infiltration); and migration inhibitory factor (MIF) (signals macrophages to remain in the local area of the DTH reaction). Activated macrophages have increased ability to present class II MHC and IL-2 and can trigger the activation of more T-DTH cells, which in turn recruit/activate more macrophages, which recruit/activate more T-DTH cells, in a runaway cycle of inflammation, without T-regulatory cells (and other factors) to inhibit the response over time. A DTH self-perpetuating response can create extensive tissue damage. Forms of metal sensitivity testing such as lymphocyte transformation test (LTT) and patch testing (for skin reactions) are the only means to predict/diagnose those individuals that will have an excessive immune response to metal exposure that may lead to premature implant failure (approximately >1-2% patients/yr) [38].

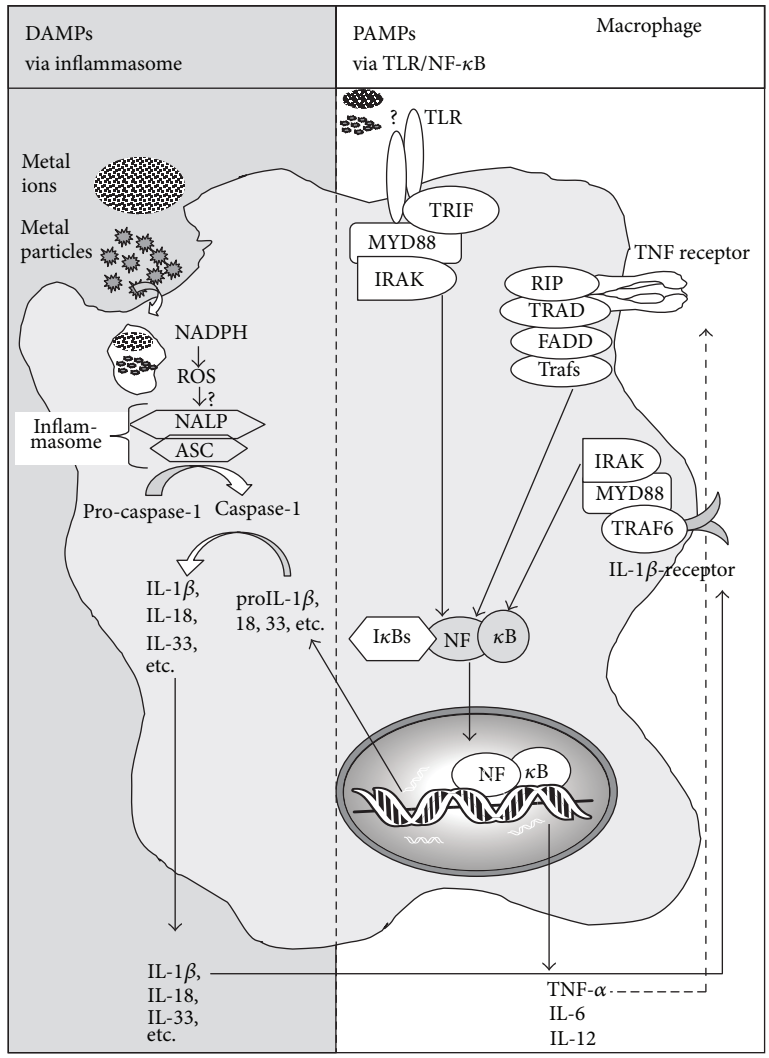

Figure 3: Schematic of intracellular innate immune responses to implant debris (metal ions and particles) that produce both DAMP and PAMP pathway activations through lysosomal destabilization (DAMPs) and either TLR or cytokine receptor activation (PAMPs), resulting in the collaborative interaction of the inflammasome and NF-κB pathways (courtesy of Bioengineering Solutions Inc.).

3. Initial Mechanisms for the Wear Particle Related Activation of the Innate Immune System

Despite new understandings of implant related cytokine/chemokines networks that are their release by different peri-implant cell types, the mechanisms mediating cellular interaction with debris particles and the subsequent activation of macrophages to produce and release the inflammatory mediators remain incomplete. Past investigations have shown the importance of PAMPs (e.g., toll-like receptors, TLRs) in vivo, in the periprosthetic tissues of patients with aseptic loosening [45–47] and in TLR-knockout mouse models (MyD88 knockout mice) where lower amounts of cytokines and osteolysis were induced by polymethylmethacrylate (PMMA) implant debris particles than wild-type mice [20, 48]. The MyD88 dependent pathways of TLR signalling result in activation of nuclear factor NF-κB, which has been long shown to play a role in particle induced osteolysis and the production of proinflammatory cytokines such as TNFα, IL-1β, and IL-12, Figure 3 [49].

Toxicity responses are another facet of innate immune activation where apoptosis and hypoxia responses have been found to be induced by implant debris [50–52]. Soluble and particulate metal debris have been shown to induce hypoxia-like pathology resulting in HIF-1α compensatory responses to metal implant debris by promoting both the induction of hypoxia (HIF-1α) and tissue angiogenesis (VEGF) providing a specific mechanism which explains why local soft tissue growths (fibrous pseudotumors) and apoptosis responses can form in some people with certain orthopedic implants [52]. The induction of apoptosis associated processes by implant debris has also been correlated with implant debris in vivo [53, 54]. And more recently ceramic and polyethylene

implant debris particles have been shown to induce some form of apoptosis of macrophages in vitro [50, 51]. This in vitro evidence has been supported by in vivo immunohistochemistry of central apoptosis-related mediators such as caspase-3 associated with macrophages, giant cells, and T-lymphocytes in local tissues (capsules and interfacial membranes) of patients with aseptic hip implants [55, 56]. The importance of apoptosis associated mediators has been made clear by murine osteolysis models that demonstrated inhibition of apoptosis by a pan-caspase inhibitor leads to decreasing bone resorption by osteoclasts [57] and presumably decreased amounts of apoptosis associated cytokines like interleukin-8 (IL-8), monocyte chemoattractant protein-1 (MCP-1), intercellular adhesion molecule-1, and type-1 interferon [58, 59].

The influence of danger signalling, that is, inflammasome activation, is a relatively new approach in orthopedics. Nonpathogen derived stimuli typically activate immune cells through a danger signal pathways, the central components of which are termed the "inflammasome" [60]. Effective immune system activation requires specific receptors that recognize both pathogen associated molecular patterns (PAMPs) and danger associated molecular patterns (DAMPs) to initiate innate proinflammatory responses, Figures 1 and 3 [61, 62]. Nonpathogen derived danger signals are triggered by DAMPs such as UV light, particulate adjuvants present in modern vaccines [63, 64], and recently have been discovered to be activated by implant debris [65]. Typical particulate DAMPs induce lysosomal destabilization, which cause an increase in NADPH (nicotinamide adenine dinucleotide phosphate-oxidase) and an increase in reactive oxygen species (ROS). The release of these intracellular contents is sensed by specific members of the NLR family, such as NALP3 (NACHT-, LRR-, and pyrin domain-containing protein 3). NALP3 protein, in association with ASC (apoptosis-associated speck-like protein containing a CARD domain), forms the intracellular multiprotein complex, that is, the inflammasome complex [66, 67]. Activation of the inflammasome (NALPs-ASC complex) leads to the cleavage of pro-caspase-1 into active caspase-1 (previously known as ICE, interleukin-1 converting enzyme). Active Caspase-1 is required for the processing and subsequent release of active proinflammatory cytokines such as IL-1β and IL-18 (and others) by cleaving intracellular pro-IL-1β, pro-IL-18, and so forth into their mature forms, IL-1b and IL-18. As IL-1β is one of the main cytokines for activation of osteolysis, an involvement in aseptic loosening is obvious, as a recent study has shown less osteolysis in caspase-1 knockout mice [68].

It is well accepted that the inflammatory factors previously described here drive osteoclast formation through progenitor recruitment and RANKL induction; however, the detailed mechanics of how this occurs remains unknown. IL-1, for example, strongly stimulates osteolysis in many contexts but does not affect OC formation directly yet is a very weak inducer of RANKL in bone cells in vitro.

4. Therapy of Aseptic Loosening by Regulation of the Innate Immune Response

New biologic treatments addressing the pathology of aseptic implant loosening are currently under development and in clinical trials. Some cytokine inhibitors have been investigated using in vitro and in vivo animal models. Potential treatments include the following.

AM630 is a selective inhibitor of cannabinoid receptor 2 that inhibits IL-1β and TNF-α [69].

LY294002 is a specific inhibitor of PI3 K that suppresses the expression of TNF-α [70].

Tetrazykline inhibits MMP-9 [71].

Simvastatin decreases ERK1/2 a phosphorylated protein which is stimulated by wear particles and involved in cell signalling activation of macrophages [72].

None of the aforementioned cytokine regulating drugs have been tested in clinical trials, due to the serious side effects and risks associated with immunosuppressive medications. Other potential candidates (for clinical treatment) include drugs indicated for the treatment of rheumatoid arthritis and other inflammatory diseases, such as traditional nonsteroidal anti-inflammatory drugs (NSAIDs), selective cyclooxygenase (COX) inhibitors (e.g., celecoxib), tumor necrosis factor (TNF) antagonists (e.g., etanercept, infliximab, adalimumab), and interleukin-1 antagonists (e.g., anakinra) [73]. However many investigators remain concerned about the application of these drugs for this pathology due to the antianabolic effects of NSAIDs and COX-2 inhibitors, and the immunosuppressive effects of the anti-inflammatory drugs [73]. Newer drugs using small interfering RNA (siRNA) have shown promise in vivo where a mouse model demonstrated that local delivery of lentivirus-mediated TNF-α small interfering RNA (siRNA) resulted in less implant debris induced TNF-α, IL-1, and IL-6 and overall in a less associated inflammation [74].

Furthermore, without clinically validated early detection biomarkers of implant loosening, by the time patients presents with pain and radiological evidence of loosening the implant is mechanically loose, and the associated continuous micromotion acts to prevent reintegration even if implant debris associated inflammation-induced osteolysis is arrested [73]. Thus diagnosis of early stages of aseptic loosening is paramount and is the focus of much continued research. Other nonimmune related counter measures to implant debris induced osteolysis have also focused on enhancing bone responses in the face of inflammation. Although beyond the scope of this review, two noteworthy anti-bone-resorption (i.e., osteoclast inhibiting) bisphosphonates (Etidronate and Alendronate) are currently being evaluated for long-term therapy [75–78], although the embrittlement of bone and cases of early fracture have tempered these efforts.

5. Conclusion

The serious pathology of aseptic osteolysis around joint replacement implants is intimately dependent on cytokines and chemokines released by innate and adaptive immune reactions and local cells around implants. These types of debris-induced inflammation are dominated by innate immune cell (macrophages) secretion of TNFα, IL-1β, IL-6, and PGE2, which causes peri-implant bone resorption. Given the increasing number of people receiving orthopedic implants the issue of biologic reactivity is growing more prevalent. There is a growing need for more targeted approaches of diagnosis and early intervention of unwanted debris-induced inflammation. New understanding of how sterile nonpathogen implant debris causes immune activation and other local reaction continue to be discovered, such as the inflammasome "danger signalling" pathway [60], and the induction of hypoxia and apoptosis related reactivity [52, 55, 56, 79]. Consequently new therapies (such as anti-TNF-infliximab, anti-IL-1β, IL-1β-receptor-antagonist anakinra, etc.) are under current investigation as targeting measurement and pharmacologic interventions. New diagnostic testing modalities (e.g., cytokines, chemokines, bone metabolism markers, and lymphocyte testing, LTT) are under investigation as candidate early diagnostic measures of debris induced inflammation. Soon these studies will lead to early detection and thus treatment of debris induced inflammation leading to improved long term implant performance.

Conflict of Interests

The authors declare that they have no conflict of interest regarding the publication of this paper.

References

[1] T. M. Wright and S. B. Goodman, *Implant Wear in Total Joint Replacement: Clinical and Biologic Issues, Material and Design Considerations*, American Academy of Orthopaedic Surgeons, Rosemont, Ill, USA, 2001.

[2] S. Kurtz, K. Ong, E. Lau, F. Mowat, and M. Halpern, "Projections of primary and revision hip and knee arthroplasty in the United States from 2005 to 2030," *Journal of Bone and Joint Surgery—Series A*, vol. 89, no. 4, pp. 780–785, 2007.

[3] P. Herberts and H. Malchau, "Long-term registration has improved the quality of hip replacement: a review of the Swedish THR Register comparing 160,000 cases," *Acta Orthopaedica Scandinavica*, vol. 71, no. 2, pp. 111–121, 2000.

[4] O. Robertsson, K. Knutson, S. Lewold, and L. Lidgren, "The Swedish Knee Arthroplasty Register 1975–1997: an update with special emphasis on 41,223 knees operated on in 1988–1997," *Acta Orthopaedica Scandinavica*, vol. 72, no. 5, pp. 503–513, 2001.

[5] M. Boehler, H. Plenk Jr., and M. Salzer, "Alumina ceramic bearings for hip endoprostheses: the Austrian experiences," *Clinical Orthopaedics and Related Research*, no. 379, pp. 85–93, 2000.

[6] S. Santavirta, M. Takagi, E. Gómez-Barrena et al., "Studies of host response to orthopedic implants and biomaterials," *Journal of Long-Term Effects of Medical Implants*, vol. 9, no. 1-2, pp. 67–76, 1999.

[7] H.-G. Willert, H. Bertram, and G. Hans Buchhorn, "Osteolysis in alloarthroplasty of the hip: the role of ultra-high molecular weight polyethylene wear particles," *Clinical Orthopaedics and Related Research*, no. 258, pp. 95–107, 1990.

[8] E. M. Schwarz, A. P. Lu, J. J. Goater et al., "Tumor necrosis factor-α/nuclear transcription factor-κB signaling in periprosthetic osteolysis," *Journal of Orthopaedic Research*, vol. 18, no. 3, pp. 472–480, 2000.

[9] M. J. Silva and L. J. Sandell, "What's new in orthopaedic research," *Journal of Bone and Joint Surgery—Series A*, vol. 84, no. 8, pp. 1490–1496, 2002.

[10] J. T. Wang, "The role of particulate orthopaedic implant materials in peri-implant osteolysis," in *Biological, Material, and Mechanical Considerations of Joint Replacement*, B. F. Morrey, Ed., pp. 1–122, Raven Press, New York, NY, USA, 1993.

[11] A. J. Rao, E. Gibon, T. Ma, Z. Yao, R. L. Smith, and S. B. Goodman, "Revision joint replacement, wear particles, and macrophage polarization," *Acta Biomaterialia*, vol. 8, no. 7, pp. 2815–2823, 2012.

[12] Y. Kadoya, P. A. Revell, A. Kobayashi, N. Al-Saffar, G. Scott, and M. A. R. Freeman, "Wear particulate species and bone loss in failed total joint arthroplasties," *Clinical Orthopaedics and Related Research*, no. 340, pp. 118–129, 1997.

[13] A. S. Shanbhag, J. J. Jacobs, J. Black, J. O. Galante, and T. T. Glant, "Macrophage/particle interactions: effect of size, composition and surface area," *Journal of Biomedical Materials Research*, vol. 28, no. 1, pp. 81–90, 1994.

[14] P. A. Revell, "Biological causes of prosthesis joint failure," in *Joint Replacement Technology*, P. A. Revell, Ed., pp. 349–396, Woodhead Publishing Limited and CRC Press LLC, Cambridge, UK, 2008.

[15] M. Lind, M. C. D. Trindade, D. J. Schurman, S. B. Goodman, and R. L. Smith, "Monocyte migration inhibitory factor synthesis and gene expression in particle-activated macrophages," *Cytokine*, vol. 12, no. 7, pp. 909–913, 2000.

[16] Y. Nakashima, D.-H. Sun, M. C. D. Trindade et al., "Induction of macrophage C-C chemokine expression by titanium alloy and bone cement particles," *Journal of Bone and Joint Surgery - Series B*, vol. 81, no. 1, pp. 155–162, 1999.

[17] B. Yaszay, M. C. D. Trindade, M. Lind, S. B. Goodman, and R. L. Smith, "Fibroblast expression of C-C chemokines in response to orthopaedic biomaterial particle challenge in vitro," *Journal of Orthopaedic Research*, vol. 19, no. 5, pp. 970–976, 2001.

[18] P.-G. Ren, Z. Huang, T. Ma, S. Biswal, R. L. Smith, and S. B. Goodman, "Surveillance of systemic trafficking of macrophages induced by UHMWPE particles in nude mice by noninvasive imaging," *Journal of Biomedical Materials Research—Part A*, vol. 94, no. 3, pp. 706–711, 2010.

[19] P.-G. Ren, A. Irani, Z. Huang, T. Ma, S. Biswal, and S. B. Goodman, "Continuous infusion of UHMWPE particles induces increased bone macrophages and osteolysis," *Clinical Orthopaedics and Related Research*, vol. 469, no. 1, pp. 113–122, 2011.

[20] Q. Gu, Q. Shi, and H. Yang, "The role of TLR and chemokine in wear particle-induced aseptic loosening," *Journal of Biomedicine and Biotechnology*, vol. 2012, Article ID 596870, 9 pages, 2012.

[21] H. Haleem-Smith, E. Argintar, C. Bush et al., "Biological responses of human mesenchymal stem cells to titanium wear

debris particles," *Journal of Orthopaedic Research*, vol. 30, no. 6, pp. 853–863, 2012.

[22] A. M. Kaufman, C. I. Alabre, H. E. Rubash, and A. S. Shanbhag, "Human macrophage response to UHMWPE, TiAlV, CoCr, and alumina particles: analysis of multiple cytokines using protein arrays," *Journal of Biomedical Materials Research—Part A*, vol. 84, no. 2, pp. 464–474, 2008.

[23] E. Gibon, T. Ma, P.-G. Ren et al., "Selective inhibition of the MCP-1-CCR2 ligand-receptor axis decreases systemic trafficking of macrophages in the presence of UHMWPE particles," *Journal of Orthopaedic Research*, vol. 30, no. 4, pp. 547–553, 2012.

[24] Z. Huang, T. Ma, P.-G. Ren, R. L. Smith, and S. B. Goodman, "Effects of orthopedic polymer particles on chemotaxis of macrophages and mesenchymal stem cells," *Journal of Biomedical Materials Research—Part A*, vol. 94, no. 4, pp. 1264–1269, 2010.

[25] D. Cadosch, O. P. Gautschi, E. Chan, H.-P. Simmen, and L. Filgueira, "Titanium induced production of chemokines CCL17/TARC and CCL22/MDC in human osteoclasts and osteoblasts," *Journal of Biomedical Materials Research—Part A*, vol. 92, no. 2, pp. 475–483, 2010.

[26] E. Gibon, Z. Yao, A. J. Rao et al., "Effect of a CCR1 receptor antagonist on systemic trafficking of MSCs and polyethylene particle-associated bone loss," *Biomaterials*, vol. 33, no. 14, pp. 3632–3638, 2012.

[27] A. Leibbrandt and J. M. Penninger, "RANK(L) as a key target for controlling bone loss," *Advances in Experimental Medicine and Biology*, vol. 647, pp. 130–145, 2009.

[28] A. Leibbrandt and J. M. Penninger, "RANKL/RANK as key factors for osteoclast development and bone loss in arthropathies," *Advances in Experimental Medicine and Biology*, vol. 649, pp. 100–113, 2009.

[29] Y. Kadoya, N. Al-Saffar, A. Kobayashi, and P. A. Revell, "The expression of osteoclast markers on foreign body giant cells," *Bone and Mineral*, vol. 27, no. 2, pp. 85–96, 1994.

[30] N. A. Athanasou, J. Quinn, and C. J. K. Bulstrode, "Resorption of bone by inflammatory cells derived from the joint capsule of hip arthroplasties," *Journal of Bone and Joint Surgery—Series B*, vol. 74, no. 1, pp. 57–62, 1992.

[31] W. Wang, D. J. Ferguson, J. M. Quinn, A. H. Simpson, and N. A. Athanasou, "Osteoclasts are capable of particle phagocytosis and bone resorption," *The Journal of Pathology*, vol. 182, no. 1, pp. 92–98, 1997.

[32] W. Wang, D. J. P. Ferguson, J. M. W. Quinn, A. H. R. W. Simpson, and N. A. Athanasou, "Biomaterial particle phagocytosis by bone-resorbing osteoclasts," *Journal of Bone and Joint Surgery—Series B*, vol. 79, no. 5, pp. 849–856, 1997.

[33] D. P. Pioletti and A. Kottelat, "The influence of wear particles in the expression of osteoclastogenesis factors by osteoblasts," *Biomaterials*, vol. 25, no. 27, pp. 5803–5808, 2004.

[34] K. Lochner, A. Fritsche, A. Jonitz et al., "The potential role of human osteoblasts for periprosthetic osteolysis following exposure to wear particles," *International Journal of Molecular Medicine*, vol. 28, no. 6, pp. 1055–1063, 2011.

[35] T. Koreny, M. Tunyogi-Csapó, I. Gál, C. Vermes, J. J. Jacobs, and T. T. Glant, "The role of fibroblasts and fibroblast-derived factors in periprosthetic osteolysis," *Arthritis and Rheumatism*, vol. 54, no. 10, pp. 3221–3232, 2006.

[36] N. Al-Saffar and P. A. Revell, "Pathology of the bone-implant interfaces," *Journal of Long-Term Effects of Medical Implants*, vol. 9, no. 4, pp. 319–347, 1999.

[37] P. A. Revell, N. Al-Saffar, and A. Kobayashi, "Biological reaction to debris in relation to joint prostheses," *Proceedings of the Institution of Mechanical Engineers, Part H: Journal of Engineering in Medicine*, vol. 211, no. 2, pp. 187–197, 1997.

[38] P. A. Revell, "The combined role of wear particles, macrophages and lymphocytes in the loosening of total joint prostheses," *Journal of the Royal Society Interface*, vol. 5, no. 28, pp. 1263–1278, 2008.

[39] B. Hercus, S. Saeed, and P. A. Revell, "Expression profile of T cell associated molecules in the interfacial tissue of aseptically loosened prosthetic joints," *Journal of Materials Science: Materials in Medicine*, vol. 13, no. 12, pp. 1153–1156, 2002.

[40] N. J. Hallab, M. Caicedo, A. Finnegan, and J. J. Jacobs, "Th1 type lymphocyte reactivity to metals in patients with total hip arthroplasty," *Journal of Orthopaedic Surgery and Research*, vol. 3, no. 1, article 6, 2008.

[41] T.-F. Li, S. Santavirta, V. Waris et al., "No lymphokines in T-cells around loosened hip prostheses," *Acta Orthopaedica Scandinavica*, vol. 72, no. 3, pp. 241–247, 2001.

[42] B. Hercus and P. A. Revell, "Phenotypic characteristics of T lymphocytes in the interfacial tissue of aseptically loosened prosthetic joints," *Journal of Materials Science: Materials in Medicine*, vol. 12, no. 10–12, pp. 1063–1067, 2001.

[43] P. A. Revell and S. E. Jellie, "Interleukin 15 production by macrophages in the implant interface membrane of aseptically loosened joint replacements," *Journal of Materials Science: Materials in Medicine*, vol. 9, no. 12, pp. 727–730, 1998.

[44] S. Saeed and P. A. Revell, "Production and distribution of interleukin 15 and its receptors (IL-15Rα and IL-R2β) in the implant interface tissues obtained during revision of failed total joint replacement," *International Journal of Experimental Pathology*, vol. 82, no. 3, pp. 201–209, 2001.

[45] T. Lähdeoja, J. Pajarinen, V.-P. Kouri, T. Sillat, J. Salo, and Y. T. Konttinen, "TOll-like receptors and aseptic loosening of hip endoprosthesis—a potential to respond against danger signals?" *Journal of Orthopaedic Research*, vol. 28, no. 2, pp. 184–190, 2010.

[46] J. Pajarinen, E. Cenni, L. Savarino et al., "Profile of toll-like receptor-positive cells in septic and aseptic loosening of total hip arthroplasty implants," *Journal of Biomedical Materials Research—Part A*, vol. 94, no. 1, pp. 84–92, 2010.

[47] M. Takagi, Y. Tamaki, H. Hasegawa et al., "Toll-like receptors in the interface membrane around loosening total hip replacement implants," *Journal of Biomedical Materials Research—Part A*, vol. 81, no. 4, pp. 1017–1026, 2007.

[48] J. I. Pearl, T. Ma, A. R. Irani et al., "Role of the Toll-like receptor pathway in the recognition of orthopedic implant wear-debris particles," *Biomaterials*, vol. 32, no. 24, pp. 5535–5542, 2011.

[49] R. Maitra, C. C. Clement, B. Scharf et al., "Endosomal damage and TLR2 mediated inflammasome activation by alkane particles in the generation of aseptic osteolysis," *Molecular Immunology*, vol. 47, no. 2-3, pp. 175–184, 2009.

[50] I. Catelas, A. Petit, D. J. Zukor, R. Marchand, L. Yahia, and O. L. Huk, "Induction of macrophage apoptosis by ceramic and polyethylene particles in vitro," *Biomaterials*, vol. 20, no. 7, pp. 625–630, 1999.

[51] D. Granchi, E. Cenni, G. Ciapetti et al., "CEll death induced by metal ions: necrosis or apoptosis?" *Journal of Materials Science: Materials in Medicine*, vol. 9, no. 1, pp. 31–37, 1998.

[52] L. Samelko, M. S. Caicedo, S. J. Lim, C. Della-Valle, J. Jacobs, and N. J. Hallab, "Cobalt-alloy implant debris induce HIF-1alpha hypoxia associated responses: a mechanism for metal-specific

orthopedic implant failure," *PLoS One*, vol. 8, no. 6, article e67127, 2013.

[53] O. L. Huk, D. J. Zukor, W. Ralston, A. Lisbona, and A. Petit, "Apoptosis in interface membranes of aseptically loose total hip arthroplasty," *Journal of Materials Science: Materials in Medicine*, vol. 12, no. 7, pp. 653–658, 2001.

[54] M. L. Wang, R. Tuli, P. A. Manner, P. F. Sharkey, D. J. Hall, and R. S. Tuan, "Direct and indirect induction of apoptosis in human mesenchymal stem cells in response to titanium particles," *Journal of Orthopaedic Research*, vol. 21, no. 4, pp. 697–707, 2003.

[55] S. Landgraeber, M. Toetsch, C. Wedemeyer et al., "Overexpression of p53/BAK in aseptic loosening after total hip replacement," *Biomaterials*, vol. 27, no. 15, pp. 3010–3020, 2006.

[56] S. Landgraeber, M. von Knoch, F. Löer et al., "Extrinsic and intrinsic pathways of apoptosis in aseptic loosening after total hip replacement," *Biomaterials*, vol. 29, no. 24-25, pp. 3444–3450, 2008.

[57] S. Landgraeber, S. Jaeckel, F. Löer et al., "Pan-caspase inhibition suppresses polyethylene particle-induced osteolysis," *Apoptosis*, vol. 14, no. 2, pp. 173–181, 2009.

[58] C. Cerri, D. Chimenti, I. Conti, T. Neri, P. Paggiaro, and A. Celi, "Monocyte/macrophage-derived microparticles upregulate inflammatory mediator synthesis by human airway epithelial cells," *Journal of Immunology*, vol. 177, no. 3, pp. 1975–1980, 2006.

[59] P. Heyder, I. Bekeredjian-Ding, M. Parcina et al., "Purified apoptotic bodies stimulate plasmacytoid dendritic cells to produce IFN-alpha," *Autoimmunity*, vol. 40, no. 4, pp. 331–332, 2007.

[60] F. Martinon, V. Pétrilli, A. Mayor, A. Tardivel, and J. Tschopp, "Gout-associated uric acid crystals activate the NALP3 inflammasome," *Nature*, vol. 440, no. 7081, pp. 237–241, 2006.

[61] R. Medzhitov, "Origin and physiological roles of inflammation," *Nature*, vol. 454, no. 7203, pp. 428–435, 2008.

[62] J. P.-Y. Ting, S. B. Willingham, and D. T. Bergstralh, "NLRs at the intersection of cell death and immunity," *Nature Reviews Immunology*, vol. 8, no. 5, pp. 372–379, 2008.

[63] C. Dostert, V. Pétrilli, R. Van Bruggen, C. Steele, B. T. Mossman, and J. Tschopp, "Innate immune activation through Nalp3 inflammasome sensing of asbestos and silica," *Science*, vol. 320, no. 5876, pp. 674–677, 2008.

[64] V. Hornung, F. Bauernfeind, A. Halle et al., "Silica crystals and aluminum salts activate the NALP3 inflammasome through phagosomal destabilization," *Nature Immunology*, vol. 9, no. 8, pp. 847–856, 2008.

[65] M. S. Caicedo, R. Desai, K. McAllister, A. Reddy, J. J. Jacobs, and N. J. Hallab, "Soluble and particulate Co-Cr-Mo alloy implant metals activate the inflammasome danger signaling pathway in human macrophages: a novel mechanism for implant debris reactivity," *Journal of Orthopaedic Research*, vol. 27, no. 7, pp. 847–854, 2009.

[66] V. Pétrilli, C. Dostert, D. A. Muruve, and J. Tschopp, "The inflammasome: a danger sensing complex triggering innate immunity," *Current Opinion in Immunology*, vol. 19, no. 6, pp. 615–622, 2007.

[67] S. Mariathasan and D. M. Monack, "Inflammasome adaptors and sensors: intracellular regulators of infection and inflammation," *Nature Reviews Immunology*, vol. 7, no. 1, pp. 31–40, 2007.

[68] L. Burton, D. Paget, N. B. Binder et al., "Orthopedic wear debris mediated inflammatory osteolysis is mediated in part by NALP3 inflammasome activation," *Journal of Orthopaedic Research*, vol. 31, no. 1, pp. 73–80, 2013.

[69] F. Zhou, J. Lu, X. Zhu et al., "Effects of a cannabinoid receptor 2 selective antagonist on the inflammatory reaction to titanium particles in vivo and in vitro," *Journal of International Medical Research*, vol. 38, no. 6, pp. 2023–2032, 2010.

[70] J. B. Huang, Y. Ding, D. S. Huang et al., "Inhibition of the PI3K/AKT pathway reduces tumor necrosis factor-alpha production in the cellular response to wear particles in vitro," *Artificial Organs*, vol. 37, no. 3, pp. 298–307, 2013.

[71] D. Chen, X. Zhang, Y. Guo et al., "MMP-9 inhibition suppresses wear debris-induced inflammatory osteolysis through down-regulation of RANK/RANKL in a murine osteolysis model," *International Journal of Molecular Medicine*, vol. 30, no. 6, pp. 1417–1423, 2012.

[72] Z. Wang, X. Gao, K. Sun, and Q. Jin, "Experimental study on simvastatin in prevention and treatment of aseptic loosening of prosthesis," *Zhongguo Xiu Fu Chong Jian Wai Ke Za Zhi*, vol. 24, no. 5, pp. 544–547, 2010.

[73] E. M. Schwarz, "WHat potential biologic treatments are available for osteolysis?" *The Journal of the American Academy of Orthopaedic Surgeons*, vol. 16, pp. S72–S75, 2008.

[74] X. Peng, K. Tao, T. Cheng, J. Zhu, and X. Zhang, "Efficient Inhibition of wear debris-induced inflammation by locally delivered siRNA," *Biochemical and Biophysical Research Communications*, vol. 377, no. 2, pp. 532–537, 2008.

[75] A. Nehme, G. Maalouf, J.-L. Tricoire, G. Giordano, P. Chiron, and J. Puget, "Effect of alendronate on periprosthetic bone loss after cemented primary total hip arthroplasty: A Prospective Randomized Study," *Revue de Chirurgie Orthopedique et Reparatrice de l'Appareil Moteur*, vol. 89, no. 7, pp. 593–598, 2003.

[76] T. S. Tapaninen, P. K. Venesmaa, J. S. Jurvelin, H. J. A. Miettinen, and H. P. J. Kröger, "Alendronate reduces periprosthetic bone loss after uncemented primary total hip arthroplasty—a 5-year follow-up of 16 patients," *Scandinavian Journal of Surgery*, vol. 99, no. 1, pp. 32–37, 2010.

[77] P. K. Venesmaa, H. P. J. Kröger, H. J. A. Miettinen, J. S. Jurvelin, O. T. Suomalainen, and E. M. Alhava, "Alendronate reduces periprosthetic bone loss after uncemented primary total hip arthroplasty: A Prospective Randomized Study," *Journal of Bone and Mineral Research*, vol. 16, no. 11, pp. 2126–2131, 2001.

[78] K. Yamaguchi, K. Masuhara, S. Yamasaki, T. Nakai, and T. Fuji, "Cyclic therapy with etidronate has a therapeutic effect against local osteoporosis after cementless total hip arthroplasty," *Bone*, vol. 33, no. 1, pp. 144–149, 2003.

[79] S. Landgraeber, M. Von Knoch, F. Löer et al., "Association between apoptotis and $CD4^+/CD8^+$ T-lymphocyte ratio in aseptic loosening after total hip replacement," *International Journal of Biological Sciences*, vol. 5, no. 2, pp. 182–191, 2009.

Hindawi Publishing Corporation
Mediators of Inflammation
Volume 2014, Article ID 136463, 14 pages
http://dx.doi.org/10.1155/2014/136463

Research Article

Effect of Tumor Necrosis Factor Family Member LIGHT (TNFSF14) on the Activation of Basophils and Eosinophils Interacting with Bronchial Epithelial Cells

Huai Na Qiu,[1] Chun Kwok Wong,[1,2,3] Jie Dong,[1] Christopher Wai-Kei Lam,[1,4] and Zhe Cai[1]

[1] *Department of Chemical Pathology, The Chinese University of Hong Kong, Prince of Wales Hospital, Shatin, New Territories, Hong Kong*
[2] *Institute of Chinese Medicine and State Key Laboratory of Phytochemistry and Plant Resources in West China, The Chinese University of Hong Kong, Hong Kong*
[3] *Shenzhen Research Institute, The Chinese University of Hong Kong, Shenzhen, China*
[4] *State Key Laboratory of Quality Research in Chinese Medicine, Macau Institute for Applied Research in Medicine and Health, Macau University of Science and Technology, Taipa, Macau*

Correspondence should be addressed to Chun Kwok Wong; ck-wong@cuhk.edu.hk

Received 30 August 2013; Revised 9 January 2014; Accepted 4 February 2014; Published 25 March 2014

Academic Editor: Charles J. Malemud

Allergic asthma can cause airway structural remodeling, involving the accumulation of extracellular matrix and thickening of smooth muscle. Tumor necrosis factor (TNF) family ligand LIGHT (TNFSF14) is a cytokine that binds herpesvirus entry mediator (HVEM)/TNFRSF14 and lymphotoxin β receptor (LTβR). LIGHT induces asthmatic cytokine IL-13 and fibrogenic cytokine transforming growth factor-β release from allergic asthma-related eosinophils expressing HVEM and alveolar macrophages expressing LTβR, respectively, thereby playing crucial roles in asthmatic airway remodeling. In this study, we investigated the effects of LIGHT on the coculture of human basophils/eosinophils and bronchial epithelial BEAS-2B cells. The expression of adhesion molecules, cytokines/chemokines, and matrix metalloproteinases (MMP) was measured by flow cytometry, multiplex, assay or ELISA. Results showed that LIGHT could significantly promote intercellular adhesion, cell surface expression of intercellular adhesion molecule-1, release of airway remodeling-related IL-6, CXCL8, and MMP-9 from BEAS-2B cells upon interaction with basophils/eosinophils, probably via the intercellular interaction, cell surface receptors HVEM and LTβR on BEAS-2B cells, and extracellular signal-regulated kinase, p38 mitogen activated protein kinase, and NF-κB signaling pathways. The above results, therefore, enhance our understanding of the immunopathological roles of LIGHT in allergic asthma and shed light on the potential therapeutic targets for airway remodeling.

1. Introduction

Allergic asthma can result in airway remodeling and pulmonary fibrosis [1]. Airway remodeling is characterized by the accumulation of extracellular matrix (ECM), such as collagen, and thickening of smooth muscle. Fibrogenic cytokine transforming growth factor (TGF-β) and asthma-related IL-13 are crucial cytokines for synergistic airway remodeling [1]. Matrix metallopeptidase 9 (MMP-9), one of the extracellular proteases family members, mediates the degradation of the extracellular matrix during tissue remodeling [2].

Granulocyte basophils have been demonstrated to bind IgE and perform essential roles of Th2 cytokine-dependent immunity and allergic inflammation [3]. Basophils are rarely found in normal tissues. However, their number increases markedly at allergic inflammatory sites in the airways of asthmatic patients, especially during asthma exacerbation in response to allergen inhalation [4–6]. The granulocyte eosinophil is another principal effector cell of allergic inflammation [7]. Allergic asthma is characterized by the accumulation and infiltration of eosinophils in tissues mediated by the specific eosinophil chemokine eotaxin and vascular

cell adhesion molecule (VCAM)-1 and intercellular adhesion molecule (ICAM)-1 on epithelial cells, with subsequent release of granular toxic proteins such as eosinophilic cationic protein from eoisnophils [7].

LIGHT (lymphotoxin-related inducible ligand that competes for glycoprotein D binding to herpesvirus entry mediator on T cells), also known as tumor necrosis factor superfamily (TNFSF)14/CD258, is one of the TNF family members. It is a homotrimer on the surface of several immune cells such as activated T and B cells. Many members including TNF-α, CD40 ligand (CD40L), Fas ligand (FasL), TNF-related activation-induced cytokine (TRANCE), and LIGHT can be cleaved from cell surfaces, and their soluble forms have been reported to be involved in various physiological processes with broad biological functions [8–11]. Since LIGHT is a membrane-expressed protein related to the membrane form of lymphotoxin (LT)$\alpha\beta$ [12], it binds the herpesvirus entry mediator (HVEM; TNFRSF14) and is also a shared ligand with membrane lymphotoxin for LTβR [12, 13]. LIGHT can optimize inflammatory cytokine IL-12 production by dendritic cells and Th1 cells [14]. It is expressed on lung inflammatory CD45+leukocytes after the allergen house dust mite challenge [15]. LIGHT directly induces airway remodeling which is dependent on the induction of the fibrogenic cytokine transforming growth factor (TGF)-β. In mouse models of chronic asthma, pharmacological inhibition of LIGHT using a fusion protein between the IgG Fc domain and LTβR can reduce lung fibrosis, smooth muscle/epithelial hyperplasia, and airway hyperresponsiveness via the suppression of the production of lung TGF-β and IL-13, which are key cytokines in airway remodeling in humans [15]. On the other hand, exogenous administration of LIGHT to the airways induces fibrosis and smooth muscle hyperplasia. LIGHT-deficient mice exhibit impairment in fibrosis and smooth muscle accumulation [15]. In line with this, sputum LIGHT levels in asthmatic patients were found to correlate with decreased lung function [16]. Apart from LIGHT, anti-human B- and T-lymphocyte attenuator (BTLA), an inhibitory receptor on T lymphocytes with similar T-cell inhibitory functions to cytotoxic T lymphocyte-associated antigen 4 (CTLA-4) and programmed death 1 (PD-1) [17], is also the ligand of HVEM [18, 19]. Although BTLA-HVEM complexes have been shown to negatively regulate T-cell immune responses [18], the expression of BTLA on asthma-related basophils, eosinophils, and bronchial epithelial cells have not been investigated.

Recent mechanistic studies have shown that LIGHT can induce IL-13 and TGF-β release from esoinophils and alveolar macrophages, respectively [15, 20]. Eosinophils express HVEM but not LTβR [15], while LIGHT can induce MMP-9 release from macrophages via LTβR [21]. We have recently demonstrated the crucial roles of the interaction of basophils and eosinophils with bronchial epithelial cells in allergic asthma [22, 23]. However, the precise role played by the elevated LIGHT in airway hyperresponsiveness is still unresolved, and the intracellular mechanisms by which LIGHT can activate bronchial epithelial cells interacting with basophils and eosinophils to release airway remodeling related molecules are not certain. Since we hypothesize that LIGHT may play an immunological role in airway remodeling through the activation of the intercellular interaction between the granulocyte and airway epithelium, the aim of the present study was to investigate the effects of LIGHT on bronchial epithelial cells interacting with basophils/eosinophils and the underlying intracellular mechanisms.

2. Materials and Methods

2.1. Reagents. The recombinant human LIGHT/TNFSF14 was purchased from R&D Systems (Minneapolis, MN, USA). IκBα phosphorylation inhibitor BAY11-7082, p38 MAPK inhibitor SB203580, c-Jun N-terminal protein kinase (JNK) inhibitor SP600125, extracellular signal-regulated kinase (ERK) inhibitor U0126, and PI3K inhibitor LY294002 were purchased from Calbiochem Corporation (San Diego, CA, USA). BAY11-7082, SB203580, SP600125, U0126, and LY294002 were dissolved in 0.1% (v/v) dimethylsulphoxide (DMSO).

2.2. Purification of Human Peripheral Blood Basophils and Eosinophils from Buffy Coat and Cell Culture. Purification of human basophils and eosinophils was performed according to our previous publications [22–24]. Fresh human buffy coat obtained from healthy volunteers of the Hong Kong Red Cross Blood Transfusion Service was diluted with PBS and centrifuged using Ficoll-Paque Plus solution (GE Healthcare Corp., Piscataway, NJ, USA) and isotonic Percoll solution (density 1.082 g/mL; GE Healthcare) for the purification of basophils and eosinophils, respectively. Basophil-rich peripheral blood mononuclear cell (PBMC) fraction or eosinophil-rich granulocyte fraction was collected and washed twice with cold PBS containing 2% fetal bovine serum (FBS) (Invitrogen Corp., Carlsbad, CA, USA). Basophils and eosinophils were purified by negative selection using basophil isolation kit and anti-CD16 magnetic beads (Miltenyi Biotec, Bergisch Gladbach, Germany), respectively, using an LS+ column (Miltenyi) within a magnetic field. With this preparation, the drop-through fraction contained purified basophils or eosinophils with a purity of at least 99% as assessed by Giemsa staining solution (Sigma-Aldrich Corp., St. Louis, MO, USA) together with specific basophil cell surface marker CD203c staining [22] or Hemacolor rapid blood smear stain (E Merck Diagnostica, Darmstadt, Germany) [23], respectively. The isolated basophils/eosinophils were cultured in RPMI1640 medium (Invitrogen) supplemented with 10% FBS (Invitrogen). The above protocol using human basophils/eosinophils purified from human buffy coat was approved by the Clinical Research Ethics Committee of The Chinese University of Hong Kong-New Territories East Cluster Hospitals with written consent from all healthy volunteers of Hong Kong Red Cross Blood Transfusion Service in accordance with the Declaration of Helsinki.

2.3. Coculture of Basophils/Eosinophils and Bronchial Epithelial Cells. The human bronchial epithelial cell line (BEAS-2B) was obtained from the American Type Culture Collection

(ATCC, Manassas, VA, USA). This cell line has been transformed by adenovirus 12-SV40 virus hybrid (Ad12SV40) and used widely as an *in vitro* bronchial epithelial cell model [24]. BEAS-2B cells were grown in Dulbecco's modified Eagle's medium nutrient mixture F12 (Invitrogen) with 10% FBS at 37°C in a humidified 5% CO_2 atmosphere until confluence to cell monolayer. In coculture, the medium of BEAS-2B cells was replaced with RPMI-1640 medium containing 10% FBS (Invitrogen) with or without basophils/eosinophils. For inhibition experiments, basophils/eosinophils and BEAS-2B cells were pretreated with signaling molecule inhibitors for 1 h before coculture and treatment by LIGHT.

2.4. Coculture of Basophils/Eosinophils and BEAS-2B Cells in the Presence of Transwell Inserts. To prevent direct interaction between basophils/eosinophils and BEAS-2B cells in the coculture, transwell inserts (pore size: 0.4 mM) (BD Biosciences Corp., San Jose, CA, USA) were used to separate these two cells into two compartments. Confluent BEAS-2B cells and basophils/eosinophils were cultured together in the presence of transwell inserts, in which basophils/eosinophils and BEAS-2B cells were placed in the upper and lower compartment, respectively [23].

2.5. Quantification of Cytokines, Chemokines, and Growth Factors Using Multiplex Immunoassay. Concentrations of cytokines IL-5, IL-6, IL-9, IL-13, epidermal growth factor (EGF), vascular endothelial growth factor (VEGF), TGF-β, and chemokine CXCL8 in the culture supernatants were measured using the human Milliplex MAP kit assay reagent (Merck Millipore Corp., Billerica, MA, USA) with Bio-Plex 200 suspension array system (Bio-Rad Laboratories, Inc., Hercules, CA, USA).

2.6. Quantification of Human MMP-9 and Periostin. Concentration of human MMP-9 in the culture supernatants was measured using the Milliplex human MMP magnetic panel assay reagent (Merck Millipore) with Bio-Plex 200 suspension array system (Bio-Rad). Human periostin was measured using ELISA reagent (RayBiotech Inc., GA, USA).

2.7. Adhesion Assay. Coculture of BEAS-2B cells (1×10^5 cells) and basophils/eosinophils (3×10^5 cells) or BEAS-2B cells alone (3×10^5 cells) were maintained in a 24-well plate with transwell inserts (pore size: 0.4 mM) (BD Biosciences) and stimulated with LIGHT (0–100 ng/mL) for 24 h. The basophils/eosinophils were removed and another batch of freshly isolated basophils/eosinophils (3×10^5 cells) was then added into the adherent BEAS-2B cells for the adhesion analysis. Cells were cultured in RPMI1640 medium containing 10% FBS and incubated at 37°C in a humidified 5% CO_2 atmosphere for 1 h and digested with trypsin and resuspended in sheath fluid. Basophils/eosinophils and BEAS-2B cells were analyzed separately based on the expression of specific basophilic cell surface marker CD203c in histograms and distinct forward light scatters (FSC) together with side light scatters (SSC) of eosinophils in dot plots using flow cytometry (FACSCalibur flow cytometer, BD Biosciences). The ratio of the measured number of adherent eosinophils/basophils onto BEAS-2B cells was calculated [22–24].

2.8. Immunofluorescence Staining and Flow Cytometric Analysis. To determine the expression of HVEM, LTβR, and intercellular adhesion molecule (ICAM)-1 on the cell surface, nonadherent basophils/eosinophils were washed and resuspended with cold PBS. Adherent bronchial epithelial cells were harvested using cell dissociation solution. After blocking with 2% human pooled serum for 20 min at 4°C and washing with PBS supplemented with 0.5% bovine serum albumin, cells were incubated with phycoerythrin (PE)-conjugated mouse anti-human HVEM antibody, PE-conjugated mouse anti-human LTβR antibody, APC-conjugated mouse anti-human BTLA/CD272 antibody (BioLegend, Inc., San Diego, CA, USA), PE-conjugated mouse IgG1 isotype, fluorescein isothiocyanate (FITC)-conjugated mouse anti-human ICAM-1 antibody, or FITC-conjugated mouse IgG2a, κ isotype (BioLegend) for 30 min at 4°C in the dark. After washing, cells were subjected to flow cytometric analysis [22].

To determine the intracellular expression of phosphorylated signaling molecules, cells were fixed with prewarmed 4% paraformaldehyde for 10 min at 37°C. After centrifugation, cells were permeabilized in ice-cold BD Phosflow Perm Buffer for 30 min and then stained with mouse anti-human phosphorylated (p) p38 MAPK, pERK1/2, pIκBα, or mouse IgG1 antibodies (BD Pharmingen Corp., San Diego, CA, USA) for 60 min followed by FITC-conjugated goat anti-mouse secondary antibody (Life Technologies, Carlsbad, CA, USA) for another 45 min at 4°C in the dark. Cells were then washed, resuspended, and subjected to flow cytometric analysis [22].

Expression of surface molecules and intracellular phosphorylated signaling molecules of 5,000 viable cells was analyzed using flow cytometry (BD FACSCalibur flow cytometer) and presented as mean fluorescence intensity (MFI). For the differential analysis of intracellular MAPK and nuclear factor (NF)-κB activity of BEAS-2B cells, nonadherent basophils/eosinophils were separated from the adherent BEAS-2B cells by washing with PBS after different treatments. Adherent BEAS-2B cells were then harvested using cell dissociation solution for the flow cytometric analysis of intracellular signaling molecules (Sigma Aldrich Corp., MO, USA). Basophils/eosinophils and BEAS-2B cells were analyzed separately based on the expression of specific basophilic cell surface marker CD203c in histograms and distinct forward light scatters (FSC) together with side light scatters (SSC) of eosinophils in dot plots using flow cytometry (FACSCalibur flow cytometer, BD Biosciences) [22–24].

2.9. Statistical Analysis. The statistical significance difference was determined by one-way analysis of variance (ANOVA) or unpaired t-test. Data were expressed as mean plus standard error of the mean (SEM) from three independent experiments. Any differences with P value <0.05 were considered significant. When ANOVA indicated a significant difference, Bonferroni's *post hoc* test was then used to assess the difference between groups. All analyses were performed using

SPSS statistical software for Windows (version 16.0; SPSS Inc., Chicago, IL, USA).

3. Results

3.1. Cell Surface Expression of HVEM, LTβR, and BTLA. As shown in Figures 1(a), 1(d), 1(g), 1(h), and 1(i), the proteins HVEM, LTβR, and BTLA were constitutively expressed on the cell surface of bronchial epithelial BEAS-2B cells but only HVEM was observed to be expressed on basophils and eosinophils. Results were similar to a previous report [15] that eosinophils expressed cell surface HVEM but not LTβR (Figures 1(d) and 1(e)). Consistent with a previous publication, a slight decrease in HVEM expression on these cells was detected after LIGHT stimulation [25] (data not shown).

3.2. Effects of LIGHT on the Expression of ICAM-1 on BEAS-2B Cells and Eosinophils. Since we observed that plasma LIGHT concentration of asthmatic patients using ELISA could be up to 100 pg/mL, the local inflammatory concentration could be 10–1000 fold higher than the circulating levels. In order to mimic the inflammatory condition, we chose 1–100 ng/mL concentration for the following *in vitro* studies that is also comparable to that adopted in a previous publication [26]. Figure 2(a) shows that LIGHT (100 ng/mL) could upregulate the cell surface expression of ICAM-1 on BEAS-2B cells alone. As shown in Figure 2(b), the cell surface expression of ICAM-1 on BEAS-2B cells alone was significantly enhanced upon stimulation by LIGHT at high concentration (100 ng/mL) ($P < 0.05$) but not with low concentration (1 or 10 ng/mL). Upon interaction with basophils, ICAM-1 level on BEAS-2B cells was also upregulated by LIGHT at 100 ng/mL only (Figure 2(b)). However, LIGHT (up to 100 ng/mL) did not show any significant effect on the expression of ICAM-1 on basophils in the coculture with BEAS-2B cells (Figure 2(b), all $P > 0.05$). In the coculture of eosinophils and BEAS-2B cells (Figure 2(c)), LIGHT could significantly induce the expression of ICAM-1 on BEAS-2B cells (LIGHT, 10 and 100 ng/mL) and eosinophils (LIGHT, 100 ng/mL) (all $P < 0.05$). As shown in Figures 2(d) and 2(e), the increased cell number of basophils or eosinophils (0.3×10^5–3×10^5 cells) could enhance the expression of ICAM-1 on BEAS-2B cells in coculture. Moreover, the transwell insert could significantly downregulate the ICAM-1 expression on BEAS-2B cells in coculture (all $P < 0.05$).

We did not observe any significant changes in cell surface expression of ICAM-1 on basophils or eosinophils alone upon treatment with LIGHT up to 100 ng/mL ($P > 0.05$) (data not shown).

3.3. Adhesion of Basophils/Eosinophils onto BEAS-2B Cells. To further address the LIGHT-induced activation in cocultured BEAS-2B and basophils/eosinophils, we estimated the ability of activated BEAS-2B in adhesion with basophils/eosinophils (Figure 3). An increased number of adherent basophils/eosinophils could only be observed in coculture upon treatment by 100 ng/mL LIGHT (Figures 3(a) and 3(b), both $P < 0.05$). Figure 3(b) shows that there was a moderate upregulation of eosinophils adhesion onto BEAS-2B cells when BEAS-2B cells alone were stimulated with LIGHT (100 ng/mL). The above results therefore were in concordance with the upregulated expression of adhesion molecule on BEAS-2B cocultured with basophils/eosinophils in the presence of LIGHT (Figure 2). Figures 3(c) and 3(d) showed that basophils/eosinophils and BEAS-2B cells could be analyzed separately based on the expression of specific basophilic cell surface marker CD203c on basophils (Figure 3(c)) and distinct forward light scatters (FSC) together with side light scatters (SSC) of eosinophils in dot plots (Figure 3(d)) using flow cytometry.

3.4. Induction of Cytokines and Chemokines upon the Interaction of Basophils/Eosinophils and BEAS-2B Cells Stimulated by LIGHT. The Milliplex human cytokine/chemokine magnetic panel assay was used to measure the airway remodeling-related cytokines and chemokines, including IL-5, IL-6, IL-9, IL-13, EGF, TGF-β, VEGF, and CXCL8. As shown in Figures 4(a) and 4(b), LIGHT (100 ng/mL) could significantly induce the release of cytokine IL-6 and chemokine CXCL8 from BEAS-2B cells. Upon coculture with basophils, the induction of IL-6 and CXCL8 by LIGHT (100 ng/mL) was found to be significantly higher than those of BEAS-2B cells alone (both $P < 0.05$). However, LIGHT did not show any significant effect on the release of IL-6 or CXCL8 from basophils alone, even at high concentration (100 ng/mL, Figures 4(a) and 4(b)). Figure 4(d) shows that LIGHT (100 ng/mL) could significantly promote the release of CXCL8 from eosinophils alone. LIGHT (10 ng/mL) could further induce the release of IL-6 and CXCL8 from coculture of eosinophils and BEAS-2B cells compared to eosinophils or BEAS-2B cells alone (all $P < 0.05$, Figures 4(c) and 4(d)). In addition, the coculture of BEAS-2B cells with eosinophils, together with LIGHT stimulation (100 ng/mL), exhibited a synergistic effect on IL-6 and CXCL8 production (all $P < 0.05$, Figures 4(c) and 4(d)). The levels of IL-5, IL-9, IL-13, EGF, VEGF, and periostin were all undetectable using the same experimental conditions (data not shown). Moreover, there was induction of IL-6 and CXCL8 production from the coculture BEAS-2B cells and eosinophils without LIGHT stimulation (Figure 4). We also found no significant induction of TGF-β in the coculture of BEAS-2B cells and basophils/eosinophils with or without LIGHT stimulation (all $P > 0.05$, data not shown).

3.5. Induction of MMP-9 upon the Interaction of Basophils and BEAS-2B Cells Stimulated by LIGHT. As shown in Figure 5, LIGHT (100 ng/mL) could significantly induce the release of MMP-9 from BEAS-2B cells ($P < 0.001$). Upon coculture with basophils, the induction of MMP-9 by LIGHT (100 ng/mL) was significantly higher than control without LIGHT treatment ($P < 0.05$). However, LIGHT did not show any significant effect on the release of MMP-9 from basophils alone, even at high concentration (100 ng/mL, $P > 0.05$). There was no significant induction of MMP-9 in eosinophils alone or the coculture of eosinophils with BEAS-2B cells with or without LIGHT stimulation (data not shown).

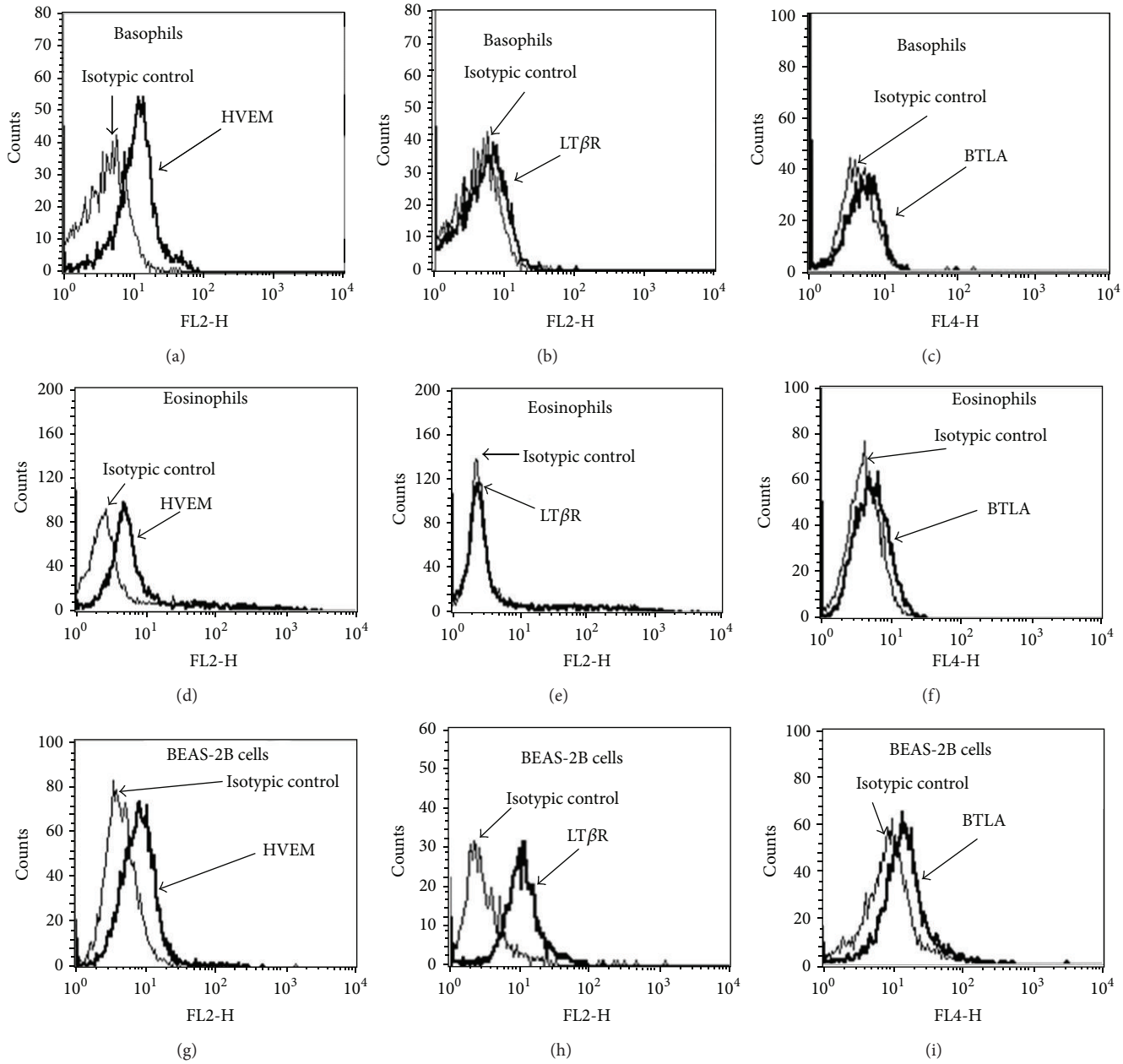

Figure 1: Protein expression of HVEM, LTβR, and BTLA on purified human basophils, purified human eosinophils, and human bronchial epithelial BEAS-2B cells. Representative histograms of the cell surface expression of HVEM, LTβR, and BTLA on (a, b, c) basophils (d, e, f), eosinophils, and (g, h, i) BEAS-2B cells determined with gating by respective side scatter and forward scatter using flow cytometry were obtained from triplicate experiments with essentially identical results.

3.6. Signaling Pathways Involved in the Interaction of Basophils/Eosinophils and BEAS-2B Cells upon LIGHT Stimulation. As shown in Figures 6(a) and 6(b), LIGHT (100 ng/mL) could significantly activate ERK and NF-κB in eosinophils (all $P < 0.05$) but not in basophils (all $P > 0.05$). Figures 6(c), 6(d), and 6(e) show that with the treatment of LIGHT (100 ng/mL), phosphorylation of p38 MAPK, ERK1/2, and IκBα was significantly enhanced in BEAS-2B cells upon their coculture with eosinophils at 30 and 60 min, and ERK1/2 was significantly phosphorylated even at 15 min. The p38 MAPK and ERK1/2 were significantly phosphorylated in BEAS-2B cells of the coculture of basophils and BEAS-2B cells at 30 and 60 min upon LIGHT (100 ng/mL) stimulation (Figures 6(c) and 6(d)).

3.7. Effects of Signaling Inhibitors on LIGHT-Induced Adhesion Molecule and Cytokines/Chemokines. The p38 MAPK inhibitor SB203580 (7.5 μM) and ERK inhibitor U0126

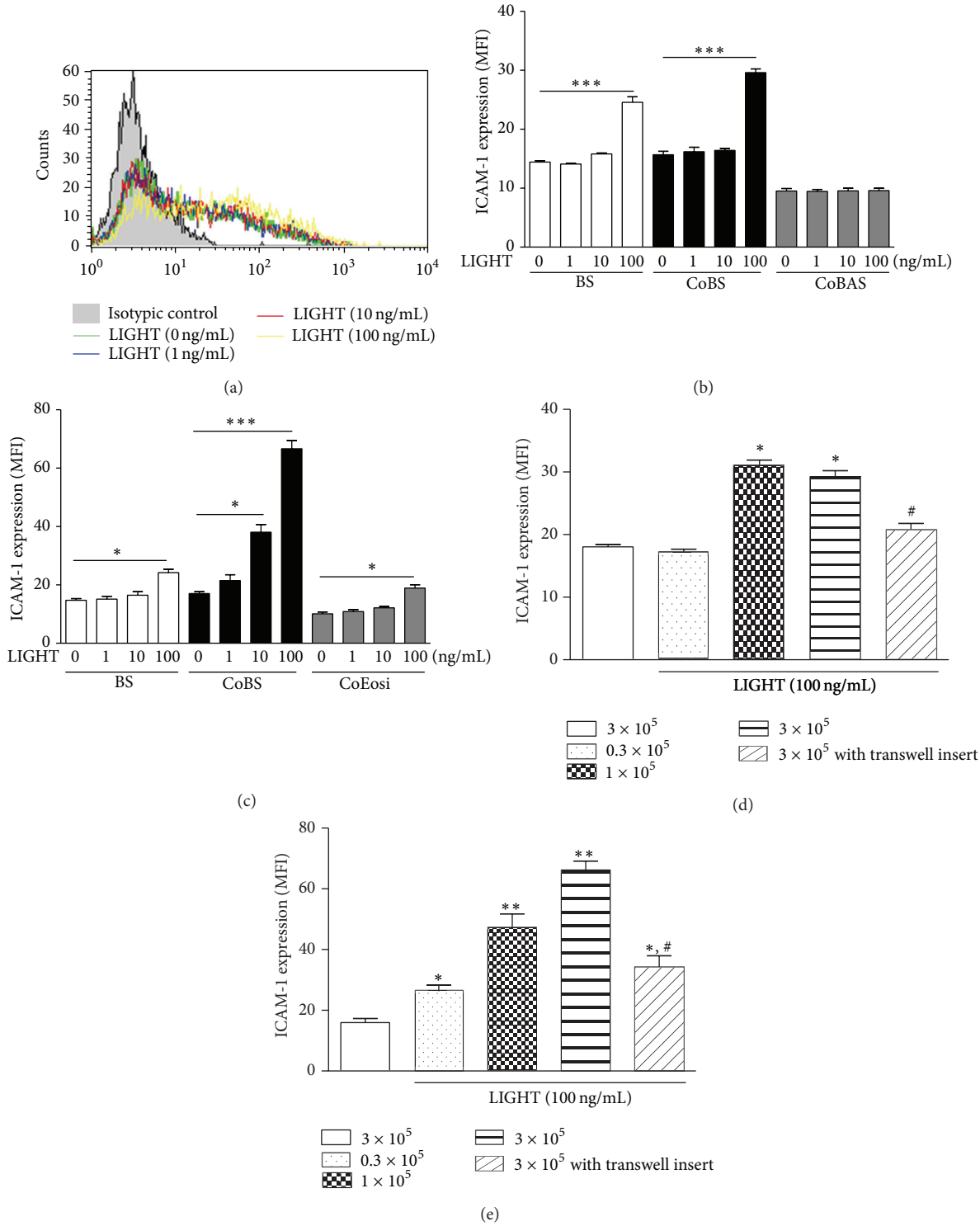

Figure 2: Effect of LIGHT on the cell surface expression of ICAM-1 on BEAS-2B cells or basophils/eosinophils. Expressions of ICAM-1 on BEAS-2B cells alone or in the coculture, and basophils/eosinophils in the coculture with or without LIGHT stimulation are presented with representative bar charts. (a) Representative histogram of the cell surface expression of ICAM-1 on BEAS-2B cells (1×10^5 cells) treated with different concentration of LIGHT (0–100 ng/mL) for 24 h is shown. (b) Basophils or (c) eosinophils (3×10^5 cells) and confluent BEAS-2B cells (1×10^5 cells) were cultured either together or separately with or without LIGHT (1–100 ng/mL) for 24 h. Surface expressions of ICAM-1 on 5,000 BEAS-2B cells, basophils, or eosinophils are expressed as the mean plus SEM of MFI of three independent experiments with three blood samples. $^{*}P < 0.05$, $^{***}P < 0.001$. (d) Basophils or (e) eosinophils (0.3×10^5–3×10^5 cells) and confluent BEAS-2B cells (1×10^5 cells) were cultured together with or without LIGHT (100 ng/mL) and transwell (pore size 0.4 μm) for 24 h. Surface expressions of ICAM-1 on 5,000 BEAS-2B cells, basophils, or eosinophils are expressed as the mean plus SEM of MFI of three independent experiments with three blood samples. $^{*}P < 0.05$; $^{**}P < 0.01$ when compared with the cocultured BEAS-2B cells and eosinophils without stimulation with LIGHT (empty bar). $^{\#}P < 0.05$ when compared with the corresponding group without transwell inserts. BS: BEAS-2B cells alone; CoBS: BEAS-2B cells in the coculture; CoBAS: basophils in the coculture; CoEosi: eosinophils in the coculture.

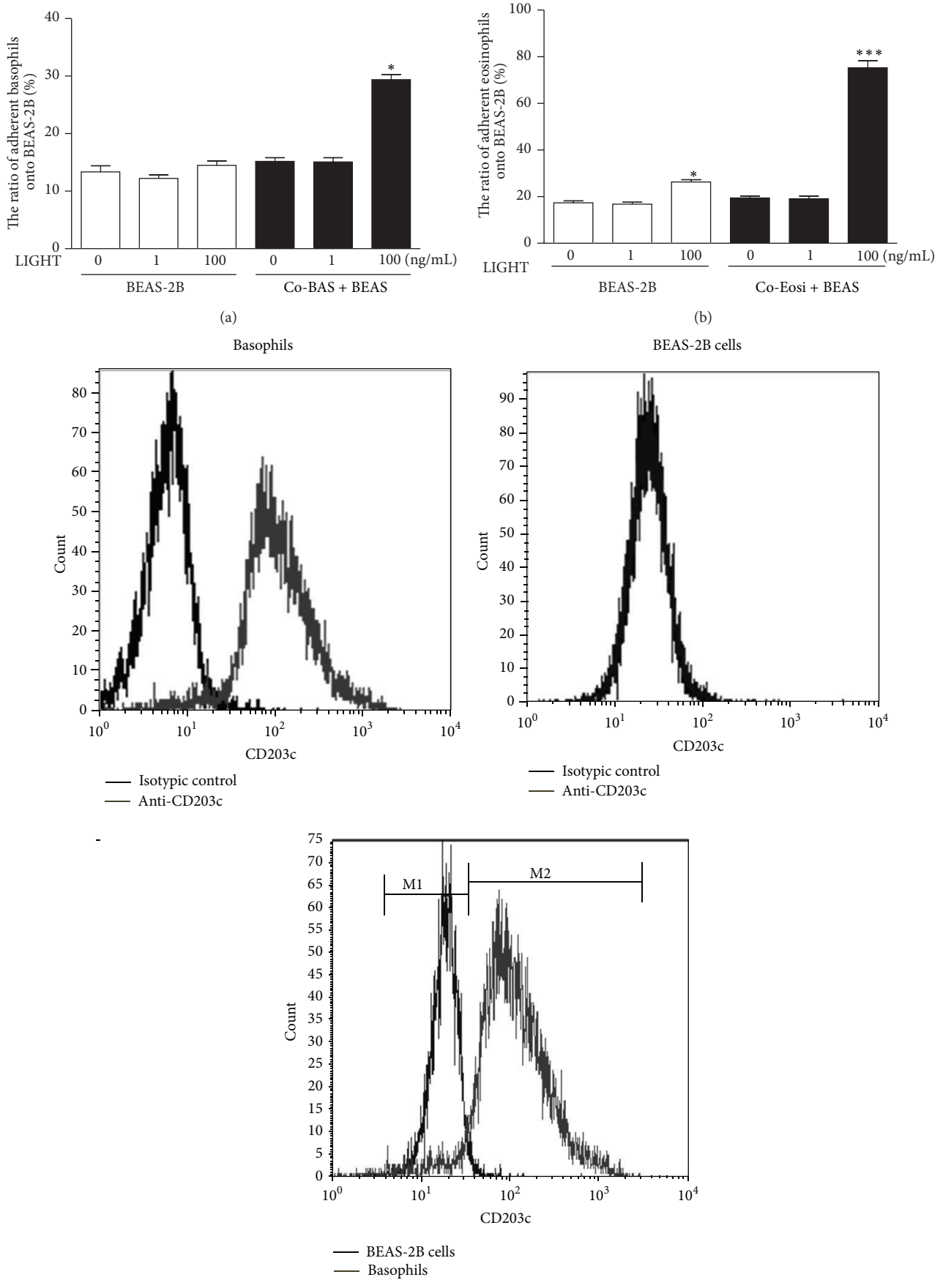

Figure 3: Continued.

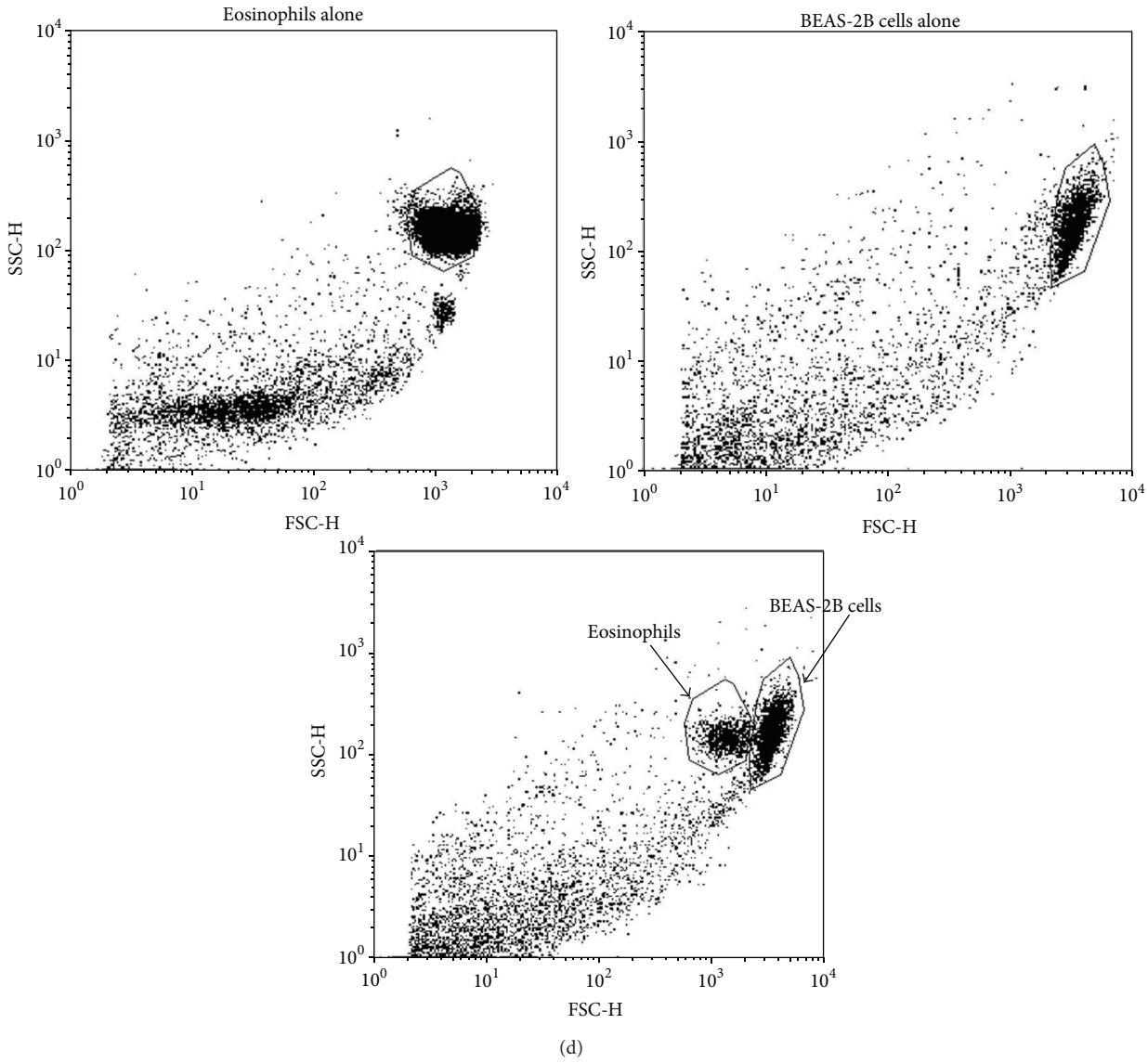

Figure 3: Adhesion of basophils or eosinophils onto BEAS-2B cells. Coculture of BEAS-2B cells (1×10^5 cells) and basophils/eosinophils (3×10^5 cells) using transwell inserts or BEAS-2B cells alone were stimulated by LIGHT (0–100 ng/mL) for 24 h. Basophils/eosinophils were removed and freshly isolated basophils/eosinophils (3×10^5 cells) were added into the corresponding well containing the adherent BEAS-2B cells (1×10^5 cells) for 1 h incubation. The ratio of (a) basophils or (b) eosinophils adherent onto BEAS-2B was analysed using flow cytometry as described in Section 2. Results are expressed as the mean plus SEM of three independent experiments with three blood samples. $^{*}P < 0.05$, $^{***}P < 0.001$. BEAS-2B: BEAS-2B cells alone were treated with LIGHT prior to adhesion analysis; Co-BAS + BEAS-2B: Coculture of BEAS-2B cells and basophils were treated with LIGHT before BEAS-2B cells were used for adhesion analysis; Co-Eosi + BEAS-2B: Coculture of BEAS-2B cells and eosinophils were treated with LIGHT before BEAS-2B cells were used for adhesion analysis. In the above adhesion assay, basophils/eosinophils and BEAS-2B cells were analyzed separately using flow cytometry. (c) Representative histograms of the flow cytometric analysis of the number of adherent basophils in coculture gated by the specific cell surface basophilic marker CD203c were shown. (d) Representative dot plots of the flow cytometric analysis of the number of adherent eosinophils in coculture gated by the SSC and FSC were shown.

(10 μM) could significantly suppress the LIGHT-induced expression of ICAM-1 on BEAS-2B cells in their coculture with basophils (Figure 7(a)) and the release of IL-6, CXCL8, and MMP-9 from the coculture (Figures 7(b), 7(c), and 7(d)). The p38 MAPK inhibitor SB203580 (7.5 μM), ERK inhibitor U0126 (10 μM), and NF-κB inhibitor BAY11-7082 (1 μM) could significantly suppress the LIGHT-induced expression of ICAM-1 on BEAS-2B cells (Figure 7(e)) and the production of IL-6 (Figure 7(f)) from the coculture of eosinophils and BEAS-2B cells.

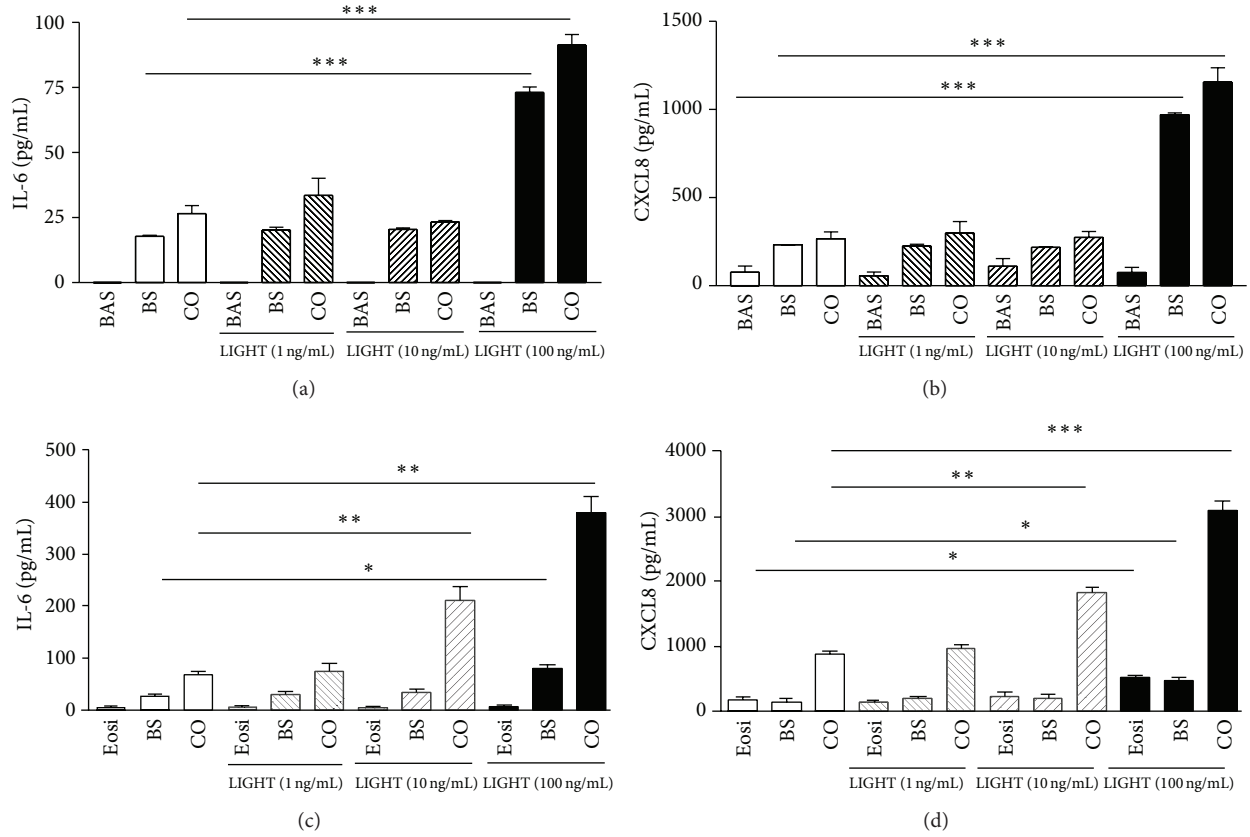

Figure 4: Effects of LIGHT on the release of IL-6 and CXCL8 from the coculture of basophils/eosinophils and BEAS-2B cells. Confluent BEAS-2B cells (1×10^5 cells) and (a, b) basophils/(c, d) eosinophils (3×10^5 cells) were cultured either together or separately with or without LIGHT for 24 h. Release of IL-6 and CXCL8 in culture supernatants was determined by Milliplex human cytokine/chemokine magnetic panel assay. Results are expressed as the mean plus SEM of three independent experiments with three blood samples. $^{*}P < 0.05$, $^{**}P < 0.01$, $^{***}P < 0.001$. BAS: basophils; Eosi: eosinophils; BS: BEAS-2B cells; CO: coculture.

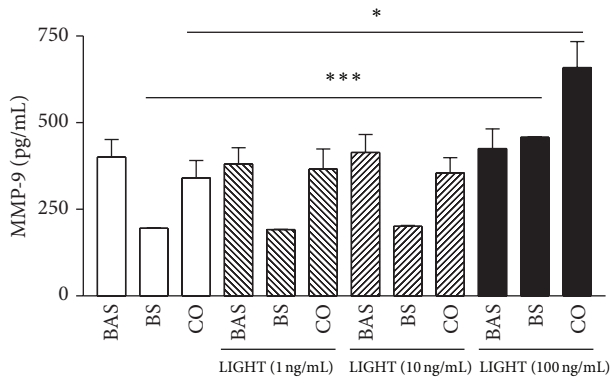

Figure 5: Effects of LIGHT on the release of MMP-9 in the coculture of basophils and BEAS-2B cells. Confluent BEAS-2B cells (1×10^5 cells) and basophils (3×10^5 cells) were cultured either together or separately with LIGHT (0–100 ng/mL) for 24 h. Release of MMP-9 in culture supernatants was measured by Milliplex human MMP panel assay. Results are expressed as the mean plus SEM of three independent experiments with three blood samples. $^{*}P < 0.05$, $^{***}P < 0.001$. BAS: basophils; BS: BEAS-2B cells; CO: coculture of basophils and BEAS-2B cells.

4. Discussion

Structural remodeling of the airway involves the accumulation of extracellular matrix proteins and thickening of smooth muscle [1]. We found that allergic asthma-related basophils and eosinophils constitutively expressed HVEM (Figure 1), a ligand of airway remodeling cytokine LIGHT. Bronchial epithelial BEAS-2B cells also expressed HVEM, LTβR, and another HVEM ligand, BTLA [17]. Therefore, LIGHT can play immunomodulatory roles for the activation of basophils/eopsinophils interacting with bronchial epithelial cells in airway remodeling. The present *in vitro* study has shown that the TNF family member LIGHT could significantly promote the cell surface expression of adhesion molecule ICAM-1, the release of airway-remodeling cytokine IL-6, chemokine CXCL8, and extracellular protease MMP-9 from human bronchial epithelial cells upon the interaction with asthma-related basophils or eosinophils. Since the increased cell number of basophils/eosinophils could enhance the expression of ICAM-1 on BEAS-2B cells, and the disruption of intercellular interaction using transwell inserts could significantly downregulate the ICAM-1

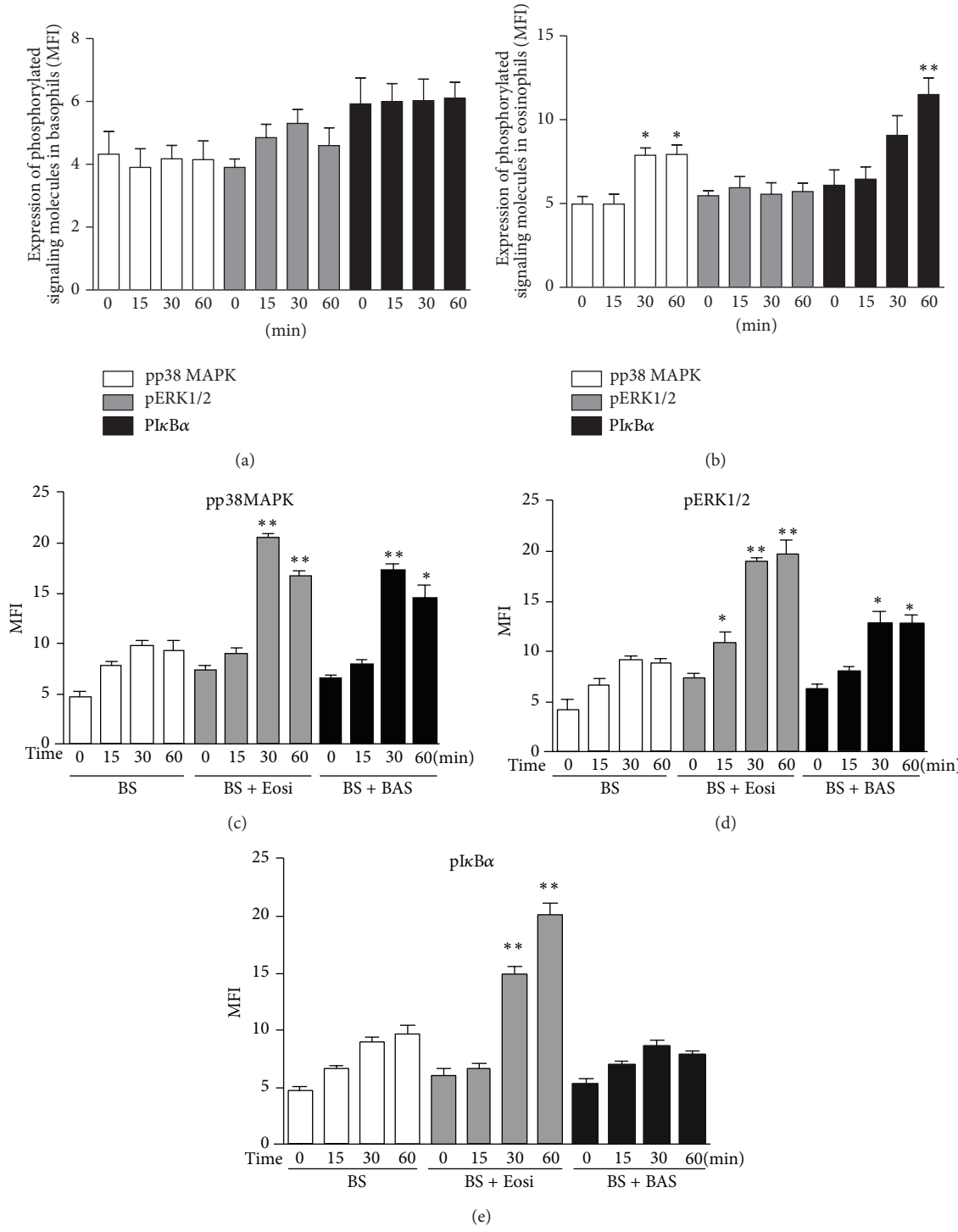

Figure 6: Phosphorylation of p38 MAPK, ERK1/2, and IκBα in BEAS-2B cells upon the coculture of basophils/eosinophils and BEAS-2B cells with the stimulation of LIGHT. BEAS-2B cells (1×10^5 cells) and basophils/eosinophils (3×10^5 cells) were cultured either together or separately with or without LIGHT stimulation (100 ng/mL) for different time points (0, 15, 30, and 60 min). The intracellular expression of phosphorylated (p) p38 MAPK, pERK1/2, and pIκBα in (a) permeabilized basophils and (b) eosinophils alone without coculture, and (c) pp38 MAPK, (d) pERK1/2, and (e) pIκBα of permeabilized BEAS-2B cells in with or without coculture with basophils/eosinophils were measured by intracellular immunofluorescence staining using flow cytometry. Results are shown in MFI and expressed as the arithmetic mean plus SEM of three independent experiments with three blood samples in bar charts. $^*P < 0.05$, $^{**}P < 0.01$ when compared with coculture control group. BAS: basophils; Eosi: eosinophils; BS: BEAS-2B cells.

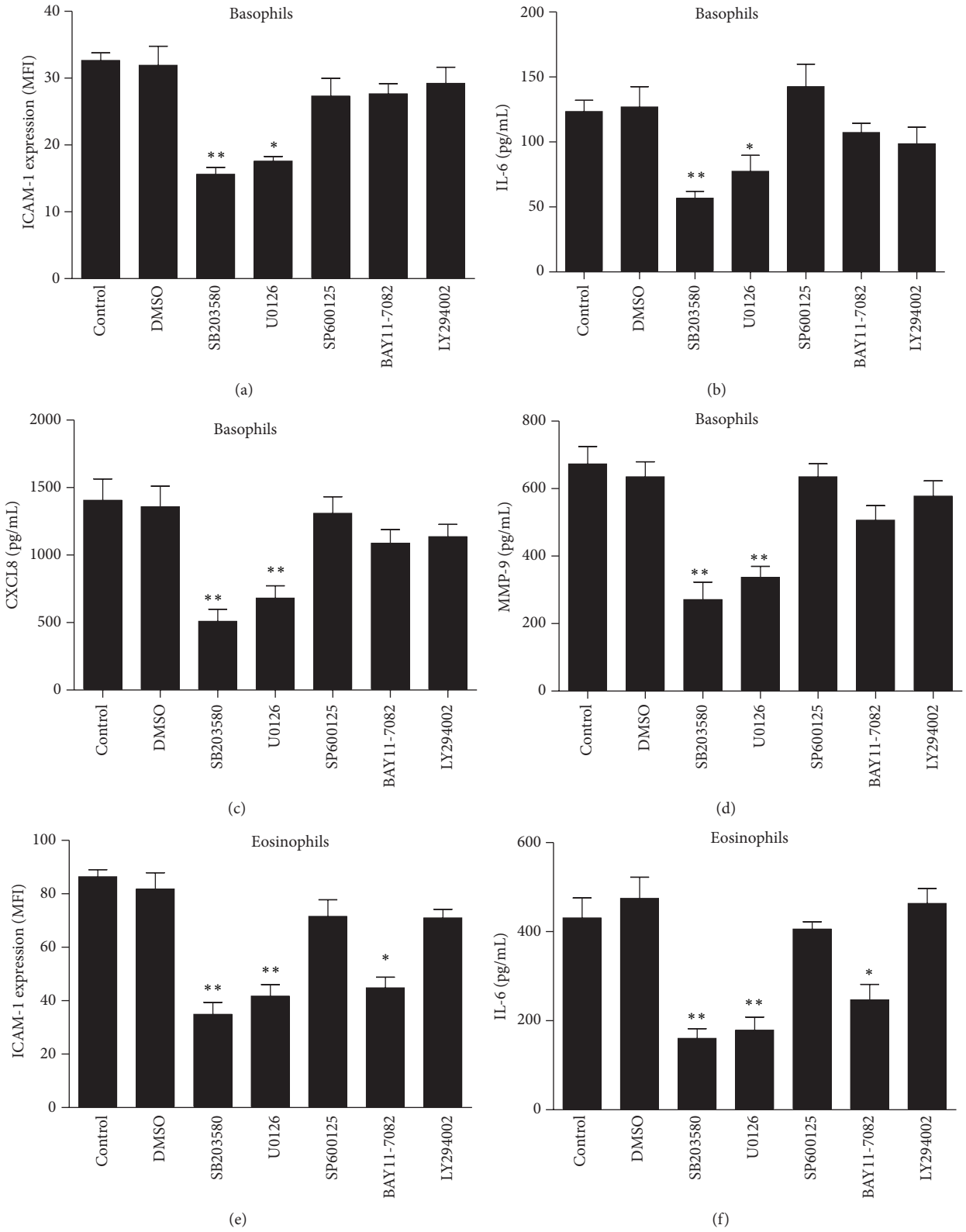

Figure 7: Effects of signaling molecule inhibitors on the cell surface expression of ICAM-1 and induction of cytokines/chemokines from coculture of BEAS-2B cells and basophils/eosinophils in the presence of LIGHT (100 ng/mL). Cocultures of (a, b, c, d) basophils or (e, f) eosinophils (3×10^5 cells) and confluent BEAS-2B cells (1×10^5 cells) were pretreated with BAY11-7082 (1 μM), SP600125 (3 μM), SB203580 (7.5 μM), U0126 (10 μM), or LY294002 (10 μM) for 1 h, followed by incubation with or without LIGHT (100 μg/mL) in the presence of inhibitors for a further 24 h. Cell surface expression of ICAM-1 on 5,000 cells was analyzed by flow cytometry as MFI. Results are expressed as mean plus SEM of three independent experiments with three blood samples in bar charts. Release of cytokines/chemokines and MMP-9 in culture supernatant was measured by Milliplex assay. Results are expressed as mean plus SEM. DMSO (0.1%) was used as the vehicle control. $^*P < 0.05$, $^{**}P < 0.01$ when compared with vehicle or negative control.

expression on BEAS-2B cells (Figures 2(d) and 2(e)), upregulated ICAM-1 expression on BEAS-2B cells was dependent on the direct interaction between basophils/eosinophils and BEAS-2B cells.

As shown in Figure 2(e), there was a remarkable increase in the ICAM-1 expression on BEAS-2B interacted with eosinophils after stimulated with LIGHT in the presence of the transwell insert, suggesting that the soluble factors were also associated with the regulation of ICAM-1. Since the direct interaction of ICAM-1 and CD18 has been shown to mediate eosinophil adhesion onto bronchial epithelial cells [27], the increased ability of BEAS-2B in adhesion with eosinophils could be partially explained by the upregulated ICAM-1 on BEAS-2B upon interaction with eosinophils with LIGHT stimulation. However, the elevated adhesion between BEAS-2B and basophils could also be observed, even the ICAM-1 expression was similar between (i) BEAS-2B coculturing with basophils using transwell inserts (Figure 2(d)) and (ii) BEAS-2B cells alone were stimulated by LIGHT (Figure 2(b)), thereby suggesting that other factors in coculture, apart from the adhesion molecule ICAM-1, were partly contributing to the intercellular adhesion. Further study may be required to fully elucidate the biochemical mechanisms for the adhesion of basophils/eosinophils onto BEAS-2B cells.

IL-6 has been shown to enhance collagen synthesis, production of tissue inhibitors of metalloproteinases (TIMPs), and airway hyperresponsiveness [28–30]. Expression of IL-6 in fibroblasts is correlated with fibrosis [28]. By causing airway smooth muscle cell proliferation and migration, CXCL8 has been shown to be a potential chemokine for airway remodeling [31]. CXCL8 released from human bronchial epithelial cells upon leukotriene D4 stimulation is involved in epithelial-mediated asthmatic airway remodeling via the activation of EGF receptor [32]. MMP-9 is significantly increased in bronchoalveolar lavage fluid (BALF) and sputum from patients with allergic asthma [33, 34]. An elevated circulation level of MMP-9 is also found in patients suffering from asthma exacerbation [35]. In addition, allergen challenge in asthmatic patients induces MMP-9 expression in the airway [36]. MMP-9-deficient mice challenged with ovalbumin show less peribronchial fibrosis and total lung collagen compared to ovalbumin-challenged wild type [37]. These results indicated the involvement of MMP-9 in mediating allergen-induced airway remodeling [37]. Together, the induced IL-6, CXCL8, and MMP-9 suggested that LIGHT may play an important role in airway remolding via the activation of basophils and eosinophils interacting with bronchial epithelial cells.

There are three isoforms of TGF-β in the normal human lung, and TGF-β1 is associated with bronchial epithelial cells, smooth muscle cells, fibroblast-like cells, and the airway extracellular matrix (ECM) [38–41]. TGF-β1 level is increased in BALF of asthmatic patients [42], and asthmatic animal models also show increased levels of TGF-β1 in BALF and tissue [43, 44]. Mice treated with anti-TGF-β antibody significantly reduce the deposition of peribronchial ECM, proliferation of airway smooth muscle cell, and mucus production in lung [45]. TGF-β induces the expression of MMPs and TIMPs, both are major ECM regulators [46]. Deposition of ECM will result in fibrosis in patients with asthma [47]. TGF-β1 plays an important role in the regulation of airway remodeling. In the present study, BEAS-2B cells were found to release TGF-β1; however, the levels of TGF-β1 seemed not to be influenced by LIGHT or the interaction with basophils or eosinophils (data not shown). It has been shown that the matricellular protein periostin can interact with cell surface integrin molecules and can be involved in tissue development and remodeling [48, 49]. However, in the present study, the level of periostin is undetectable by ELISA (data not shown). Moreover, other airway remodeling-related cytokines and growth factors including IL-5, IL-9, IL-13, EGF, and VEGF could not be detected in the present study. The expression of these mediators should be further investigated in the future *in vivo* study using murine model to better elucidate the detailed effect of LIGHT on the interaction of basophils/eosinophils and bronchial epithelial cells in airway remodeling and inflammation.

Our previous study of airway inflammation has demonstrated that the induction of IL-6 and CCL2 upon the interaction of basophils and bronchial epithelial cells under IL-17A stimulation was differentially regulated by ERK, JNK, p38 MAPK, and NF-κB pathways [24]. In the present study to investigate the signaling pathways involved in the interaction of basophils/eosinophils and human bronchial epithelial cells upon LIGHT stimulation, several specific signaling molecule inhibitors were used to block the pathways. NF-κB inhibitor BAY11-7082, ERK inhibitor U0126, and p38 MAPK inhibitor SB203580 could differentially suppress LIGHT-induced ICAM-1, IL-6, CXCL8, and MMP-9 in the coculture of basophils/eosinophils and BEAS-2B cells (Figure 7). Together with the results in Figure 6 regarding the LIGHT-mediated activation of ERK, p38 MAPK, and NF-κB in eosinophils alone and BEAS-2B cells in coculture, the results indicated that the induction of ICAM-1 and release of airway remodeling cytokine IL-6, chemokine CXCL8, and extracellular protease MMP-9 in LIGHT-activated coculture of basophils/eosinophils and BEAS-2B cells were differentially regulated by intracellular NF-κB, ERK, and p38 MAPK pathways, probably via the regulation of downstream transcription factors and/or microRNA [22, 50]. These *in vitro* mechanistic results are actually in concordance with our previous published results that the expressions of cytokines/chemokines and adhesion molecules in the coculture of eosinophils/basophils and bronchial epithelial cells are differentially regulated by distinct activation profiles of signaling molecules [22–24]. Since targeting signaling molecules can be a novel strategy for the treatment of asthma [51], the potential cross-talk between different signaling pathways and the downstream molecular regulatory mechanisms awaits further studies.

5. Conclusions

In summary, the expression of airway remodeling adhesion molecule ICAM-1 and the release of airway remodeling-related cytokine IL-6, chemokine CXCL8, and extracellular protease MMP-9 and intercellular adhesion were significantly enhanced in the coculture of basophils/eosinophils and

bronchial epithelial cells via the regulation of a distinct intracellular signal transduction mechanism. Our previous studies have also shown that the interaction of bronchial epithelial cells and basophils/eosinophils can induce the release of a variety of inflammatory mediators involved in allergic asthma via the upregulated expression of adhesion molecules and the modulation of signaling pathways [22, 23]. The release of mediators such as MMP-9, IL-6, and CXCL8 upon the activation by LIGHT should contribute to airway remodeling. However, whether LIGHT signals through HVEM on basophils/eosinophils and/or LTβR on epithelial cells are the direct or indirect consequences involving other receptor-mediated mechanisms requires further investigation. Nevertheless, the present cellular mechanistic results may somehow shed light on the potential therapeutic target for airway remodeling.

Conflict of Interests

The authors declare that there is no conflict of interests regarding the publication of this paper.

Authors' Contribution

Huai Na Qiu and Chun Kwok Wong share first authorship of this paper.

Acknowledgments

This work was supported by a direct Grant for research from the Chinese University of Hong Kong (Project code: 4054060).

References

[1] M. S. Wilson and T. A. Wynn, "Pulmonary fibrosis: pathogenesis, etiology and regulation," *Mucosal Immunology*, vol. 2, no. 2, pp. 103–121, 2009.

[2] J. J. Atkinson and R. M. Senior, "Matrix metalloproteinase-9 in lung remodeling," *American Journal of Respiratory Cell and Molecular Biology*, vol. 28, no. 1, pp. 12–24, 2003.

[3] M. C. Siracusa, M. R. Comeau, and D. Artis, "New insights into basophil biology: initiators, regulators, and effectors of type 2 inflammation," *Annals of the New York Academy of Sciences*, vol. 1217, no. 1, pp. 166–177, 2011.

[4] H. Karasuyama, K. Mukai, Y. Tsujimura, and K. Obata, "Newly discovered roles for basophils: a neglected minority gains new respect," *Nature Reviews Immunology*, vol. 9, no. 1, pp. 9–13, 2009.

[5] C. L. Kepley, P. J. McFeeley, J. M. Oliver, and M. F. Lipscomb, "Immunohistochemical detection of human basophils in postmortem cases of fatal asthma," *American Journal of Respiratory and Critical Care Medicine*, vol. 164, no. 6, pp. 1053–1058, 2001.

[6] B. M. Sullivan and R. M. Locksley, "Basophils: a nonredundant contributor to host immunity," *Immunity*, vol. 30, no. 1, pp. 12–20, 2009.

[7] P. C. Fulkerson and M. E. Rothenberg, "Targeting eosinophils in allergy, inflammation and beyond," *Nature Reviews Drug Discovery*, vol. 12, no. 2, pp. 117–129, 2013.

[8] R. A. Black, C. T. Rauch, C. J. Kozlosky et al., "A metalloproteinase disintegrin that releases tumour-necrosis factor-Ø from cells," *Nature*, vol. 385, no. 6618, pp. 729–733, 1997.

[9] N. Kayagaki, A. Kawasaki, T. Ebata et al., "Metalloproteinase-mediated release of human Fas ligand," *Journal of Experimental Medicine*, vol. 182, no. 6, pp. 1777–1783, 1995.

[10] L. Lum, B. R. Wong, R. Josien et al., "Evidence for a role of a tumor necrosis factor-α (TNF-α)-converting enzyme-like protease in shedding of TRANCE, a TNF family member involved in osteoclastogenesis and dendritic cell survival," *The Journal of Biological Chemistry*, vol. 274, no. 19, pp. 13613–13618, 1999.

[11] X. Wan, J. Zhang, H. Luo et al., "A TNF family member LIGHT transduces costimulatory signals into human T cells," *The Journal of Immunology*, vol. 169, no. 12, pp. 6813–6821, 2002.

[12] C. F. Ware, "Network communications: lymphotoxins, LIGHT, and TNF," *Annual Review of Immunology*, vol. 23, pp. 787–819, 2005.

[13] S. Scheu, J. Alferink, T. Pötzel, W. Barchet, U. Kalinke, and K. Pfeffer, "Targeted disruption of LIGHT causes defects in costimulatory T cell activation and reveals cooperation with lymphotoxin β in mesenteric lymph node genesis," *Journal of Experimental Medicine*, vol. 195, no. 12, pp. 1613–1624, 2002.

[14] G. Xu, D. Liu, I. Okwor et al., "LIGHT is critical for IL-12 production by dendritic cells, optimal $CD4^+$ Th1 cell response, and resistance to *Leishmania major*," *The Journal of Immunology*, vol. 179, no. 10, pp. 6901–6909, 2007.

[15] T. A. Doherty, P. Soroosh, N. Khorram et al., "The tumor necrosis factor family member LIGHT is a target for asthmatic airway remodeling," *Nature Medicine*, vol. 17, no. 5, pp. 596–603, 2011.

[16] A. T. Hastie, W. C. Moore, D. A. Meyers et al., "Analyses of asthma severity phenotypes and inflammatory proteins in subjects stratified by sputum granulocytes," *Journal of Allergy and Clinical Immunology*, vol. 125, no. 5, pp. 1028.e13–1036.e13, 2010.

[17] N. Watanabe, M. Gavrieli, J. R. Sedy et al., "BTLA is a lymphocyte inhibitory receptor with similarities to CTLA-4 and PD-1," *Nature Immunology*, vol. 4, no. 7, pp. 670–679, 2003.

[18] J. R. Sedy, M. Gavrieli, K. G. Potter et al., "B and T lymphocyte attenuator regulates T cell activation through interaction with herpesvirus entry mediator," *Nature Immunology*, vol. 6, no. 1, pp. 90–98, 2005.

[19] C. F. Ware and J. R. Sedý, "TNF Superfamily Networks: bidirectional and interference pathways of the herpesvirus entry mediator (TNFSF14)," *Current Opinion in Immunology*, vol. 23, no. 5, pp. 627–631, 2011.

[20] T. A. Wynn and T. R. Ramalingam, "Shedding LIGHT on severe asthma," *Nature Medicine*, vol. 17, no. 5, pp. 547–548, 2011.

[21] W. Lee, S. Kim, Y. Lee et al., "Tumor necrosis factor receptor superfamily 14 is involved in atherogenesis by inducing proinflammatory cytokines and matrix metalloproteinases," *Arteriosclerosis, Thrombosis, and Vascular Biology*, vol. 21, no. 12, pp. 2004–2010, 2001.

[22] H. N. Qiu, C. K. Wong, I. M. Chu, S. Hu, and C. W. Lam, "Muramyl dipeptide mediated activation of human bronchial epithelial cells interacting with basophils: a novel mechanism of airway inflammation," *Clinical and Experimental Immunology*, vol. 172, no. 1, pp. 81–94, 2013.

[23] C. K. Wong, S. Hu, K. M. Leung et al., "NOD-like receptors mediated activation of eosinophils interacting with bronchial epithelial cells: a link between innate immunity and allergic

asthma," *Cellular and Molecular Immunology*, vol. 10, no. 4, pp. 317–329, 2013.

[24] C. K. Wong, J. Cao, Y. B. Yin, and C. W. K. Lam, "Interleukin-17A activation on bronchial epithelium and basophils: a novel inflammatory mechanism," *European Respiratory Journal*, vol. 35, no. 4, pp. 883–893, 2010.

[25] Y. Morel, J.-M. Schiano de Colella, J. Harrop et al., "Reciprocal expression of the TNF family receptor herpes virus entry mediator and its ligand LIGHT on activated T cells: LIGHT down-regulates its own receptor," *The Journal of Immunology*, vol. 165, no. 8, pp. 4397–4404, 2000.

[26] Y. Mikami, Y. Yamauchi, M. Horie et al., "Tumor necrosis factor superfamily member LIGHT induces epithelial-mesenchymal transition in A549 human alveolar epithelial cells," *Biochemical and Biophysical Research Communications*, vol. 428, no. 4, pp. 451–457, 2012.

[27] A. Burke-Gaffney and P. G. Hellewell, "A CD18/ICAM-1-dependent pathway mediates eosinophil adhesion to human bronchial epithelial cells," *American Journal of Respiratory Cell and Molecular Biology*, vol. 19, no. 3, pp. 408–418, 1998.

[28] I. Gomes, S. K. Mathur, B. M. Espenshade, Y. Mori, J. Varga, and S. J. Ackerman, "Eosinophil-fibroblast interactions induce fibroblast IL-6 secretion and extracellular matrix gene expression: implications in fibrogenesis," *Journal of Allergy and Clinical Immunology*, vol. 116, no. 4, pp. 796–804, 2005.

[29] C. Kuhn III, R. J. Homer, Z. Zhu et al., "Airway hyperresponsiveness and airway obstruction in transgenic mice: morphologic correlates in mice overexpressing interleukin (IL)-11 and IL-6 in the lung," *American Journal of Respiratory Cell and Molecular Biology*, vol. 22, no. 3, pp. 289–295, 2000.

[30] C. L. Rochester, S. J. Ackerman, T. Zheng, and J. A. Elias, "Eosinophil-fibroblast interactions: granule major basic protein interacts with IL-1 and transforming growth factor-β in the stimulation of lung fibroblast IL-6-type cytokine production," *The Journal of Immunology*, vol. 156, no. 11, pp. 4449–4456, 1996.

[31] V. Govindaraju, M. Michoud, M. Al-Chalabi, P. Ferraro, W. S. Powell, and J. G. Martin, "Interleukin-8: novel roles in human airway smooth muscle cell contraction and migration," *American Journal of Physiology—Cell Physiology*, vol. 291, no. 5, pp. C957–C965, 2006.

[32] T. McGovern, P. Risse, K. Tsuchiya, M. Hassan, G. Frigola, and J. G. Martin, "LTD4 induces HB-EGF-dependent CXCL8 release through EGFR activation in human bronchial epithelial cells," *American Journal of Physiology—Lung Cellular and Molecular Physiology*, vol. 299, no. 6, pp. L808–L815, 2010.

[33] Y. C. Lee, H. B. Lee, Y. K. Rhee, and C. H. Song, "The involvement of matrix metalloproteinase-9 in airway inflammation of patients with acute asthma," *Clinical and Experimental Allergy*, vol. 31, no. 10, pp. 1623–1630, 2001.

[34] G. Mautino, N. Oliver, P. Chanez, J. Bousquet, and F. Capony, "Increased release of matrix metalloproteinase-9 in bronchoalveolar lavage fluid and by alveolar macrophages of asthmatics," *American Journal of Respiratory Cell and Molecular Biology*, vol. 17, no. 5, pp. 583–591, 1997.

[35] Y. Oshita, T. Koga, T. Kamimura, K. Matsuo, T. Rikimaru, and H. Aizawa, "Increased circulating 92 kDa matrix metalloproteinase (MMP-9) activity in exacerbations of asthma," *Thorax*, vol. 58, no. 9, pp. 757–760, 2003.

[36] E. A. B. Kelly, W. W. Busse, and N. N. Jarjour, "Increased matrix metalloproteinase-9 in the airway after allergen challenge," *American Journal of Respiratory and Critical Care Medicine*, vol. 162, no. 3 I, pp. 1157–1161, 2000.

[37] D. H. Lim, Y. C. Jae, M. Miller, K. McElwain, S. McElwain, and D. H. Broide, "Reduced peribronchial fibrosis in allergen-challenged MMP-9-deficient mice," *American Journal of Physiology—Lung Cellular and Molecular Physiology*, vol. 291, no. 2, pp. L265–L271, 2006.

[38] J.-D. Aubert, B. I. Dalal, T. R. Bai, C. R. Roberts, S. Hayashi, and J. C. Hogg, "Transforming growth factor β1 gene expression in human airways," *Thorax*, vol. 49, no. 3, pp. 225–232, 1994.

[39] S. E. Bottoms, J. E. Howell, A. K. Reinhardt, I. C. Evans, and R. J. McAnulty, "TGF-β isoform specific regulation of airway inflammation and remodelling in a murine model of asthma," *PLoS ONE*, vol. 5, no. 3, Article ID e9674, 2010.

[40] A. E. Redington, W. R. Roche, S. T. Holgate, and P. H. Howarth, "Co-localization of immunoreactive transforming growth factor-beta 1 and decorin in bronchial biopsies from asthmatic and normal subjects," *The Journal of Pathology*, vol. 186, no. 4, pp. 410–415, 1998.

[41] A. M. Vignola, P. Chanez, G. Chiappara et al., "Transforming growth factor-β expression in mucosal biopsies in asthma and chronic bronchitis," *American Journal of Respiratory and Critical Care Medicine*, vol. 156, no. 2 I, pp. 591–599, 1997.

[42] A. E. Redington, J. Madden, A. J. Frew et al., "Transforming growth factor-β1 in asthma: measurement in bronchoalveolar lavage fluid," *American Journal of Respiratory and Critical Care Medicine*, vol. 156, no. 2 I, pp. 642–647, 1997.

[43] J. F. Alcorn, L. M. Rinaldi, E. F. Jaffe et al., "Transforming growth factor-β1 suppresses airway hyperresponsiveness in allergic airway disease," *American Journal of Respiratory and Critical Care Medicine*, vol. 176, no. 10, pp. 974–982, 2007.

[44] S. J. McMillan and C. M. Lloyd, "Prolonged allergen challenge in mice leads to persistent airway remodelling," *Clinical and Experimental Allergy*, vol. 34, no. 3, pp. 497–507, 2004.

[45] S. J. McMillan, G. Xanthou, and C. M. Lloyd, "Manipulation of allergen-induced airway remodeling by treatment with anti-TGF-β antibody: effect on the Smad signaling pathway," *The Journal of Immunology*, vol. 174, no. 9, pp. 5774–5780, 2005.

[46] R. Halwani, S. Al-Muhsen, H. Al-Jahdali, and Q. Hamid, "Role of transforming growth factor-β in airway remodeling in asthma," *American Journal of Respiratory Cell and Molecular Biology*, vol. 44, no. 2, pp. 127–133, 2011.

[47] W. Mattos, S. Lim, R. Russell, A. Jatakanon, K. F. Chung, and P. J. Barnes, "Matrix metalloproteinase-9 expression in asthma: effect of asthma severity, allergen challenge, and inhaled corticosteroids," *Chest*, vol. 122, no. 5, pp. 1543–1552, 2002.

[48] M. Masuoka, H. Shiraishi, S. Ohta et al., "Periostin promotes chronic allergic inflammation in response to Th2 cytokines," *The Journal of Clinical Investigation*, vol. 122, no. 7, pp. 2590–2600, 2012.

[49] K. Ruan, S. Bao, and G. Ouyang, "The multifaceted role of periostin in tumorigenesis," *Cellular and Molecular Life Sciences*, vol. 66, no. 14, pp. 2219–2230, 2009.

[50] C. K. Wong, K. M. Lau, I. H. Chan et al., "MicroRNA-21$*$ regulates the prosurvival effect of GM-CSF on human eosinophils," *Immunobiology*, vol. 218, no. 2, pp. 255–262, 2013.

[51] W. Duan and W. S. F. Wong, "Targeting mitogen-activated protein kinases for asthma," *Current Drug Targets*, vol. 7, no. 6, pp. 691–698, 2006.

Hindawi Publishing Corporation
Mediators of Inflammation
Volume 2014, Article ID 703653, 12 pages
http://dx.doi.org/10.1155/2014/703653

Research Article

Monocyte Subsets in Schistosomiasis Patients with Periportal Fibrosis

Jamille Souza Fernandes,[1] Maria Ilma Araujo,[1,2,3] Diego Mota Lopes,[1] Robson da Paixão de Souza,[1] Edgar M. Carvalho,[1,2,3] and Luciana Santos Cardoso[1,2,4]

[1] *Serviço de Imunologia, Complexo Hospitalar Universitário Professor Edgard Santos, Universidade Federal da Bahia, Rua João das Botas s/n, Canela, 40110-160 Salvador, BA, Brazil*
[2] *Instituto Nacional de Ciência e Tecnologia em Doenças Tropicais (INCT-DT), CNPQ/MCT, Brazil*
[3] *Escola Bahiana de Medicina e Saúde Pública, 40050-420 Salvador, BA, Brazil*
[4] *Departamento de Análises Clínicas e Toxicológicas, Faculdade de Farmácia, UFBA, 40170-115 Salvador, BA, Brazil*

Correspondence should be addressed to Luciana Santos Cardoso; lucianac@ufba.br

Received 25 September 2013; Revised 16 January 2014; Accepted 30 January 2014; Published 13 March 2014

Academic Editor: Dennis Daniel Taub

A major issue with *Schistosoma mansoni* infection is the development of periportal fibrosis, which is predominantly caused by the host immune response to egg antigens. Experimental studies have pointed to the participation of monocytes in the pathogenesis of liver fibrosis. The aim of this study was to characterize the subsets of monocytes in individuals with different degrees of periportal fibrosis secondary to schistosomiasis. Monocytes were classified into classical ($CD14^{++}CD16^{-}$), intermediate ($CD14^{++}CD16^{+}$), and nonclassical ($CD14^{+}CD16^{++}$). The expressions of monocyte markers and cytokines were assessed using flow cytometry. The frequency of classical monocytes was higher than the other subsets. The expression of HLA-DR, IL-6, TNF-α, and TGF-β was higher in monocytes from individuals with moderate to severe fibrosis as compared to other groups. Although no differences were observed in receptors expression (IL-4R and IL-10R) between groups of patients, the expression of IL-12 was lower in monocytes from individuals with moderate to severe fibrosis, suggesting a protective role of this cytokine in the development of fibrosis. Our data support the hypothesis that the three different monocyte populations participate in the immunopathogenesis of periportal fibrosis, since they express high levels of proinflammatory and profibrotic cytokines and low levels of regulatory markers.

1. Introduction

Schistosomiasis is a chronic and debilitating disease that affects over 200 million people worldwide and it is estimated that 700 million people live in areas at risk of infection [1, 2]. It is a disease of particular socioeconomic and public health importance, since it is prevalent in tropical and subtropical areas. In Brazil, it is estimated that about 2.5 to 7 million people are infected with *S. mansoni* and 25 million live in areas at risk of infection [3, 4]. The liver pathology of *Schistosoma mansoni* infection results from the host immune response to parasite antigens from *S. mansoni* eggs that become trapped in the portal venous system [5–7]. The granulomas formed around the egg act as barriers which prevent the dispersion of *S. mansoni* egg antigens. However, with the continuous arrival of eggs, the intense inflammatory process evolves to severe fibrosis. The liver pathology leads to the interruption of normal blood flow in the venous system of the sinusoids, resulting in portal hypertension, hepatosplenomegaly, esophageal, and gastric varices, which can lead to bleeding and even death [8, 9]. This severe form of the disease occurs in about five percent of infected subjects living in endemic areas [10, 11].

Mononuclear cells are involved in the pathogenesis of chronic liver diseases, especially those associated with fibrogenesis. Monocytes, for instance, participate in the development of fibrosis through various mechanisms including secretion of cytokines and generation of products related to oxidative stress [12]. Depending on their differentiation state and local signals, monocytes and macrophages are capable of secreting a variety of growth factors and proinflammatory, profibrotic, and anti-inflammatory cytokines [13]. Recently,

Table 1: Characteristics of the studied population.

Fibrosis	Without fibrosis ($n = 17$)	Incipient fibrosis ($n = 15$)	Moderate to severe ($n = 8$)	P
Age (years)* (mean ± SD)	30 ± 13	37 ± 12	46 ± 14	$P < 0.05$[a]
Male gender n (%)**	6 (35.3)	5 (33.3)	2 (25)	$P > 0.05$
Parasite burden (epg)*** Median (min–max)	72 (24–392)	72 (24–600)	66 (24–192)	$P > 0.05$
[1]Liver size (cm)*	9.5 ± 1.3	10.3 ± 1.5	10.9 ± 2.2	$P > 0.05$
[2]Spleen size (cm)*	8.4 ± 1.7	8.3 ± 1.4	10.9 ± 2.4	$P < 0.05$[a.b]
Portal vein diameter (mm)*	6.8 ± 3.0	7.9 ± 3.3	11.3 ± 5.0	$P < 0.05$[a]

*ANOVA; **chi-square; ***Kruskal-Wallis; [a]moderate to severe fibrosis versus without fibrosis.
[b]Moderate to severe fibrosis versus incipient fibrosis.
[1]Measured by midclavicular line.
[2]The largest diameter of the organ measured by USG.

human monocytes were classified into three subpopulations according to the expression of CD14 and CD16: classical ($CD14^{++}CD16^{-}$), intermediate ($CD14^{++}CD16^{+}$), and non-classical ($CD14^{+}CD16^{++}$) [14]. The study of Liaskou et al. showed evidence implicating the intermediate monocytes in the pathogenesis of liver fibrosis caused by chronic inflammatory diseases [15]. However, to our knowledge no studies have characterized these monocyte profiles in individuals with periportal fibrosis secondary to schistosomiasis. Thus, in this study we aimed to characterize monocytes subpopulations regarding their status of activation and expression of proinflammatory, antifibrotic, profibrotic, and regulatory molecules in individuals with different degrees of periportal fibrosis.

2. Methodology

2.1. Study Design and the Endemic Area. This study was carried out in an endemic area for schistosomiasis named Água Preta, in the state of Bahia, Brazil. Água Preta is located 280 km south of Salvador, the capital of the state of Bahia. It is composed of a residential area in the center of the village and some surrounding farms. Approximately 800 individuals live in the community. They live in poor sanitary conditions and agriculture is the predominant occupation. There is one river in this region that is used for bathing, washing clothes and utensils, and leisure, exposing the residents to high risk of *S. mansoni* infection [16]. Cross-sectional parasitological surveys using Kato-Katz [17] and sedimentation techniques were conducted on three different stool samples. The inclusion criteria for this study were individuals from endemic areas who have at least one positive parasitological exam for *S. mansoni*. From the 537 individuals who agreed to participate in this study 334 were infected with *S. mansoni* (62.5%). The frequency of other helminthic infections was 43.4% for *Trichuris trichiura*, 37.4% for *Ascaris lumbricoides*, 33.7% for hookworms, and 3.5% for *Strongyloides stercoralis*. From 334 individuals who were infected with *S. mansoni*, 220 agreed to perform abdominal ultrasound, in order to determine the degree of periportal fibrosis. They also agreed to donate blood for the study of the immunological response. For this particular aim, we analyzed patients of both gender, 10 to 60 years old. Seventeen patients with grade 0 (without fibrosis), fifteen patients with grade I (incipient fibrosis), and eight with fibrosis grades II and III (moderate and severe fibrosis) were included. We had difficulty in finding patients with advanced stages of periportal fibrosis in the region of the study; only eight patients with this condition met the inclusion criteria.

Individuals under ten years old were not included, due to a low probability of developing periportal fibrosis [18], and individuals older than 60 years, due to potential senescence of the immune system. We also did not include individuals with positive serology for HIV, HTLV-1, or hepatitis virus types B and C; all of which are conditions that could interfere with the immunological response.

2.2. Ultrasound Examination. Abdominal ultrasound (USG) was performed using the Quantum 2000 Siemens and Elegra Siemens ultrasound with a convex transductor of 3.5–5.0 Mhz. Liver span was measured in the midclavicular line. The liver was also examined for smoothness of surface, echogenicity, and posterior attenuation of the sound beam and portal vein diameter outside the liver midway between its entrance into the portal hepatic vein and its first bifurcation in the liver. Periportal fibrosis was characterized as multiple diffuse echogenic areas. Grading of periportal fibrosis was determined by the mean total thickness of four portal tracts after the first division from the right and left branches of portal vein (PT1) as follows: degree 0, mean thickness <3 mm; degree I, mean thickness 3 to 5 mm; degree II, mean thickness >5 to 7 mm; and degree III, mean thickness >7 mm [19]. We decided to use the Cairo's classification because we have performed previous studies using these parameters and because the physicians who have performed the USG in our studies are very well familiar with this classification [18, 20]. The scores of periportal fibrosis were grouped according to severity: degree 0 individuals were those without periportal fibrosis, degree I individuals those with incipient periportal fibrosis, and individuals with moderate to severe periportal fibrosis were patients with degrees II and III [21]. The analysis of immune response included 17 individuals without periportal fibrosis, 15 individuals with incipient fibrosis, and 8 individuals with moderate to severe forms of the disease, characterized by grade II ($n = 06$) and III ($n = 02$) (Table 1).

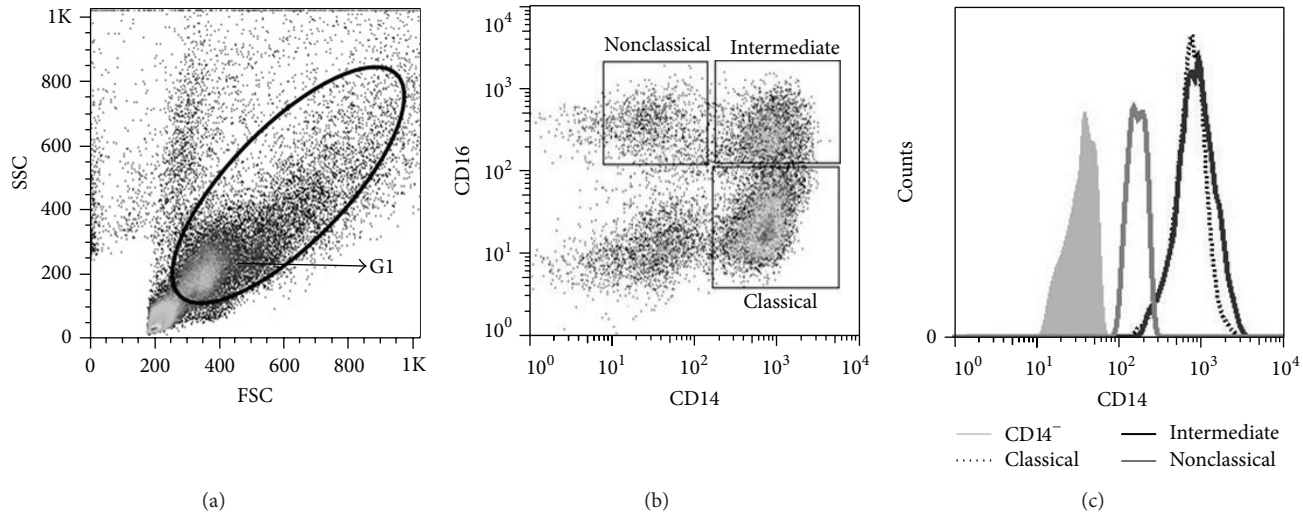

Figure 1: The monocyte population was defined by nonspecific fluorescence from the forward scatter (FSC) and side scatter (SSC) as parameters of cell size and granularity, identifying the monocyte population, region 1 (G1) (a). Strategy for classification of monocyte subsets through the expression of CD14 and CD16 (b). A representative histogram of CD14 expression in monocyte subsets (c).

2.3. Features of the Studied Subject. The features of studied individuals are shown in Table 1. The mean age of patients with moderate to severe fibrosis was higher (46 ± 14 years) compared to individuals without fibrosis (30 ± 13 years; $P < 0.05$). There were no significant differences in gender distribution or in parasite burden among groups. The sizes of the liver and spleen were also evaluated in this study. There was no significant difference in liver size among groups. However, in the group of individuals with moderate to severe fibrosis, spleen size was higher as compared to the group of individuals with incipient fibrosis and without fibrosis ($P < 0.05$). Additionally, the diameter of the portal vein was higher in subjects with moderate to severe fibrosis when compared with individuals without fibrosis (Table 1).

2.4. Cell Culture. Peripheral blood mononuclear cells (PBMCs) were isolated using Ficoll-Hypaque gradient sedimentation and adjusted to a concentration of 3×10^5/mL in RPMI 1640 medium containing 10% normal human serum (AB positive and heat inactivated), 100 U/mL of penicillin, 100 mg/mL of streptomycin, 2 mmol/L of L-glutamine, and 30 mmol/L of HEPES (all from Life Technologies GIBCO, BRL, Gaithersburg, MS). Cells were cultured either stimulated with 10 μg/mL of SEA (*Schistosoma* egg antigen) or without stimulation to assess cytokine production at 37°C in an atmosphere containing 5% CO_2 for 16 h. After incubation, the cells were stained with fluorochrome-conjugated antibody and acquired using flow cytometry (FACSCanto, BD Biosciences, San Jose, CA) as described below.

2.5. Flow Cytometry. PBMCs (3×10^5) obtained by a Ficoll-Hypaque gradient were incubated 10 μg/mL of SEA for 16 h, 37°C, and 5% of CO_2. During the last 4 h of culture, Brefeldin A (10 μg/mL; Sigma, St. Louis, MO), which impairs protein secretion by the Golgi complex, was added to the cultures. Afterwards, the cells were stained with PERCPCy5.5-labeled antibody conjugated with CD14 (anti-CD14 PERCPCy5.5; clone 61D3), anti-CD16 FITC (clone CB16), anti-IL-10R PE (polyclonal), anti-IL-4Rα PE (clone hIL-4R-M57), and anti-HLA-DR PE (clone LN3) and then washed in PBS and fixed in 4% formaldehyde for 20 min at room temperature. Intracellular staining was performed with anti-IL-12 PE (clone C8.6) mAbs, anti-IL-10 APC (clone JES3-19F1), anti-TGF-β APC (clone 9016), anti-IL-6 APC (clone MQ2-13A5), and anti-TNF-α PECy7 (MAb11), all antibodies from eBioscience. The monocyte population was defined by nonspecific fluorescence from the forward scatter (FSC) and side scatter (SSC) as parameters such as cell size and granularity, respectively. Monocyte area corresponded to the specific region graph: region 1 (G1) (Figure 1(a)). A total of 100,000 events were acquired for all experiments.

2.6. Analysis of FACS Data. The frequency of positive cells was analyzed using the program Flow Jo (Tree Star, USA). The monocytes subsets were selected based on the expression of CD14 and CD16 (Figure 1(b)). A representative histogram of CD14 expression in monocytes subsets is shown in Figure 1(c). We also evaluated the expression of CD56 in the population of monocytes and it was negative to this NK cell marker (data not shown). Limits for the quadrant markers were set based on negative populations and controls isotype (data not shown). Data were expressed as mean fluorescence intensity (MFI) parameter.

2.7. Statistical Analysis. Statistical analysis and the graphical representation were performed using the computer program Graphpad PRISM 5.0 software (La Jolla, CA, USA). Between-group comparisons were done using parametric and nonparametric methods as appropriate (ANOVA and Kruskal Wallis test). All statistical tests were two-tailed and the statistical significance was established at the 95 percent

confidence interval and significance was defined to $P < 0.05$. The Ethical Committee of Climério de Oliveira Maternity of the Federal University of Bahia, Brazil, approved the present study, and informed consent was obtained from all participants or their legal guardians.

3. Results

3.1. Monocyte Populations in Subjects with Different Degrees of Periportal Fibrosis due to Schistosomiasis. We evaluated the frequency of different subpopulations of monocytes and the activation status of these cells. The frequency of intermediate ($CD14^{++}CD16^{+}$) and nonclassical ($CD14^{+}CD16^{++}$) monocytes in cultures stimulated with SEA was higher (17% (7.72%–32.3%), 11.1% (2.71%–27.4%), resp.) in the group of individuals with incipient fibrosis when compared with the group without fibrosis (13.8% (3.88%–22.8%), and 7.56% (1.88%–24%); resp.). There was no significant difference in the frequency of classical monocytes ($CD14^{++}CD16^{-}$) among subjects with different degrees of periportal fibrosis (without fibrosis: without stimulus (WS) 56.3% (32.3%–73.9%), SEA 50.1% (32%–73.9%); incipient fibrosis: WS 45.4% (24.2%–71.6%), SEA 46.1% (22.3%–74.6%); moderate to severe fibrosis: WS 40.1% (19.2%–73.8%), SEA 46.5% (15.3%–75.6%). Furthermore, we observed that independently of the degree of fibrosis, the frequency of classical monocytes was higher in nonstimulated cultures (56.3% (32.3%–73.9%)) and also in cultures stimulated with SEA (50.1% (32%–73.9%); $P < 0.0001$) as compared to the frequency of intermediate (WS: 14.35% (6.3%–23.4%) and SEA: 13.8% (3.88%–22.8%); $P < 0.0001$) and nonclassical monocytes (WS: 5.36% (2.24%–26.2%) and SEA: 7.5% (1.88%–24%), $P < 0.0001$).

The expressions of HLA-DR on monocytes from individuals with different degrees of periportal fibrosis were evaluated. We observed that in the group of individuals with moderate to severe fibrosis the expression of HLA-DR on monocytes was higher both in classical (Figure 2(d)) (WS MFI = 1318 (404–2531), SEA MFI = 1981 (906–3419)), and intermediate monocytes (Figure 2(e)) (WS MFI = 1782 (648–3563), SEA MFI = 2033 (965–4198)) compared to the group of individuals with incipient fibrosis (classical: WS MFI = 492 (278–1623), SEA MFI = 747.5 (313–1766) and intermediate: WS MFI = 807 (278–2079), SEA MFI = 1034 (392–2022)) and without fibrosis (classical: WS MFI = 659 (263–1138), SEA MFI = 533 (315–1791), and Intermediate: WS MFI = 970 (474–1430), SEA MFI = 733 (486–2733)). However, there was no significant difference in the expression of HLA-DR on nonclassical monocytes among subjects with different degrees of periportal fibrosis (Figure 2(f)). The representative histogram for HLA-DR is shown in Figures 2(a)–2(c).

3.2. Expression of Profibrotic and Proinflammatory Molecules in Monocyte Subsets in Subjects with Different Degrees of Periportal Fibrosis Secondary to Schistosomiasis. The subsets of monocytes from individuals with different degrees of periportal fibrosis were evaluated regarding the expression of the profibrotic markers such as IL-4Rα and TGF-β and proinflammatory cytokines such as IL-6 and TNF-α.

The α receptor expression of IL-4 in the group of patients without fibrosis was higher in classical (Figure 3(a)) (WS MFI = 66.5 (38.5–199), SEA MFI = 67.15 (37.4–257)), intermediate (Figure 3(b)) (WS MFI = 110 (48.2–319), SEA MFI = 113.5 (50.9–367)), and nonclassical monocytes (Figure 3(c)) (WS MFI = 90.7 (26.3–205), SEA MFI = 103.4 (24.1–230)) compared with the group of subjects with incipient fibrosis (classical: WS MFI = 36.7 (19.5–202), SEA MFI = 38.35 (26–228); intermediate: WS MFI = 53.6 (32.5–316), SEA MFI = 54.1 (42–316); and nonclassical: WS MFI = 42.25 (21.2–235), SEA MFI = 38 (32.8–217)). The expression of this receptor was also higher in the three subpopulations of monocytes from patients with moderate to severe fibrosis (classical: SEA MFI = 49.9 (35.5–120); intermediate: WS MFI = 106 (59.7–197), SEA MFI = 103 (62.1–213), and nonclassical: SEA MFI = 62.6 (42.9–189)) compared with the group of individuals with incipient fibrosis. In the classical (Figure 3(a)) and nonclassical monocytes (Figure 3(c)) this difference was only observed in cultures stimulated with SEA.

The expression of TGF-β in the group of subjects with moderate to severe fibrosis was higher in classical (WS MFI = 62.25 (29.1–74,1) SEA MFI = 55.5 (24.1–81.8)) (Figure 3(d)), intermediate (WS MFI = 85.4 (22.5–102), SEA MFI = 64.7 (22.4–115)) (Figure 3(e)), and nonclassical monocytes (WS MFI = 28.5 (13.7–44.2)) (Figure 3(f)) compared with the group of patients without fibrosis (classical: WS MFI = 18.05 (10.4–58.2), SEA MFI = 26.2 (8.9–46.2); intermediate: WS MFI = 21.6 (13–77.9), SEA MFI = 25.6 (12.2–52.8); and nonclassical: WS MFI = 13.45 (7.6–27.7)). Furthermore, the expression of TGF-β in classical monocytes in cultures without antigenic stimulation was higher in the group of individuals with incipient fibrosis (MFI = 29.8 (21.9–86)) when compared to individuals without fibrosis (MFI = 18.05 (10.4–58.2)) (Figure 3(d)).

The expression of IL-6 (Figures 3(g)–3(i)) was higher in all three subpopulations of monocytes from the group of patients with moderate to severe fibrosis (classical: WS MFI = 79.8 (28–98.6), SEA MFI = 65.45 (26.5–135), intermediate: WS MFI = 145 (38.4–217), SEA MFI = 131 (36–258), and nonclassical: WS MFI= 99.15 (18.5–172), SEA MFI = 87.6 (17.9–231)) compared with the group of patients without fibrosis (classical: WS MFI = 18.35 (9.75–36), SEA MFI = 21.4 (8.6–62.5); intermediate: WS MFI = 17.9 (12.6–55.5), SEA MFI = 21.85 (12.3-108); and nonclassical: WS MFI = 10.8 (7.23–32.8), SEA MFI = 10.6 (6.63–39.2)) and with incipient fibrosis (classical: WS MFI = 25.4 (21.1–70.9), SEA MFI = 25.2 (20.7–87.6); intermediate: WS MFI = 33.1 (26.1–117); and nonclassical: WS MFI = 16.2 (10.1–93), SEA MFI = 11.1 (15.2–107)). We also observed that the expression of IL-6 in intermediate monocytes was higher in the group of individuals with incipient fibrosis (SEA MFI = 31.2 (26–139], related to individuals without fibrosis (SEA MFI = 21 85 (12.3–108)) (Figure 3(h)).

Regarding the expression of TNF-α, we observed that the group of subjects with moderate to severe fibrosis showed higher expression of this cytokine in classical (Figure 3(j)) (WS MFI = 321 (52–386), SEA MFI = 244 (47.4–324)), intermediate (Figure 3(k)) (WS MFI = 368 (73.1–413), SEA MFI = 261 (62.8–377)), and nonclassical monocytes (Figure 3(l))

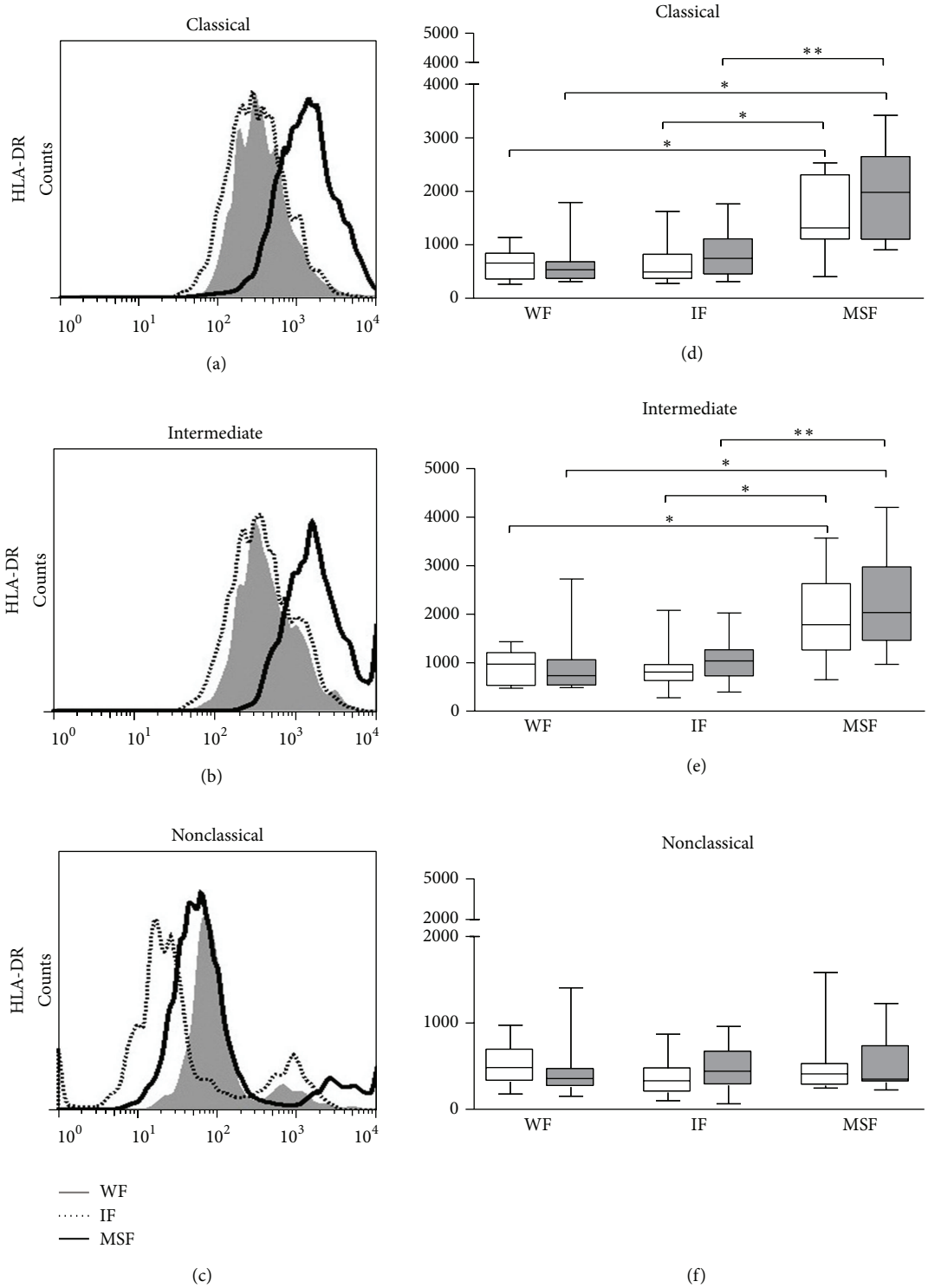

Figure 2: Representative histogram of HLA-DR expression (mean fluorescence intensity, MFI) on monocytes of patients with periportal fibrosis secondary to schistosomiasis ((a)–(c)). Expression of HLA-DR on classical ($CD14^{++}CD16^{-}$), intermediate ($CD14^{++}CD16^{+}$), and nonclassical ($CD14^{+}CD16^{++}$) monocytes, respectively, in cultures without stimulation (white bar) and stimulated with 10 μg/mL of SEA (gray bar) ((d)–(f)). Without fibrosis (WF), incipient fibrosis (IF), and moderate to severe fibrosis (MSF). $^{*}P < 0.05$ and $^{**}P < 0.005$ (Kruskal-Wallis).

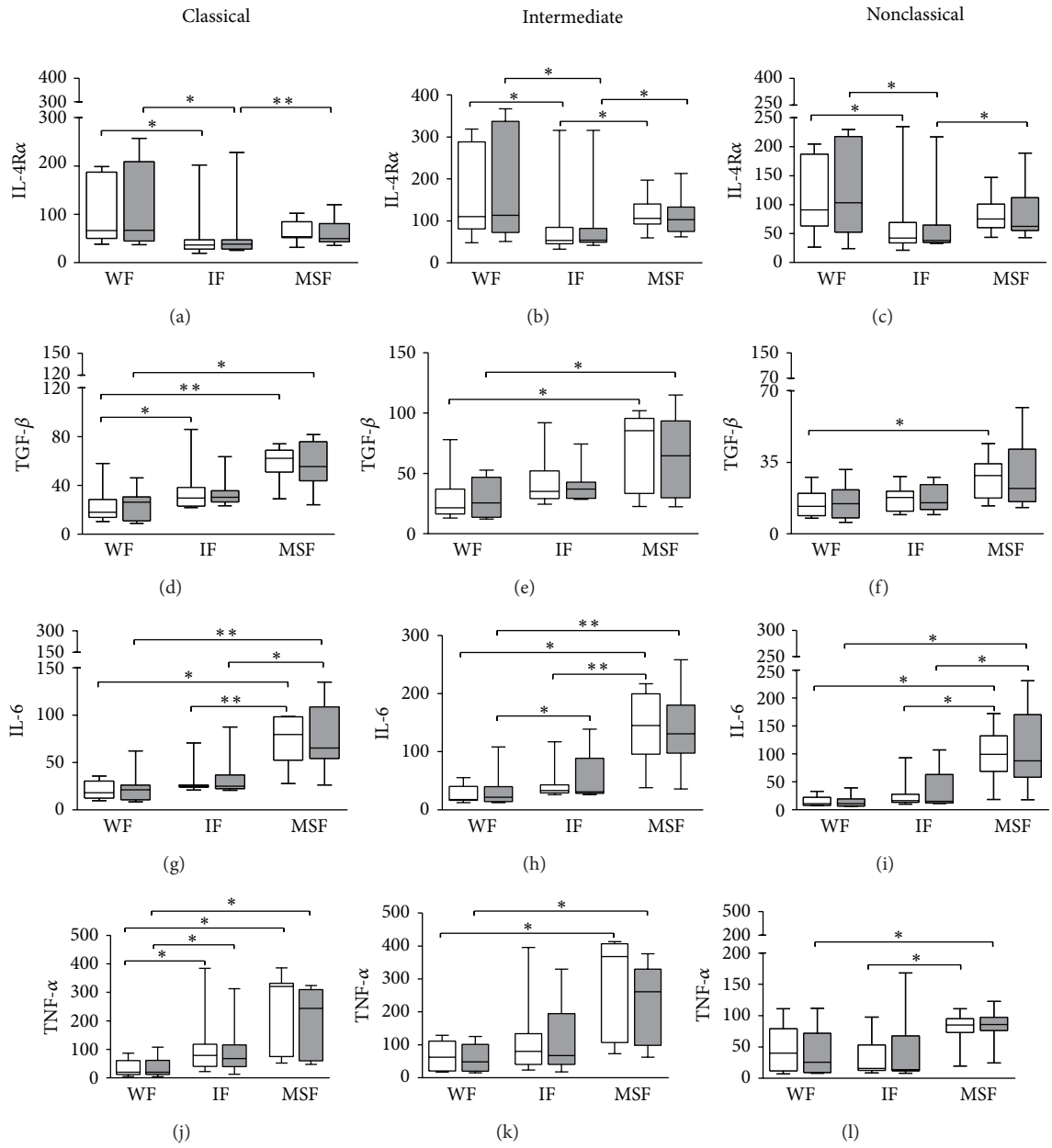

Figure 3: Mean fluorescence intensity (MFI) expression of profibrotic IL-4Rα ((a)–(c)) and TGF-β ((d)–(f)) and proinflammatory IL-6 ((g)–(i)) and TNF-α ((j)–(l)) molecules in classical ($CD14^{++}CD16^{-}$), intermediate ($CD14^{++}CD16^{+}$), and nonclassical ($CD14^{+}CD16^{++}$) monocytes, of patients with different degrees of periportal fibrosis secondary to schistosomiasis. Cultures without stimulus (white bar) and cultures stimulated with 10 μg/mL SEA (gray bar). Without fibrosis (WF), incipient fibrosis (IF), and moderate to severe fibrosis (MSF). $^{*}P < 0.05$ and $^{**}P < 0.005$ (Kruskal-Wallis).

(SEA MFI = 85.6 (24.3–123)), when compared to individuals without fibrosis (classical: WS MFI = 20.5 (5.32–86.9), SEA MFI = 20.5 (4.1–108); intermediate: WS MFI = 62.7 (17.4–129), SEA MFI = 48.7 (14.7–125); and nonclassical SEA MFI= 25.65 (8–112)). There was also a higher expression of TNF-α in nonclassical monocytes, in cultures without antigen stimulation, from the group of patients with moderate to severe fibrosis (MFI = 85.2 (19.6–111)) (Figure 3(l)) compared to individuals with incipient fibrosis (MFI = 15.7 (8.5–97.6)). Additionally, there was an increased expression of TNF-α in the classical monocytes of patients with incipient fibrosis (WS MFI = 78.8 (22.4–384), SEA MFI = 67.9 (12.9–313)) when compared with individuals without fibrosis (Figure 3(j)).

3.3. Regulatory and Antifibrotic Molecules in Monocyte Subsets in Subjects with Different Degrees of Periportal Fibrosis Secondary to Schistosomiasis. The expression of IL-12, IL-10, and IL-10R was evaluated in monocytes of schistosomiasis patients. The expression of IL-12 was higher in the classical (Figure 4(a)) (WS MFI = 464 (87.5–1310) and

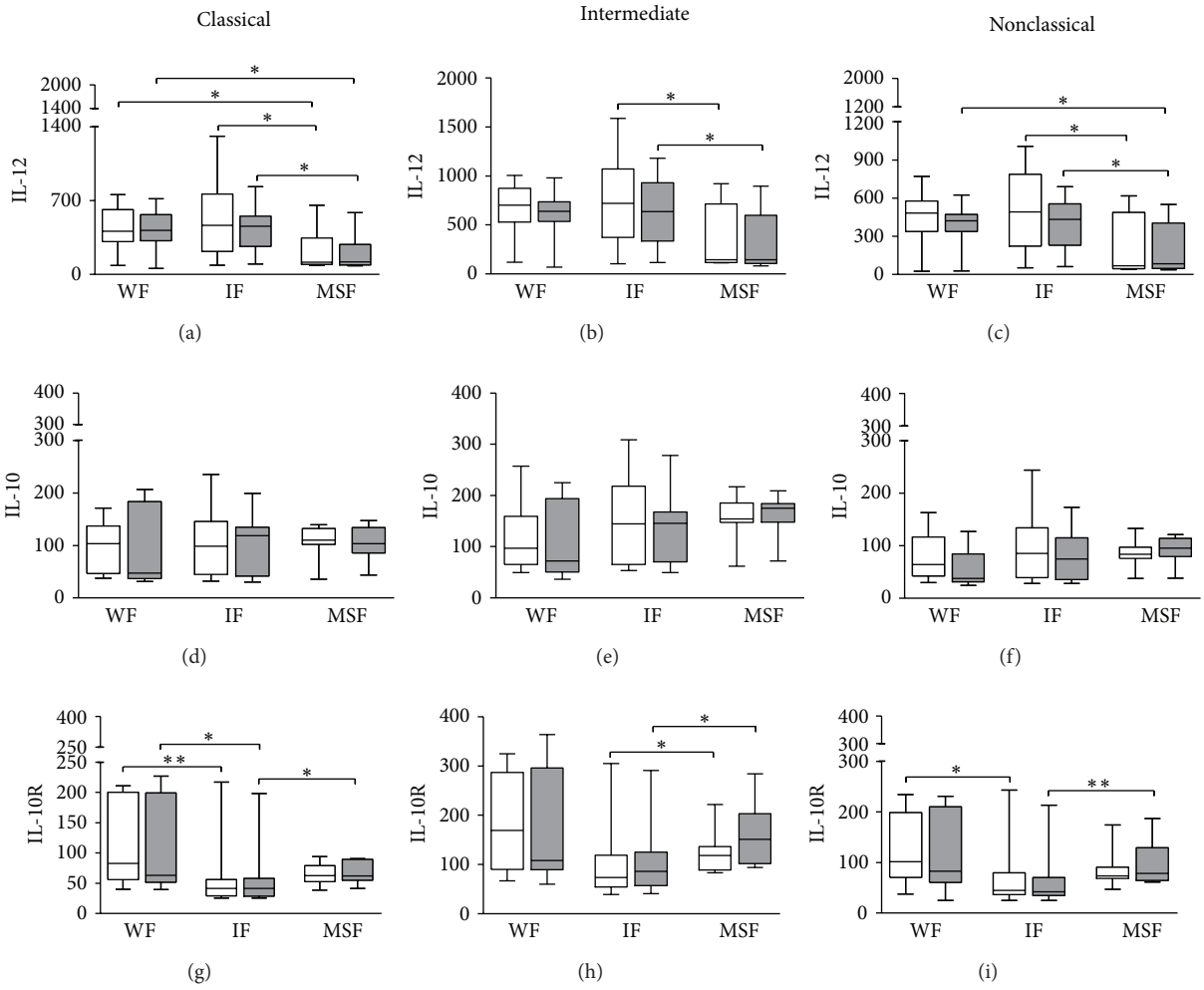

Figure 4: Mean fluorescence intensity (MFI) expression of antifibrotic IL-12 ((a)–(c)) and regulatory IL-10 ((d)–(f)) and IL-10R ((g)–(i)) molecules in classical ($CD14^{++}CD16^{-}$), intermediate ($CD14^{++}CD16^{+}$), and nonclassical ($CD14^{+}CD16^{++}$) monocytes of patients with different degrees of periportal fibrosis secondary to schistosomiasis. Cultures without stimulation (white bar) and cultures stimulated with 10 μg/mL of SEA (gray bar). Without fibrosis (WF), incipient fibrosis (IF), and moderate to severe fibrosis (MSF). $^{*}P < 0.05$ and $^{**}P < 0.005$ (Kruskal-Wallis).

SEA MFI = 456.5 (97.6–831)), intermediate (Figure 4(b)) (WS MFI = 722.5 (104–1589) and SEA MFI = 635 (117–1180)), and nonclassical monocytes (Figure 4(c)) (WS MFI = 492.5 (52.1–1006) and SEA MFI = 434 (62.1–690)) of individuals with incipient fibrosis compared with the group of subjects with moderate to severe fibrosis (classical: WS MFI = 115.5 (85.4–656) and SEA MFI = 117.5 (81–584); intermediate: WS MFI = 144 (113–922) and SEA MFI = 145.5 (83.8–896), and nonclassical: WS MFI = 67.45 (39.7–618) and SEA MFI = 84.8 (37.5–550)). Furthermore, we observed that in the group of individuals without fibrosis the expression of IL-12 was higher in both classical (WS MFI = 408 (86.2–757) and SEA MFI = 416 (57.2–716)) and the nonclassical monocytes (SEA MFI = 422 (28.4–624)) when compared with the group of patients with moderate to severe fibrosis. In nonclassical monocytes this difference was only observed in the presence of SEA.

In relation to the expression of regulatory molecule IL-10 in these monocytes there was no significant differences among subjects with different degrees of periportal fibrosis (Figures 4(d)–4(f)).

The expression of IL-10R, however, was higher in classical (Figure 4(g)) (SEA MFI = 62.3 (41.6–90.8)), intermediate (Figure 4(h)) (WS MFI = 118 (83.2–291) and SEA MFI = 151 (93.8–284)), and nonclassical monocytes (Figure 4(i)) (SEA MFI = 78.6 (61.3–187)) in the group of patients with moderate to severe fibrosis when compared with the group of subjects with incipient fibrosis (classical: SEA MFI = 41.75 (25.2–198); intermediate: WS MFI = 73.8 (38.8–305) and SEA MFI = 85.75 (40.8–291); and nonclassical: SEA MFI = 42.35 (24.6–213)). Furthermore, in the group of individuals without fibrosis the expression of IL-10R was higher in classical (WS MFI = 82.6 (40–211) and SEA MFI = 63.1 (39.7–227)) and nonclassical monocytes (WS MFI = 101.4 (37.8–234)) compared to the group of individuals with incipient fibrosis (classical: WS MFI = 41.45 (25.4–217) and SEA MFI = 41.75 (25.2–198) and nonclassical: WS MFI = 44.8 (25–243)).

4. Discussion

This study aimed to characterize the phenotype of monocytes of patients with different degrees of periportal fibrosis secondary to schistosomiasis. The mean age of individuals with moderate to severe fibrosis was higher when compared with individuals without fibrosis. This is in agreement with the literature [18, 21] and may be explained by constant reexposure to the parasite, or by the slow process of fibrosis development [22]. Parasite burden and gender distribution were similar among groups of patients with different degrees of fibrosis. However, other studies from our group have shown that individuals without fibrosis have a higher parasite burden as compared to the other groups [18, 20]. A possible explanation for this observation is that chronic infection can lead to intestinal fibrosis, which may impair the migration of eggs to the intestinal lumen and thereby decrease egg count in parasitological exams [23]. Other studies have examined the role of gender in the development of periportal fibrosis, noting an overall male bias in susceptibility [24, 25].

We did not observe a significant difference between groups of individuals with respect to liver size, likely because in those with moderate to severe periportal fibrosis, the liver parenchyma was not severely compromised. It is well known that the liver size decreases with the progression of fibrosis [19, 26–28].

We observed, however, that in patients with moderate to severe fibrosis spleen size was larger as compared to the other groups. Portal vein diameter was also higher in subjects with moderate to severe fibrosis as compared to patients without fibrosis. These findings are in agreement with other studies [29, 30].

In recent years, studies have emphasized the important role of monocytes in the inflammatory process associated with hepatic fibrosis in experimental models [31–34].

Wong et al. evaluated characteristics of classical monocytes, intermediate, and nonclassical through the gene expression profiling and observed that classical monocytes expressed genes involved in tissue repair function, the intermediate monocytes expressed genes for MHC class II [35], and nonclassical monocytes with genes involved in cytoskeleton rearrangement which may be responsible for its high motility observed *in vivo* [36]. Little is known about the role of monocytes in the pathology of human schistosomiasis, and this study aimed to characterize the monocyte subsets (classical, intermediate, and nonclassical) in schistosomiasis patients with different degrees of periportal fibrosis.

HLA-DR expression on monocytes is important to antigen presentation to T cells. We observed that in patients with moderate to severe fibrosis the expression of HLA-DR on classical and intermediate monocytes was higher as compared to the patients with incipient fibrosis and without fibrosis. However, there was no significant difference in the expression of HLA-DR on nonclassical monocytes among the groups. These results indicate that classical and intermediate monocytes might participate in periportal fibrosis development in schistosomiasis through antigen presentation and subsequently, in T cell activation. Studies using the new classification of monocytes in humans are rare. Hudig et al. observed that the different phenotypes of monocytes from human individuals is heterogeneous and may alter depending on the disease model [37]. However, there are some studies in the literature showing a low expression of HLA-DR by nonclassical monocytes, suggesting that this population has a patrolling profile and lower capacity to present antigens to T cells [35, 36, 38]. Furthermore, study of our group also observed that the addition of *Schistosoma mansoni* antigen rSm29 in PBMC cultures in the presence of soluble *Leishmania braziliensis* antigen (SLA) decreases the expression of HLA-DR in nonclassical monocytes from patients with cutaneous leishmaniasis [16].

In order to better understand the mechanisms involved in the development of periportal fibrosis in schistosomiasis, molecules of profibrotic and proinflammatory profiles were also evaluated in different subpopulations of monocytes.

The expression of IL-4Rα in the three subpopulations of monocytes was higher in patients without fibrosis and moderate to severe fibrosis when compared with individuals with incipient fibrosis. In experimental models, IL-4 and IL-13 cytokines are responsible for inducing an alternative activation of monocytes through binding to the α receptor of IL-4. The signaling through the IL-4Rα induces the expression of arginase, an enzyme responsible for the conversion of L-arginine in proline. The proline is an essential amino acid which is involved in collagen production and development of fibrosis [39]. In experimental models of *S. mansoni* infection it has been shown that the responsiveness through the IL-4Rα is important to granuloma formation and survival of the host during infection [40, 41]. However, there are few studies reporting the role of IL-4Rα in human monocytes and the role of this molecule in schistosomiasis remains controversial.

The expression of TGF-β in the three subpopulations of monocytes was also higher in subjects with moderate to severe fibrosis compared to individuals without fibrosis. This cytokine induces fibroblast proliferation and collagen deposition, suggesting its potential role in the establishment of fibrosis [42–44]. In the study conducted by Souza et al. there was no significant difference in serum levels of TGF-β in schistosomiasis patients with different degrees of periportal fibrosis [18]. In addition, other studies have not found differences in the levels of TGF-β in PBMCs cultures stimulated with SEA among groups of individuals with different degrees of periportal fibrosis [20, 21]. Possibly the expression of TGF-β by human monocytes is associated with fibrosis, while the production of this cytokine by lymphocytes is not essential. Study performed by Kanzler et al. (2001) supports the role of TGF-β in liver fibrogenesis in patients with hepatitis C infection. The authors propose that TGF-β predicts clinical disease progression [45]. However, Li et al. observed that local production of TGF-β by regulatory T cell appeared to have a protective role in fibrogenesis in individual with hepatitis C virus infection [46].

Following the same pattern of cytokine production, the expression of the inflammatory cytokine IL-6 was higher in all three subpopulations of monocytes from individuals with moderate to severe fibrosis as compared to individuals with incipient fibrosis and without fibrosis and was also higher in

intermediate monocytes of individuals with incipient fibrosis as compared to individuals without fibrosis. Khalil et al. (1996) reported an increased production of IL-6 during the course of *S. mansoni* infection and granuloma formation in an experimental model, which may indicate the involvement of this cytokine in liver pathology [47]. Another experimental study reported a high production of IL-6 by cultures of macrophages isolated from granulomas in response to SEA antigen [48]. IL-6 is a phase acute cytokine associated to fibrogenesis and collagen deposition [49–52], and Fuster et al. observed that IL-6 was strongly associated with liver fibrosis in HIV-infected patients with alcohol problems, and this cytokine may be a useful predictive marker for liver fibrosis for these patients [53].

Recently, it has been shown that the combination of TGF-β and IL-6 is crucial for the differentiation of naive T cells into Th17 cells [54–57]. IL-17 is a cytokine involved in the development of several diseases, recruiting neutrophils and macrophages to inflammatory sites [58]. The participation of IL-17 in the pathogenesis of schistosomiasis has been described in experimental models [59–61]. In our study, we observed high expression of IL-6 and TGF-β in monocytes of individuals with moderate to severe fibrosis. These cytokines may contribute to the induction of IL-17 and consequently lead to a worsening of the disease. Souza et al., however, found no difference in the levels of IL-17 in supernatants of PBMCs cultures stimulated with SEA between groups of individuals with different degrees of periportal fibrosis [18].

The expression of TNF-α was higher in monocytes of patients with moderate to severe fibrosis as compared to individuals without fibrosis or with incipient fibrosis. High levels of TNF-α produced by PBMC stimulated with *Schistosoma* antigens or in nonstimulated cells have been found in patients with periportal fibrosis [10, 18, 22, 62]. However, other studies have not observed any differences in TNF-α levels in supernatants of PBMC stimulated with SEA in patients with different degrees of fibrosis [20, 21]. In experimental studies TNF-α seems to be essential to liver fibrosis development [63]. In chronic hepatitis B virus infection $CD16^+$ subset of monocytes produces high levels of TNF, suggesting that this subset of monocytes may be closely related to liver damage in these HBV-infected patients [64]. Our study showed that monocytes express TNF-α, independent of their subpopulation, and this may be important for the development of fibrosis.

Besides the inflammatory and profibrotic role of monocytes or macrophages, these cells are also essential in preventing fibrosis in experimental models [65, 66].

In our study, the expression of IL-12 by monocytes was higher in individuals with incipient fibrosis and without fibrosis when compared to individuals with moderate to severe fibrosis. Some studies have shown that the granulomatous inflammation and hepatic fibrosis in experimental models of *S. mansoni* can be prevented by the addition of IL-12, a key cytokine that induces the Th1 immune response [67–69]. Hoffmann et al. showed that the deviation of the immune response to the Th1 type is required to reduce granuloma size and prevent hepatic fibrosis [63]. As monocytes of patients with moderate to severe fibrosis in our study showed a low expression of IL-12, these patients might present an impaired Th1 response and insufficient control of fibrosis development.

IL-10 is a cytokine with modulatory functions; however, we found no significant difference in the expression of IL-10 in monocytes from individuals with different degrees of periportal fibrosis. Some authors have shown elevated levels of this cytokine in PBMC from patients with severe periportal fibrosis [20], while others have found low levels of this cytokine in these patients [21], or no significant difference in the levels of IL-10 among groups of patients [18]. Experimental studies of double IL-10 and IL-12 knockouts resulted in severe fibrosis development [69, 70].

The expression of IL-10 receptor in this study, however, was higher in monocytes of patients with moderate to severe fibrosis and without fibrosis compared to individuals with incipient fibrosis. This was unexpected, since Herbert et al. found that the administration of anti-IL-10R monoclonal antibody in mice infected with *S. mansoni* significantly increased the production of IL-4, IFN-γ, TNF-α, and IL-17, as well as the size of hepatocellular damage [71].

The expression of IL-4Rα and IL-10R by monocytes of patients without fibrosis might contribute to the anti-inflammatory profile of monocytes in these individuals. Moreover, in a recent study from our group we observe that the lymphocytes of individuals with moderate and severe fibrosis had a lower expression of the molecule activation CD28 and low expression of regulation markers, such as CTLA-4 and $CD25^{high}$, suggesting the absence of regulation in lymphocytes of these individuals with degrees higher of fibrosis [72].

5. Conclusion

Taken together, our results indicate that monocyte subpopulations of patients with moderate to severe periportal fibrosis participate in the immunopathogenesis of the disease, since they express high levels of proinflammatory and profibrotic cytokines in combination with a low expression of regulatory molecules.

Conflict of Interests

The authors declare that they have no conflict of interests.

Acknowledgments

The authors would like to thank Dr. Irisma Souza and Dr. Delfin Gonzalez for performing the ultrasound assessment. The authors are also very grateful to all volunteers from the community of Água Preta-Gandu, who agreed to participate in this study, to the local health agent Irene Jesus for her support, and to Whitney Oriana Bagge for the corrections and suggestions made in the text. Edgar M. Carvalho and Maria Ilma Araujo are investigators supported by The Conselho Nacional de Desenvolvimento Científico e Tecnológico (CNPq). This work was supported by the Brazilian National Research Council (CNPq) Universal (482113/2010-3).

References

[1] L. S. Iarotski and A. Davis, "The schistosomiasis problem in the world: results of a WHO questionnaire survey," *Bulletin of the World Health Organization*, vol. 59, no. 1, pp. 115–127, 1981.

[2] P. Steinmann, J. Keiser, R. Bos, M. Tanner, and J. Utzinger, "Schistosomiasis and water resources development: systematic review, meta-analysis, and estimates of people at risk," *The Lancet Infectious Diseases*, vol. 6, no. 7, pp. 411–425, 2006.

[3] "Vigilância Epidemiológica e Controle da Esquistossomose," 2007, ftp://ftp.cve.saude.sp.gov.br/doc_tec/hidrica/doc/manu_esqui.pdf.

[4] BRASIL, "Guia de Vigilância Epidemiológica," 2009.

[5] K. S. Warren, "Pathophysiology and pathogenesis of hepatosplenic schistosomiasis mansoni," *Bulletin of the New York Academy of Medicine*, vol. 44, no. 3, pp. 280–294, 1968.

[6] I. Bica, D. H. Hamer, and M. J. Stadecker, "Hepatic schistosomiasis," *Infectious Disease Clinics of North America*, vol. 14, no. 3, pp. 583–604, 2000.

[7] M. G. Chiaramonte, M. Mentink-Kane, B. A. Jacobson et al., "Regulation and function of the interleukin 13 receptor α 2 during a T helper cell type 2-dominant immune response," *Journal of Experimental Medicine*, vol. 197, no. 6, pp. 687–701, 2003.

[8] A. P. Baptista and Z. A. Andrade, "Angiogenesis and schistosomal granuloma formation," *Memorias do Instituto Oswaldo Cruz*, vol. 100, no. 2, pp. 183–185, 2005.

[9] T. A. Wynn, "Common and unique mechanisms regulate fibrosis in various fibroproliferative diseases," *Journal of Clinical Investigation*, vol. 117, no. 3, pp. 524–529, 2007.

[10] S. Henri, C. Chevillard, A. Mergani et al., "Cytokine regulation of periportal fibrosis in humans infected with *Schistosoma mansoni*: IFN-γ is associated with protection against fibrosis and TNF-α with aggravation of disease," *Journal of Immunology*, vol. 169, no. 2, pp. 929–936, 2002.

[11] J. C. Bina and A. Prata, "Schistosomiasis in hyperendemic area of Taquarendi. I: *Schistosoma mansoni* infection and severe clinikal forms," *Revista da Sociedade Brasileira de Medicina Tropical*, vol. 36, no. 2, pp. 211–216, 2003.

[12] F. Marra, S. Aleffi, S. Galastri, and A. Provenzano, "Mononuclear cells in liver fibrosis," *Seminars in Immunopathology*, vol. 31, no. 3, pp. 345–358, 2009.

[13] R. Bataller and D. A. Brenner, "Liver fibrosis," *Journal of Clinical Investigation*, vol. 115, no. 2, pp. 209–218, 2005.

[14] L. Ziegler-Heitbrock, P. Ancuta, S. Crowe et al., "Nomenclature of monocytes and dendritic cells in blood," *Blood*, vol. 116, no. 16, pp. e74–e80, 2010.

[15] E. Liaskou, H. W. Zimmermann, K. K. Li et al., "Monocyte subsets in human liver disease show distinct phenotypic and functional characteristics," *Hepatology*, vol. 57, no. 1, pp. 385–398, 2013.

[16] A. M. Bafica, L. S. Cardoso, S. C. Oliveira et al., "Changes in T-cell and monocyte phenotypes in vitro by *Schistosoma mansoni* antigens in cutaneous leishmaniasis patients," *Journal of Parasitology Research*, vol. 2012, Article ID 520308, 2012.

[17] N. Katz, P. M. Coelho, and J. Pellegrino, "Evaluation of Kato's quantitative method through the recovery of *Schistosoma mansoni* eggs added to human feces," *Journal of Parasitology*, vol. 56, no. 5, pp. 1032–1033, 1970.

[18] R. P. de Souza, L. S. Cardoso, G. T. Lopes et al., "Cytokine and chemokine profile in individuals with different degrees of periportal fibrosis due to *Schistosoma mansoni* infection," *Journal of Parasitology Research*, vol. 2012, Article ID 394981, 2012.

[19] M. F. Abdel-Wahab, G. Esmat, A. Farrag, Y. A. El-Boraey, and G. T. Strickland, "Grading of hepatic schistosomiasis by the use of ultrasonography," *The American Journal of Tropical Medicine and Hygiene*, vol. 46, no. 4, pp. 403–408, 1992.

[20] A. R. De Jesus, A. Magalhães, D. Gonzalez Miranda et al., "Association of type 2 cytokines with hepatic fibrosis in human *Schistosoma mansoni* infection," *Infection and Immunity*, vol. 72, no. 6, pp. 3391–3397, 2004.

[21] L. F. Alves Oliveira, E. C. Moreno, G. Gazzinelli et al., "Cytokine production associated with periportal fibrosis during chronic schistosomiasis mansoni in humans," *Infection and Immunity*, vol. 74, no. 2, pp. 1215–1221, 2006.

[22] M. Booth, J. K. Mwatha, S. Joseph et al., "Periportal fibrosis in human *Schistosoma mansoni* infection is associated with low IL-10, low IFN-γ, high TNF-α, or low RANTES, depending on age and gender," *Journal of Immunology*, vol. 172, no. 2, pp. 1295–1303, 2004.

[23] R. R. Oliveira, K. J. Gollob, J. P. Figueiredo et al., "*Schistosoma mansoni* infection alters co-stimulatory molecule expression and cell activation in asthma," *Microbes and Infection*, vol. 11, no. 2, pp. 223–229, 2009.

[24] D. N. Silva-Teixeira, C. Contigli, J. R. Lambertucci, J. C. Serufo, and V. Rodrigues Jr., "Gender-related cytokine patterns in sera of schistosomiasis patients with symmers' fibrosis," *Clinical and Diagnostic Laboratory Immunology*, vol. 11, no. 3, pp. 627–630, 2004.

[25] Q. Mohamed-Ali, N.-E. M. A. Elwali, A. A. Abdelhameed et al., "Susceptibility to periportal (Symmers) fibrosis in human *Schistosoma mansoni* infections: evidence that intensity and duration of infection, gender, and inherited factors are critical in disease progression," *Journal of Infectious Diseases*, vol. 180, no. 4, pp. 1298–1306, 1999.

[26] S. Houston, M. Munjoma, K. Kanyimo, R. N. Davidson, and G. Flowerdew, "Use of ultrasound in a study of schistosomal periportal fibrosis in rural Zimbabwe," *Acta Tropica*, vol. 53, no. 1, pp. 51–58, 1993.

[27] M. F. Abdel-Wahab, G. Esmat, M. Milad, S. Abdel-Razek, and G. T. Strickland, "Characteristic sonographic pattern of schistosomal hepatic fibrosis," *The American Journal of Tropical Medicine and Hygiene*, vol. 40, no. 1, pp. 72–76, 1989.

[28] J. Richter, E. da Silva Monteiro, R. Moreira Braz et al., "Sonographic organometry in Brazilian and Sudanese patients with hepatosplenic schistosomiasis mansoni and its relation to the risk of bleeding from oesophageal varices," *Acta Tropica*, vol. 51, no. 3-4, pp. 281–290, 1992.

[29] M. Homeida, S. Ahmed, A. Dafalla et al., "Morbidity associated with *Schistosoma mansoni* infection as determined by ultrasound: a study in Gezira, Sudan," *The American Journal of Tropical Medicine and Hygiene*, vol. 39, no. 2, pp. 196–201, 1988.

[30] A. R. De Jesus, D. Gonzalez Miranda, R. Gonzalez Miranda et al., "Morbidity associated with *Schistosoma mansoni* infection determined by ultrasound in an endemic area of Brazil, Caatinga do Moura," *The American Journal of Tropical Medicine and Hygiene*, vol. 63, no. 1-2, pp. 1–4, 2000.

[31] J. S. Duffield, S. J. Forbes, C. M. Constandinou et al., "Selective depletion of macrophages reveals distinct, opposing roles during liver injury and repair," *Journal of Clinical Investigation*, vol. 115, no. 1, pp. 56–65, 2005.

[32] K. R. Karlmark, R. Weiskirchen, H. W. Zimmermann et al., "Hepatic recruitment of the inflammatory Gr1+ monocyte subset upon liver injury promotes hepatic fibrosis," *Hepatology*, vol. 50, no. 1, pp. 261–274, 2009.

[33] C. Mitchell, D. Couton, J.-P. Couty et al., "Dual role of CCR2 in the constitution and the resolution of liver fibrosis in mice," *The American Journal of Pathology*, vol. 174, no. 5, pp. 1766–1775, 2009.

[34] E. Seki, S. De Minicis, S. Inokuchi et al., "CCR2 promotes hepatic fibrosis in mice," *Hepatology*, vol. 50, no. 1, pp. 185–197, 2009.

[35] K. L. Wong, J. J.-Y. Tai, W.-C. Wong et al., "Gene expression profiling reveals the defining features of the classical, intermediate,and nonclassical human monocyte subsets," *Blood*, vol. 118, no. 5, pp. e16–e31, 2011.

[36] J. Cros, N. Cagnard, K. Woollard et al., "Human CD14dim monocytes patrol and sense nucleic acids and viruses via TLR7 and TLR8 receptors," *Immunity*, vol. 33, no. 3, pp. 375–386, 2010.

[37] D. Hudig, K. W. Hunter, W. J. Diamond, and D. Redelman, "Properties of human blood monocytes. II. Monocytes from healthy adults are highly heterogeneous within and among individuals," *Cytometry B*, 2013.

[38] F. L. van de Veerdonk and M. G. Netea, "Diversity: a hallmark of monocyte society," *Immunity*, vol. 33, no. 3, pp. 289–291, 2010.

[39] M. Hesse, M. Modolell, A. C. La Flamme et al., "Differential regulation of nitric oxide synthase-2 and arginase-1 by type 1/type 2 cytokines in vivo: granulomatous pathology is shaped by the pattern of L-arginine metabolism," *Journal of Immunology*, vol. 167, no. 11, pp. 6533–6544, 2001.

[40] D. R. Herbert, C. Hölscher, M. Mohrs et al., "Alternative macrophage activation is essential for survival during schistosomiasis and downmodulates T helper 1 responses and immunopathology," *Immunity*, vol. 20, no. 5, pp. 623–635, 2004.

[41] D. Jankovic, M. C. Kullberg, N. Noben-Trauth et al., "Schistosome-infected IL-4 receptor knockout (KO) mice, in contrast to IL-4 KO mice, fail to develop granulomatous pathology while maintaining the same lymphokine expression profile," *Journal of Immunology*, vol. 163, no. 1, pp. 337–342, 1999.

[42] F. Verrecchia and A. Mauviel, "Transforming growth factor-β and fibrosis," *World Journal of Gastroenterology*, vol. 13, no. 22, pp. 3056–3062, 2007.

[43] A. Fine and R. H. Goldstein, "The effect of transforming growth factor-β on cell proliferation and collagen formation by lung fibroblasts," *Journal of Biological Chemistry*, vol. 262, no. 8, pp. 3897–3902, 1987.

[44] W. A. Border and N. A. Noble, "Transforming growth factor β in tissue fibrosis," *The New England Journal of Medicine*, vol. 331, no. 19, pp. 1286–1292, 1994.

[45] S. Kanzler, M. Baumann, P. Schirmacher et al., "Prediction of progressive liver fibrosis in hepatitis C infection by serum and tissue levels of transforming growth factor-β," *Journal of Viral Hepatitis*, vol. 8, no. 6, pp. 430–437, 2001.

[46] S. Li, L. E. Vriend, I. A. Nasser et al., "Hepatitis C virus-specific T-cell-derived transforming growth factor beta is associated with slow hepatic fibrogenesis," *Hepatology*, vol. 56, no. 6, pp. 2094–2105, 2012.

[47] R. M. A. Khalil, L. Hültner, R. Mailhammer et al., "Kinetics of interleukin-6 production after experimental infection of mice with *Schistosoma mansoni*," *Immunology*, vol. 89, no. 2, pp. 256–261, 1996.

[48] S. W. Chensue, K. Warmington, J. Ruth, P. Lincoln, M.-C. Kuo, and S. L. Kunkel, "Cytokine responses during mycobacterial and schistosomal antigen-induced pulmonary granuloma formation: production of Th1 and Th2 cytokines and relative contribution of tumor necrosis factor," *The American Journal of Pathology*, vol. 145, no. 5, pp. 1105–1113, 1994.

[49] M. R. Duncan and B. Berman, "Stimulation of collagen and glycosaminoglycan production in cultured human adult dermal fibroblasts by recombinant human interleukin 6," *Journal of Investigative Dermatology*, vol. 97, no. 4, pp. 686–692, 1991.

[50] M. Lotz and P.-A. Guerne, "Interleukin-6 induces the synthesis of tissue inhibitor of metalloproteinases-1/erythroid potentiating activity (TIMP-1/EPA)," *Journal of Biological Chemistry*, vol. 266, no. 4, pp. 2017–2020, 1991.

[51] M. Mihara, Y. Moriya, and Y. Ohsugi, "IL-6-soluble IL-6 receptor complex inhibits the proliferation of dermal fibroblasts," *International Journal of Immunopharmacology*, vol. 18, no. 1, pp. 89–94, 1996.

[52] T. C. Barnes, M. E. Anderson, and R. J. Moots, "The many faces of interleukin-6: the role of IL-6 in inflammation, vasculopathy, and fibrosis in systemic sclerosis," *International Journal of Rheumatology*, vol. 2011, Article ID 721608, 2011.

[53] D. Fuster, J. I. Tsui, D. M. Cheng et al., "Interleukin-6 is associated with noninvasive markers of liver fibrosis in HIV-infected patients with alcohol problems," *AIDS Research and Human Retroviruses*, vol. 29, no. 8, pp. 1110–1116, 2013.

[54] M. Veldhoen, R. J. Hocking, C. J. Atkins, R. M. Locksley, and B. Stockinger, "TGFβ in the context of an inflammatory cytokine milieu supports de novo differentiation of IL-17-producing T cells," *Immunity*, vol. 24, no. 2, pp. 179–189, 2006.

[55] E. Bettelli, Y. Carrier, W. Gao et al., "Reciprocal developmental pathways for the generation of pathogenic effector TH17 and regulatory T cells," *Nature*, vol. 441, no. 7090, pp. 235–238, 2006.

[56] P. R. Mangan, L. E. Harrington, D. B. O'Quinn et al., "Transforming growth factor-β induces development of the T H17 lineage," *Nature*, vol. 441, no. 7090, pp. 231–234, 2006.

[57] T. Korn, E. Bettelli, M. Oukka, and V. K. Kuchroo, "IL-17 and Th17 cells," *Annual Review of Immunology*, vol. 27, pp. 485–517, 2009.

[58] H. Tallima, M. Salah, F. R. Guirguis, and R. El Ridi, "Transforming growth factor-β and Th17 responses in resistance to primary murine schistosomiasis mansoni," *Cytokine*, vol. 48, no. 3, pp. 239–245, 2009.

[59] Z. A. Andrade, "Schistosomiasis and liver fibrosis: review article," *Parasite Immunology*, vol. 31, no. 11, pp. 656–663, 2009.

[60] L. I. Rutitzky, J. R. Lopes da Rosa, and M. J. Stadecker, "Severe CD4 T cell-mediated immunopathology in murine schistosomiasis is dependent on IL-12p40 and correlates with high levels of IL-17," *Journal of Immunology*, vol. 175, no. 6, pp. 3920–3926, 2005.

[61] L. I. Rutitzky and M. J. Stadecker, "CD4 T cells producing pro-inflammatory interleukin-17 mediate high pathology in schistosomiasis," *Memorias do Instituto Oswaldo Cruz*, vol. 101, no. 1, pp. 327–330, 2006.

[62] J. K. Mwatha, G. Kimani, T. Kamau et al., "High levels of TNF, soluble TNF receptors, soluble ICAM-1, and IFN-γ, but low levels of IL-5, are associated with hepatosplenic disease in human schistosomiasis mansoni," *Journal of Immunology*, vol. 160, no. 4, pp. 1992–1999, 1998.

[63] K. F. Hoffmann, P. Caspar, A. W. Cheever, and T. A. Wynn, "IFN-γ, IL-12, and TNF-α are required to maintain reduced

liver pathology in mice vaccinated with *Schistosoma mansoni* eggs and IL-12," *Journal of Immunology*, vol. 161, no. 8, pp. 4201–4210, 1998.

[64] J.-Y. Zhang, Z.-S. Zou, A. Huang et al., "Hyper-activated pro-inflammatory CD16+ monocytes correlate with the severity of liver injury and fibrosis in patients with chronic hepatitis B," *PLoS ONE*, vol. 6, no. 3, Article ID e17484, 2011.

[65] H. W. Zimmermann and F. Tacke, "Modification of chemokine pathways and immune cell infiltration as a novel therapeutic approach in liver inflammation and fibrosis," *Inflammation and Allergy*, vol. 10, no. 6, pp. 509–536, 2011.

[66] J. A. Fallowfield, M. Mizuno, T. J. Kendall et al., "Scar-associated macrophages are a major source of hepatic matrix metalloproteinase-13 and facilitate the resolution of murine hepatic fibrosis," *Journal of Immunology*, vol. 178, no. 8, pp. 5288–5295, 2007.

[67] T. A. Wynn, A. W. Cheever, D. Jankovic et al., "An IL-12-based vaccination method for preventing fibrosis induced by schistosome infection," *Nature*, vol. 376, no. 6541, pp. 594–596, 1995.

[68] T. A. Wynn, I. Eltoum, I. P. Oswald, A. W. Cheever, and A. Sher, "Endogenous interleukin 12 (IL-12) regulates granuloma formation induced by eggs of *Schistosoma mansoni* and exogenous IL-12 both inhibits and prophylactically immunizes against egg pathology," *Journal of Experimental Medicine*, vol. 179, no. 5, pp. 1551–1561, 1994.

[69] M. M. Mentinkkane, A. W. Cheever, M. S. Wilson et al., "Accelerated and progressive and lethal liver fibrosis in mice that lack interleukin (IL)-10, IL-12p40, and IL-13Rα2," *Gastroenterology*, vol. 141, no. 6, pp. 2200–2209, 2011.

[70] K. F. Hoffmann, A. W. Cheever, and T. A. Wynn, "IL-10 and the dangers of immune polarization: excessive type 1 and type 2 cytokine responses induce distinct forms of lethal immunopathology in murine schistosomiasis," *Journal of Immunology*, vol. 164, no. 12, pp. 6406–6416, 2000.

[71] D. R. Herbert, T. Orekov, C. Perkins, and F. D. Finkelman, "IL-10 and TGF-β redundantly protect against severe liver injury and mortality during acute schistosomiasis," *Journal of Immunology*, vol. 181, no. 10, pp. 7214–7220, 2008.

[72] L. S. Cardoso, S. Barreto Ade, J. S. Fernandes et al., "Impaired lymphocyte profile in schistosomiasis patients with periportal fibrosis," *Clinical and Developmental Immunology*, vol. 2013, Article ID 710647, 2013.

Hindawi Publishing Corporation
Mediators of Inflammation
Volume 2014, Article ID 746415, 10 pages
http://dx.doi.org/10.1155/2014/746415

Research Article

The Proinflammatory Cytokine High-Mobility Group Box-1 Mediates Retinal Neuropathy Induced by Diabetes

Ahmed M. Abu El-Asrar,[1,2] Mohammad Mairaj Siddiquei,[1] Mohd Imtiaz Nawaz,[1] Karel Geboes,[3] and Ghulam Mohammad[1]

[1] *Department of Ophthalmology, College of Medicine, King Saud University, Riyadh, Saudi Arabia*
[2] *Department of Ophthalmology, King Abdulaziz University Hospital, Old Airport Road, P.O. Box 245, Riyadh 11411, Saudi Arabia*
[3] *Laboratory of Histochemistry and Cytochemistry, University of Leuven, Leuven, Belgium*

Correspondence should be addressed to Ahmed M. Abu El-Asrar; abuasrar@ksu.edu.sa

Received 15 July 2013; Revised 13 January 2014; Accepted 28 January 2014; Published 10 March 2014

Academic Editor: Charles J. Malemud

To test the hypothesis that increased expression of proinflammatory cytokine high-mobility group box-1 (HMGB1) in epiretinal membranes and vitreous fluid from patients with proliferative diabetic retinopathy and in retinas of diabetic rats plays a pathogenetic role in mediating diabetes-induced retinal neuropathy. Retinas of 1-month diabetic rats and HMGB1 intravitreally injected normal rats were studied using Western blot analysis, RT-PCR and glutamate assay. In addition, we studied the effect of the HMGB1 inhibitor glycyrrhizin on diabetes-induced biochemical changes in the retina. Diabetes and intravitreal injection of HMGB1 in normal rats induced significant upregulation of HMGB1 protein and mRNA, activated extracellular signal-regulated kinase 1 and 2 (ERK1/2), cleaved caspase-3 and glutamate; and significant downregulation of synaptophysin, tyrosine hydroxylase, glutamine synthetase, and glyoxalase 1. Constant glycyrrhizin intake from the onset of diabetes did not affect the metabolic status of the diabetic rats, but it significantly attenuated diabetes-induced upregulation of HMGB1 protein and mRNA, activated ERK1/2, cleaved caspase-3, and glutamate. In the glycyrrhizin-fed diabetic rats, the decrease in synaptophysin, tyrosine hydroxylase, and glyoxalase 1 caused by diabetes was significantly attenuated. These findings suggest that early retinal neuropathy of diabetes involves upregulated expression of HMGB1 and can be ameliorated by inhibition of HMGB1.

1. Introduction

Diabetic retinopathy (DR), a vision-threatening disease, has classically been regarded as a disease of the retinal microvasculature and a consequence of vascular cell damage. However, recent studies proved that neurodegeneration and impaired visual function are initiated early after the onset of diabetes and progress independently of the vascular lesions [1–4]. However, the molecular mechanisms underlying the diabetes-induced retinal neurodegeneration and dysfunction are still not well understood.

High-mobility group box-1 (HMGB1) is a nonhistone DNA-binding nuclear protein that has been implicated in diverse intracellular functions, including the stabilization of nucleosomal structures and the facilitation of gene transcription. Necrotic cell death can result in passive leakage of HMGB1 from the cell as the protein is then no longer bound to DNA. In addition, HMGB1 can be actively secreted by different cell types, including activated monocytes and macrophages, mature dendritic cells, natural killer cells, and endothelial cells. Extracellular HMGB1 functions as a proinflammatory cytokine and triggers the inflammatory response through the activation of multiple receptors such as the receptor for advanced glycation end products (RAGE), toll-like receptor-2 (TLR2), and TLR4 leading to activation of the transcription factors extracellular signal-regulated kinase 1 and 2 (ERK1/2) and nuclear factor Kappa B (NF-κB), which may alter gene transcription and lead to the upregulation of proinflammatory cytokines, chemokines, and adhesion molecules and intensifies cellular oxidative stress [5–10], processes that may play a role in the pathogenesis of diabetic retinal neurodegeneration and dysfunction. Strong evidence indicates that chronic, low-grade inflammation is implicated

in the pathogenesis of DR [11, 12]. Recently, it was demonstrated that HMGB1 is the main mediator bridging persistent neuroinflammation and chronic progressive dopaminergic neurodegeneration in neurodegenerative diseases, such as Parkinson's disease [13].

Recently, HMGB1 has received particular attention with respect to its pathological role in cerebral ischemia. After ischemic injury induced by transient middle cerebral artery occlusion in mice and rats, HMGB1 was found to be translocated into the cytoplasmic compartment from nuclei and released into the extracellular space from neurons [14–18]. In these studies, extracellular HMGB1 plays a key role in the development of neuronal injury through microglial activation, induction of apoptosis, excitatory amino acid release, and induction of proinflammatory mediators [14–19]. Downregulation of HMGB1 or treatment with neutralizing anti-HMGB1 monoclonal antibody remarkably suppressed infarct size, activation of microglia, and induction of proinflammatory markers and inhibited the increased permeability of the blood-brain barrier [14, 18].

In previous studies, we demonstrated that HMGB1 and RAGE were expressed by vascular endothelial cells and stromal cells in fibrovascular epiretinal membranes from patients with proliferative diabetic retinopathy (PDR). In addition, we demonstrated increased levels of HMGB1 in the vitreous samples from patients with PDR and that there were significant positive correlations between the vitreous levels of HMGB1 and the levels of the inflammatory biomarkers [20–22]. Furthermore, we demonstrated that diabetes induced significant upregulation of the expression of HMGB1 and RAGE in the retinas of rats and mice and that intravitreal administration of HMGB1 to normal rats induced activation of inflammatory signaling pathways in the retina and increased retinal vascular permeability [21, 23].

Glycyrrhizin (GA), an ingredient of the licorice roots, has long been known to exhibit glucocorticoid-like anti-inflammatory actions by inhibiting 11β-hydroxysteroid dehydrogenase. GA has been shown to have anti-inflammatory and antiviral effects. More recently, GA has also been shown to bind to and inhibit chemoattractant, mitogenic, and cytokine-like activities of HMGB1 [24]. In this study, we explored the hypothesis that HMGB1 plays a pathogenetic role in mediating diabetes-induced retinal neuropathy. To test this hypothesis, we investigated the expression of the neurodegeneration mediators and markers cleaved caspase-3, synaptophysin, tyrosine hydroxylase (TH), glutamine synthetase (GS), glutamate, and glyoxalase 1 (GLO 1) in the retinas of diabetic rats and in the retinas of normal rats after intravitreal administration of HMGB1. In addition, we analyzed whether constant GA intake suppresses retinal neuropathy induced by diabetes in rats.

2. Materials and Methods

2.1. Animals

2.1.1. Induction of Diabetes and Glycyrrhizin Treatment. All procedures with animals were performed in accordance with the Association for Research in Vision and Ophthalmology (ARVO) statement for use of animals in ophthalmic and vision research and were approved by the institutional animal care and use committee of the College of Pharmacy, King Saud University. Adult male Sprague Dawley rats of 8-9 weeks of age (200–220 g) were overnight fasted and streptozotocin (STZ) 55 mg/kg in 10 mM sodium citrate buffer, pH 4.5 (Sigma, St. Louis, MO), was injected intraperitoneally. Equal volumes of citrate buffer were injected in nondiabetic animals. Rats were considered diabetic if their blood glucose was greater than 250 mg/dL. Age-matched normal rats served as controls.

Diabetic rats were divided into 2 groups: the rats in group I received normal drinking water without any supplementation, and group II received drinking water supplemented with glycyrrhizic acid (150 mg/kg/day, Santa Cruz Biotechnology, Inc., Santa Cruz, CA) immediately after establishment of diabetes throughout the course of the experiment. Each group had 8–12 rats. After 4 weeks of diabetes, the rats were euthanized by an overdose of chloral hydrate, the eyes were removed, and retina was isolated and frozen immediately in liquid nitrogen and stored at −80°C to be analyzed by Western blot analysis or biochemical assay.

2.1.2. Intravitreal Injection of HMGB1. Sprague Dawley rats (200–220 g) were kept under deep anesthesia, and sterilized solution of recombinant HMGB1 (5 ng/5 μL; R&D Systems, Minneapolis, MN) was injected into the vitreous of the right eye as previously described by us [23]. For the control, the left eye received 5 μL of sterile phosphate buffer saline (PBS). The animals were sacrificed 4 days after intravitreal administration, and the retinas were carefully dissected, snap-frozen in liquid nitrogen, and stored at −80°C to be analyzed by Western blot analysis or biochemical assay. The breakdown of blood-retina barrier induced by intravitreal injection of HMGB1 might lead to raised levels of HMGB1 in the serum. Therefore, we determined the levels of HMGB1 in equal amounts of serum from intravitreally injected rats and normal rats using Western blot analysis.

2.1.3. Western Blot Analysis. Retinas were homogenized in a western lysis buffer (30 mM Tris-HCl; pH 7.4, 250 mM Na_3VO_4, 5 mM EDTA, 250 mM sucrose, 1% Triton X-100 with Protease inhibitor). The lysate was centrifuged at 14,000 ×g for 10 min at 4°C, and the supernatant was collected. Protein content was assayed by DC protein assay (Bio-Rad Laboratories, Hercules, CA). The tissue lysate containing 40–50 μg of protein was separated on 10% or 12% SDS-polyacrylamide gels and was transferred onto nitrocellulose membranes. The blots were blocked with 5% nonfat milk in TBST (20 mM Tris-HCl, pH 7.6, 136 mM NaCl, and 0.1% Tween-20).

For detection of HMGB1, phospho-ERK1/2, synaptophysin, cleaved caspase-3, TH, GLO1, and GS, the membrane was incubated overnight at 4°C with rabbit polyclonal anti-HMGB1 (1 : 1000, Cat. number ab18256, Abcam, UK), rabbit monoclonal anti-phospho-ERK1/2 (0.5 μg/mL, Cat. number MAB1018, R&D Systems), mouse monoclonal anti-ERK1/2

(0.5 μg/mL, Cat. number MAB1576, R&D Systems), goat polyclonal anti-synaptophysin (1 μg/mL, Cat. number AF-5555, R&D Systems), rabbit polyclonal anti-cleaved caspase-3 (1 : 300, Cat. number SC-7148, Santa Cruz), mouse monoclonal anti-TH (0.5 μg/mL, Cat. number MAB7566, R&D Systems), rabbit polyclonal anti-GLO1 (1 : 200, Cat. number ab96032, Abcam), and goat polyclonal anti-GS (1 : 500, sc-6640, Santa Cruz). After overnight incubation with primary antibodies, the membranes were washed four times with TBS-T (5 min each). For synaptophysin and GS, the membrane was incubated at room temperature for 1.5 h with anti-goat secondary horseradish peroxidase-conjugated antibody (1 : 2000, SC-2768, Santa Cruz), for HMGB1, phospo-ERK1/2 cleaved caspase-3 and GLO1, with anti-rabbit secondary horseradish peroxidase-conjugated antibody (1 : 2000, SC-2004, Santa Cruz), and for ERK1/2 and TH with anti-mouse secondary horseradish peroxidase-conjugated antibody (1 : 2000, SC-2005, Santa Cruz). After incubations with secondary antibodies, membranes were washed four times with TBS-T (5 min each) and the immunoreactivity of bands was visualized on a high-performance chemiluminescence machine (G: Box Chemi-XX8 from Syngene, Synoptic Ltd. Cambridge, UK) by using enhanced chemiluminescence plus Luminol (sc-2048, Santa Cruz) and quantified by densitometric analysis using image processing and analysis in GeneTools (Syngene by Synoptic Ltd. Cambridge, UK). For loading control, the blots were stripped and detected with a mouse monoclonal anti-β-actin (1 : 2000, SC-2048, Santa Cruz) antibody. For phosphor-ERK1/2, the loading control was total ERK1/2. All data from the three independent experiments were expressed as a ratio to optical density.

2.1.4. Real-Time Reverse Transcription Polymerase Chain Reaction (RT-PCR). Total RNA was extracted from retina using TRI reagent (Ambion, TX), according to manufacturer's protocol. cDNA was synthesized from 1 μg RNA, using a high capacity cDNA reverse transcription kit (Applied Biosystem, CA) following manufacturer's instruction. RT-PCR was performed using a SYBR green PCR master mix. The PCR primers for rat were HMGB1 forward 5′-TGATTAATGAATGAGTTCGGGC-3′ reverse 5′- TGCTCAGGAAACTTGACTGTTT-3′ and β-actin forward 5′-CCTCTATGCCAACACAGTGC-3′ reverse 5′-CATCGTACTCCTGCTTGCTG-3′. The standard PCR conditions included 2 minutes at 50°C and 10 min at 95°C followed by 40 cycles of extension at 95°C for 15 seconds and one minute at 60°C. Threshold lines were automatically adjusted to intersect amplification lines in the linear portion of the amplification curves and cycle to threshold (Ct) was recorded automatically. Data were normalized with β-actin mRNA level (housekeeping gene) and the fold change in gene expression relative to normal was calculated using the ddCt method.

2.1.5. Measurement of Glutamate in Rat Retinas. Glutamate level was measured in retinal homogenate by using glutamate assay kit (Cat. number ab83389, Abcam), according to the manufacturer's instruction. Briefly, 50 μL of standards and retinal homogenate (equal amount) was loaded in a clear 96-well plate, followed by addition of 100 μL reaction mix solution having assay buffer, glutamate developer, and glutamate enzyme mix. The plate was incubated for 30 minutes at 37°C (protected from light) and was read at 450 nm in microplate reader (Stat Fax 4200 microplate reader, awareness technology, Palm City, FL). The concentration of measured glutamate was expressed as nmol/μL/μg of protein.

2.1.6. Statistical Analysis. The Mann-Whitney test was used to compare means from two independent groups. A P value less than 0.05 indicated statistical significance. SPSS version 12.0 was used for the statistical analyses.

3. Results

3.1. Severity of Hyperglycemia in Rats. The body weights of the diabetic rats were lower and their blood glucose levels were more than fourfold higher compared with age-matched normal control rats (178 ± 22 versus 287 ± 28 g and 475 ± 32 versus 111 ± 12 mg/dL, resp.). Treatment of the diabetic rats with GA for one month did not change these metabolic variables in the diabetic rats (167 ± 25 versus 178 ± 22 g and 449 ± 36 versus 475 ± 32 mg/dL, resp.).

3.2. Effect of Diabetes on Retinal Expression of Mediators and Markers of Neurodegeneration. Western blot analysis demonstrated significant upregulation of HMGB1 expression in diabetic retinas compared to nondiabetic retinas. The expression of HMGB1 protein in the retinas of diabetic rats was upregulated by about 66% as compared to the retinas of nondiabetic rats (Figure 1(a)). Diabetes significantly increased ERK1/2 activation in the retinas by about 77% compared to nondiabetic controls (Figure 1(b)). Cleaved caspase-3, the apoptosis executer enzyme, was significantly upregulated in diabetic retinas compared to nondiabetic controls. Cleaved caspase-3 levels in the retinas of diabetic rats were increased by about 70% compared to nondiabetic controls (Figure 1(c)). The synaptic vesicle protein synaptophysin and the dopaminergic amacrine cell marker TH levels obtained in diabetic animals were significantly lower than those of nondiabetic animals. The levels decreased by about 68% and 46%, respectively (Figures 1(d) and 1(e)). GS, an enzyme that converts glutamate into glutamine, protein expression was significantly decreased in diabetic retinas compared to nondiabetic retinas. GS levels decreased by about 75% (Figure 1(f)). GLO1, an enzyme critical for the detoxification of advanced glycation end products (AGEs), protein expression was significantly decreased in diabetic retinas compared to nondiabetic rats. GLO1 expression in diabetic retinas decreased by about 51% (Figure 1(g)). Glutamate assay revealed that glutamate levels in the retinas of diabetic animals (0.04 ± 0.015 nmol/μL/μg protein) were significantly higher than those in nondiabetic controls (0.022 ± 0.004 nmol/μL/μg protein) ($P = 0.036$) (Figure 1(h)).

3.3. Effect of Intravitreal Administration of HMGB1 on Retinal Expression of Mediators and Markers of Neurodegeneration in Normal Rats. There was no significant difference in serum

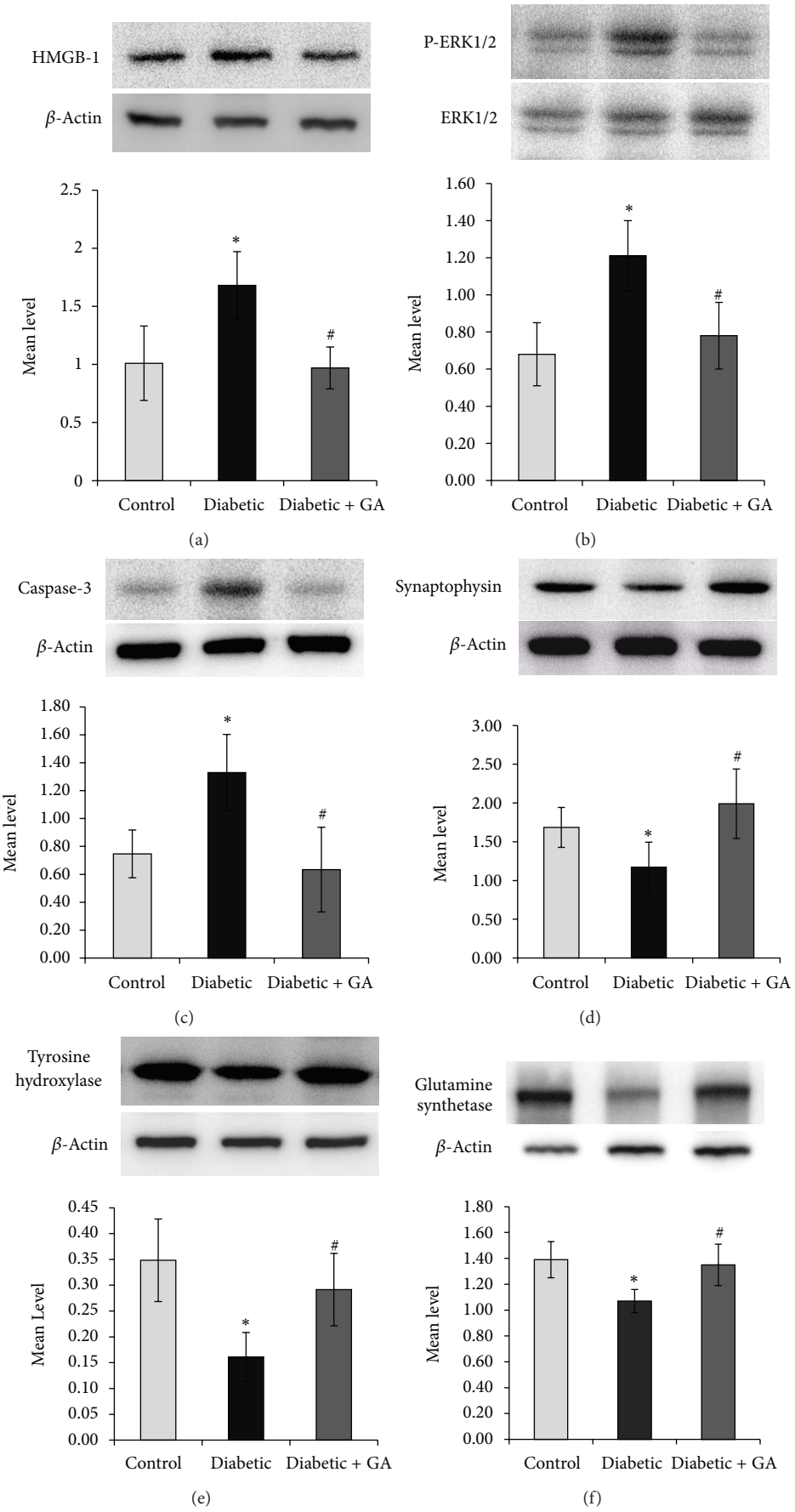

Figure 1: Continued.

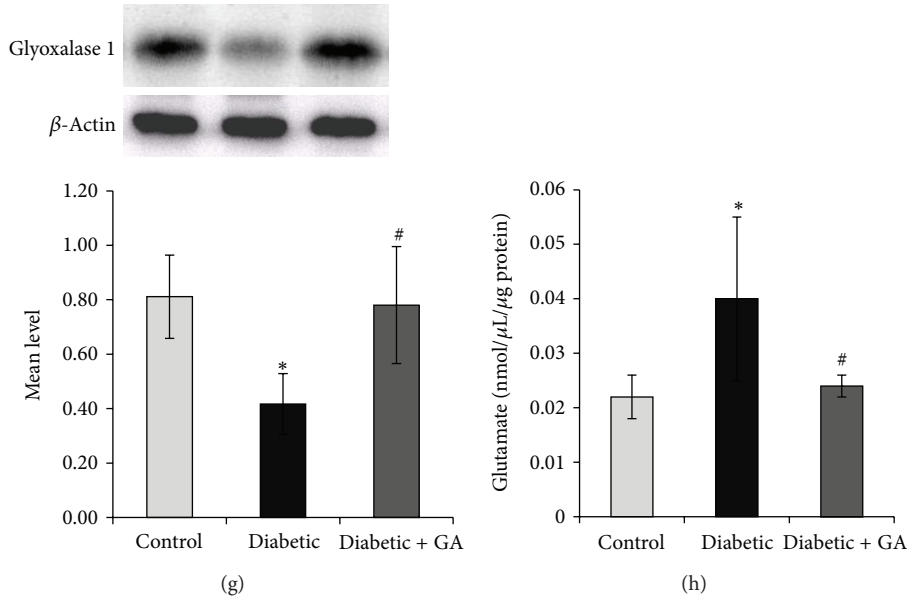

Figure 1: Western blot analysis of high-mobility group box-1 (HMGB1), extracellular signal-regulated kinase 1 and 2 (ERK1/2), cleaved caspase-3, synaptophysin, tyrosine hydroxylase, glutamine synthetase, and glyoxalase 1 in rat retinas. β-Actin was used as a housekeeping control. Protein expression of ERK1/2 activation (phosphorylation) was quantified by Western blot analysis using phospho- (P-) ERK1/2 specific antibody and was adjusted to the protein levels of unphosphorylated ERK1/2 antibody in each sample. There is a significant increase in the expression of HMGB1 (a), activated ERK1/2 (b), and cleaved caspase-3 (c) and a significant decrease in the expression of synaptophysin (d), tyrosine hydroxylase (e), glutamine synthetase (f), and glyoxalase 1 (g) in the retinas of diabetic rats compared to nondiabetic controls. Glycyrrhizic acid (GA) significantly attenuated diabetes-induced upregulation of HMGB1 (a), activated ERK1/2 (b), and cleaved caspase-3 (c) and diabetes-induced downregulation of synaptophysin (d), tyrosine hydroxylase (e), GS (f), and glyoxalase 1 (g). Glutamate assay revealed a significant increase in glutamate levels in the retinas of diabetic rats compared to nondiabetic controls. The levels of glutamate in the GA-treated diabetic rats were significantly less than those in the untreated diabetic rats (h). Each experiment was repeated at least 3 times with fresh samples. A representative set of samples is shown. Results are expressed as mean ± SD of at least 6 rats in each group. $^{*}P < 0.05$ compared with nondiabetic control rats. $^{\#}P < 0.05$ compared with diabetic rats.

levels of HMGB1 between rats intravitreally injected with HMGB1 (135.64±14.38) and normal rats (134.88±11.01) ($P = 0.225$). Intravitreal injection of HMGB1 resulted in increased HMGB1 expression by about 72% compared to the values obtained from the contralateral eye that received PBS alone (Figure 2(a)). In the same retinal samples, HMGB1 injection resulted in a 76% increase in ERK1/2 activation (Figure 2(b)), 31% increase in cleaved caspase-3 expression (Figure 2(c)), 65% decrease in synaptophysin expression (Figure 2(d)), 65% decrease in TH expression (Figure 2(e)), 70% decrease in GS expression (Figure 2(f)), and 71% decrease in GLO1 expression (Figure 2(g)). Injection of HMGB1 tended to increase retinal glutamate expression, but this was not significant (0.041 ± 0.025 versus 0.021 ± 0.004 nmol/μL/μg protein; $P = 0.07$) (Figure 2(h)).

3.4. HMGB1 Inhibitor Glycyrrhizin Attenuates the Effect of Diabetes. Western blot analysis was used to assess the effect of GA on diabetes-induced alterations of HMGB1, ERK1/2 activation, cleaved caspase-3, synaptophysin, TH, GS, and GLO1. Constant GA intake from the onset of diabetes significantly attenuated diabetes-induced upregulation of HMGB1, ERK1/2 activation, and cleaved caspase-3 by about 73%, 55%, and 78%, respectively (Figures 1(a), 1(b), and 1(c)). In the GA-fed diabetic rats, the decrease in synaptophysin, TH, GS, and GLO1 caused by diabetes was attenuated by about 58%, 55%, 79%, and 53%, respectively (Figures 1(d), 1(e), 1(f), and 1(g)). The levels of glutamate in the GA-treated diabetic rats (0.024± 0.002 nmol/μL/μg protein) were significantly less than those in the untreated diabetic rats (0.04 ± 0.015 nmol/μL/μg protein) ($P = 0.045$) (Figure 1(h)).

3.5. Retinal Expression of HMGB1 mRNA. The expression of HMGB1 mRNA in the retinas of diabetic rats was increased by about 4-fold compared to the retinas of nondiabetic rats. Intravitreal injection of HMGB1 resulted in increased HMGB1 mRNA expression by about 5-fold compared to the values obtained from the contralateral eye that received PBS alone. GA intake significantly attenuated diabetes-induced upregulation of HMGB1 mRNA by about 3.5-fold compared to untreated diabetic rats (Figure 3).

4. Discussion

In the present study, we investigated the pathological role of HMGB1 in diabetes-induced retinal neuropathy. Our previous studies showed that diabetes upregulates HMGB1

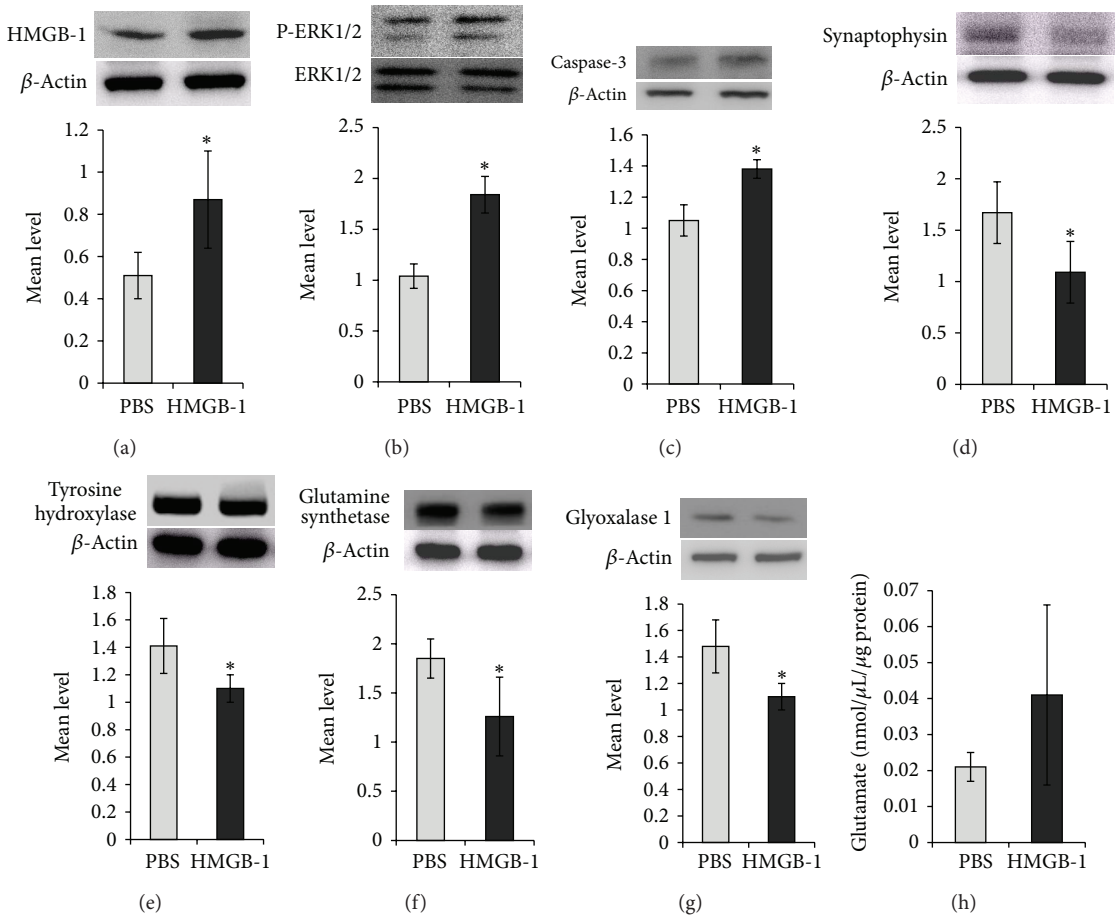

Figure 2: Western blot analysis of rat retinas. Intravitreal administration of high-mobility group box-1 (HMGB1) induced a significant upregulation of the expression of HMGB1 (a), activated extracellular signal-regulated kinase 1 and 2 (ERK1/2) (b), and cleaved caspase-3 (c) and a significant downregulation of the expression of synaptophysin (d), tyrosine hydroxylase (e), glutamine synthetase (f), and glyoxalase 1 (g) compared to intravitreal administration of phosphate buffer saline (PBS). Glutamate assay revealed that injection of HMGB1 tended to increase retinal glutamate expression, but this was not significant (h). Each experiment was repeated at least 3 times with fresh samples. A representative set of samples is shown. Results are expressed as mean ± SD of at least 6 rats in each group. $^*P < 0.05$ compared with PBS.

expression in the vitreous fluid and preretinal membranes from patients with PDR and its expression correlated with the activity of the disease and the levels of inflammatory biomarkers [20–22]. In addition, we demonstrated that HMGB1 expression was upregulated in the retinas of diabetic mice and rats [21, 23]. In the current study, we demonstrated that diabetes induced significant upregulation of cleaved caspase-3 and glutamate expression in the retinas of rats. On the other hand, diabetes induced significant downregulation of synaptophysin, TH, GS, and GLO1 in the retinas of rats. Furthermore, our data show that intravitreal injection of HMGB1 in normal rats mimics the effect of diabetes. The HMGB1 inhibitor GA attenuated diabetes-induced upregulation of HMGB1 protein and mRNA; cleaved caspase-3 and glutamate; and downregulation of synaptophysin, TH, GS, and GLO1 in the retinas of rats. Taken together, these findings suggest that HMGB1 contributes to retinal neuropathy induced by diabetes.

Diabetes induces retinal neurodegeneration as evidenced by the presence of apoptotic cells in all retinal layers [4, 25]. Activation of caspase-3 is part of the mechanism of apoptosis [25]. Several studies demonstrated that expression of active caspase-3, an indication of apoptosis, was upregulated in the diabetic retinas of human subjects [4] and rats [25]. In STZ-diabetic rat retinas, caspase-3 immunoreactivity was upregulated after 2, 8, and 16 weeks of diabetes [25]. However, Feit-Leichman et al. [26] demonstrated, in STZ-diabetic mice, upregulation of retinal caspase-3 activity at 1 month after induction of diabetes, which diminished to normal and began to increase again after approximately 6 months. They concluded that diabetes-induced degeneration of retinal capillaries can develop independent of neuronal loss. Synaptophysin is an integral protein of synaptic vesicles. It possibly serves multiple functions in synaptic vesicle formation and exocytosis, playing an important role in neurotransmitter delivery. It is widely used as one of the synaptic function markers and is also thought to be closely related to synaptogenesis and synaptic plasticity during neural tissue development. Synaptophysin knockout mice exhibited a significant decrease in synaptic vesicles in retinal rod

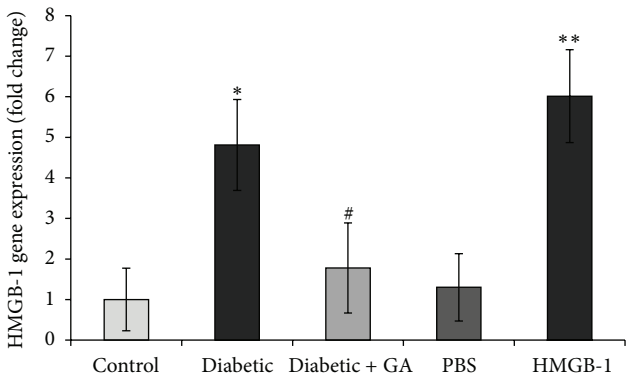

Figure 3: Gene expression of high-mobility group box-1 (HMGB1) in the retinas was quantified by RT-PCR using a primer given in the Materials and Methods section and was adjusted to the mRNA level of β-actin in each sample. Each measurement was performed at least 3 times. Results are expressed as mean ± SD of at least 6 rats in each group. GA: glycyrrhizic acid; PBS: phosphate buffer saline $^{*}P < 0.05$ compared with nondiabetic controlled rats. $^{**}P < 0.05$ compared with PBS. $^{\#}P < 0.05$ compared with diabetic rats.

photoreceptors which disturbs neurotransmitter release and synaptic network activity [27]. Previous studies demonstrated that 1 month of diabetes decreases retinal expression of synaptophysin [3, 28–30]. TH is the rate-limiting biosynthetic enzyme for dopamine synthesis. Therefore, the TH protein level is a marker of dopaminergic amacrine cells in the retina [1, 25, 31]. Several studies showed decreased TH protein levels in the diabetic retinas, reflecting reductions in the density of dopaminergic amacrine cells [1, 31–33]. The synaptically released glutamate is taken up by Müller cells where GS converts it into glutamine. Several studies found that the expression of GS was significantly decreased in the diabetic rat retinas [34, 35]. These dysfunctions resulted in elevated glutamate levels in the diabetic retinas [34, 36, 37], which might induce retinal neurodegeneration via glutamate excitotoxicity. In diabetes, there is accumulation of the AGEs precursor methylglyoxal (MG). In diabetic retinopathy, MG-derived AGEs are elevated in retina and are viewed to be causative in retinal injury and neurodegeneration [38–40]. Normally, MG is detoxified by the glyoxalase (GLO) enzyme system, composed of GLO1 and GLO2 [41]. A previous report demonstrated that GLO1 expression is reduced in the diabetic rat retinas [42]. It was also shown that GLO1 overexpression in diabetic rats prevents hyperglycemia-induced formation of MG-derived AGEs in the neural retina, prevents Müller glia dysfunction, and protects against capillary degenerative pathology [43].

In the present study, we demonstrated that, similar to diabetes, intravitreal injection of HMGB1 caused a significant upregulation of HMGB1 protein and mRNA and activated cleaved caspase-3 in the retina of normal rats. In addition, injection of HMGB1 tended to increase retinal glutamate expression, but this was not significant. In this regard, the recent finding that HMGB1 promotes glutamate release from gliosomes [19] suggests that its neurotoxicity is mediated, at least in part, by increased release of glutamate and enhanced excitotoxic neuronal death. On the other hand, *in vitro* studies demonstrated that glutamate can induce the release of HMGB1 from neuronal cells [14, 15]. Furthermore, intravitreal administration of HMGB1 induced downregulation of synaptophysin, TH, GS, and GLO1. These findings suggest that the early retinal neuropathy of diabetes involves the upregulated expression of HMGB1. Several studies showed that HMGB1 is massively released immediately after an ischemic insult and that it subsequently induces neuroinflammation in the postischemic brain [14, 15, 17]. To exert these activities, HMGB1 must transit from the nucleus, through the cytoplasm, to the outside of the cell. Several studies demonstrated that the inflammatory marker C-reactive protein [44] and the proinflammatory cytokines tumor necrosis factor-α (TNF-α) [45] and interleukin-1β (IL-1β) [46] induce translocation of HMGB1 from nucleus to the cytoplasm and its subsequent extracellular release from the cell. *In vitro* studies demonstrated that extracellular HMGB1 induced the proinflammatory biomarkers TNF-α, IL-1β, interferon-γ, intercellular adhesion molecule-1 (ICAM-1), inducible nitric oxide synthase (iNOS), and cyclooxgenase-2 in cultured neurons, astrocytes, microglia, and endothelial cells [14, 15, 17]. Moreover, cerebral microinjection of exogenous HMGB1 increased postischemic brain injury and upregulated the expression of iNOS and IL-1β [17]. These findings indicate that HMGB1 functions as a novel proinflammatory cytokine-like factor linking very early stages of cerebral ischemic injury with the activation of local neuroinflammatory response in the postischemic brain [14, 15]. Furthermore, it was also shown that extracellular HMGB1 released from the damaged brain neurons induces neuronal apoptosis and that this involves HMGB1-RAGE interaction [16]. In our laboratory, we recently demonstrated that diabetes induced significant upregulation of retinal expression of HMGB1, RAGE, activated NF-κB, activated ERK1/2, and ICAM-1 and that intravitreal administration of HMGB1 in normal rats mimics the effect of diabetes [23]. We also showed that the HMGB1 inhibitor GA was effective in preventing diabetes-induced NF-κB activation. In the present study, GA attenuated diabetes-induced ERK1/2 activation. In addition, coimmunoprecipitation studies showed that diabetes increases the interaction between HMGB1 and RAGE in the retina [23]. These findings suggest that activation of HMGB1/RAGE signaling axis with subsequent activation of NF-κB and ERK1/2 is important in promoting diabetes-induced retinal neuropathy. Recently, it was reported that chronic neuroinflammation may be a driving force of progressive neurodegeneration and that HMGB1 provides the link between chronic neuroinflammation and progressive neurodegeneration in neurodegenerative diseases, such as Parkinson's disease [13].

To confirm the neuropathological implications of HMGB1 in diabetic retinopathy, the HMGB1 inhibitor GA was administered orally after inducing diabetes in rats. GA is known to bind directly to HMGB1 and inhibit its chemoattractant and mitogenic activities [24]. Interestingly, constant intake of GA significantly reduced retinal HMGB1 protein and mRNA expression induced by diabetes. In addition, GA attenuated diabetes-induced upregulation

of cleaved caspase-3 and glutamate and counteracted the downregulation of synaptophysin, TH, GS, and GLO1 induced by diabetes without changing body weight or blood glucose levels. Our results are consistent with previous reports that demonstrated a neuroprotective effect of GA in animal models of brain ischemia [47], intracerebral hemorrhage [48], and spinal cord ischemia [49]. GA is known to possess glucocorticoid-like anti-inflammatory properties, due to its inhibitory activity on 11β-hydroxysteroid dehydrogenase [24]. Ohnishi et al. [48] demonstrated that the neuroprotective effect of GA on intracerebral hemorrhage-related pathogenic events was not mediated by glucocorticoid receptors or modulation of nitric oxide production and was reversed by exogenous HMGB1 application. These findings suggest that the protective effect of GA is mediated by its anti-HMGB1 activity and is irrelevant to the glucocorticoid system. It was demonstrated that the neuroprotective effect of GA was partly attributable to its inhibitory effect on HMGB1 release [47–49]. Furthermore, it was shown that GA affords protection in postischemic brain and spinal cord via its anti-inflammatory, antiapoptotic, antiexcitotoxic, and antioxidative effects [47, 49]. Together, these findings suggest that early retinal neuropathy induced by diabetes is, at least in part, attributable to diabetes-induced upregulation of HMGB1 expression and that inhibiting the release of HMGB1 with constant intake of GA results in less diabetes-induced retinal neuropathy. It is important to note that excessive intake of licorice may cause hypermineralocorticoidism-like syndrome characterized by sodium and water retention, potassium loss, edema, increased blood pressure, metabolic alkalosis, and depression of rennin-angiotensin-aldosterone system [50, 51].

In conclusion, our data point to a potential novel and pivotal role for HMGB1 as a mediator of diabetes-induced neuropathy in the retina. The HMGB1 inhibitor GA attenuated diabetes-induced upregulation of HMGB1 and diabetes-induced retinal neuropathy. Therefore, GA and other agents targeted to HMGB1 may provide novel therapeutic options for diabetic retinopathy.

Conflict of Interests

All the authors do not have any conflict of interests with any trademark mentioned in the paper.

Acknowledgments

The authors thank Ms. Connie B. Unisa-Marfil and Ms. Michelle B. Rasonabe for secretarial work. This work was supported by Dr. Nasser Al-Rasheed Research Chair in Ophthalmology (Abu El-Asrar AM) and National Plan for Science and Technology (NPST), King Saud University, under the Project 12-MED2604-02.

References

[1] M. Seki, T. Tanaka, H. Nawa et al., "Involvement of brain-derived neurotrophic factor in early retinal neuropathy of streptozotocin-induced diabetes in rats: therapeutic potential of brain-derived neurotrophic factor for dopaminergic amacrine cells," *Diabetes*, vol. 53, no. 9, pp. 2412–2419, 2004.

[2] A. J. Barber, "A new view of diabetic retinopathy: a neurodegenerative disease of the eye," *Progress in Neuro-Psychopharmacology and Biological Psychiatry*, vol. 27, no. 2, pp. 283–290, 2003.

[3] M. Sasaki, Y. Ozawa, T. Kurihara et al., "Neurodegenerative influence of oxidative stress in the retina of a murine model of diabetes," *Diabetologia*, vol. 53, no. 5, pp. 971–979, 2010.

[4] A. M. Abu El-Asrar, L. Dralands, L. Missotten, I. A. Al-Jadaan, and K. Geboes, "Expression of apoptosis markers in the retinas of human subjects with diabetes," *Investigative Ophthalmology and Visual Science*, vol. 45, no. 8, pp. 2760–2766, 2004.

[5] J. R. Van Beijnum, W. A. Buurman, and A. W. Griffioen, "Convergence and amplification of toll-like receptor (TLR) and receptor for advanced glycation end products (RAGE) signaling pathways via high mobility group B1 (HMGB1)," *Angiogenesis*, vol. 11, no. 1, pp. 91–99, 2008.

[6] C. J. Treutiger, G. E. Mullins, A.-S. M. Johansson et al., "High mobility group 1 B-box mediates activation of human endothelium," *Journal of Internal Medicine*, vol. 254, no. 4, pp. 375–385, 2003.

[7] C. Fiuza, M. Bustin, S. Talwar et al., "Inflammation-promoting activity of HMGB1 on human microvascular endothelial cells," *Blood*, vol. 101, no. 7, pp. 2652–2660, 2003.

[8] Z.-G. Luan, H. Zhang, P.-T. Yang, X.-C. Ma, C. Zhang, and R.-X. Guo, "HMGB1 activates nuclear factor-κB signaling by RAGE and increases the production of TNF-α in human umbilical vein endothelial cells," *Immunobiology*, vol. 215, no. 12, pp. 956–962, 2010.

[9] M. Takeuchi, J.-I. Takino, and S.-I. Yamagishi, "Involvement of the toxic AGEs (TAGE)-RAGE system in the pathogenesis of diabetic vascular complications: a novel therapeutic strategy," *Current Drug Targets*, vol. 11, no. 11, pp. 1468–1482, 2010.

[10] D. Tang, R. Kang, H. J. Zeh 3rd, and M. T. Lotze, "High-mobility group box 1, oxidative stress, and disease," *Antioxidants and Redox Signaling*, vol. 14, no. 7, pp. 1315–1335, 2011.

[11] A. M. Joussen, V. Poulaki, M. L. Le et al., "A central role for inflammation in the pathogenesis of diabetic retinopathy," *The FASEB Journal*, vol. 18, no. 12, pp. 1450–1452, 2004.

[12] K. Miyamoto, S. Khosrof, S.-E. Bursell et al., "Prevention of leukostasis and vascular leakage in streptozotocin-induced diabetic retinopathy via intercellular adhesion molecule-1 inhibition," *Proceedings of the National Academy of Sciences of the United States of America*, vol. 96, no. 19, pp. 10836–10841, 1999.

[13] H.-M. Gao, H. Zhou, F. Zhang, B. C. Wilson, W. Kam, and J.-S. Hong, "HMGB1 acts on microglia Mac1 to mediate chronic neuroinflammation that drives progressive neurodegeneration," *Journal of Neuroscience*, vol. 31, no. 3, pp. 1081–1092, 2011.

[14] J.-B. Kim, S. C. Joon, Y.-M. Yu et al., "HMGB1, a novel cytokine-like mediator linking acute neuronal death and delayed neuroinflammation in the postischemic brain," *Journal of Neuroscience*, vol. 26, no. 24, pp. 6413–6421, 2006.

[15] J. Qiu, M. Nishimura, Y. Wang et al., "Early release of HMGB-1 from neurons after the onset of brain ischemia," *Journal of Cerebral Blood Flow and Metabolism*, vol. 28, no. 5, pp. 927–938, 2008.

[16] S.-W. Kim, C.-M. Lim, J.-B. Kim et al., "Extracellular HMGB1 released by NMDA treatment confers neuronal apoptosis via RAGE-p38 MAPK/ERK signaling pathway," *Neurotoxicity Research*, vol. 20, no. 2, pp. 159–169, 2011.

[17] G. Faraco, S. Fossati, M. E. Bianchi et al., "High mobility group box 1 protein is released by neural cells upon different stresses and worsens ischemic neurodegeneration in vitro and in vivo," *Journal of Neurochemistry*, vol. 103, no. 2, pp. 590–603, 2007.

[18] K. Liu, S. Mori, H. K. Takahashi et al., "Anti-high mobility group box 1 monoclonal antibody ameliorates brain infarction induced by transient ischemia in rats," *The FASEB Journal*, vol. 21, no. 14, pp. 3904–3916, 2007.

[19] M. Pedrazzi, L. Raiteri, G. Bonanno et al., "Stimulation of excitatory amino acid release from adult mouse brain glia subcellular particles by high mobility group box 1 protein," *Journal of Neurochemistry*, vol. 99, no. 3, pp. 827–838, 2006.

[20] A. M. A. El-Asrar, L. Missotten, and K. Geboes, "Expression of high-mobility groups box-1/receptor for advanced glycation end products/osteopontin/early growth response-1 pathway in proliferative vitreoretinal epiretinal membranes," *Molecular Vision*, vol. 17, pp. 508–518, 2011.

[21] A. M. A. El-Asrar, M. I. Nawaz, D. Kangave et al., "High-mobility group box-1 and biomarkers of inflammation in the vitreous from patients with proliferative diabetic retinopathy," *Molecular Vision*, vol. 17, pp. 1829–1838, 2011.

[22] A. M. Abu El-Asrar, M. I. Nawaz, D. Kangave, M. M. Siddiquei, and K. Geboes, "Osteopontin and other regulators of angiogenesis and fibrogenesis in the vitreous from patients with proliferative vitreoretinal disorders," *Mediators of Inflammation*, vol. 2012, Article ID 493043, 8 pages, 2012.

[23] G. Mohammad, M. M. Siddiquei, A. Othman, M. Al-Shabrawey, and A. M. Abu El-Asrar, "High-mobility group box-1 protein activates inflammatory signaling pathway components and disrupts retinal vascular-barrier in the diabetic retina," *Experimental Eye Research*, vol. 107, pp. 101–109, 2013.

[24] L. Mollica, F. De Marchis, A. Spitaleri et al., "Glycyrrhizin binds to high-mobility group box 1 protein and inhibits its cytokine activities," *Chemistry and Biology*, vol. 14, no. 4, pp. 431–441, 2007.

[25] M. J. Gastinger, R. S. J. Singh, and A. J. Barber, "Loss of cholinergic and dopaminergic amacrine cells in streptozotocin-diabetic rat and Ins2Akita-diabetic mouse retinas," *Investigative Ophthalmology and Visual Science*, vol. 47, no. 7, pp. 3143–3150, 2006.

[26] R. A. Feit-Leichman, R. Kinouchi, M. Takeda et al., "Vascular damage in a mouse model of diabetic retinopathy: relation to neuronal and glial changes," *Investigative Ophthalmology and Visual Science*, vol. 46, no. 11, pp. 4281–4287, 2005.

[27] I. Spiwoks-Becker, L. Vollrath, M. W. Seeliger, G. Jaissle, L. G. Eshkind, and R. E. Leube, "Synaptic vesicle alterations in rod photoreceptors of synaptophysin-deficient mice," *Neuroscience*, vol. 107, no. 1, pp. 127–142, 2001.

[28] H. D. Vanguilder, R. M. Brucklacher, K. Patel, R. W. Ellis, W. M. Freeman, and A. J. Barber, "Diabetes downregulates presynaptic proteins and reduces basal synapsin i phosphorylation in rat retina," *European Journal of Neuroscience*, vol. 28, no. 1, pp. 1–11, 2008.

[29] T. Kurihara, Y. Ozawa, N. Nagai et al., "Angiotensin II type 1 receptor signaling contributes to synaptophysin degradation and neuronal dysfunction in the diabetic retina," *Diabetes*, vol. 57, no. 8, pp. 2191–2198, 2008.

[30] Y. Ozawa, T. Kurihara, M. Sasaki et al., "Neural degeneration in the retina of the streptozotocin-induced type 1 diabetes model," *Experimental Diabetes Research*, vol. 2011, Article ID 108328, 7 pages, 2011.

[31] K. Szabadfi, T. Atlasz, P. Kiss et al., "Protective effects of the neuropeptide PACAP in diabetic retinopathy," *Cell and Tissue Research*, vol. 348, no. 1, pp. 37–46, 2012.

[32] C. Wan, N. N. Liu, L. M. Liu, N. Cai, and L. Chen, "Effect of adenovirus-mediated brain derived neurotrophic factor in early retinal neuropathy of diabetes in rats," *International Journal of Ophthalmology*, vol. 3, pp. 145–148, 2010.

[33] F. K. Northington, R. W. Hamill, and S. P. Banerjee, "Dopamine-stimulated adenylate cyclase and tyrosine hydroxylase in diabetic rat retina," *Brain Research*, vol. 337, no. 1, pp. 151–154, 1985.

[34] E. Lieth, K. F. LaNoue, D. A. Antonetti, and M. Ratz, "Diabetes reduces glutamate oxidation and glutamine synthesis in the retina," *Experimental Eye Research*, vol. 70, no. 6, pp. 723–730, 2000.

[35] Y. Xu-hui, Z. Hong, W. Yu-hong, L. Li-juan, T. Yan, and L. Ping, "Time-dependent reduction of glutamine synthetase in retina of diabetic rats," *Experimental Eye Research*, vol. 89, no. 6, pp. 967–971, 2009.

[36] E. Lieth, A. J. Barber, B. Xu et al., "Glial reactivity and impaired glutamate metabolism in short-term experimental diabetic retinopathy. Penn State Retina Research Group," *Diabetes*, vol. 47, pp. 815–820, 1998.

[37] R. A. Kowluru, R. L. Engerman, G. L. Case, and T. S. Kern, "Retinal glutamate in diabetes and effect of antioxidants," *Neurochemistry International*, vol. 38, no. 5, pp. 385–390, 2001.

[38] A. Lecleire-Collet, L. H. Tessier, P. Massin et al., "Advanced glycation end products can induce glial reaction and neuronal degeneration in retinal explants," *British Journal of Ophthalmology*, vol. 89, no. 12, pp. 1631–1633, 2005.

[39] J. V. Glenn and A. W. Stitt, "The role of advanced glycation end products in retinal ageing and disease," *Biochimica et Biophysica Acta*, vol. 1790, no. 10, pp. 1109–1116, 2009.

[40] N. Karachalias, R. Babaei-Jadidi, N. Ahmed, and P. J. Thornalley, "Accumulation of fructosyl-lysine and advanced glycation end products in the kidney, retina and peripheral nerve of streptozotocin-induced diabetic rats," *Biochemical Society Transactions*, vol. 31, no. 6, pp. 1423–1425, 2003.

[41] M. Shinohara, P. J. Thornalley, I. Giardino et al., "Overexpression of glyoxalase-I in bovine endothelial cells inhibits intracellular advanced glycation endproduct formation and prevents hyperglycemia-induced increases in macromolecular endocytosis," *Journal of Clinical Investigation*, vol. 101, no. 5, pp. 1142–1147, 1998.

[42] A. G. Miller, G. Tan, K. J. Binger et al., "Candesartan attenuates diabetic retinal vascular pathology by restoring glyoxalase-I function," *Diabetes*, vol. 59, no. 12, pp. 3208–3215, 2010.

[43] A. K. Berner, O. Brouwers, R. Pringle et al., "Protection against methylglyoxal-derived AGEs by regulation of glyoxalase 1 prevents retinal neuroglial and vasodegenerative pathology," *Diabetologia*, vol. 55, no. 3, pp. 845–854, 2012.

[44] K.-I. Kawahara, K. K. Biswas, M. Unoshima et al., "C-reactive protein induces high-mobility group box-1 protein release through activation of p38MAPK in macrophage RAW264.7 cells," *Cardiovascular Pathology*, vol. 17, no. 3, pp. 129–138, 2008.

[45] S. Willenbrock, O. Braun, J. Baumgart et al., "TNF-α induced secretion of HMGB1 from non-immune canine mammary epithelial cells (MTH53A)," *Cytokine*, vol. 57, no. 2, pp. 210–220, 2012.

[46] K. Hayakawa, K. Arai, and E. H. Lo, "Role of ERK MAP kinase and CRM1 in IL-1β-stimulated release of HMGB1 from cortical astrocytes," *GLIA*, vol. 58, no. 8, pp. 1007–1015, 2010.

[47] S.-W. Kim, Y. Jin, J.-H. Shin et al., "Glycyrrhizic acid affords robust neuroprotection in the postischemic brain via anti-inflammatory effect by inhibiting HMGB1 phosphorylation and secretion," *Neurobiology of Disease*, vol. 46, no. 1, pp. 147–156, 2012.

[48] M. Ohnishi, H. Katsuki, C. Fukutomi et al., "HMGB1 inhibitor glycyrrhizin attenuates intracerebral hemorrhage-induced injury in rats," *Neuropharmacology*, vol. 61, no. 5-6, pp. 975–980, 2011.

[49] G. Gong, L.-B. Yuan, L. Hu et al., "Glycyrrhizin attenuates rat ischemic spinal cord injury by suppressing inflammatory cytokines and HMGB1," *Acta Pharmacologica Sinica*, vol. 33, no. 1, pp. 11–18, 2012.

[50] F. C. Stormer, R. Reistad, and J. Alexander, "Glycyrrhizic acid in liquorice—evaluation of health hazard," *Food and Chemical Toxicology*, vol. 31, no. 4, pp. 303–312, 1993.

[51] M. M. Celik, A. Karakus, C. Zeren et al., "Licorice induced hypokalemia, edema, and thrombocytopenia," *Human & Experimental Toxicology*, vol. 31, pp. 1295–1298, 2012.

Hindawi Publishing Corporation
Mediators of Inflammation
Volume 2014, Article ID 590409, 8 pages
http://dx.doi.org/10.1155/2014/590409

Research Article

Interactions between Neutrophils, Th17 Cells, and Chemokines during the Initiation of Experimental Model of Multiple Sclerosis

Dagmara Weronika Wojkowska,[1,2] Piotr Szpakowski,[1,2] Dominika Ksiazek-Winiarek,[1,2] Marcin Leszczynski,[1] and Andrzej Glabinski[1,2]

[1] *Department of Neurology, Epileptology and Stroke, Medical University of Lodz, Ulice Zeromskiego 113, 90 549 Lodz, Poland*
[2] *Department of Propedeutics of Neurology, Medical University of Lodz, Ulice Zeromskiego 113, 90 549 Lodz, Poland*

Correspondence should be addressed to Andrzej Glabinski; aglabinski@gmail.com

Received 10 September 2013; Revised 7 January 2014; Accepted 12 January 2014; Published 19 February 2014

Academic Editor: Mohammad Athar

Experimental autoimmune encephalomyelitis (EAE) is an animal model of multiple sclerosis (MS) in which activated T cell and neutrophil interactions lead to neuroinflammation. In this study the expression of CCR6, CXCR2, and CXCR6 in Th17 cells and neutrophils migrating to the brain during EAE was measured, alongside an evaluation of the production of IL-17, IL-23, CCL-20, and CXCL16 in the brain. Next, inflammatory cell subpopulations accumulating in the brain after intracerebral injections of IL-17 or CXCL1, as well as during modulation of EAE with anti-IL-23R or anti-CXCR2 antibodies, were analyzed. Th17 cells upregulate CXCR2 during the preclinical phase of EAE and a significant migration of these cells to the brain was observed. Neutrophils upregulated CCR6, CXCR2, and CXCR6 during EAE, accumulating in the brain both prior to and during acute EAE attacks. Production of IL-17, IL-23, CCL20, and CXCL16 in the CNS was increased during both preclinical and acute EAE. Intracerebral delivery of CXCL1 stimulated the early accumulation of neutrophils in normal and preclinical EAE brains but reduced the migration of Th17 cells to the brain during the preclinical stage of EAE. Modulation of EAE by anti-IL-23R antibodies ameliorated EAE by decreasing the intracerebral accumulation of Th17 cells.

1. Introduction

Multiple sclerosis (MS) a demyelinating disease of the central nervous system (CNS) is often characterized by relapsing acute episodes and in many cases evolves into a progressive chronic neurological deterioration [1]. The most commonly used animal model of MS is experimental autoimmune encephalomyelitis (EAE). The many clinical and histopathological similarities between MS and EAE allow results obtained from this model to be extrapolated to human MS [2, 3].

Immunopathogenesis of MS and EAE, despite of many decades of research, remains unclear. According to the current paradigm effector T cells play a key role in the disease development; after migration to the CNS they may initiate autoimmune inflammation and thus damage myelin. Under normal physiological conditions, the blood-brain barrier (BBB) is formed by dense tight junction (TJ) proteins that seal the space between adjacent brain endothelial cells to form a barrier between the circulating blood and the CNS. The capillary endothelial cells of the BBB are surrounded by a basal lamina, pericytes, and astrocytic end-feet with microglia in close proximity. Physiological and pathological changes in the activity of these glial cell populations may weaken BBB integrity [4]. Endothelial cells of the BBB release multiple inflammatory mediators and express various adhesion molecules such as intercellular and vascular cellular adhesion molecules (ICAM-1, VCAM-1), P- and E-selectins. These membrane proteins are required to anchor leukocytes to the vessel wall and are well-established markers of endothelial dysfunction under inflammatory conditions [5]. Migration of lymphocytes through the brain is usually

low, as the endothelial BBB limits their entry into the CNS. In the healthy brain, TJ components such as occludin, ZO-1, claudin-3, and claudin-5 are readily detectable [6]. Disruption of the BBB is a crucial event that may permit the entry of inflammatory cells into the brain, a prerequisite for the formation of MS lesions [4].

Evidence for the role of neutrophils, as well as recently discovered Th17 cells in EAE development, continues to increase [7]. Th17 cells and the cytokine IL-17 that they produce [8] mediate the disruption of BBB [9]. IL-17 enhances the activation of matrix metalloproteinase-3 (MMP-3) and attracts neutrophils to the site of inflammation. Enzymes such as MMPs, proteases, and gelatinases that may be activated by neutrophils participate in BBB disruption. The breakdown of BBB effectively increases neutrophil recruitment further, with increased protease activity subsequently attracting a large number of monocytes and macrophages to the inflammatory regions and leading to sustained myelin and axonal damage [10, 11].

In many studies, chemoattractant cytokines, or chemokines, have drawn a great deal of attention, in particular the CC and CXC ELR(−) group of chemokines which are responsible for the chemotaxis of mononuclear cells, a major component of CNS inflammatory infiltrates. However, the role of CXC ELR(+) chemokines such as CXCL1 and CXCL2, which target mainly neutrophils, has not been thoroughly described. Furthermore, cytokines that participate in Th17 cell differentiation and activation such as IL-23, as well as the chemokines CCL20 or CXCL16 and their receptors CCR6 and CXCR6, are also important mediators of this process [12–14].

The major aim of this study was thus to analyze the interactions between Th17 cells and neutrophils in the pathogenesis of early EAE and to define the role of chemokines and their receptors in this interaction.

2. Materials and Methods

2.1. Animals. All experiments used 8–12 weeks' old female SJL mice. Animals were housed at the animal facility of the Medical University of Lodz, Lodz, Poland, under standard conditions. Experimental protocols were approved by the Animal Care Committee of the Medical University of Lodz.

2.2. EAE Induction and Tissue Collection. EAE was induced by active immunization with an encephalitogenic PLP (proteolipid protein) peptide representing residues 139–151 (PLPp: 139–151, Metabion, Martinsried, Germany) emulsified with complete Freund's adjuvant (Sigma, Poznan, Poland). Pertussis toxin (Sigma, Poznan, Poland) was administered by intravenous injection on the day of immunization and again 48 h later, as previously described [2]. Animals were weighed and examined daily for clinical signs of EAE. The following clinical scoring scale was used: 0—no disease symptoms; 1—decreased tail tone or slightly clumsy gait; 2—tail atony and/or moderately clumsy gait and/or poor righting ability; 3—limb weakness; 4—limb paralysis; 5—moribund state [2].

During the preclinical phase (at days 7-8 or 10–13 days after immunization prior to any signs of EAE) and during the initial attack of EAE (the first three days of symptoms) mice were anesthetized with a ketamine/xylazine cocktail (Biowet, Pulawy, Poland) administered intraperitoneally and perfused through the left cardiac ventricle with the ice cold PBS (phosphate buffered saline) (Biomed, Krakow, Poland) containing heparin. Brains, spinal cords, and blood were collected (see below). As a control healthy, nonimmunized mice were used.

2.3. Isolation of Mononuclear Cells from the Blood and CNS. Mononuclear cells were isolated from the brain, spinal cord, and blood of immunized mice during the preclinical phase (7-8 days postimmunization; 6 mice) and during the acute attack of the disease (3-4 days after the onset of EAE symptoms; 5 mice). Cells isolated from healthy mice were used as a control (4 mice). Samples were collected from mice by cardiac blood draw using a syringe with heparin. Hematocytes were lysed for 5 min at 4°C with red blood cell lysing buffer (Sigma, Poznan, Poland). The remaining cells were isolated by centrifugation for 10 min at 400 × g (4°C) and then resuspended in PBS.

The CNS (combined brain and spinal cord) collected from animals was placed in the ice cold PBS and forced through 70 μm cell strainers (BD Bioscience, Bedford, MA, USA) to obtain single cell suspensions which were then centrifuged for 10 min at 350 × g (4°C). The CNS mononuclear cells were resuspended in 40% Percoll (Sigma, Poznan, Poland) diluted with white Hank's Buffered Salt Solution (HBSS) (Lonza, Basel, Switzerland). The suspension of cells was then carefully layered on top of the 70% Percoll diluted with red HBSS. CNS mononuclear cells were isolated by centrifugation for 40 min at 700 × g (4°C) with a slow deceleration with no brake. Cells were then collected from the 40%/70% interphase, washed, and resuspended in PBS. Cells suspensions were stained using trypan blue, counted in a Bürker chamber under a light microscope, and prepared for the flow cytometry.

2.4. Flow Cytometry Analysis. Single cell suspensions (10^6 cells) were prepared from CNS and blood and stained with fluorochrome-conjugated antibodies. All monoclonal antibodies (mAb) were purchased from BD Bioscience (Bedford, MA, USA), eBioscience (San Diego, CA, USA), and BioLegend (San Diego, CA, USA). Antibodies were directly labeled with one of the following fluorescent tags: FITC, PE, PerCP, APC, Alexa Fluor 700, and APC-Cy7. Antibodies to the following proteins were used: CD4, CD3, CD11b, CD11c, CD19, CD45, CD14, IL17, CCR6, CXCR6, CXCR2, and Gr-1. Flow cytometry was performed using a BD LSR II flow cytometer and analyzed with BD Diva software. Isotype-matched negative control mouse raised antibodies were used for all stains.

2.5. Analysis of Cytokine Level by ELISA. Study groups included 10 to 23 mice divided between the preclinical phase (11–13 days after immunization), acute EAE attack

(1–3 days of disease signs), and normal healthy mice as a control. Previously collected brains were homogenized in HEPES buffer with protease inhibitors using a homogenizer (Ultra-Turrax T8, Staufen, Germany). Samples were then centrifuged, supernatants collected, and properly diluted. To estimate the levels of IL-17, IL-23, CCL20, and CXCL16 the Quantikine kit was used as per manufacturer's instructions (R&D Systems, MN, USA).

2.6. Stereotactic Brain Microinjections. Stereotactic microinjections were conducted on ketamine/xylazine anesthetized mice on the 4th day after immunization (preclinical phase). Animals were given IL-17, CXCL1, or PBS (control group). The procedure was performed on stereotactic frame (David Kopf Instruments, Tujunga, CA) using a Hamilton syringe (32 G needle, 0.25 mm). Injections were made into the striatum of the brain (in maximal volume of 0.1 μL), which did not cause any apparent neurological impairment in the animals. After intracerebral cytokine administration, the scalp was sutured with surgical thread. Mice were sacrificed 24 h or 72 h after injection of IL-17 and CXCL1 for further analysis. Brains from animals were collected and cells for cytometric analysis were prepared as described above.

2.7. Modulation of the Course of EAE and Its Pathology Using Anti-IL23R and Anti-CXCR2 Antibodies. Immunized mice received anti-IL-23R monoclonal, blocking antibody (4 mice), anti-CXCR2 monoclonal, blocking antibody (4 mice) or PBS (control) (4 mice) on the 3rd and 6th day after immunization. Antibodies (at a concentration 20 μg/100 μL) were injected into the tail vein. All mice were weighed and examined daily for clinical signs of EAE. On the second day of the disease mice were anesthetized with a ketamine/xylazine cocktail and perfused with ice cold PBS. Brains were collected from animals and single cell suspensions (10^6 cells) were prepared. Cells were stained with fluorochrome-conjugated antibodies and a percentage of neutrophils and Th17 cells were analyzed by flow cytometry. Evans blue (EB) at a concentration of 50 mg/mL was administered intraperitoneally on the 2nd day of EAE to experimental and control mice (0.01 mL/g body weight). After 2 hours mice were anesthetized and perfused as described above. Brains were collected and homogenized (Ultra-Turrax T8, Staufen, Germany) in 1 mL of 50% TCA (trichloroacetic acid), centrifuged for 20 min at 10 000 rpm. Then supernatants were collected and diluted 1 : 3 with ethanol. Differences in BBB permeability were measured colorimetrically at a wavelength of 620 nm.

2.8. Statistical Analysis. For statistical analysis nonparametric U Mann-Whitney tests were used. A value of $P < 0.05$ was considered statistically significant. Data were shown as mean ± SEM.

3. Results

3.1. Expression of CCR6, CXCR2, and CXCR6 on Th17 Cells and Neutrophils from the CNS and Blood of Mice with EAE. A statistically significant increase in the number of Th17 cells in samples derived from the brains of mice with EAE attack was observed compared to control animals (P value = 0.03). However, the number of Th17 cells in blood during the preclinical phase of EAE was significantly lower when compared to healthy controls (P value = 0.02) (Figure 1(a)). During both the preclinical phase and attack of EAE, an increased number of neutrophils was also detected in the CNS in comparison to healthy mice (P value = 0.02; P value = 0.05, resp.) (Figure 1(a)).

CCR6 expression was present on Th17 cells, but expression levels remained constant regardless of the stage of the disease (Figure 1(b)). A significant increase of CXCR2 expression on Th17 cells was detected in the CNS during the preclinical phase in comparison to healthy mice (P value = 0.05), but this expression decreased to control levels in EAE mice (P value = 0.02) (Figure 1(b)). Numbers of CXCR6+Th17 cells were on a similar level in all analyzed groups (Figure 1(b)).

CCR6 expression on neutrophils from the CNS was increased in the preclinical phase compared to healthy controls but did not reach statistical significance. A significant decrease of CCR6 expression was, however, observed in the CNS of mice during EAE attack compared to the preclinical phase (P value = 0.05) (Figure 1(c)). Significant increases of CXCR2 expression on neutrophils were observed in the CNS during the preclinical phase (P value = 0.03), but this expression returned to control levels during EAE attack (P value = 0.04) (Figure 1(c)). CXCR6 expression on neutrophils from the CNS was also significantly elevated during the preclinical phase of EAE both when compared to healthy mice and in mice undergoing an EAE attack (P value = 0.04; P value = 0.04, resp.) (Figure 1(c)). Similarly, there was a significant increase of CXCR6 expression in the blood during the preclinical phase of EAE in comparison to controls and to EAE attack derived samples (P value = 0.05; P value = 0.02, resp.) (Figure 1(c)).

3.2. Production of IL-17, CXCL16, CCL20, and IL-23 in the CNS of Mice with EAE. A significant increase of IL-17 production was observed in the brains of mice in the preclinical phase of EAE (P value = 0.0003) as well as during the initial attack of the disease (P value = 0.005) when compared to controls (Figure 2). A significant increase of IL-23 levels was also observed in brains collected during the preclinical phase of EAE (P value = 0.003) and the EAE attack compared to normal brains (P value = 0.009) (Figure 2). Similarly, analysis of CCL20 concentration in the CNS showed a significant increase during EAE attack in comparison to healthy controls (P value = 0.006) (Figure 2). Measures of CXCL16 concentrations in brain showed significant differences between both mice undergoing an acute EAE attack (P value = 0.000008) and mice in the preclinical phase (P-value = 0.002), compared to normal controls (Figure 2).

3.3. Accumulation of Neutrophils and Th17 Cells in the Brain after Intracerebral Injection of IL-17 or CXCL1. Neutrophil accumulation in the normal brain significantly increased at

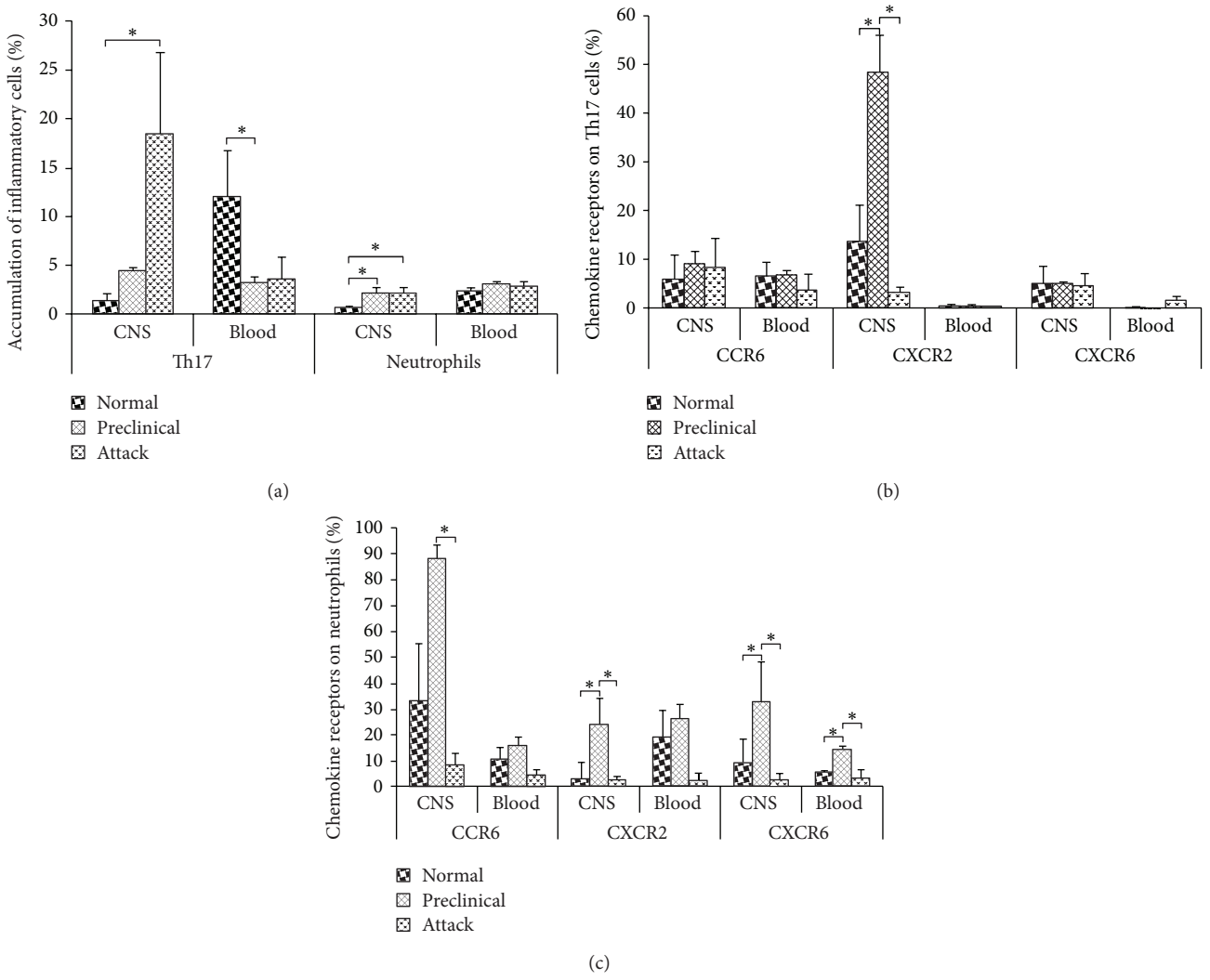

Figure 1: Flow cytometry analysis of chemokine receptors on Th17 cells and neutrophils from the CNS and blood of EAE mice. (a) Percentage of Th17 cell and neutrophils, (b) chemokine receptor expression on Th17 cells, and (c) chemokine receptor expression on neutrophils. Normal—healthy control mice, preclinical—immunized mice before disease onset, attack—second day of EAE symptoms. Data are presented as mean ± SEM. $^{*}0.05 \geq P \geq 0.01$.

24 h after either IL-17or CXCL1 stereotaxic injections (P value = 0.02 for both) (Figure 3(a)). Furthermore, neutrophil infiltration of the preclinical EAE brain after CXCL1 administration was higher than in PBS control injected mice (P value = 0.05) (Figure 3(a)).

Accumulation of Th17 cells was unchanged 24 h after IL-17 and CXCL1 injections into the normal brain. Interestingly, accumulation of Th17 cells in the brain of immunized, preclinical mice was significantly lower after IL-17 and CXCL1 intracerebral delivery than after control PBS injection (P value = 0.049 and P value = 0.03, resp.) (Figure 3(a)).

At 72 h after CXCL1 intracerebral injection, the accumulation of neutrophils in the normal brain was significantly lower than in control uninjected brain (P value = 0.01) (Figure 3(b)). At this time point, IL-17 or CXCL1 delivery to the preclinical EAE brain did not change the accumulation of neutrophils when compared to control PBS-injected animals (Figure 3(b)).

In normal brain the accumulation of Th17 cells was diminished at 72 h after IL-17 injection but increased after CXCL1 injection when compared to uninjected normal brain (P value = 0.02 and P value = 0.03, resp.) (Figure 3(b)). At that time point intracerebral CXCL1 delivery significantly reduced the accumulation of Th17 cells in the brain of preclinical mice in comparison to control PBS administration (P value = 0.01) (Figure 3(b)).

3.4. Modulation of EAE Course and Pathology by Anti-CXCR2 or Anti-IL-23R Antibodies. Modulation of EAE with a specific anti-IL-23R monoclonal antibody significantly delayed the appearance of the first clinical symptoms compared to control mice receiving PBS (P value = 0.03), as well as to mice treated with anti-CXCR2 monoclonal antibody (P value = 0.01) (Figure 4(a)). This treatment, with anti-IL23R antibodies, also significantly reduced the severity of

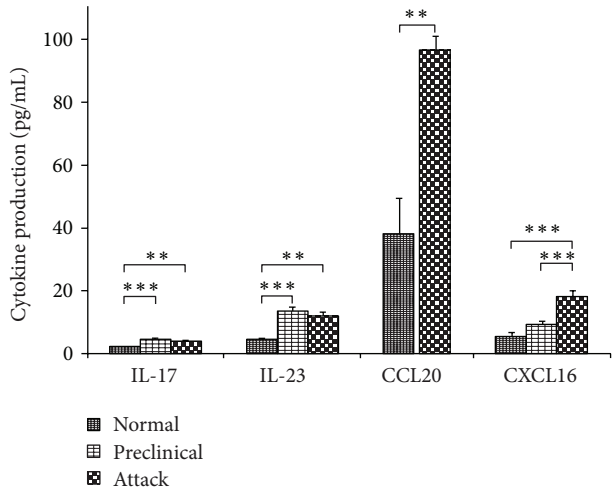

Figure 2: Cytokine production in the brain of EAE mice. Normal—healthy control mice, preclinical—immunized mice before disease onset, attack—second day of EAE symptoms. Data are presented as mean ± SEM. $^{*}0.05 \geq P \geq 0.01$; $^{**}0.01 > P \geq 0.005$; $^{***}P < 0.005$.

symptoms in this model as measured by EAE score on the second day of the disease (P value = 0.05) (Figure 4(a)).

During the second day of the EAE attack, the accumulation of neutrophils in the brain was similar in all analyzed groups. Interestingly, at that time point, the number of Th17 cells in brains of mice treated with anti-IL-23R antibody was significantly lower when compared to control mice (P value = 0.02) or mice treated with anti-CXCR2 monoclonal antibody (P value = 0.03) (Figure 4(b)).

Also at that time point, the greatest disruption of BBB permeability, as measured by Evans blue accumulation in the brain, was observed in mice treated with anti-IL-23R antibody, but this did not reach statistical significance (Figure 4(c)).

4. Discussion

Our study has demonstrated that Th17 cells and neutrophils, as well as inflammatory mediators that they produce, play a very important role in the development of autoimmune CNS inflammation during the early stages of EAE. Activated Th17 cells are the major producers of the inflammatory cytokine IL-17 [15], which is known to be produced also by neutrophils [16]. In our study an increased accumulation of Th17 cells and neutrophils in the CNS of EAE mice was observed. Moreover, the increased production of several cytokines, including IL-17, was detected in the brain during early EAE. Some studies have suggested that IL-17 may induce BBB disruption, thus facilitating the migration of inflammatory cells into the brain [4]. It has also been shown that IL-17A-induced BBB disruption involves the formation of reactive oxygen species (ROS), which are subsequently responsible for reduced expression of tight junction molecules and the deactivation of the endothelial contractile machinery [4].

IL-17 can also interact directly with astrocytes and microglia through IL-17R receptors located on these cells [17]. IL-17A deficient mice display a significantly milder disease and a significant loss of encephalitogenic capacity after adoptive transfer of *in vitro* expanded T cells [18]. These data may indicate that IL-17 is important for chemokine expression and development of neuroinflammation in EAE [19]. The increased production of chemokines attracts other inflammatory cells including neutrophils, in line with our observation after stereotaxic intracerebral IL-17 delivery to the brain. We have observed substantial neutrophil inflow to the brain at 72 h after cytokine injection. This may suggest that IL-17 interactions with other cell subpopulations are delayed, which would lead to the production of attractants for neutrophils and stimulate their migration at later time points. As Th17 cells are the main producers of IL-17, its external administration to the brain postponed the accumulation of this T cell subpopulation in EAE brain.

An important determinant of T cell differentiation into Th17 cells is the cytokine IL-23 [20], which was also upregulated in our study in the brain of mice with EAE. IL-23 promotes the development and expansion of activated CD4+ T cells that produce IL-17 upon antigen-specific stimulation [21]. Genetic analysis of these helper T cells identified a unique expression pattern of proinflammatory cytokines and other novel factors. IL-17 expression was undetectable in the CD4+ T cells of IL-23 - deficient mice (derived from either CNS or lymph nodes), suggesting that IL-23 is essential for the development of specific IL-17- producing T cells [22]. It was shown that blocking IL-23 function can alleviate EAE symptoms. Moreover, administration of anti-IL-23p19 antibodies reduced IL-17 levels in the CNS as well as the expression of IFN-gamma, IP-10, IL-17, IL-6, and TNF-alpha mRNA [23]. Our experiment modulating the course of EAE with monoclonal blocking antibodies against IL-23R confirms this hypothesis. In that experiment the first EAE symptoms were delayed and severity of the disease was decreased in the group of animals treated with the anti-IL-23R antibody. The first signs of EAE were seen 4 days later than in the control group and the average clinical scores were significantly lower. Blocking the IL-23R receptor by a monoclonal antibody also significantly reduced the Th17 cell accumulation in the brain. This observation supports the concept that a blockade of this receptor has a direct influence on the differentiation of Th17 cells.

The chemokine receptor CCR6 plays an essential role in the initiation of EAE by controlling the migration of the first wave of autoreactive Th17 cells into the normal CNS. The entry of CCR6+ T cells into the CNS most likely occurs through the blood-cerebrospinal fluid barrier, as epithelial cells of the choroid plexus constitutively express the CCR6 ligand, CCL20. This first wave of hematogenous T cells initiates the recruitment of the second wave of inflammatory T cells that enter the CNS parenchyma in a CCR6-independent manner through the activated parenchymal postcapillary venules [24]. In this context, we reported the increased production of CCL20 in the CNS during EAE attack. As previously reported, CCL20 is highly expressed in the CNS during EAE [25], suggesting that CCR6 is expressed on Th17 cells and neutrophils. As CCR6+ Th17 cells exhibit a strong chemotaxis toward CCL20, a positive feedback may occur

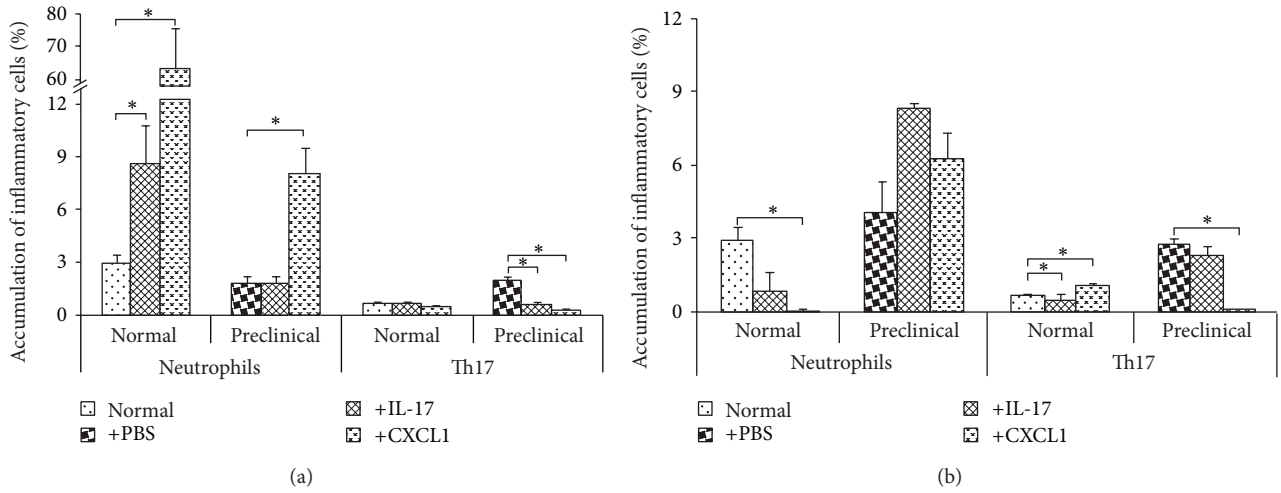

Figure 3: Accumulation of Th17 cells and neutrophils in the brain after stereotaxic intracerebral delivery of IL-17 or CXCL1. (a) 24 h after delivery, (b) 72 h after delivery. Accumulation of cells was measured in healthy control (Normal) mice and in immunized, preclinical mice by flow cytometry. Data are presented as mean ± SEM. $^{*}0.05 \geq P \geq 0.01$.

wherein Th17 cells further recruit other CCR6-expressing T cells to the site of inflammation [26].

It has been suggested that IL-17 interacts with plurality of inflammatory cells by stimulating expression of CXC ELR(+) chemokines such as CXCL1 and CXCL2, which display a strong chemotactic activity towards neutrophils [27]. Therefore, a growing amount of evidence confirms the crucial role of Th17 cells in the pathogenesis of EAE and MS and justifies the assumption that neutrophils may greatly contribute to the development of the disease. Indeed, CXCL1 has been shown to be the most highly expressed ligand for CXCR2 in the brains of mice subjected to EAE [28].

Under our conditions, however, stereotactic intracerebral microinjection of CXCL1 resulted in neutrophil infiltration into the CNS but did not reveal the presence of Th17 cells directly after delivery. IL-17 produced by Th17 cells affects the production of other inflammatory chemokines and cytokines responsible for EAE development. This might suggest that administration of CXCL1 to the brain may act directly on neutrophils bypassing the stage of IL-17 activation. It has also been shown that the inflammatory process in EAE is strongly correlated with CXCL1 expression [29, 30], and McColl et al. showed that the elimination of circulating neutrophils stimulates resistance to EAE induction [31]. This observation was confirmed by Carlson et al., who demonstrated that depletion of neutrophils in mice protects them against EAE development and this protective effect expires immediately upon reconstitution of circulating granulocytes [7]. Moreover, they found that CXCR2 knockout mice did not develop EAE [32]: but that the transfer of neutrophils expressing this receptor into these mice revoked their resistance to the disease. These data suggest the existence of a pathogenic pathway leading from Th17 cells to neutrophils, via ELR CXC chemokines(+), and highlight the crucial role of these interactions in the development of EAE and MS. However, blocking the granulocyte receptor CXCR2 can decrease demyelinated lesions while enhancing remyelination in EAE mice, as confirmed by the experiments of Liu et al. and Kerstetter et al. [32, 33].

Neutrophils can induce Th17 cells migration by CCL2 and CCL20 expression; however, Th17 cells interact with neutrophils via both an IL-17-dependent and an IL-17-independent pathway. This first pathway leads to neutrophil migration to inflammation sites by the induction of CXCL1 and CXCL2 expression, which are neutrophil chemoattractants. The second proposed pathway is based on Th17 cell production of GM-CSF, TNF-α, and IFN-γ, leading to the recruitment and activation of neutrophils [16]. As such, blocking CXCR2 on neutrophils does not necessarily lead to a noticeable reduction of neutrophils in the brain during EAE or alter the course of the disease, precisely because of the presence of the second pathway.

We also observed that CXCR2 is expressed on Th17 cells and neutrophils from the brain. Interestingly, administration of anti-CXCR2 monoclonal antibodies to immunized mice did not influence the migration of Th17 cells to the brain. This could be explained by the complexity of chemoattracting signals and the involvement of other chemokines in the regulation of cell migration and retention in brain tissues. However, our results also suggest a minor role of CXCR2-dependent attraction of effector lymphocytes at this stage of inflammation. Perhaps CXCL1 and CXCL2 can induce neutrophils, but not CXCR2+Th17 cells, to migrate into the site of inflammation.

The chemokine CXCL16 and its receptor, CXCR6, are also very important mediators of EAE development and Th17 cell interactions with neutrophils. CXCL16 is expressed by antigen-presenting cells such as monocytes, macrophages, B cells, and dendritic cells [34]. We found high levels of this chemokine in mouse brains, and moreover neutrophils demonstrated an increased expression of CXCR6. The elevated CXCL16 production in the EAE brain may help to recruit CXCR6+ cells across the BBB into gray matter foci, but additional, unknown signals provided during injury are

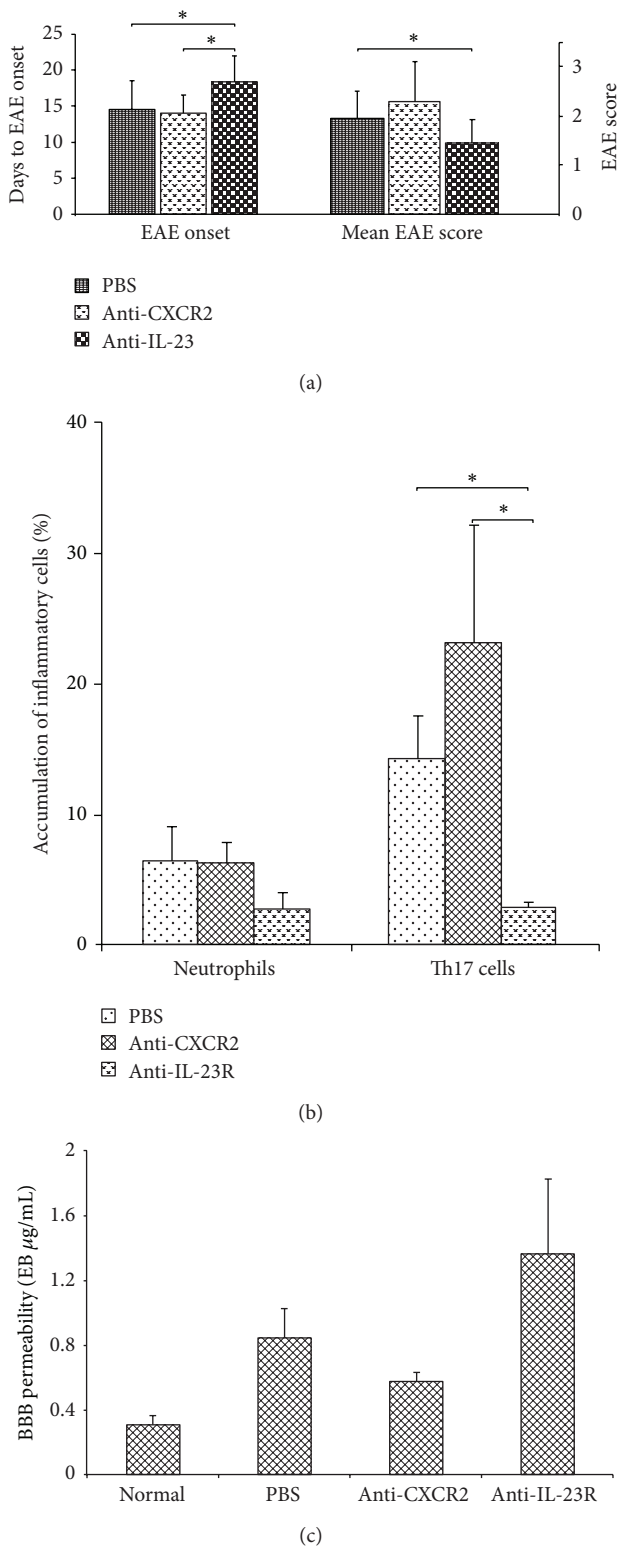

Figure 4: Modulation of EAE by anti-CXCR2 or anti-IL23R antibodies. (a) Mean time to EAE onset and mean EAE score at day 2 of the attack, (b) accumulation of Th17 cells and neutrophils in the brain, and (c) BBB permeability. Accumulation of inflammatory cell subpopulations was analyzed at the second day of EAE using flow cytometry; BBB permeability was analyzed at the same time point using Evans blue dye as described in Materials and Methods. Data are presented as mean ± SEM. $^{*}0.05 \geq P \geq 0.01$.

required for gray matter infiltration [35]. It has been shown that administration of neutralizing antibodies against CXCR6 reduced EAE severity and inflammatory cell infiltration of the CNS [36].

In summary, we characterized the chemokine receptor profile on Th17 cells and neutrophils accumulating in the CNS during early EAE and identified some of the interactions mediated by chemokines between these cell subpopulations during development in this MS model. Our data suggest that Th17 cells, neutrophils, and some chemokines could be promising targets for future MS therapies.

Conflict of Interests

The authors declare that they have no conflict of interests regarding the publication of this paper.

Acknowledgment

This work was supported by research Grant NCN N N401 456937.

References

[1] A. Compston, "The 150th anniversary of the firstdepiction of the lesions of multiplesclerosis," *Journalof Neurology, Neurosurgery and Psychiatry*, vol. 51, no. 10, pp. 1249–1252, 1988.

[2] A. Glabinski, M. Tani, V. K. Tuohy, and R. M. Ransohoff, "Murine experimental autoimmune encephalomyelitis: a model of immune-mediated inflammation and multiple sclerosis," *Methods in Enzymology*, vol. 288, pp. 182–190, 1997.

[3] D. P. McCarthy, M. H. Richards, and S. D. Miller, "Mouse models of multiple sclerosis: experimental autoimmune encephalomyelitis and theiler's virus-induced demyelinating disease," *Methods in Molecular Biology*, vol. 900, pp. 381–401, 2012.

[4] J. Huppert, D. Closhen, A. Croxford et al., "Cellular mechanisms of IL-17-induced blood-brain barrier disruption," *FASEB Journal*, vol. 24, no. 4, pp. 1023–1034, 2010.

[5] C. Gustavsson, C. Agardh, A. V. Zetterqvist, J. Nilsson, E. Agardh, and M. F. Gomez, "Vascular cellular adhesion molecule-1 (VCAM-1) expression in mice retinal vessels is affected by both hyperglycemia and hyperlipidemia," *PloS ONE*, vol. 5, no. 9, Article ID e12699, 2010.

[6] C. T. Prendergast and S. M. Anderton, "Immune cell entry to central nervous system-current understanding and prospective therapeutic targets," *Endocrine, Metabolic and Immune Disorders*, vol. 9, no. 4, pp. 315–327, 2009.

[7] T. Carlson, M. Kroenke, P. Rao, T. E. Lane, and B. Segal, "The Th17-ELR+ CXC chemokine pathway is essential for the development of central nervous system autoimmune disease," *Journal of Experimental Medicine*, vol. 205, no. 4, pp. 811–823, 2008.

[8] E. Rouvier, M.-F. Luciani, M.-G. Mattei, F. Denizot, and P. Golstein, "CTLA-8, cloned from an activated T cell, bearing AU-rich messenger RNA instability sequences, and homologous to a herpesvirus Saimiri gene," *Journal of Immunology*, vol. 150, no. 12, pp. 5445–5456, 1993.

[9] A. Saha, C. Sarkar, S. P. Singh et al., "The blood-brain barrier is disrupted in a mouse model of infantile neuronal ceroid

lipofuscinosis: amelioration by resveratrol," *Human Molecular Genetics*, vol. 21, no. 10, Article ID dds038, pp. 2233–2244, 2012.

[10] H. Park, Z. Li, X. O. Yang et al., "A distinct lineage of CD4 T cells regulates tissue inflammation by producing interleukin 17," *Nature Immunology*, vol. 6, no. 11, pp. 1133–1141, 2005.

[11] V. W. Yong, C. Power, P. Forsyth, and D. R. Edwards, "Metalloproteinases in biology and pathology of the nervous system," *Nature Reviews Neuroscience*, vol. 2, no. 7, pp. 502–511, 2001.

[12] D. J. Cua, J. Sherlock, Y. Chen et al., "Interleukin-23 rather than interleukin-12 is the critical cytokine for autoimmune inflammation of the brain," *Nature*, vol. 421, no. 6924, pp. 744–748, 2003.

[13] C. L. Langrish, B. S. McKenzie, N. J. Wilson, R. De Waal Malefyt, R. A. Kastelein, and D. J. Cua, "IL-12 and IL-23: master regulators of innate and adaptive immunity," *Immunological Reviews*, vol. 202, pp. 96–105, 2004.

[14] J. W. Lee, P. Wang, M. G. Kattah et al., "Differential regulation of chemokines by IL-17 in colonic epithelial cells," *Journal of Immunology*, vol. 181, no. 9, pp. 6536–6545, 2008.

[15] N. J. Wilson, K. Boniface, J. R. Chan et al., "Development, cytokine profile and function of human interleukin 17-producing helper T cells," *Nature Immunology*, vol. 8, no. 9, pp. 950–957, 2007.

[16] M. Pelletier, L. Maggi, A. Micheletti et al., "Evidence for a cross-talk between human neutrophils and Th17 cells," *Blood*, vol. 115, no. 2, pp. 335–343, 2010.

[17] J. Kawanokuchi, K. Shimizu, A. Nitta et al., "Production and functions of IL-17 in microglia," *Journal of Neuroimmunology*, vol. 194, no. 1-2, pp. 54–61, 2008.

[18] S. Haak, A. L. Croxford, K. Kreymborg et al., "IL-17A and IL-17F do not contribute vitally to autoimmune neuro-inflammation in mice," *Journal of Clinical Investigation*, vol. 119, no. 1, pp. 61–69, 2009.

[19] H. Park, Z. Li, X. O. Yang et al., "A distinct lineage of CD4 T cells regulates tissue inflammation by producing interleukin 17," *Nature Immunology*, vol. 6, no. 11, pp. 1133–1141, 2005.

[20] S. Aggarwal, N. Ghilardi, M. Xie, F. J. De Sauvage, and A. L. Gurney, "Interleukin-23 promotes a distinct CD4 T cell activation state characterized by the production of interleukin-17," *Journal of Biological Chemistry*, vol. 278, no. 3, pp. 1910–1914, 2003.

[21] C. Wu, N. Yosef, T. Thalhamer et al., "Induction of pathogenic TH17 cells by inducible salt-sensing kinase SGK1," *Nature*, vol. 496, no. 7446, pp. 513–517, 2013.

[22] C. L. Langrish, Y. Chen, W. M. Blumenschein et al., "IL-23 drives a pathogenic T cell population that induces autoimmune inflammation," *Journal of Experimental Medicine*, vol. 201, no. 2, pp. 233–240, 2005.

[23] Y. Chen, C. L. Langrish, B. Mckenzie et al., "Anti-IL-23 therapy inhibits multiple inflammatory pathways and ameliorates autoimmune encephalomyelitis," *Journal of Clinical Investigation*, vol. 116, no. 5, pp. 1317–1326, 2006.

[24] A. Reboldi, C. Coisne, D. Baumjohann et al., "C-C chemokine receptor 6-regulated entry of TH-17 cells into the CNS through the choroid plexus is required for the initiation of EAE," *Nature Immunology*, vol. 10, no. 5, pp. 514–523, 2009.

[25] E. Ambrosini, S. Columba-Cabezas, B. Serafini, A. Muscella, and F. Aloisi, "Astrocytes are the major intracerebral source of macrophage inflammatory protein-3α/CCL20 in relapsing experimental autoimmune encephalomyelitis and in vitro," *GLIA*, vol. 41, no. 3, pp. 290–300, 2003.

[26] K. Hirota, H. Yoshitomi, M. Hashimoto et al., "Preferential recruitment of CCR6-expressing Th17 cells to inflamed joints via CCL20 in rheumatoid arthritis and its animal model," *Journal of Experimental Medicine*, vol. 204, no. 12, pp. 2803–2812, 2007.

[27] T. Korn, E. Bettelli, M. Oukka, and V. K. Kuchroo, "IL-17 and Th17 cells," *Annual Review of Immunology*, vol. 27, pp. 485–517, 2009.

[28] M. Roy, J. F. Richard, A. Dumas, and L. Vallières, "CXCL1 can be regulated by IL-6 and promotes granulocyte adhesion to brain capillaries during bacterial toxin exposure and encephalomyelitis," *Journal of Neuroinflammation*, vol. 9, p. 18, 2012.

[29] A. R. Glabinski, V. K. Tuohy, and R. M. Ransohoff, "Expression of chemokines RANTES, MIP-1α and GRO-α correlates with inflammation in acute experimental autoimmune encephalomyelitis," *NeuroImmunoModulation*, vol. 5, no. 3-4, pp. 166–171, 1998.

[30] A. Glabinski, B. Bielecki, and R. M. Ransohoff, "Chemokine upregulation follows cytokine expression in chronic relapsing experimental autoimmune encephalomyelitis," *Scandinavian Journal of Immunology*, vol. 58, no. 1, pp. 81–88, 2003.

[31] S. R. McColl, M. A. Staykova, A. Wozniak, S. Fordham, J. Bruce, and D. O. Willenborg, "Treatment with anti-granulocyte antibodies inhibits the effector phase of experimental autoimmune encephalomyelitis," *Journal of Immunology*, vol. 161, no. 11, pp. 6421–6426, 1998.

[32] L. Liu, L. Darnall, T. Hu, K. Choi, T. E. Lane, and R. M. Ransohoff, "Myelin repair is accelerated by inactivating CXCR2 on nonhematopoietic cells," *Journal of Neuroscience*, vol. 30, no. 27, pp. 9074–9083, 2010.

[33] A. E. Kerstetter, D. A. Padovani-Claudio, L. Bai, and R. H. Miller, "Inhibition of CXCR2 signaling promotes recovery in models of multiple sclerosis," *Experimental Neurology*, vol. 220, no. 1, pp. 44–56, 2009.

[34] M. Matloubian, A. David, S. Engel, J. E. Ryan, and J. G. Cyster, "A transmembrane CXC chemokine is a ligand for HIV-coreceptor Bonzo," *Nature Immunology*, vol. 1, no. 4, pp. 298–304, 2000.

[35] J. V. Kim, N. Jiang, C. E. Tadokoro et al., "Two-photon laser scanning microscopy imaging of intact spinal cord and cerebral cortex reveals requirement for CXCR6 and neuroinflammation in immune cell infiltration of cortical injury sites," *Journal of Immunological Methods*, vol. 352, no. 1-2, pp. 89–100, 2010.

[36] N. Fukumoto, T. Shimaoka, H. Fujimura et al., "Critical roles of CXC chemokine ligand 16/scavenger receptor that binds phosphatidylserine and oxidized lipoprotein in the pathogenesis of both acute and adoptive transfer experimental autoimmune encephalomyelitis," *Journal of Immunology*, vol. 173, no. 3, pp. 1620–1627, 2004.

Hindawi Publishing Corporation
Mediators of Inflammation
Volume 2014, Article ID 590654, 9 pages
http://dx.doi.org/10.1155/2014/590654

Research Article

Regulation of Chemokine CCL5 Synthesis in Human Peritoneal Fibroblasts: A Key Role of IFN-γ

Edyta Kawka,[1,2] Janusz Witowski,[1,2] Nina Fouqet,[1] Hironori Tayama,[1] Thorsten O. Bender,[1] Rusan Catar,[1] Duska Dragun,[1] and Achim Jörres[1]

[1] *Department of Nephrology and Medical Intensive Care, Charité-Universitätsmedizin Berlin, Campus Virchow-Klinikum, Augustenburger Platz 1, 13353 Berlin, Germany*
[2] *Department of Pathophysiology, Poznan University of Medical Sciences, Swiecickiego 6, 60-781 Poznań, Poland*

Correspondence should be addressed to Achim Jörres; achim.joerres@charite.de

Received 6 September 2013; Revised 8 December 2013; Accepted 12 December 2013; Published 9 January 2014

Academic Editor: Salahuddin Ahmed

Peritonitis is characterized by a coordinated influx of various leukocyte subpopulations. The pattern of leukocyte recruitment is controlled by chemokines secreted primarily by peritoneal mesothelial cells and macrophages. We have previously demonstrated that some chemokines may be also produced by human peritoneal fibroblasts (HPFB). Aim of our study was to assess the potential of HPFB in culture to release CCL5, a potent chemoattractant for mononuclear leukocytes. Quiescent HPFB released constitutively no or trace amounts of CCL5. Stimulation of HPFB with IL-1β and TNF-α resulted in a time- (up to 96 h) and dose-dependent increase in CCL5 expression and release. IFN-γ alone did not induce CCL5 secretion over a wide range of concentrations (0.01–100 U/mL). However, it synergistically amplified the effects of TNF-α and IL-1β through upregulation of CCL5 mRNA. Moreover, pretreatment of cells with IFN-γ upregulated CD40 receptor, which enabled HPFB to respond to a recombinant ligand of CD40 (CD40L). Exposure of IFN-γ-treated HPFB, but not of control cells, to CD40L resulted in a dose-dependent induction of CCL5. These data demonstrate that HPFB synthesise CCL5 in response to inflammatory mediators present in the inflamed peritoneal cavity. HPFB-derived CCL5 may thus contribute to the intraperitoneal recruitment of mononuclear leukocytes during peritonitis.

1. Introduction

Peritoneal dialysis (PD) is an effective alternative to haemodialysis as a life-saving renal replacement therapy for patients with chronic kidney disease. However, the technique may fail as a result of repeated episodes of peritoneal infection that lead to peritoneal membrane damage and loss of its ultrafiltration capacity [1, 2]. The peritoneal cavity contains normally variable numbers of resident leukocytes, predominantly macrophages but also lymphocytes (mostly memory T cells), dendritic, and natural killer (NK) cells [3]. In contrast, acute peritonitis is characterized by a massive influx of polymorphonuclear leukocytes (PMN) [4]. PMN ingest invading microorganisms and then are gradually cleared and replaced by mononuclear cells (monocytes, macrophages, and lymphocytes) so that the intraperitoneal homeostasis is restored. The whole process is governed by a complex network of cytokines, growth factors, adhesion molecules, and molecules derived from pathogens and damaged cells [5]. In this respect, chemokines of various classes create chemotactic gradients that mediate migration of specific leukocyte subpopulations into the peritoneal cavity. In early stages of peritonitis proinflammatory cytokines (TNF-α and IL-1β) derived from resident macrophages induce the expression of CXC chemokines that attract PMN. Then, upon the influence of IFN-γ and IL-6, the pattern of chemokine expression changes so that CC chemokines predominate and mediate mononuclear cell recruitment [6].

During peritonitis chemokines are produced mainly by cytokine-stimulated mesothelial cells that cover the peritoneal membrane. However, in recent years it has become clear that fibroblasts embedded in peritoneal interstitium act not only as structural cells but may also serve as an important source of chemokines [7]. Thus, by producing various chemokines fibroblasts may modify both the intensity and the duration of the inflammatory response [8]. We have previously demonstrated that human peritoneal fibroblasts (HPFB) generate significant quantities of CXC

chemokines that attract and promote survival of PMN during PD-associated peritonitis [9]. Moreover, HPFB are able to produce CCL2, which belongs to CC chemokines and acts mainly as a monocyte chemoattractant [7].

CCL5 (CC-chemokine ligand 5) is another member of the CC chemokine family. First identified in T cells and designated RANTES (Regulated upon Activation, Normal T cell Expressed and Secreted), CCL5 is an 8 kDa protein consisting of 68 amino acids [10]. In addition to lymphocytes, it was found to be also produced by stromal cells. Acting through three types of chemokine receptors (CCR1, CCR3, and CCR5), CCL5 is broadly chemoattractive for T lymphocytes and NK cells, monocytes, basophils, and eosinophils [11]. Interestingly, once T lymphocytes reach the site of injury and become activated with specific antigens, they start producing large amounts of CCL5 after 3–5 days, which maintains and amplifies the immune response. Although there is a great deal of overlapping in biological activities of CC chemokines, the experimental studies in mice demonstrate that CCL5 deficiency is associated with impaired T-cell proliferation and function [12]. This observation indicates that CCL5 is uniquely essential for T-cell recruitment in vivo. Therefore, in the present study we have analysed how proinflammatory cytokines known to be present in the inflamed peritoneum regulate CCL5 production by peritoneal fibroblasts.

2. Materials and Methods

Unless stated otherwise, all chemicals were from Sigma-Aldrich (St Louis, MO, USA) and all culture plastics were Falcon from Becton Dickinson (Heidelberg, Germany). Cell culture media and foetal calf serum (FCS) were from Invitrogen/Life Technologies (Darmstadt, Germany), and other cell culture reagents were from Biochrom AG (Berlin, Germany). Human recombinant cytokines and anticytokine antibodies were from R&D Systems (Wiesbaden, Germany). IFN-γ specific activity was 2×10^4 WHO standard units per 1 μg protein (1 U/mL = 50 pg/mL).

2.1. Isolation and Culture of Human Peritoneal Fibroblasts (HPFB). HPFB were isolated from the specimens of apparently normal omentum obtained from consenting patients undergoing elective abdominal surgery. The tissue was treated with four rounds of digestion with trypsin, as described in detail elsewhere [13]. HPFB were identified by spindle-shape appearance, formation of parallel arrays and whorls at confluence [13], and positive immunostaining for fibroblast specific protein 1 (FSP-1) [14]. Cells were propagated in Ham's F12 culture medium supplemented with penicillin (100 U/mL), streptomycin (100 μg/mL), hydrocortisone (0.4 μg/mL), and 10% (v/v) FCS. HPFB cultures were maintained at 37°C in a humidified atmosphere of 95% air and 5% CO_2. All experiments were performed using cells from the first 3 passages and with cells derived from separate donors. Before the experiments, cells were rendered quiescent by reducing FCS concentration to 0.1% for 48 hours. Cells were then treated as specified in the figure legends. After the exposure, the supernatants were collected and stored in aliquots at −80°C until assayed.

2.2. CCL5 Protein Measurement. Concentrations of CCL5 protein secreted by HPFB were measured with the DuoSet Immunoassay Development Kit (R&D Systems). The assay was designed and performed according to the manufacturer's instructions. Sensitivity of the assay was 5 pg/mL.

2.3. Gene Expression Analysis. Expression of CCL5 gene was assessed with reverse transcription (RT) and PCR. Total RNA was extracted with RNA Bee (Tel-Test, Friendswood, TX, USA), purified with the RNeasy kit (Qiagen, Hamburg, Germany), and reverse transcribed into cDNA with random hexamer primers, as described in [15]. Conventional semi-quantitive PCR was carried out essentially as described by Robson et al. for CCL5 and β-actin [16], and by Abdel-Haq et al. for CD40 [17]. Precise quantitation of CCL5 mRNA was performed by real-time PCR. The reactions were carried out in Roche LightCycler II using 20 ng of cDNA and FastStart DNA Master SYBR Green I reagents according to the manufacturer's instructions (Roche Applied Science, Indianapolis, IN, USA). Primer pairs (TIB Molbiol, Berlin, Germany) spanned an intron to eliminate potential amplification of contaminating genomic DNA. The following primers were used: CCL5 (GenBank NM_002985.2) forward, GAGTATTTCTACACCAGTGGCAAG; reverse, TCCCGAACCCATTTCTTCTCT; GAPDH (GenBank NM_002046.4) forward, TGATGACATCAAGAAGGTGGTGAAG; reverse, TCCTTGGAGGCCATGTGGGCCAT. Cycle parameters were as follows: denaturation at 95°C for 10 s, annealing at 63°C for 5 s, and elongation at 72°C for 20 s for 40 cycles. Melting curve analyses were performed from 60°C to 95°C in 0.5°C increments. Quantitative PCR data for CCL5 were normalized based on GAPDH transcript levels. Run data were analysed by "second derivative maximum" with the quantification program Quant versions 2.7 and 3.0.

2.4. Statistical Analysis. Data are presented as mean ± SEM of the results obtained in independent experiments with cells from different donors. Statistical analyses were carried out using GraphPad Prism 5.00 software (GraphPad Software Inc., La Jolla, CA, USA). The data were compared with repeated measures analysis of variance with Newman-Keuls modification or the paired t-test, as appropriate. A P value of <0.05 was considered significant. Significant differences compared with appropriate controls were denoted with asterisks: $^{*}P < 0.05$; $^{**}P < 0.01$; $^{***}P < 0.001$.

3. Results

3.1. Induction of CCL5 Production in HPFB by IL-1β and TNF-α. The amount of CCL5 released constitutively by quiescent HPFB was barely detectable (Figure 1). In contrast, stimulation of HPFB with recombinant proinflammatory cytokines IL-1β and TNF-α resulted in a time- and dose-dependent CCL5 secretion. The release of CCL5 in response to IL-1β was significantly above the background levels within 12–24 hours of incubation and reached plateau after 72 hours. The time course of CCL5 generation in response to the same concentration of TNF-α followed a similar pattern; however, even greater amounts of CCL5 were produced (Figure 1(a)).

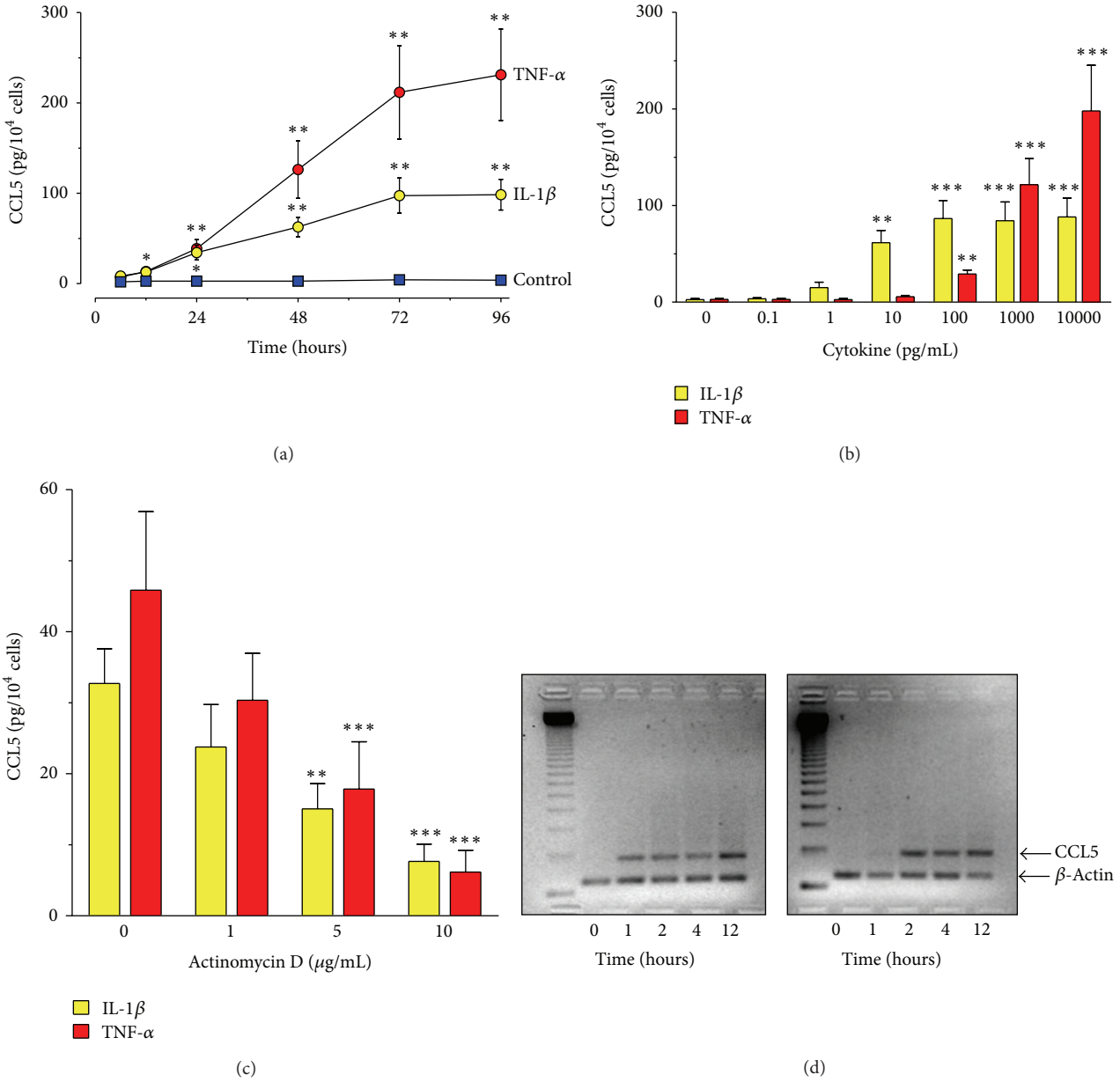

FIGURE 1: Effect of recombinant IL-1β and TNF-α on CCL5 expression and release by HPFB. Cells were exposed to either IL-1β or TNF-α. The data were derived from experiments with cells isolated from separate donors. (a) Kinetics of IL-1β-induced (1000 pg/mL) or TNF-α-induced (1000 pg/mL) CCL5 secretion ($n = 6$); (b) dose effect of IL-1β or TNF-α. Cells were stimulated for 48 hours ($n = 6$); (c) effect of actinomycin D on CCL5 release by HPFB. Cells were pretreated for 1 hour with actinomycin D and then exposed to either IL-1β or TNF-α (both at 1000 pg/mL) for 24 hours ($n = 6$); (d) time effect of IL-1β and TNF-α on CCL5 mRNA expression. HPFB were treated with cytokines at 1000 pg/mL for the times indicated. CCL5 mRNA expression was analysed by semiquantitative RT-PCR. Results of a representative experiment of three performed.

Experiments assessing the dose effect of cytokines revealed that IL-1β was effective already at concentrations as low as 1 pg/mL and the effect reached saturation at 100 pg/mL (Figure 1(b)). TNF-α was able to stimulate CCL5 release at concentrations ranging from 100 to 10000 pg/mL.

Pretreatment of HPFB with actinomycin D resulted in a dose-dependent inhibition of cytokine-induced CCL5 secretion, indicating that the stimulatory effects of IL-1β and TNF-α occurred at the transcriptional level (Figure 1(c)). Indeed, treatment of HPFB with either IL-1β or TNF-α resulted in a time-dependent upregulation of the CCL5 mRNA signal, as visualized by conventional semiquantitative PCR (Figure 1(d)).

3.2. Effect of IFN-γ on CCL5 Production by HPFB. IFN-γ at concentrations ranging from 0.01 to 100 U/mL did not induce CCL5 production by HPFB. However, it amplified synergistically CCL5 release induced by TNF-α (Figure 2)

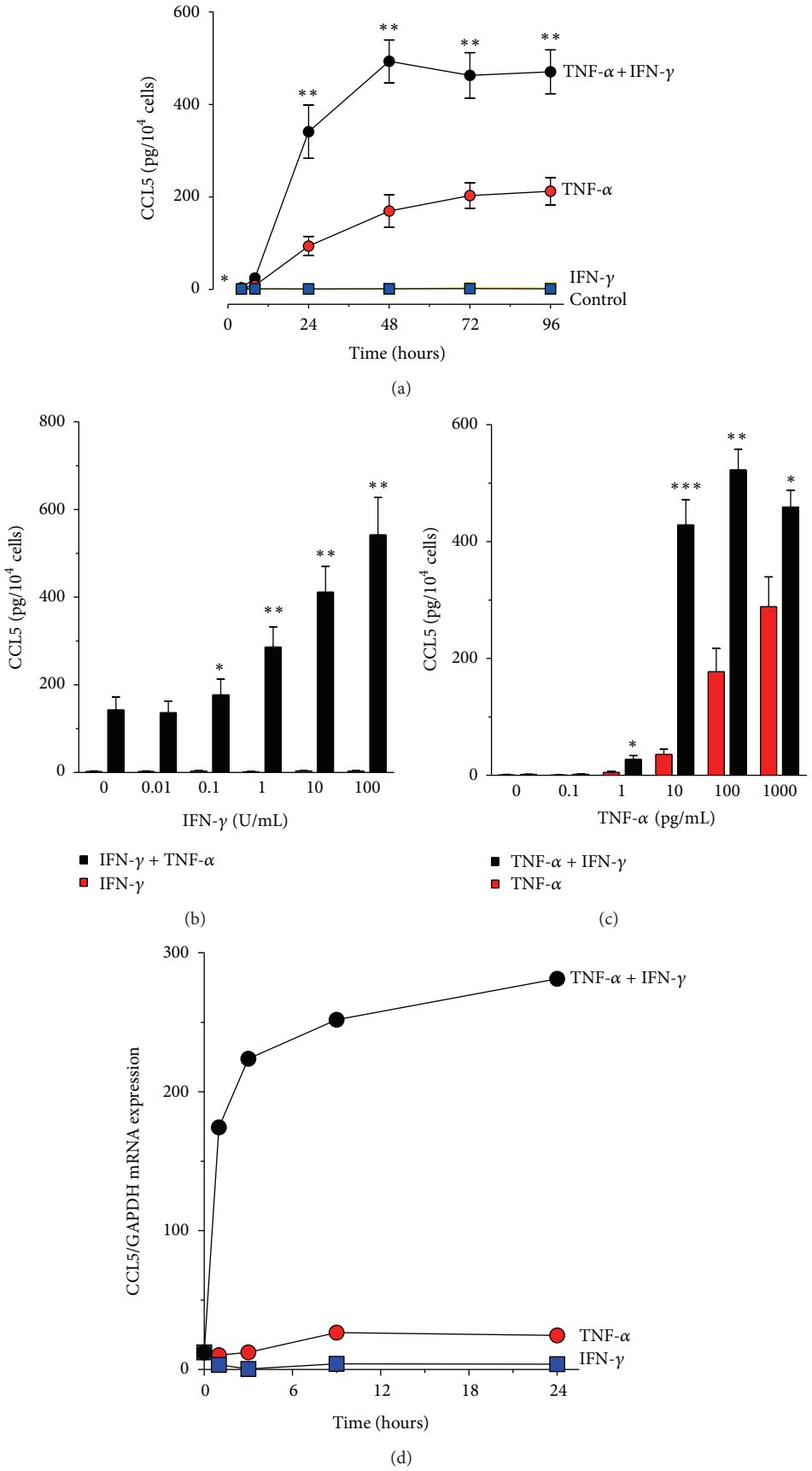

Figure 2: Continued.

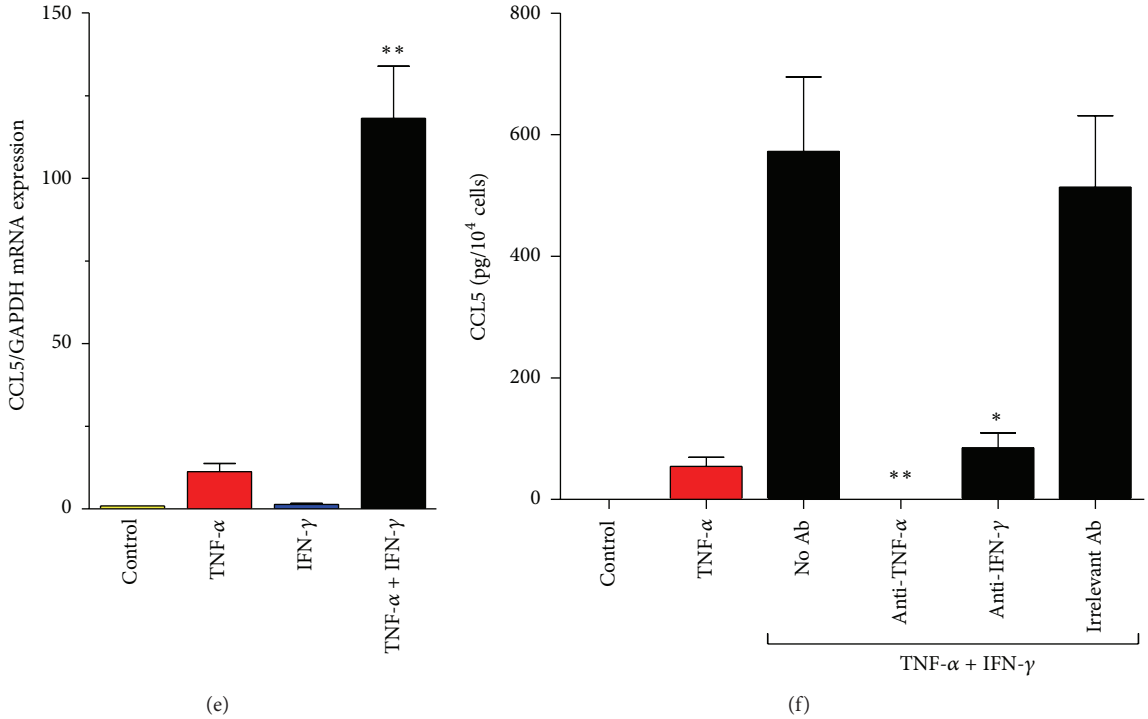

Figure 2: CCL5 induction in HPFB stimulated with TNF-α and IFN-γ. (a) Kinetics of CCL5 secretion by HPFB treated with TNF-α (1000 pg/mL) and IFN-γ (25 U/mL) alone or in combination. Asterisks represent a significant difference compared with the predictive additive values at each time point ($n = 6$); (b) dose effect of IFN-γ alone or with TNF-α (1000 pg/mL; $n = 7$); (c) dose effect of TNF-α alone or with IFN-γ (25 U/mL; $n = 5$). B and C cells were stimulated for 48 hours. Asterisks represent statistically significant differences compared to the predictive additive values; (d) kinetics of TNF-α and IFN-γ-induced CCL5 mRNA. Cells were treated with TNF-α and/or IFN-γ for the times indicated. Results of an exemplary experiment of two performed; (e) magnitude of CCL5 mRNA expression in HPFB treated for 24 hours with TNF-α and/or IFN-γ. Results of 4 experiments with cells from separate donors. Asterisks represent a significant difference compared to the predictive additive value. D and E cells were treated with TNF-α at 1000 pg/mL and IFN-γ at 25 U/mL. CCL5 mRNA expression relative to that of GAPDH was quantified with real-time PCR; (f) effect of neutralizing anti-TNF-α or anti-IFN-γ antibodies on synergistic CCL5 release by HPFB. Cells were incubated with antibodies (all at 1 μg/mL) for 48 h. Asterisks represent a significant difference compared with cells treated with a combination of TNF-α (1000 pg/mL) and IFN-γ (25 U/mL) in the absence of antibodies ($n = 4$).

and—to lesser extent—by IL-1β (not shown). The effect was time-dependent (Figure 2(a)) and related to the dose of both IFN-γ and TNF-α (Figures 2(b) and 2(c)). Concentration of IFN-γ as low as 0.1 U/mL was capable of amplifying the effect of 1000 pg/mL TNF-α. On the other hand, 25 U/mL IFN-γ magnified the effect exerted by 10 pg/mL TNF-α more than 10-fold.

Although IFN-γ alone did not induce CCL5 mRNA, it produced a rapid (within 1 hour) synergistic increase in TNF-α-driven CCL5 expression, which persisted over 24 hours (Figure 2(d)). Quantitative assessment showed that CCL5 mRNA expression in response to a combination of TNF-α + IFN-γ was approximately 10-fold greater than that induced by TNF-α alone (Figure 2(e)).

3.3. Specificity and Timing of the Effects of IFN-γ and TNF-α on CCL5 Release by HPFB. Specificity of the combined stimulation by IFN-γ and TNF-α was verified in experiments using blocking antibodies. Neutralization of IFN-γ decreased CCL5 production to a level achieved by treatment with TNF-α alone (Figure 2(f)). In turn, anti-TNF-α antibodies totally abolished CCL5 secretion in response to TNF-α + IFN-γ. Control antibody of the same class did not affect CCL5 release. To determine whether the synergistic effect of TNF-α and IFN-γ was related to the sequence of stimuli, HPFB were incubated in the presence or absence of TNF-α or IFN-γ for 24 hours, then washed, and stimulated again for further 24 hours (Table 1). These experiments showed some degree of priming with either TNF-α or IFN-γ. However, the greatest synergy was observed when both cytokines were applied together. Interestingly, the effect of combined stimulation with TNF-α and IFN-γ for the first 24 hours still persisted during the next 24 hours, even in the absence of cytokines.

3.4. Effect of CD40 Ligand (CD40L) on CCL5 Induction in HPFB. CD40L, a member of the TNF-α family, is expressed by mononuclear cells infiltrating the peritoneum during peritonitis [18]. We have therefore examined if CD40L is able to induce CCL5 in HPFB. It turned out that CD40L had almost no effect in control cells but stimulated dose-dependent CCL5 release in HPFB pretreated with IFN-γ (Figure 3). We have then used PCR to assess the expression in HPFB of CD40, a receptor for CD40L. Unstimulated cells did not express CD40 mRNA; however its presence could be

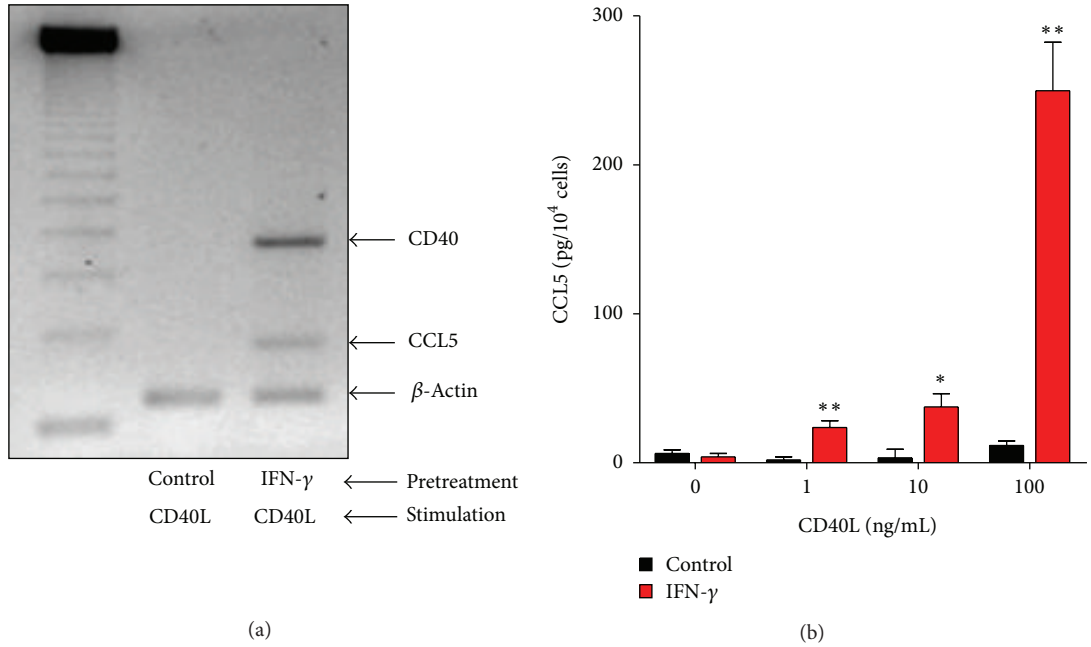

Figure 3: Effect of preexposure to IFN-γ on CD40L-induced CCL5 expression and release by HPFB. Cells were pretreated for 48 hours either with control medium or IFN-γ (100 U/mL). After that cells were stimulated with CD40L for the next 24 hours. (a) Expression of mRNA for CD40 and CCL5 was assessed by conventional RT-PCR. Results of a representative experiment of two performed. (b) CCL5 release was measured in HPFB cultures established from 5 separate donors. Asterisks represent a significant difference compared to cells not exposed to IFN-γ.

Table 1: Effect of sequential addition of TNF-α and IFN-γ on CCL5 release by HPFB.

Stimulus 1	Stimulus 2	CCL5 (pg/10^4 cells)
Medium	Medium	Undetectable
Medium	IFN-γ	Undetectable
Medium	TNF-α	4 ± 2
Medium	TNF-α + IFN-γ	24 ± 13
IFN-γ	Medium	1 ± 1
IFN-γ	TNF-α	9 ± 4
TNF-α	Medium	6 ± 4
TNF-α	IFN-γ	9 ± 7
TNF-α + IFN-γ	Medium	146 ± 20

Cells were incubated with TNF-α (1000 pg/mL) and/or IFN-γ (25 U/mL) for 24 hours (stimulus 1), washed, and incubated again for the next 24 hours in the presence or absence of these cytokines (stimulus 2). Data were derived from two independent experiments.

detected following the treatment with IFN-γ. Accordingly, subsequent stimulation with CD40L induced CCL5 mRNA expression in cells pretreated with IFN-γ.

4. Discussion

The ability of chemokines to recruit specific leukocyte subpopulations is crucial for controlling the course of inflammatory response. Thus, the regulation of chemokine production is equally important. We have shown that peritoneal fibroblasts produce significant quantities of chemokine CCL5. This observation is in keeping with the view of fibroblasts as sentinel cells providing address codes for migrating leukocytes [19]. It has previously been shown that peritoneal mesothelial cells synthesize CCL5 in response to inflammatory cytokines [16, 20, 21]. However, peritonitis may result in serious mesothelial cell damage and exfoliation [22, 23]. The function of peritoneal fibroblasts may then become essential, providing an alternative and/or additional source of chemokines. Although CCL5 production has been demonstrated in fibroblast from other locations, such as pancreas [24], skin [25, 26], gingiva [27], nasal mucosa [28, 29], and synovium [30], it is important to study the function of fibroblasts derived precisely from the tissue of interest. It is because fibroblasts display tissue-specific phenotypes that include different patterns of chemokine expression [31, 32], which may contribute to characteristic composition of leukocyte infiltrates.

Here, we show that HPFB in culture do not release CCL5 constitutively but are capable of producing this chemokine de novo in response to stimulation with proinflammatory cytokines IL-1β and TNF-α. Of those, TNF-α appears to be a more potent stimulus, which is in contrast to its effect on CXC chemokines, whose production in HPFB was found to be induced primarily by IL-1β [9]. This differential responsiveness to IL-1β and TNF-α may provide yet another level of regulation to chemokine release by HPFB.

CCL5 mediates the influx of mononuclear cells, including T cells, which are the main source of IFN–γ in the dialysed peritoneum [33]. IFN-γ can further amplify CCL5 production through synergistic induction of CCL5 mRNA. Interestingly, IFN-γ exerted this effect despite the fact that

when acting on its own, it did not stimulate CCL5. Similar results were observed in mesothelial cells [16], synovial fibroblasts [34], endothelial cells [35], and alveolar epithelial cells [36]. In contrast, in mouse macrophages IFN-γ was found to directly induce CCL5 [37]. Early induction of CCL5 gene in response to TNF-α and IFN-γ suggests that the effect is mediated by rapidly activated transcription factors that bind to CCL5 promoter. In this respect, nuclear factor κB (NF-κB) was found to be a chief mediator involved [36, 38]. It may further cooperate with interferon regulatory factors (IRF) [39, 40] and signal transducers and activators of transcription (STATs) [38].

In addition to T-cells, CCL5 attracts also eosinophils. This feature is interesting, as peritoneal eosinophilia may occur in the course of peritoneal dialysis [41] and may be related to exposure of the peritoneal membrane to foreign environment [42]. Interestingly, it has been demonstrated in an animal model of peritoneal dialysis that peritoneal eosinophilia and CCL5 elevation was particularly pronounced after exposure to dialysis fluids regarded as less biocompatible [43].

CCL5-induced leukocyte infiltrate contains T-lymphocytes that express a membrane-bound CD40L [18]. It has been demonstrated that fibroblasts from various sources express no or very little CD40 mRNA; however, it can be upregulated through IFN-γ [44]. This effect corresponds to an increase in CD40 cell surface expression [44–46]. We have found that exposure to IFN-γ increased CD40 expression in HPFB and made them responsive to CD40L. Ligation of thus induced CD40 by CD40L resulted in increased CCL5 production. Such an effect was observed previously in fibroblasts from inflamed colonic mucosa [47], but also in peritoneal mesothelial cells [45]. The underlying mechanism most likely involves NF-κB, which was shown to be activated by CD40 ligation [46]. CD40L-induced CCL5 may create positive feedback loop that further supports lymphocyte influx. In this respect, it has been shown that increased CD40L expression on peritoneal lymphocytes and macrophages supports the transition to mononuclear cell predominance in the late phase of peritonitis and timely resolution of inflammation [18].

In conclusion, our study demonstrates the great potential of peritoneal fibroblasts to generate CCL5 in response to activation by proinflammatory mediators encountered during peritonitis. By establishing a CCL5 gradient, HPFB may facilitate mononuclear leukocyte recruitment and successful resolution of inflammation. On the other hand, repeated and/or severe episodes of infection may injure the protective mesothelium and expose underlying HPFB to excessive stimulation. In those circumstances, HPFB-derived CCL5 may promote leukocyte infiltration into the peritoneal interstitium, which may lead to prolonged inflammation. In both scenarios HPFB would be actively involved in the cytokine network controlling the course of inflammation.

Conflict of Interests

The authors declare that there is no conflict of interests regarding the publication of this paper.

Authors' Contribution

Edyta Kawka and Janusz Witowski contributed equally to this study.

Acknowledgment

Edyta Kawka, Janusz Witowski, and Achim Jörres were supported by the European Training & Research in Peritoneal Dialysis (EuTRiPD) Programme, a project funded by the European Union within the Marie Curie scheme (No. 287813).

References

[1] P. J. Margetts and D. N. Churchill, "Acquired ultrafiltration dysfunction in peritoneal dialysis patients," *Journal of the American Society of Nephrology*, vol. 13, no. 11, pp. 2787–2794, 2002.

[2] G. Baroni, A. Schuinski, T. P. de Moraes et al., "Inflammation and the peritoneal membrane: causes and impact on structure and function during peritoneal dialysis," *Mediators of Inflammation*, vol. 2012, Article ID 912595, 4 pages, 2012.

[3] U. Kubicka, W. L. Olszewski, W. Tarnowski, K. Bielecki, A. Ziółkowska, and Z. Wierzbicki, "Normal human immune peritoneal cells: subpopulations and functional characteristics," *Scandinavian Journal of Immunology*, vol. 44, no. 2, pp. 157–163, 1996.

[4] T. Cichocki, Z. Hanicki, and W. Sulowicz, "Output of peritoneal cells into peritoneal dialysate. Cytochemical and functional studies," *Nephron*, vol. 35, no. 3, pp. 175–182, 1983.

[5] B. Geering, C. Stoeckle, S. Conus, and H. U. Simon, "Living and dying for inflammation: neutrophils, eosinophils, basophils," *Trends in Immunology*, vol. 34, no. 8, pp. 398–409, 2013.

[6] O. Devuyst, P. J. Margetts, and N. Topley, "The pathophysiology of the peritoneal membrane," *Journal of the American Society of Nephrology*, vol. 21, no. 7, pp. 1077–1085, 2010.

[7] J. Witowski, A. Thiel, R. Dechend et al., "Synthesis of C-X-C and C-C chemokines by human peritoneal fibroblasts: induction by macrophage-derived cytokines," *American Journal of Pathology*, vol. 158, no. 4, pp. 1441–1450, 2001.

[8] G. Parsonage, A. D. Filer, O. Haworth et al., "A stromal address code defined by fibroblasts," *Trends in Immunology*, vol. 26, no. 3, pp. 150–156, 2005.

[9] J. Witowski, H. Tayama, K. Ksiek, M. Wanic-Kossowska, T. O. Bender, and A. Jörres, "Human peritoneal fibroblasts are a potent source of neutrophil-targeting cytokines: a key role of IL-1B stimulation," *Laboratory Investigation*, vol. 89, no. 4, pp. 414–424, 2009.

[10] V. Appay and S. L. Rowland-Jones, "RANTES: a versatile and controversial chemokine," *Trends in Immunology*, vol. 22, no. 2, pp. 83–87, 2001.

[11] A. M. Krensky and Y.-T. Ahn, "Mechanisms of disease: regulation of RANTES (CCL5) in renal disease," *Nature Clinical Practice Nephrology*, vol. 3, no. 3, pp. 164–170, 2007.

[12] Y. Makino, D. N. Cook, O. Smithies et al., "Impaired T cell function in RANTES-deficient mice," *Clinical Immunology*, vol. 102, no. 3, pp. 302–309, 2002.

[13] A. Jörres, K. Ludat, J. Lang et al., "Establishment and functional characterization of human peritoneal fibroblasts in culture:

regulation of interleukin-6 production by proinflammatory cytokines," *Journal of the American Society of Nephrology*, vol. 7, no. 10, pp. 2192–2201, 1996.

[14] R. Catar, J. Witowski, P. Wagner et al., "The proto-oncogene c-Fos transcriptionally regulates VEGF production during peritoneal inflammation," *Kidney International*, vol. 84, pp. 1119–1128, 2013.

[15] A. Jörres, H. Dinter, N. Topley, G. M. Gahl, U. Frei, and P. Scholz, "Inhibition of tumour necrosis factor production in endotoxin-stimulated human mononuclear leukocytes by the prostacyclin analogue iloprost: cellular mechanisms," *Cytokine*, vol. 9, no. 2, pp. 119–125, 1997.

[16] R. L. Robson, R. M. McLoughlin, J. Witowski et al., "Differential regulation of chemokine production in human peritoneal mesothelial cells: IFN-γ controls neutrophil migration across the mesothelium in vitro and in vivo," *Journal of Immunology*, vol. 167, no. 2, pp. 1028–1038, 2001.

[17] N. Abdel-Haq, H.-N. Hao, and W. D. Lyman, "Cytokine regulation of CD40 expression in fetal human astrocyte cultures," *Journal of Neuroimmunology*, vol. 101, no. 1, pp. 7–14, 1999.

[18] A. Glik, J. Mazar, B. Rogachev, M. Zlotnik, and A. Douvdevani, "CD40 ligand expression correlates with resolution of peritonitis and mononuclear cell recruitment," *Peritoneal Dialysis International*, vol. 25, no. 3, pp. 240–247, 2005.

[19] H. M. McGettrick, C. D. Buckley, A. Filer, G. Ed Rainger, and G. B. Nash, "Stromal cells differentially regulate neutrophil and lymphocyte recruitment through the endothelium," *Immunology*, vol. 131, no. 3, pp. 357–370, 2010.

[20] C. E. Visser, J. Tekstra, J. J. E. Brouwer-Steenbergen et al., "Chemokines produced by mesothelial cells: huGRO-α, IP-10, MCP-1 and RANTES," *Clinical and Experimental Immunology*, vol. 112, no. 2, pp. 270–275, 1998.

[21] F. K. Li, A. Davenport, R. L. Robson et al., "Leukocyte migration across human peritoneal mesothelial cells is dependent on directed chemokine secretion and ICAM-1 expression," *Kidney International*, vol. 54, no. 6, pp. 2170–2183, 1998.

[22] J. D. Williams, K. J. Craig, C. Von Ruhland, N. Topley, and G. T. Williams, "The natural course of peritoneal membrane biology during peritoneal dialysis," *Kidney International, Supplement*, vol. 64, no. 88, pp. S43–S49, 2003.

[23] B. Haslinger-Löffler, B. Wagner, M. Brück et al., "Staphylococcus aureus induces caspase-independent cell death in human peritoneal mesothelial cells," *Kidney International*, vol. 70, no. 6, pp. 1089–1098, 2006.

[24] A. Andoh, H. Takaya, T. Saotome et al., "Cytokine regulation of chemokine (IL-8, MCP-1, and RANTES) gene expression in human pancreatic periacinar myofibroblasts," *Gastroenterology*, vol. 119, no. 1, pp. 211–219, 2000.

[25] A. Enzerink, P. Salmenperä, E. Kankuri, and A. Vaheri, "Clustering of fibroblasts induces proinflammatory chemokine secretion promoting leukocyte migration," *Molecular Immunology*, vol. 46, no. 8-9, pp. 1787–1795, 2009.

[26] D. Eyman, M. Damodarasamy, S. R. Plymate, and M. J. Reed, "CCL5 secreted by senescent aged fibroblasts induces proliferation of prostate epithelial cells and expression of genes that modulate angiogenesis," *Journal of Cellular Physiology*, vol. 220, no. 2, pp. 376–381, 2009.

[27] M. Mustafa, B. Wondimu, M. Bakhiet, and T. Modéer, "Production of Rantes/CCL5 in human gingival fibroblasts challenged with tumor necrosis factor α," *European Journal of Oral Sciences*, vol. 109, no. 1, pp. 44–49, 2001.

[28] F. Saji, M. Nonaka, and R. Pawankar, "Expression of RANTES by IL-1 β and TNF-α stimulated nasal polyp fibroblasts," *Auris Nasus Larynx*, vol. 27, no. 3, pp. 247–252, 2000.

[29] J. E. Meyer, I. Berner, L. M. Teran et al., "RANTES production by cytokine-stimulated nasal fibroblasts: its inhibition by glucocorticoids," *International Archives of Allergy and Immunology*, vol. 117, no. 1, pp. 60–67, 1998.

[30] M.-L. Cho, S.-Y. Min, S.-H. Chang et al., "Transforming growth factor beta 1(TGF-β1) down-regulates TNFα-induced RANTES production in rheumatoid synovial fibroblasts through NF-κB-mediated transcriptional repression," *Immunology Letters*, vol. 105, no. 2, pp. 159–166, 2006.

[31] K. M. Fries, T. Blieden, R. J. Looney et al., "Evidence of fibroblast heterogeneity and the role of fibroblast subpopulations in fibrosis," *Clinical Immunology and Immunopathology*, vol. 72, no. 3, pp. 283–292, 1994.

[32] G. Parsonage, F. Falciani, A. Burman et al., "Global gene expression profiles in fibroblasts from synovial, skin and lymphoid tissue levels distinct cytokine and chemokine expression patterns," *Thrombosis and Haemostasis*, vol. 90, no. 4, pp. 688–697, 2003.

[33] M. K. Dasgupta, M. Larabie, and P. F. Halloran, "Interferon-gamma levels in peritoneal dialysis effluents: relation to peritonitis," *Kidney International*, vol. 46, no. 2, pp. 475–481, 1994.

[34] P. Rathanaswami, M. Hachicha, M. Sadick, T. J. Schall, and S. R. McColl, "Expression of the cytokine RANTES in human rheumatoid synovial fibroblasts. Differential regulation of RANTES and interleukin-8 genes by inflammatory cytokines," *The Journal of Biological Chemistry*, vol. 268, no. 8, pp. 5834–5839, 1993.

[35] A. Marfaing-Koka, O. Devergne, G. Gorgone et al., "Regulation of the production of the RANTES chemokine by endothelial cells: synergistic induction by IFN-γ plus TNF-α and inhibition by IL-4 and IL-13," *Journal of Immunology*, vol. 154, no. 4, pp. 1870–1878, 1995.

[36] A. Casola, A. Henderson, T. Liu, R. P. Garofalo, and A. R. Brasier, "Regulation of RANTES promoter activation in alveolar epithelial cells after cytokine stimulation," *American Journal of Physiology*, vol. 283, no. 6, pp. L1280–L1290, 2002.

[37] J. Liu, X. Guan, and X. Ma, "Interferon regulatory factor 1 is an essential and direct transcriptional activator for interferon γ-induced RANTES/CC15 expression in macrophages," *The Journal of Biological Chemistry*, vol. 280, no. 26, pp. 24347–24355, 2005.

[38] Y. Ohmori, R. D. Schreiber, and T. A. Hamilton, "Synergy between interferon-γ and tumor necrosis factor-α in transcriptional activation is mediated by cooperation between signal transducer and activator of transcription 1 and nuclear factor κB," *The Journal of Biological Chemistry*, vol. 272, no. 23, pp. 14899–14907, 1997.

[39] A. H. Lee, J.-H. Hong, and Y.-S. Seo, "Tumor necrosis factor-α and interferon-γ synergistically activated the RANTES promoter through nuclear factor κB and interferon regulatory factor 1 (IRF-1) transcription factors," *Biochemical Journal*, vol. 350, no. 1, pp. 131–138, 2000.

[40] P. Génin, M. Algarté, P. Roof, R. Lin, and J. Hiscott, "Regulation of RANTES chemokine gene expression requires cooperativity between NF-κB, and IFN-regulatory factor transcription factors," *Journal of Immunology*, vol. 164, no. 10, pp. 5352–5361, 2000.

[41] M. Pérez Fontán, A. Rodríguez-Carmona, I. Galed, P. Iglesias, P. Villaverde, and E. García-Ureta, "Incidence and significance

of peritoneal eosinophilia during peritoneal dialysis-related peritonitis," *Peritoneal Dialysis International*, vol. 23, no. 5, pp. 460–464, 2003.

[42] C. Quinlan, M. Cantwell, and L. Rees, "Eosinophilic peritonitis in children on chronic peritoneal dialysis," *Pediatric Nephrology*, vol. 25, no. 3, pp. 517–522, 2010.

[43] K. Wieczorowska-Tobis, R. Brelinska, J. Witowski et al., "Evidence for less irritation to the peritoneal membrane in rats dialyzed with solutions low in glucose degradation products," *Peritoneal Dialysis International*, vol. 24, no. 1, pp. 48–57, 2004.

[44] K. M. Fries, G. D. Sempowski, A. A. Gaspari, T. Blieden, R. J. Looney, and R. P. Phipps, "CD40 expression by human fibroblasts," *Clinical Immunology and Immunopathology*, vol. 77, no. 1, pp. 42–51, 1995.

[45] A. Basok, A. Shnaider, L. Man, C. Chaimovitz, and A. Douvdevani, "CD40 is expressed on human peritoneal mesothelial cells and upregulates the production of interleukin-15 and RANTES," *Journal of the American Society of Nephrology*, vol. 12, no. 4, pp. 695–702, 2001.

[46] C. M. Gelbmann, S. N. Leeb, D. Vogl et al., "Inducible CD40 expression mediates NFκB activation and cytokine secretion in human colonic fibroblasts," *Gut*, vol. 52, no. 10, pp. 1448–1456, 2003.

[47] L. De, T. Karlson, C. V. Whiting, and P. W. Bland, "Proinflammatory cytokine synthesis by mucosal fibroblasts from mouse colitis is enhanced by interferon-γ-mediated up-regulation of CD40 signalling," *Clinical and Experimental Immunology*, vol. 148, no. 1, p. 188, 2007.

Hindawi Publishing Corporation
Mediators of Inflammation
Volume 2014, Article ID 659206, 8 pages
http://dx.doi.org/10.1155/2014/659206

Review Article

Chemokines and Chemokine Receptors in Multiple Sclerosis

Wenjing Cheng and Guangjie Chen

Department of Immunology and Microbiology, Shanghai JiaoTong University School of Medicine, Shanghai Institute of Immunology, Shanghai 200025, China

Correspondence should be addressed to Guangjie Chen; guangjie_chen@163.com

Received 29 July 2013; Accepted 18 December 2013; Published 2 January 2014

Academic Editor: Mohammad Athar

Multiple sclerosis is an autoimmune disease with classical traits of demyelination, axonal damage, and neurodegeneration. The migration of autoimmune T cells and macrophages from blood to central nervous system as well as the destruction of blood brain barrier are thought to be the major processes in the development of this disease. Chemokines, which are small peptide mediators, can attract pathogenic cells to the sites of inflammation. Each helper T cell subset expresses different chemokine receptors so as to exert their different functions in the pathogenesis of MS. Recently published results have shown that the levels of some chemokines and chemokine receptors are increased in blood and cerebrospinal fluid of MS patients. This review describes the advanced researches on the role of chemokines and chemokine receptors in the development of MS and discusses the potential therapy of this disease targeting the chemokine network.

1. Introduction

Multiple sclerosis (MS), which was first described by Carswell, has been believed to be a chronic neuroinflammatory autoimmune disease with a still unknown etiology [1–3]. It is characterized by central nervous system (CNS) dysfunction, visual disorder, and motor deficits. MS is the most common cause of neurological disability in young adults [4]. Typically, the disease usually starts at the age of 20–40, being twice common in women as men [5]. Although the course of MS is variable, it is believed that there are different four patterns including relapsing-remitting multiple sclerosis (RRMS), primary progressive multiple sclerosis (PPMS), secondary progressive multiple sclerosis (SPMS), and primary-relapsing multiple sclerosis (PRMS) [6–8].

The pathogenesis of MS is still not well understood. As a multifactorial disease, MS is caused by some combination factors including viral infection, environmental factors, genetic predisposition, and autoimmune inflammation. Furthermore, recent data suggest that autoimmune inflammation plays a more important role in the development of this disease [9]. Although both the humoral and cellular immune responses are involved in the demyelinated tissue in MS, it is widely held that the cellular immune response is more crucial during MS development. Owing to the blood brain barrier (BBB) and blood cerebrospinal fluid barrier (BCB) involved, which provide an anatomic barrier to prevent free exchange of some substances between cerebrospinal fluid and blood to the CNS, the pathogenesis of CNS disease is different from other inflammatory diseases [5]. In some cases such as viral infection or inflammatory stimulation, the lymphocytes, which are mostly myelin-specific T cells, can migrate through the BBB to the brain and spinal cord after being activated in periphery. And then in the CNS, these pathogenic cells are reactivated and release abundant of proinflammatory cytokines, which can specifically interact with their receptors and cause axonal damaging and demyelination. Furthermore, more and more available data suggest that chemokines and chemokine receptors participate in the recruitment of macrophages and T lymphocytes into the CNS and it has been considered the most critical mechanism in the pathogenesis of MS [10–12]. Although the migration of pathogenic cells within the CNS parenchyma is still not clearly understood, this process may be directed by chemotactic gradients created by chemokines that diffuse from sites of production at foci of inflammation [13].

2. Chemokines and Chemokine Receptors

2.1. The Chemokine Family: Subgroups and Functions. Chemokines, also known as chemoattractant cytokines, are a large group of small basic proteins with the molecular weight between 8 and 14 kDa and characterized by attracting leukocytes into the sites of inflammation and infection [14]. Monocyte-derived neutrophil chemotactic factor (MDNCF), which is a potentially mediator of leukocyte-specific inflammatory response, was firstly found by Yoshimura and his colleagues in 1987 [15]. Since then, the chemokine family have been extensively studied and more than 50 different chemokines have been identified in humans [16, 17]. Based on the number and spacing of their cysteine residues involved in the formation of disulfide bonds, chemokines are divided into five groups including CC (β-chemokines), CXC (α-chemokines), XC (δ-chemokines, often called as C subfamily), CX3C (γ-chemokines), and CX chemokine [18]. Although the chemokines of CC, CXC, and CX3C family have four cysteines, XC chemokines only have two [19]. CC chemokines, which are the largest group containing two adjacent cysteine residues near their N-terminus, its genes are clustered on chromosome 17 in humans. In CX3C and CXC chemokine subfamily, there are one or three additional amino acids (represented 3X or X in their names) separating the first two of the four cysteine residues, and most of the CXC chemokines are clustered on chromosome 4 in human [20]. The fifth subfamily CX chemokine, which has recently been identified in zebrafish by Nomiyama in 2008, lacks one of the two N-terminal cysteine residues but retains the third and fourth [18].

Besides the genome or protein structure-based classifications, chemokines can be categorized into two major groups, the homeostatic and inflammatory chemokines according to the mode of expression and function [21]. Homeostatic chemokines are those who can be constitutively expressed at noninflamed sites and involved in relocation of lymphocytes in physiological conditions, while inflammatory chemokines are expressed by related cells in inflammatory conditions and mediate emigration of leukocytes to inflamed sites.

By using some new techniques, for example, gene knockout, antibody blocking, and transgenic technology, many studies have demonstrated that chemokines are involved in many pathological and physiological processes, including T-cell differentiation and activation, cytokines secretion, tissue remodeling, tumor progression, and neural development [22–24]. Moreover, some independent researchers also found that many chemokines are associated with autoimmune diseases, including Graves' disease (GD), rheumatoid arthritis (RA), systemic lupus erythematosus (SLE), and MS [25, 26].

2.2. Chemokine Receptors: What Are They? Chemokines exert their functions through the interaction with their receptors which belong to GTP-binding protein coupled receptor [27]. Each chemokine receptor has a 7-transmembrane structure and couples to G-protein for signal transduction within a cell. The first chemokine receptor was identified by Holmes et al. in 1991 and now nearly 22 different chemokine receptors have been discovered in human [28]. Chemokine receptor nomenclature follows that of chemokines, with chemokine receptors named CXCRn, CCRn, CX3CRn and XCRn for the ligands of CXC, CC, CX3C, and C families, respectively [29]. However, it is still confused whether there exists a specific subgroup of chemokine receptors for CX chemokines. Individual chemokine receptor can identify more than one chemokine ligand, and correspondingly, most of the chemokines can bind to more than one receptor, which forms a complex chemokine network in immune response [30]. Furthermore, five atypical chemokine receptors CCRL1, CCRL2, CXCR7, DARC, and CCBP2, initially known as "silent" or "decoy" receptors, have been identified in recent years. Due to their deficiency of signaling and functional activities, atypical chemokine receptors cannot evoke the cell migration directly. However, a recent study showed that these atypical chemokine receptors can shape the chemokine gradients via degradation, transcytosis, or local concentration of their cognate ligands and eventually induce leukocytes recruitment indirectly in tissues [31].

3. Chemokines and Chemokine Receptors Involved in MS

As a chronic autoimmune inflammatory disease, MS is specially characterized by demyelinating and neurodegeneration. A current consensus is that the infiltration, accumulation, and activation of myelin-specific T lymphocytes and macrophages in central nervous system are a vital aspect of MS pathology [32–34]. This inflammatory process is mainly mediated by $CD4^+$ T cells, cytokines, chemokines, and chemokine receptors. Helper T cells can be divided into Th1, Th2, and Th17 subsets based on their characteristic cytokines-production patterns and effector functions. Th1 cells are responsible for cellular immunity and mainly release IFN-γ and TNF [35]. Th2 cells, which are often involved in humoral immunity, can produce cytokines such as IL-4, IL-5, and IL-10. Th17 cells mainly produce IL-17 and IL-6 and are responsible for inflammatory reaction. The chemokine receptor expression pattern would confer to each Th subset a unique characteristic of migration to corresponding ligand chemokines. Currently, a large number of researches have shown the immunoregulatory effect of chemokines and chemokine receptors on the development of MS [36–38] (Figure 1). Table 1 lists the current considerable interesting chemokines and chemokine receptors involved in MS here.

We will focus on the Th1/Th2, Th17, and Th17-1 cells and related chemokines/chemokine receptors involved in MS as follow.

3.1. Th1/Th2 Cells and Related Chemokines/Chemokine Receptors Involved in MS. In 1989, $CD4^+$ T cells were first divided into two subsets Th1 and Th2 [48]. Previous animal and human studies revealed that Th1 and Th2 lymphocytes and their related cytokines participate in the development of MS and EAE [49–51]. Th1 and Th2 cytokines can cross-inhibit each other and the progression of this disease may depend on the imbalance of Th1/Th2 ratio. It has been shown that in active phase of MS and EAE, Th1 cells can be found in lesions.

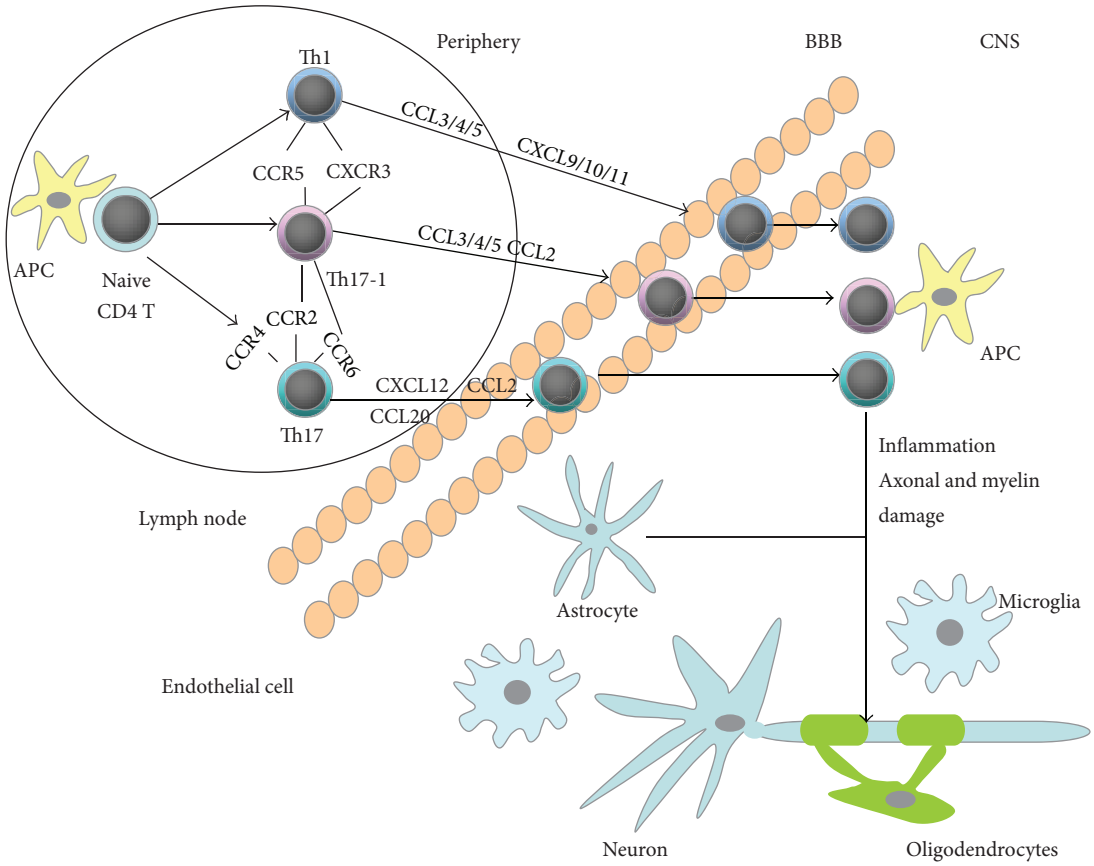

Figure 1: Migration and effector function of T cells in CNS during MS.

Table 1: Chemokines described in patients with MS.

Chemokine system name	Human ligand (old name)	Target cells	Chemokine receptors
CCL2 [33]	MCP-1	T cells, NK cells, B cells, monocytes, and dendritic cells	CCR1, CCR2
CCL3 [36]	MIP-1α	T and B cells, macrophage, and neutrophils	CCR1, CCR4, CCR5
CCL4 [39]	MIP-1β	T cells, microglia, and macrophage	CCR5
CCL5 [33]	RANTES	T cells, macrophage, eosinophils, and dendritic cells	CCR1, CCR3, CCR5
CCL7 [40]	MCP-3	T cells, B and NK cells, dendritic cells, and monocytes	CCR1, CCR2, CCR3, CCR5
CCL8 [40]	MCP-2	T cells, monocytes, and dendritic cells	CCR1, CCR2, CCR3, CCR5
CCL11 [17]	Eotaxin	T cells, dendritic cells, eosinophils, and basophils	CCR3
CCL17 [41]	TARC	T cells	CCR4
CCL19 [3]	ELC	T and B cells, and dendritic cells	CCR7
CCL20 [42]	LARC	T cells, monocytes	CCR6
CCL21 [43]	SLC	T and NK cells, dendritic cells	CCR7
CXCL1 [40]	GRO-α	monocytes, neutrophils	CXCR2
CXCL8 [41]	IL-8	monocytes, neutrophils, and fibroblasts	CXCR1, CXCR2
CXCL9 [44]	MIG	T and NK cells	CXCR3
CXCL10 [45]	IP-10	T and NK cells, macrophages, and astrocytes	CXCR3
CXCL11 [33]	I-TAC	T and NK cells	CXCR3, CXCR7
CXCL12 [46]	SDF-1	T and B cells, dendritic cells, and monocytes	CXCR4, CXCR7
CXCL13 [46]	BCA-1	T and B cells, dendritic cells, and monocytes	CXCR5
CX3CL1 [47]	Fractalkine	T and NK cells, monocytes	CX3CR1

As the level of Th1 cells is significantly increased in serum and CSF of MS patients, a shift from Th1 toward Th2 cytokine profile could have a beneficial effect on the clinical course of this disease [35]. Blockage of T-bet, which is the specific transcription factor of Th1 cells, will result in resistance to EAE in mice [39, 42].

During the last decade, a lot of studies detected the expression of chemokine receptors that are related to Th1 and Th2 cells as well as their relationship to MS and its animal model EAE [37, 52, 53]. It has been found that CCR5, CXCR3, and CXCR6 were preferentially, but not exclusively, expressed on Th1 cells, while CCR3, CCR4, CCR8, and CRTh2 (prostaglandin D_2 receptor) were associated with Th2 cells [36, 37, 45, 54]. The levels of CXCR3 and CCR5 expressed on Th1 cells are increased in CSF and brain lesions of active demyelinating MS patients [41]. A potential reason is that the migration of T cells into the brain and spinal cord is meditated by the interactions between chemokine receptor and its ligand. Accordingly, CXCL10, which is the ligand of CXCR3 and expressed by astrocytes, can be detected in active lesions of MS [55]. Meanwhile the ligands of CCR5, CCL3, CCL4 and CCL5 are also detected in active MS lesions. The levels of CXCL10, CCL3, and CCL5 are considered to reflect the Th1 reactions. The changes of these chemokines expression in CSF are thought to represent the infiltration of Th1 cells [44]. Nakajima and collaborators have studied the expression of Th1/Th2-related chemokine receptors in MS patients and found that the ratio of $CD4^+CXCR3^+/CD4^+CCR4^+$,which represents Th1/Th2 balance, was higher in active MS patients than remission MS group, indicating that there is a shift from Th2 to Th1 in pathogenesis of MS [44]. And this result is consistent with the study conducted by Uzawa et al. in 2010 [41].

3.2. Th17 Cells and Related Chemokines/Chemokine Receptors Involved in MS. As a distinct novel T helper lineage, interleukin 17-producing effector T cells (Th17 cells), was found in 2005 [56, 57]. These cells can produce IL-17 and regulate inflammatory chemokine expression and response. Differentiation of naive $CD4^+$ T cells to Th17 cells is driven by TGF-β and IL-6. STAT-3 is a necessary transcription factor to regulate the differentiation of Th17 and the expression of RORγt and RORα, which are specific transcription factors of this lineage [58, 59]. In recent years, there are increasingly evidences to support that Th17 cells have an important role in autoimmune CNS inflammation and are involved in many inflammatory diseases such as MS and rheumatoid arthritis (RA) [42, 60]. The discovery of Th17 cells opens up new areas in autoimmunity research.

The present study showed that the number of Th17 cells is increased in CSF of RRMS patients in relapse phase compared with patients during remission. This result suggested that Th17 cells play a pathogenic role in the development of MS [60]. MS was regarded as a Th1-related disease before however, it should be regarded as Th1/Th17-mediated disease based on some novel findings [61, 62]. It has been generally accepted that chemokines and chemokine receptors, which usually expressed in pathogenic cells, are required for the migration of lymphocytes into the CNS [42]. Some studies showed that human Th17 cells are enriched in $CCR4^+CCR6^+$, $CCR2^+CCR5^-$, and $CCR6^+$ populations [36, 63]. Yamazaki et al. recently found that the expression of CCR6 was regulated by TGF-β, RORγt, and RORα. Th17 cells also express the CCR6 ligand CCL20, which is induced synergistically by TGF-β and IL-6, as well as requiring STAT3, RORγt, and IL-21 [64]. In human normal tissue, the researchers found that CCL20 is constitutively expressed by epithelial cells of choroid plexus, indicating that the recruitment of CCR6-expressed Th17 cells into CNS may interact with those constitutively expressed CCL20 in the early phase of the disease [42, 65]. In EAE, the expressions of CCR6 and CCL20 were upregulated in spinal cord during disease development. The number of infiltrating T cells in CNS significantly decreased in CCR6 knock-out EAE mice, suggesting that the CCR6-deficient autoreactive Th17 cells failed to migrate into the CNS [43, 64]. Th17 cells promote migration of Th17 and Treg in vitro in a CCR6-dependent manner by producing CCL20 [64]. However, there are also some contradictory findings in EAE. For instance, two studies described that the disease is milder EAE in $CCR6^{-/-}$ mice than WT mice [42, 43], whereas in other groups, they found that $CCR6^{-/-}$ mice developed severer EAE compared to control group [64, 66, 67]. The reasons for these contradictory findings are not well understood, and these may be caused by the different mouse strains or different methods they used to induce EAE.

3.3. Th17-1 Cells and Related Chemokines/Chemokine Receptors Involved in MS. Th17-1 cells, as a novel T-cell subset, can coexpress cytokines IFN-γ and IL-17. Human memory $CD4^+$ lymphocytes have a tendency to expand into Th17-1 cells [68–70]. Dhodapkar et al. reported that dendritic cells (DC) were regarded as the most efficient inducers of human Th17-1 cells and this ability could be enhanced by the uptake of apoptotic tumor cells and some inflammatory cytokines such as IL-6, IL-1, and TNF [71, 72]. It was found that the lymphocytes have an increased propensity to expand into Th17-1 cells in the blood and brain tissue of relapsing MS patients. Th17-1 cells could preferentially cross the human BBB and accumulate in the CNS of mice during inflammatory events [70].

Just like other subsets, Th17-1 cells can also express chemokine receptors including CCR6, CCR2, and CXCR3 [45, 63]. Two studies reported that $CCR2^+CCR5^+$T cells, which were specifically involved in the development of MS but not in other noninflammatory neurologic diseases, produced a large quantity of IFN-γ and a small amount of IL-17, while $CCR2^+CCR5^-$ T cells produced a large quantity of IL-17 and a small amount of IFN-γ [36, 63]. In relapse phase of MS, the level of $CCR2^+CCR5^+$ Th17-1 cells is increased in CSF, due to that these cells have an ability to produce MMP-9 and OPN. $CCR2^+CCR5^+$ Th17-1 cells are more capable of invading the brain parenchyma than other T cells [36].

Activated Th1 cells and Th17 cells are thought to be the main culprit in MS. Th1 cells are IFN-γ producing and Th17 cells are IL-17 producing T lymphocytes. While Th17-1 cells are a novel T-cell subset producing both IFN-γ and IL-17.

A large number of chemokines and chemokine receptors have been responsible for the migration of T cells in the development of MS. Th1 cells can express CXCR3 and CCR5, which is the receptor of chemokines such as CCL3/4/5 and CXCL9/10/11. Th17 cells can express chemokine receptors including CCR2/CCR4/CCR6, and Th17-1 cells express CCR2/CCR5/CCR6/CXCR3. The interactions between these chemokine receptors and their ligands could mediate effector T cells migrating into CNS. Then these effector T cells can produce inflammatory products and cytokines that damage the myelin and axons.

4. The Therapy Targeting Chemokines/Chemokine Receptors Involved in MS

Emerging evidences have demonstrated that the levels of chemokines and their receptors are increased in the brain tissue, blood and cerebrospinal fluid in different stages of MS patients [47]. The chemokines/chemokine receptors expressed in different subsets of Th cells have the ability of attracting inflammatory cells into CNS, which will result in severe nervous system dysfunction [46, 73]. Thus, chemokine network is becoming a potential target for effective treatment of MS.

In clinical studies, some drugs targeting related chemokines and chemokine receptors have showed effective treatment through regulation of the immune responses in MS patients [74–76]. First, methylprednisolone (MP), a glucocorticosteroid drug, plays an essential role in the treatment of MS patients. This effect is mainly due to its anti-inflammatory ability. MP can inhibit the activation of T cells, promote the apoptosis of immune cells, and decrease the migration of them into the CNS [77, 78]. Jalosinski et al. found that the migratory ability of $CD4^+CCR5^+$ T cells was impaired after treatment with MP in active phase of MS patients [79]. Diminished mean level of CXCR3 ligand CXCL10 was also observed in serum of MS patients after intravenous MP treatment [80]. Second, glatiramer acetate (GA), formerly known as copolymer 1, is widely used for treatment of MS via increasing the levels of Th2-related cytokines and CCR7 expression, decreasing Th1-related cytokines as well as the expression of CCR5, CXCR3, and CXCR6 on T cells [40, 76, 81–84]. Third, IFN-β has been proven as an effective drug for treatment of RRMS patients for many years [85–87]. Dhib-Jalbut et al. demonstrated that IFN-β treatment could reduce the expression of CCL5, CCL3, and CXCR3, which was associated with Th1 cells, increasing the expression of CCR4 which was often expressed by Th2 cells in MS patients [88, 89].

Although many effective drugs have been discovered to treat MS patients, it is still hard to find a single-agent and long-lasting effective drug to suppress this disease. The underlying reasons are that the complex chemokine network contains abundant ligands and receptors, and the chemokines often display multiple functions. More research should be done to investigate the accurate regulatory roles of some special chemokines and chemokine receptors involved in MS to find out more effective targets for treating MS.

5. Conclusion

The clinical courses and outcomes are distinctly diverse for treatment of MS. The migration of pathogenic cells such as T cells and macrophages to the site of lesions in CNS is a vital aspect in pathogenesis of MS. Chemokine, a small protein with chemoattractant property, may facilitate the infiltration of pathogenic cells into the brain and spinal cord. The pathogenesis of MS is becoming more and more unambiguous through studying these proteins, which could be new therapeutic targets for this disease. To obtain more effective treatment for the autoimmune disease, we need to identify the ideal therapeutic target or molecule which is solely expressed on some autoimmune effector cells. Only then, we will be able to balance therapeutic effectiveness against the immunosuppression which is untoward. Although the complexity of chemokine network is bewildering, we hope that further therapy of MS targeting chemokine network could open up new vistas.

Abbreviations

BBB: Blood brain barrier
BCB: Blood cerebrospinal fluid barrier
CNS: Central nervous system
EAE: Experimental autoimmune encephalomyelitis

GA: Glatiramer acetate
GD: Graves' disease
GRTh2: Prostaglandin D_2 receptor
IL: Interleukin
IFN-β: Interferon-β
MDNCF: Monocyte-derived neutrophil chemotactic factor
MS: Multiple sclerosis
MP: Methylprednisolone
MMP-9: Matrix metalloproteinase-9
RA: Rheumatoid arthritis
SLE: Systemic lupus erythematosus
TGF-β: Transforming growth factor-β
TNF: Tumor necrosis factor
ROR-α: Retinoic acid-related orphan receptor-α
ROR-γt: Retinoic acid-related orphan receptor-γt
OPN: Osteopontin
DC: Dendritic cells
TGF-β: Transforming growth factor-β
DARC: Duffy antigen receptor group.

Conflict of Interests

The authors declare that there is no conflict of interests regarding the publication of the article.

Acknowledgments

This work was supported by Grants from National Nature Science Foundation of China (81373208), Shanghai Commission of Science and Technology (11JC1411602), Shanghai Municipal Education Commission (12ZZ103), and Shanghai Board of Health Foundation (2011177).

References

[1] A. Compston and A. Coles, "Multiple sclerosis," *The Lancet*, vol. 359, no. 9313, pp. 1221–1231, 2002.

[2] W. F. Hickey, "The pathology of multiple sclerosis: a historical perspective," *Journal of Neuroimmunology*, vol. 98, no. 1, pp. 37–44, 1999.

[3] A. Szczuciński and J. Losy, "Chemokines and chemokine receptors in multiple sclerosis. Potential targets for new therapies," *Acta Neurologica Scandinavica*, vol. 115, no. 3, pp. 137–146, 2007.

[4] A. Mathew, J. M. Pakan, E. C. Collin et al., "An ex-vivo multiple sclerosis model of inflammatory demyelination using hyperbranched polymer," *Biomaterials*, vol. 34, no. 23, pp. 5872–5882, 2013.

[5] V. H. Perry, D. C. Anthony, S. J. Bolton, and H. C. Brown, "The blood-brain barrier and the inflammatory response," *Molecular Medicine Today*, vol. 3, no. 8, pp. 335–341, 1997.

[6] J. H. Noseworthy, C. Lucchinetti, M. Rodriguez, and B. G. Weinshenker, "Multiple sclerosis," *The New England Journal of Medicine*, vol. 343, no. 13, pp. 938–952, 2000.

[7] D. E. McFarlin and H. F. McFarland, "Multiple sclerosis (first of two parts)," *The New England Journal of Medicine*, vol. 307, no. 19, pp. 1183–1188, 1982.

[8] D. E. McFarlin and H. F. McFarland, "Multiple sclerosis (second of two parts)," *The New England Journal of Medicine*, vol. 307, no. 20, pp. 1246–1251, 1982.

[9] B. Hemmer, J. J. Archelos, and H.-P. Hartung, "New concepts in the immunopathogenesis of multiple sclerosis," *Nature Reviews Neuroscience*, vol. 3, no. 4, pp. 291–301, 2002.

[10] N. Berghmans, H. Heremans, S. Li et al., "Rescue from acute neuroinflammation by pharmacological chemokine-mediated deviation of leukocytes," *Journal of Neuroinflammation*, vol. 9, article 243, 2012.

[11] T. Matsushita, T. Tateishi, N. Isobe et al., "Characteristic cerebrospinal fluid cytokine/chemokine profiles in neuromyelitis optica, relapsing remitting or primary progressive multiple sclerosis," *PLoS One*, vol. 8, no. 4, Article ID e61835, 2013.

[12] F. Sellebjerg, L. Börnsen, M. Khademi et al., "Increased cerebrospinal fluid concentrations of the chemokine CXCL13 in active MS," *Neurology*, vol. 73, no. 23, pp. 2003–2010, 2009.

[13] R. M. Ransohoff, "The chemokine system in neuroinflammation: an update," *Journal of Infectious Diseases*, vol. 186, supplement 2, pp. S152–S156, 2002.

[14] G. Hassanshahi, A. Jafarzadeh, and A. J. Dickson, "Expression of stromal derived factor alpha (SDF-1α) by primary hepatocytes following isolation and heat shock stimulation," *Iranian Journal of Allergy, Asthma and Immunology*, vol. 7, no. 2, pp. 61–68, 2008.

[15] T. Yoshimura, K. Matsushima, S. Tanaka et al., "Purification of a human monocyte-derived neutrophil chemotactic factor that has peptide sequence similarity to other host defense cytokines," *Proceedings of the National Academy of Sciences of the United States of America*, vol. 84, no. 24, pp. 9233–9237, 1987.

[16] I. F. Charo and R. M. Ransohoff, "The many roles of chemokines and chemokine receptors in inflammation," *The New England Journal of Medicine*, vol. 354, no. 6, pp. 610–621, 2006.

[17] A. Rot and U. H. von Andrian, "Chemokines in innate and adaptive host defense: basic chemokinese grammar for immune cells," *Annual Review of Immunology*, vol. 22, pp. 891–928, 2004.

[18] H. Nomiyama, N. Osada, and O. Yoshie, "The evolution of mammalian chemokine genes," *Cytokine and Growth Factor Reviews*, vol. 21, no. 4, pp. 253–262, 2010.

[19] G. S. Kelner, J. Kennedy, K. B. Bacon et al., "Lymphotactin: a cytokine that represents a new class of chemokine," *Science*, vol. 266, no. 5189, pp. 1395–1399, 1994.

[20] H. Nomiyama, N. Osada, and O. Yoshie, "A family tree of vertebrate chemokine receptors for a unified nomenclature," *Developmental and Comparative Immunology*, vol. 35, no. 7, pp. 705–715, 2011.

[21] H. Nomiyama, K. Hieshima, N. Osada et al., "Extensive expansion and diversification of the chemokine gene family in zebrafish: identification of a novel chemokine subfamily CX," *BMC Genomics*, vol. 9, article 222, 2008.

[22] L. Cartier, O. Hartley, M. Dubois-Dauphin, and K.-H. Krause, "Chemokine receptors in the central nervous system: role in brain inflammation and neurodegenerative diseases," *Brain Research Reviews*, vol. 48, no. 1, pp. 16–42, 2005.

[23] N. Godessart and S. L. Kunkel, "Chemokines in autoimmune disease," *Current Opinion in Immunology*, vol. 13, no. 6, pp. 670–675, 2001.

[24] K. Biber, M. W. Zuurman, I. M. Dijkstra, and H. W. G. M. Boddeke, "Chemokines in the brain: neuroimmunology and beyond," *Current Opinion in Pharmacology*, vol. 2, no. 1, pp. 63–68, 2002.

[25] X. Li, Y. Qi, X. Ma et al., "Chemokine (C-C motif) ligand 20, a potential biomarker for graves' disease, is regulated by osteopontin," *PLoS One*, vol. 8, no. 5, Article ID e64277, 2013.

[26] J. Sellam, S. Rouanet, H. Hendel-Chavez et al., "CCL19, a B-cell chemokine, is related to the decrease of blood memory B-cells and predicts the clinical response to rituximab in rheumatoid arthritis," *Arthritis Rheum*, vol. 65, no. 9, pp. 2253–2261, 2013.

[27] J. Vomaske, M. Denton, C. Kreklywich et al., "Cytomegalovirus CC chemokine promotes immune cell migration," *Journal of Virology*, vol. 86, no. 21, pp. 11833–11844, 2012.

[28] W. E. Holmes, J. Lee, W.-J. Kuang, G. C. Rice, and W. I. Wood, "Structure and functional expression of a human interleukin-8 receptor. Science. 1991. 253: 1278–1280," *Journal of Immunology*, vol. 183, no. 5, pp. 2895–2897, 2009.

[29] A. Reaux-Le Goazigo, J. Van Steenwinckel, W. Rostene, and S. Melik Parsadaniantz, "Current status of chemokines in the adult CNS," *Progress in Neurobiology*, vol. 104, pp. 67–92, 2013.

[30] R. Horuk, "Chemokine receptors," *Cytokine and Growth Factor Reviews*, vol. 12, no. 4, pp. 313–335, 2001.

[31] C. Cancellieri, A. Vacchini, M. Locati, R. Bonecchi, and E. M. Borroni, "Atypical chemokine receptors: from silence to sound," *Biochemical Society Transactions*, vol. 41, no. 1, pp. 231–236, 2013.

[32] H. J. Fischer, N. Schweingruber, F. Luhder, and H. M. Reichardt, "The potential role of T cell migration and chemotaxis as targets of glucocorticoids in multiple sclerosis and experimental autoimmune encephalomyelitis," *Molecular and Cellular Endocrinology*, vol. 380, no. 1-2, pp. 99–107, 2013.

[33] R. Sporici and T. B. Issekutz, "CXCR3 blockade inhibits T-cell migration into the CNS during EAE and prevents development of adoptively transferred, but not actively induced, disease,"

European Journal of Immunology, vol. 40, no. 10, pp. 2751–2761, 2010.

[34] S. Wüst, J. van den Brandt, D. Tischner et al., "Peripheral T cells are the therapeutic targets of glucocorticoids in experimental autoimmune encephalomyelitis," *Journal of Immunology*, vol. 180, no. 12, pp. 8434–8443, 2008.

[35] C. Oreja-Guevara, J. Ramos-Cejudo, L. S. Aroeira, B. Chamorro, and E. Diez-Tejedor, "TH1/TH2 cytokine profile in relapsing-remitting multiple sclerosis patients treated with Glatiramer acetate or Natalizumab," *BMC Neurology*, vol. 12, article 95, 2012.

[36] W. Sato, A. Tomita, D. Ichikawa et al., "CCR2(+)CCR5(+) T cells produce matrix metalloproteinase-9 and osteopontin in the pathogenesis of multiple sclerosis," *The Journal of Immunology*, vol. 189, no. 10, pp. 5057–5065, 2012.

[37] Y. Shimizu, K. Ota, S. Kubo et al., "Association of Th1/Th2-related chemokine receptors in peripheral T cells with disease activity in patients with multiple sclerosis and neuromyelitis optica," *European Neurology*, vol. 66, no. 2, pp. 91–97, 2011.

[38] D. A. Hendrickx, N. Koning, K. G. Schuurman et al., "Selective upregulation of scavenger receptors in and around demyelinating areas in multiple sclerosis," *Journal of Neuropathology & Experimental Neurology*, vol. 72, no. 2, pp. 106–118, 2013.

[39] E. Bettelli, B. Sullivan, S. J. Szabo, R. A. Sobel, L. H. Glimcher, and V. K. Kuchroo, "Loss of T-bet, but not STAT1, prevents the development of experimental autoimmune encephalomyelitis," *The Journal of Experimental Medicine*, vol. 200, no. 1, pp. 79–87, 2004.

[40] R. A. Høglund, A. L. Hestvik, T. Holmøy, and A. A. Maghazachi, "Expression and functional activity of chemokine receptors in glatiramer acetate-specific T cells isolated from multiple sclerosis patient receiving the drug glatiramer acetate," *Human Immunology*, vol. 72, no. 2, pp. 124–134, 2011.

[41] A. Uzawa, M. Mori, S. Hayakawa, S. Masuda, F. Nomura, and S. Kuwabara, "Expression of chemokine receptors on peripheral blood lymphocytes in multiple sclerosis and neuromyelitis optica," *BMC Neurology*, vol. 10, article 113, 2010.

[42] A. Reboldi, C. Coisne, D. Baumjohann et al., "C-C chemokine receptor 6-regulated entry of TH-17 cells into the CNS through the choroid plexus is required for the initiation of EAE," *Nature Immunology*, vol. 10, no. 5, pp. 514–523, 2009.

[43] A. Liston, R. E. Kohler, S. Townley et al., "Inhibition of CCR6 function reduces the severity of experimental autoimmune encephalomyelitis via effects on the priming phase of the immune response," *Journal of Immunology*, vol. 182, no. 5, pp. 3121–3130, 2009.

[44] H. Nakajima, K. Fukuda, Y. Doi et al., "Expression of Th1/Th2-related chemokine receptors on peripheral T cells and correlation with clinical disease activity in patients with multiple sclerosis," *European Neurology*, vol. 52, no. 3, pp. 162–168, 2004.

[45] E. V. Acosta-Rodriguez, L. Rivino, J. Geginat et al., "Surface phenotype and antigenic specificity of human interleukin 17-producing T helper memory cells," *Nature Immunology*, vol. 8, no. 6, pp. 639–646, 2007.

[46] M. Krumbholz, D. Theil, S. Cepok et al., "Chemokines in multiple sclerosis: CXCL12 and CXCL13 up-regulation is differentially linked to CNS immune cell recruitment," *Brain*, vol. 129, no. 1, pp. 200–211, 2006.

[47] B. Broux, K. Pannemans, X. Zhang et al., "CX_3CR1 drives cytotoxic $CD4^+CD28^-$ T cells into the brain of multiple sclerosis patients," *Journal of Autoimmunity*, vol. 38, no. 1, pp. 10–19, 2012.

[48] T. R. Mosmann and R. L. Coffman, "TH1 and TH2 cells: different patterns of lymphokine secretion lead to different functional properties," *Annual Review of Immunology*, vol. 7, pp. 145–173, 1989.

[49] P. D. Cravens, B. C. Kieseier, R. Hussain et al., "The neonatal CNS is not conducive for encephalitogenic Th1 T cells and B cells during experimental autoimmune encephalomyelitis," *Journal of Neuroinflammation*, vol. 10, article 67, 2013.

[50] S. A. Imam, M. K. Guyton, A. Haque et al., "Increased calpain correlates with Th1 cytokine profile in PBMCs from MS patients," *Journal of Neuroimmunology*, vol. 190, no. 1-2, pp. 139–145, 2007.

[51] P. Pellegrini, R. Totaro, I. Contasta, A. M. Berghella, A. Carolei, and D. Adorno, "CD30 antigen and multiple sclerosis: CD30, an important costimulatory molecule and marker of a regulatory subpopulation of dendritic cells, is involved in the maintenance of the physiological balance between TH1/TH2 immune responses and tolerance: the role of IFNβ-1a in the treatment of multiple sclerosis," *NeuroImmunoModulation*, vol. 12, no. 4, pp. 220–234, 2005.

[52] E. Julià, M. C. Edo, A. Horga, X. Montalban, and M. Comabella, "Differential susceptibility to apoptosis of $CD4^+$ T cells expressing CCR5 and CXCR3 in patients with MS," *Clinical Immunology*, vol. 133, no. 3, pp. 364–374, 2009.

[53] T. Misu, H. Onodera, K. Fujihara et al., "Chemokine receptor expression on T cells in blood and cerebrospinal fluid at relapse and remission of multiple sclerosis: imbalance of Th1/Th2-associated chemokine signaling," *Journal of Neuroimmunology*, vol. 114, no. 1-2, pp. 207–212, 2001.

[54] R. Bonecchi, G. Bianchi, P. P. Bordignon et al., "Differential expression of chemokine receptors and chemotactic responsiveness of type 1 T helper cells (Th1s) and Th2s," *The Journal of Experimental Medicine*, vol. 187, no. 1, pp. 129–134, 1998.

[55] J. E. Simpson, J. Newcombe, M. L. Cuzner, and M. N. Woodroofe, "Expression of the interferon-γ-inducible chemokines IP-10 and Mig and their receptor, CXCR3, in multiple sclerosis lesions," *Neuropathology and Applied Neurobiology*, vol. 26, no. 2, pp. 133–142, 2000.

[56] L. E. Harrington, R. D. Hatton, P. R. Mangan et al., "Interleukin 17-producing $CD4^+$ effector T cells develop via a lineage distinct from the T helper type 1 and 2 lineages," *Nature Immunology*, vol. 6, no. 11, pp. 1123–1132, 2005.

[57] H. Park, Z. Li, X. O. Yang et al., "A distinct lineage of CD4 T cells regulates tissue inflammation by producing interleukin 17," *Nature Immunology*, vol. 6, no. 11, pp. 1133–1141, 2005.

[58] X. O. Yang, B. P. Pappu, R. Nurieva et al., "T helper 17 lineage differentiation is programmed by orphan nuclear receptors ROR alpha and ROR gamma," *Immunity*, vol. 28, no. 1, pp. 29–39, 2008.

[59] A. Laurence, C. M. Tato, T. S. Davidson et al., "Interleukin-2 signaling via STAT5 constrains T helper 17 cell generation," *Immunity*, vol. 26, no. 3, pp. 371–381, 2007.

[60] V. Brucklacher-Waldert, K. Stuerner, M. Kolster, J. Wolthausen, and E. Tolosa, "Phenotypical and functional characterization of T helper 17 cells in multiple sclerosis," *Brain*, vol. 132, no. 12, pp. 3329–3341, 2009.

[61] Y. Sonobe, S. Jin, J. Wang et al., "Chronological changes of $CD4^+$ and $CD8^+$ T cell subsets in the experimental autoimmune encephalomyelitis, a mouse model of multiple sclerosis," *Tohoku Journal of Experimental Medicine*, vol. 213, no. 4, pp. 329–339, 2007.

[62] J. S. Tzartos, M. A. Friese, M. J. Craner et al., "Interleukin-17 production in central nervous system-infiltrating T cells and

glial cells is associated with active disease in multiple sclerosis," *American Journal of Pathology*, vol. 172, no. 1, pp. 146–155, 2008.

[63] W. Sato, T. Aranami, and T. Yamamura, "Cutting edge: human Th17 cells are identified as bearing $CCR2^{+}CCR5^{-}$ phenotype," *Journal of Immunology*, vol. 178, no. 12, pp. 7525–7529, 2007.

[64] T. Yamazaki, X. O. Yang, Y. Chung et al., "CCR6 regulates the migration of inflammatory and regulatory T cells," *Journal of Immunology*, vol. 181, no. 12, pp. 8391–8401, 2008.

[65] M. El-Behi, A. Rostami, and B. Ciric, "Current views on the roles of Th1 and Th17 cells in experimental autoimmune encephalomyelitis," *Journal of Neuroimmune Pharmacology*, vol. 5, no. 2, pp. 189–197, 2010.

[66] A. Elhofy, R. W. DePaolo, S. A. Lira, N. W. Lukacs, and W. J. Karpus, "Mice deficient for CCR6 fail to control chronic experimental autoimmune encephalomyelitis," *Journal of Neuroimmunology*, vol. 213, no. 1-2, pp. 91–99, 2009.

[67] R. Villares, V. Cadenas, M. Lozano et al., "CCR6 regulates EAE pathogenesis by controlling regulatory $CD4^{+}$ T-cell recruitment to target tissues," *European Journal of Immunology*, vol. 39, no. 6, pp. 1671–1681, 2009.

[68] Y. K. Lee, H. Turner, C. L. Maynard et al., "Late developmental plasticity in the T Helper 17 lineage," *Immunity*, vol. 30, no. 1, pp. 92–107, 2009.

[69] R. E. Eid, D. A. Rao, J. Zhou et al., "Interleukin-17 and interferon-γ are produced concomitantly by human coronary artery-infiltrating T cells and act synergistically on vascular smooth muscle cells," *Circulation*, vol. 119, no. 10, pp. 1424–1432, 2009.

[70] H. Kebir, I. Ifergan, J. I. Alvarez et al., "Preferential recruitment of interferon-γ-expressing TH17 cells in multiple sclerosis," *Annals of Neurology*, vol. 66, no. 3, pp. 390–402, 2009.

[71] K. M. Dhodapkar, S. Barbuto, P. Matthews et al., "Dendritic cells mediate the induction of polyfunctional human IL17-producing cells (Th17-1 cells) enriched in the bone marrow of patients with myeloma," *Blood*, vol. 112, no. 7, pp. 2878–2885, 2008.

[72] A. Kimura, T. Naka, and T. Kishimoto, "IL-6-dependent and -independent pathways in the development of interleukin 17-producing T helper cells," *Proceedings of the National Academy of Sciences of the United States of America*, vol. 104, no. 29, pp. 12099–12104, 2007.

[73] G. Michałowska-Wender, J. Losy, J. Biernacka-Łukanty, and M. Wender, "Impact of methylprednisolone treatment on the expression of macrophage inflammatory protein 3α and B lymphocyte chemoattractant in serum of multiple sclerosis patients," *Pharmacological Reports*, vol. 60, no. 4, pp. 549–554, 2008.

[74] T. Berger, "Current therapeutic recommendations in multiple sclerosis," *Journal of the Neurological Sciences*, vol. 287, supplement 1, pp. S37–S45, 2009.

[75] J. Schmidt, J. M. Metselaar, M. H. M. Wauben, K. V. Toyka, G. Storm, and R. Gold, "Drug targeting by long-circulating liposomal glucocorticosteroids increases therapeutic efficacy in a model of multiple sclerosis," *Brain*, vol. 126, no. 8, pp. 1895–1904, 2003.

[76] E. Y. Tsareva, O. G. Kulakova, A. N. Boyko et al., "Allelic combinations of immune-response genes associated with glatiramer acetate treatment response in Russian multiple sclerosis patients," *Pharmacogenomics*, vol. 13, no. 1, pp. 43–53, 2012.

[77] J. S. Sloka and M. Stefanelli, "The mechanism of action of methylprednisolone in the treatment of multiple sclerosis," *Multiple Sclerosis*, vol. 11, no. 4, pp. 425–432, 2005.

[78] P.-B. Andersson and D. E. Goodkin, "Glucocorticosteroid therapy for multiple sclerosis: a critical review," *Journal of the Neurological Sciences*, vol. 160, no. 1, pp. 16–25, 1998.

[79] M. Jalosinski, K. Karolczak, A. Mazurek, and A. Glabinski, "The effects of methylprednisolone and mitoxantrone on CCL5-induced migration of lymphocytes in multiple sclerosis," *Acta Neurologica Scandinavica*, vol. 118, no. 2, pp. 120–125, 2008.

[80] G. Michałowska-Wender, J. Losy, A. Szczuciński, J. Biernacka-Łukanty, and M. Wender, "Effect of methylprednisolone treatment on expression of sPECAM-1 and CXCL10 chemokine in serum of MS patients," *Pharmacological Reports*, vol. 58, no. 6, pp. 920–923, 2006.

[81] S. Dhib-Jalbut, "Mechanisms of action of interferons and glatiramer acetate in multiple sclerosis," *Neurology*, vol. 58, no. 8, supplement 4, pp. S3–S9, 2002.

[82] M. K. Racke, A. E. Lovett-Racke, and N. J. Karandikar, "The mechanism of action of glatiramer acetate treatment in multiple sclerosis," *Neurology*, vol. 74, supplement 1, pp. S25–S30, 2010.

[83] C. Farina, M. S. Weber, E. Meinl, H. Wekerle, and R. Hohlfeld, "Glatiramer acetate in multiple sclerosis: update on potential mechanisms of action," *The Lancet Neurology*, vol. 4, no. 9, pp. 567–575, 2005.

[84] R. A. Hoglund, T. Holmoy, H. F. Harbo, and A. A. Maghazachi, "A one year follow-up study of natural killer and dendritic cells activities in multiple sclerosis patients receiving glatiramer acetate (GA)," *PLoS One*, vol. 8, no. 4, Article ID e62237, 2013.

[85] H. Nakajima, T. Hosokawa, Y. Doi et al., "Interferon-beta1b increases Th2 response in neuromyelitis optica," *International Journal of Molecular Sciences*, vol. 13, no. 10, pp. 12213–12223, 2012.

[86] G. Comi, M. Filippi, F. Barkhof et al., "Effect of early interferon treatment on conversion to definite multiple sclerosis: a randomised study," *The Lancet*, vol. 357, no. 9268, pp. 1576–1582, 2001.

[87] R. A. Rudick, D. E. Goodkin, L. D. Jacobs et al., "Impact of interferon beta-1a on neurologic disability in relapsing multiple sclerosis," *Neurology*, vol. 49, no. 2, pp. 358–363, 1997.

[88] S. Dhib-Jalbut, S. Sumandeep, R. Valenzuela, K. Ito, P. Patel, and M. Rametta, "Immune response during interferon beta-1b treatment in patients with multiple sclerosis who experienced relapses and those who were relapse-free in the START study," *Journal of Neuroimmunology*, vol. 254, pp. 131–140, 2013.

[89] Y. C. Q. Zang, J. B. Halder, A. K. Samanta, J. Hong, V. M. Rivera, and J. Z. Zhang, "Regulation of chemokine receptor CCR5 and production of RANTES and MIP-1α by interferon-β," *Journal of Neuroimmunology*, vol. 112, no. 1-2, pp. 174–180, 2001.

Hindawi Publishing Corporation
Mediators of Inflammation
Volume 2014, Article ID 292376, 12 pages
http://dx.doi.org/10.1155/2014/292376

Review Article

The Inflammatory Chemokine CCL5 and Cancer Progression

Donatella Aldinucci[1] and Alfonso Colombatti[1,2]

[1] *Experimental Oncology 2, Aviano National Cancer Institute (CRO), Via Franco Gallini 2, 33081 Aviano, Italy*
[2] *Department of Medical and Biological Science Technology, Microgravity Ageing Training Immobility Excellence Center (MATI), Piazzale M. Kolbe, 33100 Udine, Italy*

Correspondence should be addressed to Donatella Aldinucci; daldinucci@cro.it

Received 10 September 2013; Accepted 10 December 2013; Published 2 January 2014

Academic Editor: Mohammad Athar

Until recently, inflammatory chemokines were viewed mainly as indispensable "gate keepers" of immunity and inflammation. However, updated research indicates that cancer cells subvert the normal chemokine system and these molecules and their receptors become important constituents of the tumor microenvironment with very different ways to exert tumor-promoting roles. The CCR5 and the CCL5 ligand have been detected in some hematological malignancies, lymphomas, and a great number of solid tumors, but extensive studies on the role of the CCL5/CCR axis were performed only in a limited number of cancers. This review summarizes updated information on the role of CCL5 and its receptor CCR5 in cancer cell proliferation, metastasis, and the formation of an immunosuppressive microenvironment and highlights the development of newer therapeutic strategies aimed to inhibit the binding of CCL5 to CCR5, to inhibit CCL5 secretion, or to inhibit the interactions among tumor cells and the microenvironment leading to CCL5 secretion.

1. Introduction

Epidemiological and experimental studies provided clear evidence that unresolved pathogen infections and chronic inflammation promote tumor development and led to the inclusion of inflammation among the hallmarks of cancer [1, 2]. On the other hand, cancer cells not only make themselves "invisible" to the immune system, but also favor the formation of an immunosuppressive microenvironment unable to eliminate cancer cells [3]. As a result, the reduced secretion of molecules acting as tumor-promoting factors and the normalization of the tumor microenvironment [4] are main goals to develop appropriate antitumor strategies.

The tumor microenvironment is composed of stromal and inflammatory cells that are recruited and/or locally induced to proliferate or differentiate by tumor cells or by normal cells "educated" by tumor cells. They communicate directly through cell-cell contact but also indirectly through paracrine signals [4]. These signals are predominantly constituted by cytokines and chemokines (chemotactic cytokines), key orchestrators of leukocytes trafficking under homeostatic conditions as well as during inflammation and cancer [5] and part of the molecular pathways driving cancer cell survival, motility, and invasiveness [6].

Chemokines, identified on the basis of their ability to induce chemotaxis, have a fundamental role not only in inflammation and immune surveillance but also in cancer progression [7]. Chemokines, secreted by the tumor cells from primary tumors or metastatic sites or by the normal cells recruited and/or locally activated, can behave as growth factors [8], increase metastasis formation and angiogenesis, [9] or induce the formation of an immunosuppressive microenvironment. This last complex capacity is obtained by recruiting activating tumor-associated macrophages (TAM) [10], myeloid-derived suppressor cells (MDSC), T-regulatory cells (T-reg) [11], or mesenchymal stem cells (MSCs) [12] and by inhibiting the antitumor activity of Th1 cells and cytotoxic T lymphocytes (CTL) [13].

In response to chemokines present in remote organs, tumor cells that express the corresponding receptor disseminate with higher efficiency [14]. Furthermore, tumor cells

acquire higher adhesive, migratory, and invasive properties in response to chemokines that are expressed at preferential metastatic sites [15]. As a consequence, the presence of inflammatory cells such as reactive leukocytes and the expression of a large number of inflammatory mediators (e.g., cytokines, chemokines, and enzymes) in the primary tumor are mostly associated with poor prognosis and metastasis formation [16].

A variety of chemokines and chemokine receptors have been detected in neoplastic tissues [1, 4]. We will focus our attention primarily on the C-C chemokine ligand 5 (CCL5), also known as Regulated upon Activation, Normal T-cell Expressed, and Secreted (RANTES), and its receptors C-C chemokine receptor type 5 (CCR5).

CCR5 is a seven-transmembrane G-protein-coupled receptor, mediating diverse signaling cascades in response to its ligands. CCR5, a promiscuous receptor, binds with high-affinity CCL5, CCL3 (MIP-1a), and CCL4 (MIP-1b) and is the major coreceptor for HIV [17].

CCL5 belongs to the C-C chemokine family whose members also include CCL3 and CCL4 [18]. CCL5, a target gene of NF-κB activity, is expressed by T lymphocytes, macrophages, platelets, synovial fibroblasts, tubular epithelium, and certain types of tumor cells [18]. NF-κB activation by different stimuli such as CD40L [19] or IL-15 [20] induces CCL5 production.

CCL5 plays an active role in recruiting a variety of leukocytes into inflammatory sites including T cells, macrophages, eosinophils, and basophils. In collaboration with certain cytokines that are released by T cells such as IL-2 and IFN-γ, CCL5 also induces the activation and proliferation of particular natural killer cells to generate C-C chemokine-activated killer cells [18]. CCL5 produced by $CD8^+$ T cells and other immune cells has been shown to inhibit HIV entry into target cells.

CCL5 activity is mediated through its binding to CCR1, CCR3, and mainly CCR5 [18]. CCR4 [21, 22] and CD44 are auxiliary receptors for CCL5 [21, 23].

The exact functions of CCL5 in tumor biology are still unclear. CCL5 production is relevant to inducing proper immune responses against tumors [2], but, on the other hand, CCL5 is associated with cancer progression and metastasis.

CCL5/CCR5 interactions may favor tumor development in multiple ways: acting as growth factors, stimulating angiogenesis, modulating the extracellular matrix, inducing the recruitment of additional stromal and inflammatory cells, and taking part in immune evasion mechanisms [3].

A schematic view of the consequences of the CCL5/CCR5 interactions in cancer is shown in Figure 1.

This review summarizes updated information on the role of the CCL5/CCR5 axis in tumor development and/or progression, focusing primarily on multiple myeloma (MM), classical Hodgkin lymphoma (cHL), prostate, breast, gastric, colon, and ovarian cancer, and melanoma.

Based on the findings obtained so far, we propose that inflammatory chemokines and their receptors are attractive therapeutic targets in malignancy.

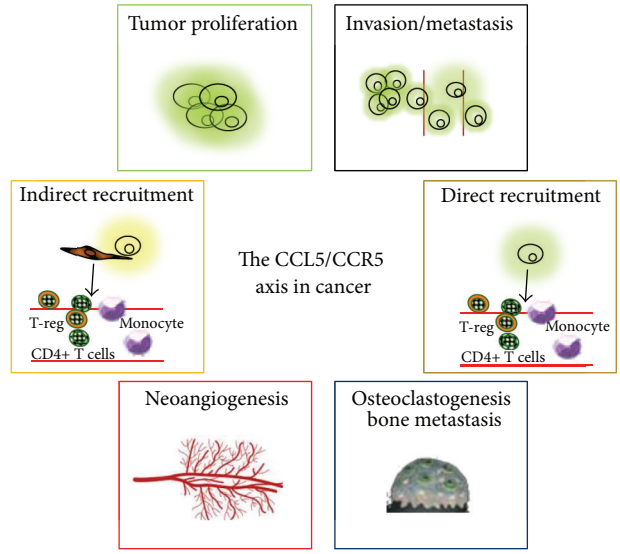

Figure 1: Effects of the CCL5/CCR5 interactions in cancer. Cancer cells secrete CCL5 or induce fibroblasts to secrete CCL5 which act in a paracrine or autocrine fashion on CCR5-positive tumor cells to sustain their proliferation, to recruit immunosuppressive cells (T-reg cells, monocyte), to induce osteoclasts activation and bone metastasis, to induce neoangiogenesis, and to guide tumor cells to disseminate to distant organs.

2. Mechanism Leading to Cancer Cell Proliferation and Metastasis Formation via the CCL5/CCR5 Axis

The binding of chemokine to their G-protein-coupled receptors (GPCRs) activates a series of downstream effectors that facilitate internalization of the receptor and signal transduction leading to integrin activation (adhesion) and polarization of the actin cytoskeleton [24]. The consequences are directional sensing, cell polarization, accumulation of small GTPases, Rac, Cdc42, and PI3K at the leading edge, actin polymerization, and F-actin formation. These changes cause actomyosin contraction and tail retraction and finally cell migration [24].

More specifically, CCL5 contributes to the activation of the $\alpha v\beta 3$ integrin and to cell migration through PI3K/Akt, which in turn activates IKKalpha/beta and NF-κB [25]. NF-κB activation also can elevate the secretion of MMP-9 [26] or promote invasion by increasing the secretion of both MMP-2 and -9 and by activating the ERK and Rac signaling [27]. CCL5 induces migration also by upregulating the activities of MMP-9 through STAT3 [28]. In other instances CCL5/CCR5 acts via MEK, ERK, and then NF-κB, resulting in the activations of $\alpha v\beta 3$ integrin and contributing to cell migration [29].

Chemokines, by activating the tyrosine kinase receptors, the Jak-STAT, or the MAPK/ERK signaling pathway, also promote tumor cell proliferation [30]. Exogenous CCL5 stimulates cell proliferation by inducing the mTOR pathway, leading to a rapid upregulation of cyclin D1, c-Myc, and Dad-1 expression. An additional mechanism based on the CCL5-CCR5 interaction can lead to increased cell proliferation:

increased glucose uptake, increased ATP production, and enhanced glycolysis, associated with extracellular acidification [31].

3. The CCL5/CCR5 Axis in Hematological Malignancies

Many studies were published during the last several years on the expression of CCL5 and CCR5 in hematological malignancies, but, only for multiple myeloma (MM) and at least in part for cHL, we have a comprehensive view of the role played by the CCL3-CCL5/CCR5 pair.

3.1. Multiple Myeloma. The MM cell localization in the bone marrow and the cross-talk with the bone niche trigger dramatic alterations in the bone marrow (BM) microenvironment, critical for tumor progression, resistance to therapies, and osteolytic bone destruction [32]. The interaction between osteoclasts (OCs) and MM cells plays a key role in the pathogenesis of MM-related osteolytic bone disease. MM cells promote OCs formation and, in turn, OCs enhance tumor cell proliferation via cell-cell contact [33].

The CCR5-ligand CCL3 is detected in MM cell line and freshly isolated MM cells [34, 35] and is one of the most important OC-activating factors produced by MM cells and a contributor of MM-associated osteolytic bone disease [36]. MM cells from patients with multiple bone lesions secrete higher amounts of CCL3 (and CCL4) than those with less-advanced bone involvement [37]. Consistently, CCL3 serum levels are elevated in newly diagnosed MM patients and correlate with the extent of bone disease, bone resorption, and disease prognosis [38]. Increased expression of CCL3 in bone biopsies correlates with extensive bone disease, increased angiogenesis, and advanced stage in newly diagnosed patients with MM [39]. CCL3, secreted by MM cells, stimulates OC activity and also inhibits osteoblast formation, further contributing to the imbalance between bone resorption and bone formation [40]. MM cells also secrete CCL5, suggesting a possible role of this chemokine in the pathogenesis of MM since, like CCL3, it is a potent activator of both CCR1 and CCR5 receptors [41] expressed by stromal cells and OC precursors [35].

Several studies have evaluated the expression of CCR5 and CCR1 by MM cell lines and by cells derived from patients [34, 35, 42–45] and demonstrated that their engagement determines MM cell survival, migration, and homing to the BM. In fact, MM cells migrate in the presence of CCL5 and the extent of migration depends on the CCR5 expression levels [35, 43, 45].

Inhibition of CCR1 and CCR5 receptors by antagonists or neutralizing antibodies partially reduce osteoclastogenesis, osteolytic lesions, and MM-induced angiogenesis [34, 35, 42]. Recently, Dairaghi et al. [46] demonstrated that CCR1 blockade by the selective antagonist CCX721 reduces tumor burden and osteolysis in vivo in a mouse model of myeloma bone disease, likely by inhibiting the cross-talk of MM cells with OCs and OC precursors [46]. Thus the development of CCR1 antagonists for the treatment of MM and associated osteolytic bone disease is a further therapeutic possibility.

Overall, the current observations propose two major mechanisms by which CCL3 and/or CCL5 released by tumor cells and their receptors support MM progression: the first is the ability to disrupt bone homeostasis and induce bone destruction, and the second is the bone marrow homing of MM cells [35] due to the expression of CCR5 and CCR1. Therefore, counteracting the consequences of these chemokine/chemokine receptors interactions may represent a new therapeutic option in MM.

3.2. Hodgkin Lymphoma. The microenvironment is essential for growth and survival of classical Hodgkin Lymphoma (HL) tumor cells [8] and chemokines play a primary role in its formation. They may exert a direct action on tumor cells by increasing cell survival and proliferation, recruit cells capable of sustaining the growth of tumor cells by providing a suppressive environment that suppresses cytotoxic immune responses, or redirect HL cells to advantageous microenvironmental sites within the lymphoid tissues.

cHL cells secrete cytokines/chemokines and express a variety of cytokine/chemokine receptors [8, 47] and it is now widely assumed that the clinical and histological features of cHL are primarily due to the effects of a plethora of cytokines and chemokines secreted by cHL cells such as CCL5 [48, 49], CCL17 [47], CCL22 [50], CCL28 [51], and CCL20 [39, 52] or by the surrounding cellular infiltrate. The recruitment and proliferation of nontumor cells may be also mediated by molecules produced by "normal" cells of the microenvironment, activated by tumor cells [8]. For example: cHL cells (i) do not express eotaxin but produce IL-13 and TNF-α which are capable of inducing eotaxin expression in cocultured dermal fibroblasts in a concentration leading to a specific chemotactic response of Th2 cells [53]; (ii) produce molecules capable of inducing CCL5 secretion in HL-derived fibroblasts [49]; (iii) express CD40 and its engagement by CD40L rosetting T-cells increase CCL5 secretion [49]. Together these lines of evidence suggest that the cross-talk between tumor cells and fibroblasts or the activation by surrounding CD40L+ T-cells may be involved in the influx and further proliferation of inflammatory cells typical of the HL microenvironment. Accordingly, when compared with control lymph nodes or tissues diagnosed with reactive lymphoid hyperplasia, cHL tissues display higher levels of chemokines such as CCL5 and CCL3 [47, 48]. Both chemokines are significantly higher in EBV-positive than in EBV-negative HL tissues [47], consistent with the fact that the EBV gene LMP1 is necessary to induce the expression of CCL5 in EBV-negative cell lines [54].

Both CCR5 [49] and CCL5 [48, 49] are also constitutively expressed by cHL-derived cell lines (L-428, KM-H2, L-1236, and L-540), by tumor cells from cHL lymph node tissues, and by bystander cells including lymphocytes and macrophages [49]. CCR5 receptor is functional since human recombinant CCL5 increases the clonogenic growth of cHL tumor cells. As a consequence, CCL5 secreted by the microenvironment may be a paracrine growth factor for cHL cell. Consistent

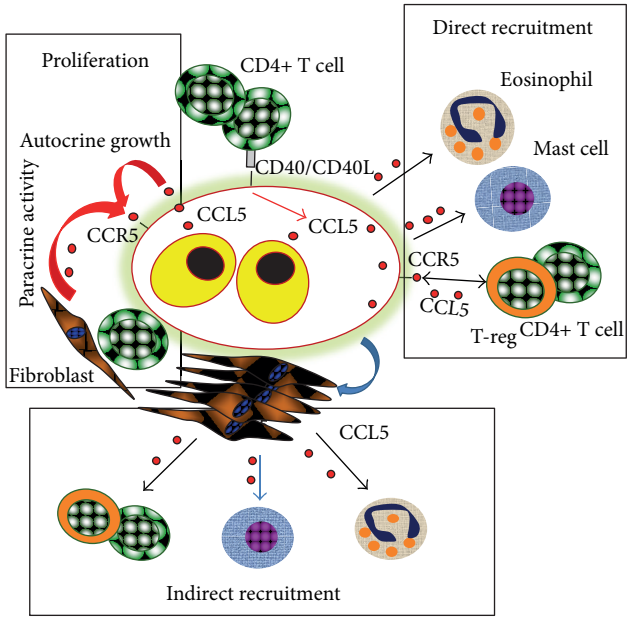

FIGURE 2: Interactions among cHL cells and the microenvironment. Proposed role of the CCL5/CCR5 axis in Hodgkin Lymphoma leading to tumor cell proliferation and microenvironment formation. CCL5 produced by cHL cells may represent an autocrine growth factor. CCL5 secreted by T cells or fibroblasts may represent a paracrine growth factor. CD40L increases CCL5 secretion by cHL cells and they induce fibroblasts to secrete CCL5. CCL5 secreted by cHL (direct recruitment) or fibroblasts activated by HL cells (indirect recruitment) may in turn recruit CD4+ T cells, T-reg cells, eosinophils, and mast cells.

with the fact that cHL cell lines expressed the CCR5 receptor and its ligand, neutralizing anti-CCL5 mAbs decrease the spontaneous clonogenic growth, suggesting that CCL5 may represent an autocrine growth factor for cHL cells. CD40 engagement [19] and cocultivation with fibroblasts from HL-involved lymph nodes (HLF) [49] increase CCL5. On the other hand, the silencing of IRF4, a transcription factor iperexpressed by cHL cells and whose expression is linked to proliferation and survival [55], decreases CCL5 secretion. CCL5 secreted by cHL cells increases the migration of mast cells [48], eosinophils, CD4+ T cells [49], and likely T-reg cells [56], highlighting its involvement in the formation of the microenvironment [8].

As a consequence CCL5 and the CCR5 ligands secreted by tumor cells or by the surrounding T-cells, macrophages, or fibroblasts may support cHL progression by increasing proliferation and by recruiting cells involved in the microenvironment formation. A schematic view of the possible mechanisms (paracrine and autocrine) leading to cHL cells proliferation and microenvironment formation by CCL5 is shown in Figure 2.

4. The CCL5/CCR5 Axis in Solid Tumors

A number of solid tumor types express CCL5 and/or CCR5, but only some malignancies were widely studied, thus providing evidence of the involvement of this pair in cancer progression and development. We briefly summarize the role of CCL5/CCR5 in melanoma and gastric, ovarian, cervical, colorectal, and prostate cancer. However, since the most extensive results were obtained in breast cancer, major emphasis is given to this malignancy.

4.1. Breast Cancer. CCL5, while being minimally expressed by normal breast epithelial duct cells, is highly expressed by breast tumor cells at primary tumor sites, regional lymph nodes, and metastatic sites, indicating that CCL5 expression is acquired in the course of malignant transformation [18] and that CCL5 plays a role in breast cancer development and/or progression. Increased positivity and expression levels of CCL5 by breast tumor cells are significantly associated with [57] disease progression, relapse, and/or metastasis, compared to patients in remission [58, 59]. In this tumor the major source of CCL5 is the tumor cells [57]; however, CCL5 is also expressed by infiltrating leukocytes and mesenchymal stem cells (MSCs) of the tumor microenvironment [15, 57, 60]. CCL5 is also present in interstitial fluids perfusing the tumor, in pleural effusions, and in serum [18].

A functional CCR5 receptor is expressed by a subpopulation of human breast cancer cell lines and displays a functional response to CCL5. In addition, oncogene transformation induces CCR5 expression, and the subpopulation of cells that express a functional CCR5 also displays increased cell migration [61] and invasiveness [62]. A microarray analysis on 2,254 human breast cancer specimens found increased expression of CCL5 and its receptor CCR5, but not CCR3, in the basal and HER-2 genetic subtypes [62]. In contrast, when a similar analysis was performed in nonneoplastic breast samples, no correlation between CCL5 and CCR5 expression levels was found, indicating that CCL5/CCR5 signaling may be preferentially activated during the development of specific breast cancer subtypes [62]. CCL5 expression is strongly associated with the progression of breast cancer, particularly the triple-negative breast cancer (TNBC), and may represent an immunotherapeutic target in the TNBC [63].

Hypoxia is a major selective factor that promotes the growth of tumors with a diminished susceptibility to radiation and chemotherapy and is associated with cancer progression, cancer metastasis, and thus poor prognosis. Hypoxia induces a strong increase of both CCL5 and CCR5 expressions by breast cancer cells [64]. Under this experimental condition CCL5 stimulates cell migration rather than cell proliferation and neutralization of CCL5 inhibits the hypoxia-induced migration of cancer cells. Similarly, overexpression of CCR5 increases cell migration, and knockdown of CCR5 attenuates hypoxia-mediated cell migration. Hypoxia-inducible factor-1α (HIF-1α) is involved in CCR5 and CCL5 regulation under hypoxia and HIF-1α mRNA levels are highly correlated with CCR5 mRNA and CCL5 mRNA levels in clinical samples [64].

CCL5 also concurs with the cross-talk between breast cancer cells and MSCs: cancer cells stimulate CCL5 secretion by MSCs and osteoblasts of the tumor microenvironment and CCL5 in turn induces tumor cell migration and promotes

invasion and metastasis [15, 60]. MSCs-derived CCL5 promotes mammary tumor cell invasion and the activation of matrix metalloproteinases (MMPs), consistent with the fact that CCL5 is capable of upregulating the release of MMP-9 [65].

Tumor infiltrating cells seem bona fide prognostic and even predictive biomarkers and could be incorporated into diagnostic and therapeutic algorithms of breast cancer [18]. CCL5 supports breast malignancy by changing the equilibrium between leukocyte infiltrates in tumors, leading to dominance of cells with tumor-promoting rather than tumor-killing activities. In fact, CCL5 shifts the balance between different leukocyte cell types by increasing the presence of deleterious TAMs [10] that secrete proangiogenic factors, suppress the antitumor response [66], and inhibit the antitumor T-cell activities.

CCL5, together with tumor-derived colony-stimulating factors, promotes mammary tumor progression generating MDSCs in the bone marrow, helping to maintain the immunosuppressive capacity of human MDSCs [67]. CCL5 neutralization could decrease the immunosuppression activity of MDSCs, improve the efficacy against poorly immunogenic tumors, and reduce progression and metastasis.

CCL5 expression by breast tumor cells represents a valuable prognostic factor for detection of stage II breast cancer patients who are at risk for disease progression [68]. Its expression is associated with the absence of estrogen receptor, thus increasing the prognostic value of each of these two markers in patients (in the order III > II > I) at risk for progression [68]. CCL5 serum levels are elevated in breast cancer patients compared to healthy individuals [69] and tend to be higher in lymph-node-positive patients, larger tumor size, the presence of lymphovascular invasion and multifocal tumors [70].

CCL5 is also involved in drug resistance [71]. Tamoxifen resistance is a major therapeutic problem in breast cancer and a significant correlation between STAT3-RANTES autocrine signaling and acquisition of tamoxifen resistance has been reported: STAT3 and RANTES in tamoxifen-resistant MCF-7 cells regulate each other via autocrine signaling, leading to the induction of an antiapoptotic signal. This latter facilitates the maintenance of drug resistance, thus suggesting a novel strategy for the management of patients with tamoxifen-resistant tumors [71].

To conclude, based on several studies done in patients, animal model systems, and in vitro systems, the CCL5/CCR5 axis seems to have a crucial role in cancer progression and may represent an important breast cancer therapeutic target with minimal adverse impact [63].

4.2. Melanoma. Melanoma cell lines and melanoma tissues express a number of chemokines that support their growth and are implicated in tumor progression [72]. Furthermore, organ-specific patterns of melanoma metastasis correlate with the expression of specific chemokine receptors [72].

CCL5 and CCR5 are expressed by melanoma cells, primary melanomas, and cutaneous metastasis. CCL5 is higher in melanoma cells than in normal melanocytes and is associated with a higher malignancy state and increased tumor formation [73, 74]. CCR5 is exclusively expressed in primary melanomas and some cutaneous metastases [75]. Recently, to better evaluate the significance of CCR5 expression in melanoma development, tumor growth in CCR5 knockout ($CCR5^{-/-}$) and wild type ($CCR5^{+/+}$) mice was investigated. CCR5 deficiency caused apoptotic melanoma cell death through inhibition of NF-κB and upregulation of IL-1Rα [76], thus suggesting a tumor-promoting role of CCR5. Already a previous study by Mellado et al. had shown that CCR5 plays a key role in inducing apoptotic death in tumor infiltrated lymphocytes (TIL) in a CCL5-dependent manner: CXCL12 released by melanoma cells induced the expression of CCL5 by TIL, which in turn activated their death program [77]. This activity is upregulated also by CCL3 and CCL4: they act via CCR5 to induce cytochrome-c release into the cytosol, leading to activation of caspase-9 and -3. Recently, using a mouse model of melanoma, Schlecker et al. [13] demonstrated that tumor-infiltrating monocyte-MDSCs directly attract high numbers of T-regs via CCR5 and that intratumoral injection of CCL4 or CCL5 increases tumor-infiltrating T-regs, but CCR5 deficiency led to their profound decrease. Moreover, melanoma growth is delayed in CCR5-deficient mice, likely because of a profound decrease of T-regs, emphasizing the importance of CCR5 in the control of antitumor immune responses.

The conclusion is that the CCL5/CCR5 axis seems associated with melanoma progression due to increased levels of immunosuppressive cells.

4.3. Gastric Cancer. Increased CCL5 levels are expressed by human gastric cancer cell lines characterized by a high metastatic potential [78] suggesting a tumor-promoting role of CCL5 in gastric cancer. This possibility is supported by the effects of supernatants derived from low- and high-metastatic gastric cancer cell lines on the activities of peripheral blood mononuclear cells (PBMC). Supernatants from high-metastatic gastric cancer cell lines increase CCL5 expression in PBMC, as compared to PBMC stimulated by supernatants of low-metastatic cells. In turn, tumor cells cocultured with PBMC have higher invasion properties than noncocultured cells, and this process is highly inhibited by antibodies to CCL5 [79], suggesting that the cross-talk with PBMC, likely through CCL5, increases the invasion potential of tumor cells.

Several authors have then analyzed CCL5 expression in gastric cancer and found a possible correlation with the formation of metastasis. The possibility that CCL5 could serve as a predictor of metastasis was based on a study analyzing CCL5 circulating levels prior to anticancer treatment: CCL5 levels are higher in patients than in healthy controls; furthermore, the expression is higher in stage IV patients than in stages I or II-III [80] and in metastatic sites [81]. In fact, CCL5 and CCR5 are highly expressed in gastric cancer with lymph node metastasis, and CCL5 levels in the lymph nodes with cancer invasion are substantially increased, confirming the role of CCL5/CCR5 axis in metastasis formation [81].

Following infection with *Helicobacter pylori* in a gastric cancer model system CCL5 is elevated and its levels are

reduced by treatment with anti-inflammatory drugs [82]. This is in accordance with the finding that IL-2 and IFN-γ (Th1 cells) are lower and IL-10 (Th2 cells) is higher in lymph node metastasis than in cancer without metastasis, suggesting a shift toward an immunosuppressive microenvironment [82].

Expression of CCR5 by gastric tumor cells is associated with a lower survival rate [83]. Gastric cancer cells exploit CCL5, not only for their own growth, but also to assist in evasion of the host immune system [84]. CCL5 serum levels correlate with the clinical stage and treatment with CCL5 promotes tumor growth. Gastric cancer cells stimulate CD4+ T lymphocytes to secrete CCL5 and they may also induce Fas-FasL-mediated apoptosis of CD8+ T lymphocytes using CCL5 [84].

The conclusion is that the CCL5/CCR5 axis seems associated with gastric cancer progression due to increased growth and metastasis formation.

4.4. Colon Cancer. The CCL5/CCR5 axis plays also a role in colon cancer since CCL5 and its receptors are overexpressed within primary as well as liver and pulmonary metastases compared to healthy tissues [85]. CCL5 increases the in vitro growth and the migratory responses of colon cancer cells from both human and mouse origins. In addition, systemic treatment of mice with neutralizing anti-CCL5 antibodies reduced the extent of subcutaneous tumors, liver metastases, and peritoneal carcinosis. More recently, a novel mechanism of immune escape mediated by CCL5 was defined by Chang et al. [11]. Knockdown of CCL5 from CT26 mouse colon tumor cells decreases apoptosis of tumor-infiltrating CD8+ T cells and reduces tumor growth in mice. Here, CCL5 not only promotes migration of T-reg cells to tumors but also enhances the killing ability on CD8+ T cells. This augmented function is associated with the increased release of TGF-β by T-reg cells [11].

While a treatment with TAK-779, a CCR5 antagonist, only partially compromises colon progression, CCL5 neutralization renders the tumors more sensitive to a PDGFRβ-directed strategy in mice. It is of note that this combination regimen offers the greatest protection against liver metastases and fully suppresses macroscopic peritoneal carcinosis. The conclusion is that CCL5/CCR5 signaling recruits T-regs which in turn eliminate CD8+ T cells, thereby defining a novel mechanism of immune escape in colorectal cancer and pointing to the potential value of CCL5 as a therapeutic target [11].

4.5. Prostate Cancer. The CCL5/CCR5 axis is involved also in prostate cancer (PCa) progression: both are expressed in human prostate cancer (PCa) cell lines, primary cultures of prostatic adenocarcinoma cells, and PCa tissues [86]. CCL5 stimulates PCa cell proliferation and invasion and both are inhibited by the CCR5 antagonist TAK-779 [87]. CCL5 increases PCa proliferation in synergy with IL-6 and it is also induced by the antibody-mediated aggregation of the prostate specific membrane antigen (PSMA) [88]. PSMA is a type-II integral membrane protein capable of activating the NF-κB transcription factor [88], predominantly localized to the epithelial cells of the prostate gland and whose expression increases several fold in high-grade prostate cancers and in metastatic and in androgen-insensitive prostate carcinoma [88].

Serum CCL5 levels do not differ among prostate cancer patients with or without paclitaxel resistance but the expression of the CCR1 receptor increases in paclitaxel-resistant PC3 prostate cancer cells [27]. Interaction between CCR1 and CCL5 promotes the invasion of taxane-resistant PC3 prostate cancer cells by increasing the secretion of MMP-2 and -9 via ERK and Rac activation [27] suggesting that CCR1 could be a novel therapeutic target for taxane-resistant prostate cancer.

4.6. Ovarian Cancer. CCL5 expression is detected not only in malignant ovarian biopsies, but also in normal biopsies, with minimal expression in ovarian cancer cell lines [89]. The cell types expressing CCL5 in the biopsies are not yet determined, but it is likely that infiltrating leukocytes constitute the major origin of this chemokine in ovarian tumors [89].

However, recently Long et al. [26] demonstrated that CCL5 is expressed in ovarian cancer stem cells (CSLCs) characterized by the expression of CD133 antigen that identifies a specific subpopulation of human ovarian cancer cell line and ovarian cancer tissue in which migration and invasion are particularly enhanced. In comparison to CD133-negative non-CSLCs, CCL5 and its receptors, CCR1, CCR3, and CCR5, are consistently upregulated in CD133-positive cells, and blocking of CCL5, CCR1, or CCR3 effectively inhibits the invasive capacity of CSLCs. The enhanced invasiveness is mediated through NF-κB activation along with elevated MMP-9 secretion, suggesting that the autocrine activation of CCR1 and CCR3 by CCL5 represents one of the major mechanisms underlying the metastatic property of ovarian cancer cells [26].

Evidence supporting an association between CCL5 and ovarian carcinoma progression was also provided by a study analyzing chemokine levels in plasma of patients at different stages of disease. CCL5 levels are higher in ovarian cancer patients than in patients diagnosed with benign ovarian cysts and elevated in stages III-IV of ovarian cancer compared to stages I-II [90]. CCL5, along with CCL3 and CCL4, is present in ascitic fluids of ovarian carcinoma patients, and their levels positively correlate with the extent of T lymphocytes infiltration [91]. CCR5 and CCR1 are mainly detected in T lymphocytes and monocytes but only low expression of CCR5 is detected in the tumor cells [26, 91].

Cancer-associated fibroblasts (CAFs) are fibroblasts altered by the continuous exposure to cancer cells residing within the tumor microenvironment [92]. CAFs promote cancer cell invasion, proliferation, and metastasis by secreting cytokines and chemokines, which stimulate receptor tyrosine kinase signaling and epithelial-mesenchymal transition (EMT) programs [2].

The cultivation of ovarian cancer cells with normal fibroblasts generates CAFs possibly through the secretion of molecules that regulate the expression of miRNAs, non-coding RNA molecules that regulate gene expression at a posttranscriptional level [93]. The cross-talk between ovarian cancer cells and fibroblasts decreases *miR-31* and *miR-214*

and increases *miR-155* expression, reprogramming normal fibroblasts into tumor-promoting cancer-associated fibroblasts. CCL5 is a key target of *miR-214* and the downregulation of *miR-214* increases CCL5 production, leading to increased tumor growth [94]. Anti-CCL5 antibodies block the effect of CAFs on tumor growth and cell migration [94] and CCL5-transfected normal fibroblasts increase the invasion of ovarian cancer cells [94], suggesting that CCL5 is a candidate effector molecule in CAFs, contributing to tumor cell recruitment and growth. The conclusion is that CCL5 is a protumorigenic chemokine and a key target of *miR-214*, thus showing that microRNA perturbation in the stromal microenvironment can affect tumor growth by increasing the secretion of CCL5 by CAFs and suggesting that CCL5 is a possible therapeutic target in ovarian cancer.

However, at present several outstanding questions remain and the roles played by CCL5 and its receptors in ovarian cancer are far from being resolved. Many additional aspects should be studied in this disease since they may provide important considerations and new strategies for therapeutic intervention.

5. Possible Clinical Applications: CCL5 and CCR5 as Therapeutic Targets in Cancer

A fundamental objective in cancer therapy is to disrupt the interactions leading to tumor growth or to the formation of a protumorigenic and immunosuppressive microenvironment. Accordingly, our knowledge on the role of chemokine receptors in proliferation and invasion of malignant cells and the role of chemokines in the recruitment of tumor-promoting myeloid cells or lymphocytes could be exploited in new approaches to treatment.

5.1. Inhibition of CCR5/CCL5 Interactions. CCR5 is an essential coreceptor for HIV virus entry to host cells and has therefore become an attractive target for anti-HIV therapeutics development. A number of specific small molecule CCR5 antagonists that are being used as antiviral therapies, but are also effective in blocking CCR5 signal transduction, were identified by high-throughput screening efforts. Maraviroc and vicriviroc are CCR5 antagonists that exert potent blocking activities for chemokine function and HIV entry [87]. There are several lines of evidence suggesting possible clinical applications of CCR5 antagonists in cancer treatment. Maraviroc or vicriviroc reduces in vitro invasion of basal breast cancer cells without affecting cell proliferation or viability [95, 96]. Maraviroc, that has already been licensed by FDA for the use in humans, prevents the development of hepatocellular carcinoma [97] in a mouse model and decreases pulmonary metastasis in a preclinical mouse model of breast cancer [62, 96], suggesting that CCR5 antagonists could be used as an adjuvant therapy to reduce the risk of metastasis in patients with the basal breast cancer subtype.

The nonpeptide CCR5 antagonist TAK-779 is a small molecular weight quaternary ammonium derivative, that binds exclusively to CCR5. It inhibits HIV infection [87] but also the CCL5-induced proliferation and invasion of PCa cells; this suggests that this antagonist may potentially be an effective inhibitor 9 of tumor growth and progression [86].

Anibamine [98, 99] is the first natural product reported as a CCR5 antagonist and thus provides a novel structural skeleton distinct from other lead compounds that have generally been identified from high-throughput screening efforts. Anibamine produces significant inhibition of PCa and ovarian cancer cell line OVCAR-3 proliferation without any significant cytotoxicity in NIH 3T3 fibroblastic cells [99, 100], suppresses adhesion and invasion of the highly metastatic M12 PCa cell line, and decreases PCa growth in mice [98, 99]. Based on these results, anibamine and also one of its synthetic analogues are potential leads to develop novel agents against prostate and ovarian cancer. Anibamine is currently undergoing further preclinical characterization [99, 100].

5.2. Inhibition of CCL5 Secretion. Inhibition of CCL5 secretion by cancer cell or by the tumor microenvironment may represent an additional system to affect cancer progression. MSCs are recruited by developing breast tumors where they can enhance the metastatic potential of weakly tumorigenic breast cancer cells through the secretion of CCL5 [15]. Zoledronic acid significantly affects the secretion of CCL5 and interleukin 6 in MSCs [101] suggesting that the drug could contribute to antitumor activity by affecting the ability of MSCs to interact with breast cancer cells. Alternatively, chemotherapy drugs could affect both proliferation and the formation of an immunosuppressive microenvironment by decreasing the secretion of CCL5 by cancer cells, as reported for the PI3Kδ-specific inhibitor GS-1101 in cHL cells [9].

5.3. Inhibition of Cross-Talk (CCL5 Secretion). Another therapeutical modality that deserves some consideration deals with the potential utilization of the cross-talk between cancer cells and cellular constituent of the microenvironment. Along this line we recently found that the EGFR-tyrosine kinase inhibitor gefitinib negatively affects EGFR activation by PC3-CM leading to decreased secretion of CCL5 by MSCs [102].

Overall, anti-CCL5 drugs could affect both tumor cell proliferation and/or the formation of an immunosuppressive microenvironment by decreasing the secretion of CCL5 by cancer cells.

A schematic view of the possible therapeutic application is shown in Figure 3.

6. Conclusions

The investigation of the roles played by CCL5/CCR5 in tumor development and metastasis is only in its infancy. While promalignancy effects are strongly implicated in MM and breast cancer, their contribution to other malignancies such as cHL, melanoma, gastric, prostate, and ovarian and colon cancer deserves further studies.

Furthermore, one has to take into account the fact that the CCL5/CCR5 axis acts in conjunction with other chemokines to affect the malignant phenotype (e.g., the CXCL12/CXCR4

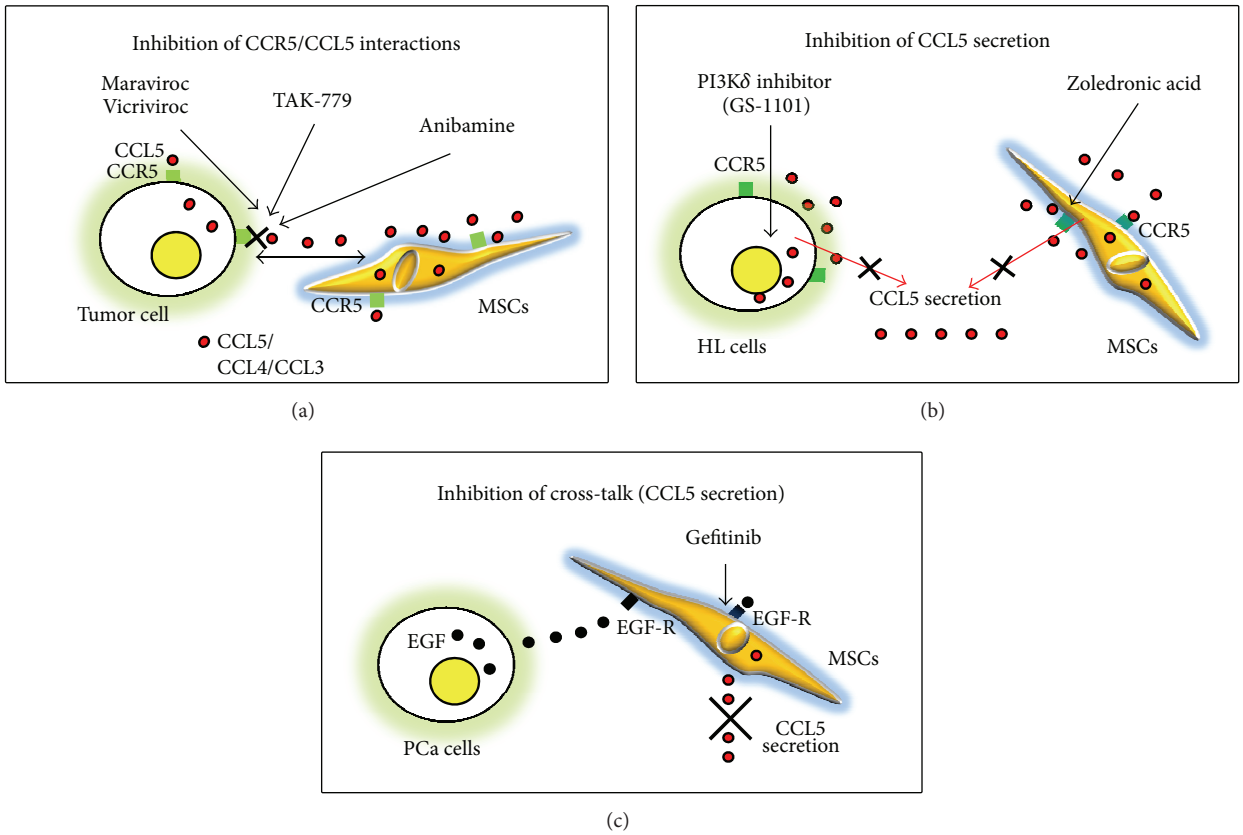

Figure 3: CCL5 and CCR5 as therapeutic targets in cancer. Different strategies proposed to disrupt the CCL5/CCR5 axis. (a) CCL5/CCL5 interaction may be inhibited by CCR5 antagonists. (b) CCL5 secretion by tumor cells or by MSCs of the tumor microenvironment may be decreased by treatment with chemotherapeutic agents. (c) The interactions between tumor cells and MSCs, mediated by EGF/EGFR pair, leading to increased CCL5 secretion by MSCs, may be inhibited by the EGFR-tyrosine kinase inhibitor gefitinib.

pair), exemplifying the multifactorial nature of malignancies and the need to target several mediators simultaneously. Also, in considering CCL5/CCR5 as therapeutic targets, we should evaluate the effects of anti-CCL5/CCR5 treatments on the immune integrity of the host. The optimal therapeutic modalities would have to accommodate two opposing demands: the need to inhibit the detrimental involvement of CCL5 and CCR5 in specific malignant diseases protecting their potentially beneficial activities in immunity, including the anticancer immune responses.

Overall, our current knowledge leads us to suggest the CCL5/CCR5 axis as a potential therapeutic target in several cancer diseases. However, bringing this proposal into practical application requires further research to more clearly elucidate the effects of CCL5 on cancer progression and the formation of an immunosuppressive microenvironment to insure that such treatments are supported by the appropriate rationale.

Finally, as postulated by Schall and Proudfoot, [103] the right target selection, time of intervention, and, in particular, functional dose may be the key to developing successful chemokine-targeted drugs not only for inflammatory diseases but also for cancer.

Conflict of Interests

The authors declare that there is no conflict of interests.

Acknowledgment

This work is supported by Ministero della Salute, Ricerca Finalizzata FSN, I.R.C.C.S., Rome, Italy.

References

[1] A. Mantovani, "Molecular pathways linking inflammation and cancer," *Current Molecular Medicine*, vol. 10, no. 4, pp. 369–373, 2010.

[2] D. Hanahan and L. M. Coussens, "Accessories to the crime: functions of cells recruited to the tumor microenvironment," *Cancer Cell*, vol. 21, no. 3, pp. 309–322, 2012.

[3] M. H. Kershaw, J. A. Westwood, and P. K. Darcy, "Gene-engineered T cells for cancer therapy," *Nature Reviews Cancer*, vol. 13, no. 8, pp. 525–541, 2013.

[4] R. K. Jain, "Normalizing tumor microenvironment to treat cancer: bench to bedside to biomarkers," *Journal of Clinical Oncology*, vol. 31, no. 17, pp. 2205–2218, 2013.

[5] A. Zlotnik and O. Yoshie, "The chemokine superfamily revisited," *Immunity*, vol. 36, no. 5, pp. 705–716, 2012.

[6] J. Candido and T. Hagemann, "Cancer-related inflammation," *Journal of Clinical Immunology*, vol. 33, supplement 1, pp. S79–S84, 2013.

[7] F. R. Balkwill, "The chemokine system and cancer," *Journal of Pathology*, vol. 226, no. 2, pp. 148–157, 2012.

[8] D. Aldinucci, A. Gloghini, A. Pinto, R. de Filippi, and A. Carbone, "The classical Hodgkin's lymphoma microenvironment and its role in promoting tumour growth and immune escape," *Journal of Pathology*, vol. 221, no. 3, pp. 248–263, 2010.

[9] S. A. Meadows, F. Vega, A. Kashishian et al., "PI3Kδ inhibitor, GS-1101 (CAL-101), attenuates pathway signaling, induces apoptosis, and overcomes signals from the microenvironment in cellular models of Hodgkin lymphoma," *Blood*, vol. 119, no. 8, pp. 1897–1900, 2012.

[10] J. Cook and T. Hagemann, "Tumour-associated macrophages and cancer," *Current Opinion in Pharmacology*, vol. 13, no. 4, pp. 595–601, 2013.

[11] L.-Y. Chang, Y.-C. Lin, J. Mahalingam et al., "Tumor-derived chemokine CCL5 enhances TGF-β-mediated killing of $CD8^+$ T cells in colon cancer by T-regulatory cells," *Cancer Research*, vol. 72, no. 5, pp. 1092–1102, 2012.

[12] X. Yang, J. Hou, Z. Han et al., "One cell, multiple roles: contribution of mesenchymal stem cells to tumor development in tumor microenvironment," *Cell & Bioscience*, vol. 3, no. 1, pp. 5–3, 2013.

[13] E. Schlecker, A. Stojanovic, C. Eisen et al., "Tumor-infiltrating monocytic myeloid-derived suppressor cells mediate CCR5-dependent recruitment of regulatory T cells favoring tumor growth," *The Journal of Immunology*, vol. 189, no. 12, pp. 5602–5611, 2012.

[14] A. Ben-Baruch, "The tumor-promoting flow of cells into, within and out of the tumor site: regulation by the inflammatory axis of TNFα and chemokines," *Cancer Microenvironment*, vol. 5, no. 2, pp. 151–164, 2012.

[15] A. E. Karnoub, A. B. Dash, A. P. Vo et al., "Mesenchymal stem cells within tumour stroma promote breast cancer metastasis," *Nature*, vol. 449, no. 7162, pp. 557–563, 2007.

[16] P. Allavena, G. Germano, F. Marchesi, and A. Mantovani, "Chemokines in cancer related inflammation," *Experimental Cell Research*, vol. 317, no. 5, pp. 664–673, 2011.

[17] M. Oppermann, "Chemokine receptor CCR5: insights into structure, function, and regulation," *Cellular Signalling*, vol. 16, no. 11, pp. 1201–1210, 2004.

[18] G. Soria and A. Ben-Baruch, "The inflammatory chemokines CCL2 and CCL5 in breast cancer," *Cancer Letters*, vol. 267, no. 2, pp. 271–285, 2008.

[19] D. Aldinucci, A. Gloghini, A. Pinto, A. Colombatti, and A. Carbone, "The role of CD40/CD40L and interferon regulatory factor 4 in Hodgkin lymphoma microenvironment," *Leukemia and Lymphoma*, vol. 53, no. 2, pp. 195–201, 2012.

[20] M. J. Chenoweth, M. F. Mian, N. G. Barra et al., "IL-15 can signal via IL-15Rα, JNK, and NF-κB To drive RANTES production by myeloid cells," *Journal of Immunology*, vol. 188, no. 9, pp. 4149–4157, 2012.

[21] J. Udi, J. Schuler, D. Wider et al., "Potent in vitro and in vivo activity of sorafenib in multiple myeloma: induction of cell death, CD138-downregulation and inhibition of migration through actin depolymerization," *British Journal of Haematology*, vol. 161, no. 1, pp. 104–116, 2013.

[22] V. Appay and S. L. Rowland-Jones, "RANTES: a versatile and controversial chemokine," *Trends in Immunology*, vol. 22, no. 2, pp. 83–87, 2001.

[23] B. Roscic-Mrkic, M. Fischer, C. Leemann et al., "RANTES (CCL5) uses the proteoglycan CD44 as an auxiliary receptor to mediate cellular activation signals and HIV-1 enhancement," *Blood*, vol. 102, no. 4, pp. 1169–1177, 2003.

[24] A. J. Ridley, M. A. Schwartz, K. Burridge et al., "Cell migration: integrating signals from front to back," *Science*, vol. 302, no. 5651, pp. 1704–1709, 2003.

[25] C.-Y. Huang, Y.-C. Fong, C.-Y. Lee et al., "CCL5 increases lung cancer migration via PI3K, Akt and NF-κB pathways," *Biochemical Pharmacology*, vol. 77, no. 5, pp. 794–803, 2009.

[26] H. Long, R. Xie, T. Xiang et al., "Autocrine CCL5 signaling promotes invasion and migration of $CD133^+$ ovarian cancer stem-like cells via NF-kappaB-mediated MMP-9 upregulation," *Stem Cells*, vol. 30, no. 10, pp. 2309–2319, 2012.

[27] T. Kato, Y. Fujita, K. Nakane et al., "CCR1/CCL5 interaction promotes invasion of taxane-resistant PC3 prostate cancer cells by increasing secretion of MMPs 2/9 and by activating ERK and Rac signaling," *Cytokine*, vol. 64, no. 1, pp. 251–257, 2013.

[28] J. E. Kim, H. S. Kim, Y. J. Shin et al., "LYR71, a derivative of trimeric resveratrol, inhibits tumorigenesis by blocking STAT3-mediated matrix metalloproteinase 9 expression," *Experimental and Molecular Medicine*, vol. 40, no. 5, pp. 514–522, 2008.

[29] S.-W. Wang, H.-H. Wu, S.-C. Liu et al., "CCL5 and CCR5 interaction promotes cell motility in human osteosarcoma," *PLoS ONE*, vol. 7, no. 4, Article ID e35101, 2012.

[30] D. Raman, T. Sobolik-Delmaire, and A. Richmond, "Chemokines in health and disease," *Experimental Cell Research*, vol. 317, no. 5, pp. 575–589, 2011.

[31] D. F. Gao and E. N. Fish, "89: a role for CCL5 in breast cancer cell metabolism," *Cytokine*, vol. 63, no. 3, p. 264, 2013.

[32] I. Borrello, "Can we change the disease biology of multiple myeloma?" *Leukemia Research*, vol. 36, supplement 1, pp. S3–S12, 2012.

[33] M. Abe, K. Hiura, J. Wilde et al., "Osteoclasts enhance myeloma cell growth and survival via cell-cell contact: a vicious cycle between bone destruction and myeloma expansion," *Blood*, vol. 104, no. 8, pp. 2484–2491, 2004.

[34] Y. Oba, J. W. Lee, L. A. Ehrlich et al., "MIP-1α utilizes both CCR1 and CCR5 to induce osteoclast formation and increase adhesion of myeloma cells to marrow stromal cells," *Experimental Hematology*, vol. 33, no. 3, pp. 272–278, 2005.

[35] E. Menu, E. de Leenheer, H. de Raeve et al., "Role of CCR1 and CCR5 in homing and growth of multiple myeloma and in the development of osteolytic lesions: a study in the 5TMM model," *Clinical and Experimental Metastasis*, vol. 23, no. 5-6, pp. 291–300, 2006.

[36] G. D. Roodman and S. J. Choi, "MIP-1 alpha and myeloma bone disease," *Cancer Treatment and Research*, vol. 118, pp. 83–100, 2004.

[37] T. Hashimoto, M. Abe, T. Oshima et al., "Ability of myeloma cells to secrete macrophage inflammatory protein (MIP)-1α and MIP-1β correlates with lytic bone lesions in patients with multiple myeloma," *British Journal of Haematology*, vol. 125, no. 1, pp. 38–41, 2004.

[38] E. Terpos, M. Politou, R. Szydlo, J. M. Goldman, J. F. Apperley, and A. Rahemtulla, "Serum levels of macrophage inflammatory protein-1 alpha (MIP-1α) correlate with the extent of bone disease and survival in patients with multiple myeloma," *British Journal of Haematology*, vol. 123, no. 1, pp. 106–109, 2003.

[39] M. Roussou, A. Tasidou, M. A. Dimopoulos et al., "Increased expression of macrophage inflammatory protein-1α on trephine biopsies correlates with extensive bone disease, increased angiogenesis and advanced stage in newly diagnosed patients with multiple myeloma," *Leukemia*, vol. 23, no. 11, pp. 2177–2181, 2009.

[40] S. Vallet, S. Pozzi, K. Patel et al., "A novel role for CCL3 (MIP-1α) in myeloma-induced bone disease via osteocalcin downregulation and inhibition of osteoblast function," *Leukemia*, vol. 25, no. 7, pp. 1174–1181, 2011.

[41] Y. Cao, T. Luetkens, S. Kobold et al., "The cytokine/chemokine pattern in the bone marrow environment of multiple myeloma patients," *Experimental Hematology*, vol. 38, no. 10, pp. 860–867, 2010.

[42] M. Abe, K. Hiura, J. Wilde et al., "Role for macrophage inflammatory protein (MIP)-1α and MIP-1β in the development of osteolytic lesions in multiple myeloma," *Blood*, vol. 100, no. 6, pp. 2195–2202, 2002.

[43] S. Lentzsch, M. Gries, M. Janz, R. Bargou, B. Dörken, and M. Y. Mapara, "Macrophage inflammatory protein 1-alpha (MIP-1α) triggers migration and signaling cascades mediating survival and proliferation in multiple myeloma (MM) cells," *Blood*, vol. 101, no. 9, pp. 3568–3573, 2003.

[44] S. Vallet and K. C. Anderson, "CCR1 as a target for multiple myeloma," *Expert Opinion on Therapeutic Targets*, vol. 15, no. 9, pp. 1037–1047, 2011.

[45] C. Möller, T. Strömberg, M. Juremalm, K. Nilsson, and G. Nilsson, "Expression and function of chemokine receptors in human multiple myeloma," *Leukemia*, vol. 17, no. 1, pp. 203–210, 2003.

[46] D. J. Dairaghi, B. O. Oyajobi, A. Gupta et al., "CCR1 blockade reduces tumor burden and osteolysis in vivo in a mouse model of myeloma bone disease," *Blood*, vol. 120, no. 7, pp. 1449–1457, 2012.

[47] E. Maggio, A. van den Berg, A. Diepstra, J. Kluiver, L. Visser, and S. Poppema, "Chemokines, cytokines and their receptors in Hodgkin's lymphoma cell lines and tissues," *Annals of Oncology*, vol. 13, supplement 1, pp. 52–56, 2002.

[48] M. Fischer, M. Juremalm, N. Olsson et al., "Expression of CCL5/RANTES by Hodgkin and reed-sternberg cells and its possible role in the recruitment of mast cells into lymphomatous tissue," *International Journal of Cancer*, vol. 107, no. 2, pp. 197–201, 2003.

[49] D. Aldinucci, D. Lorenzon, L. Cattaruzza et al., "Expression of CCR5 receptors on Reed-Sternberg cells and Hodgkin lymphoma cell lines: involvement of CCL5/Rantes in tumor cell growth and microenvironmental interactions," *International Journal of Cancer*, vol. 122, no. 4, pp. 769–776, 2008.

[50] M. Niens, L. Visser, I. M. Nolte et al., "Serum chemokine levels in Hodgkin lymphoma patients: highly increased levels of CCL17 and CCL22," *British Journal of Haematology*, vol. 140, no. 5, pp. 527–536, 2008.

[51] H. Hanamoto, T. Nakayama, H. Miyazato et al., "Expression of CCL28 by Reed-Sternberg cells defines a major subtype of classical Hodgkin's disease with frequent infiltration of eosinophils and/or plasma cells," *American Journal of Pathology*, vol. 164, no. 3, pp. 997–1006, 2004.

[52] K. R. N. Baumforth, A. Birgersdotter, G. M. Reynolds et al., "Expression of the Epstein-Barr virus-encoded Epstein-Barr virus nuclear antigen 1 in Hodgkin's lymphoma cells mediates up-regulation of CCL20 and the migration of regulatory T cells," *American Journal of Pathology*, vol. 173, no. 1, pp. 195–204, 2008.

[53] F. Jundt, I. Anagnostopoulos, K. Bommert et al., "Hodgkin/Reed-Sternberg cells induce fibroblasts to secrete eotaxin, a potent chemoattractant for T cells and eosinophils," *Blood*, vol. 94, no. 6, pp. 2065–2071, 1999.

[54] J. N. Uchihara, A. M. Krensky, T. Matsuda et al., "Transactivation of the CCL5/RANTES gene by Epstein-Barr virus latent membrane protein 1," *International Journal of Cancer*, vol. 114, no. 5, pp. 747–755, 2005.

[55] D. Aldinucci, M. Celegato, C. Borghese, A. Colombatti, and A. Carbone, "IRF4 silencing inhibits Hodgkin lymphoma cell proliferation, survival and CCL5 secretion," *British Journal of Haematology*, vol. 152, no. 2, pp. 182–190, 2011.

[56] D. Aldinucci, A. Pinto, A. Gloghini, and A. Carbone, "Chemokine receptors as therapeutic tools in Hodgkin lymphoma: CCR4 and beyond," *Blood*, vol. 115, no. 3, pp. 746–747, 2010.

[57] G. Luboshits, S. Shina, O. Kaplan et al., "Elevated expression of the CC chemokine regulated on activation, normal T cell expressed and secreted (RANTES) in advanced breast carcinoma," *Cancer Research*, vol. 59, no. 18, pp. 4681–4687, 1999.

[58] Y. Niwa, H. Akamatsu, H. Niwa, H. Sumi, Y. Ozaki, and A. Abe, "Correlation of tissue and plasma RANTES levels with disease course in patients with breast or cervical cancer," *Clinical Cancer Research*, vol. 7, no. 2, pp. 285–289, 2001.

[59] I. Bièche, F. Lerebours, S. Tozlu, M. Espie, M. Marty, and R. Lidereau, "Molecular profiling of inflammatory breast cancer: identification of a poor-prognosis gene expression signature," *Clinical Cancer Research*, vol. 10, no. 20, pp. 6789–6795, 2004.

[60] Z. Mi, S. D. Bhattacharya, V. M. Kim, H. Guo, L. J. Talbotq, and P. C. Kuo, "Osteopontin promotes CCL5-mesenchymal stromal cell-mediated breast cancer metastasis," *Carcinogenesis*, vol. 32, no. 4, pp. 477–487, 2011.

[61] Y. Zhang, F. Yao, X. Yao et al., "Role of CCL5 in invasion, proliferation and proportion of $CD44^+$/CD24- phenotype of MCF-7 cells and correlation of CCL5 and CCR5 expression with breast cancer progression," *Oncology Reports*, vol. 21, no. 4, pp. 1113–1121, 2009.

[62] M. Velasco-Velazquez, X. Jiao, M. de la Fuente et al., "CCR5 antagonist blocks metastasis of basal breast cancer cells," *Cancer Research*, vol. 72, no. 15, pp. 3839–3850, 2012.

[63] D. Lv, Y. Zhang, H. J. Kim, L. Zhang, and X. Ma, "CCL5 as a potential immunotherapeutic target in triple-negative breast cancer," *Cellular & Molecular Immunology*, vol. 10, no. 4, pp. 303–310, 2013.

[64] S. Lin, S. Wan, L. Sun et al., "Chemokine C-C motif receptor 5 and C-C motif ligand 5 promote cancer cell migration under hypoxia," *Cancer Science*, vol. 103, no. 5, pp. 904–912, 2012.

[65] M. Swamydas, K. Ricci, S. L. Rego, and D. Dreau, "Mesenchymal stem cell-derived CCL-9 and CCL-5 promote mammary tumor cell invasion and the activation of matrix metalloproteinases," *Cell Adhesion & Migration*, vol. 7, no. 3, pp. 315–324, 2013.

[66] E. Azenshtein, G. Luboshits, S. Shina et al., "The CC chemokine RANTES in breast carcinoma progression: regulation of expression and potential mechanisms of promalignant activity," *Cancer Research*, vol. 62, no. 4, pp. 1093–1102, 2002.

[67] Y. Zhang, D. Lv, H. J. Kim et al., "A novel role of hematopoietic CCL5 in promoting triple-negative mammary tumor progression by regulating generation of myeloid-derived suppressor cells," *Cell Research*, vol. 23, no. 3, pp. 394–408, 2013.

[68] N. Yaal-Hahoshen, S. Shina, L. Leider-Trejo et al., "The chemokine CCL5 as a potential prognostic factor predicting

disease progression in stage II breast cancer patients," *Clinical Cancer Research*, vol. 12, no. 15, pp. 4474–4480, 2006.

[69] Z. A. Dehqanzada, C. E. Storrer, M. T. Hueman et al., "Assessing serum cytokine profiles in breast cancer patients receiving a HER2/neu vaccine using Luminex technology," *Oncology Reports*, vol. 17, no. 3, pp. 687–694, 2007.

[70] A. Smeets, B. Brouwers, S. Hatse et al., "Circulating CCL5 levels in patients with breast cancer: is there a correlation with lymph node metastasis?" *ISRN Immunology*, vol. 2013, Article ID 453561, 5 pages, 2013.

[71] E. H. Yi, C. S. Lee, J. K. Lee et al., "STAT3-RANTES autocrine signaling is essential for tamoxifen resistance in human breast cancer cells," *Molecular Cancer Research*, vol. 11, no. 1, pp. 31–42, 2013.

[72] A. S. Payne and L. A. Cornelius, "The role of chemokines in melanoma tumor growth and metastasis," *Journal of Investigative Dermatology*, vol. 118, no. 6, pp. 915–922, 2002.

[73] U. Mrowietz, U. Schwenk, S. Maune et al., "The chemokine RANTES is secreted by human melanoma cells and is associated with enhanced tumour formation in nude mice," *British Journal of Cancer*, vol. 79, no. 7-8, pp. 1025–1031, 1999.

[74] S. Mattei, M. P. Colombo, C. Melani, A. Silvani, G. Parmiani, and M. Herlyn, "Expression of cytokine/growth factors and their receptors in human melanoma and melanocytes," *International Journal of Cancer*, vol. 56, no. 6, pp. 853–857, 1994.

[75] H. Seidl, E. Richtig, H. Tilz et al., "Profiles of chemokine receptors in melanocytic lesions: de novo expression of CXCR6 in melanoma," *Human Pathology*, vol. 38, no. 5, pp. 768–780, 2007.

[76] J. K. Song, M. H. Park, D.-Y. Choi et al., "Deficiency of C-C chemokine receptor 5 suppresses tumor development via inactivation of NF-κB and upregulation of IL-1Ra in Melanoma model," *PLoS ONE*, vol. 7, no. 5, Article ID e33747, 2012.

[77] M. Mellado, A. M. de Ana, M. C. Moreno, C. Martínez, and J. M. Rodríguez-Frade, "A potential immune escape mechanism by melanoma cells through the activation of chemokine-induced T cell death," *Current Biology*, vol. 11, no. 9, pp. 691–696, 2001.

[78] R. Fukui, H. Nishimori, F. Hata et al., "Metastases-related genes in the classification of liver and peritoneal metastasis in human gastric cancer," *Journal of Surgical Research*, vol. 129, no. 1, pp. 94–100, 2005.

[79] K. Okita, T. Furuhata, Y. Kimura et al., "The interplay between gastric cancer cell lines and PBMCs mediated by the CC chemokine RANTES plays an important role in tumor progression," *Journal of Experimental and Clinical Cancer Research*, vol. 24, no. 3, pp. 439–446, 2005.

[80] H. K. Kim, K. S. Song, Y. S. Park et al., "Elevated levels of circulating platelet microparticles, VEGF, IL-6 and RANTES in patients with gastric cancer: possible role of a metastasis predictor," *European Journal of Cancer*, vol. 39, no. 2, pp. 184–191, 2003.

[81] Z. Cao, X. Xu, X. Luo et al., "Role of RANTES and its receptor in gastric cancer metastasis," *Journal of Huazhong University of Science and Technology—Medical Science*, vol. 31, no. 3, pp. 342–347, 2011.

[82] K. B. Hahm, Y. J. Song, T. Y. Oh et al., "Chemoprevention of Helicobacter pylori-associated gastric carcinogenesis in a mouse model: is it possible?" *Journal of Biochemistry and Molecular Biology*, vol. 36, no. 1, pp. 82–94, 2003.

[83] H. Sugasawa, T. Ichikura, H. Tsujimoto et al., "Prognostic significance of expression of CCL5/RANTES receptors in patients with gastric cancer," *Journal of Surgical Oncology*, vol. 97, no. 5, pp. 445–450, 2008.

[84] H. Sugasawa, T. Ichikura, M. Kinoshita et al., "Gastric cancer cells exploit $CD4^+$ cell-derived CCL5 for their growth and prevention of $CD8^+$ cell-involved tumor elimination," *International Journal of Cancer*, vol. 122, no. 11, pp. 2535–2541, 2008.

[85] B. Cambien, P. Richard-Fiardo, B. F. Karimdjee et al., "CCL5 neutralization restricts cancer growth and potentiates the targeting of PDGFRβ in colorectal carcinoma," *PLoS ONE*, vol. 6, no. 12, Article ID e28842, 2011.

[86] G. G. Vaday, D. M. Peehl, P. A. Kadam, and D. M. Lawrence, "Expression of CCL5 (RANTES) and CCR5 in prostate cancer," *Prostate*, vol. 66, no. 2, pp. 124–134, 2006.

[87] K. Maeda, D. Das, H. Nakata, and H. Mitsuya, "CCR5 inhibitors: emergence, success, and challenges," *Expert Opinion on Emerging Drugs*, vol. 17, no. 2, pp. 135–145, 2012.

[88] M. Colombatti, S. Grasso, A. Porzia et al., "The prostate specific membrane antigen regulates the expression of IL-6 and CCL5 in prostate tumour cells by activating the MAPK pathways," *PLoS ONE*, vol. 4, no. 2, Article ID e4608, 2009.

[89] R. P. M. Negus, G. W. H. Stamp, J. Hadley, and F. R. Balkwill, "Quantitative assessment of the leukocyte infiltrate in ovarian cancer and its relationship to the expression of C-C chemokines," *American Journal of Pathology*, vol. 150, no. 5, pp. 1723–1734, 1997.

[90] S. Tsukishiro, N. Suzumori, H. Nishikawa, A. Arakawa, and K. Suzumori, "Elevated serum RANTES levels in patients with ovarian cancer correlate with the extent of the disorder," *Gynecologic Oncology*, vol. 102, no. 3, pp. 542–545, 2006.

[91] D. Milliken, C. Scotton, S. Raju, F. Balkwill, and J. Wilson, "Analysis of chemokines and chemokine receptor expression in ovarian cancer ascites," *Clinical Cancer Research*, vol. 8, no. 4, pp. 1108–1114, 2002.

[92] S. Madar, I. Goldstein, and V. Rotter, "'Cancer associated fibroblasts'—more than meets the eye," *Trends in Molecular Medicine*, vol. 19, no. 8, pp. 447–453, 2013.

[93] R. Schickel, B. Boyerinas, S.-M. Park, and M. E. Peter, "MicroRNAs: key players in the immune system, differentiation, tumorigenesis and cell death," *Oncogene*, vol. 27, no. 45, pp. 5959–5974, 2008.

[94] A. K. Mitra, M. Zillhardt, Y. Hua et al., "MicroRNAs reprogram normal fibroblasts into cancer-associated fibroblasts in ovarian cancer," *Cancer Discovery*, vol. 2, no. 12, pp. 1100–1108, 2012.

[95] M. Baba, O. Nishimura, N. Kanzaki et al., "A small-molecule, nonpeptide CCR5 antagonist with highly potent and selective anti-HIV-1 activity," *Proceedings of the National Academy of Sciences of the United States of America*, vol. 96, no. 10, pp. 5698–5703, 1999.

[96] M. Velasco-Velazquez and R. G. Pestell, "The CCL5/CCR5 axis promotes metastasis in basal breast cancer," *Oncoimmunology*, vol. 2, no. 4, 2013.

[97] L. Ochoa-Callejero, L. Perez-Martinez, S. Rubio-Mediavilla, J. A. Oteo, A. Martinez, and J. R. Blanco, "Maraviroc, a CCR5 antagonist, prevents development of hepatocellular carcinoma in a mouse model," *PLoS ONE*, vol. 8, no. 1, Article ID e53992, 2013.

[98] F. Zhang, C. K. Arnatt, K. M. Haney et al., "Structure activity relationship studies of natural product chemokine receptor CCR5 antagonist anibamine toward the development of novel anti prostate cancer agents," *European Journal of Medicinal Chemistry*, vol. 55, pp. 395–408, 2012.

[99] X. Zhang, K. M. Haney, A. C. Richardson et al., "Anibamine, a natural product CCR5 antagonist, as a novel lead for the development of anti-prostate cancer agents," *Bioorganic and Medicinal Chemistry Letters*, vol. 20, no. 15, pp. 4627–4630, 2010.

[100] Y. Zhang, C. K. Arnatt, F. Zhang, J. Wang, K. M. Haney, and X. Fang, "The potential role of anibamine, a natural product CCR5 antagonist, and its analogues as leads toward development of anti-ovarian cancer agents," *Bioorganic & Medicinal Chemistry Letters*, vol. 22, no. 15, pp. 5093–5097, 2012.

[101] M. Gallo, A. de Luca, L. Lamura, and N. Normanno, "Zoledronic acid blocks the interaction between mesenchymal stem cells and breast cancer cells: implications for adjuvant therapy of breast cancer," *Annals of Oncology*, vol. 23, no. 3, pp. 597–604, 2012.

[102] C. Borghese, L. Cattaruzza, E. Pivetta et al., "Gefitinib inhibits the cross-talk between mesenchymal stem cells and prostate cancer cells leading to tumor cell proliferation and inhibition of docetaxel activity," *Journal of Cellular Biochemistry*, vol. 114, no. 5, pp. 1135–1144, 2013.

[103] T. J. Schall and A. E. I. Proudfoot, "Overcoming hurdles in developing successful drugs targeting chemokine receptors," *Nature Reviews Immunology*, vol. 11, no. 5, pp. 355–363, 2011.

Hindawi Publishing Corporation
Mediators of Inflammation
Volume 2013, Article ID 564687, 7 pages
http://dx.doi.org/10.1155/2013/564687

Clinical Study

CD38 Ligation in Peripheral Blood Mononuclear Cells of Myeloma Patients Induces Release of Protumorigenic IL-6 and Impaired Secretion of IFNγ Cytokines and Proliferation

Giorgio Fedele,[1] Marco Di Girolamo,[2] Umberto Recine,[3] Raffaella Palazzo,[1] Francesca Urbani,[1] Alberto L. Horenstein,[4] Fabio Malavasi,[4] and Clara Maria Ausiello[1]

[1] *Department of Infectious, Parasitic and Immune-mediated Diseases, Anti-infectious Immunity Unit, Istituto Superiore di Sanità, 00161 Rome, Italy*
[2] *Department of Internal Medicine S. Giovanni Calibita, Fatebenefratelli General Hospital, 00186 Rome, Italy*
[3] *Onco-hematological unit, Department of General Medicine, S. Spirito Hospital, 00193 Rome, Italy*
[4] *Laboratory of Immunogenetics, Department of Medical Sciences and Research Center for Experimental Medicine (CeRMS), University of Torino Medical School and "Città della Salute e della Scienza" Hospital, 10126 Torino, Italy*

Correspondence should be addressed to Giorgio Fedele; giorgio.fedele@iss.it and Clara Maria Ausiello; ausiello@iss.it

Received 4 September 2013; Revised 5 November 2013; Accepted 20 November 2013

Academic Editor: Salahuddin Ahmed

CD38, a surface receptor that controls signals in immunocompetent cells, is densely expressed by cells of multiple myeloma (MM). The immune system of MM patients appears as functionally impaired, with qualitative and quantitative defects in T cell immune responses. This work answers the issue whether CD38 plays a role in the impairment of T lymphocyte response. To this aim, we analyzed the signals implemented by monoclonal antibodies (mAb) ligation in peripheral blood mononuclear cells (PBMC) obtained from MM patients and compared to benign monoclonal gammopathy of undetermined significance (MGUS). PBMC from MM both failed to proliferate and secrete IFNγ induced by CD38 ligation while it retained the ability to respond to TCR/CD3. The impaired CD38-dependent proliferative response likely reflects an arrest in the progression of cell cycle, as indicated by the reduced expression of PCNA. CD38 signaling showed an enhanced ability to induce IL-6 secretion. PBMC from MM patients displays a deregulated response possibly due to defects of CD38 activation pathways and CD38 may be functionally involved in the progression of this pathology via the secretion of high levels of IL-6 that protects neoplastic cells from apoptosis.

1. Introduction

CD38 is a multifunctional surface molecule, expressed in a variety of cells and tissues. The molecule is densely expressed by normal plasma cells and by cells of multiple myeloma (MM), a clonal malignant disorder of terminally differentiated B lymphocytes. The disease is characterized by bone marrow plasmacytosis, bone lytic lesions, and by a secondary hypergammaglobulinemia. MM usually develops from an asymptomatic premalignant stage of clonal plasma cell proliferation, termed "monoclonal gammopathy of undetermined significance" (MGUS) [1, 2].

CD38 is simultaneously a receptor and adhesion molecule as well as an ectoenzyme that catalyses the synthesis of ADP ribose (ADPR), cyclic ADPR (cADPR), and nicotinic acid adenine dinucleotide phosphate (NAADP), starting from nicotinamide adenine dinucleotide (NAD^+). cADPR and NAADP are two potent second messenger for Ca^{2+} release [3, 4]. As a receptor, CD38 is engaged by CD31, identified as a counter-receptor [5], or by surrogate agonistic monoclonal antibodies (mAbs) [6]. The effects mediated by CD38 ligation include production of pro-inflammatory and regulatory cytokines by monocytes [7], NK cells [8], activated B [9] and T lymphocytes [10] and dendritic cells (DC) [11], proliferation of T lymphocytes [12], and protection of mature B lymphocytes and DC from apoptosis [13, 14].

The role of CD38 has been informative in different pathological disorders, such as in AIDS (where CD38 is one of the earliest indicators of infection [15]) and B cell chronic lymphocytic leukemia (B-CLL) [16]. There are several

issues suggesting that CD38 plays significant roles in MM. First, CD38 is expressed by normal and tumoral plasma cells at high levels, in cells which tend to eliminate the majority of surface molecules. Second, plasma cells from MM and MGUS express CD31, the CD38 ligand, in a significant proportion of cases [17–20]. Another finding linking CD38 and plasma cell biology is the release of interleukin IL-6 driven by CD38 signaling [7, 10]. Indeed, IL-6 produced by bone marrow stromal cells is an autocrine growth factor for human myeloma cells and it is involved in the genesis of several of the clinical symptoms observed in MM patients [20, 21]. However, still elusive is the functional role exerted by CD38 in plasma cells and in myeloma [2, 19].

The immune system of MM patients is functionally impaired, with quantitative and qualitative defects mainly in the context of cellular responses. Defects in antigen presenting cell (APC) functions have been reported in these patients. Indeed, high potency blood DC failed to up-regulate the expression of the costimulatory molecule CD80 in response to stimulation by human CD40 ligand, a defect caused by transforming growth factor β1 (TGFβ1) and by (IL)-10 produced by malignant plasma cells [22]. DC functions were restored by inhibiting p38 or activating MEK/ERK MAPK and neutralizing IL-6 in progenitor cells [23]. Also, T lymphocytes from MM patients displayed an altered phenotype, characterized by enhanced expression of CD38 and HLA Class II [24], impaired responses to mitogens [25], and increased susceptibility to apoptosis (enhanced expression of Fas (APO-1/CD95) and decreased expression of the anti-apoptotic factor Bcl-2) [26, 27]. $CD8^+$ T lymphocytes in MM patients are characterized by increased expression of nonfunctional killer inhibitory receptor CD94 [28].

Some of these defects may be linked to the superior ability of DC obtained from MM patients to maintain regulatory T cells [29]. Active MM patients show a deregulated cytokine network [30, 31], with increased synthesis, release of IL-6 production [25], and impaired Th1 response. The picture is further complicated by the finding of differences in Th1 response between active MM and MGUS patients as well as MM in remission [31].

Trying to dissect the role of CD38 in the immune response and at the same time to elucidate its role in MM pathogenesis, we designed a pilot study, where CD38-mediated signaling in MM and MGUS patients are compared. The rational stems from the notion that 25% of the patients with MGUS eventually develop MM or related plasma cell disorder. However, whether the changes that occur in the clonal plasma cell are important in the progression of MGUS to active myeloma is not yet clear. A critical feature shared by MM and MGUS is the extremely low rate of clonal plasma cell proliferation until late stages of MM are reached [32].

The approach adopted was a functional evaluation of CD38 engagement and signals in peripheral blood mononuclear cells (PBMC) obtained from MM patients and compared to a MGUS picture.

2. Patients, Materials, and Methods

2.1. Patients. PBMC were obtained from 11 patients with MM (mean age 74 years, 64% males) and 7 patients with MGUS (mean age 67 years, 71% males). Blood samples were taken before therapy. MM patients were staged according to the criteria of Durie and Salmon [33]. All stages were included: 4 patients of IA stage (36%), 3 patients of IIA stage (27%), and 4 patients of IIIA stage (36%). Fifteen healthy donors, sex and age matched were included as reference controls. All experiments were conducted in accordance with the Declaration of Helsinki [34]. Ethics approval was obtained from the Ethical Committee of two Hospitals, and written informed consent was provided by patients and healthy donors involved in the study.

2.2. Monoclonal Antibodies and Reagents. Agonistic anti-CD38 mAb [IB4 (IgG_{2a})] [35] and the reference anti-TCR/CD3 mAb [CBT3G (IgG_{2a})] were high-grade purified [36]. Proliferation tests and cytokine assays were performed by using the IB4 mAb at 20 μg/mL, while CBT3G mAb was used at 1 μg/mL.

2.3. PBMC Isolation and Proliferation and Cytokine Assays. PBMC obtained from heparinized venous peripheral blood by centrifugation on density gradient (Lympholyte-H, Cedarlane, Hornby, ON, Canada) were washed twice and suspended in RPMI-1640 medium (Gibco Life Technologies, Paisley, UK) supplemented with 5% pooled AB serum and antibiotics (Penicillin 50 IU/mL, Streptomycin 50 μg/mL, Gibco) (hereinafter referred to as complete medium).

PBMC proliferation was measured by using 2×10^5 cells/well in 0.2 mL complete medium in triplicate, in 96 flat-bottomed microwell trays (Falcon, BD Biosciences, San Jose, CA) in the presence of the relevant stimulus. The plates were incubated at 37°C in a 5% CO_2 for 5 days. Eighteen hours before harvesting, the plates were pulsed with Methyl-^{3}H-thymidine (0.5 μCi/well, specific activity: 2.5 Ci/mmole, GE Healthcare, Piscataway, NJ) and DNA synthesis was evaluated by counting ^{3}H-thymidine incorporation [35]. Proliferation data were expressed as stimulation index (SI), defined as the ratio between the counts per minute of the stimulated cultures and the background value of unstimulated cultures.

Cytokine release was assessed by culturing PBMC in 5 mL tubes (Falcon) at a concentration of 2×10^6 cells/mL in 0.5 mL of complete medium at 37°C in a 5% CO_2 atmosphere. Supernatants were collected after 18 hours and used to measure IFNγ and IL-6. The enzyme immunoassay system adopted (Quantikine, R&D Systems, Inc., Minneapolis, MN) displayed a sensitivity of 3 pg/mL for IFNγ, 0.7 pg/mL for IL-6, respectively.

2.4. mRNA Cytokine Expression by TaqMan Real-Time Reverse Transcriptase-PCR Analysis. TaqMan Real-time Reverse Transcriptase-PCR (Life Technologies, Paisley, UK) analysis was used to measure cytokine mRNA expression. Total RNA was extracted from PBMC, and reverse transcription was carried out as previously described [35]. TaqMan assays were performed according to the manufacturer's instructions with an ABI 7700 thermocycler (Life Technologies). PCR was performed, by amplifying the target cDNA (IL-6 and PCNA transcripts) and with beta-actin cDNA as endogenous

Table 1: Proliferation induced by CD38 ligation is specifically reduced in MM and MGUS patients.[a]

Stimulus	MM ($n = 11$)	MGUS ($n = 7$)	Controls ($n = 15$)
Anti-CD38	3.4 ± 1.2 $P = 0.007$	2.3 ± 0.8 $P = 0.005$	20.1 ± 5.3
Anti-CD3	36.6 ± 6.9	24.8 ± 10	44.0 ± 7.2
None	0.7 ± 0.1	0.4 ± 0.1	0.9 ± 0.4

[a]PBMC from MM, MGUS patients, and healthy individuals were treated with indicated stimulus and ^{3}H-Thymidine incorporation assayed. Results are expressed as mean ± SE of cpm ($\times 10^3$). Number (n) of individuals tested and statistical significance (Student's t-test) of differences between MM or MGUS patients versus healthy controls are indicated.

Table 2: Altered response in IFNγ and IL-6 cytokine release upon CD38 ligation in MM patients.[a]

Stimulus	MM		Controls	
	IFNγ (10)	IL-6 (10)	IFNγ (10)	IL-6 (10)
Anti-CD38	60 ± 19	2929 ± 878 $P = 0.041$	295 ± 156	820 ± 162
Anti-CD3	1072 ± 253	1638 ± 677	10361 ± 179	478 ± 99
None	45 ± 17	1088 ± 482	4.2 ± 1	236 ± 103

[a]PBMC from MM patients and healthy individuals were treated with indicated stimulus and IFNγ and IL-6 assayed by specific ELISA. Results are expressed as mean ± SE of pg/mL. Number (n) of individuals tested and statistical significance (Student's t-test) of differences between MM and healthy controls are indicated.

control. Specific primers and probes were obtained from Life Technologies. Data obtained were analyzed with PE Relative Quantification software (Life Technologies). Specific mRNA transcript levels were expressed as fold increase compared to basal condition [11].

2.5. Statistical Analyses. Statistical descriptive analyses were carried out using the SPSS Inc (Chicago, IL) statistical package. Differences between mean values were assessed by two-tailed Student's t-test. The association between proliferation and IL-6 secretion was measured by applying a linear regression model and by calculating the Pearson correlation coefficient. $P < 0.05$ was considered statistically significant.

3. Results

3.1. CD38-Mediated Signals in PBMC Purified from MM and MGUS Patients. CD38-mediated signals were comparatively evaluated in PBMC obtained from MM and MGUS patients, using healthy individuals as reference. The pathway driven by CD38 was also compared to the activation ruled by TCR/CD3. Previous [12, 35] and present studies (Table 1) indicate that CD38 ligation in PBMC by agonistic anti-CD38 mAb is followed by high levels of proliferation in healthy individuals. The same signals in PBMC obtained from MM and MGUS patients give a proliferation impact lower than that observed in controls ($P < 0.01$). The results indicate that the effect is specific for CD38 signals, while the cascade mediated by the TCR/CD3 pathway is unaffected (Table 1).

CD38 ligation by mAb in cultured PBMC induces multiple cytokines (including IFNγ and IL-6), some of them identical to those induced via TCR/CD3 activation [37]. Thus, IFNγ and IL-6 released after CD38 and CD3 activations were studied comparatively.

Due to the limited numbers of PBMC recovered from patients and to the decision to give priority to the proliferation measurement, cytokine assays were feasible in 10 out of 11 MM patients, 4 out of 7 MGUS patients, and 10 out of 15 healthy individuals.

Agonistic anti-CD38 mAb (and control anti-CD3 mAb) are able to induce release in PBMC from healthy individuals of high levels of IFNγ and IL-6. The results obtained in patients indicate that the ability to release IFNγ after CD38 engagement is decreased, while the IL-6 levels increased in MM (Table 2) and MGUS (data not shown) patients. Because of a high interdonor variability, expected when dealing with patients with different genetic background and immunological history, and the small sample of patients studied, the statistical significance was reached only when the IL-6 levels observed in CD38-activated PBMC of MM patients were compared to control group. The high IL-6 levels observed in untreated PBMC from MM patients are due to the high spontaneous IL-6 secretion observed in 4/10 MM patients tested and probably reflect the presence of malignant cells producing IL-6. After looking at other cytokines not directly associated with tumor progression (e.g., TNFα and IL-5), we observed that the production in untreated MM is almost overlapping with that scored by control PBMC (data not shown). These findings seem to confirm that IL-6 likely parallels the tumoral growth [20]. The levels of IFNγ and IL-6 release obtained after TCR/CD3 activation of PBMC were similar, irrespective of the source of PBMC (Table 2).

Figures 1(a) and 1(b) show the IFNγ and IL-6 levels plotted with respect to lymphocyte proliferation levels detected after CD38 ligation in MM patients and in controls. The secretion of IFNγ is greatly reduced in PBMC from MM patients (Figure 1(a)); on the contrary, the secretion of IL-6 is significantly enhanced (Figure 1(b)), as compared to PBMC of control group. Figure 1(b) depicts a clear dichotomy between MM patients and healthy subjects in their response to CD38 stimulation. In PBMC of MM patients, the proliferation is almost absent while IL-6 production is elevated with a low correlation ($r = 0.49$, $P = 0.014$) between these two parameters. In healthy subjects, there is a clear correlation between PBMC proliferation and IL-6 levels ($r = 0.65$, $P < 0.0001$) with consistent levels of proliferation and reduced levels of IL-6 (Figure 1(b)). No correlation is found between IFNγ and proliferation (Figure 1(a)) both in patients and healthy subjects.

The increased levels of IL-6 induced by CD38 engagement in PBMC from MM and MGUS patients were confirmed at a transcriptional level. IL-6 mRNA expression measured by real-time quantitative RT-PCR highlights the same increase induced by CD38 triggering in MM and MGUS patients as compared to controls, paralleling the results of protein secretion (Figure 2(a))

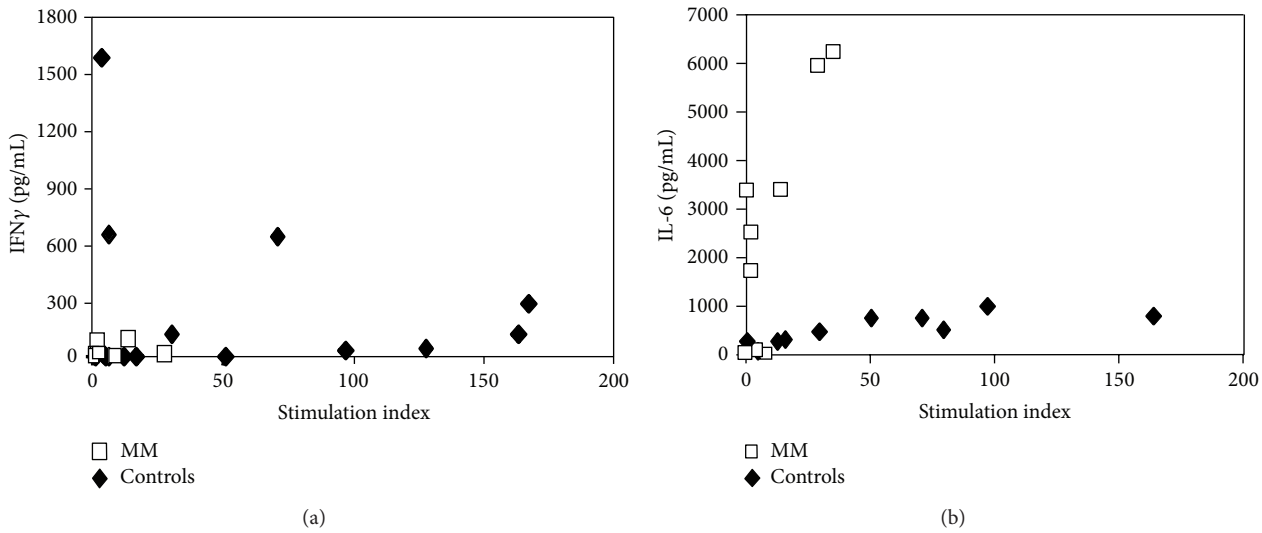

Figure 1: Proliferation, IFNγ, and IL-6 induction by CD38 mAb engagement in PBMC obtained from MM patients or healthy individuals. PBMC (2×10^5 cells/well in 0.2 mL) obtained from MM patients or healthy controls were cultured in the presence of agonistic anti-CD38 IB4 (20 μg/mL). Proliferation (SI) was measured after 5 days by ^{3}H-Thymidine incorporation. IFNγ (pg/mL) and IL-6 (pg/mL) were measured by ELISA after 18 hours of culture. (a) Dispersion of proliferation (SI) respect to IFNγ (pg/mL) values in each of all PBMC donors tested. (b) Dispersion of proliferation (SI) respect IL-6 (pg/mL) values in each of all PBMC donors tested. For the definition of SI and technical details, see text.

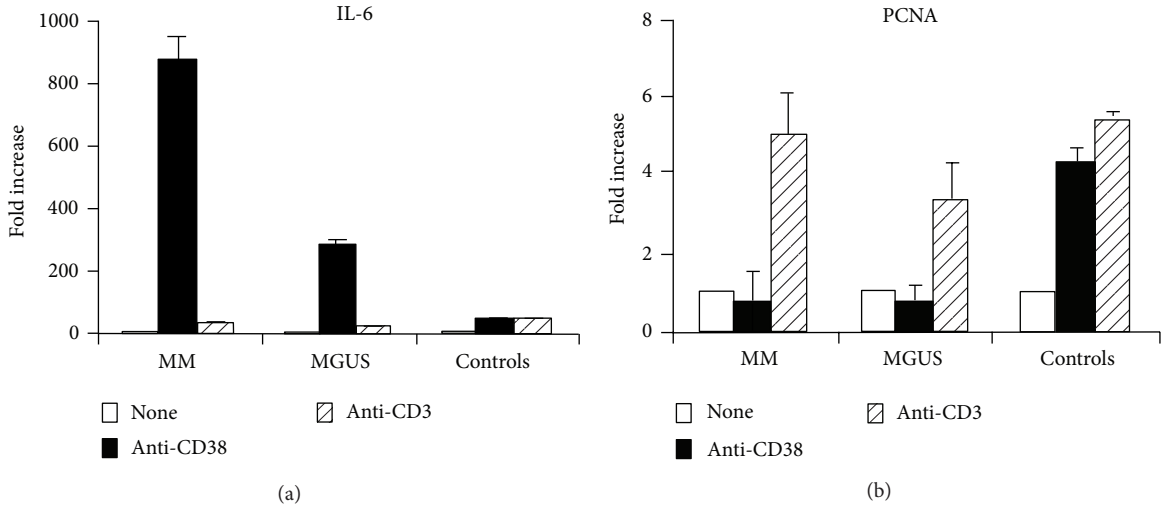

Figure 2: IL-6 and PCNA induction by CD38 molecules engagement in PBMC obtained from MM, MGUS patients, or healthy individuals. (a) PBMC (1×10^6/mL) obtained from MM, MGUS patients, or healthy controls were cultured in the presence of agonistic anti-CD38, anti-CD3, or unstimulated (none). Taqman Real Time quantitative RT-PCR for IL-6 gene expression was performed at 18 hours time-point. mRNA transcript levels were expressed as fold increase over the unstimulated PBMC. (b) PBMC (1×10^6/mL) obtained from MGUS, MM patients, or healthy individuals were cultured in the presence of agonistic anti-CD38, anti-CD3, or unstimulated (none). Taqman Real Time quantitative RT-PCR for PCNA gene expression was performed at 18 hours time-point. mRNA transcript levels were expressed as fold increase over the unstimulated PBMC. For further technical details, see text.

3.2. The Impaired CD38-Dependent Proliferative Response in MM and MGUS Patients Is due to an Arrest in the Cell Cycle Progression. The finding that CD38 ligation by agonistic mAb was unable to induce proliferation in PBMC of MM and MGUS patients was hypothesized as due to a cell cycle arrest. To this aim, we tested the presence of proliferating cell nuclear antigen (PCNA), a cell marker used in MM patients to evaluate the proliferation of clonal plasma cells, and a parameter which also parallels the tumor histological grade [38]. PCNA expression was assessed by using real-time quantitative RT-PCR in CD38-activated PBMC. Results show that PCNA expression is not increased when PBMC from MM and MGUS are reacted with the agonistic anti-CD38 mAb, confirming the presence of a proliferative defect

(Figure 2(b)). Conversely, PCNA expression is increased when the PBMC from MM and MGUS are exposed to an anti-CD3 mAb. This finding confirms that the ability of these cells to proliferate is maintained via TCR/CD3.

4. Discussion

The results obtained in this study support the view that PBMC from MM patients displays an altered response to signals mediated via CD38. Two lines of evidence indicate that CD38 is not a mere diagnostic marker but is also a key element in the pathogenetic events underlying myeloma development. First, the activation pathway ruled by CD38 appears as directly involved in the induction of a defective proliferative response in MM patients. Second, CD38 signals lead to the production of increased levels of IL-6, a key cytokine in the biology of MM [20, 21].

PBMC of MM and MGUS failed to proliferate after CD38 engagement, while the ability to proliferate in response to TCR/CD3 is maintained. This finding is suggestive of a specific defect in the CD38 activation pathways. The impaired CD38 proliferative response mediated by PBMC from MM and MGUS patients goes in parallel with an arrest in cell cycle progression, as indicated by the reduced expression of PCNA.

The experimental setting adopted does not allow to identify the cell population responsible for cytokine release in response to CD38 ligation. Yet, the cytokine data along with proliferation data (likely attributable to T cells) might highlight unresponsiveness to CD38 stimulation by T lymphocytes and provide support to the view that this pathway is deregulated in MM patients. However, these questions should be addresses more in depth by using multiparametric flow cytometry assays, allowing a better definition of the cells involved.

Myeloma cells may be directly involved in the inhibition of the T immune response of the patient [39, 40]. Campbell and colleagues [40] reported that myeloma cell lines suppress the proliferation of T lymphocytes, blocked in G1 arrest and refractory to respond to IL-2. Their conclusions are that MM cells have developed a strategy of suppression of T lymphocyte responses, which become unable to enter the IL-2/CD25 pathway of autocrine growth.

The lack of response to CD38 engagement by PBMC is not a general feature; indeed, CD38 ligation by agonistic mAb in PBMC obtained from MM leads to levels of IL-6 significantly increased as compared to the controls. Results in line with these are reported by Lapena and colleagues [25]. T lymphocytes from the MM patients activated by PHA release IL-6 in amounts significantly higher than those in the controls; at the same time, the proliferative response was decreased [25], in line with other results [31].

IL-6 is a major survival factor for malignant plasma cells *in vivo* and *in vitro*. Myeloma cell lines are protected from apoptosis by IL-6, due to the induction of specific antiapoptotic genes [41]. Besides, protecting from apoptosis, IL-6 plays a pivotal role in disease progression of MM patients. Indeed, autocrine IL-6 production detected in plasma cells from MM patients parallels a high labeling index [42].

This study reports that PBMC from MM and MGUS patients shares an impaired ability to transduce proliferative signals via CD38, suggesting that CD38 activation pathway defects are already present in the MGUS pathology and are not feature acquired by MM. A longitudinal study following the parameters here analyzed from the diagnoses of MGUS to the overt MM may help in detecting relevant defects in the above transition.

In conclusion, the present results support the role of CD38 in the genesis of tumor transformation of plasma cells. On one side, CD38 signaling pathways are able to rule IL-6 produced by PBMC, becoming a key step in the progression of the disease.

On the other side, it is apparent that myeloma induces a suppression of T cell responses, an event beneficial for tumor growth and survival. Myeloma is a tumor growing in closed system where the enzymatic activity of CD38 may be complemented by those exerted by PC-1/CD203a and CD73 [18, 43]. The consequence is that CD38 would be a component of one of the multiple strategies adopted by tumor to evade the immune response. This unconventional ectoenzyme network is able to provide the generation of local tolerance in different disease models, such as the BM microenvironment in pathology (e.g., myeloma or CLL) [44]. Conceivably, CD38/PC-1/CD73 pathway may tip the balance from activation to anergy and suppression [43, 45]. The fallouts of these observations are two-fold. One is to follow distribution and response to CD38 in the transition (if any) from MGUS to MM, and also to follow the proliferative response and IL-6 secretion in specific compartments of PBMC, such as T and B regulatory cells, DC subsets, NK-cells, and monocytes in order to link the alterations described to specific cell populations.

A second aspect concerns the applications in therapy. Targeted immunotherapy based on mAbs (murine, humanized, or human) specific for relevant tumor antigens has become a feasible and highly promising approach in hematological malignancies, mainly because it can be combined with conventional treatments to further increase the potency of antitumor effects. CD38 is a particularly attractive target on malignant plasma cells at all stages of disease and in CLL patients with a poor clinical prognosis or refractory to therapies. As such, this molecule is a promising target for antibody therapy also in different tumors [46].

Acknowledgments

This work was supported by grants from PRIN (Progetto di Ricerca di Rilevanza Nazionale), from FIRB (Fondo Investimenti Ricerca di Base) (both from Italian Ministry of Education, University and Research), from the "ex-60%" Program (University of Torino), from the Italian Ministry of Health (Bando Giovani Ricercatori 2008 no. GR-2008-1138053), and partly from AIRC 5 × 1000.

References

[1] R. A. Kyle and S. V. Rajkumar, "Multiple myeloma," *Blood*, vol. 111, no. 6, pp. 2962–2972, 2008.

[2] N. G. Kastrinakis, V. G. Gorgoulis, P. G. Foukas, M. A. Dimopoulos, and C. Kittas, "Molecular aspects of multiple myeloma," *Annals of Oncology*, vol. 11, no. 10, pp. 1217–1228, 2000.

[3] H. C. Lee, "Enzymatic functions and structures of CD38 and homologs," *Chemical Immunology*, vol. 75, pp. 39–59, 2000.

[4] F. Malavasi, S. Deaglio, A. Funaro et al., "Evolution and function of the ADP ribosyl cyclase/CD38 gene family in physiology and pathology," *Physiological Reviews*, vol. 88, no. 3, pp. 841–886, 2008.

[5] S. Deaglio, M. Morra, R. Mallone et al., "Human CD38 (ADP-ribosyl cyclase) is a counter-receptor of CD31, an Ig superfamily member," *Journal of Immunology*, vol. 160, no. 1, pp. 395–402, 1998.

[6] F. Malavasi, S. Deaglio, E. Ferrero et al., "CD38 and CD157 as receptors of the immune system: a bridge between innate and adaptive immunity," *Molecular Medicine*, vol. 12, no. 11-12, pp. 334–341, 2006.

[7] R. Lande, F. Urbani, B. di Carlo et al., "CD38 ligation plays a direct role in the induction of IL-1β, IL-6, and IL-10 secretion in resting human monocytes," *Cellular Immunology*, vol. 220, no. 1, pp. 30–38, 2002.

[8] R. Mallone, A. Funaro, M. Zubiaur et al., "Signaling through CD38 induces NK cell activation," *International Immunology*, vol. 13, no. 4, pp. 397–409, 2001.

[9] A. Funaro, M. Morra, L. Calosso, M. G. Zini, C. M. Ausiello, and F. Malavasi, "Role of the human CD38 molecule in B cell activation and proliferation," *Tissue Antigens*, vol. 49, no. 1, pp. 7–15, 1997.

[10] C. M. Ausiello, A. la Sala, C. Ramoni, F. Urbani, A. Funaro, and F. Malavasi, "Secretion of IFN-γ, IL-6, granulocyte-macrophage colony-stimulating factor and IL-10 cytokines after activation of human purified T lymphocytes upon CD38 ligation," *Cellular Immunology*, vol. 173, no. 2, pp. 192–197, 1996.

[11] G. Fedele, L. Frasca, R. Palazzo, E. Ferrero, F. Malavasi, and C. M. Ausiello, "CD38 is expressed on human mature monocyte-derived dendritic cells and is functionally involved in CD83 expressioin and IL-12 induction," *European Journal of Immunology*, vol. 34, no. 5, pp. 1342–1350, 2004.

[12] A. Funaro, G. C. Spagnoli, C. M. Ausiello et al., "Involvement of the multilineage CD38 molecule in a unique pathway of cell activation and proliferation," *Journal of Immunology*, vol. 145, no. 8, pp. 2390–2396, 1990.

[13] S. Zupo, E. Rugari, M. Dono, G. Taborelli, F. Malavasi, and M. Ferrarini, "CD38 signaling by agonistic monoclonal antibody prevents apoptosis of human germinal center B cells," *European Journal of Immunology*, vol. 24, no. 5, pp. 1218–1222, 1994.

[14] L. Frasca, G. Fedele, S. Deaglio et al., "CD38 orchestrates migration, survival, and Th1 immune response of human mature dendritic cells," *Blood*, vol. 107, no. 6, pp. 2392–2399, 2006.

[15] A. Savarino, F. Bottarel, F. Malavasi, and U. Dianzani, "Role of CD38 in HIV-1 infection: an epiphenomenon of T-cell activation or an active player in virus/host interactions?" *AIDS*, vol. 14, no. 9, pp. 1079–1089, 2000.

[16] S. Deaglio, T. Vaisitti, S. Aydin, E. Ferrero, and F. Malavasi, "In-tandem insight from basic science combined with clinical research: CD38 as both marker and key component of the pathogenetic network underlying chronic lymphocytic leukemia," *Blood*, vol. 108, no. 4, pp. 1135–1144, 2006.

[17] A. Chillemi, G. Zaccarello, V. Quarona et al., "Anti-CD38 antibody therapy: windows of opportunity yielded by the functional characteristics of the target molecule," *Molecular Medicine*, vol. 19, pp. 99–108, 2013.

[18] V. Quarona, G. Zaccarello, A. Chillemi et al., "CD38 and CD157: a long journey from activation markers to multifunctional molecules," *Cytometry B*, vol. 84, no. 4, pp. 207–217, 2013.

[19] A. Chillemi, G. Zaccarello, V. Quarona et al., "CD38 and bone marrow microenvironment," *Frontiers in Bioscience*, vol. 19, pp. 152–162, 2014.

[20] K. Gadó, G. Domján, H. Hegyesi, and A. Falus, "Role of interleukin-6 in the pathogenesis of multiple myeloma," *Cell Biology International*, vol. 24, no. 4, pp. 195–209, 2000.

[21] K. Bommert, R. C. Bargou, and T. Stühmer, "Signalling and survival pathways in multiple myeloma," *European Journal of Cancer*, vol. 42, no. 11, pp. 1574–1580, 2006.

[22] R. D. Brown, B. Pope, A. Murray et al., "Dendritic cells from patients with myeloma are numerically normal but functionally defective as they fail to up-regulate CD80 (B7-1) expression after huCD40LT stimulation because of inhibition by transforming growth factor-β1 and interleukin-10," *Blood*, vol. 98, no. 10, pp. 2992–2998, 2001.

[23] S. Wang, S. Hong, J. Yang et al., "Optimizing immunotherapy in multiple myeloma: restoring the function of patients' monocyte-derived dendritic cells by inhibiting p38 or activating MEK/ERK MAPK and neutralizing interleukin-6 in progenitor cells," *Blood*, vol. 108, no. 13, pp. 4071–4077, 2006.

[24] M. Massaia, A. Bianchi, C. Attisano et al., "Detection of hyperreactive T cells in multiple myeloma by multivalent cross-linking of the CD3/TCR complex," *Blood*, vol. 78, no. 7, pp. 1770–1780, 1991.

[25] P. Lapena, A. Prieto, J. Garcia-Suarez et al., "Increased production of interleukin-6 by T lymphocytes from patients with multiple myeloma," *Experimental Hematology*, vol. 24, no. 1, pp. 26–30, 1996.

[26] M. A. Frassanito, F. Silvestris, N. Silvestris et al., "Fas/Fas ligand (FasL)-deregulated apoptosis and IL-6 insensitivity in highly malignant myeloma cells," *Clinical and Experimental Immunology*, vol. 114, no. 2, pp. 179–188, 1998.

[27] M. Massaia, P. Borrione, C. Attisano et al., "Dysregulated Fas and bcl-2 expression leading to enhanced apoptosis in T cells of multiple myeloma patients," *Blood*, vol. 85, no. 12, pp. 3679–3687, 1995.

[28] B. Besostri, E. Beggiato, A. Bianchi et al., "Increased expression of non-functional killer inhibitory receptor CD94 in CD8+ cells of myeloma patients," *British Journal of Haematology*, vol. 109, no. 1, pp. 46–53, 2000.

[29] D. K. Banerjee, M. V. Dhodapkar, E. Matayeva, R. M. Steinman, and K. M. Dhodapkar, "Expansion of FOXP3high regulatory T cells by human dendritic cells (DCs) in vitro and after injection of cytokine-matured DCs in myeloma patients," *Blood*, vol. 108, no. 8, pp. 2655–2661, 2006.

[30] H. Murakami, H. Ogawara, and H. Hiroshi, 'Th1/Th2 cells in patients with multiple myeloma," *Hematology*, vol. 9, no. 1, pp. 41–45, 2004.

[31] M. A. Frassanito, A. Cusmai, and F. Dammacco, "Deregulated cytokine network and defective Th1 immune response in multiple myeloma," *Clinical and Experimental Immunology*, vol. 125, no. 2, pp. 190–197, 2001.

[32] S. V. Rajkumar, R. Fonseca, G. W. Dewald et al., "Cytogenetic abnormalities correlate with the plasma cell labeling index and extent of bone marrow involvement in myeloma," *Cancer Genetics and Cytogenetics*, vol. 113, no. 1, pp. 73–77, 1999.

[33] B. G. M. Durie and S. E. Salmon, "A clinical staging system for multiple myeloma: correlation of measured myeloma cell mass

with presenting clinical features, response to treatment, and survival," *Cancer*, vol. 36, no. 3, pp. 842–854, 1975.

[34] World Medical Association, "World Medical Association Declaration of Helsinki: ethical principles for medical research involving human subjects," *Journal of the American Medical Association*, vol. 310, no. 20, pp. 2191–2194, 2013.

[35] C. M. Ausiello, F. Urbani, R. Lande et al., "Functional topography of discrete domains of human CD38," *Tissue Antigens*, vol. 56, no. 6, pp. 539–547, 2000.

[36] A. L. Horenstein, F. Crivellin, A. Funaro, M. Said, and F. Malavasi, "Design and scaleup of downstream processing of monoclonal antibodies for cancer therapy: from research to clinical proof of principle," *Journal of Immunological Methods*, vol. 275, no. 1-2, pp. 99–112, 2003.

[37] C. M. Ausiello, F. Urbani, A. la Sala, A. Funaro, and F. Malavasi, "CD38 ligation induces discrete cytokine mRNA expression in human cultured lymphocytes," *European Journal of Immunology*, vol. 25, no. 5, pp. 1477–1480, 1995.

[38] A. I. Chaidos, M. C. Bai, S. A. Kamina, P. E. Kanavaros, N. J. Agnantis, and K. L. Bourantas, "Incidence of apoptosis and cell proliferation in multiple myeloma: correlation with bcl-2 protein expression and serum levels of interleukin-6 (IL-6) and soluble IL-6 receptor," *European Journal of Haematology*, vol. 69, no. 2, pp. 90–94, 2002.

[39] G. Cook, J. D. M. Campbell, C. E. Carr, K. S. Boyd, and I. M. Franklin, "Transforming growth factor β from multiple myeloma cells inhibits proliferation and IL-2 responsiveness in T lymphocytes," *Journal of Leukocyte Biology*, vol. 66, no. 6, pp. 981–988, 1999.

[40] J. D. M. Campbell, G. Cook, S. E. Robertson et al., "Suppression of IL-2-induced T cell proliferation and phosphorylation of STAT3 and STAT5 by tumor-derived TGFβ is reversed by IL-15," *Journal of Immunology*, vol. 167, no. 1, pp. 553–561, 2001.

[41] M. Jourdan, J.-L. Veyrune, J. de Vos, N. Redal, G. Couderc, and B. Klein, "A major role for Mcl-1 antiapoptotic protein in the IL-6-induced survival of human myeloma cells," *Oncogene*, vol. 22, no. 19, pp. 2950–2959, 2003.

[42] K. A. Donovan, M. Q. Lacy, M. P. Kline et al., "Contrast in cytokine expression between patients with monoclonal gammopathy of undetermined significance or multiple myeloma," *Leukemia*, vol. 12, no. 4, pp. 593–600, 1998.

[43] A. L. Horenstein, A. Chillemi, G. Zaccarello et al., "CD38/CD203a/CD73 ectoenzymatic pathway independent from CD39 runs a novel adenosinergic loop in human T lymphocytes," *OncoImmunology*, vol. 2, no. 9, Article ID e26246, 2013.

[44] F. Malavasi, S. Deaglio, R. Damle, G. Cutrona, M. Ferrarini, and N. Chiorazzi, "CD38 and chronic lymphocytic leukemia: a decade later," *Blood*, vol. 118, no. 13, pp. 3470–3478, 2011.

[45] R. Bahri, A. Bollinger, T. Bollinger, Z. Orinska, and S. Bulfone-Paus, "Ectonucleotidase CD38 demarcates regulatory, memory-like CD8+ T cells with IFN-g-mediated suppressor activities," *PLoS ONE*, vol. 7, no. 9, pp. 1–12, 2012.

[46] J. H. Ellis, K. A. Barber, A. Tutt et al., "Engineered anti-CD38 monoclonal antibodies for immunotherapy of multiple myeloma," *Journal of Immunology*, vol. 155, no. 2, pp. 925–937, 1995.

Hindawi Publishing Corporation
Mediators of Inflammation
Volume 2013, Article ID 436894, 10 pages
http://dx.doi.org/10.1155/2013/436894

Research Article

Differential Influence of Inositol Hexaphosphate on the Expression of Genes Encoding TGF-β Isoforms and Their Receptors in Intestinal Epithelial Cells Stimulated with Proinflammatory Agents

Małgorzata Kapral, Joanna Wawszczyk, Stanisław Sośnicki, and Ludmiła Węglarz

Department of Biochemistry, Medical University of Silesia, Jedności 8, 41-200 Sosnowiec, Poland

Correspondence should be addressed to Małgorzata Kapral; mkapral@sum.edu.pl

Received 6 August 2013; Revised 8 November 2013; Accepted 27 November 2013

Academic Editor: Dennis Daniel Taub

Transforming growth factor β (TGF-β) is a multifunctional cytokine recognized as an important regulator of inflammatory responses. The effect of inositol hexaphosphate (IP6), a naturally occurring phytochemical, on the mRNA expression of TGF-β1, TGF-β2, TGF-β3 and TβRI, TβRII, and TβRIII receptors stimulated with bacterial lipopolysaccharides (*Escherichia coli* and *Salmonella typhimurium*) and IL-1β in intestinal cells Caco-2 for 3 and 12 h was investigated. Real-time qRT-PCR was used to validate mRNAs level of examined genes. Bacterial endotoxin promoted differential expression of TGF-βs and their receptors in a time-dependent manner. IL-1β upregulated mRNA levels of all TGF-βs and receptors at both 3 h and 12 h. IP6 elicited the opposed to LPS effect by increasing downregulated transcription of the examined genes and suppressing the expression of TGF-β1 at 12 h. IP6 counteracted the stimulatory effect of IL-1β on TGF-β1 and receptors expression by decreasing their mRNA levels. IP6 enhanced LPS- and IL-1β-stimulated mRNA expression of TGF-β2 and -β3. Based on these studies it may be concluded that IP6 present in the intestinal milieu may exert immunoregulatory effects and chemopreventive activity on colonic epithelium under inflammatory conditions or during microbe-induced infection/inflammation by modulating the expression of genes encoding TGF-βs and their receptors at transcriptional level.

1. Introduction

Inflammatory bowel disease (IBD) is a chronic inflammation of the gastrointestinal tract thought to be a result of dysregulated or aberrant immune response to intestinal flora and multiple environmental factors with regard to genetic predisposition [1]. Exposure of intestinal epithelial cells (IEC) to bacterial components and products can potentially initiate intestinal inflammation by their release of cytokines chemokines and recruitment of inflammatory cells. IEC can also respond to a broad array of cytokines with altered gene expression and growth characteristics [2]. Cytokine that plays a crucial role in the inflammatory diseases such as IBD is IL-1β. Enhanced level of this cytokine has been determined in mucosal tissues infected with enteropathogenic bacteria, as well as in mucosal biopsies with active IBD. IL-1β activates intracellular signaling cascades in IEC leading to the increase of expression and secretion of proinflammatory cytokines and chemokines, uncontrolled intestinal inflammation, and disruption of epithelial function [3, 4]. Lipopolysaccharide (LPS) or endotoxin, the key component of the cell wall of Gram-negative bacteria, stimulates activation of transcription factors and production of proinflammatory cytokines. The expression of LPS specific Toll-like receptor 4 (TLR-4) in human colorectal cancer cells highlighted a key function of TLR system in the development of colitis-associated tumors, suggesting a role of this receptor in colorectal cancer development and progression [2]. Cytokines with

anti-inflammatory properties have been implicated in the prevention of inappropriate immune activation by intestinal flora.

Transforming growth factor β is a strong anti-inflammatory cytokine with multipotent mechanism of action [5]. In mammals three isoforms (TGF-β1, -β2, and -β3) have been described, which share 75% amino acid sequence homology but are encoded by different genes [6]. TGF-βs have strong impact on the inflammatory responses and tumor microenvironment including fibroblasts, endothelial cells and immune cells. TGF-βs suppress cytotoxic T-cell differentiation and inhibit NK cell and neutrophil effector functions. Also, they have been shown to suppress MHC I and MHC II expression [7]. On the other hand, overexpression of TGF-β could induce the secretion of proinflammatory cytokines, for example, TNF-α [8], IL-1β, IL-6, and IL-8 [7]. This indicates complexity of TGF-β signalling immune regulation within different contexts [9]. TGF-β signalling is mediated by three specific types of cell surface proteins: TGF-β receptor I (TβRI), II (TβRII), and III (TβRIII). TβRIII is a coreceptor modulating intracellular TGF-βs activities [10]. TGF-β initiates its signaling by binding to TβRII, which has intrinsic serine-threonine kinase activity. Then, TβRII recruits and phosphorylates TβRI, establishing heterotetrameric complex consisting of two TβRII and two TβRI [11]. TβRI initiates phosphorylation of the adaptor proteins SMAD2 and SMAD3 which is followed by the formation of complex with SMAD4 [5]. Nuclear SMAD complexes bind to SMAD-binding elements on DNA, affecting transcriptional activity which is dependent on their interaction with coactivators [12]. SMAD7 differs structurally from other members of SMAD family and functions as a negative regulator of TGF-β signaling. Its gene expression is induced by TGF-β; thus SMAD7 represents negative feedback loop, restraining TGF-β activity [13]. It recruits the GADD34 complex to the TβRI, thus preventing SMAD2/SMAD3 phosphorylation and TGF-β signal transduction. SMAD7 also contributes to TβRI dephosphorylation and ubiquitination and proteasomal degradation of the TGF-β receptor complex [14]. Many factors modulate the TGF-β-mediated cellular response. Transcription factors, histone readers, modifiers, and chromatin remodelers that bind to activated SMAD determine what genes and how they will be affected by signal transduction complexes. TGF-β can also activate other non-SMAD signalling pathways, including PI3K, MAPK, TRAF6, and mTORC [15]. Some of the important downstream targets of TGF-β signaling include cell cycle checkpoint genes, the activation of which leads to growth arrest. Yet, TGF-β signaling can also directly stimulate the production of several mitogenic growth factors which can drive the carcinogenic process [16]. A number of inflammatory diseases including inflammatory bowel disease and cancer are associated with abnormal TGF-βs regulation [5, 17, 18]. Monteleone et al. [19] have shown marked overexpression of SMAD7 in the inflamed tissue of IBD patients. Moreover it was associated with a reduction in SMAD3 phosphorylation, which is crucial for anti-inflammatory action of TGF-β. Proinflammatory stimuli, such as TNF-α, IL-1β, and INF-γ, also induce SMAD7 expression [20]. Chronic inflammation has been recognized to be associated with a high cancer risk and may be involved in all stages of tumor development, that is, initiation, promotion, and progression [21]. The control of colitis by certain anti-inflammatory agents reduced colon cancer incidence [22].

Colorectal cancer is one of the most common cancers, accounting for 8% of all cancer deaths, making it the fourth cause of cancer deaths[23]. Due to high mortality and extensive anticancer drugs toxicity there has been growing interest in substances that may have chemopreventive action, that is, can prevent or delay the development of cancer [24, 25]. Diet has been proved to play a significant role in the aetiology of colorectal cancer. Consumption of dietary components with anti-inflammatory activity has been associated with reduced risk of developing colorectal cancer. One of the essential components of high fiber diet is inositol hexaphosphate (IP6) [26]. It is a naturally occurring hexaphosphorylated carbohydrate, found in both plant and mammalian cells [27]. With intracellular concentration of about 100 μM, IP6 participates in a variety of cellular functions such as signal transduction, regulation of cell proliferation, and differentiation [28]. IP6 has been shown in *in vitro* studies to inhibit growth of human breast, colon, prostate, and liver cancer cells. Its anticancer properties have been documented to result from its antiproliferative, proapoptotic, and antiangiogenic effects. IP6 is also known for its antioxidant properties, prevention against formation of kidney stones, high blood cholesterol level and heart and liver diseases [27]. Its antioxidant action was recognized in experimental models of myocardial reperfusion injury, pulmonary inflammation, and peptic ulcer induction [28]. Therefore, IP6 is believed to have potential to serve as preventive agent for chronic inflammation and carcinogenesis [29]. Recently, it has been revealed that IP6 has strong impact on transcriptional activity of TGF-βs and their receptor genes in colon cancer cells [30].

The aim of the present study was to examine the potential of IP6 to affect proinflammatory agents-influenced changes in transcriptional activity of the genes encoding TGF-β1, TGF-β2, and TGF-β3 and their receptors TβRI, TβRII, and TβRIII in human colon Caco-2 cells.

2. Materials and Methods

2.1. Cell Culture and Cell Stimulation Assays. The Caco-2 human intestinal epithelial cells (DSMZ, Braunschweig, Germany) were routinely cultured in RPMI 1640 medium (Sigma Aldrich) supplemented with 10% fetal bovine serum (GibcoBRL), 100 U/mL penicillin and 100 μg/mL streptomycin (both from Sigma Aldrich) and 10 mM HEPES (GibcoBRL). They were maintained at 37°C in a 5% CO_2 atmosphere within a humidified incubator. Cells were seeded into six-well plates (Nunc International) at a density of 4.5×10^5 per well and allowed to grow to 80% confluency in 3 mL of medium. After three days the culture media were changed to media with 2% FBS and cells were then cultured for 2 days. They were then stimulated with 100 μg/mL LPS (*Escherichia coli* serotype 055:B5, *Salmonella enterica* serotype typhimurium;

both from Sigma Aldrich), or 1 ng/mL IL-1β (Sigma Aldrich) for 30 min. Afterwards cells were treated with 2.5 mM IP6 as dipotassium salt (distilled water dissolved and pH 7.4 adjusted) (Sigma Aldrich) for 3 and 12 h. In separate cultures, cells were incubated with LPS or IL-1β at the indicated concentrations and for the indicated times. The untreated Caco-2 cells were used as the control.

2.2. RNA Extraction. Total RNA was extracted from cells using TRIzol reagent (Invitrogen) according to the manufacturer's specifications. Integrity of the RNA extracts was qualitatively checked by electrophoresis in 1.0% agarose gel stained with ethidium bromide. RNA concentration was determined spectrophotometrically on the basis of absorbance values at a wavelength of 260 nm using a GeneQuant pro (Amersham Biosciences).

2.3. Real-Time qRT-PCR Assay. Detection of the expression of genes encoding TGF-β isoforms and their receptors was carried out using a qRT-PCR technique with a SYBR Green chemistry (SYBR Green Quantitect RT-PCR Kit, Qiagen) and Opticon DNA Engine Continuous Fluorescence detector (MJ Research) as described previously [31]. Oligonucleotide primers specific for TGF-β1, TGF-β2, TGF-β3, TβRI, TβRII, and TβRIII mRNAs were designed using Primer Express 2.0 software (PE Applied Biosystems, USA) (Table 1). The thermal profile for one-step RT-PCR was as follows: 50°C for 30 min for reverse transcription and 95°C for 15 min followed by 45 cycles at 94°C for 15 s, 55°C for 30 s, and 72°C for 45 s for amplification. Following RT-PCR, the samples were subjected to temperature ramp from 60°C to 95°C at the rate of 0.2°C/s with continuous fluorescence monitoring for melting curve analysis. Each gene analysis was performed in triplicate. A commercially available standard of β-actin (TaqMan DNA Template Reagent Kit, Applied Biosystems) was used to estimate the mRNA copy numbers of examined genes. The obtained results of mRNA copy number were recalculated per μg of total RNA. The expression level of examined genes in cultured cells was expressed as the fold change relative to the control. The value of fold change >1 reflects increased expression of the target gene, and a value of fold change <1 points to a decrease in the gene expression. Finally, specificity of RT-PCR reaction was confirmed by determining the characteristic temperature of melting for each amplimer and by 6% polyacrylamide gel (PAA) electrophoresis of RT-PCR products with their visualization using silver staining.

2.4. Statistical Analysis. The results were collected based on three independent experiments. Statistical analysis was performed with the use of Statistica PL 9.0 software. All the results are expressed as means ± SD. Comparison of two data sets was performed by unpaired t-test. Significance level was assumed for $P < 0.05$.

3. Results

The colon cancer cells Caco-2 showed constitutive expression of genes encoding all three TGF-β isoforms and their receptors.

3.1. Changes of TGF-β1 Expression by the Effect of Proinflammatory Agents and IP6. In the time course of the experiment, differential TGF-β1 expression after exposure of Caco-2 to *E. coli* LPS was observed. At 3 h, it decreased in comparison to control ($P = 0.025$) and IP6 up regulated LPS-evoked effect ($P = 0.032$). A significantly higher TGF-β1 mRNA level was determined following cell treatment with LPS for 12 h than in unstimulated cells ($P = 0.047$). LPS-stimulated transcription of this gene was remarkably down-regulated by IP6 at that time ($P = 0.01$) (Figures 1(a) and 1(b)). Endotoxin of *S. typhimurium* had no influence on TGF-β1 mRNA level after 3 h treatment ($P = 0.487$) but longer exposure of cells to it (12 h) caused significant decrease in transcription of the gene ($P < 0.001$) (Figure 1(a)). The levels of TGF-β1 mRNA in cells stimulated with *S.* Typhi. LPS and cells treated with both LPS and IP6 revealed no statistically significant differences after 3 and 12 h ($P > 0.05$) (Figure 1(b)). Incubation of Caco-2 with IL-1β for both 3 and 12 h up-regulated TGF-β1 gene as compared with untreated cells ($P < 0.05$) (Figure 1(a)). After 3 h, 2.5 mM IP6 did not change TGF-β1 expression stimulated by IL-1β ($P = 0.268$). Furthermore, significant decrease in the expression of this gene was revealed in cells exposed to IL-1β and IP6 for 12 h ($P = 0.047$) in comparison to the cultures treated with IL-1β only (Figure 1(b)).

3.2. Changes of TGF-β2 Expression by the Effect of Proinflammatory Agents and IP6. LPS of *E. coli* gradually down-regulated TGF-β2 expression within 3–12 h ($P < 0.05$) (Figure 2(a)) and IP6 was able to enhance it markedly at both time points in comparison to LPS effects only ($P < 0.05$) (Figure 2(b)). In response to LPS of *Salmonella* Caco-2 exhibited significantly higher transcription of this gene than control after 3 h ($P = 0.001$). However, the prolongation of time to 12 h led to insignificantly reduced TGF-β2 expression ($P = 0.130$) (Figure 2(a)). IP6 enhanced LPS-stimulated transcription of this gene after 3 h ($P < 0.001$). Subsequently (12 h), the combination of IP6 and LPS gave rise to 2-fold increase in TGF-β2 mRNA level ($P = 0.002$) compared to LPS-treated cells (Figure 2(b)). The TGF-β2 transcript was over 2-fold higher by the treatment with IL-1β for 3 h ($P = 0.007$) and 12 h ($P = 0.001$) as compared to control (Figure 2(a)). When IP6 was added to IL-1β-prestimulated cultures, the level of TGF-β2 mRNA markedly raised at 3 h in comparison to those treated with IL-1β alone ($P < 0.0001$) (Figure 2(b)).

3.3. Changes of TGF-β3 Expression by the Effect of Proinflammatory Agents and IP6. E. coli LPS diminished transcriptional activity of TGF-β3 gene in Caco-2 cells in a time-dependent manner. The decrease of the TGF-β3 mRNA level was statistically significant compared to control at 12 h ($P < 0.0001$) (Figure 3(a)). IP6 enhanced the expression of this

Table 1: Characteristics of primers used in experiment.

Gene	Primer sequence	Product amplified (bp)	TM (°C)
TGF-β1	F: 5′-TGAACCGGCCTTTCCTGCTTCTCATG-3′ R: 5′-GCGGAAGTCAATGTACAGCTGCCGC-3′	151	85
TGF-β2	F: 5′-TACTACGCCAAGGAGGTTTACAAA-3′ R: 5′-TTGTTCAGGCACTCTGGCTTT-3′	201	80
TGF-β3	F: 5′-CTGGATTGTGGTTCCATGCA-3′ R: 5′-TCCCCGAATGCCTCACAT-3′	121	81
TβRI	F: 5′-ACTGGCAGCTGTCATTGCTGGACCAG-3′ R: 5′-CTGAGCCAGAACCTGACGTTGTCATATCA-3′	201	81
TβRII	F: 5′-GGCTCAACCACCAGGGCATCCAGAT-3′ R: 5′-CTCCCCGAGAGCCTGTCCAGATGCT-3′	139	84
TβRIII	F: 5′-ACCGTGATGGGCATTGCGTTTGCA-3′ R: 5′-GTGCTCTGCGTGCTGCCGATGCTGT-3′	173	85

bp: base pair; TM: temperature of melting.

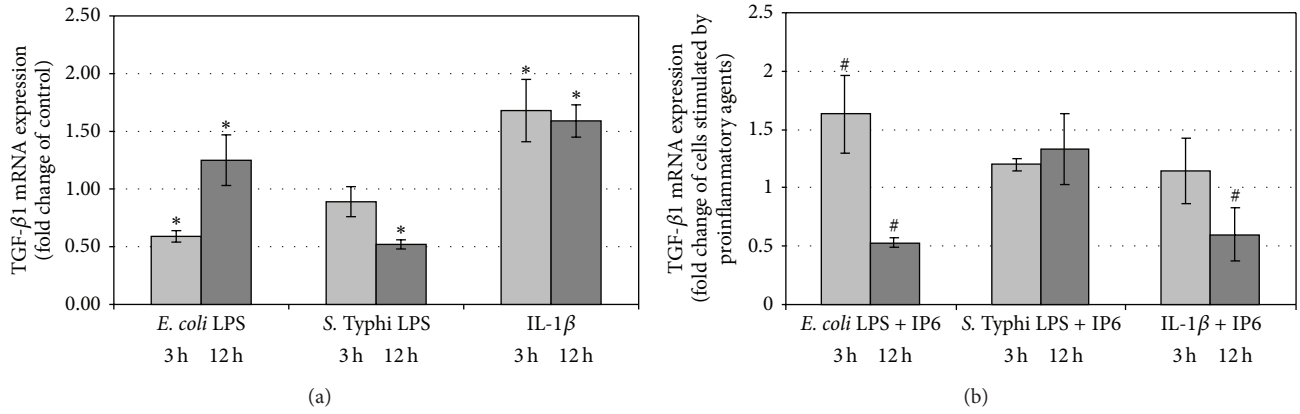

Figure 1: Expression of TGF-β1 gene in Caco-2 cells as determined by real-time RT-PCR. Changes in TGF-β1 mRNA expression in Caco-2 cells after treatment with (a) proinflammatory agents and (b) proinflammatory agents and 2.5 mM IP6 for 3 h and 12 h. The results are presented as mean ± SD of three separate experiments; $^{*}P < 0.05$ versus control Caco-2 cells; $^{\#}P < 0.05$ versus proinflammatory agents-stimulated cells.

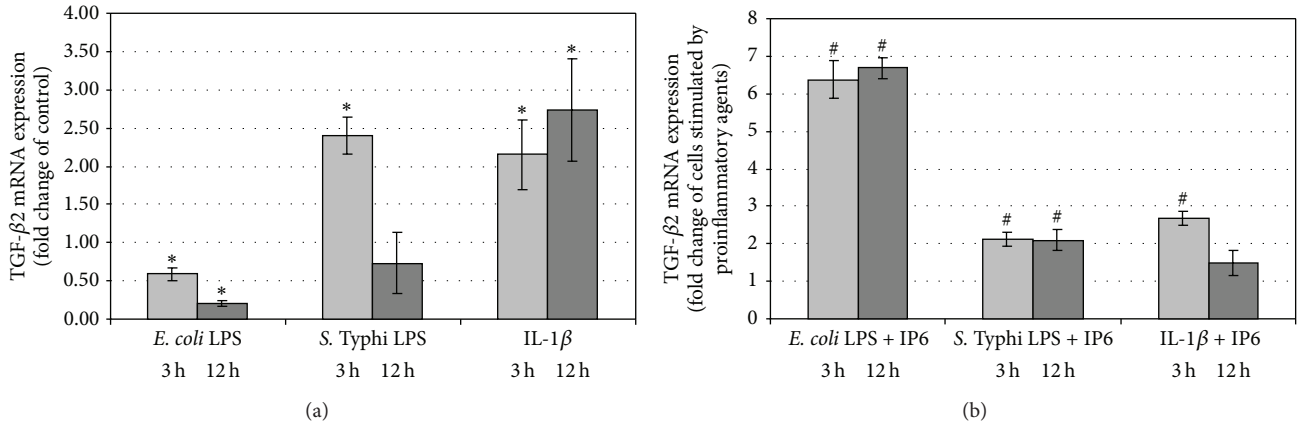

Figure 2: Expression of TGF-β2 gene in Caco-2 cells as determined by real-time RT-PCR. Changes in TGF-β2 mRNA expression in Caco-2 cells after treatment with (a) proinflammatory agents and (b) proinflammatory agents and 2.5 mM IP6 for 3 h and 12 h. The results are presented as mean ± SD of three separate experiments; $^{*}P < 0.05$ versus Caco-2 cells; $^{\#}P < 0.05$ versus proinflammatory agents-stimulated cells.

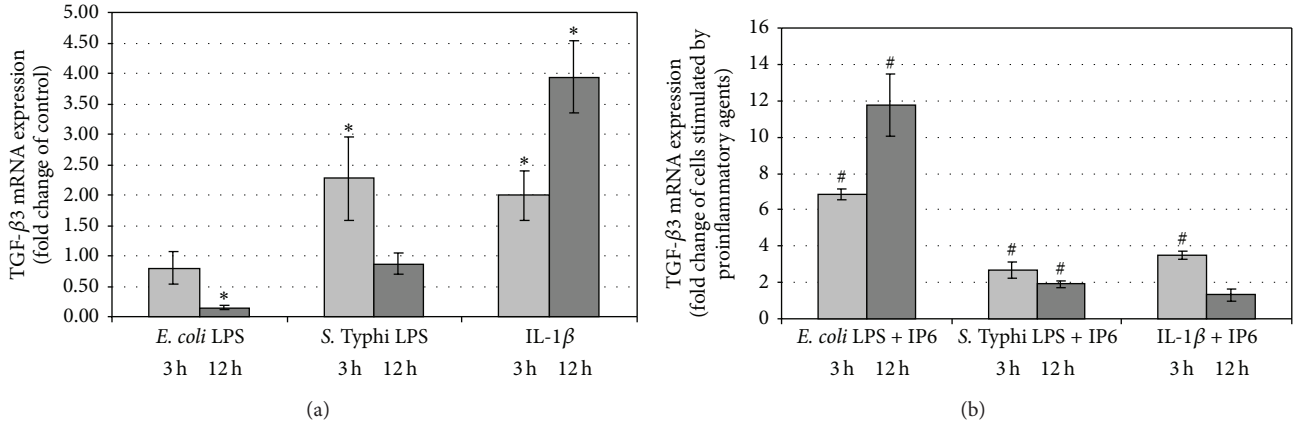

Figure 3: Expression of TGF-β3 gene in Caco-2 cells as determined by real-time RT-PCR. Changes in TGF-β3 mRNA expression in Caco-2 cells after treatment with (a) proinflammatory agents and (b) proinflammatory agents and 2.5 mM IP6 for 3 h and 12 h. The results are presented as mean ± SD of three separate experiments; $^{*}P < 0.05$ versus control Caco-2 cells; $^{\#}P < 0.05$ versus proinflammatory agents-stimulated cells.

gene after 3 h ($P < 0.0001$) and 12 h ($P < 0.0001$) with reference to LPS-stimulated cells (Figure 3(b)). Cell cultures treated with LPS of *S.* Typhi manifested above 2-fold increase in TGF-β3 mRNA expression compared to control culture at 3 h ($P = 0.016$) and IP6 markedly enhanced LPS-induced expression of this isoform ($P = 0.008$). Incubation of cells with *S.* Typhi LPS for 12 h did not change mRNA level of TGF-β3 compared to control ($P = 0.286$). In cells exposed to LPS and IP6 statistically significant increase in mRNA for TGF-β3 in relation to cells treated with *S.* Typhi LPS only ($P = 0.005$) was observed (Figures 3(a) and 3(b)). IL-1β induced transcriptional activity of this gene by 2-fold after 3 h ($P = 0.009$) and about 4-fold after 12 h ($P < 0.0001$) as compared to unstimulated cells (Figure 3(a)). IP6 modified IL-1β effects by significant increasing of TGF-β3 mRNA expression at 3 h ($P < 0.001$) (Figure 3(b)).

3.4. The Effect of IP6 on TβRI Expression in Caco-2 Cells Stimulated by Bacterial Endotoxins and IL-1β. Lipopolysaccharide of *E. coli* downregulated transcriptional activity of the gene encoding type I TGF-β receptor in Caco-2 at 3 h ($P < 0.001$) (Figure 4(a)) while IP6 strongly induced it ($P < 0.0001$) (Figure 4(b)). At 12 h, the expression of the gene in control and LPS-stimulated cultures was comparable ($P = 0.075$), and there were no changes in TβRI mRNA amount in the cells treated with LPS and IP6 ($P = 0.479$) (Figures 4(a) and 4(b)). Caco-2 exposed to LPS of *Salmonella* Typhi for 3 h produced significantly higher quantity of TβRI transcript than control ($P < 0.001$). The amount of TβRI mRNA in cells treated with LPS/IP6 and LPS-stimulated cells was similar ($P > 0.05$). Treatment of Caco-2 cells with *Salmonella* Typhi LPS for 12 h resulted in statistically significant decrease in TβRI gene transcription ($P = 0.016$) which was remarkably up-regulated by IP6 ($P < 0.004$) (Figures 4(a) and 4(b)). By comparison, IL-1β induced transcriptional activity of TβRI gene in Caco-2 cells. The extent of stimulation by this cytokine was 3.9- and 2.6-fold after 3 h and 12 h, respectively, compared to the control ($P < 0.05$) (Figure 4(a)). Nevertheless, 2.5 mM IP6 did not significantly change mRNA TβRI expression in IL-1β-treated cultures throughout the time period of the experiment ($P > 0.05$) (Figure 4(b)).

3.5. The Effect of IP6 on TβRII Expression in Caco-2 Cells Stimulated by Bacterial Endotoxins and IL-1β. Over the period of the experiment, a statistically significant decrease in the expression of TβRII in cultures treated with LPS of *E. coli* in relation to control ($P < 0.05$) was detected. By comparison, IP6 stimulated LPS-decreased transcription of TβRII for both 3 h ($P = 0.017$) and 12 h ($P = 0.003$) (Figures 5(a) and 5(b)). The transcription of TβRII did not differ in the control cells and the cells stimulated with LPS of *Salmonella* for 3 h ($P = 0.129$). Moreover, cultures treated with LPS and LPS/IP6 revealed similar level of TβRII transcript at this time point ($P = 0.468$). Cell culturing with *Salmonella tyhpi* LPS for 12 h decreased TβRII mRNA level as compared to the control ($P < 0.001$). Transcriptional activity of this gene was upregulated in response to 2.5 mM IP6 ($P = 0.001$) (Figures 5(a) and 5(b)). Exposure of Caco-2 to IL-1β for both 3 h and 12 h resulted in above 3-fold up-regulation of TβRII gene as compared with untreated cells ($P < 0.05$). At 3 h, TβRII gene was found to be expressed at the same level in IL-1β-stimulated cells and cells treated with both IL-1β and IP6 ($P = 0.312$). In longer-lasting cultures, transcriptional activity of this gene was significantly suppressed by IP6 in cells treated with IL-1β/IP6 in comparison to those challenged with IL-1β alone ($P = 0.023$) (Figures 5(a) and 5(b)).

3.6. The Effect of IP6 on TβRIII Expression in Caco-2 Cells Stimulated by Bacterial Endotoxins and IL-1β. In 3 h and 12 h lasting cultures, the expression of TβRIII was significantly lowered by LPS of *E. coli* compared to control cells ($P < 0.05$) (Figure 6(a)). LPS-treated cells exposed to IP6 presented an increase in transcriptional activity of the gene in comparison to cells incubated with LPS only ($P < 0.001$). The considerable, that is, 3.5-fold and 2.6-fold enhancement

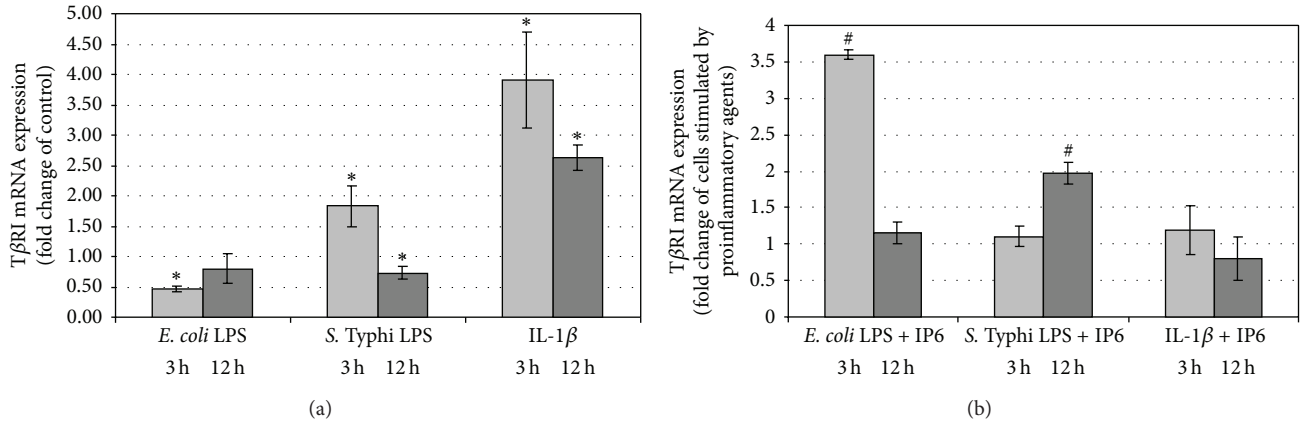

FIGURE 4: Expression of TβRI gene in Caco-2 cells as determined by real-time RT-PCR. Changes in TβRI mRNA expression in Caco-2 cells after treatment with (a) proinflammatory agents and (b) proinflammatory agents and 2.5 mM IP6 for 3 h and 12 h. The results are presented as mean ± SD of three separate experiments; $^{*}P < 0.05$ versus control Caco-2 cells; $^{\#}P < 0.05$ versus proinflammatory agents-stimulated cells.

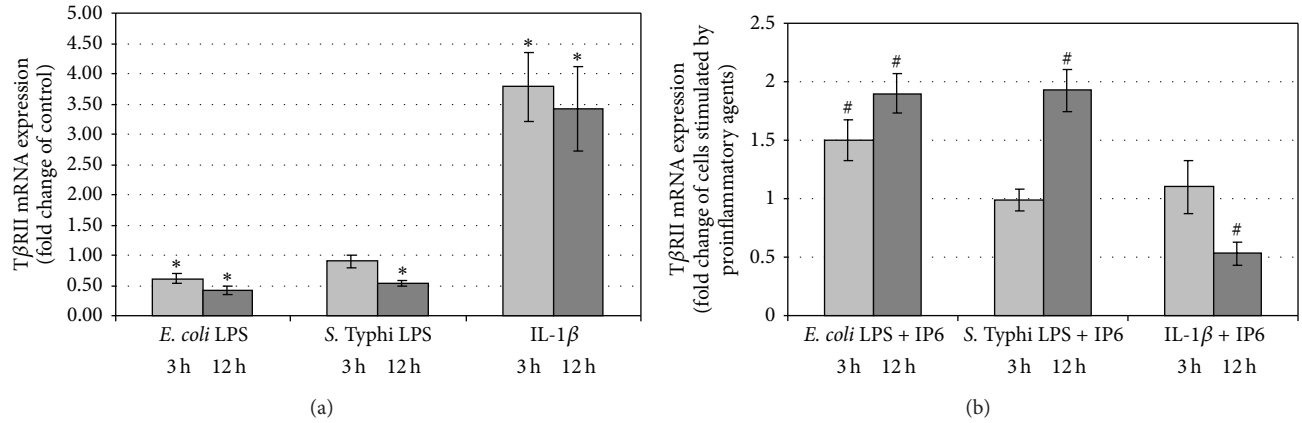

FIGURE 5: Expression of TβRII gene in Caco-2 cells as determined by real-time RT-PCR. Changes in TβRII mRNA expression in Caco-2 cells after treatment with (a) proinflammatory agents and (b) proinflammatory agents and 2.5 mM IP6 for 3 h and 12 h. The results are presented as mean ± SD of three separate experiments; $^{*}P < 0.05$ versus control Caco-2 cells; $^{\#}P < 0.05$ versus proinflammatory agents-stimulated cells.

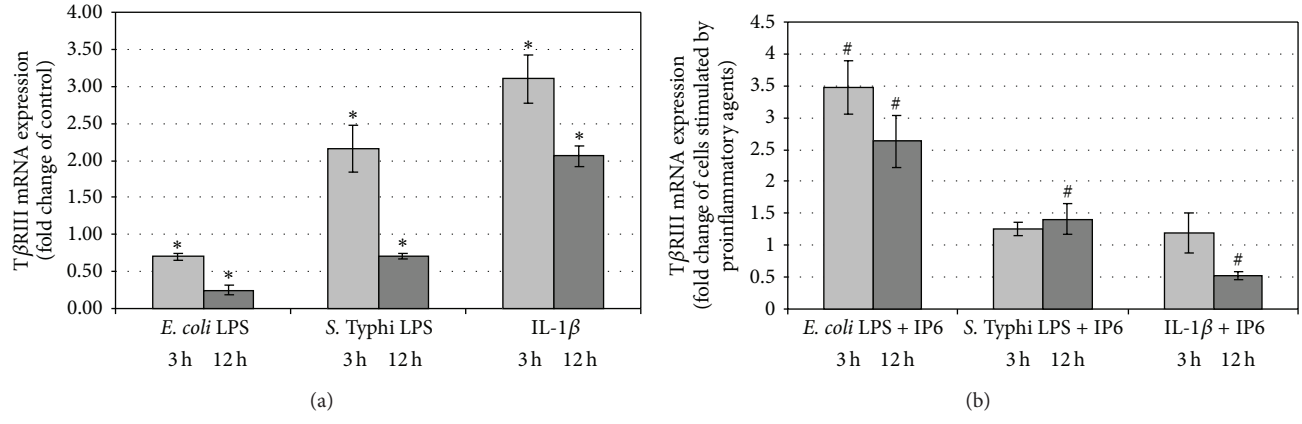

FIGURE 6: Expression of TβRIII gene in Caco-2 cells as determined by real-time RT-PCR. Changes in TβRIII mRNA expression in Caco-2 cells after treatment with (a) proinflammatory agents and (b) proinflammatory agents and 2.5 mM IP6 for 3 h and 12 h. The results are presented as mean ± SD of three separate experiments; $^{*}P < 0.05$ versus control Caco-2 cells; $^{\#}P < 0.05$ versus proinflammatory agents-stimulated cells.

of TβRIII mRNA expression was observed after 3 h and 12 h, respectively, ($P < 0.05$) (Figures 6(a) and 6(b)). Cells exposed to LPS of *S.* Typhi for 3 h produced significantly higher quantity of TβRIII transcript ($P < 0.001$) which has not been changed by IP6 ($P > 0.05$). Furthermore, after 12 h, endotoxin of *S.* Typhi reduced transcription of the gene encoding type III receptor ($P = 0.043$), which was markedly up-regulated by IP6 ($P = 0.041$). Treatment of cells with IL-1β for both 3 h and 12 h showed a significant ($P < 0.0001$) increase in the expression of TβRIII in comparison with control. However, no statistically significant change in its mRNA level in cultures with IL-β/IP6 and IL-1β only was detected after 3 h ($P = 0.130$). After 12 h, a marked decrease in IL-1β-enhanced TβRIII transcript level was observed in response to IP6 ($P < 0.001$) (Figures 6(a) and 6(b)).

4. Discussion and Conclusions

The researches over the past few years have shown unique and essential roles for TGF-β in regulating inflammatory and adaptive immune responses. In particular, TGF-β antagonizes the activation of the key proinflammatory cytokines including IL-1β and TNF-α [13, 32].

The anti-inflammatory treatment strategies can rely on inhibition of proinflammatory cytokine production, receptor binding, signaling, or induction/up-regulation of anti-inflammatory and immunoregulatory cytokines [2]. Various synthetic and natural compounds showing anti-inflammatory properties have been identified. Studies conducted *in vitro* and *in vivo* have demonstrated that phytochemicals, such as curcumin, resveratrol, and genistein, exert chemopreventive effect by targeting the constituents of inflammatory signal pathways [32, 33].

IP6, a natural phytochemical, has recently been described as having immunoregulatory properties. The studies of Cherng et al. [34] showed that IP6 significantly suppressed the secretion of IL-10 and augmented IFN-γ production in human peripheral blood mononuclear cells. This compound can modulate the inflammatory response of IEC by regulating their expression and secretion of cytokines and chemokines. Our previous studies revealed that IP6 down-regulated both the IL-1β-stimulated increase of IL-8 release from enterocytes and the cellular response to bacterial LPS [35]. Moreover, it appeared to influence the expression of TNF-α, proinflammatory cytokine, and its receptors TNFRI and TNFRII in colon cancer cells [36]. IP6 could also inhibit IL-1β-stimulated expression of IL-6 and IL-8 at the transcriptional level in IEC [37].

In the present study, we evaluated the influence of IP6 on the expression of TGF-β1, -β2, and -β3 and their receptors TβRI, TβRII, and TβRIII in human intestinal cells under inflammatory conditions. The intestinal epithelium plays important roles in maintaining immune homeostasis in the gut and participates in maintenance of tolerance toward the microflora and food antigens [38]. The cells of intestinal epithelium are capable of producing and releasing IL-1β, IL-6, TNF-α, and TGF-β, either spontaneously or during the course of intestinal mucosa inflammation [35, 38–40]. Therefore, we used LPS derived from *E. coli* and *S.* Typhi, as well as IL-1β as a relevant *in vitro* model, to study the regulation of TGF-β isoforms and their receptors expression in colon epithelial cells. The cell line Caco-2 (enterocyte-like) utilized in the present experiment is a well-established and widely used model of human intestinal barrier [41].

Lipopolysaccharide released from Gram-negative bacteria cell surface is one of the most potent innate immune-activating stimuli known [42]. Over the last years, the effects of enteropathogenic and enteroinvasive bacteria and members of the normal intestinal microflora on the expression of TGF-βs were examined. However, these studies revealed that commensal and pathogenic species induced fundamentally different cytokine responses in human intestinal epithelial cell lines [43]. The results of Zeuthen et al. [38] showed that the presence and composition of enteric bacteria affects the production of IEC-derived TGF-β and that the modulatory effect of this cytokine is highly dependent on the bacterial stimulus. The authors indicated relatively high production of TGF-β1 in nonstimulated Caco-2 cells and its further increase by stimulation with both G-positive and G-negative commensals [38]. The results of Yoshioka et al. [40] studies demonstrated that intestinal epithelial DLD1 cells increased TGF-β1 and LoVo cells increased TGF-β2 secretion, at 12 h in response to *E. coli* LPS. However, no significant changes in TGF-βs production in hepatocellular carcinoma and myelomonocytic cell lines were observed following stimulation with LPS. Considerable upexpression of mRNAs for TGF-β1, TGF-β2, and TGF-β3 was detected in human intestinal line HT-29 after 3 h coculture with enterotoxigenic *E. coli.* Furthermore, the infection the cells with both enteropathogenic *E. coli* and *S. typhimurium* led to the high induction of TGF-β3 mRNA only. There were insignificant differences in TGF-β1 and TGF-β2 mRNAs in control and cells exposed to both pathogens. Additionally, the authors indicated significantly reduced expression of all TGF-β isoforms in HT-29 incubated with commensal bacteria. The majority of bacteria also reduced TGF-β1 expression in Caco-2 cell line. Also, a significant increase in TGF-β2 and decrease in TGF-β3 mRNAs in these cells co-cultured with commensal *E. coli* were determined [43].

In our study, LPS derived from *E. coli* down-regulated mRNA levels of TGF-β2 and TGF-β3 and all types of receptors in Caco-2 cells over the course of the experiment. In the case of TGF-β1, its reduced transcriptional activity was seen after 3 h of incubation. However, a longer stimulation of cells with LPS caused up-expression of this isoform. IP6 elicited the opposed to *E. coli* LPS effect by increasing downregulated transcription of the examined genes and by suppressing the expression of TGF-β1 at 12 h. Then, endotoxin of *S.* Typhi promoted differential expression profile of TGF-βs and their receptors in a time-dependent manner. The addition of *S.* Typhi. LPS to the cell cultures was manifested by higher transcriptional activity of TGF-β2, -β3, TβRI, and TβRII at 3 h, but longer stimulation of Caco-2 resulted in up-regulation of TGF-β1 and all receptors. IP6 had no effect on LPS-altered expression of TGF-β1. However, it enhanced LPS-increased mRNA expression of TGF-β2 and -β3. Likewise, this agent was capable of activating LPS-downregulated transcription of TβRI, II and III after 12 h.

According to the published data, the proinflammatory cytokines like IL-1, TNF-α, and IFN-γ increased the production of TGF-β isoforms [44]. The main source of IL-1 in IBD patients is the monocyte/macrophage system and active IL-1β is released into the colonic mucosa [45]. Low concentrations of IL-1β have been shown to induce local inflammatory response followed by the activation of protective immune response [46].

As shown in this study, IL-1β stimulation of the epithelial cells up-regulated mRNA levels of all TGF-β isoforms and their receptors at both 3 h and 12 h. IP6 counteracted the stimulatory effect of IL-1β on TGF-β1, TβRII, and TβRIII genes expression in Caco-2 cells by decreasing their mRNA levels in 12 h lasting cultures. Furthermore, IP6 acted synergistically with IL-1β by enhancing the transcription of TGF-β2 and -β3 isoforms at 3 h.

TGB-βs exert their effects via activation of heteromeric receptor complexes of TβRI and TβRII. They can also interact with the type III receptor. This receptor acts as an enhancer of TGF-βs activities by promoting their access to the signaling receptors, especially that of TGF-β2 isoform which has a low affinity for the type II receptor [47]. The differential impact of IP6 on the expression of mRNA TGF-βs and their receptors in colon epithelium under inflammatory conditions may be related to the role which these isoforms play. The three isoforms of TGF-β are distributed in specific spatial and temporal patterns in the tissues and demonstrate distinct biological activities. The TGF-β2 and -β3 isoforms, whose expression was enhanced by IP6, are the effective inhibitors of epithelial proliferation. TGF-β3 may be most effective in inducing epithelial wound repair [48]. TGF-β2 suppresses IFN-γ and IL-1 at the transcriptional level and plays a critical role in the development of tolerance and the prevention of autoimmunity and anti-inflammatory responses [49]. Also, the increased expression of TGF-β1 mRNA in Caco-2 cells treated with IP6 for 3 h following *E. coli* endotoxin pretreatment may indicate its anti-inflammatory activity in relation to this LPS. A variety of pathogenic and proinflammatory stimuli upregulate SMAD7 mRNA expression, which in turn suppresses the TGF-β pathway, through activation of NF-κB. Bitzer et al. [13] show that p65/RelA subunit of NF-κB is required for transcriptional activation of SMAD7 by bacterial LPS and the proinflammatory cytokines (IL-1β, TNF-α). Inositol hexaphosphate exerts influence on cells via phosphatidylinositol-3 kinase (PI3K), MAPK, PKC, AP-1, and NF-κB [28, 29]. Our previously published data demonstrated that IP6 modulated the expression of p65 subunit of nuclear factor κB and its IκBα inhibitor in the intestinal epithelial cells [31].

Diseases characterized by chronic inflammation frequently result in irreversible organ dysfunction due to extensive tissue fibrosis. Intestinal fibrosis is often a part of the natural course of IBD. TGF-β, in particular the TGF-β1 isoform, is a potent profibrogenic agent inducing collagen synthesis and regulating the balance between matrix-degrading metalloproteinases (MMPs) and their inhibitors (TIMPs) [50]. According to Hong et al. [5], natural or synthesized agents that suppress and blockade TGF-β signaling generally demonstrate anti-inflammatory and anti-fibrotic activities. Rahal et al. [51] underline that, there are no IBD therapies that have been shown to specifically decrease fibrosis. They investigated the ability of resveratrol, a naturally occurring phytochemical, to decrease inflammation and fibrosis in an animal model of CD and showed the reduction of inflammatory cytokines as a promising trend in decreasing tissue fibrosis. The results of the present study demonstrate that IP6 is able to significantly downregulate TGF-β1, TβRII, and TβRIII activities in colon epithelial cells stimulated with proinflammatory agents IL-1β and *E. coli* LPS. Moreover, in the recently published studies, we reported that IP6 influenced constitutive expression of both MMP and TIMP genes and downregulated IL-1β-stimulated transcription of some of these genes in the intestinal epithelial cells [52]. Taken together, we postulate that IP6 can attenuate inflammation and fibrosis in intestinal epithelium. Our results were consistent with the report of Kamp et al., [53] who concluded that IP6 reduced pulmonary inflammation and fibrosis in the respiratory bronchioles of rats.

In summary, the present findings suggest that IP6 can suppress the inflammation and exert chemopreventive activity through the modulation of expression of genes encoding TGF-βs and their receptors. The current data confirm our previous conclusions that IP6 present in the intestinal milieu may exert immunoregulatory effects on colonic epithelium under inflammatory conditions or during microbe-induced infection/inflammation in order to maintain the colonic mucosa in a noninflammatory state or to counteract infection [35, 37]. Inositol hexaphosphate with its anti-inflammatory and antifibrotic properties seems to be an ideal drug candidate to adjunct therapy of IBD and inflammation-associated colon cancer. Therefore, it is tempting to hypothesize that supplementing the diet of IP6 could be beneficial for preventing or reducing the inflammatory reactions and fibrosis in the intestine.

Conflict of Interests

The authors report no conflict of interests related to this study or the findings specified in this paper.

Acknowledgment

This work was supported by Grant no. KNW-1-048/k/3/0 from the Medical University of Silesia (Katowice, Poland).

References

[1] D. C. Baumgart and S. R. Carding, "Inflammatory bowel disease: cause and immunobiology," *The Lancet*, vol. 369, no. 9573, pp. 1627–1640, 2007.

[2] U. Böcker, O. Yezerskyy, P. Feick et al., "Responsiveness of intestinal epithelial cell lines to lipopolysaccharide is correlated with Toll-like receptor 4 but not Toll-like receptor 2 or CD14 expression," *International Journal of Colorectal Disease*, vol. 18, no. 1, pp. 25–32, 2003.

[3] R. M. Al-Sadi and T. Y. Ma, "IL-1β causes an increase in intestinal epithelial tight junction permeability," *Journal of Immunology*, vol. 178, no. 7, pp. 4641–4649, 2007.

[4] M. Ligumsky, P. L. Simon, F. Karmeli et al., "Role of interleukin 1 in inflammatory bowel disease-enhanced production during active disease," *Gut*, vol. 31, no. 6, pp. 686–689, 1990.

[5] S. Hong, H.-J. Lee, S. J. Kim, and K.-B. Hahm, "Connection between inflammation and carcinogenesis in gastrointestinal tract: focus on TGF-β signaling," *World Journal of Gastroenterology*, vol. 16, no. 17, pp. 2080–2093, 2010.

[6] R. L. Elliott and G. C. Blobe, "Role of transforming growth factor beta in human cancer," *Journal of Clinical Oncology*, vol. 23, no. 9, pp. 2078–2093, 2005.

[7] B. Bierie and H. L. Moses, "Transforming growth factor beta (TGF-β) and inflammation in cancer," *Cytokine and Growth Factor Reviews*, vol. 21, no. 1, pp. 49–59, 2010.

[8] R. Paduch and P. Niedziela, "TGF-beta1 influence on TNF-alpha production and sTNF-Rs shedding in a coculture of colon carcinoma cell spheroids with normal cells," *In Vitro Cellular and Developmental Biology*, vol. 45, no. 7, pp. 371–377, 2009.

[9] L. Yang, Y. Pang, and H. L. Moses, "TGF-β and immune cells: an important regulatory axis in the tumor microenvironment and progression," *Trends in Immunology*, vol. 31, no. 6, pp. 220–227, 2010.

[10] L. Kubiczkova, L. Sedlarikova, R. Hajek et al., "TGF-β—an excellent servant but a bad master," *Journal of Translational Medicine*, vol. 10, pp. 183–207, 2012.

[11] C.-H. Heldin, K. Miyazono, and P. Ten Dijke, "TGF-β signalling from cell membrane to nucleus through SMAD proteins," *Nature*, vol. 390, no. 6659, pp. 465–471, 1997.

[12] A. Moustakas and C.-H. Heldin, "The regulation of TGFβ signal transduction," *Development*, vol. 136, no. 22, pp. 3699–3714, 2009.

[13] M. Bitzer, G. von Gersdorff, D. Liang et al., "A mechanism of suppression of TGF-β/SMAD signaling by NF-κB/RelA," *Genes and Development*, vol. 14, no. 2, pp. 187–197, 2000.

[14] A. Rizzo, M. J. Waldner, C. Stolfi et al., "Smad7 expression in T cells prevents colitis-associated cancer," *Cancer Research*, vol. 71, no. 24, pp. 7423–7432, 2011.

[15] J. Massague, "TGFβ signalling in context," *Nature Reviews Molecular Cell Biology*, vol. 13, no. 10, pp. 616–630, 2012.

[16] M. W. Saif and E. Chu, "Biology of colorectal cancer," *Cancer Journal*, vol. 16, no. 3, pp. 196–201, 2010.

[17] K.-B. Hahm, Y.-H. Im, T. W. Parks et al., "Loss of transforming growth factor β signalling in the intestine contributes to tissue injury in inflammatory bowel disease," *Gut*, vol. 49, no. 2, pp. 190–198, 2001.

[18] J. F. S. Santibañez, M. Quintanilla, and C. Bernabeu, "TGF-β/TGF-β receptor system and its role in physiological and pathological conditions," *Clinical Science*, vol. 121, no. 6, pp. 233–251, 2011.

[19] G. Monteleone, A. Kumberova, N. M. Croft, C. McKenzie, H. W. Steer, and T. T. MacDonald, "Blocking Smad7 restores TGF-β1 signaling in chronic inflammatory bowel disease," *The Journal of Clinical Investigation*, vol. 108, no. 4, pp. 601–609, 2001.

[20] G. Monteleone, R. Caruso, and F. Pallone, "Role of Smad7 in inflammatory bowel diseases," *World Journal of Gastroenterology*, vol. 18, no. 40, pp. 5664–5668, 2012.

[21] S. P. Hussain and C. C. Harris, "Inflammation and cancer: an ancient link with novel potentials," *International Journal of Cancer*, vol. 121, no. 11, pp. 2373–2380, 2007.

[22] H. Lu, W. Ouyang, and C. Huang, "Inflammation, a key event in cancer development," *Molecular Cancer Research*, vol. 4, no. 4, pp. 221–233, 2006.

[23] J. Ferlay, H.-R. Shin, F. Bray, D. Forman, C. Mathers, and D. M. Parkin, "Estimates of worldwide burden of cancer in 2008: GLOBOCAN 2008," *International Journal of Cancer*, vol. 127, no. 12, pp. 2893–2917, 2010.

[24] B. Rousseau, B. Chibaudel, J.-B. Bachet et al., "Stage II and stage III colon cancer: treatment advances and future directions," *Cancer Journal*, vol. 16, no. 3, pp. 202–209, 2010.

[25] P. A. Thompson and E. W. Gerner, "Current concepts in colorectal cancer prevention," *Expert Review of Gastroenterology and Hepatology*, vol. 3, no. 4, pp. 369–382, 2009.

[26] I. Vucenik and A. M. Shamsuddin, "Protection against cancer by dietary IP6 and inositol," *Nutrition and Cancer*, vol. 55, no. 2, pp. 109–125, 2006.

[27] M. Gu, K. Raina, C. Agarwal, and R. Agarwal, "Inositol hexaphosphate downregulates both constitutive and ligand-induced mitogenic and cell survival signaling, and causes caspase-mediated apoptotic death of human prostate carcinoma PC-3 cells," *Molecular Carcinogenesis*, vol. 49, no. 1, pp. 1–12, 2010.

[28] A. Matejuk and A. Shamsuddin, "IP6 in cancer therapy: past, present and future," *Current Cancer Therapy Reviews*, vol. 6, no. 1, pp. 1–12, 2010.

[29] J. Liao, D. N. Seril, A. L. Yang, G. G. Lu, and G.-Y. Yang, "Inhibition of chronic ulcerative colitis associated adenocarcinoma development in mice by inositol compounds," *Carcinogenesis*, vol. 28, no. 2, pp. 446–454, 2007.

[30] M. Kapral, J. Wawszczyk, A. Hollek et al., "Induction of the expression of genes encoding TGF-β, isoforms and their receptors by inositol hexaphosphate in human colon cancer cells," *Acta Poloniae Pharmaceutica*, vol. 70, no. 2, pp. 357–363, 2013.

[31] M. Kapral, B. Parfiniewicz, B. Strzałka-Mrozik, A. Zachacz, and L. Węglarz, "Evaluation of the expression of transcriptional factor NF-κB induced by phytic acid in colon cancer cells," *Acta Poloniae Pharmaceutica*, vol. 65, no. 6, pp. 697–702, 2008.

[32] Y. S. Kim, M. R. Young, G. Bobe, N. H. Colburn, and J. A. Milner, "Bioactive food components, inflammatory targets, and cancer prevention," *Cancer Prevention Research*, vol. 2, no. 3, pp. 200–208, 2009.

[33] C. D. Davis, "Nutritional interactions: credentialing of molecular targets for cancer prevention," *Experimental Biology and Medicine*, vol. 232, no. 2, pp. 176–183, 2007.

[34] J.-M. Cherng, W. Chiang, and L.-C. Chiang, "Immunomodulatory activities of edible beans and related constituents from soybean," *Food Chemistry*, vol. 104, no. 2, pp. 613–618, 2007.

[35] L. Węglarz, J. Wawszczyk, A. Orchel, M. Jaworska-Kik, and Z. Dzierzewicz, "Phytic acid modulates in vitro IL-8 and IL-6 release from colonic epithelial cells stimulated with LPS and IL-1β," *Digestive Diseases and Sciences*, vol. 52, no. 1, pp. 93–102, 2007.

[36] K. Cholewa, B. Parfiniewicz, I. Bednarek et al., "The influence of phytic acid on TNF-α and its receptors genes' expression in colon cancer Caco-2 cells," *Acta Poloniae Pharmaceutica*, vol. 65, no. 1, pp. 75–79, 2008.

[37] J. Wawszczyk, M. Kapral, A. Hollek et al., "The effect of phytic acid on the expression of NF-κB, IL-6 and IL-8 in IL-1β-stimulated human colonic epithelial cells," *Acta Poloniae Pharmaceutica*, vol. 69, no. 6, pp. 1313–1319, 2012.

[38] L. H. Zeuthen, L. N. Fink, and H. Frokiaer, "Epithelial cells prime the immune response to an array of gut-derived commensals towards a tolerogenic phenotype through distinct

actions of thymic stromal lymphopoietin and transforming growth factor-β," *Immunology*, vol. 123, no. 2, pp. 197–208, 2008.

[39] D. Haller, C. Bode, W. P. Hammes, A. M. A. Pfeifer, E. J. Schiffrin, and S. Blum, "Non-pathogenic bacteria elicit a differential cytokine response by intestinal epithelial cell/leucocyte co-cultures," *Gut*, vol. 47, no. 1, pp. 79–87, 2000.

[40] T. Yoshioka, Y. Morimoto, H. Iwagaki et al., "Bacterial lipopolysaccharide induces transforming growth factor β and hepatocyte growth factor through toll-like receptor 2 in cultured human colon cancer cells," *Journal of International Medical Research*, vol. 29, no. 5, pp. 409–420, 2001.

[41] J. van de Walle, A. Hendrickx, B. Romier, Y. Larondelle, and Y.-J. Schneider, "Inflammatory parameters in Caco-2 cells: effect of stimuli nature, concentration, combination and cell differentiation," *Toxicology in Vitro*, vol. 24, no. 5, pp. 1441–1449, 2010.

[42] M. Rossol, H. Heine, U. Meusch et al., "LPS-induced cytokine production in human monocytes and macrophages," *Critical Reviews in Immunology*, vol. 31, no. 5, pp. 379–446, 2011.

[43] B. Bahrami, S. Macfarlane, and G. T. Macfarlane, "Induction of cytokine formation by human intestinal bacteria in gut epithelial cell lines," *Journal of Applied Microbiology*, vol. 110, no. 1, pp. 353–363, 2011.

[44] I. Drygiannakis, V. Valatas, O. Sfakianaki et al., "Proinflammatory cytokines induce crosstalk between colonic epithelial cells and subepithelial myofibroblasts: implication in intestinal fibrosis," *Journal of Crohn's and Colitis*, vol. 7, no. 4, pp. 286–300, 2013.

[45] M. E. McAlindon, C. J. Hawkey, and Y. R. Mahida, "Expression of interleukin 1β and interleukin 1β converting enzyme by intestinal macrophages in health and inflammatory bowel disease," *Gut*, vol. 42, no. 2, pp. 214–219, 1998.

[46] R. N. Apte and E. Voronov, "Interleukin-1 - major pleiotropic cytokine in tumor-host interactions," *Seminars in Cancer Biology*, vol. 12, no. 4, pp. 277–290, 2002.

[47] G. de Crescenzo, S. Grothe, J. Zwaagstra, M. Tsang, and M. D. O'Connor-McCourt, "Real-time monitoring of the interactions of transforming growth factor-β (TGF-β) isoforms with latency-associated protein and the ectodomains of the TGF-β type II and III receptors reveals different kinetic models and stoichiometries of binding," *The Journal of Biological Chemistry*, vol. 276, no. 32, pp. 29632–29643, 2001.

[48] B. C. Mckaig, K. Hughes, P. J. Tighe, and A. Y. R. Mahida, "Differential expression of TGF-β isoforms by normal and inflammatory bowel disease intestinal myofibroblasts," *American Journal of Physiology: Cell Physiology*, vol. 282, no. 1, pp. C172–C182, 2002.

[49] Y.-J. Lee, Y. Han, H.-T. Lu et al., "TGF-β suppresses IFN-γ induction of class II MHC gene expression by inhibiting class II transactivator messenger RNA expression," *Journal of Immunology*, vol. 158, no. 5, pp. 2065–2075, 1997.

[50] A. Di Sabatino, C. L. Jackson, K. M. Pickard et al., "Transforming growth factor β signalling and matrix metalloproteinases in the mucosa overlying Crohn's disease strictures," *Gut*, vol. 58, no. 6, pp. 777–789, 2009.

[51] K. Rahal, P. Schmiedlin-Ren, J. Adler et al., "Resveratrol has antiinflammatory and antifibrotic effects in the peptidoglycan-polysaccharide rat model of Crohn's disease," *Inflammatory Bowel Diseases*, vol. 18, no. 4, pp. 613–623, 2012.

[52] M. Kapral, J. Wawszczyk, M. Jurzak, A. Hollek, and L. Weglarz, "The effect of inositol hexaphosphate on the expression of selected metalloproteinases and their tissue inhibitors in IL-1β-stimulated colon cancer cells," *International Journal of Colorectal Disease*, vol. 27, no. 11, pp. 1419–1428, 2012.

[53] D. W. Kamp, V. A. Israbian, A. V. Yeldandi, R. J. Panos, P. Graceffa, and S. A. Weitzman, "Phytic acid, an iron chelator, attenuates pulmonary inflammation and fibrosis in rats after intratracheal instillation of asbestos," *Toxicologic Pathology*, vol. 23, no. 6, pp. 689–695, 1995.

Hindawi Publishing Corporation
Mediators of Inflammation
Volume 2013, Article ID 450950, 7 pages
http://dx.doi.org/10.1155/2013/450950

Clinical Study

Enhanced Inflammatory Activity of Endometriotic Lesions from the Rectovaginal Septum

Dominic Bertschi,[1] Brett D. McKinnon,[1,2] Jakob Evers,[1] Nick A. Bersinger,[1,2] and Michael D. Mueller[1]

[1] *Department of Obstetrics and Gynecology, Inselspital, Berne University Hospital, 3010 Berne, Switzerland*
[2] *Department of Clinical Research, University of Berne, 3010 Berne, Switzerland*

Correspondence should be addressed to Brett D. McKinnon; brett.mckinnon@dkf.unibe.ch

Received 9 August 2013; Accepted 22 November 2013

Academic Editor: Charles J. Malemud

Endometriosis is characterised by the growth of ectopic lesions at multiple locations outside the uterine cavity and may be considered a collection of distinct but related conditions. The exact aetiology of endometriosis is still not clear although a role for inflammation is increasingly accepted. We therefore investigated the inflammatory activity of eutopic tissue and that of the matching ectopic lesions from different locations by measuring the genetic expression of inflammatory chemokines and cytokines. The gene expression in matching eutopic and ectopic tissue was compared, as was the gene expression in lesions from different locations. A significantly higher mRNA expression of the chemokines ENA-78 and RANTES and the cytokines IL-6 and TNFα was observed in endometriotic lesions of the rectovaginal septum (RVS) compared to that of matching eutopic tissue. Comparisons across lesion locations showed a significantly higher expression of IL-6 and TNFα in the RVS compared to lesions from either the ovaries or the peritoneum. These results show that the production of some inflammatory chemokines and cytokines is significantly increased in the ectopic endometrial tissue compared to matching eutopic tissue. Furthermore, IL-6 and TNFα are produced in significantly higher quantities in RVS lesions compared to other lesions.

1. Introduction

Endometriosis is defined as the presence of endometrial tissue outside the uterine cavity. The most common symptoms leading to a diagnosis are dysmenorrhoea, pelvic pain, and reduced fertility [1]. It is a very prevalent disease affecting up to 10% of the reproductive-aged female population [2].

The precise aetiology of endometriosis is not yet clear. Currently, the most widely accepted theory is the implantation theory: retrograde menstruation can result in viable endometrial cells and fragments entering the peritoneal cavity [3] and once attached [4], they promote a chronic pelvic inflammatory response [5]. Retrograde menstruation however cannot explain all cases, as endometriotic lesions have been identified in diverse locations such as the brain [6]. It is broadly accepted however that most of the ectopic lesions can be separated into three main regions: (i) ovarian, (ii) rectovaginal septum (RVS), and (iii) peritoneum. Biochemical and pathological differences between the lesions found in these locations have led to suggestions that endometriosis may represent a collection of related but distinct conditions [7]. It is possible that the variability between these distinct but related lesions is what contributes to the enigmatic nature of the disease.

The contribution of inflammation to the progression of endometriosis is increasingly being recognised. Endometriotics lesions that are established at ectopic sites secrete chemokines which attract macrophages into the peritoneal cavity, further stimulating the inflammatory response and release of cytokines [8]. Significantly increased numbers of activated macrophages have been identified in the peritoneal fluid of women with endometriosis [9], as has an increased concentration of various chemokines and cytokines. Significantly elevated levels of epithelial neutrophil-activating

peptide (ENA-78) [10], monocyte chemotactic protein (MCP-1) [11], interleukin (IL)-8 [12], tumor necrosis factor (TNF)-α [13], IL-6 [14, 15], and regulated on activation normal T cell expressed and secreted (RANTES) [12] have all been found in the peritoneal fluid of patients with endometriosis. Underlining the inflammatory nature of the condition is the fact that TNFα [16], ENA-78 [17], and IL-6 [18, 19] are also elevated in the serum of women with endometriosis. Less data is however available on the inflammatory response of the lesion itself and whether there is variability based on the type or lesion location. A difference in the production of specific cytokines may provide an insight into the inflammatory activity of lesions that grow in different locations.

In order to gain a better understanding of this complex disease and the differences that can occur between various lesions, this study investigated the production of several chemokines and cytokines in matching eutopic endometrial and ectopic endometriotic tissue and compared their gene expression levels in the three most common presentations of the disease.

2. Patients and Methods

2.1. Sample Collection and Patient Data. Informed consent was collected prior to surgery from all women included in the study. Laparoscopic surgery was performed for the investigation of pelvic pain or infertility, and any endometriotic lesions identified were removed and their location was noted. Where possible, an endometrial biopsy was also collected using a soft curette (Pipelle-de-cornier, Laboratoire CCD, France). All tissue collected during the surgery was stored in RNAlater (Invitrogen Life Technologies, Zug, Switzerland) at −80°C until further use. Exclusion criteria for the study included prior or current infections, liver dysfunction, or the use of hormonal treatments, including any hormonal contraceptive or gonadotropin releasing hormone analogues (GnRHa) within the past 3 months. All laparoscopies were performed in the proliferative phase of the menstrual cycle. Institutional review board approval was obtained from the ethical committee prior to the commencement of the study.

After the informed consent was obtained and exclusion criteria were satisfied, we collected eutopic endometrial biopsies from 17 patients. A single matching ectopic lesion was collected from 15 women, two lesions were collected from another, and three lesions in the final case, resulting in 20 ectopic lesions with matching eutopic samples. The primary indication for surgery was dysmenorrhea for ten of these women, pelvic pain for four women, and infertility for the remaining three. The average age of the patients was 32.94 ± 1.454, range 24–41, and the body mass index (BMI) was 23.39 ± 0.914, range 18.90–33.10.

For the further comparison of the mRNA expression across ectopic sites additional lesions were collected from another 23 patients to make a total of 40 patients. A single lesion was collected from 34 patients, two lesions were collected from five patients, and three lesions were collected from one patient, resulting in a total of 47 ectopic endometriotic lesions. In some cases the isolated mRNA was insufficient to determine the concentration of all genes of interest and as such n values are included with each mean and SEM. The primary indication for surgery was dysmenorrhea for 17 women, pelvic pain for another 14, and idiopathic infertility for the remaining nine. The average age was 35.58 ± 1.265, range 22–58, and the BMI was 23.79 ± 0.811, range 18.00–47.30. No significant difference in either age or BMI was observed in the three groups based on lesion location.

2.2. Determination of Gene Expression in Eutopic Endometrium and Ectopic Endometriotic Tissue. Approximately 30 mg of tissue from both the eutopic endometrial biopsies and ectopic endometriotic lesions was excised and homogenized in the FastPrep 120 tissue homogenizer (30 seconds at 4.0 m/sec) in cell lysis buffer (Qiagen, Düsseldorf, Germany). RNA isolation was performed with the RNAeasy minikit (Qiagen) and after isolation the TurboDNase kit (Ambion, Life Technologies, Zug, Switzerland) was used for genomic DNase digestion. One microgram of the total RNA was reverse transcribed in a 25 μL reaction volume with the Moloney murine leukemia virus (MMLV) reverse transcriptase (Promega, Dübendorf, Switzerland) and random primers. The resulting cDNA was diluted 1 : 20 and the absence of genomic DNA was confirmed with a reverse transcriptase control.

The quantitative real time polymerase chain reaction (qPCR) was performed with the SYBR green Fast Advance Master Mix (Qiagen) and a Rotor-Gene RG 2000 (Corbett Research, NSW, Australia), under the following conditions, 95°C for 5 min, followed by 40 cycles of 95°C for 5 second, and 60°C for 10 seconds. Specificity of the reaction was confirmed via melt curve analysis and the product size was confirmed on a 4% agarose gel.

The Genbank accession number and the primer sequences for all genes examined by qPCR are shown in Table 1.

2.3. Statistical Analysis. The most stable reference genes and the optimal combination to provide minimal variability were selected via the geNORM software program and a geometric mean of the four reference genes selected was used to normalise the expression of the genes of interest for both the eutopic and ectopic tissue [20]. The reaction efficiency of each assay was determined via linear regression [21] and the fold change calculated with the qBASEplus software (Biogazelle, Zwijnaarde, Belgium).

The difference between the matched eutopic and ectopic mRNA expression at different locations and the difference between mRNA in different ectopic locations were determined by a one-way Analysis of Variance (ANOVA) test with a *post hoc* Bonferroni's multiple comparisons test between selected groups. All values are presented as mean ± SEM and all statistical analysis was performed with Graphpad Prism 5.0 and significance was set at a value of $P < 0.05$.

3. Results

3.1. Cytokine mRNA Concentrations in Matching Eutopic and Ectopic Endometrial Tissue. For the chemokines a one-way ANOVA test confirmed a significant variation between

Table 1: Primer sequences of the reference genes and genes of interest.

Cytokine	Genbank accession no.	Sense	Antisense
GAPDH	NM_002046	5′-TGC ACC ACC AAC TGC TTA GC-3′	5′-GGC ATG GAC TGT GGT CAT GAG-3′
ACTB	NM_001101	5′-CTG GAA CGG TGA AGG GTG ACA-3′	5′-AAG GGA CTT CCT GTA ACA ATG CA-3′
YWHAZ	NM_003406	5′- ACT TTT GGT ACA TTG TGG CTT CAA -3′	5′-CGC CAG GAC AAA CCA GTA T-3′
RPL13A	NM_012423	5′CCT GGA GGA GAA GAG GAA AGA-3′	5′-TTG AGG ACC TCT GTG TAT TTG TCA A-3′
IL-6	NM_00600	5′-GCA CTG GCA GAA AAC AAC CT-3′	5′-CAG GGG TGG TTA TTG CAT CT-3′
IL-8	NM_000584	5′-ACT GAG AGT GAT TGA GAG TGG AC-3′	5′-AAC CCT CTG CAC CCA GTT TTC -3′
ENA-78	NM_02994	5′-CTC CAA TCT TCG CTC CTC CAA-3′	5′-GGA GGC TCA TAG TGG TCA AGA G-3′
TNFα	NM_000594	5′-GCC CAT GTT GTA GCA AAC CC-3′	5′-TAT CTC TCA GCT CCA CGC CA-3′
MCP-1	NM_002982	5′-GGG CAT TGA TTG CAT CTG GC-3′	5′-CTG CTC ATA GCA GCC ACC TT-3′
PAPP-A	NM_002581	5′-AGT GGT ATC CTC ACC CTG CT-3′	5′-GTT GCA AAA GGC TCG GTT GT-3′
RANTES	NM_002985	5′-CTG CTT TGC CTA TGC CC-3′	5′-TCG GGT GAC AAA GAC GAC TG-3′

the mRNA concentrations of the ectopic endometriotic tissue with eutopic endometrial tissue for ENA-78 ($P = 0.0039$) and RANTES ($P = 0.0490$), but not for MCP-1 ($P = 0.1251$) or IL-8 ($P = 0.7991$) (Figure 1). A Bonferroni's multiple comparisons test was performed to compare the mean of each location against the eutopic mean. No significant difference was observed for MCP-1 mRNA expression between the eutopic tissue (0.107 ± 0.015, $n = 17$) and the ovarian lesions (2.751 ± 1.943, $n = 8$, $P < 0.05$), the peritoneal (0.590 ± 0.167, $n = 7$, $P < 0.01$) or the RVS (1.865 ± 0.712, $n = 4$, $P < 0.01$) lesions (Figure 1(a)). For ENA-78 there was a significantly stronger expression in the RVS lesions (5.905 ± 3.569, $n = 4$, $P < 0.01$) compared to the eutopic tissue (0.613 ± 0.250, $n = 17$), but no difference was observed in lesions from either the ovaries (0.811 ± 0.290, $n = 8$), or the peritoneum (1.444 ± 0.504, $n = 7$) (Figure 1(b)). For IL-8 there was no significant variation in the mRNA expression in either the peritoneum (0.396 ± 0.114, $n = 8$), the ovarian (0.409 ± 0.084, $n = 8$), or the RVS (1.574 ± 0.385, $n = 5$) compared to the eutopic tissue (3.979 ± 3.337, $n = 20$) (Figure 1(c)). A significantly higher expression of RANTES mRNA was observed in the RVS (0.582 ± 0.264, $n = 5$, $P < 0.05$) compared to the eutopic tissue (0.239 ± 0.0432, $n = 17$), but not in either the peritoneum (0.220 ± 0.030, $n = 5$) or the ovarian tissue (0.190 ± 0.045, $n = 8$) (Figure 1(d)).

For the inflammatory cytokines a one-way ANOVA test confirmed a significant variation between the mRNA concentrations in the eutopic tissue with the mRNA concentration in the ectopic tissue for TNFα ($P = 0.0014$) and IL-6 ($P < 0.0001$) (Figure 2). A *post hoc* Bonferroni's multiple comparisons test indicated that TNFα mRNA expression in both the peritoneal (1.939 ± 0.667, $n = 8$, $P < 0.05$) and the RVS (3.128 ± 1.608, $n = 4$, $P < 0.01$) samples was significantly higher than that observed for their matching eutopic tissue (0.444 ± 0.106, $n = 17$), although no difference was observed with the ovarian lesions (0.291 ± 0.034, $n = 8$) (Figure 2(a)). For IL-6 there was a significantly higher expression in the RVS region (9.308 ± 3.714, $n = 5$, $P < 0.0001$), but not the ovaries (0.689 ± 0.237, $n = 7$) or the peritoneal region (0.667 ± 0.237, $n = 7$) compared to the eutopic tissue (0.152 ± 0.091, $n = 17$) (Figure 2(b)).

3.2. Cytokine mRNA Concentrations of Ectopic Endometriotic Lesions from Different Locations. A significant variation was observed between the mRNA expression of TNFα ($P = 0.0265$) and IL-6 ($P < 0.0001$), amongst the endometriotic lesions from different locations. A *post-hoc* Bonferroni's multiple comparisons test indicated that the TNFα mRNA expression in the RVS (2.590 ± 1.357, $n = 5$) was significantly higher than in the ovarian lesions (0.813 ± 0.144, $n = 24$, $P < 0.05$), but not in the peritoneal lesions (1.711 ± 0.460, $n = 12$). For IL-6 the mRNA expression in the RVS lesions (10.150 ± 3.148, $n = 6$) was significantly higher than the expression in both the ovaries (1.260 ± 0.323, $n = 24$, $P < 0.0001$) and the peritoneum (1.211 ± 0.400, $n = 13$, $P < 0.0001$) (Figure 3).

In contrast no significant difference in mRNA expression was observed for any of the four chemokines examined in this study. MCP-1 expression in the RVS (1.700 ± 0.576, $n = 5$) was not significantly higher than either the ovarian (1.393 ± 0.632, $n = 25$) or the peritoneal samples (0.814 ± 0.215, $n = 13$), which was also the case for ENA-78 (Peritoneal; 1.497 ± 0.465, $n = 13$, ovarian; 2.988 ± 1.429, $n = 25$, RVS; 4.822 ± 2.969, $n = 5$), IL-8 (peritoneum; 1.548 ± 1.188, $n = 13$, ovaries; 1.352 ± 0.471, $n = 25$, RVS; 2.017 ± 0.543, $n = 6$), and RANTES (peritoneal; 0.288 ± 0.064, $n = 11$, ovarian; 0.364 ± 0.054, $n = 22$, RVS; 0.528 ± 0.222, $n = 6$) (Figure 3).

4. Discussion

The study showed that the mRNA expression of the chemokines ENA-78 and RANTES, as well as the inflammatory cytokines TNFα and IL-6, was significantly increased in the ectopic lesion compared to those in the matched eutopic tissue in women with endometriosis. For IL-6, ENA-78, and RANTES this increase was most significant in the RVS region, whereas for TNFα, it was in both the peritoneal lesions and the RVS lesions. In addition, when compared across lesion

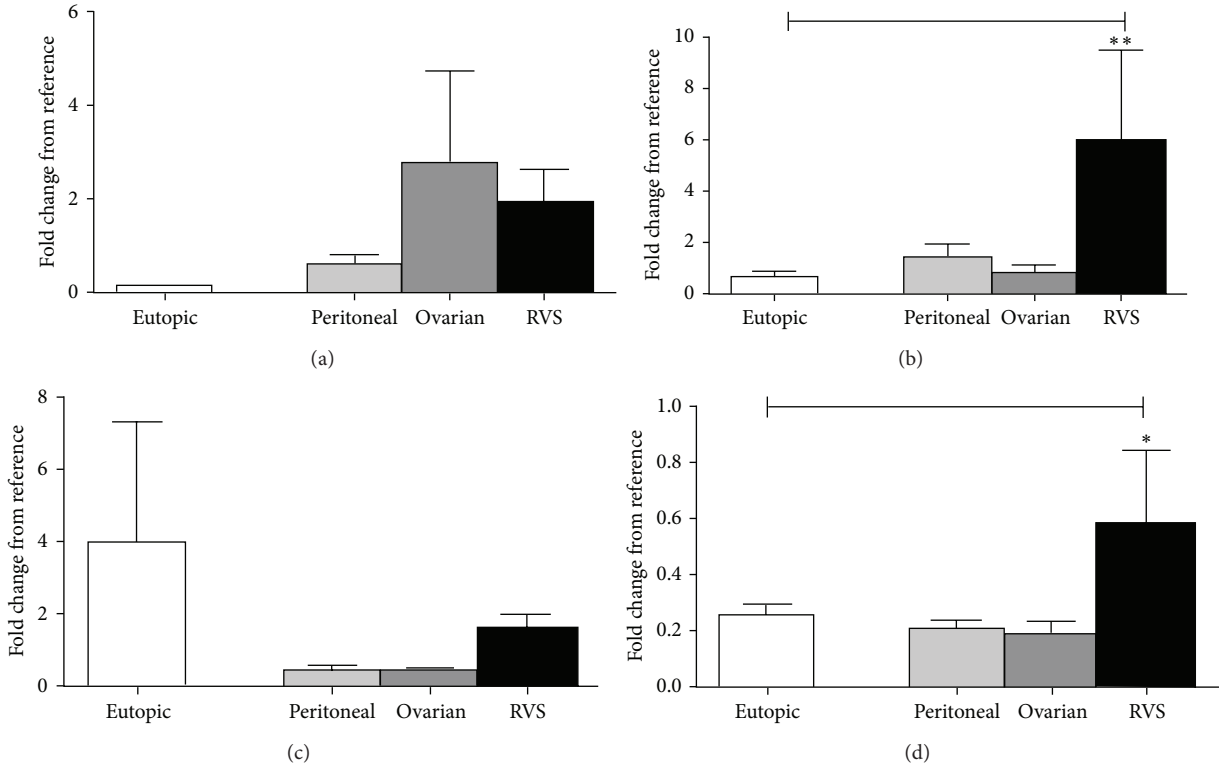

Figure 1: Chemokine production in eutopic endometrium and matching ectopic endometriotic lesions from different locations. (a) No significant difference was observed in the mRNA expression of MCP-1. (b) ENA-78 mRNA expression was significantly stronger in the RVS lesions compared to its matching eutopic tissue. (c) No significant difference in IL-8 mRNA expression was observed between the eutopic endometrium and the ectopic lesions from different locations. (d) RANTES expression was significantly higher in the RVS lesions compared to the eutopic endometrium. All values are represented by mean ± SEM. $^{*} < .05$, $^{**} < .01$.

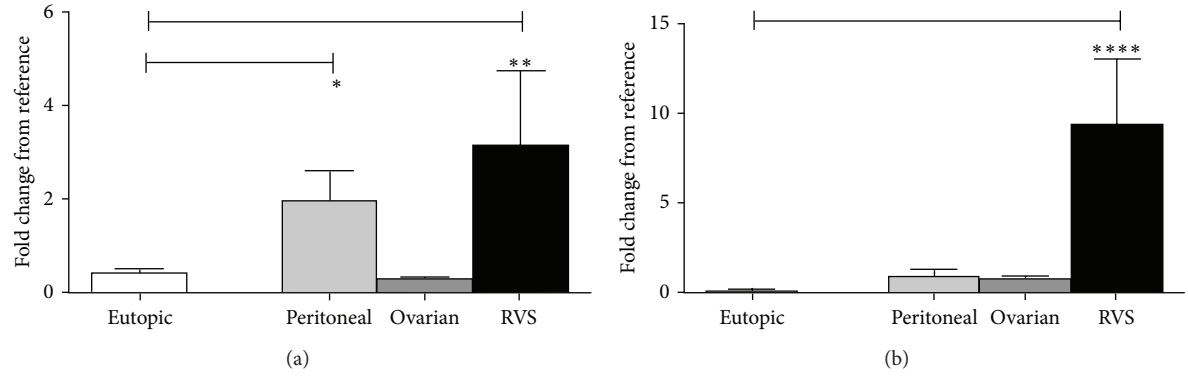

Figure 2: Inflammatory cytokine mRNA expression in eutopic and matching ectopic endometriotic lesions from different locations. (a) The mRNA expression of TNFα was significantly higher in the peritoneal and RVS lesions compared to their matching eutopic endometrium. (b) The mRNA expression of IL-6 was significantly higher only in the RVS lesions. All values are represented by mean ± SEM. $^{*} < .05$, $^{**} < .01$, $^{****} < .0001$.

locations IL-6 was the most highly expressed in the RVS region compared to either the ovaries or the peritoneum. The results suggest therefore that different inflammatory proteins have separate roles in different lesions and understanding these roles may help to specifically target certain presentations of endometriosis. In addition, the increased production of many of these proteins by the RVS lesions provides some molecular evidence towards the notion that lesions developing in the RVS are strongly inflammatory.

Increased expression of chemokines by ectopic endometrial implants is an important early stage in the pathogenesis of endometriosis. Chemokines secreted by the ectopic lesions stimulate the infiltration of macrophages that further contribute to the development of the disease. In this

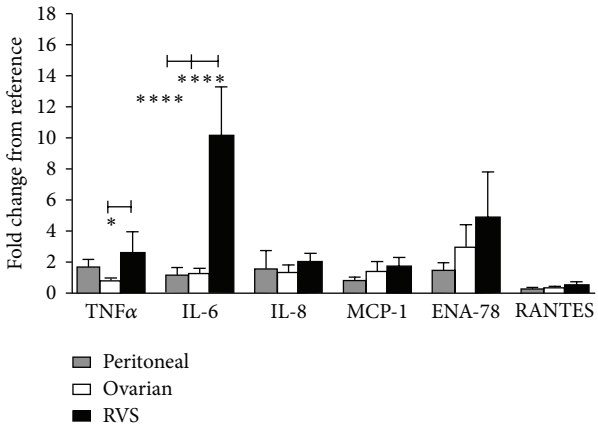

Figure 3: Comparison of cytokine and chemokine concentrations in endometriotic lesions from different locations. A comparison of the mRNA expression between endometriotic lesions from different locations indicated that TNFα expression in the RVS was significantly higher than expression in the ovarian lesions. IL-6 mRNA expression was significantly higher in the RVS than either the ovarian or the peritoneal lesions. There was no significant difference between the lesions with any of the other cytokines. All values are represented by mean ± SEM. $^{*} < .05$, $^{****} < .0001$.

study we found a significant increase in the expression of RANTES and ENA-78 in the RVS lesions compared to the matching eutopic tissue. RANTES production by ectopic lesions recruits leukocytes [22], which then in turn stimulates RANTES production [23] creating a feedback loop. Previous studies support this result as RANTES correlates with deep infiltrating endometriosis (DIE), which is most commonly found in the RVS [24]. ENA-78 may also play a significant role in the pathogenesis of endometriosis via the activation of macrophages and the adhesion of endometriotic cells to the underlying tissue [25]. Previous studies have shown that both endometrial epithelial [26] and stromal cells [27] produce significant amounts of ENA-78, which is stimulated by IL-1β, although this is the first evidence to indicate a significant upregulation in production of ENA-78 by RVS lesions.

IL-8 has strong chemotactic properties for neutrophils and T lymphocytes and is a potent angiogenic agent [28]. While numerous studies have shown an upregulation of IL-8 in the peritoneal fluid of women with endometriosis [29, 30] the source is not clear. An increase in peritoneal macrophages may be responsible for a higher concentration of IL-8, as would an increased production of IL-8 by the endometriotic lesions themselves.. Previous evidence shows that both cultured epithelial and stromal endometrial and endometriotic cells produce IL-8 [26, 27], although one study found that the ectopic tissue produced less IL-8 than the eutopic tissue [31]. Another study on cultured epithelial and stromal cells showed that IL-8 secretion is increased after exposure to IL-1β [26]. The lack of a significant difference for IL-8 in this study may be a reflection of the need to stimulate IL-8 production in endometriotic tissue.

TNFα mRNA expression was also significantly up-regulated in both the RVS and the peritoneal lesions compared to those in their matching eutopic tissue. For IL-6 a significant variation was only observed in the RVS lesion. TNFα has an essential role in the inflammatory process. The primary function of TNFα is to initiate a cascade of other cytokines that can further stimulate a proinflammatory response. In endometriosis it correlates with both the stage of the disease [32], and the menstrual pain reported [33]. Consistent with its early role in the inflammatory cycle it also stimulates cytokines, such as IL-6. The increased expression of TNFα is consistent with an important role for this cytokine in the early pathogenesis of endometriosis that may be common for different types of lesions. The fact that IL-6 is only significantly higher in RVS lesions may suggest that the inflammatory pathway between these two lesions may diverge prior to this point.

IL-6 is a multifunctional cytokine that can stimulate cell proliferation [34] and angiogenesis [35] and is hormonally regulated [36]. Different studies have shown both an increase [14, 15] or no change in the peritoneal fluid of women with endometriosis compared to women without [37]. IL-6 production has previously been identified in ectopic lesions, however results differ as to whether there is a change in production once the tissue becomes pathological. Some studies have found no significant difference between eutopic endometrium and endometriotic tissue from ovarian endometriosis [31], whereas others with ovarian endometriosis only [38], or non-detailed locations, have shown significant increases [39]. Furthermore, an *in vitro* study from endometrial stromal cells isolated from chocolate ovarian cysts showed a significant ability to produce IL-6 with production comparable to that of peritoneal macrophages [40]. None of these previous studies however have addressed the production of IL-6 in lesions from different locations.

A limitation of this study that should be mentioned is the small number of samples available for the RVS region. This is primarily due to the strict exclusion criteria for this study. As evidence indicates that the use of GnRHa can have an effect on the cytokine concentrations in the peritoneal fluid [41, 42] we excluded all samples from women with previous GnRHa use in the last 3 months. As women with RVS lesions are more likely to experience painful symptoms and to have previously sought treatment for endometriosis, a large proportion of women presenting to our tertiary care facility with RVS lesions had previous GnRHa or contraceptive use and thus were excluded from the study. However, although we only had a small number of samples, the ability to use matched eutopic and ectopic samples and our strict exclusion criteria should provide more weight to these results. Further studies with more samples should be performed to confirm our findings of differential cytokine production from lesions from different locations.

In conclusion, this study gives new insights in the production of chemokines and cytokines in endometriotic lesions from different locations and our results support the supposition that the RVS lesions are an intensely inflammatory form of endometriotic lesions. Assessing lesions from different locations uniquely may be vital in understanding the pathological changes of the disease and potentially for their mode of treatment.

Conflict of Interests

None of the authors have a conflict of interests.

References

[1] N. Sinaii, K. Plumb, L. Cotton et al., "Differences in characteristics among 1,000 women with endometriosis based on extent of disease," *Fertility and Sterility*, vol. 89, no. 3, pp. 538–545, 2008.

[2] B. Eskenazi and M. L. Warner, "Epidemiology of endometriosis," *Obstetrics and Gynecology Clinics of North America*, vol. 24, no. 2, pp. 235–258, 1997.

[3] J. A. Sampson, "Metastatic or embolic endometriosis, due to the menstrual dissemination of endometrial tissue into the venous circulation," *The American Journal of Pathology*, vol. 3, no. 2, pp. 93–110. 43, 1927.

[4] C. A. Witz, "Cell adhesion molecules and endometriosis," *Seminars in Reproductive Medicine*, vol. 21, no. 2, pp. 173–181, 2003.

[5] R. O. Burney and L. C. Giudice, "Pathogenesis and pathophysiology of endometriosis," *Fertility and Sterility*, vol. 98, no. 3, pp. 511–519, 2012.

[6] L. L. Thibodeau, G. R. Prioleau, and E. E. Manuelidis, "Cerebral endometriosis. Case report," *Journal of Neurosurgery*, vol. 66, no. 4, pp. 609–610, 1987.

[7] M. Nisolle and J. Donnez, "Peritoneal endometriosis, ovarian endometriosis, and adenomyotic nodules of the rectovaginal septum are three different entities," *Fertility and Sterility*, vol. 68, no. 4, pp. 585–596, 1997.

[8] D. I. Lebovic, M. D. Mueller, and R. N. Taylor, "Immunobiology of endometriosis," *Fertility and Sterility*, vol. 75, no. 1, pp. 1–10, 2001.

[9] J. Halme, S. Becker, and M. G. Hammond, "Increased activation of pelvic macrophages in infertile women with mild endometriosis," *American Journal of Obstetrics and Gynecology*, vol. 145, no. 3, pp. 333–337, 1983.

[10] M. D. Mueller, L. Mazzucchelli, C. Buri, D. I. Lebovic, E. Dreher, and R. N. Taylor, "Epithelial neutrophil-activating peptide 78 concentrations are elevated in the peritoneal fluid of women with endometriosis," *Fertility and Sterility*, vol. 79, supplement 1, pp. 815–820, 2003.

[11] N. A. Bersinger, H. Dechaud, B. McKinnon, and M. D. Mueller, "Analysis of cytokines in the peritoneal fluid of endometriosis patients as a function of the menstrual cycle stage using the Bio-Plex platform," *Archives of Physiology and Biochemistry*, vol. 118, no. 4, pp. 210–218, 2012.

[12] N. A. Bersinger, S. von Roten, D. M. Wunder, L. Raio, E. Dreher, and M. D. Mueller, "PAPP-A and osteoprotegerin, together with interleukin-8 and RANTES, are elevated in the peritoneal fluid of women with endometriosis," *American Journal of Obstetrics and Gynecology*, vol. 195, no. 1, pp. 103–108, 2006.

[13] M. A. Bedaiwy, S. A. El-Nashar, R. K. Sharma, and T. Falcone, "Effect of ovarian involvement on peritoneal fluid cytokine concentrations in endometriosis patients," *Reproductive BioMedicine Online*, vol. 14, no. 5, pp. 620–625, 2007.

[14] T. Harada, H. Yoshioka, S. Yoshida et al., "Increased interleukin-6 levels in peritoneal fluid of infertile patients with active endometriosis," *American Journal of Obstetrics and Gynecology*, vol. 176, no. 3, pp. 593–597, 1997.

[15] I. Velasco, P. Acién, A. Campos, M. I. Acién, and E. Ruiz-Maciá, "Interleukin-6 and other soluble factors in peritoneal fluid and endometriomas and their relation to pain and aromatase expression," *Journal of Reproductive Immunology*, vol. 84, no. 2, pp. 199–205, 2010.

[16] S. Galo, P. Žúbor, N. Szunyogh et al., "TNF-α serum levels in women with endometriosis: prospective clinical study," *Ceska Gynekologie*, vol. 70, no. 4, pp. 286–290, 2005.

[17] Z. Cai, Y. He, and D. Peng, "Changes of serum epithelial neutrophil-activating peptide-78 in patients with endometriosis," *Di Yi Jun Yi Da Xue Xue Bao*, vol. 25, no. 4, pp. 464–465, 2005.

[18] M. A. Bedaiwy, T. Falcone, R. K. Sharma et al., "Prediction of endometriosis with serum and peritoneal fluid markers: a prospective controlled trial," *Human Reproduction*, vol. 17, no. 2, pp. 426–431, 2002.

[19] A. Mihalyi, O. Gevaert, C. M. Kyama et al., "Non-invasive diagnosis of endometriosis based on a combined analysis of six plasma biomarkers," *Human Reproduction*, vol. 25, no. 3, pp. 654–664, 2010.

[20] J. Vandesompele, K. De Preter, F. Pattyn et al., "Accurate normalization of real-time quantitative RT-PCR data by geometric averaging of multiple internal control genes," *Genome Biology*, vol. 3, no. 7, Article ID RESEARCH0034, 2002.

[21] J. M. Ruijter, C. Ramakers, W. M. H. Hoogaars et al., "Amplification efficiency: linking baseline and bias in the analysis of quantitative PCR data," *Nucleic Acids Research*, vol. 37, no. 6, article e45, 2009.

[22] D. Hornung, I. P. Ryan, V. A. Chao, J. Vigne, E. D. Schriock, and R. N. Taylor, "Immunolocalization and regulation of the chemokine RANTES in human endometrial and endometriosis tissues and cells," *Journal of Clinical Endocrinology and Metabolism*, vol. 82, no. 5, pp. 1621–1628, 1997.

[23] D. I. Lebovic, V. A. Chao, and R. N. Taylor, "Peritoneal macrophages induce RANTES (regulated on activation, normal T cell expressed and secreted) chemokine gene transcription in endometrial stromal cells," *Journal of Clinical Endocrinology and Metabolism*, vol. 89, no. 3, pp. 1397–1401, 2004.

[24] Y. Yang, X. Zhang, C. Zhou, X. Huang, J. Lin, and H. Xu, "Elevated immunoreactivity of RANTES and CCR1 correlate with the severity of stages and dysmenorrhea in women with deep infiltrating endometriosis," *Acta Histochemica*, vol. 115, no. 5, pp. 434–439, 2013.

[25] M. Nishida, K. Nasu, and H. Narahara, "Role of chemokines in the pathogenesis of endometriosis," *Frontiers in Bioscience*, vol. 3, pp. 1196–1204, 2011.

[26] N. A. Bersinger, F. Frischknecht, R. N. Taylor, and M. D. Mueller, "Basal and cytokine-stimulated production of epithelial neutrophil activating peptide-78 (ENA-78) and interleukin-8 (IL-8) by cultured human endometrial epithelial and stromal cells," *Fertility and Sterility*, vol. 89, supplement, no. 5, pp. 1530–1536, 2008.

[27] N. A. Bersinger, A. R. Günthert, B. McKinnon, S. Johann, and M. D. Mueller, "Dose-response effect of interleukin (IL)-1β, tumour necrosis factor (TNF)-α, and interferon-γ on the in vitro production of epithelial neutrophil activating peptide-78 (ENA-78), IL-8, and IL-6 by human endometrial stromal cells," *Archives of Gynecology and Obstetrics*, vol. 283, no. 6, pp. 1291–1296, 2011.

[28] A. Arici, "Local cytokines in endometrial tissue: the role of interleukin-8 in the pathogenesis of endometriosis," *Annals of the New York Academy of Sciences*, vol. 955, pp. 101–109, 118, 396–406, 2002.

[29] I. P. Ryan, J. F. Tseng, E. D. Schriock, O. Khorram, D. V. Landers, and R. N. Taylor, "Interleukin-8 concentrations are elevated in peritoneal fluid of women with endometriosis," *Fertility and Sterility*, vol. 63, no. 4, pp. 929–932, 1995.

[30] A. Arici, S. I. Tazuke, E. Attar, H. J. Kliman, and D. L. Olive, "Interleukin-8 concentration in peritoneal fluid of patients with endometriosis and modulation of interleukin-8 expression in human mesothelial cells," *Molecular Human Reproduction*, vol. 2, no. 1, pp. 40–45, 1996.

[31] A. Bergqvist, H. Nejaty, B. Fröysa et al., "Production of interleukins 1β, 6 and 8 and tumor necrosis factor alpha in separated and cultured endometrial and endometriotic stromal and epithelial cells," *Gynecologic and Obstetric Investigation*, vol. 50, no. 1, pp. 1–6, 2000.

[32] J. Eisermann, M. J. Gast, J. Pineda, R. R. Odem, and J. L. Collins, "Tumor necrosis factor in peritoneal fluid of women undergoing laparoscopic surgery," *Fertility and Sterility*, vol. 50, no. 4, pp. 573–579, 1988.

[33] B. Scholl, N. A. Bersinger, A. Kuhn, and M. D. Mueller, "Correlation between symptoms of pain and peritoneal fluid inflammatory cytokine concentrations in endometriosis," *Gynecological Endocrinology*, vol. 25, no. 11, pp. 701–706, 2009.

[34] S. Miki, M. Iwano, Y. Miki et al., "Interleukin-6 (IL-6) functions as an in vitro autocrine growth factor in renal cell carcinoma," *FEBS Letters*, vol. 250, no. 2, pp. 607–610, 1989.

[35] B. Motro, A. Itin, L. Sachs, and E. Keshet, "Pattern of interleukin 6 gene expression in vivo suggests a role for this cytokine in angiogenesis," *Proceedings of the National Academy of Sciences of the United States of America*, vol. 87, no. 8, pp. 3092–3096, 1990.

[36] A. Akoum, A. Lemay, I. Paradis, N. Rheault, and R. Maheux, "Secretion of interleukin-6 by human endometriotic cells and regulation by proinflammatory cytokines and sex steroids," *Human Reproduction*, vol. 11, no. 10, pp. 2269–2275, 1996.

[37] A. Rapkin, M. Morgan, C. Bonpane, and O. Martinez-Maza, "Peritoneal fluid interleukin-6 in women with chronic pelvic pain," *Fertility and Sterility*, vol. 74, no. 2, pp. 325–328, 2000.

[38] A. Bergqvist, C. Bruse, M. Carlberg, and K. Carlström, "Interleukin 1β, interleukin-6, and tumor necrosis factor-α in endometriotic tissue and in endometrium," *Fertility and Sterility*, vol. 75, no. 3, pp. 489–495, 2001.

[39] A. Salmassi, Y. Acil, A. G. Schmutzler, K. Koch, W. Jonat, and L. Mettler, "Differential interleukin-6 messenger ribonucleic acid expression and its distribution pattern in eutopic and ectopic endometrium," *Fertility and Sterility*, vol. 89, supplement, no. 5, pp. 1578–1584, 2008.

[40] T. Tsudo, T. Harada, T. Iwabe et al., "Altered gene expression and secretion of interleukin-6 in stromal cells derived from endometriotic tissues," *Fertility and Sterility*, vol. 73, no. 2, pp. 205–211, 2000.

[41] W. Küpker, A. Schultze-Mosgau, and K. Diedrich, "Paracrine changes in the peritoneal environment of women with endometriosis," *Human Reproduction Update*, vol. 4, no. 5, pp. 719–723, 1998.

[42] K. Nirgianakis, N. A. Bersinger, B. McKinnon, P. Kostov, S. Imboden, and M. D. Mueller, "Regression of the inflammatory microenvironment of the peritoneal cavity in women with endometriosis by GnRHa treatment," *European Journal of Obstetrics & Gynecology and Reproductive Biology*, vol. 170, no. 2, pp. 550–554, 2013.

Hindawi Publishing Corporation
Mediators of Inflammation
Volume 2013, Article ID 903948, 13 pages
http://dx.doi.org/10.1155/2013/903948

Research Article

The Role of T Cell Immunoglobulin Mucin Domains 1 and 4 in a Herpes Simplex Virus-Induced Behçet's Disease Mouse Model

Ju A. Shim,[1] Eun-So Lee,[2] Bunsoon Choi,[1] and Seonghyang Sohn[1,3]

[1] *Laboratory of Cell Biology, Ajou University Institute for Medical Sciences, Suwon 443-721, Republic of Korea*
[2] *Department of Dermatology, Ajou University, School of Medicine, Suwon 443-721, Republic of Korea*
[3] *Brain Korea 21 Project for Medical Science, Suwon 443-721, Republic of Korea*

Correspondence should be addressed to Seonghyang Sohn; sohnsh@ajou.ac.kr

Received 31 May 2013; Revised 24 October 2013; Accepted 18 November 2013

Academic Editor: Dennis Daniel Taub

The T cell immunoglobulin mucin (TIM) proteins regulate T cell activation and tolerance. TIM-1 plays an important role in the regulation of immune responses and the development of autoimmune diseases. TIM-4 is a natural ligand of TIM-1, and the interaction of TIM-1 and TIM-4 is involved in the regulation of T helper (Th) cell responses and modulation of the Th1/Th2 cytokine balance. Behçet's disease (BD) is a chronic, multisystemic inflammatory disorder with arthritic, intestinal, mucocutaneous, ocular, vascular, and central nervous system involvement. Tim-1 expression was lower in a herpes simplex virus-induced BD mouse model compared to that in asymptomatic BD normal (BDN) mice. Tim-4 expression was higher in BD mice than that in BDN mice. In this study, we investigated the Tim expression in a BD mouse model with BD-like symptoms. Tim-1 and Tim-4 expression was regulated by an expression vector or siRNA injected into the BD mouse model. The *Tim-1* vector injected into BD mice resulted in changes in BD-like symptoms and decreased the severity score. Treatment with Tim-4 siRNA also improved BD-like symptoms and decreased the severity score accompanied by upregulation of regulatory T cells. We showed that regulating Tim-1 or Tim-4 affected BD-like symptoms in mice.

1. Introduction

The T cell immunoglobulin and mucin domain (TIM) family is located on chromosome 11B1.1 in mice and consists of several members (*Tim*-1–8). In humans it is located on chromosome 5q33.2 and consists of three members (*TIM*-1, 3, and 4) [1]. Individual TIM family members may serve as susceptibility markers for asthma, allergies, and autoimmune diseases, as well as potential cell surface markers for T helper (Th) type 1 and Th2 cells [1, 2]. Therefore, the human *TIM* gene family is critical in the regulation of Th1/Th2 mediated immunological reactions [2].

TIM-1 was first identified as a hepatitis A virus cellular receptor 1 [3, 4] and a kidney injury molecule, KIM-1 [5, 6]. TIM-1 is expressed on $CD4^+$ T cells after activation and its expression is sustained preferentially in Th2 but not Th1 cells [1, 7]. TIM-1 plays an important role regulating immune responses and the development of autoimmune disease. The high-avidity anti-Tim-1 antibody enhances the severity of experimental autoimmune encephalitis by increasing autopathogenic Th1 and Th17 responses, whereas the low-avidity antibody inhibits autopathogenic Th1 and Th17 responses [8].

TIM-4 is a natural ligand of TIM-1 [7] and is exclusively expressed on antigen-presenting cells, including dendritic cells (DCs) and macrophages [9, 10], where it mediates phagocytosis of apoptotic cells and plays an important role maintaining tolerance [11, 12]. TIM-1 and TIM-4 interact to regulate Th cell responses and modulate the Th1/Th2 cytokine balance [7]. DC-derived TIM-4 maintains TIM-1 in Th2 cells in a stable status and plays a critical role sustaining Th2 polarization [13]. TIM-4 binding to TIM-1 has different effects on T cell proliferation. A higher dose of Tim-4-Ig consistently leads to an increase in T cell proliferation upon ligation with the T-cell receptor, whereas a lower concentration of Tim-4-Ig inhibits T cell proliferation [7]. Human TIM-1 is also associated with other types of immune dysfunction, such as atopic dermatitis, allergy, rheumatoid arthritis, asthma, and

systemic lupus erythematosus (SLE) [14–18], suggesting that Tim-1 may regulate immune responses. In addition, TIM-4 expression in peripheral blood mononuclear cells (PBMCs) also increases in patients with SLE [13].

Behçet's Disease (BD) is a Th1-polarized [19], chronic, multisystemic inflammatory disorder with arthritis, gastrointestinal, mucocutaneous, ocular, vascular, and central nervous system involvement. This disease takes a chronic course with periodic exacerbations and progressive deterioration [20]. The etiology of BD is unclear; however, viral infection has long been postulated as one of the main factors. Since Behçet first proposed a viral etiology [21], his hypothesis has been verified by detecting virus in saliva [22], intestinal ulcers [23], and genital ulcers [24, 25] of patients with BD. Subsequently, herpes simplex virus (HSV) inoculation of the earlobes of ICR mice resulted in the development of BD-like symptoms [26]. Manifestations in mice inoculated with HSV include multiple symptoms such as oral ulcers, genital ulcers, skin ulcers, eye symptoms, intestinal ulcers, arthritis, and neural involvement, as well as skin crusting. The frequencies of these symptoms are similar to those of patients with BD [27].

TIM-1 and TIM-4 have not been studied much in BD until now. In this study, we investigated the Tim expression in a BD mouse model with BD-like symptoms. The expression Tim-1 and Tim-4 was analyzed in BD mice and the changes in BD-like symptoms were observed by regulating of Tim-1 or Tim-4 expression. Furthermore, the changes in cellular phenotypes and cytokine levels on immune cells were confirmed after upregulation of Tim-1 or downregulation of Tim-4 in BD mice.

2. Materials and Methods

2.1. Antibodies and Reagents. Mouse anti-CD4, anti-Tim-1, anti-Tim-4, anti-CD8a, anti-CD122, anti-CD11b, anti-CD11c, and anti-CD25 antibodies as well as an anti-Foxp3 staining kit were purchased from eBioscience (San Diego, CA, USA).

2.2. Animal Experiments. ICR male mice (4-5 weeks old) were infected with HSV type 1 (1×10^6 pfu/mL, F strain) grown in Vero cells as described previously [26]. We used anesthetic composed of a mixture of Zoletil (Virbac Lab, Carros, France) and Rompun (Bayer, Seoul, Korea). The ratio of Zoletil and Rompun was 1 : 4, and it was administered at a dose of 40 μL/mouse (tiletamine 10 mg/kg, zolazepam 10 mg/kg, and xylazine hydrochloride 36 mg/kg) via intramuscular injection. Virus inoculation was conducted twice at 10 day intervals, after which the animals were observed for 16 weeks. Animals were handled in accordance with a protocol approved by the animal care committee of Ajou University School of Medicine (Institutional approved number: AMC-102).

2.3. BD-Like Symptoms. Multiple symptoms were observed in the mice after HSV inoculation, and 12% of the HSV-injected mice developed BD-like symptoms. Disappearance of symptoms or a >20% decrease in dimension of lesion size was classified as effective. Determination of the BD severity score was followed by determining the value of the BD activity index, as outlined on the BD activity form (http://www.behcet.ws/pdf/BehcetsDiseaseActivityForm.pdf). Symptoms exhibited by patients, including mouth ulceration, genital ulceration, erythema, skin pustules, skin ulceration, joints-arthritis, diarrhea, blurred or red eye (right, left), reduced vision (right, left), loss of balance, discoloration of skin, and swelling of the face were selected and analyzed in the BD mouse model. The score of each symptom was one, and the total score was used to determine the BD severity score.

2.4. Tim-1 DNA Constructs. A *Tim-1* construct with an extracellular Flag epitope tag was generated [28]. A cDNA clone containing the entire coding sequence of murine *Tim-1* was constructed. Briefly, the *Tim-1* open reading frame (excluding the start codon and signal sequence) was amplified from this clone by polymerase chain reaction and ligated into a pCDEF3 expression plasmid [29]. All DNA constructs were verified by automated DNA sequencing. All plasmids used were purified by two passes through Endo-Free columns (Qiagen, Chatsworth, CA, USA) as described previously [30].

2.5. Preparation of Tim-4 Small Interfering RNA (siRNA). Tim-4 siRNA (siTim-4) was synthesized by Genolution Pharmaceuticals, Inc. (Seoul, Korea). The synthesized sequences of Tim-4 siRNA were sense: 5′- CUA AAU CAC AUC AGA UCA ACA GCA GUU -3′, and antisense: 5′- CUG CUG UUG AUC UGA UGU GAU UUA GUU -3′. The Tim-4 siRNA with transfection reagent jetPEI (PolyPlus-transfection, Llkirch, France) was used to inject into mice.

2.6. Tim-1 Vector and Tim-4 siRNA Administration of BD Mice. Ten μg of *Tim-1* vector was intraperitoneally injected four times at 2 day intervals into BD mice when the BD-like symptoms appeared, followed by 2 weeks of observations. The control was injected with the pCDEF3 empty vector. Five μg of siRNA Tim-4 was intraperitoneally injected three times at 2 day intervals into BD mice to downregulate Tim-4, followed by a 2-week observation. Scrambled siRNA was used as the negative control (Genolution Pharmaceuticals, Inc., Seoul, Korea).

2.7. Flow Cytometry. PBMCs and lymph node cells were isolated from mice and erythrocytes were removed from cell suspensions in ACK solution, then washed with phosphate buffered saline (PBS). The cells were surface-stained with anti-mouse antibodies (CD4, CD8, CD11b, CD11c, CD25, CD122, Tim-1, and Tim-4) for 30 min at 4°C in the dark. An anti-mouse Foxp3-staining buffer set was used according to the manufacturer's instructions to detect Foxp3 intracellularly. Briefly, cells were fixed using Fix/perm buffer after washing with 1x permeabilization buffer and then incubated with anti-mouse Foxp3 antibody. For analysis, the cells were gated and then the population of stained cells was analyzed by a flow cytometer (FACS Canto II; Becton Dickinson, Franklin Lakes, NJ, USA) with ≥10,000 gated lymphocytes.

2.8. Enzyme Linked Immunosorbent Assay (ELISA). Serum was collected 14 days after the first administration of the *Tim-1* vector and Tim-4 siRNA into BD mice. Serum was analyzed using commercial ELISA kits for the detecting mouse interleukin (IL)-6 (R&D Systems, Minneapolis, MN), tumor necrosis factor (TNF)-α (R&D Systems), IL-17 (R&D Systems), IL-4 (R&D System), and interferon (IFN)-γ (R&D Systems), according to the manufacturer's instructions. The ELISA reader was Bio-Rad model 170–6850 microplate reader, and samples were read at a wavelength of 450 nm.

2.9. Statistical Analysis. All data are expressed as mean ± standard deviation. Statistical differences between the experimental groups were determined using Student's *t*-test with a Bonferroni correction. Statistical analysis was conducted using MedCalc version 9.3.0.0. A $P < 0.05$ was considered significant.

3. Results

3.1. The Frequencies of Tim-1 and Tim-4 Expressing Cells in Normal Healthy, BD Normal (BDN), and BD Mice. The frequencies of Tim-1$^+$, CD4$^+$Tim-1$^+$, and CD8$^+$Tim-1$^+$ cells were analyzed in cells from lymph nodes (LN), spleen (SP), and PBMCs of normal healthy (Nor) and BDN (HSV-1 was inoculated but no symptoms) mice and compared with those in BD mice by FACS. In LN, the frequencies of Tim-1$^+$, CD4$^+$Tim-1$^+$, and CD8$^+$Tim-1$^+$ cells in BD mice were significantly lower than those in BDN mice (BDN versus BD (%): Tim-1$^+$, 20.1 ± 11.5 (n = 12) versus 11.1 ± 6.7 (n = 12), P = 0.01; CD4$^+$Tim-1$^+$, 3.4 ± 1.9 (n = 9) versus 2.2 ± 1.6 (n = 9), P = 0.09; CD8$^+$Tim-1$^+$, 1.9 ± 1.1 (n = 9) versus 1.1 ± 0.6 (n = 9), P = 0.04) (Figure 1(a)). In SP, the BD mice showed significantly lower frequencies than Nor or BDN mice (Nor versus BDN versus BD (%): Tim-1$^+$, 21.3±6.5 (n = 6) versus 18.3 ± 8.5 (n = 10) versus 12.2 ± 5.9 (n = 10), Nor versus BD P = 0.006, BDN versus BD P = 0.04; CD4$^+$Tim-1$^+$, 3.1 ± 1.6 (n = 6) versus 1.9 ± 1.0 (n = 8) versus 1.7 ± 0.5 (n = 8), Nor versus BD P = 0.02, BDN versus BD P = 0.35). CD8$^+$Tim-1$^+$ cells showed similar frequencies among three groups (Figure 1(b)). In PBMCs, the frequencies of BD mice were slightly lower than those of BDN, but not significantly (BDN (n = 9) versus BD (n = 9) (%): Tim-1$^+$, 27.6 ± 17.1 versus 23.6 ± 8.4, P = 0.54; CD4$^+$Tim-1$^+$, 8.3 ± 5.9 versus 5.7 ± 4.4, P = 0.31; CD8$^+$Tim-1$^+$, 7.6 ± 5.0 versus 5.2 ± 4.3, P = 0.29). BD mice had significantly higher levels than those of Nor mice (Figure 1(c)). These data indicate that the frequencies of Tim-1 expressing cells in BD mice were downregulated compared to those in BDN mice.

The frequencies of Tim-4$^+$ cells were also analyzed in LN, SP, and PBMCs of Nor, BDN, and BD mice. In LN, the frequencies of Tim-4$^+$ cells in BD mice were significantly higher than those in Nor and BDN mice (Nor versus BDN, versus BD (%): 1.3 ± 0.8 (n = 11) versus 3.2 ± 0.9 (n = 15) versus 5.8 ± 2.0 (n = 15), Nor versus BDN P = 0.000005, Nor versus BD, P = 0.0000001, BDN versus BD P = 0.00003) (Figure 2(a)). In SP, the frequencies of Tim-4$^+$ cells in BD mice were also significantly higher than those in Nor mice (Nor versus BD (%): 3.9 ± 2.8 (n = 11) versus 6.7 ± 4.3 (n = 17), P = 0.035). However, the difference between BDN and BD mice was not significant (Figure 2(b)). In PBMCs, the frequencies of Tim-4$^+$ cells in BD mice were higher than those in Nor mice (Figure 2(c)). Moreover, in peritoneal macrophages, the frequencies of Tim-4$^+$ cells in BD mice were significantly higher than those in Nor and BDN mice (Nor versus BDN versus BD (%): 6.1 ± 2.0 (n = 5) versus 8.6 ± 4.0 (n = 9) versus 26.6 ± 17.0 (n = 5), Nor versus BDN, P = 0.11, Nor versus BD, P = 0.02, BDN versus BD, P = 0.005). No differences between Nor and BDN mice were observed (Figure 2(d)). In addition, we also examined the frequencies of CD11b$^+$Tim-4$^+$ and CD11c$^+$Tim-4$^+$ cells in LN and SP. In LN, both markers in BD mice were higher than those in Nor and BDN mice (Nor (n = 5) versus BDN (n = 6) versus BD (n = 5) (%): CD11b$^+$Tim-4$^+$, 1.1±0.3 versus 1.7 ± 0.7 versus 3.0 ± 1.4, Nor versus BDN, P = 0.05, Nor versus BD, P = 0.01, BDN versus BD, P = 0.04; CD11c$^+$Tim-4$^+$, 0.1 ± 0.0 versus 0.5 ± 0.1 versus 0.7 ± 0.5, nor versus BDN, P = 0.00003, Nor versus BD, P = 0.01, BDN versus BD, P = 0.14) (Figure 2(e)). In splenocytes, expression of CD11c$^+$Tim-4$^+$ cells was similar to that in LN in Nor (0.3 ± 0.1%, n = 5), BDN (0.6±0.4%, n = 6) and BD mice (1.0±0.6%, n = 8) (Nor versus BDN, P = 0.07, Nor versus BD, P = 0.07, BDN versus BD, P = 0.1). In contrast, the frequencies of CD11b$^+$Tim-4$^+$ cells in BD mice were significantly lower than those in Nor, but higher than those in BDN mice (Figure 2(f)). These data suggest that the frequencies of Tim-4 expressing cells in BD mice were upregulated compared to those in BDN mice.

3.2. Administration of the Tim-1 Vector Upregulates the Frequencies of Tim-1$^+$ Cells In In Vivo LN. We investigated the change in BD-like symptoms according to the regulation of Tim-1 expression. The *Tim-1* expression vector was administered to BD mice to upregulate Tim-1 expression. The *Tim-1* vector was injected intraperitoneally at 10, 30, and 50 μg/mouse into Nor mice twice at 2 day intervals. The frequencies of Tim-1$^+$ cells from LN were compared to those of the control vector injected group the day after the last injection. The expression of Tim-1$^+$ cells in the 10 μg *Tim-1* vector injected group (19.1 ± 5.1%, n = 4) was significantly higher than that in the control vector injected group (10 μg: 9.4±2.6%, n = 4, P = 0.01; 50 μg: 10.4±5.4%, n = 4, P = 0.06) (Figure 3). However, the 30 (n = 3) and 50 μg (n = 4) *Tim-1* vector injected groups showed lower expression than that in the 10 μg injected group. Thus, 10 μg of the *Tim-1* vector was used for subsequent experiments.

3.3. Administration of Tim-1 Vector Affected BD-Like Symptoms. Ten μg of *Tim-1* vector was injected intraperitoneally into BD mice four times at 2 day intervals, followed by observations for 2 weeks. Skin and genital ulcers improved after administering the *Tim-1* vector when compared to those in the control vector-injected group (Figure 4(a)). Additionally, the severity score was 2.83 ± 0.41 before and 2.83 ± 0.75 at 1 week in the control vector group and 2.67 ± 1.21 at 2 weeks after the first injection of control vector (n = 6). The severity score in the *Tim-1* vector group was 3.17 ± 0.75 before

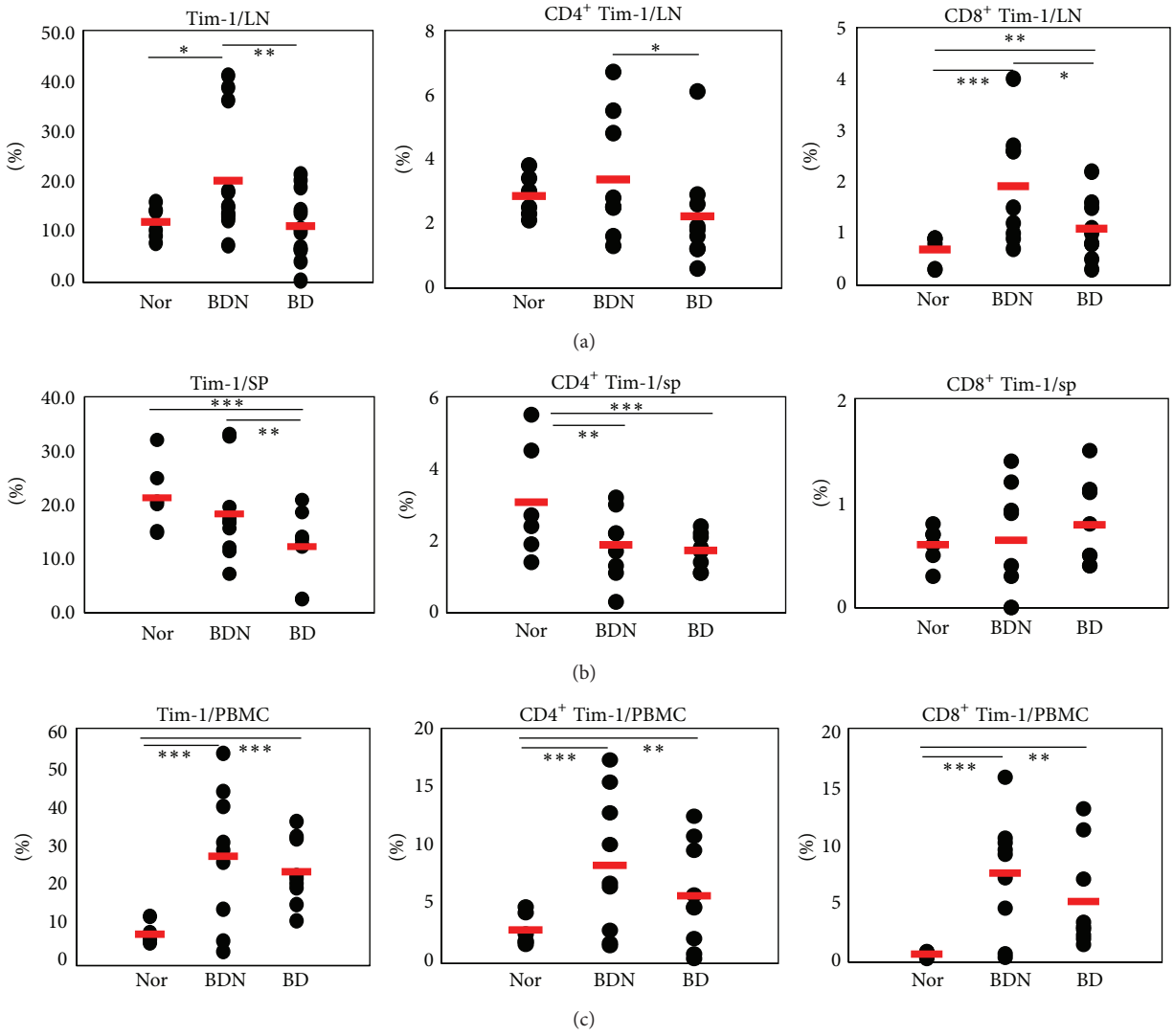

FIGURE 1: The frequencies of Tim-1$^+$ cell phenotypes in normal healthy, Behçet's disease (BD) normal (BDN), and BD mice. The frequencies of Tim-1$^+$, CD4$^+$Tim-1$^+$ and CD8$^+$Tim-1$^+$, cells in BD mice were compared to Nor and BDN mice by FACS analysis in (a) lymph nodes, (b) spleen, and (c) peripheral blood mononuclear cells (PBMCs) (n = 6–12) ($^*P < 0.1$, $^{**}P < 0.05$, $^{***}P < 0.01$). Nor: normal healthy mice, BDN: BD normal mice.

injection, 1.50 ± 1.22 at 1 week after injection ($P = 0.004$), and 1.33 ± 1.51 at 2 weeks after injection in BD mice ($P = 0.03$, n = 6) (Figure 4(b)). The severity score decreased after injecting the *Tim-1* vector, whereas the control vector injection did not result in a difference.

Two weeks after the first administration of the *Tim-1* vector to BD mice, isolated LN and PBMCs were analyzed for Tim-1$^+$ cells by FACS. In LN, the frequencies of Tim-1$^+$ cells in *Tim-1* vector injected group were slightly higher compared to those in the control vector injected group (Con versus Tim-1 (%): 10.3 ± 1.7 (n = 4) versus 11.9 ± 3.2 (n = 5), P = 0.19). However, CD4$^+$Tim-1$^+$ and CD8$^+$Tim-1$^+$ cells were similar to those in the control vector injected group (Figure 4(c)). The frequencies of Tim-4$^+$ cells were also not different (Figure 4(d)). In PBMCs, Tim-1$^+$ cells were slightly lower in the *Tim-1* vector injected group, but CD4$^+$Tim-1$^+$, CD8$^+$Tim-1$^+$, and Tim-4$^+$ cells were not different (Figures 4(c)-4(d)). Interestingly, CD4$^+$ T cells in the Tim-1 vector injected group were slightly higher than those in the control vector injected group (Con versus Tim-1 (%): 21.3 ± 10.7 (n = 8) versus 27.6 ± 13.7 (n = 8), P = 0.36) (Figure 4(c)).

3.4. Tim-1 Vector Administration Affects the Regulatory Cellular Phenotypes. Several cellular phenotypes in the LN and PBMCs were analyzed in BD mice after administering the *Tim-1* vector. The frequencies of CD4$^+$CD25$^+$, CD4$^+$Foxp3$^+$, and CD4$^+$CD25$^+$Foxp3$^+$ (regulatory T, Treg) cells in LN were not significantly changed in the *Tim-1* vector compared to those in the control vector injected group (Con (n = 5) versus Tim-1 (n = 6) (%): CD4$^+$CD25$^+$, 6.5 ± 1.6 versus 6.1 ± 2.3, P = 0.35; CD4$^+$Foxp3$^+$, 5.3 ± 1.5 versus 4.7 ± 1.7, P = 0.29; Treg, 5.2 ± 1.4 versus 4.7 ± 1.7, P = 0.3) (Figure 5(a)). But,

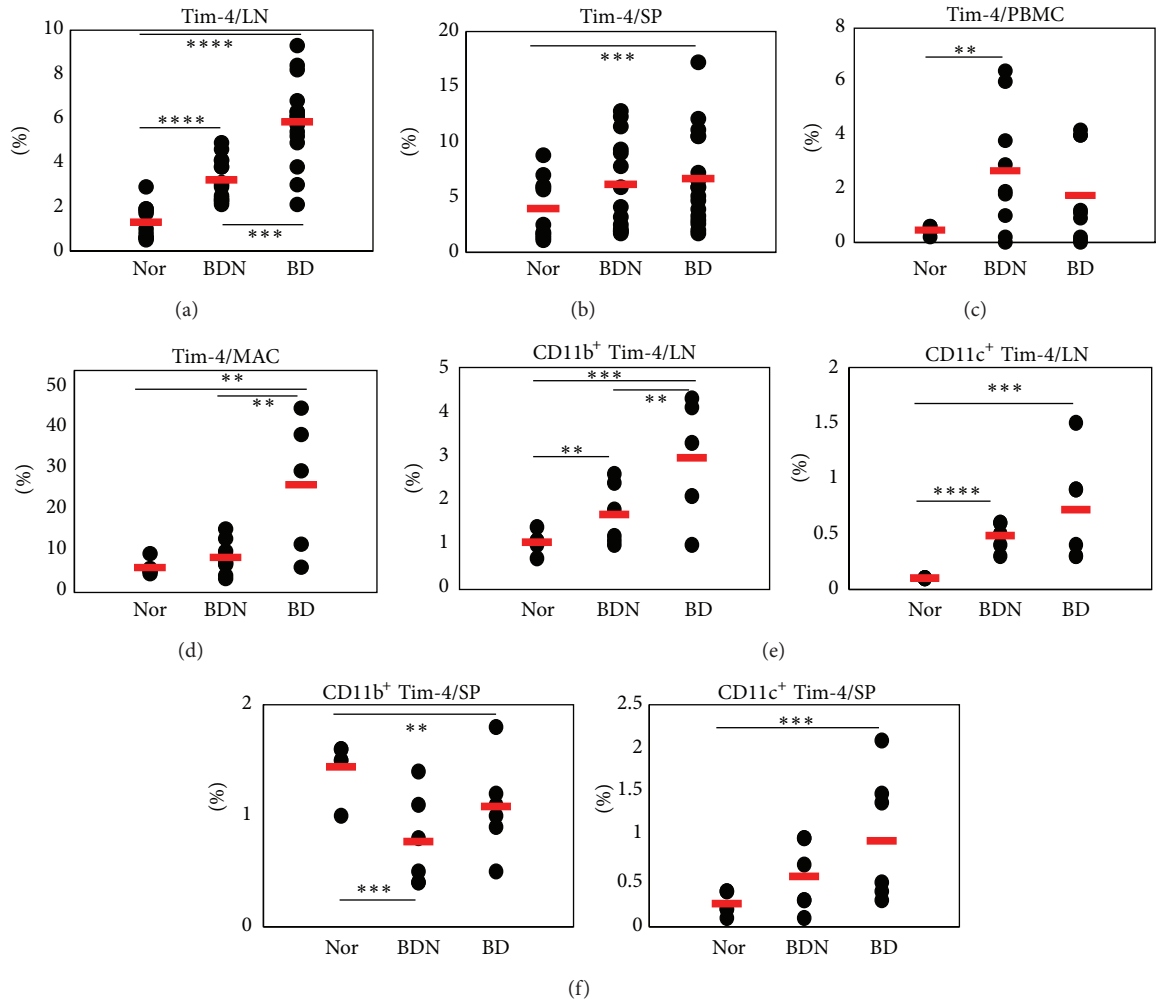

FIGURE 2: The frequencies of Tim-4$^+$ cell phenotypes in normal healthy, BDN and Behçet's disease (BD) mice. The frequencies of Tim-4$^+$ cells in BD mice were compared to Nor and BDN mice by FACS analysis in (a) lymph nodes, (b) spleen, (c) PBMCs, and (d) peritoneal macrophages. The expression of CD11b$^+$Tim-4$^+$ and CD11c$^+$Tim-4$^+$ cells in BD mice were also compared to those in Nor and BDN mice in (e) lymph nodes and (f) spleen ($n = 5$–17) ($^{**}P < 0.05$, $^{***}P < 0.01$, $^{****}P < 0.001$) Nor: normal healthy mice, BDN: BD normal mice.

in PBMCs, CD4$^+$CD25$^+$, CD4$^+$Foxp3$^+$, and Treg cells in the *Tim-1* vector injected group were significantly higher than those in the control vector injected group (Con ($n = 8$) versus Tim-1 ($n = 8$) (%): CD4$^+$CD25$^+$, 0.31±0.18 versus 0.61±0.21, $P = 0.01$; CD4$^+$Foxp3$^+$, 0.10 ± 0.10 versus 0.31 ± 0.12, $P = 0.004$; Treg, 0.04 ± 0.08 versus 0.16 ± 0.10, $P = 0.03$) (Figure 5(a)).

CD8$^+$CD122$^+$ T cells are newly identified, regarded as Treg cells [31], and are involved in anti-inflammatory responses [32]. Another type of Treg cells, CD8$^+$CD122$^+$ T cells, were also analyzed in LN of the *Tim-1* vector injected group (Con ($n = 5$) versus Tim-1 ($n = 6$) (%): 1.3 ± 0.3 versus 1.6 ± 0.7, $P = 0.25$) (Figure 5(b)). In PBMCs, CD122$^+$ and CD8$^+$CD122$^+$ T cells in the *Tim-1* vector injected group were also higher than those in the control vector injected group (Con ($n = 8$) versus Tim-1 ($n = 8$) (%): CD122$^+$, 1.2 ± 1.0 versus 9.8 ± 7.9, $P = 0.04$; CD8$^+$CD122$^+$, 1.9 ± 1.5 versus 2.4 ± 2.1, $P = 0.58$).

Our study indicated that the *Tim-1* vector upregulated Treg cells and CD122$^+$ cells in BD mice. Up-regulation of these cellular phenotypes may be involved in improved BD-like symptoms after injection of the Tim-1 vector.

3.5. Proinflammatory Cytokines are Downregulated by Tim-1 Vector Administration in BD Mice. Sera were analyzed by ELISA at 2 weeks after *Tim-1* vector administration into BD mice to determine the levels of cytokines. The IL-17 level in *Tim-1* vector injected group was significantly lower than that in the control group (Con ($n = 7$) versus Tim-1 ($n = 7$) (pg/mL): 11.53 ± 4.45 versus 6.84 ± 2.17, $P = 0.03$). TNF-α also decreased significantly in the *Tim-1* vector injected group compared to that in the control group (Con ($n = 11$) versus Tim-1 ($n = 11$) (pg/mL): 16.5±13.8 versus 6.9±5.1, $P = 0.04$). The IL-6 level in the *Tim-1* vector injected group decreased (Con ($n = 8$) versus Tim-1 ($n = 8$) (pg/mL): 145.7 ± 176.9 versus 72.2 ± 38.8, $P = 0.27$). In contrast, IL-4 increased

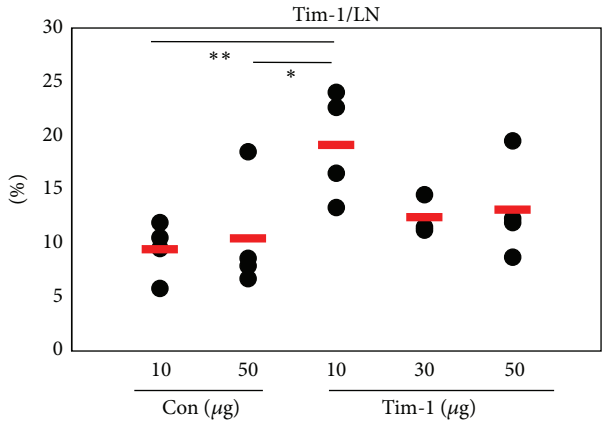

FIGURE 3: Administration of *Tim-1* vector increased the frequencies of Tim-1$^+$ cells. The *Tim-1* vector was injected intraperitoneally at 10, 30, and 50 μg/mouse into Nor mice twice at 2 day intervals to observe up-regulation of Tim-1 expression. The day of the last injection, the frequencies of Tim-1$^+$ cells in LN were compared to the control vector injected group by FACS analysis. The control was injected with the pCDEF3 empty vector (10 or 50 μg/mouse) (n = 3-4) ($^{**}P < 0.05$). Con: control vector injection to normal (Nor) mice, Tim-1: *Tim-1* vector injection to Nor mice.

slightly in the *Tim-1* vector injected group (Con (n = 8) versus Tim-1 (n = 9) (pg/mL): 9.3 ± 5.4 versus 10.8 ± 5.0, P = 0.53). But, IFN-γ levels did not differ between the *Tim-1* and control vector injected group (Figure 6). Consequently, these results indicate that the *Tim-1* vector might downregulate proinflammatory cytokines in BD mice.

3.6. Tim-4 siRNA Treatment Downregulated the Expression of Tim-4 in Normal Healthy Mice. In BD mice, the frequencies of Tim-4$^+$ cells were higher than those in Nor and BDN mice in LN cells and peritoneal macrophages (Figure 2). siTim-4 was injected into Nor mice intraperitoneally to downregulate Tim-4$^+$ cells, and the frequencies of Tim-4$^+$ cells were analyzed in peritoneal macrophages by FACS. Tim-4 siRNA (siTim-4) at 2, 5, or 10 μg/mouse or negative control (NC) scrambled siRNA (2 and 5 μg/mouse) was injected (NC: 5 μg versus siTim-4–2, 5, and 10 μg (n = 4): 8.9 ± 1.4% versus 6.6 ± 3.4% (P = 0.42), 3.7±0.9% (P = 0.013), 2.8±2.2% (P = 0.04)) (Figure 7(a)). siTim-4 downregulated Tim-4$^+$ macrophages dose dependently and showed a significant difference in the 5 μg and 10 μg administered groups. Therefore, 5 μg injections were used for the following experiment. To determine the time-dependent efficacy of Tim-4 siRNA, 5 μg of siTim-4 was injected, and the frequencies of Tim-4$^+$ macrophages were analyzed by FACS after 24, 48, and 72 hours. siTim-4 significantly downregulated Tim-4$^+$ macrophages until 72 hours compared to that of NC. The frequencies of Tim-4$^+$ at 48 hours were lowest (NC versus siTim-4 (n = 2): 24 h, 7.9 ± 0.6% versus 4.9 ± 0.2%, P = 0.02; 48 h, 8.9 ± 1.4% versus 2.9 ± 0.4%, P = 0.03; 72 h, 15.4 ± 0.1% versus 4.2 ± 3.0%, P = 0.03) (Figure 7(b)).

3.7. Administration of siTim-4 Changes BD-Like Symptoms. Five μg of siTim-4 was injected intraperitoneally three times at 2 day intervals into BD mice and the mice were observed for 2 weeks (Figure 8(a)). After administration of siTim-4, BD-like symptoms, such as skin and genital ulcers, were compared to the control group. In the negative control group, the severity score was 2.25 ± 0.46 before, 2.00 ± 1.07 at one week (P = 0.35), and 1.88 ± 1.13 at 2 weeks after the first injection of BD mice (P = 0.28, n = 8). In the siTim-4 treated group, the score was 2.63 ± 0.52 before, 1.25 ± 0.81 at 1 week (P = 0.001), and 1.25 ± 0.89 at 2 weeks after injection into BD mice (P = 0.001, n = 8) (Figure 8(b)). At 1 and 2 weeks after the first administration of siTim-4 to BD mice, macrophages were isolated from the peritoneal cavity and analyzed for Tim-4 by FACS. The frequencies of Tim-4$^+$ cells at 1 and 2 weeks after siTim-4 treatment tended to be lower than those in the negative control group, but the difference was not significant (1 week: 18.6 ± 4.8% versus 15.7 ± 3.7%, P = 0.31, 2 weeks: 20.7 ± 6.5% versus 18.8 ± 3.3%, P = 0.42) (Figure 8(b)). However, in LN, Tim-4$^+$, CD11b$^+$Tim-4$^+$, CD11c$^+$Tim-4$^+$, Tim-1$^+$, CD4$^+$Tim-1$^+$, and CD8$^+$Tim-1$^+$ cells in the siTim-4 treated group were similar to those in the control treated group at 1 week after the first siTim-4 injection (Figures 8(c)-8(d)). Even at 2 weeks after the first injection, those markers were not different (data not shown). In these results, BD-like symptoms improved with siTim-4 treatment and decreased the severity score.

3.8. Treg Cells are Upregulated in siTim-4 Treated BD Mice. The frequencies of CD4$^+$CD25$^+$, CD4$^+$Foxp3$^+$, and Treg (CD4$^+$CD25$^+$ Foxp3$^+$) cells were analyzed by FACS at 1 and 2 weeks after the first treatment with siTim-4 in BD mice (Figure 9). After 1 week, Treg cells increased slightly in siTim-4 treated BD mice compared with those in the NC treated group (NC versus siTim-4: CD4$^+$CD25$^+$, 5.82 ± 2.01% versus 6.84 ± 2.03%, P = 0.45, n = 5; CD4$^+$Foxp3$^+$, 4.64 ± 1.9% versus 5.82 ± 2.4%, P = 0.41, n = 5; Treg, 3.28 ± 1.57% versus 4.08 ± 1.73%, P = 0.47, n = 5). After 2 weeks, Treg cells were significantly higher in siTim-4 treated BD mice than those in the NC treated group (NC versus siTim-4: CD4$^+$CD25$^+$, 4.8 ± 0.6% versus 5.9 ± 1.2%, P = 0.03, n = 6; CD4$^+$Foxp3$^+$, 4.1 ± 0.7% versus 5.2 ± 1.2%, P = 0.03, n = 7; Treg, 2.7 ± 0.5% versus 3.5 ± 0.9%, P = 0.04, n = 7). These results suggest that the increased number of Treg cells is associated with knock down of Tim-4 in BD mice.

3.9. Treatment with siTim-4 Decreases Serum Levels of IL-17 in BD Mice. After administering siTim-4 to BD mice, the serum level of IL-17 was analyzed by ELISA and compared with NC siRNA treated BD mice. The level of IL-17 tended to decrease in the siTim-4 treated group compared to that in the NC treated group, but the difference was not significant (NC versus siTim-4 (n = 8): 19.4 ± 11.5 pg/mL versus 15.6 ± 8.1 pg/mL, P = 0.25) (Figure 10).

4. Discussion

BD mice downregulated Tim-1 levels and upregulated Tim-4 levels in LN, SP, PBMCs, and peritoneal macrophages compared to those in BDN mice. Administration of the

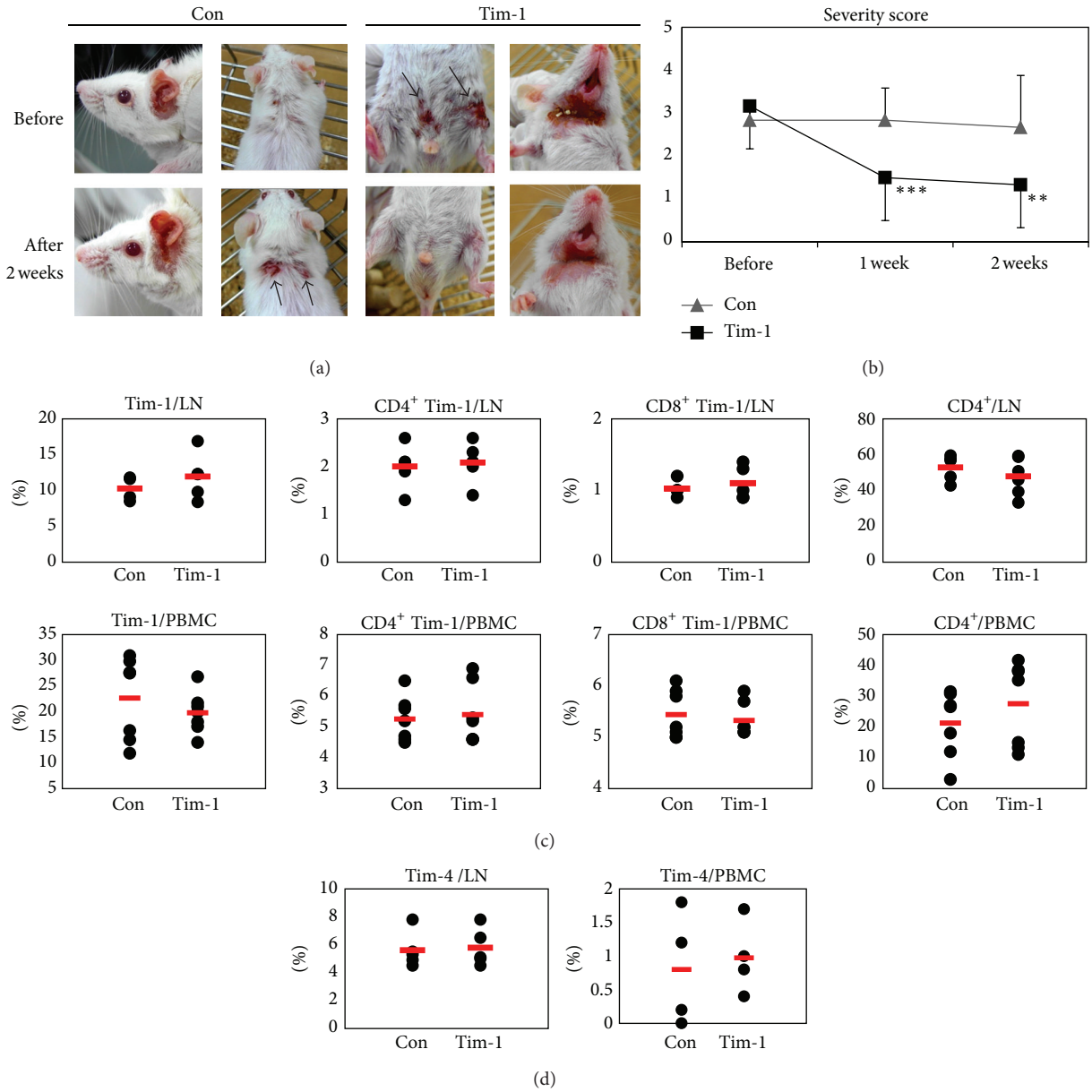

FIGURE 4: Administration of Tim-1 improved the Behçet's disease (BD)-like symptoms, but the frequencies of Tim-1 expressing cells remained unchanged. Ten μg/mouse of *Tim-1* vector was injected intraperitoneally four times at 2 day intervals into BD mice, followed by 2 weeks of observations. (a) Photographs of mice were taken before and at 1 and 2 weeks after the first treatment of the *Tim-1* vector and control vector injected groups. (b) Severity scores were compared before and at 1 and 2 weeks after treatment. (c) Two weeks after first *Tim-1* vector injection, the frequencies of Tim-1$^+$, CD4$^+$Tim-1$^+$, CD8$^+$Tim-1$^+$, CD4$^+$ T cells, and (d) Tim-4$^+$ cells in LN and PBMCs were evaluated by FACS analysis (n = 5-6) ($^*P < 0.1$). Con: control vector injection to BD mice, Tim-1: *Tim-1* vector injection to BD mice.

Tim-1 vector upregulated the frequencies of Tim-1$^+$ cells, and Tim-4 siRNA downregulated the frequencies of Tim-4$^+$ cells. Administering the *Tim-1* vector improved BD-like symptoms, such as genital and skin ulcers, and decreased the severity score. TIM-1 expression is lower in patients with active SLE compared to that in inactive patients [18]. Human TIM-1 is associated with immune dysfunction, such as atopic dermatitis, allergy, rheumatoid arthritis, asthma, and SLE [14–18]. Our data indicate that the Tim-1 related T cells phenotype did not change much after administering the *Tim-1* vector. Interestingly, the frequencies of CD4$^+$ T cells in PBMCs increased in the *Tim-1* vector injected group compared to those in the control vector injected group. Actually, TIM-1 is expressed on CD4$^+$ T cells after activation and its expression is preferentially sustained on Th2 but not Th1 cells [1, 7]. Xiao et al. reported that Tim-1-Fc triggers a significant increase in the frequencies of CD4$^+$ T cells [33]. In our study, Treg cells were upregulated in the

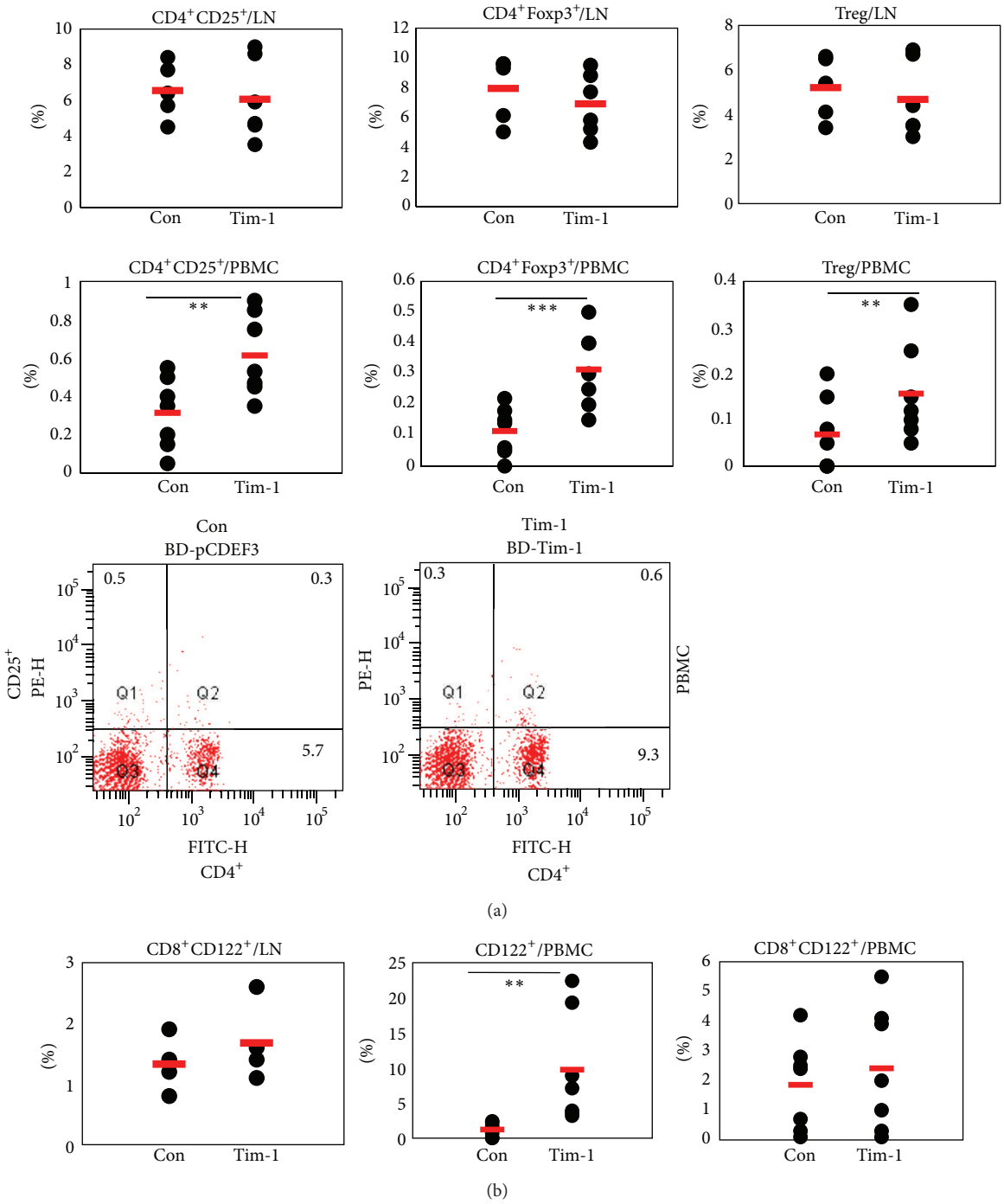

FIGURE 5: The frequencies of Treg cells in PBMCs were affected in *Tim-1* vector injected Behçet's disease (BD) mice. Two types of Treg cells were confirmed in LN and PBMCs after *Tim-1* administration to BD mice. (a) The frequencies of $CD4^+CD25^+$, $CD4^+Foxp3^+$, and Treg cells were compared between the control and *Tim-1* vector injected groups. Bottom panel shows $CD4^+CD25^+$ in PBMCs by FACS. (b) $CD8^+CD122^+$ T cells tended to be upregulated compared to those in the control group, but the difference was not significant. $CD122^+$ cells increased significantly in the *Tim-1* vector injected group ($n = 5$–8) ($^{**}P < 0.05$, $^{***}P < 0.01$). Con: control vector injection to BD mice, Tim-1: *Tim-1* vector injection to BD mice.

Tim-1 vector injected BD group. Other Treg cells, $CD8^+CD122^+$ T cells, were also higher in PBMCs and LN of the *Tim-1* vector injected group compared to those in the control group. $CD8^+CD122^+$ T cells are newly identified and regarded as Treg cells [31] and have an effect on anti-inflammatory responses [32]. Our results suggest that the function of Tim-1 influenced the BD-like symptoms and is associated with Treg and $CD8^+CD122^+$ T cells.

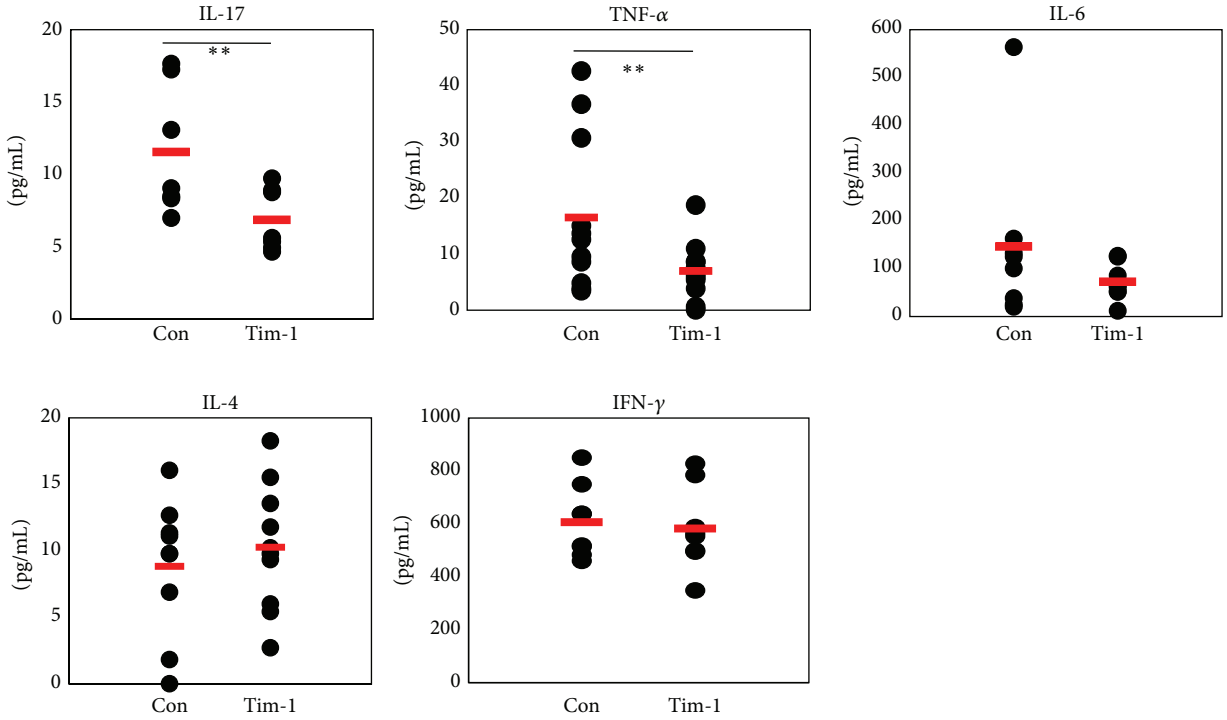

Figure 6: Administration of the *Tim-1* vector decreased proinflammatory cytokines in Behçet's disease (BD) mice. Serum was isolated from blood at 2 weeks after the first injection of the *Tim-1* vector. The levels of interleukin (IL)-17, tumor necrosis factor (TNF)-α, IL-6, interferon (IFN)-γ, and IL-4 were analyzed in the sera of *Tim-1* and control vector injected BD mice by ELISA ($n = 7$~11) ($^{**}P < 0.05$). Con: control vector injection to BD mice, Tim-1: *Tim-1* vector injection to BD mice.

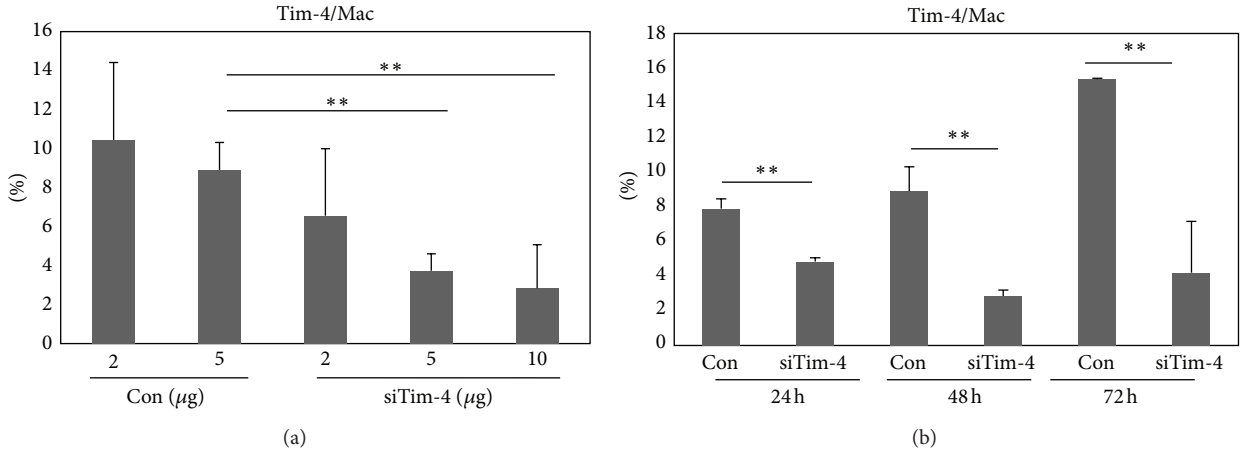

Figure 7: The expression of Tim-4$^+$ cells was downregulated after siTim-4 treatment. Tim-4 siRNA was administered intraperitoneally and the frequencies of Tim-4$^+$ cells were analyzed in peritoneal macrophages in normal (Nor) mice by FACS. (a) siTim-4 2, 5, and 10 μg/mouse or negative control siRNA (Con) (2 and 5 μg/mouse) were injected intraperitoneally into Nor mice. (b) Five μg of siTim-4 was injected, and the frequencies of Tim-4$^+$ peritoneal macrophages were analyzed 24, 48, and 72 hours later. Scrambled siRNA was used as the negative control ($n = 3$-4) ($^{**}P < 0.05$). Con: control siRNA injection into normal mice, siTim-4: Tim-4 siRNA injection to normal mice, Mac: peritoneal macrophage.

Recent studies suggest that IL-17 may play a dominant role in provoking chronic autoimmune inflammation and is considered essential for T cell-mediated colitis and promotion of inflammation [34–36]. The association of IL-17 and IL-22 was also reported in patients with BD [37, 38]. TNF-α overexpression has been implicated in acute and chronic inflammatory diseases, such as septic shock, bowel disease, Crohn's disease, rheumatoid arthritis, atopic dermatitis, psoriasis, and BD [39]. Overproduction of IL-6 plays a role in rheumatoid arthritis, juvenile idiopathic

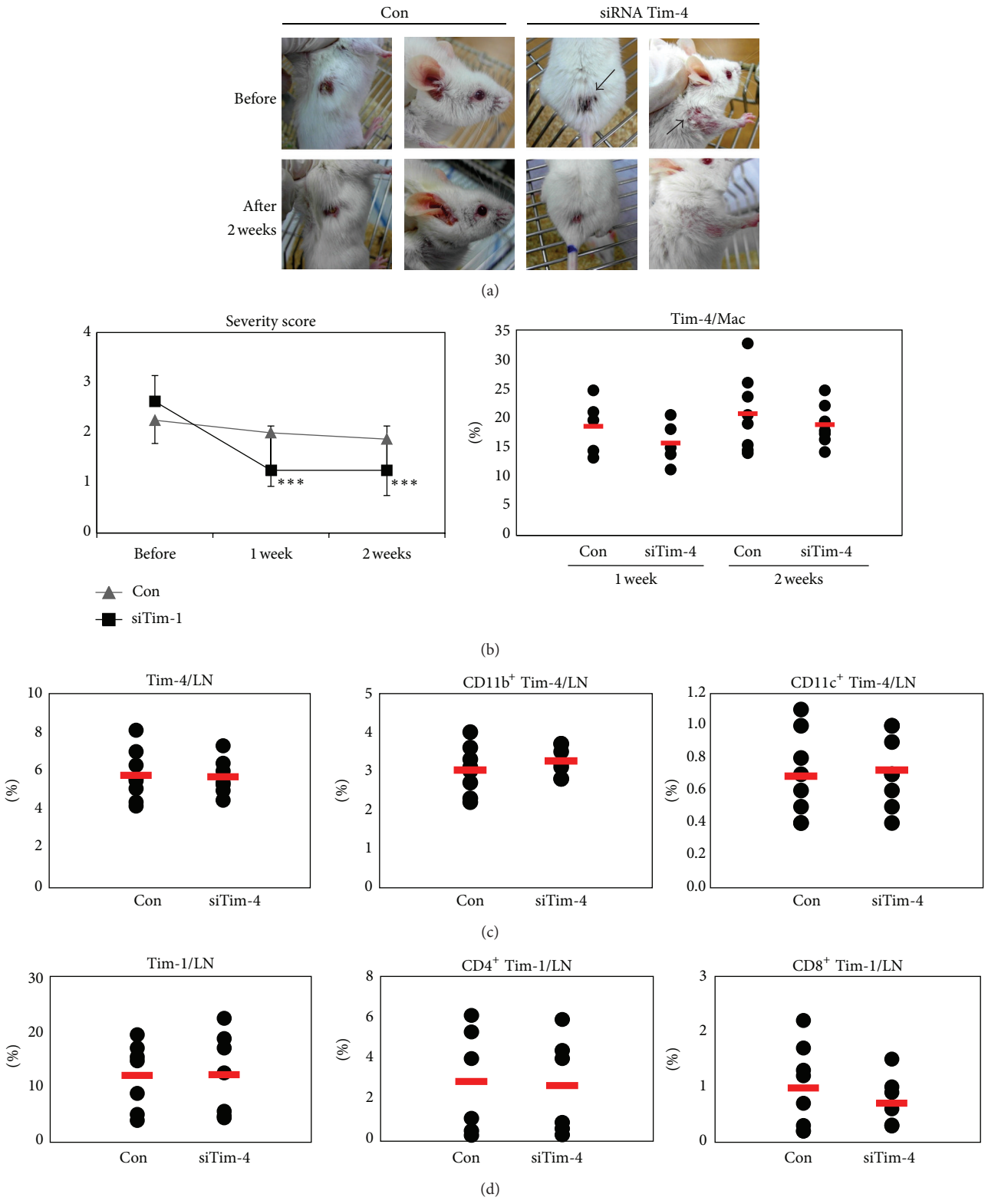

FIGURE 8: Behçet's disease (BD)-like symptoms were changed after siTim-4 administration. Five μg/mouse of Tim-4 siRNA was injected intraperitoneally three times at 2 day intervals into BD mice and they were observed for 2 weeks. (a) Photographs of mice taken before and at 1 and 2 weeks after treatment with siTim-4 and the control treated group (Con: negative control siRNA treated groups). (b) The severity score was compared before and at 1 and 2 weeks after treatment between the siTim-4 and control treated groups. The frequencies of Tim-4$^+$ cells in peritoneal cavity were compared between the siTim-4 and control treated groups. (c, d) The frequencies of Tim-4$^+$, CD11b$^+$Tim-4$^+$, CD11c$^+$Tim-4$^+$, Tim-1$^+$, CD4$^+$Tim-1$^+$, and CD8$^+$Tim-1$^+$ cells in LN were compared to the siTim-4 and control treated groups (n = 7-8) ($^{**}P < 0.05$). Con: negative control injection to BD mice, siTim-4: Tim-4 siRNA injection to BD mice, LN: lymph node.

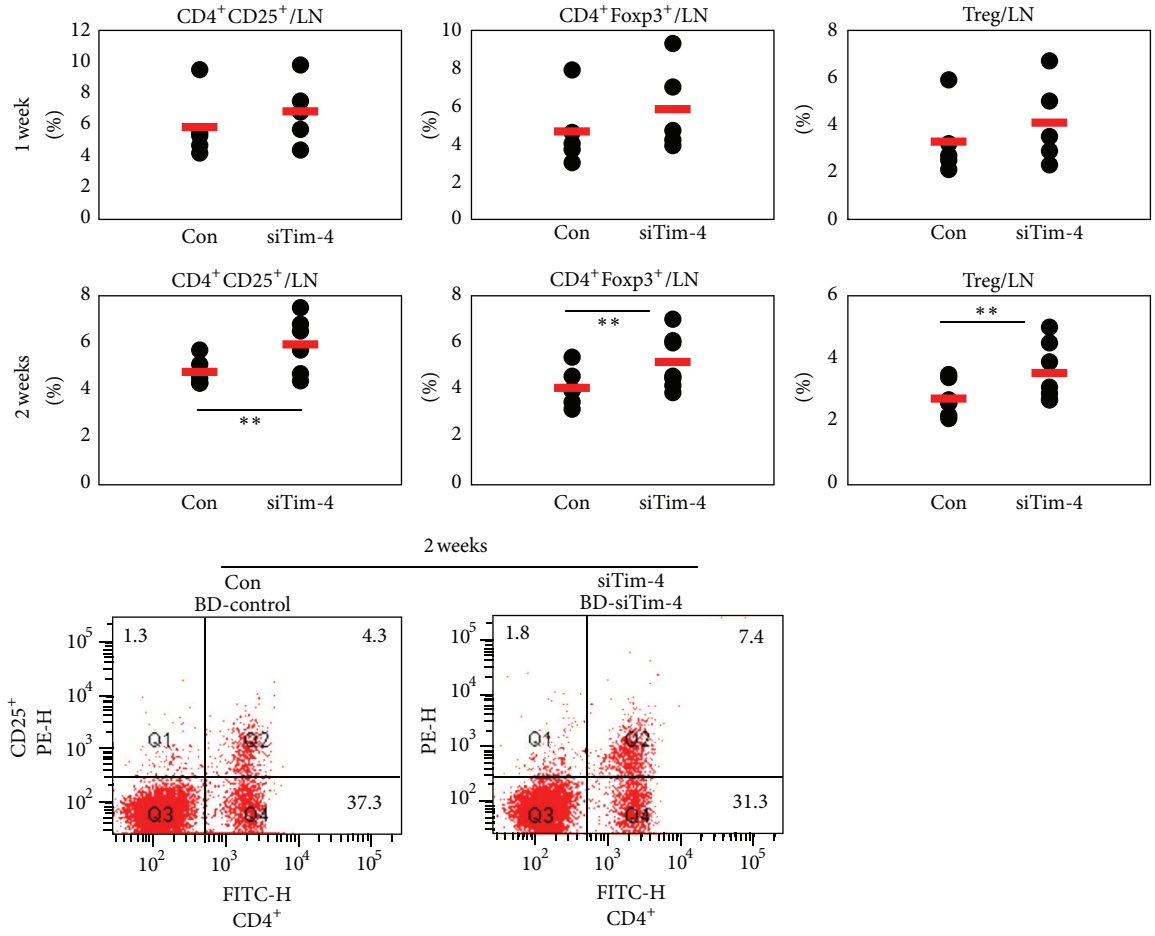

FIGURE 9: The frequencies of Treg cells were upregulated after treatment with siTim-4 in Behçet's disease (BD) mice. Treg cells were confirmed by flow cytometry in lymph nodes of BD mice after treatment with siTim-4. At 1 and 2 weeks after the first treatment with siTim-4, the frequencies of $CD4^+CD25^+$, $CD4^+Foxp3^+$, and $CD4^+CD25^+Foxp3^+$ Treg cells were compared between the siTim-4 and control groups (negative control siRNA treated groups) ($n = 5$–7) ($^{**}P < 0.05$). The bottom panel shows $CD4^+CD25^+$ in PBMCs at 2 weeks by FACS dot plot. Con: negative control siRNA injection to BD mice, siTim-4: Tim-4 siRNA injection to BD mice.

arthritis [40], inflammatory bowel disease [41], and SLE [42]. The anti-Tim-1 antibody (high avidity/agonistic) is a down-regulator of pro-inflammatory Th-17 cells. TIM-1-TIM-4 interaction is involved in the regulation of Th cell responses and modulation of the Th1/Th2 cytokine balance [7]. Our data also indicate that administering the *Tim-1* vector decreased proinflammatory cytokines, such as IL-17, TNF-α, and IL-6, but the Th2 type cytokine IL-4 was upregulated in the *Tim-1* vector injected group. Recently, upregulated cytokine IL-22 in ocular BD patients was also downregulated by anti-IL-6 and anti-TNF-α [37]. These results were similar to our results.

BD mice displayed markedly increased Tim-4 levels in LN and peritoneal macrophages compared to those in Nor and BDN mice. The frequencies of $Tim\text{-}4^+$ cells were downregulated when Tim-4 siRNA was administered to Nor mice compared to those in the NC group. siTim-4 administration to BD mice tended to decrease $Tim\text{-}4^+$ cells in peritoneal macrophages. siTim-4 administered BD mice displayed improved symptoms such as skin and genital ulcers and arthritis and showed a decreased severity score. But, $Tim\text{-}4^+$ cells related T cell phenotypes were not changed after siTim-4 treatment. TIM-4 is a ligand for TIM-1 [7] and is not expressed in T cells but is exclusively expressed in antigen-presenting cells, including DCs and macrophages [9, 10]. Two groups have reported that Tim-4 deficient mice with a 129 or b6 background develop little or no autoimmunity [9, 43]. In conjunction with improved symptoms, Treg cells in the siTim-4 treated group were significantly upregulated compared to those in the control group, and IL-17 level decreased. In our previous study, adoptive transfer of Treg cells to BD mice also improved BD-like symptoms [44]. In addition, the frequencies of Treg cells are lower in patients with autoimmune and inflammatory diseases, such as Crohn's disease [45], multiple sclerosis [46], and SLE [47], than those in healthy controls and inactive patients. The TIM-1-TIM-4 interaction is important for regulating T cell proliferation and modulating the Th1/Th2 cytokine balance [7]. Our data suggest that upregulated Treg cells induced by siTim-4 might contribute to improve BD-like symptoms.

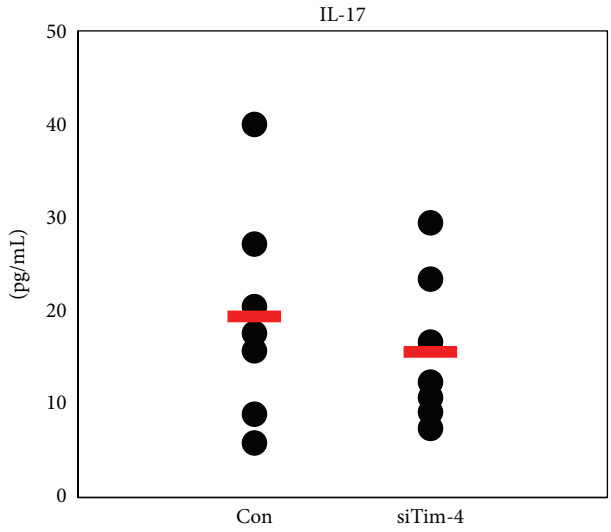

Figure 10: Administration of siTim-4 decreased serum level of IL-17 in Behçet's disease (BD) mice. Serum obtained at 2 weeks after the first injection of siTim-4 and control (Con) in BD mice. The level of IL-17 was analyzed by ELISA ($n = 8$). Con: negative control siRNA injection to BD mice, siTim-4: Tim-4 siRNA injection to BD mice.

In conclusion, the frequencies of Tim-1$^+$ cells in BD mice were downregulated compared to those in BDN mice. Administering the *Tim-1* vector to BD mice improved the BD-like symptoms and decreased the severity score by up-regulating Treg cells and down-regulating pro-inflammatory cytokines. In addition, treatment with siTim-4 upregulated Treg cells and improved BD-like symptoms, which were related to the Tim-1 and Tim-4 expression and the Tim-1-Tim-4 interaction. Furthermore, Tim-4 siRNA downregulated the level of IL-17, which may have been involved in improving the BD-like symptoms. Consequently, regulation of Tim-1 and Tim-4 was effective for improving BD-like symptoms in mice.

Conflict of Interests

There is no conflict of interest for this study.

Authors' Contribution

The *Tim-1* vector was kindly provided by Professor Lawrence P. Kane from the University of Pittsburgh.

Acknowledgment

This study was supported by a Korea Science and Engineering Foundation (KOSEF) Grant R01-2008-000-20474-0, the Korean Health Technology R&D Project, Ministry for Health, Welfare, and Family Affairs (A100535), and 2010-0011130 and 2013R1A1A3008248 from the National Research Foundation of Korea (NRF) by the Ministry of Education, Science, and Technology. Ju A. Shim performed the experiment, Eun-So Lee discussed the results, Seonghyang Sohn designed the study, Ju A. Shim and Seonghyang Sohn wrote the paper.

References

[1] V. K. Kuchroo, D. T. Umetsu, R. H. DeKruyff, and G. J. Freeman, "The TIM gene family: emerging roles in immunity and disease," *Nature Reviews Immunology*, vol. 3, no. 6, pp. 454–462, 2003.

[2] J. H. Meyers, C. A. Sabatos, S. Chakravarti, and V. K. Kuchroo, "The TIM gene family regulates autoimmune and allergic diseases," *Trends in Molecular Medicine*, vol. 11, no. 8, pp. 362–369, 2005.

[3] G. Kaplan, A. Totsuka, P. Thompson, T. Akatsuka, Y. Moritsugu, and S. M. Feinstone, "Identification of a surface glycoprotein on African green monkey kidney cells as a receptor for hepatitis A virus," *EMBO Journal*, vol. 15, no. 16, pp. 4282–4296, 1996.

[4] D. Feigelstock, P. Thompson, P. Mattoo, Y. Zhang, and G. G. Kaplan, "The human homolog of HAVcr-1 codes for a hepatitis A virus cellular receptor," *Journal of Virology*, vol. 72, no. 8, pp. 6621–6628, 1998.

[5] W. K. Han, V. Bailly, R. Abichandani, R. Thadhani, and J. V. Bonventre, "Kidney Injury Molecule-1 (KIM-1): a novel biomarker for human renal proximal tubule injury," *Kidney International*, vol. 62, no. 1, pp. 237–244, 2002.

[6] T. Ichimura, J. V. Bonventre, V. Bailly et al., "Kidney injury molecule-1 (KIM-1), a putative epithelial cell adhesion molecule containing a novel immunoglobulin domain, is up-regulated in renal cells after injury," *The Journal of Biological Chemistry*, vol. 273, no. 7, pp. 4135–4142, 1998.

[7] J. H. Meyers, S. Chakravarti, D. Schlesinger et al., "TIM-4 is the ligand for TIM-1, and the TIM-1-TIM-4 interaction regulates T cell proliferation," *Nature Immunology*, vol. 6, no. 5, pp. 455–464, 2005.

[8] S. E. Umetsu, W.-L. Lee, J. J. McIntire et al., "TIM-1 induces T cell activation and inhibits the development of peripheral tolerance," *Nature Immunology*, vol. 6, no. 5, pp. 447–454, 2005.

[9] R. Rodriguez-Manzanet, J. H. Meyers, S. Balasubramanian et al., "TIM-4 expressed on APCs induces T cell expansion and survival," *Journal of Immunology*, vol. 180, no. 7, pp. 4706–4713, 2008.

[10] M. Mizui, T. Shikina, H. Arase et al., "Bimodal regulation of T cell-mediated immune responses by TIM-4," *International Immunology*, vol. 20, no. 5, pp. 695–708, 2008.

[11] N. Kobayashi, P. Karisola, V. Peña-Cruz et al., "TIM-1 and TIM-4 glycoproteins bind phosphatidylserine and mediate uptake of apoptotic cells," *Immunity*, vol. 27, no. 6, pp. 927–940, 2007.

[12] M. Miyanishi, K. Tada, M. Koike, Y. Uchiyama, T. Kitamura, and S. Nagata, "Identification of Tim4 as a phosphatidylserine receptor," *Nature*, vol. 450, no. 7168, pp. 435–439, 2007.

[13] C.-Q. Zhao, T.-L. Li, S.-H. He et al., "Specific immunotherapy suppresses Th2 responses via modulating TIM1/TIM4 interaction on dendritic cells," *Allergy*, vol. 65, no. 8, pp. 986–995, 2010.

[14] S.-C. Chae, J.-H. Song, J.-C. Heo, Y.-C. Lee, J.-W. Kim, and H.-T. Chung, "Molecular variations in the promoter and coding regions of human Tim-1 gene and their association in Koreans with asthma," *Human Immunology*, vol. 64, no. 12, pp. 1177–1182, 2003.

[15] S.-C. Chae, J.-H. Song, Y.-C. Lee, J.-W. Kim, and H.-T. Chung, "The association of the exon 4 variations of Tim-1 gene with allergic diseases in a Korean population," *Biochemical and*

Biophysical Research Communications, vol. 312, no. 2, pp. 346–350, 2003.

[16] S.-C. Chae, Y.-R. Park, J.-H. Song, S.-C. Shim, K.-S. Yoon, and H.-T. Chung, "The polymorphisms of Tim-1 promoter region are associated with rheumatoid arthritis in a Korean population," *Immunogenetics*, vol. 56, no. 10, pp. 696–701, 2005.

[17] N. S. Page, G. Jones, and G. J. Stewart, "Genetic association studies between the T cell immunoglobulin mucin (TIM) gene locus and childhood atopic dermatitis," *International Archives of Allergy and Immunology*, vol. 141, no. 4, pp. 331–336, 2006.

[18] Y. Wang, J. Meng, X. Wang et al., "Expression of human TIM-1 and TIM-3 on lymphocytes from systemic lupus erythematosus patients," *Scandinavian Journal of Immunology*, vol. 67, no. 1, pp. 63–70, 2008.

[19] F. Ilhan, T. Demir, P. Türkçüoğlu, B. Turgut, N. Demir, and A. Gödekmerdan, "Th1 polarization of the immune response in uveitis in Behçet's disease," *Canadian Journal of Ophthalmology*, vol. 43, no. 1, pp. 105–108, 2008.

[20] T. Shimizu, G. E. Ehrlich, G. Inaba, and K. Hayashi, "Behcet disease (Behcet syndrome)," *Seminars in Arthritis and Rheumatism*, vol. 8, no. 4, pp. 223–260, 1979.

[21] H. Behçet, "Über rezidivierende, aphthöse, durch ein virus verursachte Geschwüre am Mund, am Auge und an den Genitalien," *Dermatologische Wochenschrift*, vol. 105, pp. 1152–1157, 1937.

[22] S. Lee, D. Bang, Y. H. Cho, E.-S. Lee, and S. Sohn, "Polymerase chain reaction reveals herpes simplex virus DNA in saliva of patients with Behçet's disease," *Archives of Dermatological Research*, vol. 288, no. 4, pp. 179–183, 1996.

[23] E. S. Lee, S. Lee, D. Bang, S. Sohn, C. Park, and K. Lee, "Herpes simplex virus detection by polymerase chain reaction in intestinal ulcer of patients with Behçet's disease," *Journal of Investigative Dermatology*, vol. 101, no. 3, p. 474, 1993.

[24] D. Bang, K. H. Yoon, H. G. Chung, E. H. Choi, E.-S. Lee, and S. Lee, "Epidemiological and clinical features of Behcet's disease in Korea," *Yonsei Medical Journal*, vol. 38, no. 6, pp. 428–436, 1997.

[25] E. Lee, S. Lee, D. Bang, and S. Sohn, "Detection of herpes simplex virus DNA by polymerase chain reaction in genital ulcer of patients with Behçet's disease," *Revue du Rhumatisme*, vol. 63, p. 532, 1996.

[26] S. Sohn, E.-S. Lee, D. Bang, and S. Lee, "Behcet's disease-like symptoms induced by the Herpes simplex virus in ICR mice," *European Journal of Dermatology*, vol. 8, no. 1, pp. 21–23, 1998.

[27] H. J. Kim, D. Bang, S. H. Lee et al., "Behcet's syndrome in Korea: a look at the clinical picture," *Yonsei Medical Journal*, vol. 29, no. 1, pp. 72–78, 1988.

[28] A. J. de Souza, T. B. Oriss, K. J. O'Malley, A. Ray, and L. P. Kane, "T cell Ig and mucin 1 (TIM-1) is expressed on in vivo-activated T cells and provides a costimulatory signal for T cell activation," *Proceedings of the National Academy of Sciences of the United States of America*, vol. 102, no. 47, pp. 17113–17118, 2005.

[29] J. Wu, Y. Song, A. B. H. Bakker et al., "An activating immunoreceptor complex formed by NKG2D and DAP10," *Science*, vol. 285, no. 5428, pp. 730–732, 1999.

[30] M. Ulker, K. D. Lewis, L. E. Hood, and I. Stroynowski, "Activated T cells transcribe an alternatively spliced mRNA encoding a soluble form of Qa-2 antigen," *EMBO Journal*, vol. 9, no. 12, pp. 3839–3847, 1990.

[31] O. Saitoh, N. Abiru, M. Nakahara, and Y. Nagayama, "CD8+CD122+ T cells, a newly identified regulatory T subset, negatively regulate graves' hyperthyroidism in a murine model," *Endocrinology*, vol. 148, no. 12, pp. 6040–6046, 2007.

[32] M. Rifa'i, Z. Shi, S.-Y. Zhang et al., "CD8+CD122+ regulatory T cells recognize activated T cells via conventional MHC class I—$\alpha\beta$TCR interaction and become IL-10-producing active regulatory cells," *International Immunology*, vol. 20, no. 7, pp. 937–947, 2008.

[33] L. Xiao, Z.-R. Fu, F. Liu et al., "Suppression of allograft rejection by Tim-1-Fc through cross-linking with a novel Tim-1 binding partner on T cells," *PLoS ONE*, vol. 6, no. 7, Article ID e21697, 2011.

[34] D. J. Cua, J. Sherlock, Y. Chen et al., "Interleukin-23 rather than interleukin-12 is the critical cytokine for autoimmune inflammation of the brain," *Nature*, vol. 421, no. 6924, pp. 744–748, 2003.

[35] C. L. Langrish, Y. Chen, W. M. Blumenschein et al., "IL-23 drives a pathogenic T cell population that induces autoimmune inflammation," *The Journal of Experimental Medicine*, vol. 201, no. 2, pp. 233–240, 2005.

[36] D. Yen, J. Cheung, H. Scheerens et al., "IL-23 is essential for T cell-mediated colitis and promotes inflammation via IL-17 and IL-6," *The Journal of Clinical Investigation*, vol. 116, no. 5, pp. 1310–1316, 2006.

[37] S. Sugita, Y. Kawazoe, A. Imai et al., "Role of IL-22- and TNF-α-producing Th22 cells in uveitis patients with Behcet's disease," *Journal of Immunology*, vol. 190, no. 11, pp. 5799–5808, 2013.

[38] T. Cai, Q. Wang, Q. Zhou et al., "Increased expression of IL-22 is associated with disease activity in Behcet's disease," *PlosOne*, vol. 8, no. 3, Article ID e59009, 2013.

[39] C. K. Edwards III, "Drug discovery and development for inflammatory diseases," *Expert Opinion on Therapeutic Targets*, vol. 8, no. 2, pp. 151–163, 2004.

[40] N. Nishimoto and T. Kishimoto, "Humanized antihuman IL-6 receptor antibody, tocilizumab," *Handbook of Experimental Pharmacology*, no. 181, pp. 151–160, 2008.

[41] J. Mudter and M. F. Neurath, "IL-6 signaling in inflammatory bowel disease: pathophysiological role and clinical relevance," *Inflammatory Bowel Diseases*, vol. 13, no. 8, pp. 1016–1023, 2007.

[42] H.-Y. Chun, J.-W. Chung, H.-A. Kim et al., "Cytokine IL-6 and IL-10 as biomarkers in systemic lupus erythematosus," *Journal of Clinical Immunology*, vol. 27, no. 5, pp. 461–466, 2007.

[43] K. Wong, P. A. Valdez, C. Tan, S. Yeh, J.-A. Hongo, and W. Ouyang, "Phosphatidylserine receptor Tim-4 is essential for the maintenance of the homeostatic state of resident peritoneal macrophages," *Proceedings of the National Academy of Sciences of the United States of America*, vol. 107, no. 19, pp. 8712–8717, 2010.

[44] J. Shim, E.-S. Lee, S. Park, D. Bang, and S. Sohn, "CD4+ CD25+ regulatory T cells ameliorate Behcet's disease-like symptoms in a mouse model," *Cytotherapy*, vol. 13, no. 7, pp. 835–847, 2011.

[45] I. Ricciardelli, K. J. Lindley, M. Londei, and S. Quaratino, "Anti tumour necrosis-α therapy increases the number of FOXP3 + regulatory T cells in children affected by Crohn's disease," *Immunology*, vol. 125, no. 2, pp. 178–183, 2008.

[46] J. Huan, N. Culbertson, L. Spencer et al., "Decreased FOXP3 levels in multiple sclerosis patients," *Journal of Neuroscience Research*, vol. 81, no. 1, pp. 45–52, 2005.

[47] H.-Y. Lee, Y.-K. Hong, H.-J. Yun, Y.-M. Kim, J.-R. Kim, and W.-H. Yoo, "Altered frequency and migration capacity of CD4+ CD25+ regulatory T cells in systemic lupus erythematosus," *Rheumatology*, vol. 47, no. 6, pp. 789–794, 2008.

Hindawi Publishing Corporation
Mediators of Inflammation
Volume 2013, Article ID 245804, 9 pages
http://dx.doi.org/10.1155/2013/245804

Research Article

IRF5 Is a Specific Marker of Inflammatory Macrophages *In Vivo*

Miriam Weiss,[1] Katrina Blazek,[1] Adam J. Byrne,[1,2] Dany P. Perocheau,[1] and Irina A. Udalova[1]

[1] *Kennedy Institute of Rheumatology, University of Oxford, Roosevelt Drive, Headington, Oxford OX3 7FY, UK*
[2] *Leukocyte Biology Section, National Heart and Lung Institute, Sir Alexander Fleming Building, Faculty of Medicine, Imperial College, South Kensington, London SW7 2AZ, UK*

Correspondence should be addressed to Miriam Weiss; miriam.weiss@stx.ox.ac.uk
and Irina A. Udalova; irina.udalova@kennedy.ox.ac.uk

Received 31 August 2013; Revised 29 November 2013; Accepted 30 November 2013

Academic Editor: Salahuddin Ahmed

Macrophages are an integral part of the innate immune system and key players in pathogen clearance and tissue remodelling. Both functions are accomplished by a pivotal network of different macrophage subtypes, including proinflammatory M1 and anti-inflammatory M2 macrophages. Previously, our laboratory identified the transcription factor interferon regulatory factor 5 (IRF5) as the master regulator of the M1 macrophage polarisation. IRF5 was found to be highly expressed in human M1 compared to M2 macrophages. Furthermore, IRF5 dictates the expression of proinflammatory genes such as *IL12b* and *IL23a* whilst repressing anti-inflammatory genes like *IL10*. Here we show that murine bone marrow derived macrophages differentiated *in vitro* with GM-CSF are also characterised by high levels of IRF5 mRNA and protein and express proinflammatory cytokines upon LPS stimulation. These macrophages display characteristic expression of M1-marker MHC II but lack the M2-marker CD206. Significantly, we develop intracellular staining of IRF5- expressing macrophages and utilise it to recapitulate the *in vitro* results in an *in vivo* model of antigen-induced arthritis, emphasising their physiological relevance. Thus, we establish the species-invariant role of IRF5 in controlling the inflammatory macrophage phenotype both *in vitro* and in *in vivo*.

1. Introduction

Macrophages are immune cells involved in recognition of pathogenic stimuli and the initiation and resolution of inflammation. They can adapt to various different environmental signals giving rise to several subtypes with distinct functions [1]. These subtypes can be classified as M1 (classically activated) and M2 (alternatively activated) macrophages. In addition, there are several phenotypes associated with M2 macrophages, for example, M2-like or tumour associated macrophages [2]. M1 macrophages secrete high levels of IL-12 and IL-23 but low levels of IL-10, whereas M2 macrophages secrete low levels of IL-12 and IL-23 but high levels of IL-10 [3].

Several reports have described the *in vitro* differentiation of lineage-defined macrophages. In general, these methods utilise M-CSF (macrophage colony stimulating factor; CSF-1) to differentiate bone marrow derived progenitors, followed by priming with various stimuli. Addition of interferon-γ followed by lipopolysaccharide (LPS) stimulation has been used to acquire M1 macrophages whereas addition of IL-4 or IL-13 without LPS yields M2 macrophages [3]. Another established method uses GM-CSF (granulocyte/macrophage colony stimulating factor) in order to generate M1 macrophages or alternatively M-CSF treatment for M2 differentiation, usually followed by LPS challenge for both subtypes [4, 5]. In the physiological situation, M-CSF is detected in low steady state levels whereas GM-CSF has been shown to be increased upon stimulation with inflammatory stimuli, such as IL-1, TNF, or LPS [6, 7].

Macrophages are also known to play a key role in autoimmune diseases such as rheumatoid arthritis (RA), a degenerative disease characterised by joint inflammation and bone destruction [8]. At the site of inflammation, macrophages are present in high numbers and it has been found that depletion ameliorates disease severity [9–11]. More

specifically, M1 macrophages contribute to RA pathogenesis by secreting proinflammatory cytokines and thereby taking part in the Th1/Th17 response [12, 13].

Distinct macrophage subtypes are not only characterised by their differences in cytokine release but also display differential expression of key transcription factors. Recently, we identified the transcription factor interferon regulatory factor 5 (IRF5) as the major regulator of proinflammatory M1 macrophage polarisation [14]. IRF5 directly induces the expression of proinflammatory cytokines such as IL-6, IL-12b, and IL-23a whilst repressing transcription of anti-inflammatory cytokines such as IL-10 [14, 15]. IRF5 is involved in various inflammatory processes such as the type I interferon response to virus infection and pathogen recognition receptor signalling [16]. Upon viral infection, IRF5 is phosphorylated and thereby translocated to the nucleus where it binds to the regulatory regions of its target genes [17]. Nonviral stimulation of toll-like receptors (TLR) including TLR4, 7, and 9 also leads to activation of IRF5 [16]. Moreover, polymorphisms in the *IRF5* gene have been found to associate with RA [18, 19].

Despite the major role IRF5 plays in macrophage activation, it has rarely been used to track inflammatory macrophages in disease. In this study, we aim to characterise murine macrophages and IRF5 expression in both *in vitro* and *in vivo* models of inflammation. We therefore used the murine model of antigen-induced arthritis (AIA) in which mice are immunised with methylated BSA (mBSA) prior to intra-articular injection of mBSA in one knee, leading to localised inflammation and a Th17 response [20, 21]. First, we analysed *in vitro* differentiated macrophages regarding their IRF5 expression, LPS response, and surface receptor expression. We then used flow cytometry to label intracellular IRF5 in both the *in vitro* macrophages and those derived from the affected knee of the AIA mouse model.

2. Material and Methods

2.1. Animals and Antigen-Induced Arthritis. For this study wild type mice were bred on a C57Bl/6 background. The experimental animal procedures used in this work were approved by the Kennedy Institute of Rheumatology Ethics Committee and the UK Home Office.

We induced arthritis as described previously; briefly, at day zero, mice were sedated using inhaled isoflurane anaesthesia and subsequently immunised with 100 μg of mBSA emulsified in 0.2 mL of complete Freund's adjuvant, administered intra-dermally at the base of the tail. At day seven, we induced arthritis by means of an intraarticular injection of mBSA (200 μg in 10 μL of sterile PBS), or PBS alone using a sterile 33-gauge microcannula, in sedated animals. At day nine, the mice were sacrificed and the knee joints were excised.

2.2. In Vitro Differentiation of Macrophages. For the generation of *in vitro* differentiated macrophages, bone marrow from wild type mice was cultured in RPMI-1640 medium with L-glutamine (PAA Laboratories) supplemented with 10% FCS, 1% penicillin/streptomycin, 0.01% 2-mercaptoethanol, and with either recombinant murine GM-CSF (20 ng/mL; Peprotech) or recombinant human M-CSF (100 ng/mL; Peprotech). After eight days, adherent cells were washed with PBS and replated, then stimulated with LPS (100 ng/mL; Alexis Biochemicals).

2.3. RNA Extraction and Quantitative Real-Time PCR. Total RNA was extracted using RNeasy Mini Kit (Qiagen) as per the manufacturer's instructions. Contaminating genomic DNA was removed from RNA samples using the RNase-Free DNase Set (Qiagen). Total RNA was reverse-transcribed into cDNA using the High Capacity cDNA Reverse Transcription Kit (Life Technologies) as per the manufacturer's instructions. Real-time PCR reactions were performed on an ABI 7900HT (Life Technologies) with TaqMan primer sets for murine *Fizz1*, *iNOS*, *Il10*, *Il12b*, *Il23a*, *Irf5*, and *Hprt* (Life Technologies) and gene expression was analysed using the change-in-threshold ΔΔCt-method.

2.4. Western Blot. For protein isolation, cells were harvested with Versene (EDTA) 0.02% (Lonza). Pellets were resuspended with macrophage lysis buffer (20 mM Tris pH 8, 300 mM NaCl, 1% NP40, and 10% glycerol) containing freshly added protease inhibitors (Roche). Samples were incubated on ice for 30 min before cellular debris was removed by centrifugation for 15 min, at 13,000 rpm/4°C. Lysates were transferred into new tubes and stored at −80°C. To determine the protein concentration of whole cell lysates a BCA test (Thermo Scientific) was performed according to the manufacturer's instructions.

5–7 μg of total protein were resolved by Novex Tris-glycine gel (Life Technologies), transferred onto a PVDF membrane (GE Healthcare) by wet western blotting, and subjected to incubation with rabbit anti-IRF5 (Abcam) or mouse anti β-actin (Sigma), followed by detection with horseradish-peroxidase- (HRP-) conjugated secondary antibodies and chemiluminescent substrate solution ECL (GE Healthcare).

2.5. Enzyme Linked Immunosorbent Assay (ELISA). Supernatants of stimulated cells were transferred into tubes, centrifuged for 5 min at 3,300 rpm, and stored at −20°C until needed. Cytokine secretion was quantified for murine IL-10 (eBioscience), IL-12p70 (eBioscience), and IL-23 (eBioscience) according to the manufacturer's instructions. Absorbance was read at 450 nm by a spectrophotometric ELISA plate reader (Labsystems Multiscan Biochromic) and analysed using Ascent Labsystems software. All samples were analysed in triplicate in a volume of 50 μL.

2.6. Flow Cytometry. Single cell suspensions of *in vitro* differentiated macrophages and knees were washed with FACS buffer (1% BSA, 0.01% sodium azide in PBS, and pH 7.4) and stained with the following antibodies: APC conjugated anti-CD206 antibody (BioLegend), APC-Cy7 conjugated anti-CD11b antibody (BD Biosciences), PE conjugated anti-MCH II [I-A/I-E] antibody (BD Biosciences), PerCP

conjugated anti-CD45 antibody (BD Biosciences), and PE-Cy7 conjugated anti-F4/80 (eBioscience). For intracellular FACS staining, cells were fixed with fixation/permeabilisation solution (eBioscience) and washed with permeabilisation buffer (eBioscience). Samples were then stained with rabbit anti-IRF5 antibody (Abcam) followed by secondary staining with goat anti-rabbit Alexa Fluor 488 (Life Technologies). FACS analysis was performed using a FACS Canto II (BD Biosciences), and the data were analysed with Flow Jo software, version 7.6 (Treestar).

2.7. Statistical Analyses. Statistical analysis was performed using GraphPad v5.0 (GraphPad Software) using two-way ANOVA (with Bonferroni's multiple comparisons) or unpaired one-tailed Mann-Whitney *U* tests (comparisons between two groups). *P* values less than 0.05 were considered significant.

3. Results and Discussion

3.1. High Levels of IRF5 Expression in Murine GM-CSF Differentiated Bone Marrow Derived Macrophages. In order to assess the expression of IRF5 *in vitro*, bone marrow derived macrophages were differentiated with either GM-CSF or M-CSF (GM-BMDM and M-BMDM, resp.). After nine days of differentiation, macrophages were challenged with LPS for 0 h, 1 h, 4 h, 8 h, and 24 h and analysed for mRNA and protein levels of IRF5.

In unstimulated murine cells, IRF5 levels were considerably higher in GM-CSF differentiated compared to M-CSF differentiated macrophages (Figure 1(a)). Interestingly, this expression pattern is also exhibited by their unstimulated human macrophage counterparts, with significantly higher IRF5 expression in GM-CSF *in vitro* differentiated human macrophages compared to those differentiated with M-CSF [14].

Upon LPS stimulation, IRF5 mRNA and protein expression were induced in M-CSF differentiated murine cells and further induced in GM-CSF differentiated murine cells. *Irf5* mRNA levels increased between 4 and 8 h but protein levels were already higher after 1 h of poststimulation (Figure 1(a)) we therefore hypothesised that the LPS-induced production of IRF5 was most likely due to a combination of two factors: (1) increased mRNA levels and (2) protein stabilisation, possibly related to activation by phosphorylation or ubiquitination [22, 23]. IRF5 has been shown to be essential for the proinflammatory phenotype of human monocyte derived GM-CSF macrophages upon LPS stimulation. However, mRNA and protein levels in human M-CSF derived macrophages are not further induced upon LPS stimulation, suggesting some species-specific or cell source-specific differences in LPS-regulated IRF5 production.

3.2. Distinct Cytokine Expression Profiles of M-CSF and GM-CSF Derived BMDMs. Next, to determine the inflammatory properties of *in vitro* differentiated murine macrophages, expression and secretion of the cytokines IL-10, IL-12, and IL-23 were analysed.

As expected, each macrophage subtype was found to display differential behaviour to LPS stimulation regarding their cytokine expression (Figures 1(b) and 1(c)). Transcription and secretion of the anti-inflammatory cytokine IL-10 were elevated in M-CSF differentiated macrophages compared to GM-CSF treated cells. LPS stimulation of M-BMDMs resulted in increased IL-10 expression on both transcript and protein level. At 24 h, *Il10* mRNA returned to an almost basal level, whereas protein secretion remained high. IL-10 protein secretion was significantly higher following 8 h LPS stimulation in M-BMDMs whereas GM-BMDMs only showed basal IL-10 expression.

Proinflammatory cytokines IL-12 and IL-23 were found to be expressed at much higher levels in GM-CSF derived macrophages whereas M-BMDMs show only minimal expression of proinflammatory cytokines, although with similar kinetics of expression as in GM-BMDMs (Figure S1A in Supplementary Material available online at http://dx.doi.org/10.1155/2013/245804). The differences in cytokine expression were statistically significant on both the transcript and protein levels. *Il12b* mRNA was induced upon LPS stimulation in GM-BMDMs, with the highest levels observed 8 h after stimulation. Secretion of IL12p70 was increased from 4 h of stimulation onwards. Although M-BMDMs expressed low levels of *Il23a* mRNA following 1 h of stimulation, they did not secrete heterodimeric IL-23 protein at any time point. In GM-BMDMs *Il23a* mRNA expression peaked following 1 h of LPS stimulation, while IL-23 protein secretion extended to 24 h after LPS stimulation.

We also noted that IRF5 levels increased in M-BMDMs upon LPS stimulation but did not result in significant induction of proinflammatory cytokines. Thus, we hypothesised that this could be due to a lower functional activity of IRF5 in M-BMDMs, as IRF5 protein is subject to posttranslational modifications such as phosphorylation and ubiquitination [22–24]. However, the status of posttranslational modifications for IRF5 in LPS stimulated macrophages is yet to be determined. Furthermore, the availability of activating cofactors potentially required for IRF5 mediated induction of proinflammatory cytokines might be different in M-BMDMs compared to GM-BMDMs.

Thus, consistent with its proposed role as a master regulator of the M1 macrophage phenotype and in accordance with data for human *in vitro* differentiated macrophages [14], GM-CSF differentiated BMDMs express high levels of IRF5 and produce IL-12 as well as IL-23 following stimulation with LPS, whereas M-CSF differentiated BMDMs express lower levels of IRF5 and produce IL-10. These data confirm the study of Fleetwood et al. [4] that suggested that GM-CSF and M-CSF induce a distinct M1 or M2 BMDM phenotype, respectively.

3.3. Specific Intracellular IRF5 Staining of M-CSF and GM-CSF Derived BMDMs. In order to establish intracellular IRF5 staining, expression was measured by fluorescence activated cell sorting (FACS) of unstimulated and LPS stimulated GM- and M-BMDMs at day nine of differentiation. Known cell surface receptor markers of M1 and M2 macrophages,

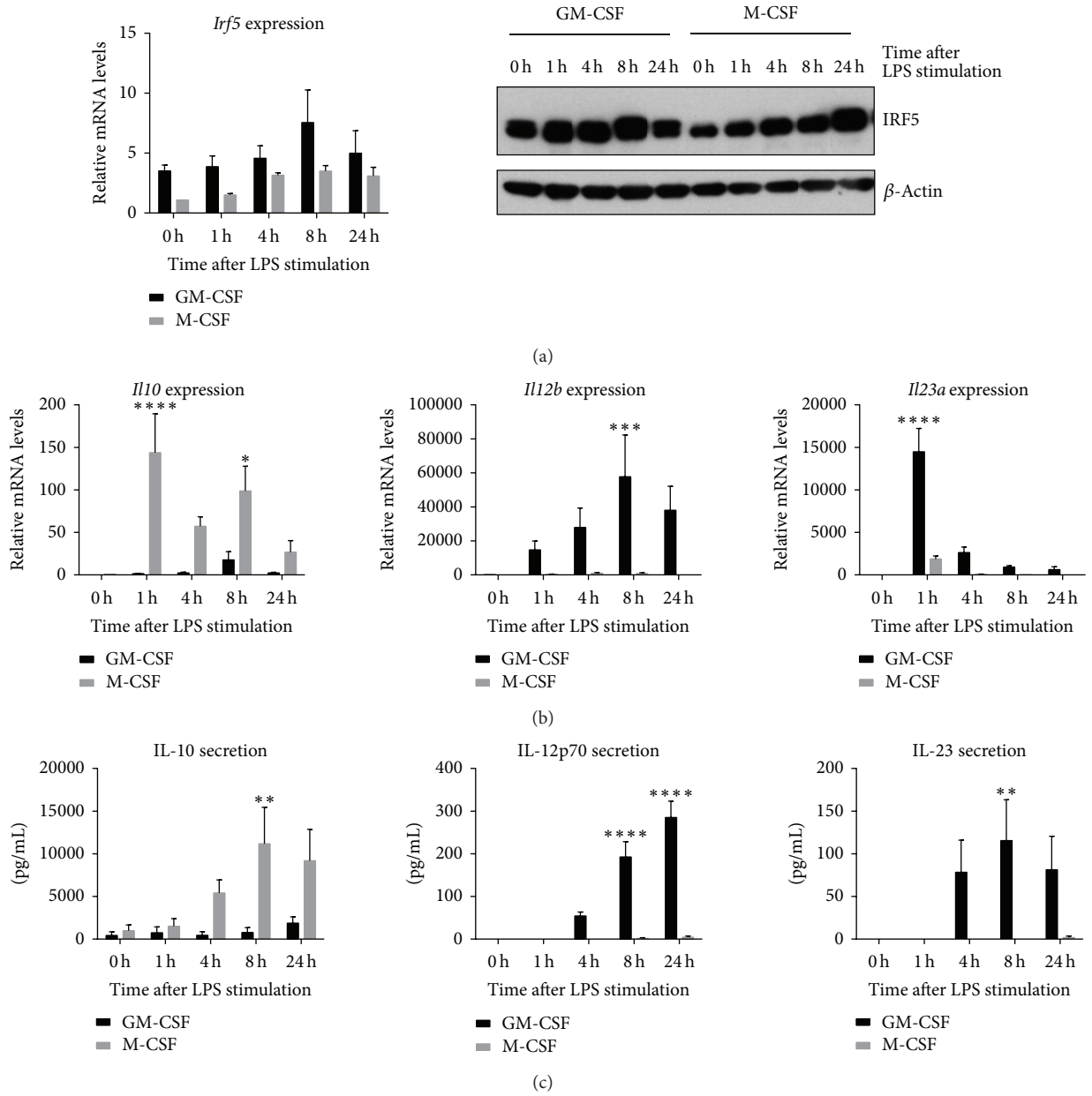

Figure 1: IRF5 levels and cytokine response of *in vitro* differentiated macrophages. BMDMs were differentiated with GM-CSF (20 ng/mL) or M-CSF (100 ng/mL) for eight days. All cells were challenged with LPS for the indicated time periods. (a) Transcript levels were measured with real-time PCR. Error bars represent the standard error for $n = 6$. Protein levels of IRF5 and β-actin were determined by western blot. Experiment is representative for three independent experiments. (b) and (c) At each time point RNA (top panel) and supernatants (bottom panel) were collected. Error bars represent the standard error for $n = 5$. Statistical analysis was performed by 2-way ANOVA and Bonferroni's multiple comparison. $^{*}P \leq 0.05$; $^{**}P \leq 0.01$; $^{***}P \leq 0.001$; $^{****}P \leq 0.0001$.

MHCII, and CD206 (mannose receptor), respectively, as well as the pan macrophage marker F4/80 were used as controls for specificity of IRF5 staining.

Around 70% of the M-CSF derived macrophages were F4/80^{high} and CD206^{high} (Figure 2(a)). GM-CSF differentiated macrophages on the other hand were generally F4/80^{low} and only 1-2% of them expressed CD206. Although F4/80 is reported to be highly expressed on all tissue macrophages, GM-CSF derived cells only showed a low percentage of F4/80+ cells. This could be because GM-CSF can also induce differentiation into DCs, effectively leading to generation of DC-like macrophages [25]. Conversely, 80% of unstimulated GM-CSF derived BMDMs expressed MHC II, whereas in CD206 positive M2 macrophages only 10% of cells exhibit expression of this marker (Figure 2(b)). A similar distribution was observed for IRF5, where over 70% of unstimulated GM-BMDMs were IRF5+ compared to only 5% of unstimulated M-BMDMs. In summary, most unstimulated M-BMDMs display the M2 marker CD206 and F4/80 whereas GM-BMDMs lack the latter but express M1 markers MHC II and

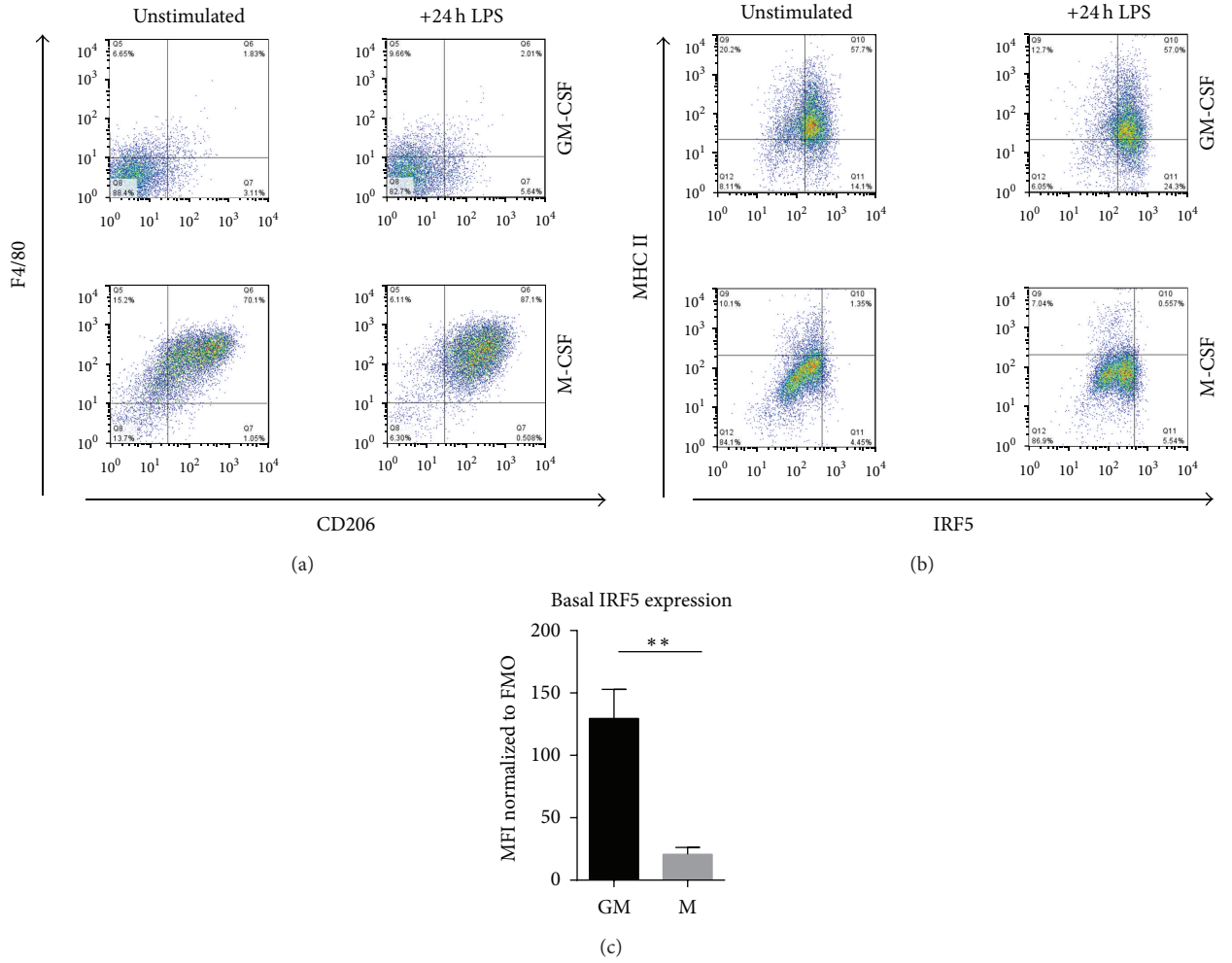

Figure 2: Surface receptor expression of polarised macrophages and intracellular IRF5 staining. Macrophages were *in vitro* differentiated with GM-CSF or M-CSF for eight days and then stimulated with LPS for 24 h. FACS samples were collected before and after stimulation. (a) and (b) Samples were stained for the expression of F4/80, CD206, MHC II, and IRF5. (c) Macrophages were stained for intracellular IRF5 and staining in unstimulated cells was quantified by mean fluorescence intensity (MFI). Error bars represent the standard error for $n = 6$. Statistical analysis was performed by one-tailed Mann-Whitney U test. $^{**}P \leq 0.01$.

IRF5. Basal IRF5 levels in unstimulated cells were quantified using mean fluorescence intensity (MFI) (Figure 2(c)). The MFI for IRF5 in GM-CSF derived macrophages was found to be sixfold higher than in M-CSF differentiated macrophages. The quantified differences in the IRF5 levels were further confirmed by the analysis of IRF5 mRNA and protein levels in these samples (Figure S1B).

LPS stimulation only minimally increased expression of F4/80 and CD206 in GM-BMDMs, whilst in M-BMDMs the percentage of $F4/80^{high}$ $CD206^{high}$ cells increased to almost 90%. MHC II expression decreased after 24 h of LPS stimulation in both cell types, consistent with the previous reports indicating that LPS does not induce expression of MHC II in macrophages [26–28]. Of significance, the population of $IRF5^{+}$ cells increased to over 80% in LPS-stimulated GM-BMDMs but remained unchanged in M-BMDMs contrary to the observed increase in IRF5 protein levels detected by Western Blot analysis (Figure 1(a)). Although the same antibody is used for both techniques, in a Western Blot, proteins are denatured, whereas in FACS proteins are in a native configuration. It is possible that in M-BMDMs native IRF5 protein is in a conformation that does not allow its recognition by this antibody unless denatured. The structure of proteins can be affected by posttranslational modifications such as phosphorylation or ubiquitination which also dictate protein activity. As highlighted above, the manner in which IRF5 is modified in stimulated macrophages is the subject of ongoing research.

Thus, we have developed intracellular IRF5 staining and demonstrated that M1 macrophages have a higher percentage of IRF5+ cells than M2 macrophages. It is worth noting though that FACS staining for IRF5 in macrophages is challenging due to relatively high background from secondary antibodies and macrophage autofluorescence. A reporter IRF5 mouse strain, similar to the described RelA-GFP knock-in [29], would further facilitate analysis of IRF5 expression

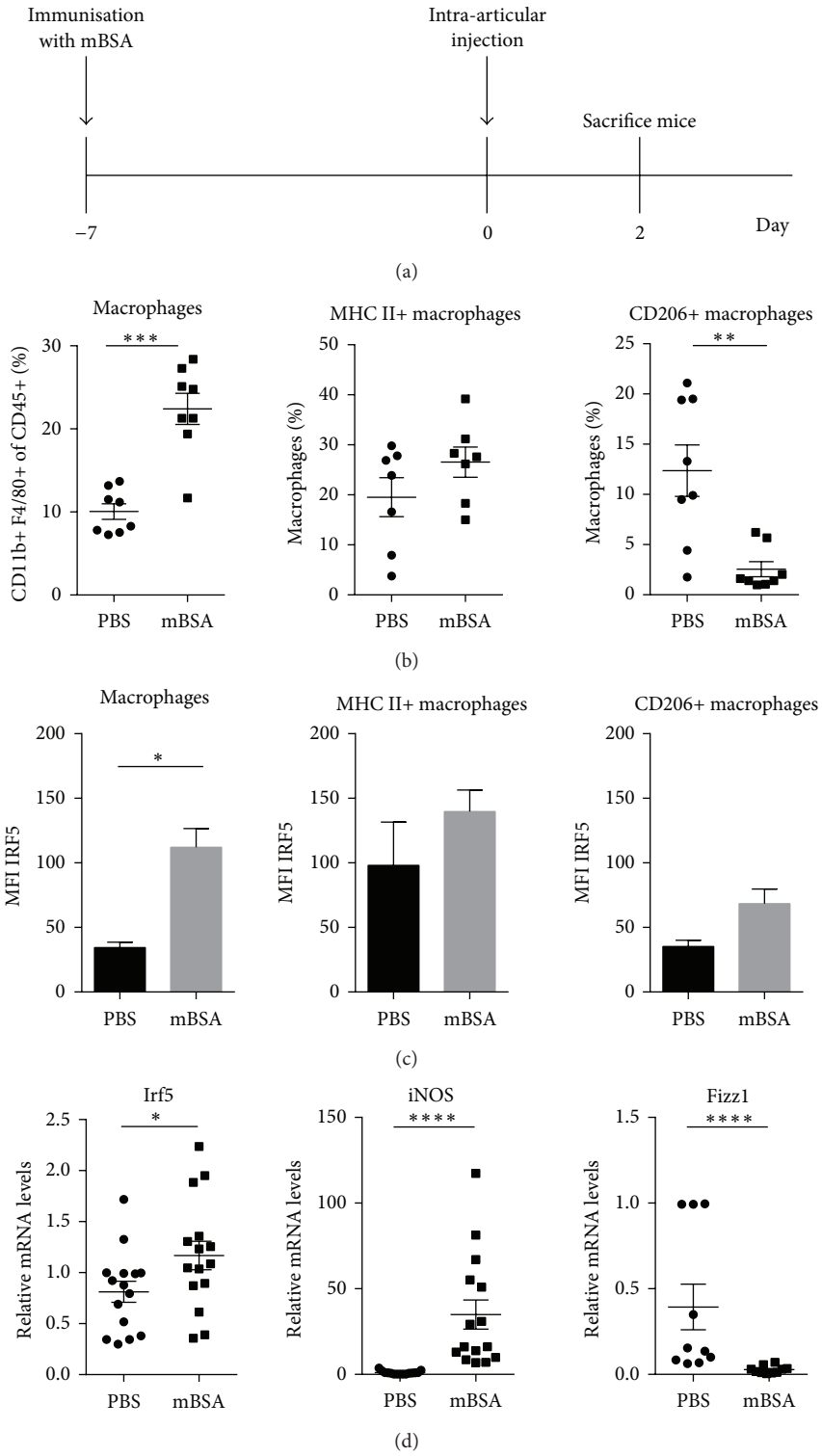

Figure 3: Macrophage populations and IRF5 expression at the site of inflammation in a mouse model of arthritis. Mice were immunised with mBSA in complete Freud's adjuvant prior to intra-articular injection of mBSA or PBS. Knees were collected at day two of disease. (a) Schematic of the experimental set-up for antigen-induced arthritis. (b) Samples from three independent experiments were stained for flow cytometry with antibodies against CD45, CD11b, F4/80, CD206, and MHC II. (c) IRF5 FACS staining was quantified calculating the mean fluorescence intensity in knees of three wild type mice. (d) Total RNA was isolated from knees of three independent experiments and analysed by real-time PCR for expression of Irf5, iNOS, and Fizz1. Statistical analysis was performed throughout by one-tailed Mann-Whitney U test. $^{*}P \leq 0.05$; $^{**}P \leq 0.01$; $^{***}P \leq 0.001$; $^{****}P \leq 0.0001$.

in macrophage populations and possibly other cell types in *in vivo* models. In addition, it would be helpful in the analysis of the intracellular localisation of IRF5 in response to stimulation.

3.4. IRF5 Expressing Macrophages at the Site of Inflammation in an Experimental Model of Arthritis. Finally, we utilised a murine model of antigen-induced arthritis to explore the possibility of using IRF5 as a marker of inflammatory macrophages in a disease setting. Mice were immunised with mBSA and after seven days arthritis was induced by intra-articular injection of mBSA (affected knee) or PBS (control knee) (Figure 3(a)). Affected knees and control knees were harvested two days after injection and subjected to FACS analysis. In addition, RNA was isolated from knees to study mRNA levels of *Irf5* and macrophage markers at the site of inflammation. The chosen markers were *iNOS* and *Fizz1* for M1 and M2 macrophages, respectively [30, 31].

Macrophages were defined as CD45+, CD11b+, and F4/80+ cells. Within this population, we identified proinflammatory (MHC II+ CD206−) and anti-inflammatory (MHC II-CD206+) macrophage subsets. The percentage of total macrophage populations, as well as the proinflammatory macrophage subset, was significantly increased in inflamed knees compared to control knees (Figure 3(b)). In contrast, the percentage of CD206+ macrophages was found to be significantly reduced after antigen challenge. These results also demonstrate that there are a large number of macrophages which do not fit either category. This probably reflects the extent of macrophage plasticity and the wide spectrum of *in vivo* macrophage subtypes [32]. This especially holds true in a disease setting where incoming macrophages might be at different stages of polarisation and where the inflammatory environment can be constantly changing.

Quantification of IRF5 FACS staining in macrophages demonstrated that increased IRF5 expression can be detected in affected knees (Figure 3(c)). When IRF5 levels were assessed in each macrophage population individually, it was observed that proinflammatory macrophages express relatively high levels of IRF5. CD206+ macrophages express less IRF5 but also show a minor increase in inflamed knees, suggesting that the remaining CD206+ macrophages at the site of inflammation express more IRF5 than they did prior to challenge. The *in vivo* data confirm the findings in *in vitro* differentiated macrophages that proinflammatory macrophages do express higher levels of IRF5 than CD206+ macrophages.

Analysis of whole knee RNA extracts supported these observations and demonstrated that *Irf5* transcript levels are significantly augmented in affected knees (Figure 3(d)). Expression of the M1 marker *iNOS* was significantly higher in mBSA injected knees whereas *Fizz1* expression is diminished. Taken together, these results indicate that there is an increasing amount of proinflammatory macrophages at the site of inflammation which correlates with an increase in IRF5 mRNA and protein. We therefore conclude that IRF5 is an appropriate marker for detection of inflammatory macrophages in this arthritis disease model. However, it has to be kept in mind that although IRF5 levels within macrophage populations increase, this may not necessarily translate into elevated protein activity since the phosphorylation status and cellular localisation are not taken into account. It has been shown that IRF5 undergoes posttranslational modifications and is regulated by phosphorylation and ubiquitination [22–24]. However, the role of IRF5 activation in the context of disease has not been studied extensively and further research will be required to elucidate this [33].

Recently, IRF5 was used as an indicator for M1 macrophage infiltrate in house dust mite induced asthma animal models [34]. Although this study did not describe the phenotype of the IRF5 expressing macrophages in detail, it demonstrated that IRF5 can potentially be used as a marker in a different disease setting and tissue. This is particularly important since IRF5 associates not only with RA but also with several other autoimmune diseases such as inflammatory bowel disease, asthma, and systemic lupus erythematosus [35–38].

It has recently become clear that in addition to macrophages derived from infiltrating monocytes generated in bone marrow, tissue-resident macrophages of different origin may also play a crucial role in inflammation [39, 40]. Moreover, transcriptional profiling of macrophages from different origins demonstrated heterogeneity of macrophage populations and revealed tissue-specific transcriptional signatures [32]. This suggests that identification of subset specific transcription factors is needed to tease out the contribution of different macrophage subtypes in inflammatory processes, especially in disease-related chronic inflammation or autoimmunity that so far received less attention [41]. We hypothesise that IRF5 could play a critical role in tracking inflammatory macrophages in various inflammatory diseases.

4. Conclusions

To conclude, this study clearly demonstrates that IRF5 is highly expressed in murine proinflammatory macrophages and may be utilised as a reliable marker for macrophages at sites of inflammation. Murine GM-BMDMs express IRF5 and proinflammatory cytokines *in vitro* when challenged with LPS. We show that it is possible to label intracellular IRF5 in these proinflammatory macrophages, as well as in macrophages in an inflamed knee during the progression of an experimental mouse model of antigen-induced arthritis. Thus, this study describes a useful method for tracking proinflammatory macrophages and demonstrates its feasibility in a murine disease model.

References

[1] D. M. Mosser and J. P. Edwards, "Exploring the full spectrum of macrophage activation," *Nature Reviews Immunology*, vol. 8, no. 12, pp. 958–969, 2008.

[2] S. K. Biswas and A. Mantovani, "Macrophage plasticity and interaction with lymphocyte subsets: cancer as a paradigm," *Nature Immunology*, vol. 11, no. 10, pp. 889–896, 2010.

[3] S. Gordon, "Alternative activation of macrophages," *Nature Reviews Immunology*, vol. 3, no. 1, pp. 23–35, 2003.

[4] A. J. Fleetwood, T. Lawrence, J. A. Hamilton, and A. D. Cook, "Granulocyte-macrophage colony-stimulating factor (CSF) and macrophage CSF-dependent macrophage phenotypes display differences in cytokine profiles and transcription factor activities: implications for CSF blockade in inflammation," *Journal of Immunology*, vol. 178, no. 8, pp. 5245–5252, 2007.

[5] F. A. W. Verreck, T. de Boer, D. M. L. Langenberg et al., "Human IL-23-producing type 1 macrophages promote but IL-10-producing type 2 macrophages subvert immunity to (myco)bacteria," *Proceedings of the National Academy of Sciences of the United States of America*, vol. 101, no. 13, pp. 4560–4565, 2004.

[6] J. A. Hamilton, "Colony-stimulating factors in inflammation and autoimmunity," *Nature Reviews Immunology*, vol. 8, no. 7, pp. 533–544, 2008.

[7] F. A. W. Verreck, T. de Boer, D. M. L. Langenberg, L. van der Zanden, and T. H. M. Ottenhoff, "Phenotypic and functional profiling of human proinflammatory type-1 and anti-inflammatory type-2 macrophages in response to microbial antigens and IFN-γ- and CD40L-mediated costimulation," *Journal of Leukocyte Biology*, vol. 79, no. 2, pp. 285–293, 2006.

[8] A. Kennedy, U. Fearon, D. J. Veale, and C. Godson, "Macrophages in synovial inflammation," *Frontiers in Immunology*, vol. 2, article 52, 2011.

[9] T. J. M. Smeets, M. C. Kraan, S. Galjaard, P. P. Youssef, M. D. Smith, and P. P. Tak, "Analysis of the cell infiltrate and expression of matrix metalloproteinases and granzyme B in paired synovial biopsy specimens from the cartilage-pannus junction in patients with RA," *Annals of the Rheumatic Diseases*, vol. 60, no. 6, pp. 561–565, 2001.

[10] P. Barrera, "Synovial macrophage depletion with clodronate-containing liposomes in rheumatoid arthritis," *Arthritis & Rheumatism*, vol. 43, no. 9, pp. 1951–1959, 2000.

[11] P. L. E. M. van Lent, A. E. M. Holthuysen, N. van Rooijen, L. B. A. van de Putte, and W. B. van den Berg, "Local removal of phagocytic synovial lining cells by clodronate- liposomes decreases cartilage destruction during collagen type II arthritis," *Annals of the Rheumatic Diseases*, vol. 57, no. 7, pp. 408–413, 1998.

[12] K. Nistala, S. Adams, H. Cambrook et al., "Th17 plasticity in human autoimmune arthritis is driven by the inflammatory environment," *Proceedings of the National Academy of Sciences of the United States of America*, vol. 107, no. 33, pp. 14751–14756, 2010.

[13] M. Chabaud, E. Lubberts, L. Joosten, W. van den Berg, and P. Miossec, "IL-17 derived from juxta-articular bone and synovium contributes to joint degradation in rheumatoid arthritis," *Arthritis Research*, vol. 3, no. 3, pp. 168–177, 2001.

[14] T. Krausgruber, K. Blazek, T. Smallie et al., "IRF5 promotes inflammatory macrophage polarization and TH1-TH17 responses," *Nature Immunology*, vol. 12, no. 3, pp. 231–238, 2011.

[15] A. Takaoka, H. Yanai, S. Kondo et al., "Integral role of IRF-5 in the gene induction programme activated by Toll-like receptors," *Nature*, vol. 434, no. 7030, pp. 243–249, 2005.

[16] K. Honda and T. Taniguchi, "IRFs: master regulators of signalling by Toll-like receptors and cytosolic pattern-recognition receptors," *Nature Reviews Immunology*, vol. 6, no. 9, pp. 644–658, 2006.

[17] B. J. Barnes, P. A. Moore, and P. M. Pitha, "Virus-specific activation of a novel Interferon Regulatory Factor, IRF-5, results in the induction of distinct interferon α genes," *Journal of Biological Chemistry*, vol. 276, no. 26, pp. 23382–23390, 2001.

[18] E. A. Stahl, S. Raychaudhuri, E. F. Remmers et al., "Genome-wide association study meta-analysis identifies seven new rheumatoid arthritis risk loci," *Nature Genetics*, vol. 42, no. 6, pp. 508–514, 2010.

[19] K. Dawidowicz, Y. Allanore, M. Guedj et al., "The Interferon Regulatory Factor 5 gene confers susceptibility to rheumatoid arthritis and influences its erosive phenotype," *Annals of the Rheumatic Diseases*, vol. 70, no. 1, pp. 117–121, 2011.

[20] D. L. Asquith, A. M. Miller, I. B. McInnes, and F. Y. Liew, "Animal models of rheumatoid arthritis," *European Journal of Immunology*, vol. 39, no. 8, pp. 2040–2044, 2009.

[21] P. J. Egan, A. van Nieuwenhuijze, I. K. Campbell, and I. P. Wicks, "Promotion of the local differentiation of murine Th17 cells by synovial macrophages during acute inflammatory arthritis," *Arthritis and Rheumatism*, vol. 58, no. 12, pp. 3720–3729, 2008.

[22] M. Y. Balkhi, K. A. Fitzgerald, and P. M. Pitha, "Functional regulation of MyD88-activated Interferon regulatory factor 5 by K63-linked polyubiquitination," *Molecular and Cellular Biology*, vol. 28, no. 24, pp. 7296–7308, 2008.

[23] H. C. C. Foreman, S. van Scoy, T. F. Cheng, and N. C. Reich, "Activation of interferon regulatory factor 5 by site specific phosphorylation," *PLoS ONE*, vol. 7, no. 3, Article ID e33098, 2012.

[24] M. Y. Balkhi, K. A. Fitzgerald, and P. M. Pitha, "IKKα negatively regulates IRF-5 function in a MyD88-TRAF6 pathway," *Cellular Signalling*, vol. 22, no. 1, pp. 117–127, 2010.

[25] K. Inaba, M. Inaba, N. Romani et al., "Generation of large numbers of dendritic cells from mouse bone marrow cultures supplemented with granulocyte/macrophage colony-stimulating factor," *Journal of Experimental Medicine*, vol. 176, no. 6, pp. 1693–1702, 1992.

[26] A. Celada, M. J. Klemsz, and R. A. Maki, "Interferon-γ activates multiple pathways to regulate the expression of the genes for major histocompatibility class II I-Aβ, tumor necrosis factor and complement component C3 in mouse macrophages," *European Journal of Immunology*, vol. 19, no. 6, pp. 1103–1109, 1989.

[27] M. Rescigno, S. Citterio, C. Thèry et al., "Bacteria-induced neobiosynthesis, stabilization, and surface expression of functional class I molecules in mouse dendritic cells," *Proceedings of the National Academy of Sciences of the United States of America*, vol. 95, no. 9, pp. 5229–5234, 1998.

[28] S. C. Sicher, G. W. Chung, M. A. Vazquez, and C. Y. Lu, "Augmentation or inhibition of IFN-γ-induced MHC class II expression by lipopolysaccharides: the roles of TNF-α and nitric oxide, and the importance of the sequence of signaling," *Journal of Immunology*, vol. 155, no. 12, pp. 5826–5834, 1995.

[29] R. de Lorenzi, R. Gareus, S. Fengler, and M. Pasparakis, "GFP-p65 knock-in mice as a tool to study NF-κB dynamics *in vivo*," *Genesis*, vol. 47, no. 5, pp. 323–329, 2009.

[30] J. MacMicking, Q. W. Xie, and C. Nathan, "Nitric oxide and macrophage function," *Annual Review of Immunology*, vol. 15, pp. 323–350, 1997.

[31] S. Gordon and F. O. Martinez, "Alternative activation of macrophages: mechanism and functions," *Immunity*, vol. 32, no. 5, pp. 593–604, 2010.

[32] E. L. Gautier, "Gene-expression profiles and transcriptional regulatory pathways that underlie the identity and diversity of mouse tissue macrophages," *Nature Immunology*, vol. 13, no. 11, pp. 1118–1128, 2012.

[33] R. C. Stone, D. Feng, J. Deng et al., "Interferon Regulatory Factor 5 activation in monocytes of systemic lupus erythematosus

patients is triggered by circulating autoantigens independent of type i interferons," *Arthritis and Rheumatism*, vol. 64, no. 3, pp. 788–798, 2012.

[34] C. Draijer, P. Robbe, C. E. Boorsma, M. N. Hylkema, and B. N. Melgert, "Characterization of macrophage phenotypes in three murine models of house-dust-mite-induced asthma," *Mediators of Inflammation*, vol. 2013, Article ID 632049, 10 pages, 2013.

[35] V. Dideberg, G. Kristjansdottir, L. Milani et al., "An insertion-deletion polymorphism in the interferon regulatory factor 5 (IRF5) gene confers risk of inflammatory bowel diseases," *Human Molecular Genetics*, vol. 16, no. 24, pp. 3008–3016, 2007.

[36] G. Gathungu, C. K. Zhang, W. Zhang, and J. H. Cho, "A two-marker haplotype in the IRF5 gene is associated with inflammatory bowel disease in a North American cohort," *Genes and Immunity*, vol. 13, no. 4, pp. 351–355, 2012.

[37] C. Wang, M. J. Rose-Zerilli, G. H. Koppelman et al., "Evidence of association between Interferon Regulatory Factor 5 gene polymorphisms and asthma," *Gene*, vol. 504, no. 2, pp. 220–225, 2012.

[38] W. D. Xu, H. F. Pan, Y. Xu, and D. Q. Ye, "Interferon regulatory factor 5 and autoimmune lupus," *Expert Reviews in Molecular Medicine*, vol. 15, article e6, 2013.

[39] L. C. Davies, M. Rosas, S. J. Jenkins et al., "Distinct bone marrow-derived and tissue-resident macrophage lineages proliferate at key stages during inflammation," *Nature Communications*, vol. 4, article 1886, 2013.

[40] S. J. Jenkins, D. Ruckerl, P. C. Cook et al., "Local macrophage proliferation, rather than recruitment from the blood, is a signature of TH2 inflammation," *Science*, vol. 332, no. 6035, pp. 1284–1288, 2011.

[41] L. C. Davies, S. J. Jenkins, J. E. Allen, and P. R. Taylor, "Tissue-resident macrophages," *Nature Immunology*, vol. 14, no. 10, pp. 986–995, 2013.

Hindawi Publishing Corporation
Mediators of Inflammation
Volume 2013, Article ID 636812, 11 pages
http://dx.doi.org/10.1155/2013/636812

Research Article

Modulation of Conjunctival Goblet Cell Function by Inflammatory Cytokines

L. Contreras-Ruiz,[1] A. Ghosh-Mitra,[2] M. A. Shatos,[2] D. A. Dartt,[2] and S. Masli[1]

[1] *Department of Ophthalmology, Boston University School of Medicine, Boston, MA 02118, USA*
[2] *Department of Ophthalmology, Harvard Medical School, Schepens Eye Research Institute and Massachusetts Eye and Ear, Boston, MA 02114, USA*

Correspondence should be addressed to S. Masli; smasli@bu.edu

Received 19 August 2013; Accepted 13 November 2013

Academic Editor: Mohammad Athar

Ocular surface inflammation associated with Sjögren's syndrome is characterized by a loss of secretory function and alteration in numbers of mucin secreting goblet cells. Such changes are a prominent feature of ocular surface inflammatory diseases and are attributed to inflammation; however, the exact effect of the inflammatory cytokines on conjunctival goblet cell function remains largely unknown. In this study, we developed a primary culture of mouse goblet cells from conjunctival tissue and evaluated the effects on their function by inflammatory cytokines detected in the conjunctiva of mouse model of Sjögren's syndrome (Thrombospondin-1 deficient mice). We found that apoptosis of goblet cells was primarily induced by TNF-α and IFN-γ. These two cytokines also inhibited mucin secretion by goblet cells in response to cholinergic stimulation, whereas IL-6 enhanced such secretion. No changes in secretory response were detected in the presence of IL-13 or IL-17. Goblet cells proliferated to varying degrees in response to all the tested cytokines with the greatest response to IL-13 followed by IL-6. Our results therefore reveal that inflammatory cytokines expressed in the conjunctiva during an ocular surface disease directly disrupt conjunctival goblet cell functions, compromising the protective function of tears, thereby contributing to ocular surface damage.

1. Introduction

Mucin-secreting goblet cells are widely distributed throughout mammalian mucosal surfaces, such as the gastrointestinal, urogenital, and respiratory tracts, where they play a key role in hydrating, lubricating, and clearing pathogens from the underlying epithelium [1]. The importance of goblet cells as major producers of mucins is well established, with critical emphasis placed on the number of functional goblet cells and on the amount and rate at which they synthesize mucins. In fact, alterations in goblet cell numbers and mucin secretion are prominent features of mucosa associated diseases, with increased goblet cell numbers and hypersecretion in conditions such as asthma or cystic fibrosis [2, 3], and mucin depletion and diminished goblet cell density in intestinal diseases such as inflammatory bowel disease or ulcerative colitis [4, 5].

In the eye, goblet cells are the principal secretory cell in the conjunctival epithelium, where they function in lubricating the ocular surface epithelia during the blink response stabilizing the tear film, and as a physical barrier to pathogen penetration [6]. Alterations in goblet cell secretion lead to an unstable tear film and a vulnerable ocular surface. Goblet cell loss has been reported in several inflammatory diseases of the ocular surface, including Stevens-Johnson syndrome, ocular mucous membrane pemphigoid, alkali burn, neutrophilic keratitis, graft-versus-host-disease, and Sjögrens's syndrome (SS) [7–9].

Although the mechanisms leading to goblet cell changes in the eye are not entirely understood, evidence in other mucosal tissues suggests that inflammation may have an important contribution. It is known that IL-13 is involved in lung goblet cell hyperplasia and mucus hypersecretion [10], while IFN-γ inhibited IL-13-induced goblet cell hyperplasia in a mouse model of airway inflammation [11] and it is a potent inhibitor of mucin secretion in a human colonic goblet cell line [12]. Although both IL-13 and IFN-γ have been

reported in ocular inflammatory conditions it is not known whether conjunctival goblet cells respond similarly to those in the lungs with mucus hypersecretion or with inhibition of secretion [13, 14]. It was also previously reported that overexpression of IL-17A induces respiratory mucous metaplasia [15]. However, the role of inflammation in conjunctival goblet cell function has remained unaddressed, partly due to lack of *in vitro* cell cultures that allow study of goblet cells without altering their phenotype and function. Therefore, we have developed a primary culture of mouse goblet cells from conjunctival tissue to evaluate the effects of inflammatory cytokines on goblet cells with respect to processes such as mucin secretion, proliferation, and apoptosis.

We have previously described extensively an autoimmune SS-associated ocular phenotype in Thrombospondin-1 (TSP-1) deficient mice that resembles the changes detectable in SS patients [16]. These mice spontaneously and progressively develop inflammation in the conjunctiva, with appearance of inflammatory infiltrates, tissue expression of Th1 and Th17 inflammatory cytokines, along with the development of inflammatory T cell effectors in their draining lymph nodes [17]. Similar to SS patients, significant changes in goblet cell numbers are detected in TSP-1 deficient mice along with reduced tear mucin level.

Our primary purpose in this study was to evaluate whether inflammation in TSP-1 deficient conjunctiva disrupts the functions of goblet cells. We used cultured goblet cells from mouse conjunctiva to study the effect of inflammatory cytokines detected in TSP-1 null conjunctiva on secretory and proliferative properties of goblet cells. The studies described herein indicate that mouse goblet cells, as shown previously with rat and human goblet cells [18, 19], can be isolated from mouse conjunctiva retaining *in vivo* characteristics of mouse goblet cells, and that the proinflammatory cytokines expressed in TSP-1 null conjunctiva induce their proliferation in varying degrees. Greatest proliferation was induced by IL-13 with IL-6 following closely. Both TNF-α and IFN-γ induced goblet cell apoptosis while inhibiting mucin secretion induced by cholinergic stimulation. Contrary to this effect IL-6 enhanced such mucin secretion by goblet cells. Our results therefore reveal that inflammation can directly disrupt conjunctival goblet cell functions resulting in an altered tear composition with a compromised protective function, which contributes to ocular surface damage.

2. Materials and Methods

2.1. Mice. C57BL/6 (H-2b) mice, 4 to 22 weeks old, were purchased from Charles River Laboratories (Wilmington, MA). TSP-1 null mice (C57BL/6 background), originally received from Dr. J. Lawler (BIDMC, Harvard Medical School, Boston, MA) were bred in-house in a pathogen-free facility at Schepens Eye Research Institute, Boston, MA. All experiments were conducted in accordance with institutional guidelines and ARVO Statement for the Use of Animals in Ophthalmic and Vision Research.

2.2. RT-PCR. Total RNA was isolated from conjunctivas harvested from WT or TSP-1 null mice (6, 8, and 12 weeks, $n = 3$ to 5) using TRIzol Reagent (Life Technologies, Carlsbad, CA) according to the manufacturer's instructions. cDNA was synthesized by reverse transcribing RNA using oligo (dT) and M-MLV RT (Promega, Madison, WI). Real-time PCR assay was performed on the Eppendorf Realplex2 system (Eppendorf AG, Hamburg, Germany) using SYBR Green PCR Master Mix (Applied Biosystems, Carlsbad, CA) to determine relative quantitative expression levels of Interleukin (IL)-13 and GATA3 genes. IL-13 primers (F-5′-AGAATGGCCTGTTACACTCA-3′ and R-5′-TTTCCGGTTTCTAGTTTGA-3′), GATA3 primers (F-5′-GCCTGGCGCCGTCTTGATA-3′ and R-5′-CCCGGTCAGATTGCG TAGCTC-3′), and glyceraldehyde-3-phosphate dehydrogenase primers (F-5′-CGAGAATGGGAAGCTTGTCA-3′ and R-5′-AGACACCAGTAGACTCCACGACAT-3′) were used. Amplification reactions were set up in quadruplicates with the thermal profile: 95°C for three minutes, 40 cycles at 95°C for ten seconds, 53°C for ten seconds, and 72°C for ten seconds. To verify the specificity of the amplification reaction, a melting curve analysis was performed. Fluorescence signal generated at each cycle was analyzed using system software. The threshold cycle values were used to determine relative quantification of gene expression with glyceraldehyde-3-phosphate dehydrogenase as a reference gene.

2.3. Isolation and Culture of Goblet Cells. Goblet cells from mouse conjunctival pieces were grown in organ culture, as described previously for rat and humans [18, 19]. Conjunctival tissues were excised from 4- to 22-week-old male mice and placed into Hank's balanced salt solution (Lonza, Walkersville, MD). Tissues were finely minced into small pieces that were anchored onto scored 24-well culture plates. Approximately 65 to 90 explants were obtained from each animal and four pieces of tissue were anchored per culture well. The culture dishes contained just enough medium to cover the bottom of the well so that the tissue would receive nutrients through surface tension. Explants were fed every other day with RPMI-1640 medium (Lonza, Walkersville, MD) supplemented with 10% heat-inactivated fetal calf serum (Thermo Fisher Scientific, Waltham, MA), 1 mM sodium pyruvate, 10 mM HEPES, 100 μg/mL penicillin-streptomycin, and 1X nonessential amino-acid mixture (Lonza, Walkersville, MD) and grown under routine culture conditions of 5% CO_2 at 37°C. Cells were permitted to grow from the tissue explant for 14 days until reaching 85% confluence; and then the explant was removed and discarded.

2.4. Immunofluorescence. Cultured conjunctival goblet cells were fixed in ice-cold methanol and examined for the presence of cytokeratin (CK)-4, CK-7, and MUC5AC. Cells were incubated at room temperature for one hour with blocking buffer composed of phosphate-buffered saline (PBS) with 2% bovine serum albumin and 0.02% Triton-X (all from Sigma-Aldrich). Afterwards, the cells were incubated overnight at 4°C with the primary antibodies anti-CK-7 (10 μg/mL), which recognizes a goblet cell-specific keratin [20], anti-CK-4 (10 μg/mL), a specific marker for stratified, squamous, nongoblet epithelial cells [20], and MUC5AC (2 μg/mL),

specific for mucin produced by goblet cells [21] (all from Abcam, Cambridge, MA). After rinsing in PBS, the cells were incubated with AlexaFluor 488- or 568-conjugated secondary antibodies (6 μg/mL; Life Technologies, Carlsbad, CA) for one hour at room temperature, washed, and mounted for microscopy examination in a Nikon Eclipse E-800 fluorescence microscope (Nikon, Melville, NY).

2.5. Flow Cytometry. Cultured conjunctival goblet cells were stained with eFluor 780-conjugated Fixable Viability Dye (eBioscience, San Diego, CA). Intracellular MUC5AC was evaluated with anti-MUC5AC antibody (Abcam) and DyLight 649-conjugated secondary antibody (Abcam) using an intracellular staining kit (eBioscience) as per the manufacturer's instructions. Fluorescence-labeled cells were analyzed using BD LSRII Flow Cytometer (BD Bioscience, San Jose, CA). Further analysis of the data was performed using FlowJo v9.4.10 software (Tree Star, Inc., Ashland, OR).

2.6. Cytokine Treatments. To evaluate the effect of inflammatory conditions on goblet cell function, cultured conjunctival goblet cells were grown for 14 days until 85% confluence was reached. Prior to any cytokine exposure, cells were maintained for 24 h in serum-free medium. After this, cultured conjunctival goblet cells were treated with 10 ng/mL of the recombinant cytokines IL-13, IFN-γ, TNF-α, IL-6, and IL-17A (R&D Systems, Minneapolis, MN) for 24 h. Viability of cells in response to stimulatory cytokines (63% IL-13-treated, 66% in IL-6-treated) was comparable to that in response to inhibitory cytokines (65% IFN-γ-treated, 71% TNF-α-treated) and untreated control cells (66%).

2.7. MUC5AC Secretion: ELISA. Treated and control cultures of conjunctival goblet cells were stimulated with the cholinergic agonist carbachol (10^{-3} M, Sigma-Aldrich) for one hour and then MUC5AC secretion was measured in the supernatants using the Mucin-5 Subtype AC (MUC5AC) ELISA kit (TSZ ELISA, Waltham, MA) according to the manufacturer's instructions. The cells were also collected and cell homogenates were analyzed for the total amount of protein using the BCA Protein Assay Kit (Pierce, Rockford, IL). MUC5AC secretion was normalized to total protein in the homogenate, and the result was presented as MUC5AC ng/mg of cellular protein.

2.8. Cell Proliferation and Apoptosis. Treated and control cultured goblet cells were pulsed with the thymidine analog, 5-bromo-2-deoxyuridine (BrdU, 1 mM) (EMD Millipore, Billerica, MA) for 24 h. Afterwards, the cells were fixed and permeabilized using an intracellular staining kit (eBioscience), treated with DNase (Sigma-Aldrich) to expose incorporated BrdU and stained with a biotin-conjugated anti-BrdU antibody (1 μg/10^6 cells; Invitrogen) for one hour at 4°C. After rinsing in PBS, cells were incubated with streptavidin-FITC-conjugated reagent (1 μg/10^6 cells; BD Bioscience) for one hour at 4°C and stained with the DNA dye 7-amino-actinomycin-D (7-AAD) (eBioscience). BrdU content (FITC) and total DNA content (7-AAD) were determined using BD LSRII Flow Cytometer and FlowJo software, and the percentage of cells in each of the G_0-G_1, S, G_2-M phases and apoptotic cells were calculated.

2.9. Statistical Analysis. Student's t-test was used to determine significant differences between mean values of experimental and control groups. Error bars in figures represent ± standard error of the mean (SEM). $P < 0.05$ was considered statistically significant.

3. Results

3.1. Th2 Inflammatory Response in TSP-1 Null Conjunctiva. In human SS pathology a dynamic balance between Th1 and Th2 cytokines was reported with the latter found to prevail in low-grade infiltration of salivary glands [22]. Similarly Th2-mediated pathology was reported in the MRL/lpr mouse model of SS [23]. To determine if the spontaneous ocular surface inflammation noted in TSP-1 deficient mice involves Th2 cytokines, we examined conjunctival expression of the transcription factor GATA-3, an essential mediator of these cytokines. We also correlated this expression with that of a representative Th2 cytokine IL-13. Real-time PCR analysis on RNA isolated from conjunctiva derived from WT or TSP-1 null mice at ages 6, 8, and 12 weeks was performed to study the expression levels of GATA-3 and IL-13. Although no differences in GATA3 expression were detectable at 6 weeks of age, at 8 and 12 weeks the expression was significantly increased in TSP-1 deficient conjunctiva compared with the WT control tissues (Figure 1(a)). Consistent with this result, overexpression of IL-13 was detected in TSP-1 null conjunctiva at all ages compared to the aged-matched WT control tissues (Figure 1(b)). Together these results suggest involvement of Th2-mediated pathology in the ocular surface inflammation in TSP-1 null mice similar to that reported by others in SS.

3.2. Primary Mouse Conjunctival Goblet Cell Culture. It has been reported that IL-13 is involved in lung goblet cell hyperplasia and mucus hypersecretion [10]. Increased expression of IL-13 in TSP-1 null conjunctiva is consistent with increased goblet cell numbers detected in the earlier stages of ocular surface inflammation between 8 and 12 weeks of age [16]. However, by 15 weeks of age a significant decline in filled goblet cells is detected in TSP-1 null conjunctiva as compared to age-matched WT controls [17]. To allow for an investigation of a direct effect of conjunctival cytokines, if any, on goblet cell proliferation or mucin secretion, we established *in vitro* cultures of goblet cells derived from conjunctival tissue explants based on a method originally described using rat and human tissue [18, 19].

Cells were grown from WT conjunctival explants. After 14 days of culture, epithelial morphology of most of the cells was apparent with the presence of distinct secretory granules. To determine if these were goblet cells extensive characterization with goblet cell-specific markers was performed. These included goblet cell derived soluble mucin, MUC5AC, and an intermediate filament associated solely with goblet cells, cytokeratin 7 (CK-7). Any presence of stratified

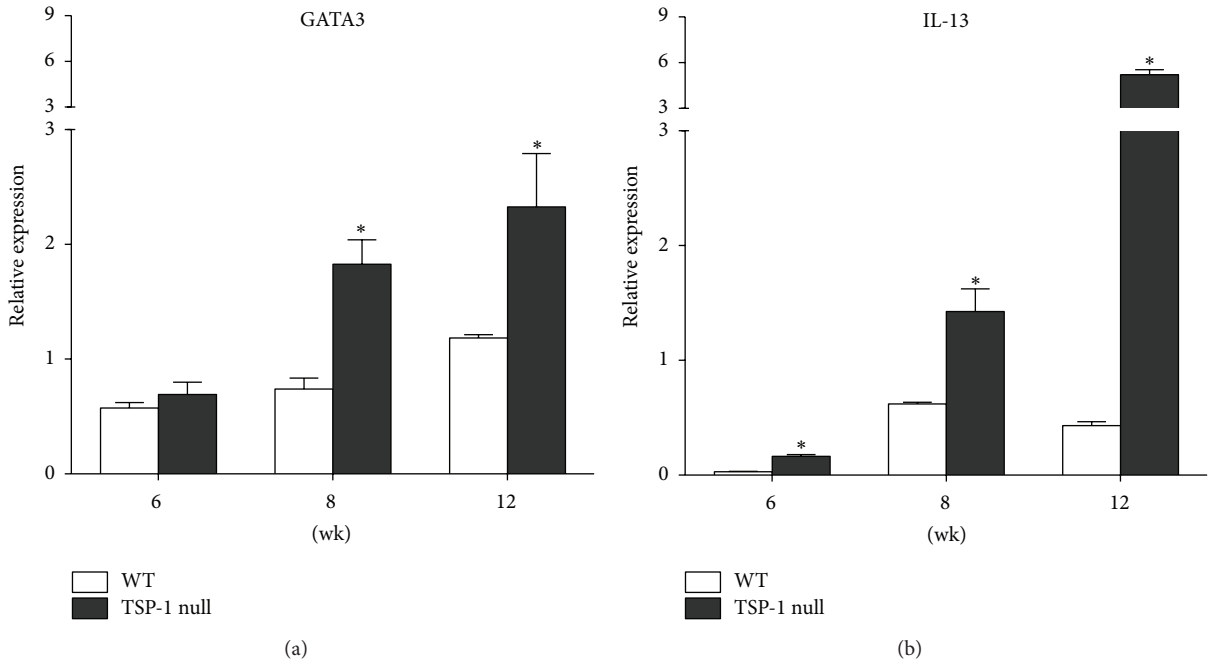

Figure 1: Th2-type inflammatory response is increased in TSP-1 null conjunctiva. Conjunctiva tissues were collected from WT and TSP-1 null mice at 6, 8, and 12 weeks. Extracted RNA was analyzed in a real time PCR assay to determine the levels of message for the Th2 cytokine IL-13 and the Th2-associated transcription factor GATA3 $^{*}P < 0.05$.

squamous epithelial cells was ruled out by staining for their marker cytokeratin 4 (CK-4). As seen in Figure 2(a), most cells in culture stained positively for goblet cell specific markers MUC5AC and CK-7 with a detectable intense cytosolic signal for both these markers. On the other hand, no signal was detected when cells were stained for CK-4 resembling the isotype control staining with no fluorescence signal. Furthermore, flow cytometric analysis of cultured cells stained for intracellular MUC5AC was performed to establish a quantitative estimate of goblet cells in the culture. As shown in Figure 2(b), a strong signal was detected in positive control HT-29 cell line as all the cells stained positively for MUC5AC, and similarly most cells (>85%) from primary cultures were positively stained for MUC5AC. These results confirmed that almost all cells in our conjunctival explant-derived primary cultures were goblet cells that can be further used in an *in vitro* assay.

3.3. Deficiency of TSP-1 in Goblet Cells Does Not Alter Their Ability to Secrete MUC5AC in Response to Cholinergic Stimulation. Cultured goblet cells respond to *in vitro* cholinergic stimulation induced by carbachol by releasing their vesicular content of MUC5AC into the culture supernatant. In rat and human goblet cell cultures this was determined using an assay that detects glycosylated carbohydrates [18, 19]. We used MUC5AC ELISA to assess the secretory function of WT and TSP-1 null goblet cells in primary cultures. These cells were generated from either 4-week or 22-week-old mice. Upon carbachol stimulation MUC5AC in the culture supernatant was compared to that collected from unstimulated cells. As shown in Figure 3, both 4-week-old WT and TSP-1 null conjunctiva-derived primary cultures of goblet cells responded to carbachol stimulus by secreting significantly increased amounts of MUC5AC in culture supernatants. A similar response was noted in cultures generated from 22-week-old WT mice. However, such increased release of MUC5AC was inhibited when goblet cell cultures were derived from 22-week-old TSP-1 null mice, suggesting a loss of their secretory ability. These results implicate active ocular surface inflammation in older TSP-1 null mice as a potential cause of the disrupted secretory function of goblet cells.

3.4. Expression of Cytokine Receptors in Primary Cultures of Conjunctival Goblet Cells. During ocular surface inflammation the conjunctival cytokine environment in TSP-1 null mice includes Th1 (TNFα, IFNγ) and Th17 (IL-17A, IL-6) besides Th2 cytokines, and these are largely detectable by 6 weeks of age with a progressive increase by 12 weeks [17]. To determine if these cytokines may inhibit the secretory function of TSP-1 null goblet cells as detected in our results, we first assessed the presence of receptors for the cytokines that were detected in TSP-1 null conjunctiva during ocular surface inflammation. Cultured goblet cells from WT mice were stained with immunofluorescence-conjugated antibodies for the indicated receptors and stained cells were analyzed by flow cytometry. Expression of each receptor was evaluated by comparing mean fluorescence intensity (MFI) of the staining with receptor-specific antibody to that of a corresponding isotype control antibody. As shown in Figure 4, receptors for all the cytokines tested were detectable on goblet cells as indicated by the significantly increased receptor specific MFI. These results suggest that cytokines such as IL-13, IFN-γ, TNF-α, IL-6, and IL-17 that are detectable during

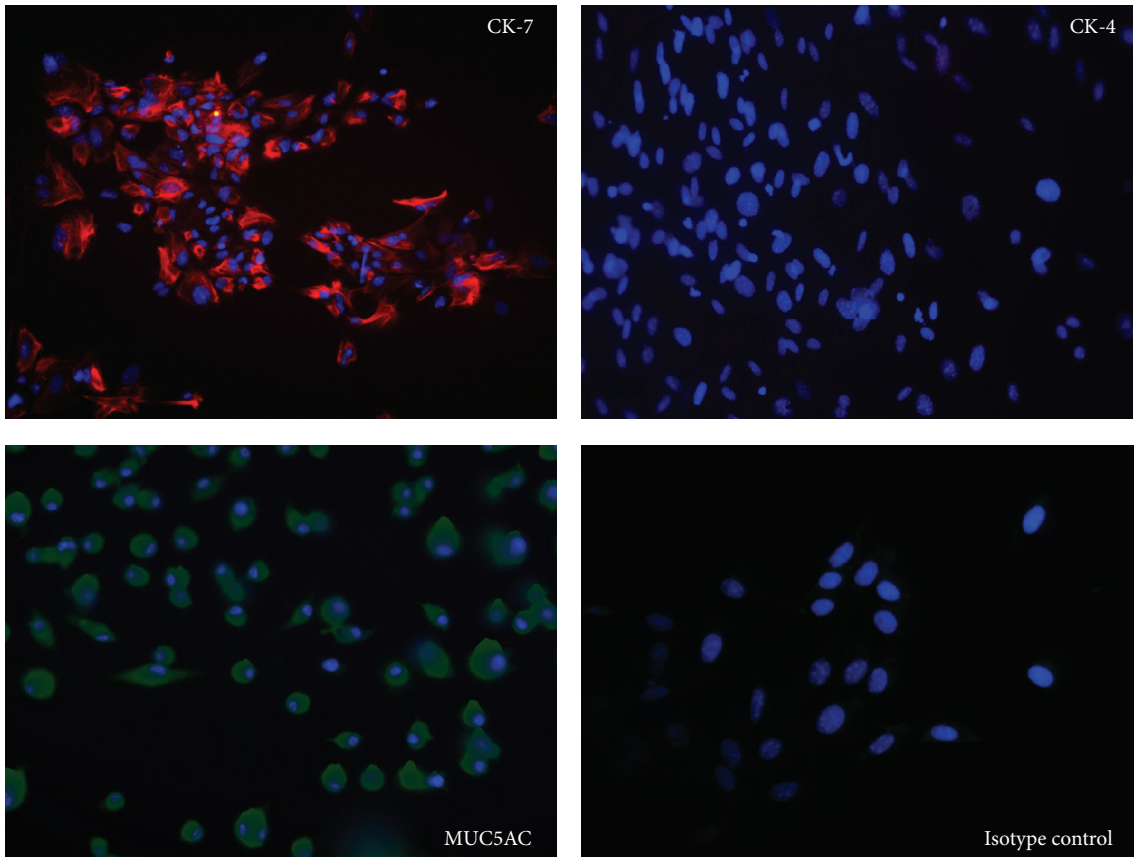

(a)

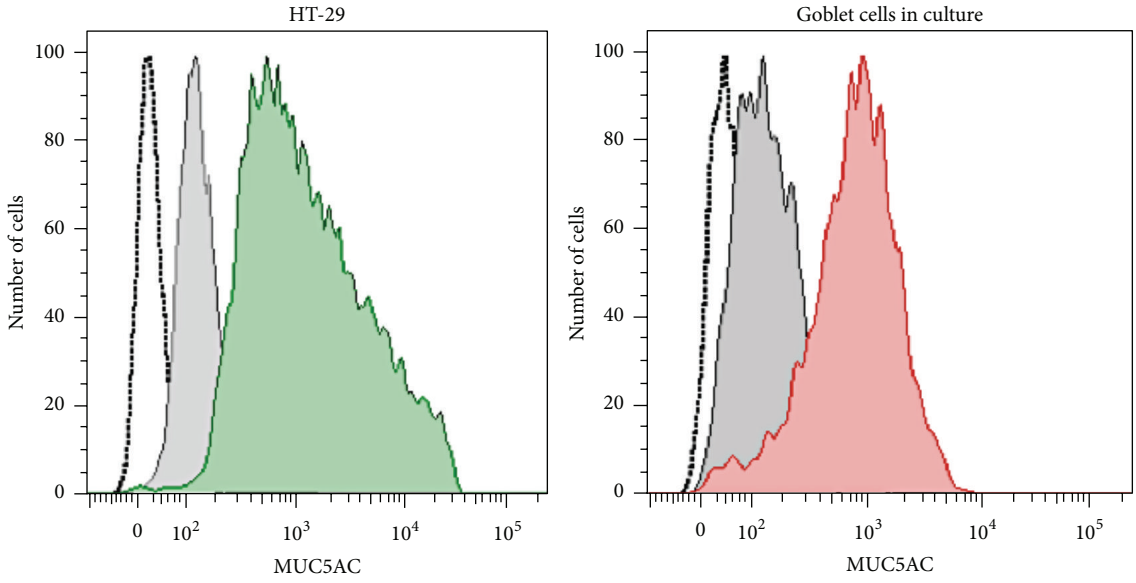

(b)

Figure 2: Primary mouse goblet cell cultures express goblet cell specific markers. (a) Cells were grown from WT conjunctival explants for 14 days, and the expression of goblet cell specific (CK-7-red and MUC5AC-green) and stratified squamous cell specific (CK-4-red) markers was analyzed by immunofluorescence. Nuclei were counterstained with DAPI (blue). Magnification = ×20. (b) Flow cytometric analysis of goblet cells for the expression of MUC5AC. Unstained cells (empty histogram), isotype controls (filled grey histogram), colonic HT-29 cells (filled green histogram), and cultured goblet cells (filled red histogram).

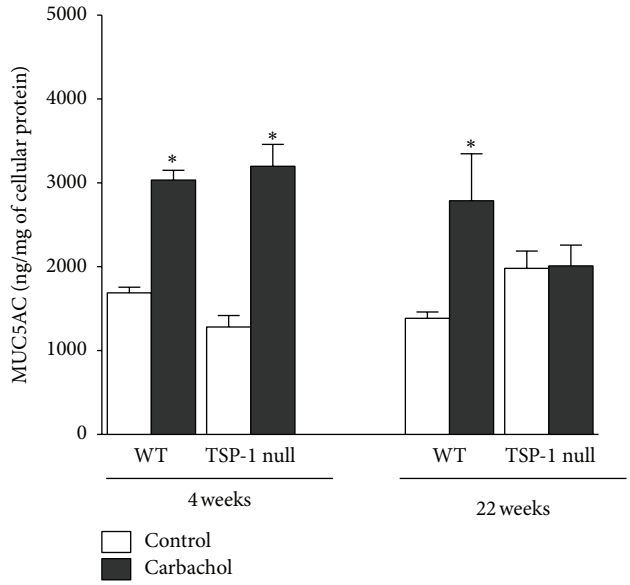

Figure 3: Conjunctival inflammation associated with TSP-1 deficiency prevents carbachol-mediated MUC5AC secretion. Cultured goblet cells were grown from conjunctival explants of WT and TSP-1 null mice at 4 and 22 weeks of age. Goblet cells were stimulated with the cholinergic agonist carbachol, and MUC5AC secretion evaluated by ELISA in the supernatant. $^{*}P < 0.05$.

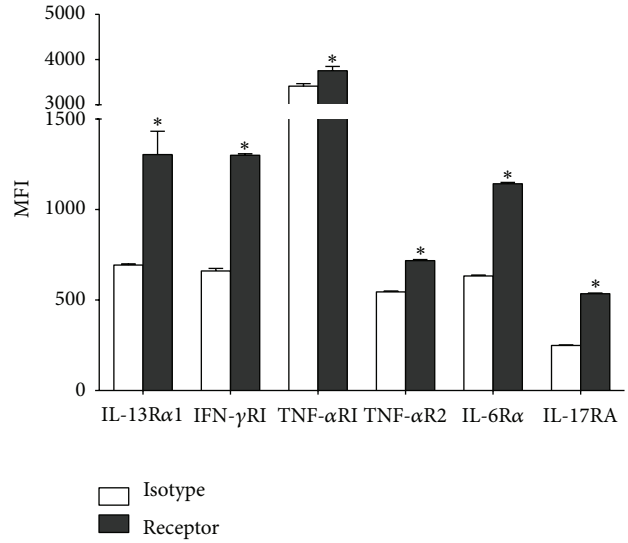

Figure 4: Expression of cytokine receptors in primary cultures of conjunctival goblet cells. The expression of the cytokine receptors IL-13Rα1, IFN-γRI, TNF-αR1, TNF-αR2, IL-6Rα, and IL-17RA was detected using flow cytometry in primary cultures of conjunctival goblet cells. Results are presented as mean fluorescence intensity (MFI) for the cytokine receptors (black bars) and the corresponding isotype controls (white bars). $^{*}P < 0.05$.

ocular surface inflammation in TSP-1 null mice have the potential to influence goblet cells directly via their respective receptors.

3.5. Inflammatory Cytokines Alter MUC5AC Secretion by Goblet Cells in Response to Cholinergic Stimulation. To determine if proinflammatory cytokines detected in TSP-1 null conjunctiva may alter the secretory function of goblet cells, we exposed goblet cell cultures derived from WT conjunctiva explants to Th1 (IFN-γ and TNF-α), Th2 (IL-13), and Th17 (IL-17A and IL-6) cytokines for 24 hr, prior to their cholinergic stimulation with carbachol. As shown in Figure 5, carbachol-mediated mucin secretion of goblet cells exposed to both Th1 cytokines (IFN-γ and TNF-α) was significantly reduced as compared to those secreted by untreated cells. In contrast carbachol-induced secretion was significantly enhanced if cells were treated with IL-6. Carbachol stimulation of IL-17A or IL-13 exposed goblet cells did not alter their mucin secretion in comparison to untreated goblet cells.

These results suggest that during ocular inflammation, presence of Th1 cytokines in the tissue environment could directly inhibit goblet cell secretory function. These results are consistent with reduced levels of MUC5AC detected in pilocarpine-induced tears (cholinergic stimulation) collected from TSP-1 null mice with ocular surface inflammation as compared to those from WT control mice [17]. Together, our results suggest that in an inflammatory environment in TSP-1 null conjunctiva the inhibitory effects of Th1 cytokines predominate over the enhancing effect of IL-6 on goblet cell secretory function.

3.6. Inflammatory Cytokines Alter Goblet Cell Proliferation and Apoptosis. Changes in goblet cell numbers in TSP-1 null mice range from a significant increase during the early stages of ocular inflammation between 8 and 12 weeks to a significant decline with the disease progression by 15 weeks of age [16, 17]. Similar changes are reported in the conjunctiva of SS patients [24, 25]. The basis of these observed changes in goblet cell numbers remains unclear especially since the densities are determined based on the mucin content of goblet cells as detected by Alcian Blue and Periodic Acid Schiff (AB/PAS) staining. It is not clear whether the increase in the number of goblet cells is due to inhibited mucin release or actual proliferation of these cells. Similarly, it remains unclear whether the loss of goblet cells represents a mere inability to detect them by AB/PAS staining after complete release of their mucin content or whether the cell loss is due to cell death.

To address some of these possibilities we evaluated proliferation and apoptotic cell death in goblet cells treated with selected cytokines. We treated goblet cell cultures derived from WT conjunctiva explants with Th1 (IFN-γ or TNF-α), Th2 (IL-13), and Th17 (IL-17A or IL-6) cytokines and pulsed these cultures with BrdU, as described in methods. Nuclear incorporation of BrdU was detected using fluorescence conjugated anti-BrdU antibody in combination with vital dye 7-AAD. Flow cytometric staining pattern of BrdU and 7-AAD was examined to identify cell cycle stages. Gates were set to identify and enumerate proliferating cells ($S + G_2$), resting cells ($G_0 + G_1$), and apoptotic cells. As shown in Figure 6(a), among goblet cells exposed to IL-13 as compared with untreated cultures, a more than twofold increase in

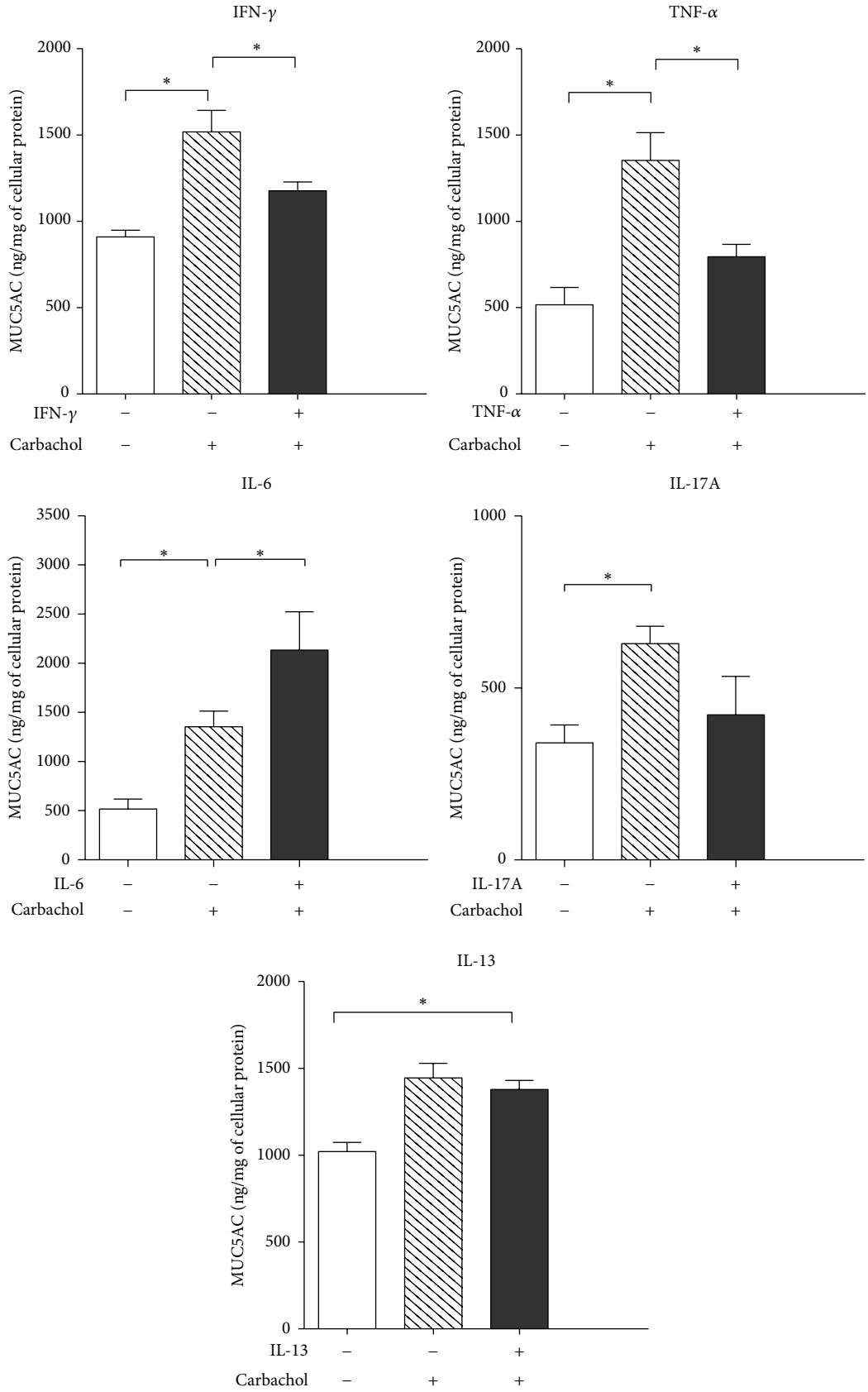

Figure 5: Inflammatory cytokines alter carbachol-mediated MUC5AC secretion by goblet cells. Cultured goblet cells were treated for 24 h with IFN-γ, TNF-α, IL-6, or IL-17A (10 ng/mL), stimulated with the cholinergic agonist carbachol (10^{-3} M) for 1 h, and MUC5AC secretion in the supernatants was evaluated by ELISA. $^{*}P < 0.05$.

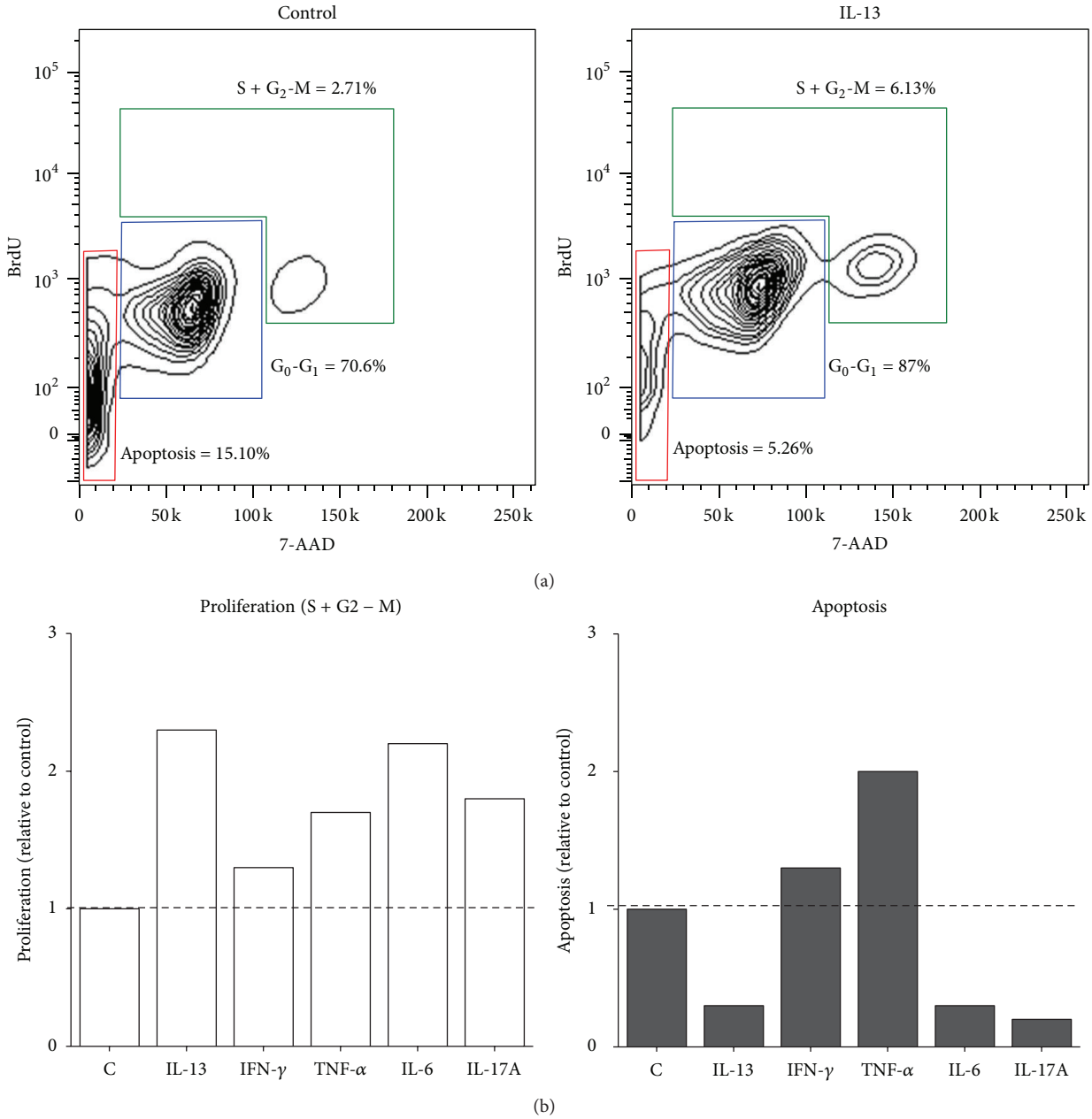

FIGURE 6: Inflammatory cytokines alter proliferation and apoptosis rate of cultured conjunctival goblet cells. Cultured goblet cells were pulsed with BrdU and treated for 24 h with 10 ng/mL of IL-13, IFN-γ, TNF-α, IL-6, or IL-17A. Cells stained with fluorescence-conjugated anti-BrdU antibody and viability dye 7-AAD was analyzed by flow cytometry to identify stages of cell cycles. (a) Representative flow cytometry plots are shown and percentage of cells in each of the G_0-G_1, S + G_2-M phases and apoptotic cells are indicated for untreated control and IL-13 treated cells. (b) Bar graphs show changes in proliferation (S + G_2-M phases) and apoptosis relative to untreated controls.

proliferating cells (6.13% versus 2.71%) was detected with nearly a threefold reduction in apoptotic cells (5.26% versus 15.1%). These results are consistent with the role of IL-13 described in the differentiation and proliferation of goblet cells in other tissues [10, 26]. Contrary to such an effect of the Th2 cytokine, as shown in Figure 4(b), a relatively lesser degree (<twofold) of proliferation was detected among goblet cells treated with Th1 cytokines (IFN-γ: 3.54% and TNF-α: 4.56% versus 2.71%), which was however, accompanied with increased apoptotic cells (IFN-γ: 30.1% and TNF-α: 19.8% versus 15.1%). These results are consistent with the inhibitory effect of Th1 cytokines detected on mucin secretion of goblet cells. The effect of Th17 cytokines resembled that of IL-13 in that an increased proportion of proliferating goblet cells (IL-6: 5.95% and IL-17A: 4.87% versus 2.71%) with reduced apoptotic cells (IL-6: 4.53% and IL-17A: 3.55% versus 15.1%) were detected.

Together our results suggest that inflammatory cytokines indeed alter proliferation as well as apoptosis of conjunctival goblet cells in that increased expression of IL-13 and

IL-6 in the conjunctiva may contribute to an initial increase in goblet cell numbers (as seen in TSP-1 null mice) by inducing their proliferation, while goblet cell loss may be attributed to Th1 cytokines that cause their apoptosis. Further investigation is needed to determine whether the inhibitory effect of cytokines on goblet cell mucin secretion leads to their apoptotic cell death.

4. Discussion

Ocular surface inflammation in TSP-1 deficient mice is characterized by tissue expression of Th1, Th17, and Th2 cytokines and loss of secretory function with alteration in numbers of mucin secreting goblet cells [17]. In this present study, we developed a primary culture of mouse goblet cells from conjunctival tissue and evaluated the effects of inflammatory cytokines on goblet cells with respect to processes such as mucin secretion, proliferation, and apoptosis. We demonstrated that inflammation has an essential role in the disruption of conjunctival goblet cell functions, and that the proinflammatory cytokines expressed in TSP-1 null conjunctiva induced significant changes in proliferation, apoptosis, and mucin secretion of these cells.

In our experiments Th1 cytokines IFN-γ and TNF-α inhibited cholinergic stimulus induced mucin secretion and led to goblet cell apoptosis. Significantly increased expression for these cytokines is detectable in TSP-1 deficient conjunctiva as compared to WT tissues, and this expression progressively increases with age similar to that of IL-13 [17]. Such increase was also accompanied with reduced MUC5AC levels in tears secreted in response to cholinergic stimulation in TSP-1 null mice compared to age-matched WT controls. In SS patients, overexpression of both Th1 cytokines is noted in the conjunctiva, which is also correlated with a decline in goblet cell numbers [27, 28]. Similar decline in goblet cells is also detected in TSP-1 null conjunctiva [17]. Thus, our *in vitro* findings are consistent with *in vivo* results and hence support a role for Th1 cytokines in inflammation-mediated conjunctival goblet cell loss during SS. Furthermore, inhibition of mucin secretion by these cytokines also explains reduced tear MUC5AC detected in TSP-1 null mice as well as SS patients [17, 29]. The inhibitory and proapoptotic effect of IFN-γ and TNF-α in conjunctival goblet cells are similar to that reported in airway goblet cells [30, 31]. However, these reports are based on mucous staining of the cells and do not address secretory aspects of mucins. Studies that examined mucous secretion from intestinal colonic goblet cell lines reported stimulatory effect of IFN-γ and TNF-α on mucin secretion [32, 33]. These results differ from our observations that address stimulated mucin secretion as against basal levels examined in colonic goblet cells. Furthermore, differential effect of these cytokines on intestinal epithelial apoptosis was reported with its induction by TNF-α but not IFN-γ [34]. These results clearly indicate tissue specific differences in responses to inflammatory cytokines.

Chronic inflammatory responses in many autoimmune diseases, including SS, involve Th17 cytokines IL-17 and IL-6 [35–38]. Increased mucin expression by airway epithelial cells exposed to these cytokines *in vitro* was correlated with the mucus hypersecretion detected in chronic airway diseases [3]. In our experiments, while both IL-6 and IL-17 induced proliferation of conjunctival goblet cells, only IL-6 enhanced mucin secretion induced by cholinergic stimulus. Considering reduced tear MUC5AC levels in TSP-1 null mice, our *in vitro* results suggest that the stimulatory effect of IL-6 is likely countered by some inhibitory signal *in vivo*. Temporal analysis of TSP-1 deficient conjunctiva has indicated significantly increased expression of TNF-α and IFN-γ until 12 weeks of age [17]. Therefore, possibly the inhibitory effects of the latter two cytokines predominate over stimulatory effects of IL-6. It is also possible that goblet cell proliferation in response to Th17 cytokines represents a mechanism to replenish lost goblet cells in the conjunctiva. The relative expression of cytokines and tear MUC5AC levels at later stages of the disease may provide further insights into chronic inflammatory processes in Sjögren's pathology.

The expression of the representative Th2 cytokine IL-13 was detected in exocrine gland and peripheral blood mononuclear cells from patients with primary SS [22, 39]. Consistent with these reports, our results also point to an involvement of Th2-mediated pathology in the ocular surface inflammation in TSP-1 null mice, with increased expression of the Th2-associated transcription factor GATA3 and the inflammatory cytokine IL-13 in TSP-1 null conjunctiva. The effects of IL-13 on goblet cell hyperplasia have been extensively studied in the gastrointestinal and respiratory tracts. It is known to induce airway goblet cell differentiation, hyperplasia, and mucus hypersecretion in different inflammatory diseases [10]. In the intestinal epithelium, mucin (MUC5AC) secretion induced by IL-13 is critical for worm expulsion during enteric nematode infections [40, 41]. Although the effect of IL-13 on regulation of conjunctival goblet cell density is not completely understood, the fact that IL-13 deficient mice have a significantly lower number of filled conjunctival goblet cells than wild type mice [42] suggested a potential role of IL-13 in regulating conjunctival goblet cells. In this study, we show that IL-13 has a direct effect on stimulating conjunctival goblet cell proliferation without affecting their mucin secretion. Increased expression of IL-13 in TSP-1 null conjunctiva coincides with an initial increase in goblet cell numbers between 8 and 12 weeks of age prior to their decline [16]. This change is also concurrent with significantly reduced tear MUC5AC levels in TSP-1 null mice [17]. Together our results indicate that although conjunctival goblet cells may resemble airway goblet cells in their hyperplastic response to IL-13, this proliferation may not be accompanied by mucin hypersecretion in tears.

Goblet cell density is a critical parameter that reflects the overall health of the ocular surface [43]. Alterations in mucin secretion and goblet cell number are prominent features of ocular surface diseases [7–9]. The information about the mechanisms leading to goblet cell changes is limited, because it is often extrapolated from studies using whole conjunctival tissue. Goblet cell cultures derived from airway epithelia of hamsters, rats, and humans have been in use for several years in addition to colonic neoplastic cell lines [44–48], but tissue specific differences among goblet cells cannot be overlooked. Unlike conjunctival mucosa, goblet cells in

the lungs are not abundant under normal conditions but are induced by a variety of inflammatory stimuli to differentiate them from pulmonary epithelial cell type, Clara cells [49]. In the gastrointestinal mucosa goblet, cell numbers and mucin secretion are modulated by intestinal and colonic microbes [50]. No equivalent alterations in conjunctival goblet, cells have been noted as yet.

Shatos et al. reported the first conjunctival goblet cell culture, achieving the isolation and growth of goblet cells from rat and human conjunctiva [18, 19]. Our study demonstrates that conjunctival goblet cells can be also isolated from mouse conjunctiva using the same explant culture system, retaining goblet cell specific markers and functional activity. This culture serves as an *in vitro* model to study the effect of inflammation on goblet cells in a direct, controlled, and reproducible manner.

5. Conclusion

This study demonstrates that inflammatory cytokines associated with the ocular manifestation of Sjögren's syndrome contribute to the pathology by inducing apoptosis and altering mucin secretion and proliferation of conjunctival goblet cells. In addition, this study demonstrates successful and consistent generation of mouse conjunctival goblet cell primary culture for *in vitro* studies.

Conflict of Interests

The authors declare that there is no conflict of interests regarding the publication of this paper.

Acknowledgments

The authors appreciate technical assistance provided by Bruce Turpie. This research was supported by National Institute of Health Grant no. EY015472 and Department of Defense Grant no. W81XWH-10-1-0392.

References

[1] C. W. Davis and B. F. Dickey, "Regulated airway goblet cell mucin secretion," *Annual Review of Physiology*, vol. 70, pp. 487–512, 2008.

[2] C. L. Ordoñez, R. Khashayar, H. H. Wong et al., "Mild and moderate asthma is associated with airway goblet cell hyperplasia and abnormalities in mucin gene expression," *American Journal of Respiratory and Critical Care Medicine*, vol. 163, no. 2, pp. 517–523, 2001.

[3] Y. Chen, P. Thai, Y. H. Zhao, Y. S. Ho, M. M. DeSouza, and R. Wu, "Stimulation of airway mucin gene expression by interleukin (IL)-17 through IL-6 paracrine/autocrine loop," *Journal of Biological Chemistry*, vol. 278, no. 19, pp. 17036–17043, 2003.

[4] D. A. McCormick, L. W. L. Horton, and A. S. Mee, "Mucin depletion in inflammatory bowel disease," *Journal of Clinical Pathology*, vol. 43, no. 2, pp. 143–146, 1990.

[5] Y. S. Kim and S. B. Ho, "Intestinal goblet cells and mucins in health and disease: recent insights and progress," *Current Gastroenterology Reports*, vol. 12, no. 5, pp. 319–330, 2010.

[6] I. K. Gipson and T. Inatomi, "Cellular origin of mucins of the ocular surface tear film," in *Lacrimal Gland, Tear Film, and Dry Eye Syndromes 2*, D. A. Sulliva, D. A. Dartt, and M. A. Meneray, Eds., vol. 438 of *Advances in Experimental Medicine and Biology*, pp. 221–227, Springer, New York, NY, USA, 1998.

[7] T. Nakamura, K. Nishida, A. Dota, M. Matsuki, K. Yamanishi, and S. Kinoshita, "Elevated expression of transglutaminase 1 and keratinization-related proteins in conjunctiva in severe ocular surface disease," *Investigative Ophthalmology and Visual Science*, vol. 42, no. 3, pp. 549–556, 2001.

[8] J. P. Gilbard and S. R. Rossi, "Tear film and ocular surface changes in a rabbit model of neurotrophic keratitis," *Ophthalmology*, vol. 97, no. 3, pp. 308–312, 1990.

[9] S. C. G. Tseng, L. W. Hirst, and A. E. Maumenee, "Possible mechanisms for the loss of goblet cells in mucin-deficient disorders," *Ophthalmology*, vol. 91, no. 6, pp. 545–552, 1984.

[10] M. Kondo, J. Tamaoki, K. Takeyama, J. Nakata, and A. Nagai, "Interleukin-13 induces goblet cell differentiation in primary cell culture from guinea pig tracheal epithelium," *American Journal of Respiratory Cell and Molecular Biology*, vol. 27, no. 5, pp. 536–541, 2002.

[11] J. G. Ford, D. Rennick, D. D. Donaldson et al., "IL-13 and IFN-γ: interactions in lung inflammation," *Journal of Immunology*, vol. 167, no. 3, pp. 1769–1777, 2001.

[12] A. Jarry, D. Merlin, A. Velcich, U. Hopfer, L. H. Augenlicht, and C. L. Laboisse, "Interferon-γ modulates cAMP-induced mucin exocytosis without affecting mucin gene expression in a human colonic goblet cell line," *European Journal of Pharmacology: Molecular Pharmacology*, vol. 267, no. 1, pp. 95–103, 1994.

[13] V. P. J. Saw, I. Offiah, R. J. Dart et al., "Conjunctival interleukin-13 expression in mucous membrane pemphigoid and functional effects of interleukin-13 on conjunctival fibroblasts in vitro," *American Journal of Pathology*, vol. 175, no. 6, pp. 2406–2415, 2009.

[14] A. Leonardi, I. A. Fregona, M. Plebani, A. G. Secchi, and V. L. Calder, "Th1- and Th2-type cytokines in chronic ocular allergy," *Graefe's Archive for Clinical and Experimental Ophthalmology*, vol. 244, no. 10, pp. 1240–1245, 2006.

[15] X. O. Yang, H. C. Seon, H. Park et al., "Regulation of inflammatory responses by IL-17F," *Journal of Experimental Medicine*, vol. 205, no. 5, pp. 1063–1075, 2008.

[16] B. Turpie, T. Yoshimura, A. Gulati, J. D. Rios, D. A. Dartt, and S. Masli, "Sjögren's syndrome-like ocular surface disease in thrombospondin-1 deficient mice," *American Journal of Pathology*, vol. 175, no. 3, pp. 1136–1147, 2009.

[17] L. Contreras-Ruiz, B. Regenfuss, F. A. Mir, J. Kearns, and S. Masli, "Conjunctival inflammation in thrombospondin-1 deficient mouse model of Sjogren's syndrome," *PLoS One*, vol. 8, no. 9, Article ID e75937, 2013.

[18] M. A. Shatos, J. D. Ríos, Y. Horikawa et al., "Isolation and characterization of cultured human conjunctival goblet cells," *Investigative Ophthalmology and Visual Science*, vol. 44, no. 6, pp. 2477–2486, 2003.

[19] M. A. Shatos, J. D. Rios, V. Tepavcevic, H. Kano, R. Hodges, and D. A. Dartt, "Isolation, characterization, and propagation of rat conjunctival goblet cells in vitro," *Investigative Ophthalmology and Visual Science*, vol. 42, no. 7, pp. 1455–1464, 2001.

[20] K. L. Krenzer and T. F. Freddo, "Cytokeratin expression in normal human bulbar conjunctiva obtained by impression cytology," *Investigative Ophthalmology and Visual Science*, vol. 38, no. 1, pp. 142–152, 1997.

[21] T. Inatomi, S. Spurr-Michaud, A. S. Tisdale, Q. Zhan, S. T. Feldman, and I. K. Gipson, "Expression of secretory mucin genes by human conjunctival epithelia," *Investigative Ophthalmology and Visual Science*, vol. 37, no. 8, pp. 1684–1692, 1996.

[22] D. I. Mitsias, A. G. Tzioufas, C. Veiopoulou et al., "The Th1/Th2 cytokine balance changes with the progress of the immunopathological lesion of Sjogren's syndrome," *Clinical and Experimental Immunology*, vol. 128, no. 3, pp. 562–568, 2002.

[23] D. A. Jabs, R. A. Prendergast, A. L. Campbell et al., "Autoimmune Th2-mediated dacryoadenitis in MRL/MpJ mice becomes Th1-mediated in IL-4 deficient MRL/MpJ mice," *Investigative Ophthalmology and Visual Science*, vol. 48, no. 12, pp. 5624–5629, 2007.

[24] R. A. Ralph, "Conjunctival goblet cell density in normal subjects and in dry eye syndromes," *Investigative Ophthalmology*, vol. 14, no. 4, pp. 299–302, 1975.

[25] J. D. Nelson and J. C. Wright, "Conjunctival goblet cell densities in ocular surface disease," *Archives of Ophthalmology*, vol. 102, no. 7, pp. 1049–1051, 1984.

[26] S. Kanoh, T. Tanabe, and B. K. Rubin, "IL-13-induced MUC5AC production and goblet cell differentiation is steroid resistant in human airway cells," *Clinical and Experimental Allergy*, vol. 41, no. 12, pp. 1747–1756, 2011.

[27] P. J. Pisella, F. Brignole, C. Debbasch et al., "Flow cytometric analysis of conjunctival epithelium in ocular rosacea and keratoconjunctivitis sicca," *Ophthalmology*, vol. 107, no. 10, pp. 1841–1849, 2000.

[28] F. Brignole, P. J. Pisella, M. Goldschild, M. De Saint Jean, A. Goguel, and C. Baudouin, "Flow cytometric analysis of inflammatory markers in conjunctival epithelial cells of patients with dry eyes," *Investigative Ophthalmology and Visual Science*, vol. 41, no. 6, pp. 1356–1363, 2000.

[29] P. Argüeso, M. Balaram, S. Spurr-Michaud, H. T. Keutmann, M. R. Dana, and I. K. Gipson, "Decreased levels of the goblet cell mucin MUC5AC in tears of patients with Sjögren syndrome," *Investigative Ophthalmology and Visual Science*, vol. 43, no. 4, pp. 1004–1011, 2002.

[30] L. Cohn, R. J. Homer, N. Niu, and K. Bottomly, "T helper 1 cells and interferon γ regulate allergic airway inflammation and mucus production," *Journal of Experimental Medicine*, vol. 190, no. 9, pp. 1309–1318, 1999.

[31] Z. O. Q. Shi, M. J. Fischer, G. T. De Sanctis, M. R. Schuyler, and Y. Tesfaigzi, "IFN-γ, but not fas, mediates reduction of allergen-induced mucous cell metaplasia by inducing apoptosis," *Journal of Immunology*, vol. 168, no. 9, pp. 4764–4771, 2002.

[32] M. G. Smirnova, J. P. Birchall, and J. P. Pearson, "TNF-α in the regulation of MUC5AC secretion: some aspects of cytokine-induced mucin hypersecretion on the in vitro model," *Cytokine*, vol. 12, no. 11, pp. 1732–1736, 2000.

[33] A. Jarry, F. Muzeau, and C. Laboisse, "Cytokine effects in a human colonic goblet cell line. Cellular damage and its partial prevention by 5 aminosalicylic acid," *Digestive Diseases and Sciences*, vol. 37, no. 8, pp. 1170–1178, 1992.

[34] K. Juuti-Uusitalo, L. J. Klunder, K. A. Sjollema et al., "Differential effects of TNF (TNFSF2) and IFN-γ on intestinal epithelial cell morphogenesis and barrier function in three-dimensional culture," *PLoS One*, vol. 6, no. 8, Article ID e22967, 2011.

[35] B. Afzali, G. Lombardi, R. I. Lechler, and G. M. Lord, "The role of T helper 17 (Th17) and regulatory T cells (Treg) in human organ transplantation and autoimmune disease," *Clinical and Experimental Immunology*, vol. 148, no. 1, pp. 32–46, 2007.

[36] C. Q. Nguyen, M. H. Hu, Y. Li, C. Stewart, and A. B. Peck, "Salivary gland tissue expression of interleukin-23 and interleukin-17 in Sjögren's syndrome: findings in humans and mice," *Arthritis and Rheumatism*, vol. 58, no. 3, pp. 734–743, 2008.

[37] M. E. Doyle, L. Boggs, R. Attia et al., "Autoimmune dacryoadenitis of NOD/LtJ mice and its subsequent effects on tear protein composition," *American Journal of Pathology*, vol. 171, no. 4, pp. 1224–1236, 2007.

[38] A. Sakai, Y. Sugawara, T. Kuroishi, T. Sasano, and S. Sugawara, "Identification of IL-18 and Th17 cells in salivary glands of patients with Sjögren's syndrome, and amplification of IL-17-mediated secretion of inflammatory cytokines from salivary gland cells by IL-18," *Journal of Immunology*, vol. 181, no. 4, pp. 2898–2906, 2008.

[39] G. M. Villarreal, J. Alcocer-Varela, and L. Llorente, "Differential interleukin (IL)-10 and IL-13 gene expression in vivo in salivary glands and peripheral blood mononuclear cells from patients with primary Sjögren's syndrome," *Immunology Letters*, vol. 49, no. 1-2, pp. 105–109, 1996.

[40] S. Z. Hasnain, C. M. Evans, M. Roy et al., "Muc5ac: a critical component mediating the rejection of enteric nematodes," *Journal of Experimental Medicine*, vol. 208, no. 5, pp. 893–900, 2011.

[41] I. Khan and S. M. Collins, "Immune-mediated alteration in gut physiology and its role in host defence in nematode infection," *Parasite Immunology*, vol. 26, no. 8-9, pp. 319–326, 2004.

[42] C. S. De Paiva, J. K. Raince, A. J. McClellan et al., "Homeostatic control of conjunctival mucosal goblet cells by NKT-derived IL-13," *Mucosal Immunology*, vol. 4, no. 4, pp. 397–408, 2011.

[43] S. Kinoshita, T. C. Kiorpes, J. Friend, and R. A. Thoft, "Goblet cell density in ocular surface disease. A better indicator than tear mucin," *Archives of Ophthalmology*, vol. 101, no. 8, pp. 1284–1287, 1983.

[44] R. Wu, W. R. Martin, C. B. Robinson et al., "Expression of mucin synthesis and secretion in human tracheobronchial epithelial cells grown in culture," *American Journal of Respiratory Cell and Molecular Biology*, vol. 3, no. 5, pp. 467–478, 1990.

[45] R. Wu, E. Nolan, and C. Turner, "Expression of tracheal differentiated functions in serum-free hormone-supplemented medium," *Journal of Cellular Physiology*, vol. 125, no. 2, pp. 167–181, 1985.

[46] L. Kaartinen, P. Nettesheim, K. B. Adler, and S. H. Randell, "Rat tracheal epithelial cell differentiation in vitro," *In Vitro Cellular and Developmental Biology—Animal*, vol. 29, no. 6, pp. 481–492, 1993.

[47] J. Fogh, J. M. Fogh, and T. Orfeo, "One hundred and twenty seven cultured human tumor cell lines producing tumors in nude mice," *Journal of the National Cancer Institute*, vol. 59, no. 1, pp. 221–226, 1977.

[48] D. J. McCool, J. F. Forstner, and G. G. Forstner, "Synthesis and secretion of mucin by the human colonic tumour cell line LS180," *Biochemical Journal*, vol. 302, part 1, pp. 111–118, 1994.

[49] G. Chen, T. R. Korfhagen, Y. Xu et al., "SPDEF is required for mouse pulmonary goblet cell differentiation and regulates a network of genes associated with mucus production," *Journal of Clinical Investigation*, vol. 119, no. 10, pp. 2914–2924, 2009.

[50] B. Deplancke and H. R. Gaskins, "Microbial modulation of innate defense: goblet cells and the intestinal mucus layer," *American Journal of Clinical Nutrition*, vol. 73, no. 6, pp. S1131–S1141, 2001.

Hindawi Publishing Corporation
Mediators of Inflammation
Volume 2013, Article ID 165453, 10 pages
http://dx.doi.org/10.1155/2013/165453

Research Article

Induction of Tumor Necrosis Factor (TNF) Release from Subtypes of T Cells by Agonists of Proteinase Activated Receptors

Haiwei Yang,[1] Tao Li,[2] Jifu Wei,[1] Huiyun Zhang,[2] and Shaoheng He[1,3]

[1] *Department of Urology, The First Affiliated Hospital of Nanjing Medical University, Nanjing, 300 Guangzhou Road, Jiangsu 210029, China*
[2] *Department of Infectious Diseases, The First Affiliated Hospital of Shantou University Medical College, Shantou 515041, China*
[3] *Allergy and Clinical Immunology Research Centre, The First Affiliated Hospital of Liaoning Medical University, Jinzhou, Liaoning 121001, China*

Correspondence should be addressed to Shaoheng He; shoahenghe@hotmail.com

Received 2 July 2013; Revised 22 November 2013; Accepted 22 November 2013

Academic Editor: Mohammad Athar

Serine proteinases have been recognized as playing an important role in inflammation via proteinase activated receptors (PARs). However, little is known about the influence of serine proteinases and PARs on TNF secretion from highly purified T cells. We challenged T cells from human peripheral blood with serine proteinases and agonist peptides of PARs and measured the levels of TNF in culture supernatants by ELISA. The results showed that thrombin and trypsin, but not tryptase, stimulated approximately up to 2.5-fold increase in TNF release from T cells following 16 h incubation. Proteinase inhibitors and PAR-1 antagonist SCH 79797 almost completely abolished thrombin- and trypsin-induced TNF release from T cells. Agonist peptides of PAR-1, but not PAR-2 induced TNF release from T cells. Moreover, trypsin- and thrombin-induced upregulated expression of TNF was observed in CD4+, IL-4+, or CD25+ T cells, but not in IFN+ or IL-17+ T cells. The signaling pathways MAPK/ERK and PI3K/Akt are involved in the thrombin- and trypsin-induced TNF release from T cells. In conclusion, thrombin and trypsin can induce TNF release from IL-4+ and CD25+ T cells through activation of PAR-1 and therefore contribute to regulation of immune response and inflammation of the body.

1. Introduction

Proteinase-activated receptors (PARs) belong to a family of G-protein-coupled receptors with seven transmembrane domains activated via proteolytic cleavage by serine proteinases [1]. A total of four PARs have been identified and cloned. Among them, PAR-1 [2, 3], PAR-3 [4], and PAR-4 [5] are targets for thrombin, trypsin, and cathepsin G, whereas PAR-2 is resistant to thrombin but can be activated by trypsin, mast cell tryptase [6, 7], neutrophil elastase [8], and insect-derived proteinase [9].

PARs are expressed by various cells involved in inflammatory and immunological responses, such as vascular endothelial cells, epithelial cells, mast cells, T cells, monocyte, eosinophils, and neutrophils [10, 11]. In these cells, activation of PARs affects their main functions such as proliferation, degranulation, and release of inflammatory mediators [10, 11]. In our previous study [12], we have showed the expression of PAR-1, PAR-2, and PAR-3 on T cells, and thrombin-, trypsin-, and tryptase-induced interleukin (IL-6) release from T cells. It has also been reported that cytoplasmic free calcium and phospholipase C and protein kinase C activation are increased in T-leukemic cell lines following stimulation with thrombin or the thrombin receptor agonist peptide [13]. Thrombin and thrombin receptor agonist also enhanced CD69 expression and IL-2 productions by cross-linking T cell receptors in both Jurkat T cells and peripheral blood lymphocytes [14]. We, therefore, anticipated that thrombin, trypsin, and tryptase might induce TNF release from T cells through PARs.

TNF is a major proinflammatory cytokine that is thought to be important in the pathogenesis of asthma [15], food allergy [16], ocular allergy [17], and atopic dermatitis [18]. It has been reported that the increased number of TNF expressing cells and levels of TNF is observed in the bronchoalveolar lavage (BAL) and in the airways of asthmatics [19]. Inhaled TNF increases airway responsiveness to methacholine in asthmatic subjects associated with a sputum neutrophilia [20]. Since PARs, TNF, and T cells all play roles in inflammation, we believe, there must be some linkages between them. The aim of the present study is to investigate roles of thrombin, tryptase, trypsin, elastase, and agonist peptides of PARs in the secretion of TNF from purified human T cells and subtypes of T cells.

2. Materials and Methods

2.1. Reagents. Human thrombin, trypsin (specific activity: ~10,000 BAEE U/mg protein), soybean trypsin inhibitor (SBTI), and bovine serum albumin (BSA, fraction V) were purchased from Sigma (St Louis, MO, USA). Recombinant hirudin and human neutrophil elastase (specific activity: 20 MeO-Suc-Ala-Ala-Pro-Val-pNA U/mg protein) were obtained from Calbiochem (San Diego, CA, USA). Recombinant human Lung β tryptase (specific activity: ~1,000 Nα CBZ-L-Lysine Thiobenzyl Ester U/mg protein) was from Promega (Madison, WI, USA). SCH 79797 was from Tocris Cookson (Ellisville, Mo, USA). Agonist peptides of PARs, and their reverse forms, and PAR-2 antagonist peptide FSLLRY-NH_2 were synthesized in CL Bio-Scientific Inc. (Xi An, China). The sequences of the active and reverse peptides were PAR-1, SFLLR-NH_2 and RLLFS-NH_2, TFLLRN-NH_2 and NRLLFT-NH_2; PAR-2, SLIGKV-NH_2 and VKGILS-NH_2 as well as trans cinnamoyl (tc)-LIGRLO-NH_2 and tc-OLRGIL-NH_2; PAR-3, TFRGAP-NH_2 and PAGRFT-NH_2. RPMI 1640 and newborn calf serum (NCS) were obtained from GIBCO (Carlsbad, CA, USA). Ficoll-Paque Plus was from Amersham Biosciences (Uppsala, Sweden). PE-conjugated mouse anti-human CD3 monoclonal antibody, PE-conjugated goat-anti rabbit IgG, and TNF OptEIA ELISA kits were purchased from BD PharMingen (San Jose, CA, USA). TRIzol reagent and SYBR Green I Stain were purchased from Invitrogen (Carlsbad, CA, USA). Cellular activation of signaling kits for extracellular signal-regulated kinase (ERK), 2-(2-diamino)-3-methoxyphenyl-4H-1-benzopyran-4-one (PD98059), Akt, PI3K, and P38 2-(4-morpholinyl)-8-phenyl-4H-1-benzopyran-4-one (LY294002) was purchased from Cell Signaling Technology (Beverly, MA, USA). ExScript RT reagent kit and SYBR *Premix Ex Taq* (perfect real time) were obtained from TaKaRa (DaLian, China). Rabbit anti-human PAR-1 and rabbit anti-huamn PAR-2 polyclonal antibodies were purchased from Santa Cruz Biotechnology (Santa Cruz, CA, USA). FITC-conjugated mouse anti-human CD4 monoclonal, PE-conjugated mouse anti-human CD8 monoclonal, Percp-cy5.5-conjugated mouse anti-human TNF monoclonal, FITC-conjugated mouse anti-human IFN monoclonal, PE-conjugated mouse anti-human IL-4 monoclonal, APC-conjugated mouse anti-human CD25 monoclonal, and APC-conjugated mouse anti-human IL-17 monoclonal antibodies were purchased from eBioscience. Lymphocyte Isolation Kit I was from Miltenyi Biotec (Bergisch Gladbach, Germany). All other reagents were of analytic grade and obtained from Sigma (St Louis, MO, USA).

2.2. Isolation and Culture of T Cells. Human T cells were isolated from peripheral blood mononuclear cells (PBMCs) by a MACS system with T Cell Isolation Kit I according to the manufacturer's protocol. In brief, PBMCs were isolated from fresh blood donated by healthy volunteers, 100 mL from each individual per visit. The informed consent from each volunteer and agreement with the ethical committee of the First Affiliated Hospital of Nanjing Medical University were obtained. After being separated from red blood cells by Ficoll-Paque density gradient, PBMCs were collected and incubated with microbead-linked anti-CD3 monoclonal antibody for 15 min at 8°C. CD3+ T cells were separated from other cells by passing through a magnetic cell separation system. For purity analysis, the cells were resuspended in PBS and incubated with PE-conjugated monoclonal antibody against human CD3 for 1 h. The purity of T cells was consistently more than 95% and cell viability was more than 98%. The purified CD3+ T cells were then used for the further cell challenge tests.

2.3. Purified T-Cell Challenge. T cells were cultured in 24-well culture plates at a density of 5×10^5 cells/well in RPMI 1640 medium containing 10% NCS at 37°C for 2 h with 5% CO_2, respectively. The culture supernatants were then removed and cells were washed twice with fresh serum-free RPMI 1640 medium at 300 g for 10 min. For challenge experiments, cells were exposed to various doses of thrombin (0.01–3.0 μg/mL, 1 U = 0.5 μg, 1 U/mL = 5.6 nM, U = NIH unit), trypsin (0.01–0.3 μg/mL, 1 μg/mL = 42 nM), tryptase (0.25–2.0 μg/mL, 1 μg/mL = 7.4 nM), and elastase (0.01–0.3 μg/mL, 1 μg/mL = 34 nM, 1 U/mL = 1700 nM) with or without their inhibitors; and to agonist peptides of PAR-1, PAR-2 and PAR-3 (all at 0.1–100 μM) and their reverse peptides, respectively, for 16 h before the culture, supernatants were harvested and stored at −40°C till use. The cell pellet was used for flow cytometry analysis.

2.4. Real-Time PCR Analysis of TNF Gene Expression in Purified T Cells. Quantitative expression of TNF mRNAs in T cells was determined by real-time PCR following the manufacture's protocol. Briefly, after synthesizing cDNA from the total RNA by using ExScriptTM RT reagent kit, real-time PCR was performed by using SYBR Premix Ex Taq on the ABI Prism 7000 Sequence Detection System (Perkin Elmer Applied Systems, Foster City, CA, USA). Each reaction contains 12.5 μL of 2 × SYBR green Master Mix, 1 μL of 10 μM of primers, 1 μL of the cDNA, to a total volume of 25 μL. The thermal cycling conditions included an initial denaturation step at 50°C for 2 min, 95°C for 10 min; 40 cycles at 95°C for 15 s, annealing temperatures at 60°C for 30 s, and extension at 72°C for 30 s.

The sequences of PCR primers for TNF and β-actin were 5′-CCCCAGGGACCTCTCTCTAATC-3′ (forward) and 5′-GGTTTGCTACAACATGGGCTACA-3′ (reverse); 5′-AGGGGCCGGACTCGTCATACT-3′ (forward), and 5′-GGCGGCAACACCATGTACCCT-3′ (reverse), respectively.

Consequently, at the end of the PCR cycles, specificities of the amplification products were controlled by dissociation curve analysis. Expression of mRNA in each sample was finally determined after correction with β-actin expression. The gene specific threshold cycle (Ct) for each sample (ΔCt) was corrected by subtracting the Ct for the housekeeping gene β-actin. Untreated controls were chosen as the reference samples, and the ΔCt for all experimental samples was subtracted by the ΔCt for the control samples ($\Delta\Delta$Ct). The magnitude change of test gene mRNA was expressed as $2 - \Delta\Delta$Ct. Each measurement of a sample was conducted in duplicate.

2.5. Western Blot Analysis of Signal Transduction Pathways in Purified T Cells. T cells were preincubated with 50 μM of PD98059, 20 μM of LY294002, or medium alone for 30 min before adding thrombin 3.0 μg/mL, trypsin 0.3 μg/mL, or medium alone for 30 min, 2 h, or 6 h. The cells were lysed in a buffer containing 20 mM of Tris-HCl (pH 7.4), 137 mM of NaCl, 10% glycerol, 1% Triton X-100, 2 mM of EDTA, 25 mM of β-glycerophosphate, 2 mM of sodium pyrophosphate, and 0.5 mM of dithiothreitol at 4°C for 30 min. Cell debris was removed by centrifugation of the lysate at 12,000 ×g for 10 min. The supernatants were mixed with equal volumes of 2x sodium dodecyl sulphate (SDS) sample buffer and heated to 100°C for 10 min. An equal volume of sample was fractionated by SDS-PAGE on a 10% acrylamide gel and transferred onto polyvinylidene difluoride (PVDF) membranes with a Bio-Rad transfer system, according to the manufacturer's instructions. After blocking nonspecific binding sites with 5% BSA in TBST (50 mM of Tris, 0.15 M of NaCl, 0.1% Tween 20, pH 7.6) for 1 h, membranes were probed with phospho-ERK1/2, phospho-Akt, phospho-p38, or phospho-PI3k antibodies at 4°C overnight, followed by incubation with HRP-conjugated secondary antibodies. Immunoreactive bands were visualized by using enhanced chemiluminescence reagents according to the manufacturer's protocol. Densitometry analysis of immunoblots was carried out using Quantity One software (Bio-Rad, USA).

2.6. Determination of Cytokines. The levels of TNF in culture supernatants were measured with OptEIA ELISA kits according to the manufacturer's instructions. The plates were read on a plate reader (Molecular Devices, Menlo Park, CA) with the Softmax data analysis program. The minimum detectable concentration of TNF was 2.2 pg/mL.

2.7. Flow Cytometry Analysis. To test the PAR1 and 2 expressions after treatment of trypsin and thrombin, isolated T cells were pelleted by centrifugation at 450 g for 10 min after cells were stimulated with thrombin 3.0 μg/mL, trypsin 0.3 μg/mL, or medium alone for 16 h. For PAR1 and PAR2 staining, cells were incubated with rabbit anti-human PAR1 or PAR2 antibodies at 37°C for 1 h. After washing, cells were incubated with PE-conjugated goat anti-rabbit IgG antibody 37°C for 45 min. After washing, cells were analyzed on a fluorescence-activated cell sorting (FACS) arial flow cytometer with CellDevia software (BD Biosciences, USA).

To test the secretion of TNF from subtypes of T cells, isolated T cells were pelleted by centrifugation at 450 g for 10 min and then fixed and permeabilized by using a cell fixation/permeabilization kit (BD Pharmingen). Briefly, thoroughly resuspended cells were added in 100 μL of BD Cytofix/Cytoperm solution and incubated for 20 min at 4°C. Cells were then incubated with fluorescence labeled anti-human CD4, CD8, CD25, TNF, IFN, IL-4, and IL-17 monoclonal antibodies or isotope control, respectively (at a final concentration of 4 μg/mL) at 4°C for 30 min. After washing, cells were analyzed on a fluorescence-activated cell sorting (FACS) Arial flow cytometer with CellDevia software (BD Biosciences, USA).

2.8. Statistical Analysis. The results were shown as mean ± SEM. Differences between groups were tested for significance using the Student's t-test. $P < 0.05$ was taken as statistically significant. All statistics were performed with SPSS 13.0 for window (SPSS Inc., Chicago, IL, USA).

3. Results

3.1. Induction of TNF Release from Purified T Cells by Serine Proteinases. The purity of T cells was consistently more than 95% (date was shown in Supplementary Material, Figure S1). It has been shown that thrombin, trypsin, and tryptase can induce proinflammatory cytokine IL-6 release from T cells [12], but little is known of serine proteinase-induced TNF release from T cells. Here, we showed that thrombin at concentrations of 1.0 and 3.0 μg/mL provoked TNF release from T cells following 16 h incubation period in a dose-dependent manner. Approximately up to 2.5-fold increase in TNF release was observed when T cells were incubated with thrombin for 16 h. At 6 h following incubation, data (not shown) on both basal and induced TNF release from T cells were inconsistent. This is most likely due to the limitation of the assay sensitivity and relatively low secretion of TNF. PAR-1 agonist peptides, SFLLR-NH_2 at the concentration of 100 μM and TFLLRN-NH_2 at the concentration of 5 μM, induced a significant release of TNF at 16 h following incubation. However, RLLFS-NH_2, a reverse peptide of SFLLR-NH_2, and NRLLFT-NH_2, a reverse peptide of TFLLRN-NH_2, had little effect on release of TNF from T cells (Figure 1(a)).

Hirudin, a specific thrombin inhibitor, was able to inhibit thrombin-induced secretion of TNF. Approximately up to 82.4% inhibition of thrombin-induced secretion of TNF was observed when 3.0 μg/mL of thrombin and 10 U/mL of hirudin were added to T cells for 16 h. Hirudin alone at the concentrations tested had little effect on TNF secretion from T cells. SCH 79797, a PAR-1 antagonist at the concentration of 1 μM, inhibited 89% thrombin-induced TNF release from T cells (Figure 1(a)).

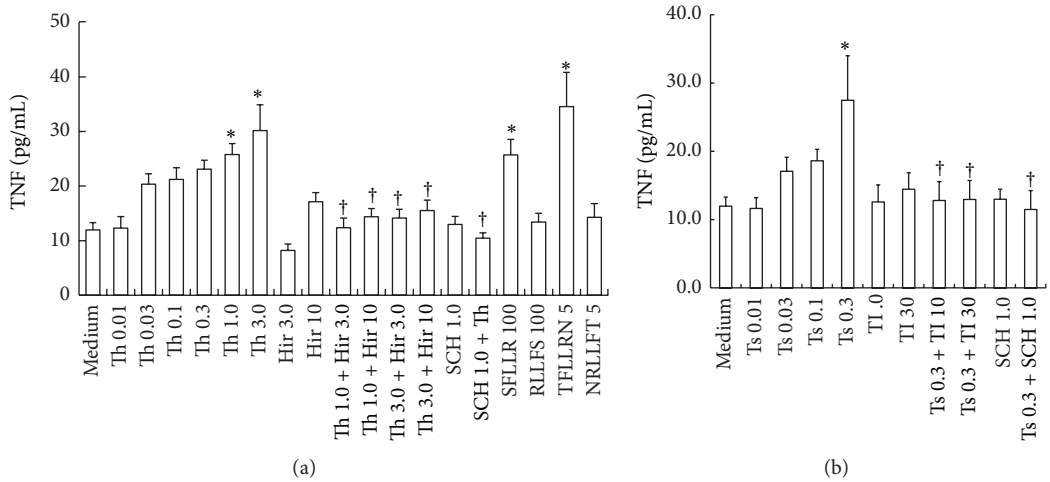

Figure 1: Induction of TNF secretion from human purified T cells by thrombin and trypsin. Cells were incubated with (a) various concentrations of thrombin (Th, μg/mL), SFLLR (μM), TFLLRN (μM), and their reverse peptides RLLFS (μM), NRLLFT (μM), and (b) trypsin (Ts, μg/mL) in the presence or absence of their inhibitors, respectively, for 16 h at 37°C. Values shown are mean ± SEM for four to six independent experiments from different donors. $^*P < 0.05$ compared with the response to medium alone control. $^\dagger P < 0.05$ compared with the response to the corresponding proteinase alone. Hir = hirudin (U/mL), TI = SBTI (μg/mL), and SCH = SCH 79797 (μM).

Similarly, trypsin at the concentration of 0.3 μg/mL induced 2.3-fold increase in TNF release from T cells at 16 h (Figure 1(b)). However, tryptase at the concentrations up to 2 μg/mL and elastase at the concentrations up to 6 U/mL had little effect on TNF release from T cells (data not shown). Inhibitors of trypsin, SBTI at the concentrations of 10 and 30 μg/mL, eliminated 0.3 μg/mL trypsin-induced TNF release by a value up to 94.8 and 94.2%, respectively. SBTI alone at the concentrations tested had little effect on TNF secretion from T cells. SCH 79797, a PAR-1 antagonist at the concentration of 1 μM, inhibited 96.8% trypsin-induced TNF release from T cells (Figure 1(b)).

SLIGKV, an agonist peptide of PAR-2 and TFRGAP-NH_2, an agonist peptide of PAR-3 at the concentrations up to 100 μM, did not appear to have any effect on TNF release from T cells (data not shown).

3.2. Real-Time PCR Analysis of Expression of TNF mRNA in Purified T Cells. In order to confirm the findings above, we investigated the influence of the serine proteinases on the expression of TNF mRNA in T cells. It was found that the expression of TNF mRNA was upregulated when T cells were incubated with thrombin at 1 and 3 μg/mL for 2 and 6 h. The maximum enhanced expression of TNF mRNA was 4.2-fold over baseline control (Figure 2(a)) after 6 h incubation. Hirudin, a specific thrombin inhibitor at the concentration of 3 U/mL, completely abolished thrombin-induced upregulated expression of TNF mRNA after 6 h incubation (Figure 2(b)).

Trypsin at the concentration of 0.3 μg/mL also induced increased expression of TNF mRNA by a value up to approximately 4.0-fold in T cells (Figure 2(a)), which was completely blocked by SBTI (Figure 2(b)). Similarly, SCH 79797 at the concentration of 1 μM inhibited both thrombin- and trypsin-induced upregulated expression of TNF mRNA in T cells by a value up to 72 and 72.5%, respectively (Figure 2(b)).

SFLLR-NH_2 at the concentration of 100 μM and TFLLRN-NH_2 at the concentration of 5 μM significantly increase the expression of TNF mRNA at 2 and 6 h following incubation (Figure 2(a)). But RLLFS-NH_2, a reverse peptide of SFLLR-NH_2, and NRLLFT-NH_2, a reverse peptide of TFLLRN-NH_2, had little effect on expression of TNF mRNA in T cells (data not shown).

At the same time, neither thrombin nor trypsin showed obvious effect on the expression of PAR-1 and PAR-2 (data not shown).

3.3. Upregulated Expression of TNF in Subtypes of T Cells. It is wellknown that there are numerous subtypes of T cells and each of them has distinctive functions. We, therefore, investigated subtypes of T cells by flow cytometer analysis in order to determine the subtypes that upregulate TNF in response to trypsin or thrombin. The results showed that trypsin and thrombin induced upregulated expression of TNF in CD4+ T cells, but not CD8+ T cells, following 16 h incubation period. Among CD4+ T cells, trypsin and thrombin enhanced TNF expression in IL-4+ or CD25+ T cells, but not in IFN+ or IL-17+ T cells. SCH 79797 was able to inhibit enhanced TNF expression induced by trypsin and thrombin (Figures 3(a) and 3(b)).

3.4. Effect of PD98059 and LY294002 on Release and Gene Expression of TNF. In order to examine signal transduction pathways of thrombin and trypsin, T cells were preincubated with PD98059, LY294002, or medium alone for 30 min before adding thrombin 3.0 μg/mL, trypsin 0.3 μg/mL, or medium

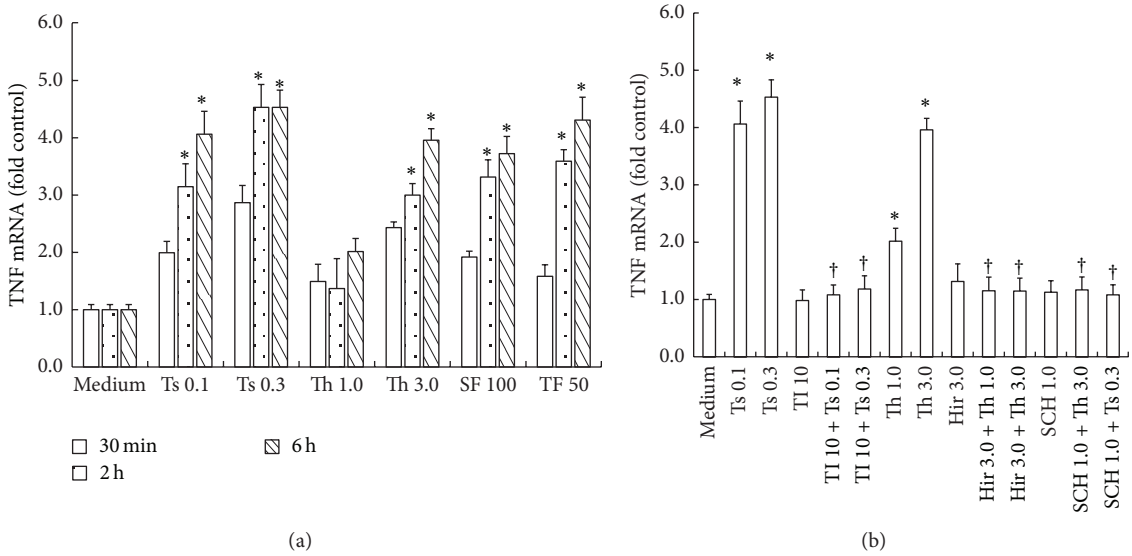

Figure 2: Induction of upregulated expression of TNF mRNA in purified T cells by thrombin and trypsin. (a) Cells were incubated with various concentrations of thrombin (Th, μg/mL), trypsin (Ts, μg/mL), SFLLR-NH_2 (SF, μM), and TFLLRN-NH_2 (TF, μM) for 30 min, 2 h or 6 h at 37°C. (b) Cells were incubated with Th (μg/mL) and Ts (μg/mL) in the presence or absence of their inhibitors, respectively for 6 h at 37°C. Values shown are mean ± SEM for four to six independent experiments from different donors. $^*P < 0.05$ compared with the response to medium alone control. $^\dagger P < 0.05$ compared with the response to the corresponding proteinase alone. Hir = hirudin (U/mL), TI = SBTI (μg/mL), and SCH = SCH 79797 (μM).

alone for 16 h. Following 16 h incubation period, PD98059 an inhibitor of MAPK pathway, and LY294002, an inhibitor of PI3K, completely blocked thrombin- and trypsin-induced release of TNF (Figure 4(a)).

Furthermore, PD98059 inhibited thrombin- and trypsin-induced upregulation of expression of TNF mRNA by a value up to 91.2 and 98.6%, and LY294002 eliminated thrombin- and trypsin-induced expression of TNF mRNA by 95.5 and 83.2% in T cells following 6 h incubation (Figure 4(b)).

3.5. Effect of PD98059 on Phosphorylation of ERK in Purified T Cells. Thrombin (3 μg/mL) and trypsin-(0. 3 μg/mL) induced enhanced phosphorylation of ERK1/2 in T cells following 0.5, 2, and 6 h incubation periods. However, thrombin and trypsin did not significantly affect phosphorylation of P38 in T cells following 0.5, 2, and 6 h incubation periods (Date was shown in Supplementary Material, Figure S2). PD98059 was able to completely block thrombin- and trypsin-induced phosphorylation of ERK1/2 when it was preincubated with T cells for 30 min. PD98059 also inhibited basal phosphorylation of ERK1/2 in T cells (Figure 5).

3.6. Effect of LY294002 on Akt Phosphorylation in Purified T Cells. Thrombin at a concentration of 3 μg/mL and trypsin at a concentration of 0.3 μg/mL induced significantly increased phosphorylation of Akt in T cells following 0.5, 2, and 6 h incubation periods. However, thrombin and trypsin did not significantly affect phosphorylation of PI3k in T cells following 0.5, 2, and 6 h incubation periods (date was shown in Supplementary Material, Figure S3). LY294002 was able to block thrombin- and trypsin-induced phosphorylation of Akt when it was incubated with T cells for 30 min. LY294002 also diminished basal phosphorylation of Akt in T cells (Figure 6).

4. Discussion

We discovered in the present study that serine proteinases thrombin and trypsin, but not tryptase induced TNF release from human T cells. Since TNF is a potent proinflammatory cytokine, our observation is likely to add some novel information for, understanding of actions of serine proteinases in causing inflammation.

As little as 1.0 μg/mL of thrombin was able to induce significant TNF release from T cells, suggesting this proteinase is a potent secretagogue of TNF. This concentration of thrombin should be easily achieved in blood, particularly when the processes of platelet aggregation and coagulation are initiated [21]. Inhibition of thrombin-induced TNF release by a specific inhibitor of thrombin and hirudin indicates that action of thrombin on T cells was dependent on the enzymatic activity of this serine proteinase. There are 3 receptors for thrombin on cells, including PAR-1, PAR-3, and PAR-4 [2, 3]. Since PAR-1 agonist peptides SFLLR-NH2, and TFLLRN-NH2, but not PAR-3 agonist peptide TFRGAP-NH2 were capable of stimulating TNF release, a PAR-1 antagonist SCH 79797 [22] almost completely abolished thrombin-induced TNF release from T cells, and purified human T cells do not express PAR-4; the action of thrombin on T cells is most likely through activation of PAR-1. Our previous report which found thrombin-induced IL-6 secretion from human peripheral blood T cells may support our current findings [16].

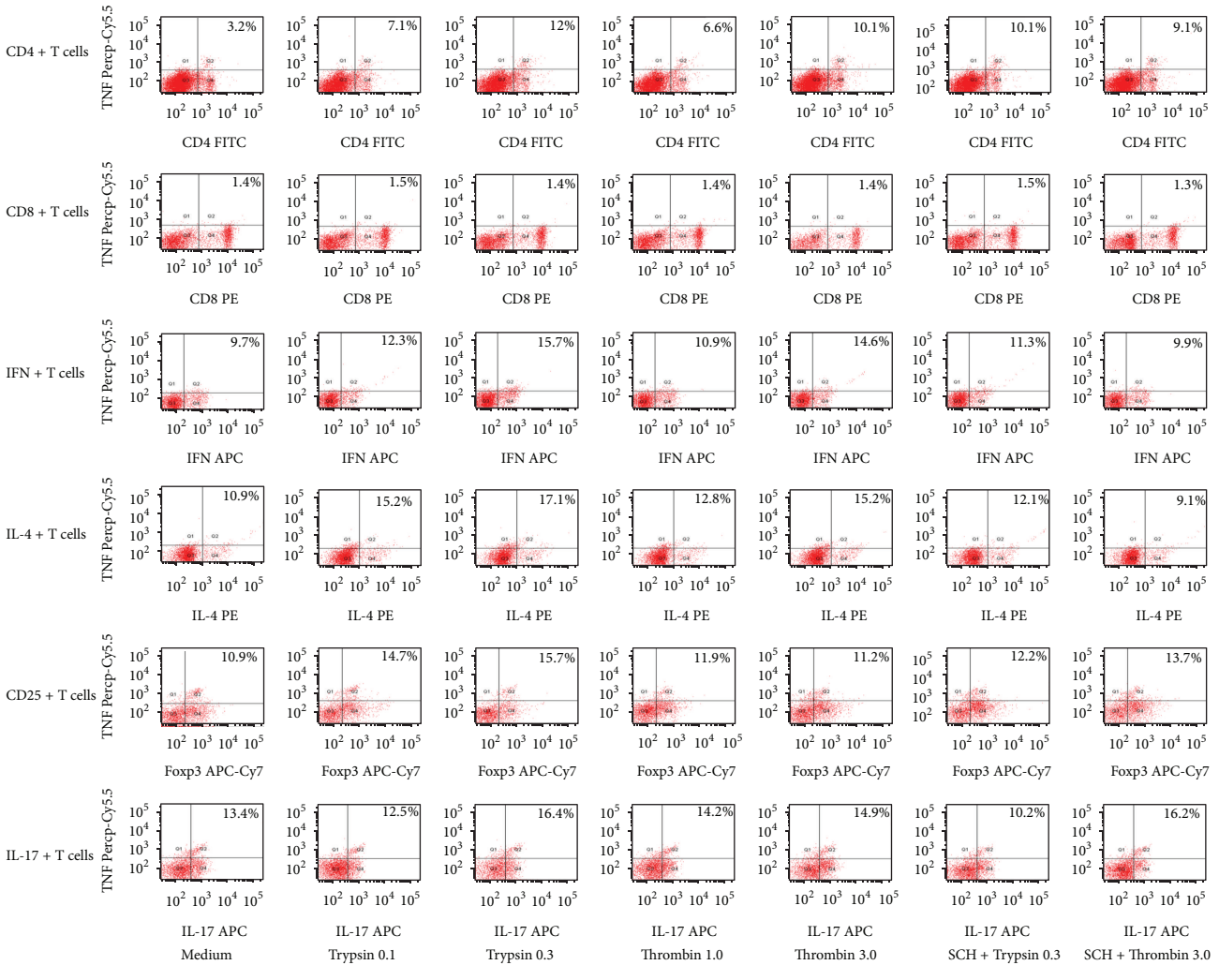

(a)

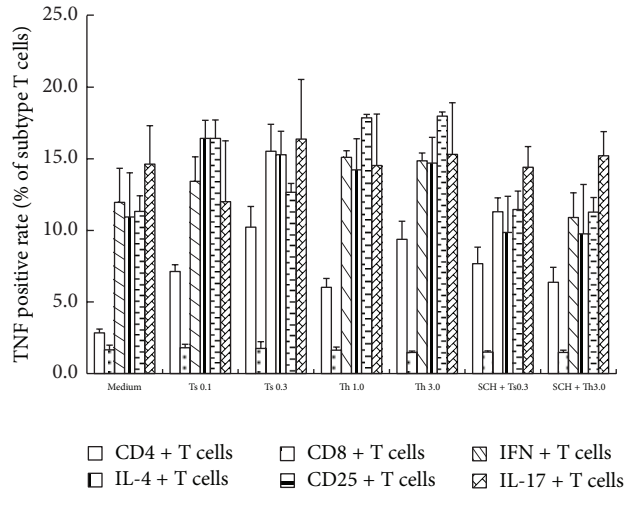

(b)

Figure 3: Induction of upregulated expression of TNF in subtypes of purified T cells. Isolated T cells were incubated with trypsin or thrombin for 16 h at 37°C before being analyzed by flow cytometer. (a) Numbers within the large gated regions indicate the percentage of TNF expression cells among different subtypes of T cells. (b) The mean ± SEM data represented the percentage of TNF + cells in different subtypes of T cells indicated for four separate experiments. $^{*}P < 0.05$ in comparison with medium alone control. $^{\dagger}P < 0.05$ compared with the response to the corresponding uninhibited control.

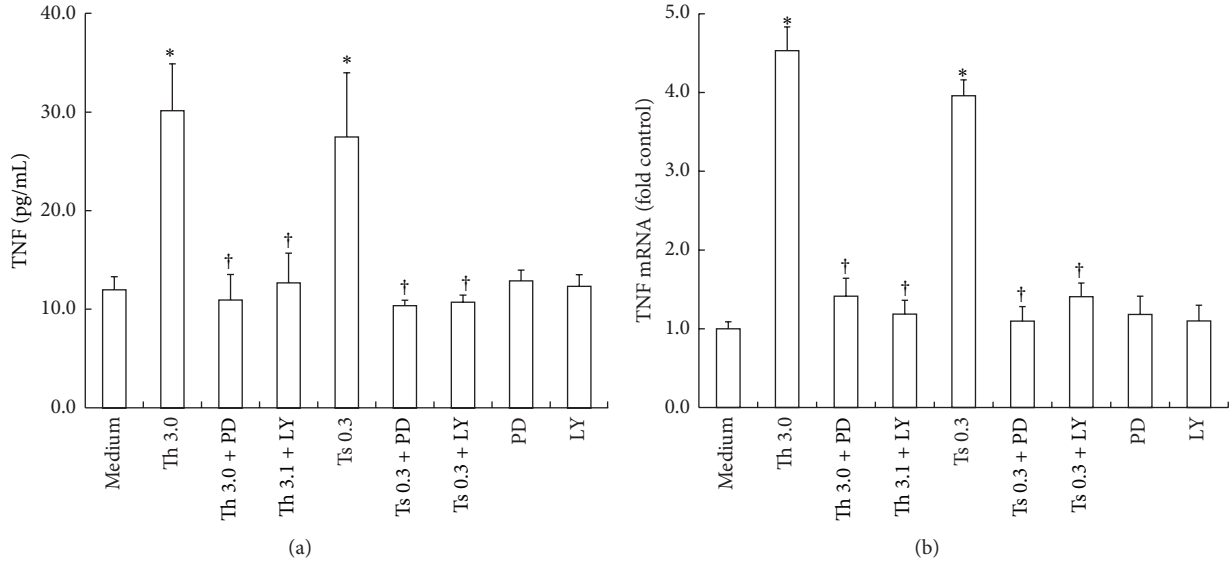

Figure 4: Effect of PD98059 and LY294002 on release and gene expression of TNF in purified T cells. PD98059 (PD, 50 μM) or LY294002 (LY, 20 μM) was preincubated with T cells at 37°C for 30 min before 3.0 μg/mL of thrombin and 0.3 μg/mL of trypsin being added for 6 or 16 h. (a) Cells were collected for analysis of TNF release from T cells at 16 h following incubation. (b) Cells were collected for analysis of gene expression of TNF in T cells at 6 h following incubation. Values shown are mean ± SEM for four to six independent experiments from different donors. $^{*}P < 0.05$ compared with the response to medium alone control. $^{\dagger}P < 0.05$ compared with the response to the corresponding proteinase alone. Th = thrombin (μg/mL), Ts = trypsin (μg/mL), LY = LY294002 (μM), and PD = PD98059 (μM).

While little information is available on induction of TNF release from T cells by trypsin, the ability of trypsin to stimulate IL-6 secretion from T cells [16] may support the anticipation that trypsin is capable of inducing cytokine release from T cells. As little as 0.3 μg/mL of trypsin was able to provoke TNF secretion from T cells proved that it is a potent stimulus of TNF release. As for thrombin, inhibitor of trypsin SBTI was able to inhibit trypsin-induced TNF release from T cells, indicating that an intact catalytic site is required for the serine proteinase to stimulate TNF release. Since PAR-1 is one of three receptors of trypsin, PAR-1 agonist peptides SFLLR-NH_2 and TFLLRN-NH_2 are capable of stimulating TNF release from T cells, and SCH 79797 almost completely abolished trypsin-induced TNF release from T cells, the action of trypsin on T cells is most likely through activation of PAR-1. PAR-2 is also a receptor of trypsin. Since PAR-2 agonist peptide SLIGKV-NH_2 and tryptase are not capable of stimulating TNF release from T cells, the action of trypsin on T cells is not likely through activation of PAR-2.

Trypsin- and thrombin-induced upregulated expression of TNF was observed in CD4+, IL-4+ or CD25+ T cells, indicating that IL-4+, and CD25+ T cells are major sources of TNF. While little information on the relationship between CD25+ T cells and TNF is available, a study which found that the percentage of CD4(+)CD25(+) T cells were significantly high, but the percentage of FoxP3(+) cells were low in allergic rhinitis patients, and that IL-4, IL-5, and TNF levels in nasal lavage fluids were high indicates that the increased TNF release may be from CD4(+)CD25(+), nonregulatory T cells [23]. We believe that the current study is the first work that demonstrates coexpression of CD25 and TNF in the subtype of CD4(+) T cells. Similarly, we clearly found that IL-4+ T cells express enhanced TNF, though little information on coexpression of IL-4 and TNF in T cells is available. This finding implicates that trypsin and thrombin may be involved in the inflammation through induction of TNF release from IL-4+ or CD25+ T cells. It was demonstrated that nickel-specific CD4+ T cell lines [24] and Th17 cells [25] corelease IL-17 and TNF, but trypsin- and thrombin-induced TNF release appears not from IL-17+ T cells as TNF expression in IL-17+ T cells was not upregulated by these two proteinases.

MAPK/ERK pathway is the signaling pathway that is most likely involved in the thrombin- and trypsin-induced TNF release from highly purified T cells, as PD98059, an inhibitor of MAPK/ERK pathway, almost completely blocked thrombin- and trypsin-provoked phophorylation of ERK and TNF release. While little information on signaling pathways associated with PAR-1 signaling in purified T cells is available, the previous reports that PAR-1 agonists activated MAPK/ERK and p38 MAPK signaling pathways in dermal [26] and cardiac fibroblasts [27] may support our current observation that MAPK/ERK pathway is the signaling pathway that is most likely involved in the thrombin- and trypsin-induced TNF release. In addition, PI3K/Akt signaling pathway seems also to be involved in thrombin and trypsin induced TNF secretion, as LY294002 an inhibitor of PI3K/Akt signaling pathway partially diminished thrombin and trypsin induced TNF secretion and completely abolished thrombin and trypsin provoked phosphorylation of Akt. This finding is in the same line with the report, which showed that thrombin stimulated enhance PI3K activity in hamster

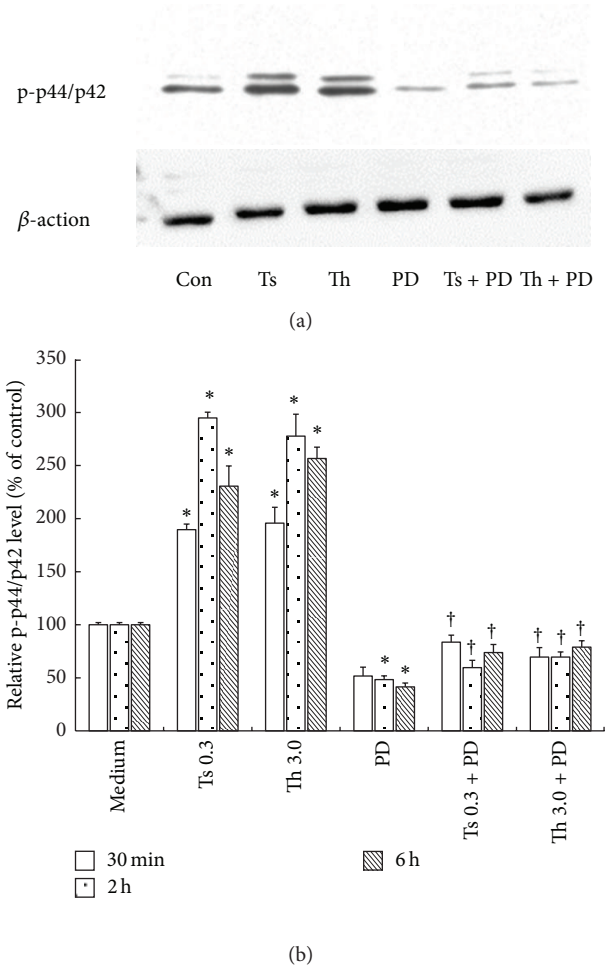

Figure 5: Western blot analysis of influence of PD98059 on thrombin- and trypsin-induced phosphorylation of ERK in purified T cells. PD98059 (PD, 50 μM) was preincubated with T cells at 37°C for 30 min before 3.0 μg/mL of thrombin and 0.3 μg/mL of trypsin being added for 30 min and 2 and 6 h. (a) Cells were treated with thrombin and trypsin for 2 h. (b) The relative levels of phospho-ERK1/2 were expressed as the ratio to β-actin, an internal control (house keeping protein). The values shown are mean ± SD for four separate experiments. $^{*}P < 0.05$ compared with the response to medium alone. $^{\dagger}P < 0.05$ compared with the response to the corresponding proteinase alone.

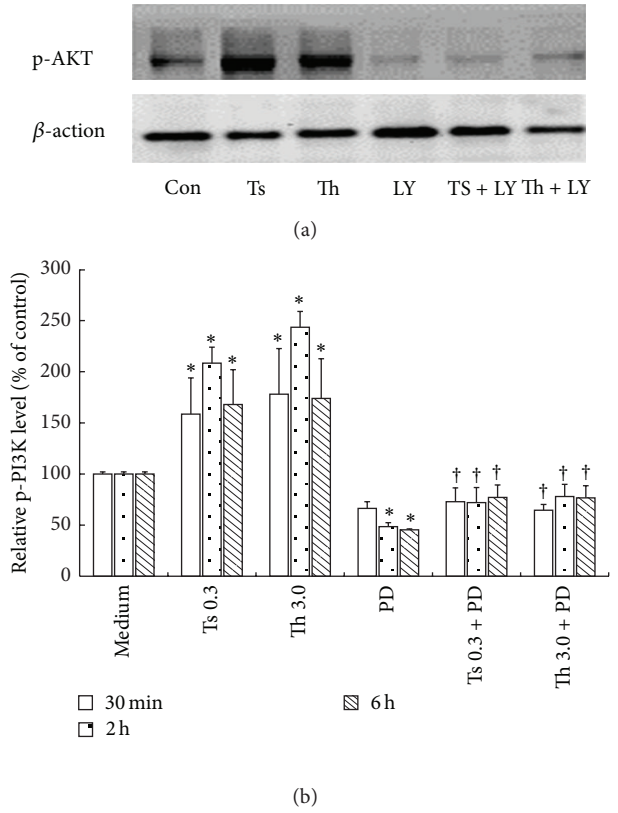

Figure 6: Western blot analysis of influence of LY294002 on thrombin- and trypsin-induced phosphorylation of AKT in purified T cells. LY294002 (LY, 20 μM) was preincubated with T cells at 37°C for 30 min before 3.0 μg/mL of thrombin and 0.3 μg/mL of trypsin being added for 0.5, 2, and 6 h. (a) Cells were treated with thrombin and trypsin for 2 h. (b) The relative levels of phospho-Akt were expressed as the ratio to β-actin, an internal control (housekeeping protein). The values shown are mean ± SD for four separate experiments. $^{*}P < 0.05$ compared with the response to medium alone. $^{\dagger}P < 0.05$ compared with the response to the corresponding proteinase alone.

embryonic fibroblasts [28], but different from our previous report, which showed that thrombin did not enhanced PI3K activity in human dermal fibroblasts [29]. The discrepancy between these studies may be due to the difference in cell origin and species.

TNF is a member of a growing family of peptide mediators comprising at least 19 cytokines, including lymphotoxin-α, Fas ligand, and CD40 ligand. The family is now considered as central mediators of a broad range of biological activities in protective immune responses against a variety of infectious pathogens. On the other hand, TNF also exerts host-damaging effects in sepsis and autoimmune disease [30, 31]. These findings indicate that TNF is one of key mediators of inflammation; therefore, our current study is of importance in understanding TNF-related inflammation and the mechanism of proteinase-induced cytokine production in T cells.

5. Conclusions

In conclusion, it is discovered in the present study that serine proteinases thrombin and trypsin are potent stimuli of TNF secretion from highly purified T cells. Their actions on T cells depend on their enzymatic activities and are likely through activation of PAR-1. Stimulation of TNF secretion from T cells by serine proteinases further proved that these proteinases are actively involved in the pathogenesis of inflammation and regulation of immune response in man.

Acknowledgments

This project was sponsored by the Grants from the National Natural Science Foundation of China (nos. 30972714, 30972822, 81001329, 81172836, 81030054, and 81273274) and a project funded by the Priority Academic Program Development of Jiangsu Higher Education Institutions.

References

[1] S. R. Coughlin, "Thrombin signalling and protease-activated receptors," *Nature*, vol. 407, no. 6801, pp. 258–264, 2000.

[2] T.-K. H. Vu, D. T. Hung, V. I. Wheaton, and S. R. Coughlin, "Molecular cloning of a functional thrombin receptor reveals a novel proteolytic mechanism of receptor activation," *Cell*, vol. 64, no. 6, pp. 1057–1068, 1991.

[3] M. L. Kahn, Y.-W. Zheng, W. Huang et al., "A dual thrombin receptor system for platelet activation," *Nature*, vol. 394, no. 6694, pp. 690–694, 1998.

[4] H. Ishihara, A. J. Connolly, D. Zeng et al., "Protease-activated receptor 3 is a second thrombin receptor in humans," *Nature*, vol. 386, no. 6624, pp. 502–506, 1997.

[5] W.-F. Xu, H. Andersen, T. E. Whitmore et al., "Cloning and characterization of human protease-activated receptor 4," *Proceedings of the National Academy of Sciences of the United States of America*, vol. 95, no. 12, pp. 6642–6646, 1998.

[6] M. Molino, E. S. Barnathan, R. Numerof et al., "Interactions of mast cell tryptase with thrombin receptors and PAR-2," *Journal of Biological Chemistry*, vol. 272, no. 7, pp. 4043–4049, 1997.

[7] M. Steinhoff, C. U. Corvera, M. S. Thoma et al., "Proteinase-activated receptor-2 in human skin: tissue distribution and activation of keratinocytes by mast cell tryptase," *Experimental Dermatology*, vol. 8, no. 4, pp. 282–294, 1999.

[8] A. Uehara, K. Muramoto, H. Takada, and S. Sugawara, "Neutrophil serine proteinases activate human nonepithelial cells to produce inflammatory cytokines through protease-activated receptor 2," *Journal of Immunology*, vol. 170, no. 11, pp. 5690–5696, 2003.

[9] G. Sun, M. A. Stacey, M. Schmidt, L. Mori, and S. Mattoli, "Interaction of mite allergens Der p3 and Der p9 with protease-activated receptor-2 expressed by lung epithelial cells," *Journal of Immunology*, vol. 167, no. 2, pp. 1014–1021, 2001.

[10] S. Verrall, M. Ishii, M. Chen, L. Wang, T. Tram, and S. R. Coughlin, "The thrombin receptor second cytoplasmic loop confers coupling to G(q)- like G proteins in chimeric receptors: additional evidence for a common transmembrane signaling and G protein coupling mechanism in G protein- coupled receptors," *Journal of Biological Chemistry*, vol. 272, no. 11, pp. 6898–6902, 1997.

[11] L. Hou, G. L. Howells, S. Kapas, and M. G. Macey, "The protease-activated receptors and their cellular expression and function in blood-related cells," *British Journal of Haematology*, vol. 101, no. 1, pp. 1–9, 1998.

[12] T. Li and S. He, "Induction of IL-6 release from human T cells by PAR-1 and PAR-2 agonists," *Immunology and Cell Biology*, vol. 84, no. 5, pp. 461–466, 2006.

[13] A. Tordai, J. W. Fenton II, T. Andersen, and E. W. Gelfand, "Functional thrombin receptors on human T lymphoblastoid cells," *Journal of Immunology*, vol. 150, no. 11, pp. 4876–4886, 1993.

[14] B. Mari, V. Imbert, N. Belhacene et al., "Thrombin and thrombin receptor agonist peptide induce early events of T cell activation and synergize with TCR cross-linking for CD69 expression and interleukin 2 production," *Journal of Biological Chemistry*, vol. 269, no. 11, pp. 8517–8523, 1994.

[15] P. J. Busse, T. F. Zhang, B. Schofield, S. Kilaru, S. Patil, and X.-M. Li, "Decrease in airway mucous gene expression caused by treatment with anti-tumor necrosis factor alpha in a murine model of allergic asthma," *Annals of Allergy, Asthma & Immunology*, vol. 103, no. 4, pp. 295–303, 2009.

[16] M. Heyman and J. F. Desjeux, "Cytokine-induced alteration of the epithelial barrier to food antigens in disease," *Annals of the New York Academy of Sciences*, vol. 915, pp. 304–311, 2000.

[17] A. Leonardi, "The central role of conjunctival mast cells in the pathogenesis of ocular allergy," *Current Allergy and Asthma Reports*, vol. 2, no. 4, pp. 325–331, 2002.

[18] C. Vestergaard, C. Johansen, U. Christensen, H. Just, T. Hohwy, and M. Deleuran, "TARC augments TNF-α-induced CTACK production in keratinocytes," *Experimental Dermatology*, vol. 13, no. 9, pp. 551–557, 2004.

[19] S. Waserman, J. Dolovich, M. Conway, and J. S. Marshall, "TNFalpha dysregulation in asthma: relationship to ongoing corticosteroidtherapy," *Canadian Respiratory Journal*, vol. 7, pp. 229–237, 2000.

[20] P. S. Thomas, "Tumour necrosis factor-α: the role of this multifunctional cytokine in asthma," *Immunology and Cell Biology*, vol. 79, no. 2, pp. 132–140, 2001.

[21] M. D. Rand, J. B. Lock, C. van't Veer, D. P. Gaffney, and K. G. Mann, "Blood clotting in minimally altered whole blood," *Blood*, vol. 88, no. 9, pp. 3432–3445, 1996.

[22] H.-S. Ahn, C. Foster, G. Boykow, A. Stamford, M. Manna, and M. Graziano, "Inhibition of cellular action of thrombin by N3-cyclopropyl-7-{[4-(1- methylethyl)phenyl]methyl}-7H-pyrrolo[3,2-f]quinazoline-1,3-diamine (SCH 79797), a nonpeptide thrombin receptor antagonist," *Biochemical Pharmacology*, vol. 60, no. 10, pp. 1425–1434, 2000.

[23] S. Genc, H. Eroglu, U. C. Kucuksezer et al., "The decreased CD4+CD25+ FoxP3+ T cells in nonstimulated allergic rhinitis patients sensitized to house dust mites," *Journal of Asthma*, vol. 49, no. 6, pp. 569–574, 2012.

[24] C. Albanesi, A. Cavani, and G. Girolomoni, "IL-17 is produced by nickel-specific T lymphocytes and regulates ICAM-1 expression and chemokine production in human keratinocytes: synergistic or antagonist effects with IFN-γ and TNF-α," *Journal of Immunology*, vol. 162, no. 1, pp. 494–502, 1999.

[25] M. A. McArthur and M. B. Sztein, "Unexpected heterogeneity of multifunctional T cells in response to superantigen stimulation in humans," *Clinical Immunology*, vol. 146, no. 2, pp. 140–152, 2013.

[26] A. Sabri, J. Short, J. Guo, and S. F. Steinberg, "Protease-activated receptor-1-mediated DNA synthesis in cardiac fibroblast is via epidermal growth factor receptor transactivation: distinct PAR-1 signaling pathways in cardiac fibroblasts and cardiomyocytes," *Circulation Research*, vol. 91, no. 6, pp. 532–539, 2002.

[27] Z.-M. Bian, S. G. Elner, A. Yoshida, and V. M. Elner, "Human RPE-monocyte co-culture induces chemokine gene expression through activation of MAPK and NIK cascade," *Experimental Eye Research*, vol. 76, no. 5, pp. 573–583, 2003.

[28] R. Goel, P. J. Phillips-Mason, A. Gardner, D. M. Raben, and J. J. Baldassare, "α-Thrombin-mediated Phosphatidylinositol 3-Kinase Activation through Release of G$\beta\gamma$ Dimers from Gαq

and Gα i2," *Journal of Biological Chemistry*, vol. 279, no. 8, pp. 6701–6710, 2004.

[29] L. Wang, J. Luo, Y. Fu, and S. He, "Induction of interleukin-8 secretion and activation of ERK1/2, p38 MAPK signaling pathways by thrombin in dermal fibroblasts," *International Journal of Biochemistry and Cell Biology*, vol. 38, no. 9, pp. 1571–1583, 2006.

[30] R. M. Locksley, N. Killeen, and M. J. Lenardo, "The TNF and TNF receptor superfamilies: integrating mammalian biology," *Cell*, vol. 104, no. 4, pp. 487–501, 2001.

[31] K. Pfeffer, "Biological functions of tumor necrosis factor cytokines and their receptors," *Cytokine and Growth Factor Reviews*, vol. 14, no. 3-4, pp. 185–191, 2003.

Hindawi Publishing Corporation
Mediators of Inflammation
Volume 2013, Article ID 378703, 12 pages
http://dx.doi.org/10.1155/2013/378703

Research Article

The Mechanism of Sevoflurane Preconditioning-Induced Protections against Small Intestinal Ischemia Reperfusion Injury Is Independent of Mast Cell in Rats

Xiaoliang Gan,[1,2] Guangjie Su,[1] Weicheng Zhao,[1,3] Pinjie Huang,[1] Gangjian Luo,[1] and Ziqing Hei[1]

[1] *Department of Anesthesiology, The Third Affiliated Hospital, Sun Yat-sen University, Guangzhou 510630, China*
[2] *Department of Anesthesiology, Zhongshan Ophthalmic Center, Sun Yat-sen University, Guangzhou 510060, China*
[3] *Department of Anesthesiology, The First People's Hospital of Foshan, Foshan 528000, China*

Correspondence should be addressed to Ziqing Hei; heiziqing@sina.com

Received 5 September 2013; Revised 1 November 2013; Accepted 4 November 2013

Academic Editor: Mohammad Athar

The study aimed to investigate whether sevoflurane preconditioning can protect against small intestinal ischemia reperfusion (IIR) injury and to explore whether mast cell (MC) is involved in the protections provided by sevoflurane preconditioning. Sprague-Dawley rats exposed to sevoflurane or treated with MC stabilizer cromolyn sodium (CS) were subjected to 75-minute superior mesenteric artery occlusion followed by 2-hour reperfusion in the presence or absence of MC degranulator compound 48/80 (CP). Small intestinal ischemia reperfusion resulted in severe intestinal injury as demonstrated by significant elevations in intestinal injury scores and $p47^{phox}$ and $gp91^{phox}$, ICAM-1 protein expressions and malondialdehyde and IL-6 contents, and MPO activities as well as significant reductions in SOD activities, accompanied with concomitant increases in mast cell degranulation evidenced by significant increases in MC counts, tryptase expression, and β-hexosaminidase concentrations, and those alterations were further upregulated in the presence of CP. Sevoflurane preconditioning dramatically attenuated the previous IIR-induced alterations except MC counts, tryptase, and β-hexosaminidase which were significantly reduced by CS treatment. Furthermore, CP exacerbated IIR injury was abrogated by CS but not by sevoflurane preconditioning. The data collectively indicate that sevoflurane preconditioning confers protections against IIR injury, and MC is not involved in the protective process.

1. Introduction

Small intestinal ischemia reperfusion (IIR) injury occurs frequently in many clinical conditions, including bowel transplantation [1] and liver transplantation, as well as all kinds of shock [2]. Although the advanced treatments have been applied in clinical, the mortality associated with IIR is still high [3]. Mast cells are widely present throughout gastrointestinal tract; previous studies including ours have demonstrated that mast cells play a critical role in the pathogenesis of IIR injury [4, 5], and mast cell inhibition provides a promising therapeutic method against IIR injury.

Sevoflurane, a novel inhaled anesthetic, has been widely used in patients undergoing surgery. In addition to its anesthesia effect, several studies so far have demonstrated that sevoflurane preconditioning confers protections against hypoxic and ischemic cerebral and spinal cord injuries [6, 7], moreover, sevoflurane preconditioning also provides promising benefits against ischemia/reperfusion injury in the heart and kidneys [8, 9]. The protective mechanisms were associated with the reduction of leukocytes infiltration [10], downregulation of apoptosis [6], and enhancement of antioxidant enzymes [11]. However, to our knowledge, there is no evidence supporting the role of sevoflurane preconditioning in IIR injury, and the underlying mechanism is incompletely understood.

Several studies so far have demonstrated that sevoflurane can be safely used in patients diagnosed to have mastocytosis

(a group of rare disorders caused by the presence of too many mast cells) without triggering mast cell degranulation with release of histamine, prostaglandin, tryptase, and heparin [12]. By contrast, Annecke reported that sevoflurane preconditioning can attenuate heart ischemia reperfusion injury without inhibiting mast cell release histamine [13]. However, the direct relationship between sevoflurane preconditioning and mast cell degranulation remains to be elucidated.

Therein, we aimed to investigate whether sevoflurane preconditioning can provide protections against IIR injury; in particular, we studied whether mast cell was involved in the protections provided by sevoflurane preconditioning by using a specific mast cell degranulator (Compound 48/80) and a specific stabilizer (cromolyn sodium) in a rodent model.

2. Materials and Methods

2.1. Animal Experiments. Female Sprague-Dawley (SD) rats weighing 180–200 g, purchased from the Animal Center of Guangdong Province (Guangzhou, China), were housed individually in wire-bottomed cages and were placed under pathogen free condition for one week before use. The experimental protocol and design were approved by the Sun Yat-sen University Animal Experimentation Committee and performed according to Sun Yat-sen University Guidelines for Animal Experimentation. All the animals were allowed free access to water and food ad libitum except 16 h before surgery. Rats were randomly divided into seven groups: (1) Sham-operated (SH), (2) sole IIR (IIR), (3) IIR + Compound 48/80 (IIR + CP), (4) IIR + cromolyn sodium (IIR + CS), (5) IIR + cromolyn sodium + Compound 48/80 (IIR + CS + CP), (6) sevoflurane + IIR (SEV + IIR), and (7) sevoflurane + IIR + Compound 48/80 (SEV + IIR + CP). In sevoflurane pretreated groups, the rats were exposed to rats 2.3% sevoflurane in a gas-tight anesthesia chamber for 1 hour according to previous studies for 3 subsequent days [7]; the other rats were exposed to oxygen alone. At the 4th day, the rats were anesthetized by intraperitoneal injection of 10% of chloral hydrate (3.5 mL/kg) after fasting for 16 h, and the abdomen was opened by a midline incision in a supine position; the superior mesenteric artery (SMA) was isolated and occluded for 75 min with a small clamp, and then the clamp was released to maintain the rats for 2 h during reperfusion in all IIR groups. However, in the Sham-operated group, the SMA was just isolated but not clamped and maintained the same period during the surgery. The cromolyn sodium (mast cell stabilizer, 50 mg/kg) was injected intravenously at 15 min after ischemia, and the Compound 48/80 (mast cell degranulator, 0.75 mg/kg) was intravenously injected via the tail vein at 5 min before the release of the clamp in the Compound 48/80 groups. Meanwhile, the same volumes of physiological saline were administrated in the control groups. The doses of agents were adjusted in accordance with our previous study [5]. During the surgery, all the rats body temperature was maintained at 38°C using heated pad. And 10 mL/kg 37°C normal saline was injected subcutaneously to avoid dehydration after the abdomen had been closed.

2.2. Collection of Intestinal Mucosa. At the end of the experiment, the whole small intestine was removed carefully, and a segment of 1.0 cm intestine was cut from 10 cm to terminal ileum and fixed in 10% formaldehyde and then embedded in paraffin for section. The remaining small intestine was washed thoroughly with 0°C normal saline and then opened longitudinally to expose the intestinal epithelium, after being rinsed completely with 0°C normal saline and dried with suction paper. The mucosal layer was harvested by gentle scraping of the epithelium with a glass slide with a plate on the ice and then was stored at −70°C for further measurements.

2.3. Intestinal Histology. Five-μm thick sections were prepared from paraffin-embedded intestine tissue, the segment of small intestine was stained with hematoxylin-eosin. And the damages of intestinal mucosa were evaluated by two histologists who were initially blinded to the experiment according to the Chiu's standard [14]. Criteria of Chiu grading system consists from 5 subdivisions according to the changes of villus and gland of intestinal mucosa: grade 0, normal mucosa; grade 1, development of subepithelial Gruenhagen's space at the tip of villus; grade 2, extension of the space with moderate epithelial lifting; grade 3, massive epithelial lifting with a few denuded villi; grade 4, denuded villi with exposed capillaries; and grade 5, disintegration of the lamina propria, ulceration and hemorrhage.

2.4. Detection of the Content of Malondialdehyde (MDA) in Small Intestinal Mucosa. Small intestinal mucosa was homogenized with normal saline. The tissue content of MDA, an index of oxidative stress mediated tissue lipid peroxidation, was determined by the TBA method (Jiancheng Bioengineering Ltd, Nanjing, China) as described in [15]. The values of MDA in tissue homogenate were expressed as nmol/mL. The content of final MDA in small intestinal mucosa was normalized for tissue weight.

2.5. Detection of Superoxide Dismutase (SOD) Activity in Small Intestinal Mucosa. Small intestinal mucosa was made into a homogenate with normal saline, frozen at −20°C for 5 min and centrifuged for 15 min at 4000 r/min. Supernatants were transferred into fresh tubes for the evaluation of SOD activity. SOD activity was assessed by SOD detection kits according to the manufacturer's instructions (Jiancheng Bioengineering Ltd, Nanjing, China). Presented data were normalized for tissue weight.

2.6. Measurement of β-Hexosaminidase Level in Serum. At the end of the experiment, 2 mL of blood was obtained from inferior vena cava and was centrifuged for 15 min at 4000 r/min. The supernatant, serum, was stored at −20°C for the determination of β-hexosaminidase level using the modification of a previously described method [16]. Briefly, 50 μL of serum was incubated with 50 μL of 1 mM p-nitrophenyl-N-acetyl-β-D-glucosaminide dissolved in 0.1 M

citrate buffer (pH 5) in 96-well plate at 37°C for 1 h. The reaction was terminated with 200 μL/well of 0.1 M carbonate buffer (pH 10.5). The absorbance at 405 nm was measured using a microplate reader.

2.7. Western Blotting. Intestinal mucosa samples were homogenized with lysis buffer for 30 seconds in a mortar and pestle with liquid nitrogen. Homogenates were centrifuged at 13000 rpm for 10 min at 4°C and the supernatant was collected as the source of sample of protein. The proteins were processed with standard methods for western blot analysis as described in [17]. Rat monoclonal antitryptase antibody, rat monoclonal anti-gp91^{phox} and anti-p47^{phox} antibodies, and rat monoclonal anti-ICAM-1 and α-tubulin antibodies were obtained from Santa Cruz (Santa Cruz, CA, USA). The secondary antibody conjugated to horseradish peroxidase was diluted at 1 : 2,000 (Santa Cruz, CA, USA). Immunoblots were incubated with an enhanced chemiluminescence detection system (KeyGen Biotech, China) and the densitometry analysis was performed using Quantity One software.

2.8. Determination of IL-6 Production in Small Intestinal Mucosa by Enzyme Immunoassay. Briefly, intestinal protein was measured by BCA Protein Assay Kit provided by KenGen Biotech Company, Nanjing, China; the results were expressed as g/L. And the levels of IL-6 were measured by commercial ELISA kits following manufacturer's instructions (R&D systems Inc., USA). The absorbance was read at 450 nm by a biokinetics microplate reader Model EL340 (Biotek Instruments, USA); the results were expressed as pg/L; then the levels of IL-6 in the intestine were calculated as pg/mg protein.

2.9. Determination of Myeloperoxidase (MPO) Activity in Small Intestinal Mucosa. Myeloperoxidase (MPO) activity was determined with the O-dianisidine method [18], using a MPO detection kit (Nanjing Jiancheng Bioengineering Institute) as we described [19]. MPO activity was defined as the quantity of enzyme degrading 1 μmol of peroxide per minute at 37°C and was expressed in units per gram weight of wet tissue.

2.10. Assessment of Mast Cell Counts in Small Intestine. Five μm thick sections were prepared from paraffin-embedded intestine tissue; after deparaffinization, endogenous peroxidase was quenched with 3% H_2O_2 in deionized water for 10 min. Nonspecific binding sites were blocked by incubating the sections in 10% of normal rabbit serum for 1 h. The sections were then incubated with polyclonal rat antimast cell tryptase (dilution 1 : 2000, Santa Cruz, CA, USA) for 20 min at 37°C, followed by incubation with biotinylated mouse anti-rat IgG at room temperature for 10–15 min. After 3 × 5 min PBS rinses, the horseradish-peroxidase-conjugated streptavidin solution was added and incubated at room temperature for 10–15 min. The antibody binding sites were visualized by incubation with a diaminobenzidine-H_2O_2 solution. The sections incubated with PBS instead of the primary antibody were used as negative controls. Brown-yellow granules in cytoplasm were recognized as positive staining for tryptase. We calculated the tryptase positive mast cells in five randomly selected areas at ×200 magnification by Image-Pro Plus 5.0 (USA).

2.11. Statistical Analysis. The data (except for the survival curves) were expressed as mean ± SEM. Analysis of variance was performed using Graphpad Prism software. One-way analysis of variance was used for multiple comparisons, followed by Bonferroni's and Student's t-test for unpaired values. The survival rate was expressed as the percentage of live animals, and the Mantel Cox log rank test was used to determine differences between survival curves. A P value less than 0.05 is considered a significant difference.

3. Results

3.1. Effects of Sevoflurane Preconditioning on Survival Rates in Rats Challenged to IIR in the Presence or Absence of Mast Cell Activator. Initially, we sought to explore the role of sevoflurane preconditioning in the IIR injury; pretreatment of rats with sevoflurane displayed no significant differences in comparison with IIR group. And we also sought to investigate whether mast cell inhibition is involved in the benefits induced by sevoflurane preconditioning; the mast cell special stabilizer and activator were addressed as positive and negative control groups. As illustrated in Figure 1, activation of mast cell by Compound 48/80 resulted in significant decreases in 2 h survival rates after the clamp releasing as compared with sole IIR group, and stabilizing mast cell dramatically abolished the reductions in 2 h survival induced by Compound 48/80; by contrast, pretreatment of sevoflurane did not attenuate Compound 48/80 mediated exacerbation of postischemic survival rate in rats subjected to IIR. These data further demonstrate that mast cell degranulation exacerbates IIR injury, and the results gave us the first impression that sevoflurane preconditioning may not contribute to mast cell stabilization.

3.2. Effects of Sevoflurane Preconditioning on Small Intestinal Structure in Rats Undergoing IIR in the Presence or Absence of Mast Cell Activator. Because there were no differences in the 2 h survival among IIR group, IIR + CS group, and SEV + IIR group, we, next, sought to define the further effects of sevoflurane preconditioning on the IIR injury and its relationships with mast cell. The sections of small intestine obtained for evaluation of the injury severity by HE staining at the end of the experiment, 75 min ischemia followed by 2 h reperfusion, resulted in severe damages to small intestine; as depicted in Figure 2, multiple erosions and bleeding were observed in IIR group, while Compound 48/80 further aggravated IIR injury demonstrated by more multiple erosions and bleedings and more inflammatory cell sequestrations seen in the IIR + CP group, whereas the villus and glands were normal and no inflammatory cell infiltration was observed in mucosal epithelial layer in Sham-operated group. Mast cell stabilizer and sevoflurane similarly significantly attenuated the injuries

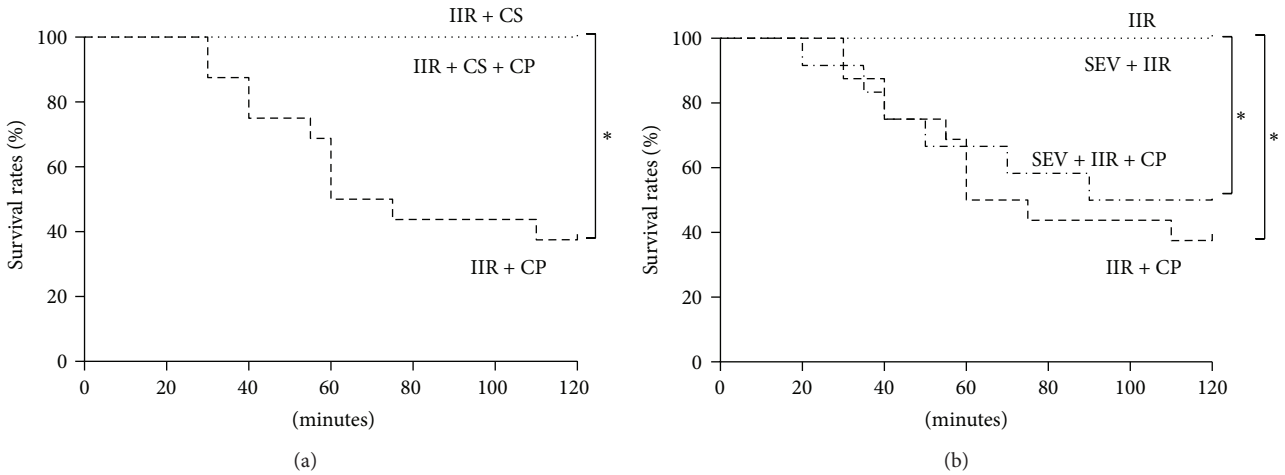

Figure 1: Survival rates after IIR injury. SH group (Sham-operated group), IIR group (75 min intestinal ischemia and 2 h reperfusion), IIR + CP group (IIR group + Compound 48/80 1 mg/kg), IIR + CS group (50 mg/kg cromolyn sodium treated IIR group), IIR + CS + CP group (50 mg/kg cromolyn sodium treated IIR group + Compound 48/80 1 mg/kg), SEV + IIR group (2.3% sevoflurane pretreated IIR group), SEV + IIR + CP group (2.3% sevoflurane pretreated IIR group + Compound 48/80 1 mg/kg). The survival rates in 2 h after reperfusion were 100% in all groups except IIR + CP and SEV + IIR + CP groups. Results are expressed as percentage of live animals, $n = 6$ per group, whereas $n = 16$ in IIR + CP group and $n = 12$ in SEV + IIR + CP group. * indicated that P value was less than 0.05.

in small intestine and only slight edema of mucosa villus and infiltration of few necrotic epithelial inflammatory cells were found in mucosa epithelial layer under microscopy assessment in CS or sevoflurane treated groups. However, cromolyn sodium, but not sevoflurane, blocked Compound 48/80-induced exacerbation in small intestinal morphology changes after 2 h reperfusion. Consistent with morphological changes, the Chiu's scores markedly increased in IIR group as compared with Sham-operated group while treated with mast cell degranulator Compound 48/80 after ischemia resulted in further increases in Chiu's scores. Cromolyn sodium and sevoflurane similarly lowered the Chiu's scores; of note, cromolyn sodium, but not sevoflurane, significantly limited the changes induced by Compound 48/80 ($P < 0.05$, IIR + CS + CP versus IIR + CP group).

3.3. Effects of Sevoflurane Preconditioning on Mast Cell Degranulation in Small Intestine in Rats Undergoing IIR in the Presence or Absence of Mast Cell Activator. Tryptase and β-hexosaminidase are the unique markers released from mast cell and the elevations can be recognized as mast cell degranulation. As shown in Figure 3, after 2 h of reperfusion, we found that tryptase protein expression and β-hexosaminidase level, as well as mast cell counts, were greatly increased in group IIR as compared with Sham-operated group, and Compound 48/80 resulted in further mast cell degranulation as significant increases in tryptase protein expression, β-hexosaminidase level, and mast cell counts were more observed in group IIR + CP than in group IIR; as expected, mast cell stabilizer CS not only attenuated the upregulations induced by IIR, but also abolished the exacerbations mediated by Compound 48/80. Interestingly, pretreatment of rats with sevoflurane exhibited no reductions in tryptase protein expression, β-hexosaminidase level, and mast cell counts induced by IIR challenge; furthermore, the alterations were further aggravated in the presence of Compound 48/80 despite sevoflurane preconditioning, which was comparable to IIR + CP group. Collectively, the findings from the current study indicated that mast cell degranulation aggravated IIR injury and mast cell stabilization is not involved in the protections provided by sevoflurane preconditioning.

3.4. Effects of Sevoflurane Preconditioning on Neutrophil Rolling in Small Intestine in Rats Undergoing IIR in the Presence or Absence of Mast Cell Activator. IIR injury is characterized by neutrophil infiltration into the inflamed tissues [20], as illustrated in Figure 4; in agreement with previous results [20], we also found that IIR led to marked increases in MPO activities and ICAM-1 protein expressions as compared with Sham-operated group; furthermore, Compound 48/80 led to further increases in MPO activities and ICAM-1 protein expression in group IIR + CP than in group IIR. Administrations with cromolyn sodium and sevoflurane similarly significantly inhibited neutrophil infiltration/activation demonstrated by downregulation of MPO activities and ICAM-1 protein expression induced by IIR. Of note, mast cell stabilizer, but not sevoflurane, blocked Compound 48/80 mediated exacerbation of IIR by reducing neutrophil infiltration.

3.5. Effects of Sevoflurane Preconditioning on Inflammation in Small Intestine in Rats Undergoing IIR in the Presence or Absence of Mast Cell Activator. Inflammatory cytokine, interleukin 6 (IL-6), has been demonstrated to be implicated in the pathogenesis of IIR injury [21]. As shown in Figure 5, in the current study, rats undergoing 75 min ischemia and 2 h reperfusion showed significant increases in IL-6 levels in

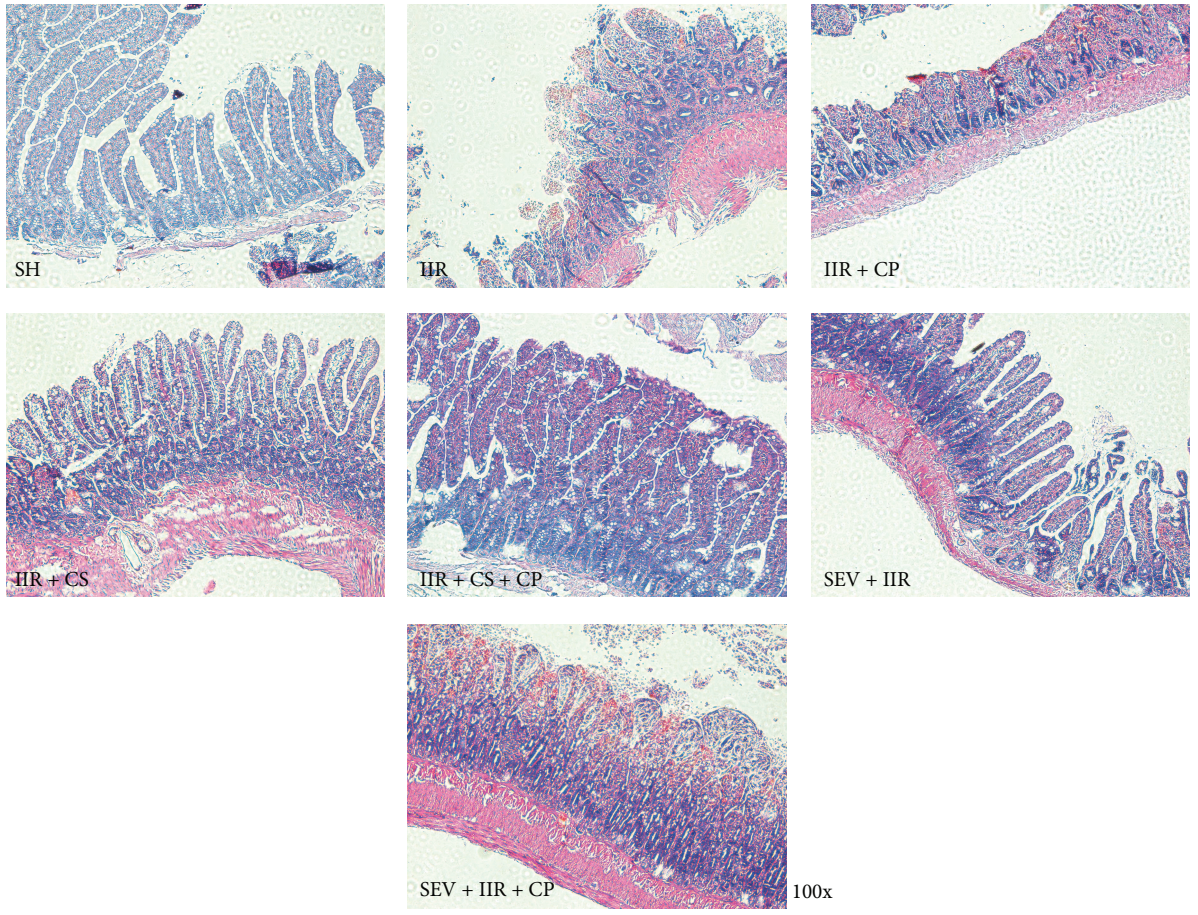

(a)

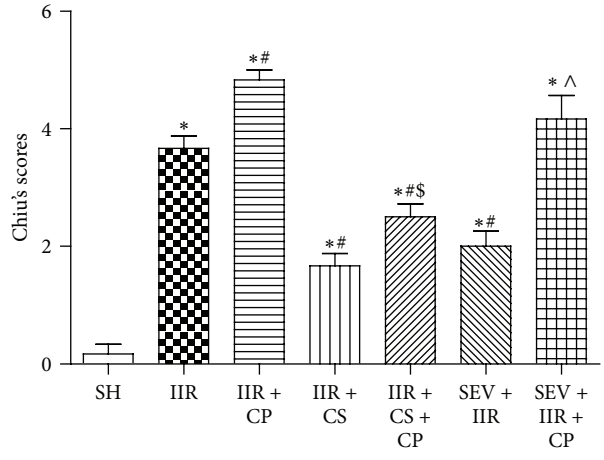

(b)

Figure 2: Morphological changes of intestine and intestinal histological score under light microscope after IIR injury. (a) is representative image of SH group (Sham-operated group), IIR group (75 min intestinal ischemia and 2 h reperfusion), IIR + CP group (IIR group + Compound 48/80 1 mg/kg), IIR + CS group (50 mg/kg cromolyn sodium treated IIR group), IIR + CS + CP group (50 mg/kg cromolyn sodium treated IIR group + Compound 48/80 1 mg/kg), SEV + IIR group (2.3% sevoflurane pretreated IIR group), and SEV + IIR + CP group (2.3% sevoflurane pretreated IIR group + Compound 48/80 1 mg/kg), (HE staining, ×100). Bar graph in (b) quantified the intestine histological scores. Results are expressed as Mean ± SEM. $n = 6$ per group. $^{*}P < 0.05$ versus SH group, $^{\#}P < 0.05$ versus IIR group, $^{\$}P < 0.05$ versus IIR + CP group, $^{\&}P < 0.05$ versus IIR + CS group, and $^{\wedge}P < 0.05$ versus SEV + IIR group.

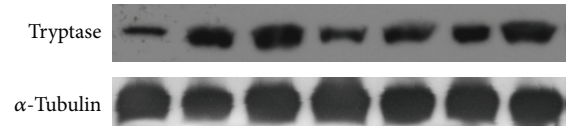

(a)

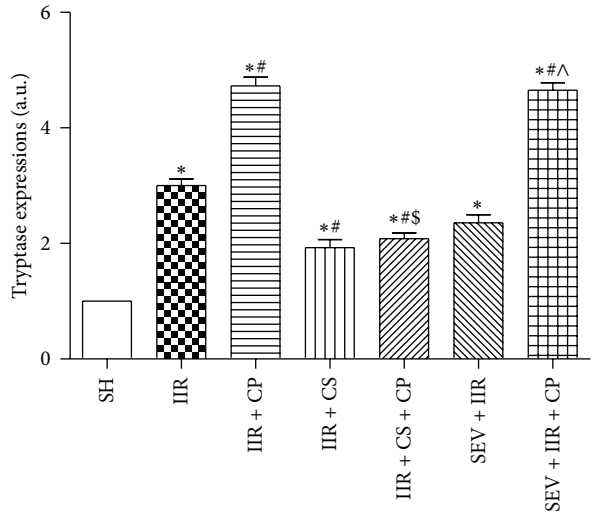

(b)

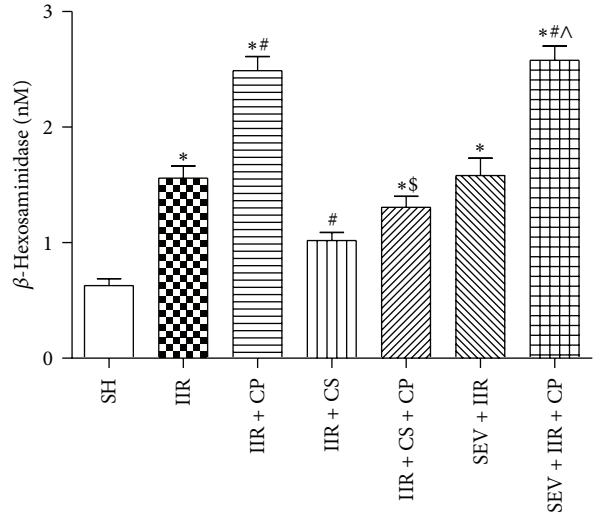

(c)

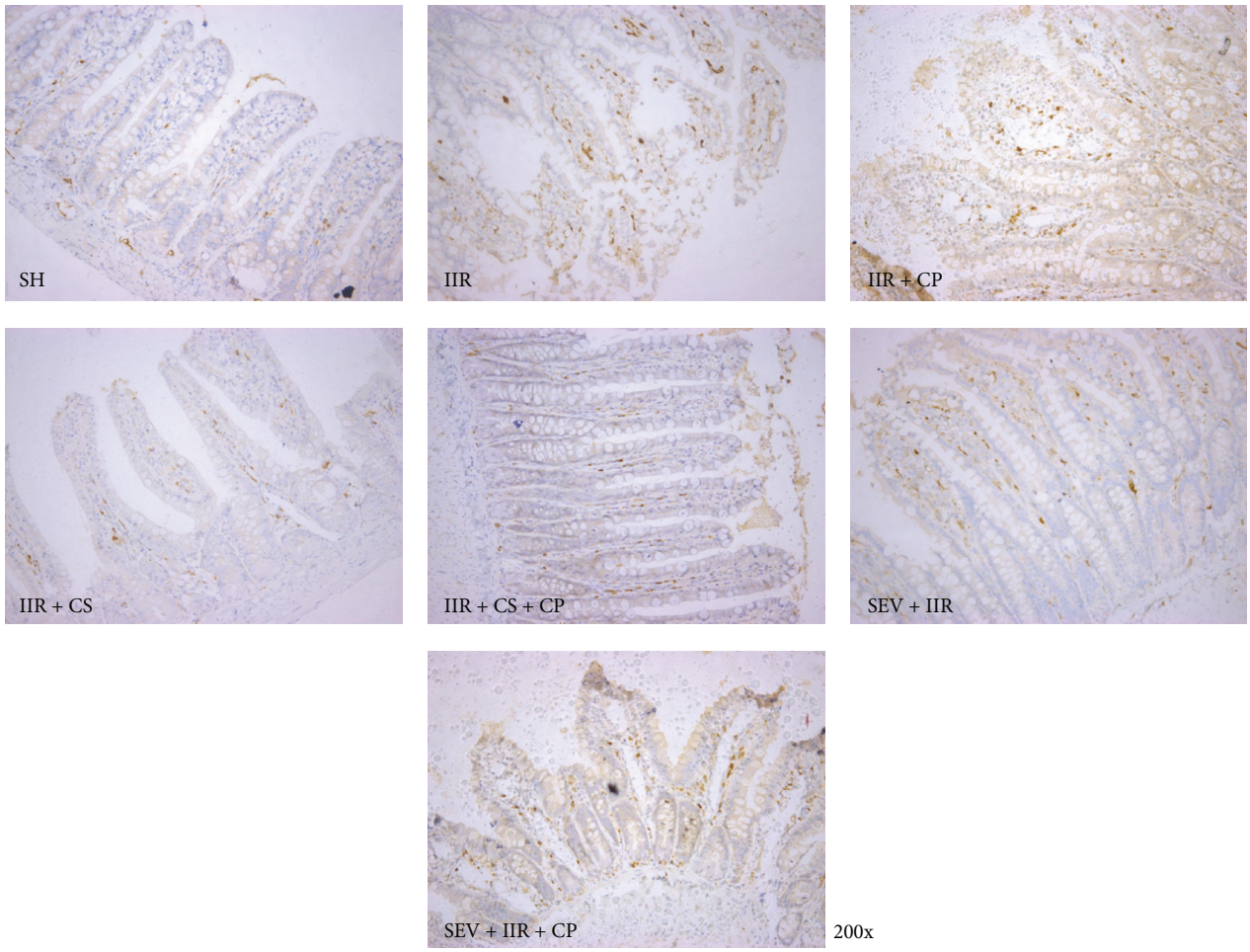

(d)

Figure 3: Continued.

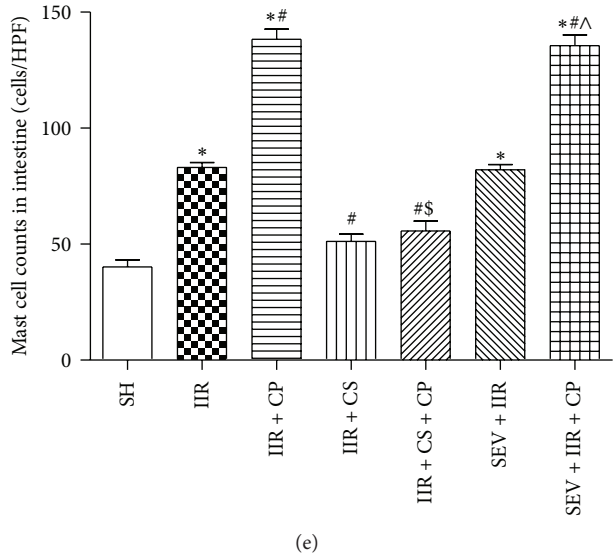

(e)

Figure 3: Tryptase protein expression in intestine mucosa, and β-hexosaminidase levels in serum, intestinal mast cell counts after IIR injury. SH group (Sham-operated group), IIR group (75 min intestinal ischemia and 2 h reperfusion), IIR + CP group (IIR group + Compound 48/80 1 mg/kg), IIR + CS group (50 mg/kg cromolyn sodium treated IIR group), IIR + CS + CP group (50 mg/kg cromolyn sodium treated IIR group + Compound 48/80 1 mg/kg), SEV + IIR group (2.3% sevoflurane pretreated IIR group), and SEV + IIR + CP group (2.3% sevoflurane pretreated IIR group + Compound 48/80 1 mg/kg). Representative band of tryptase protein expression in intestinal mucosa is displayed in (a). Bar graphs (b) quantified tryptase protein expression ($n = 3$). Bar graph (c) quantified β-hexosaminidase levels ($n = 6$). Representative images of immunohistochemical staining for tryptase in intestine are displayed in (d) (SP staining, ×200); brown-yellow granules in the cytoplasm were recognized as mast cells. Bar graph in (e) quantified mast cell counts in small intestine ($n = 6$). Results are expressed as Mean ± SEM. $^{*}P < 0.05$ versus SH group, $^{\#}P < 0.05$ versus IIR group, $^{\$}P < 0.05$ versus IIR + CP group, $^{\&}P < 0.05$ versus IIR + CS group, and $^{\wedge}P < 0.05$ versus SEV + IIR group.

small intestinal mucosa in group IIR as compared with Sham-operated group; moreover, administration with Compound 48/80 further resulted in dramatic enhancements in IL-6 levels in group IIR + CP ($P < 0.05$ versus group IIR). Mast cell stabilizer cromolyn sodium and sevoflurane similarly greatly abrogated the increases in IL-6 levels; however, cromolyn sodium, but not sevoflurane, blocked the enhancements in IL-6 levels resulted from IIR in the presence of the MC activator Compound 48/80.

3.6. Effects of Sevoflurane Preconditioning on Oxidative Stress in Small Intestine in Rats Undergoing IIR in the Presence or Absence of Mast Cell Activator. Since mast cell inhibition is not involved in the protection induced by sevoflurane preconditioning, we sought other underlying mechanisms by which sevoflurane preconditioning provides benefits against IIR. Ischemia reperfusion injury is also characterized by up-regulation of free radical species [17]. In line with previous results [22], as shown in Figure 6, 75 min ischemia followed by 2 h reperfusion resulted in substantial increases in MDA contents and reductions in SOD activities as compared with Sham-operated group. Meanwhile, IIR also caused great increases in $gp91^{phox}$ and $p47^{phox}$ protein expression when compared with Sham-operated group. Moreover, Compound 48/80 further aggravated the changes of oxidative stress induced by IIR ($P < 0.05$ IIR + CP versus IIR); by contrast, cromolyn sodium and sevoflurane similarly attenuated IIR mediated oxidative stress demonstrated by downregulating MDA contents and $gp91^{phox}$ and $p47^{phox}$ protein expressions and up-regulating SOD activities in cromolyn sodium and sevoflurane treated groups by comparison with group IIR. Furthermore, cromolyn sodium limited the further increases of oxidative stress induced by Compound 48/80. As expected, sevoflurane preconditioning exhibited no protective effects against Compound 48/80 exacerbated oxidative stress.

4. Discussion

We have shown in the current study, to our knowledge, for the first time that sevoflurane preconditioning attenuated the small intestinal ischemia reperfusion injury; inhibiting neutrophil sequestration may represent the major mechanism whereby sevoflurane preconditioning alleviates IIR injury. Further, we showed that the subsequent mast cell activation contributed to the exacerbation of IIR injury demonstrated by significant increases in intestinal injury score and elevations in postischemic oxidative stress and neutrophil sequestrations, leading to significantly reduced postischemic survival; stabilizing mast cell by cromolyn sodium not only dramatically attenuated IIR injury, but also totally blocked the exacerbated injury induced by mast cell activation. By contrast, we showed that sevoflurane preconditioning offers no protections in mast cell mediated IIR injury.

Mast cell, containing a large range of mediators, presents throughout gastrointestinal tract. Although mast cell may

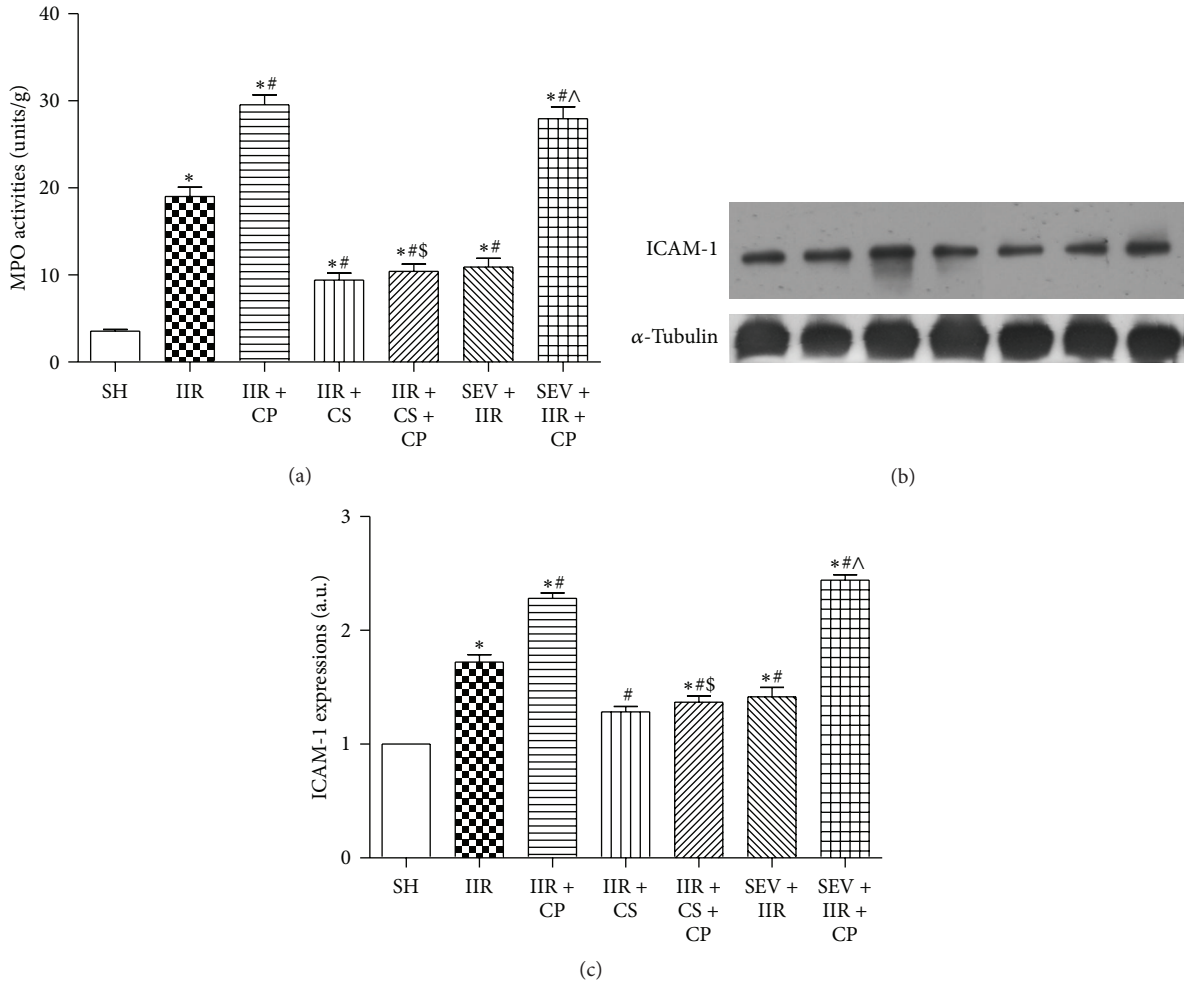

Figure 4: MPO activities and ICAM-1 protein expression in intestine mucosa after IIR injury. SH group (Sham-operated group), IIR group (75 min intestinal ischemia and 2 h reperfusion), IIR + CP group (IIR group + Compound 48/80 1 mg/kg), IIR + CS group (50 mg/kg cromolyn sodium treated IIR group), IIR + CS + CP group (50 mg/kg cromolyn sodium treated IIR group + Compound 48/80 1 mg/kg), SEV + IIR group (2.3% sevoflurane pretreated IIR group), and SEV + IIR + CP group (2.3% sevoflurane pretreated IIR group + Compound 48/80 1 mg/kg). Bar graph (a) quantified MPO activities in intestinal mucosa ($n = 6$). Representative band of ICAM-1 protein expressions is displayed in (b). Bar graphs (c) quantified ICAM-1 protein expressions ($n = 3$). Results are expressed as Mean ± SEM. $^{*}P < 0.05$ versus SH group, $^{\#}P < 0.05$ versus IIR group, $^{\$}P < 0.05$ versus IIR + CP group, $^{\&}P < 0.05$ versus IIR + CS group, and $^{\wedge}P < 0.05$ versus SEV + IIR group.

function as host defense to prevent bacterial invasion [23], prolonged MC activation has been demonstrated to contribute to the development of a variety of disorders and to play a critical role in the pathogenesis of IIR injury by releasing histamine, tryptase, and TNF-α [24]. Ramos et al. reported that mast cell degranulation plays a significant role in the development of sepsis by regulating cell death, which resulted in multiorgan dysfunction [25]. Consistent with the previous findings that stabilizing MC from degranulation would be one of the potential strategies for combating IIR injury [26], our current study further revealed that inhibiting mast cell from activation/degranulation by cromolyn sodium significantly limited the IIR injury evidenced as increases in postischemic survival and reductions in tryptase protein expression and β-hexosaminidase levels, which causes or exacerbates IIR injury; this notion is further supported by the fact that mast cell stabilizer cromolyn sodium abolished the exacerbated injury induced by Compound 48/80. The data from the current study further confirmed that mast cell activation plays a central role in exacerbating IIR injury, although the mechanism governing mast cell activation during IIR is yet to be explored.

Uncontrollable inflammation and neutrophils sequestration in inflamed tissues also contribute to IIR injury, and selectins and intercellular adhesion molecules (ICAMs) by the activated endothelium induce neutrophils migration to injurious site [27]. Compton et al. have reported that tryptase released from mast cell degranulation plays a central role in attracting leukocytes infiltration and migration to ischemic tissues [28]. And treatment with mast cell stabilizer cromolyn sodium can reduce the expressions of ICAM-1 in the lungs in a rat model of pancreatitis-associated lung injury and

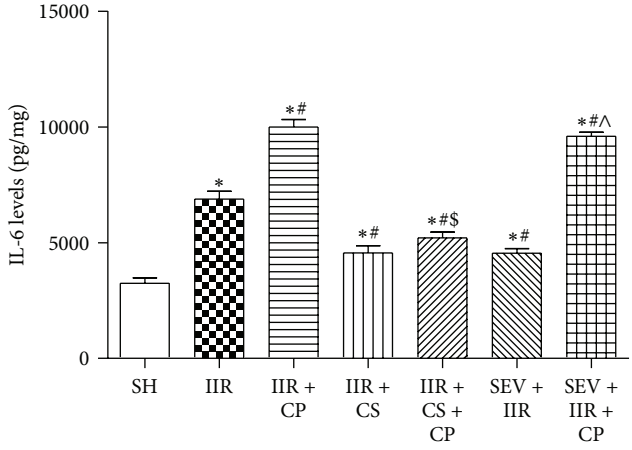

Figure 5: Levels of IL-6 in intestine after IIR injury. SH group (Sham-operated group), IIR group (75 min intestinal ischemia and 2 h reperfusion), IIR + CP group (IIR group + Compound 48/80 1 mg/kg), IIR + CS group (50 mg/kg cromolyn sodium treated IIR group), IIR + CS + CP group (50 mg/kg cromolyn sodium treated IIR group + Compound 48/80 1 mg/kg), SEV + IIR group (2.3% sevoflurane pretreated IIR group), and SEV + IIR + CP group (2.3% sevoflurane pretreated IIR group + Compound 48/80 1 mg/kg). Bar graph quantified IL-6 levels in intestinal mucosa. Results are expressed as Mean ± SEM. $n = 6$ per group. $^{*}P < 0.05$ versus SH group, $^{\#}P < 0.05$ versus IIR group, $^{\$}P < 0.05$ versus IIR + CP group, $^{\&}P < 0.05$ versus IIR + CS group, and $^{\wedge}P < 0.05$ versus SEV + IIR group.

downregulate IL-6 level [29]. These findings point to the importance of mast cell degranulation, through increased release of proinflammatory mediator, in inducing neutrophil migration to inflamed tissues. In the present study, we found that, during IIR, mast cell degranulation resulted in more neutrophils infiltration into small intestine evidenced as significant elevations in MPO activities, ICAM-1 protein expression, and IL-6 concentration; most importantly, cromolyn sodium abolished the alterations induced by IIR and prevented Compound 48/80-mediated exacerbation of IIR injury.

Previous study reported that sevoflurane preconditioning prevents from acute lung injury induced by aortic ischemia and reperfusion through reducing pulmonary neutrophil accumulation [10]. We also found that sevoflurane preconditioning significantly downregulated the MPO activities, ICAM-1 protein expression, and IL-6 concentrations, indicating that inhibiting neutrophil sequestration and the subsequent systemic inflammation may be the potential mechanism of attenuating IIR injury. It is well known that the delay in diagnosis and treatment of IIR injury contributes to the continued high in-hospital mortality rate [30]; the findings from the current study suggested that preventive administration of sevoflurane may be a promising approach in alleviating postoperative intestinal ischemia and mortality.

Sevoflurane is a preferable clinical choice in patients diagnosed to have mastocytosis, a group of rare disorders caused by the presence of too many mast cells and CD34+ mast cell precursors, without inducing mast cell degranulation [12]. It is well known that sevoflurane can mimic the effect of brief ischaemic episodes and protect from ischemia/reperfusion injury; Annecke and the groups have demonstrated that sevoflurane preconditioning significantly alleviates ischemia reperfusion injury in an ex vivo model of heart without alterations of histamine, and the findings suggested the benefits provided by sevoflurane preconditioning are not involved in mast cell [13]. Under the current study, we adjusted exposure of rats with 1 MAC sevoflurane for 1 h in three consequent days in the presence or absence of mast cell activator. The results from the current study showed that sevoflurane preconditioning greatly attenuated IIR injury demonstrated by reductions in injury scores and down-regulations of neutrophil infiltrations and inflammation; however, those protections are reversed by mast cell activator Compound 48/80, whereas mast cell stabilizer cromolyn sodium still confers protections challenged by Compound 48/80. The data from the present study indicated that the protective roles of sevoflurane preconditioning are independent of inhibiting mast cell.

Overproduction of reactive oxidative species (ROS) by NADPH oxidase is generally considered to play a critical role in the pathogenesis of ischemia reperfusion injury, and there are a number of NADPH homologs, such as Nox1, Nox2 (also named as $gp91^{phox}$), and Nox3-4 [31]. It is should be noted that Nox2 is predominantly expressed within epithelial cells. Guan et al. demonstrated that intracellular NADPH concentration, in villus tip cells in intestine were significantly rapidly increased even after short-term ischemia [32]. Bedirli et al. recently reported that sevoflurane preconditioning dramatically attenuated the oxidative stress in a rat model of sepsis [33]; moreover, Yang et al. have demonstrated that sevoflurane preconditioning confers neuroprotection by increasing antioxidant enzymes [11]. In agreement with the previous results, we also found that 75 min small intestinal ischemia and 2 h reperfusion led to significant increases in MDA level and $gp91^{phox}$ and $p47^{phox}$ proteins expression, and resulted in significant decreases in SOD activities, furthermore, preconditioning of IIR-rats with sevoflurane significantly reduced the IIR mediated alterations, indicating that sevoflurane preconditioning confers protections against IIR injury possibly through reducing oxidative stress.

In addition to IgE/Fcε, the classical signal pathway of mast cell activation and several distinct nonimmunological stimuli also contribute to mast cell activation [34], including trauma and physical stress. Yoshimaru et al. proved in vitro that upregulated ROS activates mast cell by NADPH oxidase [35], Collaco et al. have demonstrated that inhibiting ROS can dramatically stabilize mast cell in vitro [36]; we previously found significant increases of mast cell activation and concomitant elevations in oxidative stress in a rodent challenged by IIR [22]. The results indicate that there is linkage between mast cell activation and superoxide production. Our current study extended findings of previous studies [22] by showing that NADPH oxidase is overexpressed during IIR which contributed to increased oxidative stress and MC activation, leading to exacerbation of IIR injury, and pretreating of rats with mast cell stabilizer cromolyn sodium not only

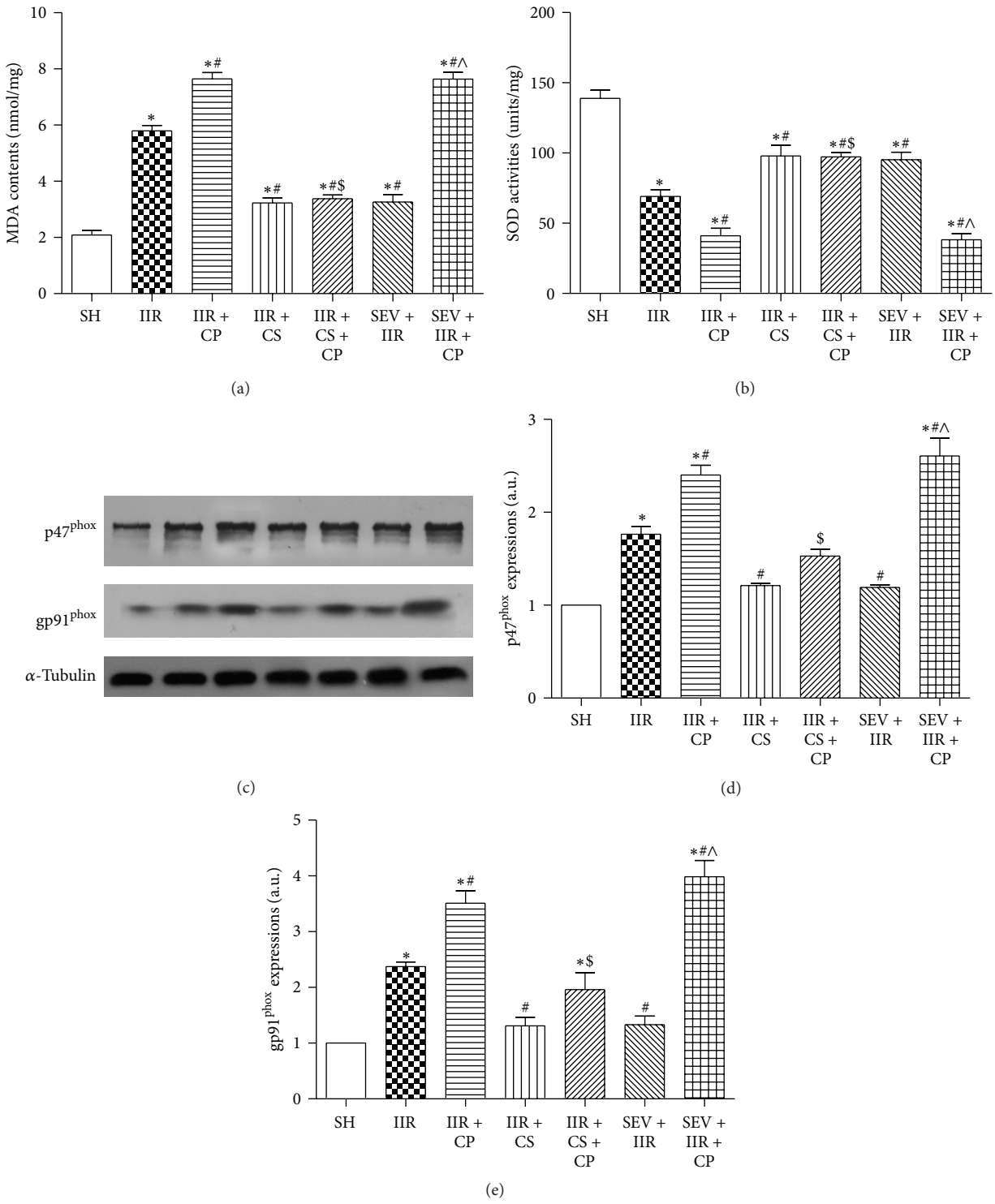

Figure 6: MDA contents and SOD activities and $p47^{phox}$ and $gp91^{phox}$ protein expressions in intestine mucosa after IIR injury. SH group (Sham-operated group), IIR group (75 min intestinal ischemia and 2 h reperfusion), IIR + CP group (IIR group + Compound 48/80 1 mg/kg), IIR + CS group (50 mg/kg cromolyn sodium treated IIR group), IIR + CS + CP group (50 mg/kg cromolyn sodium treated IIR group + Compound 48/80 1 mg/kg), SEV + IIR group (2.3% sevoflurane pretreated IIR group), and SEV + IIR + CP group (2.3% sevoflurane pretreated IIR group + Compound 48/80 1 mg/kg). Bar graph (a) quantified MDA contents and bar graph (b) quantified SOD activities, $n = 6$ per group. Representative bands of $p47^{phox}$ and $gp91^{phox}$ protein expressions are displayed in (c). Bar graphs (d) and (e) quantified $p47^{phox}$ and $gp91^{phox}$ protein expressions, respectively ($n = 3$). Results are expressed as Mean ± SEM. $^{*}P < 0.05$ versus SH group, $^{\#}P < 0.05$ versus IIR group, $^{\$}P < 0.05$ versus IIR + CP group, $^{\&}P < 0.05$ versus IIR + CS group, and $^{\wedge}P < 0.05$ versus SEV + IIR group.

reduced MC activation, but also attenuated NADPH oxidase overexpression and reduced ROS production and consequently attenuated IIR injury and increased survival rate. Pretreatments of rats with sevoflurane displayed significant elevations in oxidative stress during IIR in the presence of mast cell activator Compound 48/80; the results are in line with the findings of Kaida et al. who reported that mast cell degranulation per se contributes to increased oxidative stress [37].

The limitation of the current study is that we did not show the direct relationships between the sevoflurane preconditioning and neutrophil migration in the development of IIR injury; several studies so far have confirmed that sevoflurane preconditioning can inhibit neutrophil infiltrate into ischemic area [10]; therein, the present study did not focus on the underlying mechanism by which sevoflurane preconditioning affects neutrophil sequestration.

In a summary, we have shown that mast cell activation, through increased release of mediators, contributes to deleterious injury induced by IIR and that mast cell stabilizer inhibits mast cell activation, attenuates IIR injury, and enhances postischemic mortality; sevoflurane preconditioning attenuates IIR injury possibly through blocking neutrophil sequestration and reducing oxidative stress but not through inhibiting mast cell, while the underlying mechanism merits further study.

Conflict of Interests

The authors declare no conflict of interests.

Authors' Contribution

Xiaoliang Gan and Guangjie Su contributed equally to the work.

Acknowledgment

This study was supported by the National Natural Science Foundation of China (NSFC), Grant no. 30901408.

References

[1] A. Nickkholgh, P. Contin, K. Abu-Elmagd et al., "Intestinal transplantation: review of operative techniques," *Clinical Transplantation*, vol. 27, supplement 25, pp. 56–65, 2013.

[2] D. C. Reino, D. Palange, E. Feketeova et al., "Activation of toll-like receptor 4 is necessary for trauma hemorrhagic shock-induced gut injury and polymorphonuclear neutrophil priming," *Shock*, vol. 38, pp. 107–114, 2012.

[3] E. Alhan, A. Usta, A. Cekic, K. Saglam, S. Turkyilmaz, and A. Cinel, "A study on 107 patients with acute mesenteric ischemia over 30 years," *International Journal of Surgery*, vol. 10, pp. 510–513, 2012.

[4] J. Karhausen, M. Qing, A. Gibson et al., "Intestinal mast cells mediate gut injury and systemic inflammation in a rat model of deep hypothermic circulatory arrest," *Critical Care Medicine*, vol. 41, no. 9, pp. e200–e210, 2013.

[5] X. Gan, D. Liu, P. Huang, W. Gao, X. Chen, and Z. Hei, "Mast-cell-releasing tryptase triggers acute lung injury induced by small intestinal ischemia-reperfusion by activating PAR-2 in rats," *Inflammation*, vol. 35, pp. 1144–1153, 2012.

[6] N. Bedirli, E. U. Bagriacik, H. Emmez, G. Yilmaz, Y. Unal, and Z. Ozkose, "Sevoflurane and isoflurane preconditioning provides neuroprotection by inhibition of apoptosis-related mRNA expression in a rat model of focal cerebral ischemia," *Journal of Neurosurgical Anesthesiology*, vol. 24, pp. 336–344, 2012.

[7] R. Ye, Q. Yang, X. Kong et al., "Sevoflurane preconditioning improves mitochondrial function and long-term neurologic sequelae after transient cerebral ischemia: role of mitochondrial permeability transition," *Critical Care Medicine*, vol. 40, pp. 2685–2693, 2012.

[8] J. Frädorf, R. Huhn, N. C. Weber et al., "Sevoflurane-induced preconditioning: impact of protocol and aprotinin administration on infarct size and endothelial nitric-oxide synthase phosphorylation in the rat heart in vivo," *Anesthesiology*, vol. 113, no. 6, pp. 1289–1298, 2010.

[9] D. Obal, S. Dettwiler, C. Favoccia, K. Rascher, B. Preckel, and W. Schlack, "Effect of sevoflurane preconditioning on ischaemia/reperfusion injury in the rat kidney in vivo," *European Journal of Anaesthesiology*, vol. 23, no. 4, pp. 319–326, 2006.

[10] R. Kalb, P. Schober, L. A. Schwarte, J. Weimann, and S. A. Loer, "Preconditioning, but not postconditioning, with Sevoflurane reduces pulmonary neutrophil accumulation after lower body ischaemia/reperfusion injury in rats," *European Journal of Anaesthesiology*, vol. 25, no. 6, pp. 454–459, 2008.

[11] Q. Yang, H. Dong, J. Deng et al., "Sevoflurane preconditioning induces neuroprotection through reactive oxygen species-mediated up-regulation of antioxidant enzymes in rats," *Anesthesia and Analgesia*, vol. 112, no. 4, pp. 931–937, 2011.

[12] F. M. Konrad, K. E. Unertl, and T. H. Schroeder, "Mastocytosis. A challenge in anaesthesiology," *Anaesthesist*, vol. 58, no. 12, pp. 1239–1243, 2009.

[13] T. Annecke, D. Chappell, C. Chen et al., "Sevoflurane preserves the endothelial glycocalyx against ischaemia-reperfusion injury," *British Journal of Anaesthesia*, vol. 104, no. 4, pp. 414–421, 2010.

[14] C. J. Chiu, H. J. Scott, and F. N. Gurd, "Intestinal mucosal lesion in low-flow states. II. The protective effect of intraluminal glucose as energy substrate," *Archives of Surgery*, vol. 101, no. 4, pp. 484–488, 1970.

[15] Z. Xia, J. Gu, D. M. Ansley, F. Xia, and J. Yu, "Antioxidant therapy with Salvia miltiorrhiza decreases plasma endothelin-1 and thromboxane B2 after cardiopulmonary bypass in patients with congenital heart disease," *Journal of Thoracic and Cardiovascular Surgery*, vol. 126, no. 5, pp. 1404–1410, 2003.

[16] H. Oda, M. Fujimoto, M. S. Patrick et al., "RhoH plays critical roles in FcεRI-dependent signal transduction in mast cells," *Journal of Immunology*, vol. 182, no. 2, pp. 957–962, 2009.

[17] T. Wang, S. Qiao, S. Lei et al., "N-acetylcysteine and allopurinol synergistically enhance cardiac adiponectin content and reduce myocardial reperfusion injury in diabetic rats," *PLoS ONE*, vol. 6, no. 8, Article ID e23967, 2011.

[18] J. E. Krawisz, P. Sharon, and W. F. Stenson, "Quantitative assay for acute intestinal inflammation based on myeloperoxidase activity. Assessment of inflammation in rat and hamster models," *Gastroenterology*, vol. 87, no. 6, pp. 1344–1350, 1984.

[19] B. Xu, X. Gao, J. Xu et al., "Ischemic postconditioning attenuates lung reperfusion injury and reduces systemic proinflammatory

cytokine release via heme oxygenase 1," *Journal of Surgical Research*, vol. 166, no. 2, pp. e157–e164, 2011.

[20] M. Ghyczy, C. Torday, J. Kaszaki, A. Szabó, M. Czóbel, and M. Boros, "Oral phosphatidylcholine pretreatment decreases ischemia-reperfusion induced methane generation and the inflammatory response in the small intestine," *Shock*, vol. 30, no. 5, pp. 596–602, 2008.

[21] K. Yoshiya, P. H. Lapchak, T.-H. Thai et al., "Depletion of gut commensal bacteria attenuates intestinal ischemia/reperfusion injury," *American Journal of Physiology*, vol. 301, no. 6, pp. G1020–G1030, 2011.

[22] Z.-Q. Hei, X.-L. Gan, G.-J. Luo, S.-R. Li, and J. Cai, "Pretreatment of cromolyn sodium prior to reperfusion attenuates early reperfusion injury after the small intestine ischemia in rats," *World Journal of Gastroenterology*, vol. 13, no. 38, pp. 5139–5146, 2007.

[23] A. B. Penissi, M. I. Rudolph, and R. S. Piezzi, "Role of mast cells in gastrointestinal mucosal defense," *Biocell*, vol. 27, no. 2, pp. 163–172, 2003.

[24] N. G. Frangogiannis, C. W. Smith, and M. L. Entman, "The inflammatory response in myocardial infarction," *Cardiovascular Research*, vol. 53, no. 1, pp. 31–47, 2002.

[25] L. Ramos, G. Peña, B. Cai, E. A. Deitch, and L. Ulloa, "Mast cell stabilization improves survival by preventing apoptosis in sepsis," *Journal of Immunology*, vol. 185, no. 1, pp. 709–716, 2010.

[26] Z. Q. Hei, X. L. Gan, P. J. Huang, J. Wei, N. Shen, and W. L. Gao, "Influence of Ketotifen, Cromolyn Sodium, and Compound 48/80 on the survival rates after intestinal ischemia reperfusion injury in rats," *BMC Gastroenterology*, vol. 8, article 42, 2008.

[27] F. Spiller, M. I. L. Orrico, D. C. Nascimento et al., "Hydrogen sulfide improves neutrophil migration and survival in sepsis via K+ATP channel activation," *American Journal of Respiratory and Critical Care Medicine*, vol. 182, no. 3, pp. 360–368, 2010.

[28] S. J. Compton, J. A. Cairns, S. T. Holgate, and A. F. Walls, "Human mast cell tryptase stimulates the release of an IL-8-dependent neutrophil chemotactic activity from human umbilical vein endothelial cells (HUVEC)," *Clinical and Experimental Immunology*, vol. 121, no. 1, pp. 31–36, 2000.

[29] X. Zhao, M. Dib, X. Wang, B. Widegren, and R. Andersson, "Influence of mast cells on the expression of adhesion molecules on circulating and migrating leukocytes in acute pancreatitis-associated lung injury," *Lung*, vol. 183, no. 4, pp. 253–264, 2005.

[30] W. T. Kassahun, T. Schulz, O. Richter, and J. Hauss, "Unchanged high mortality rates from acute occlusive intestinal ischemia: six year review," *Langenbeck's Archives of Surgery*, vol. 393, no. 2, pp. 163–171, 2008.

[31] G. R. Drummond, S. Selemidis, K. K. Griendling, and C. G. Sobey, "Combating oxidative stress in vascular disease: NADPH oxidases as therapeutic targets," *Nature Reviews Drug Discovery*, vol. 10, no. 6, pp. 453–471, 2011.

[32] Y. Guan, R. T. Worrell, T. A. Pritts, and M. H. Montrose, "Intestinal ischemia-reperfusion injury: reversible and irreversible damage imaged in vivo," *American Journal of Physiology*, vol. 297, no. 1, pp. G187–G196, 2009.

[33] N. Bedirli, C. Y. Demirtas, T. Akkaya et al., "Volatile anesthetic preconditioning attenuated sepsis induced lung inflammation," *Journal of Surgical Research*, vol. 178, pp. e17–e23, 2012.

[34] C. Wolber, F. Baur, and J. R. Fozard, "Interaction between adenosine and allergen or compound 48/80 on lung parenchymal strips from actively sensitized Brown Norway rats," *European Journal of Pharmacology*, vol. 498, no. 1-3, pp. 227–232, 2004.

[35] T. Yoshimaru, Y. Suzuki, T. Inoue, O. Niide, and C. Ra, "Silver activates mast cells through reactive oxygen species production and a thiol-sensitive store-independent Ca^{2+} influx," *Free Radical Biology and Medicine*, vol. 40, no. 11, pp. 1949–1959, 2006.

[36] C. R. Collaco, D. J. Hochman, R. M. Goldblum, and E. G. Brooks, "Effect of sodium sulfite on mast cell degranulation and oxidant stress," *Annals of Allergy, Asthma and Immunology*, vol. 96, no. 4, pp. 550–556, 2006.

[37] S. Kaida, Y. Ohta, Y. Imai, K. Ohashi, and M. Kawanishi, "Compound 48/80 causes oxidative stress in the adrenal gland of rats through mast cell degranulation," *Free Radical Research*, vol. 44, no. 2, pp. 171–180, 2010.

Hindawi Publishing Corporation
Mediators of Inflammation
Volume 2013, Article ID 720536, 19 pages
http://dx.doi.org/10.1155/2013/720536

Research Article

Progression of Luminal Breast Tumors Is Promoted by Ménage à Trois between the Inflammatory Cytokine TNFα and the Hormonal and Growth-Supporting Arms of the Tumor Microenvironment

Polina Weitzenfeld, Nurit Meron, Tal Leibovich-Rivkin, Tsipi Meshel, and Adit Ben-Baruch

Ela Kodesz Institute for Research on Cancer Development and Prevention, Department of Cell Research and Immunology, George S. Wise Faculty of Life Sciences, Tel Aviv University, 69978 Tel Aviv, Israel

Correspondence should be addressed to Adit Ben-Baruch; aditbb@tauex.tau.ac.il

Received 21 August 2013; Accepted 9 October 2013

Academic Editor: Salahuddin Ahmed

Breast cancer progression is strongly linked to inflammatory processes, aggravating disease course. The impacts of the inflammatory cytokine TNFα on breast malignancy are not fully substantiated, and they may be affected by cooperativity between TNFα and other protumoral mediators. Here, we show that together with representatives of other important arms of the tumor microenvironment, estrogen (hormonal) and EGF (growth-supporting), TNFα potently induced metastasis-related properties and functions in luminal breast tumor cells, representing the most common type of breast cancer. Jointly, TNFα + Estrogen + EGF had a stronger effect on breast cancer cells than each element alone, leading to the following: (1) extensive cell spreading and formation of FAK/paxillin-enriched cellular protrusions; (2) elevated proportion of tumor cells coexpressing high levels of CD44 and β1 and VLA6; (3) EMT and cell migration; (4) resistance to chemotherapy; (5) release of protumoral factors (CXCL8, CCL2, MMPs). Importantly, the tumor cells used in this study are known to be nonmetastatic under all conditions; nevertheless, they have acquired high metastasizing abilities *in vivo* in mice, following a brief stimulation by TNFα + Estrogen + EGF. These dramatic findings indicate that TNFα can turn into a strong prometastatic factor, suggesting a paradigm shift in which clinically approved inhibitors of TNFα would be applied in breast cancer therapy.

1. Introduction

The majority of breast cancer patients are diagnosed with luminal tumors that are characterized by the expression of estrogen receptors (ER) and progesterone receptors (PR) and the absence or only weak amplification of HER2 (this latter parameter depends on the subclass, whether luminal A or luminal B) [1, 2]. Although ER-expressing and PR-expressing patients typically experience a favorable outcome and a relatively good prognosis, eventually many of them become unresponsive to endocrine therapies and develop metastases at remote organs [1–3]. To date, the mechanisms that contribute to tumor progression and more importantly to metastasis formation in these patients are poorly understood.

Tumor cell dissemination to remote organs is a multifactorial process that is linked to upregulation of extracellular matrix (ECM) and adhesion receptors, to increased spreading and migration, and to epithelial-to-mesenchymal transition (EMT) [4–10]. Moreover, strong induction of metastatic traits is endowed on the tumor cells by elements of the tumor microenvironment that promote many different metastasis-related functions including tumor cell spreading and EMT [11–13].

The tumor milieu is an extremely complex and dynamic contexture comprised of many cell types, ECM components, and secreted factors. Recently, intensive research indicates that there is an intimate link between inflammation and cancer, where inflammatory cells and cytokines promote

processes of tumor growth and progression. In this respect, much emphasis has been attributed to the inflammatory cytokine tumor necrosis factor α (TNFα). TNFα was shown to induce antitumor effects when administered in high concentrations directly into tumors. Thus, TNFα was considered for quite some time as a potential therapeutic modality, whose introduction to patients would limit disease course. However, recent investigations challenged this view and indicated that chronic and consistent presence of TNFα in tumors leads to procancerous consequences in many malignant diseases [14–17].

Specifically in breast cancer, studies in animal model systems have shown that TNFα exerted causative procancerous activities through a diverse set of mechanisms [18–21]. Along these lines, we and others have shown that TNFα was highly expressed in breast tumors [22–25], that the incidence of TNFα expression was significantly increased in advanced stages of breast cancer (detected in approximately 90% of the patients with recurrent disease) [22], and that TNFα induced EMT and invasion of breast tumor cells [22, 26, 27]. Moreover, by virtue of its inflammatory actions as inducer of inflammatory chemokines, TNFα indirectly led to high presence of protumoral leukocyte subpopulations in tumors [28].

The opposing roles of TNFα in cancer may be due to interactions that the cytokine has with other procancerous elements that reside at the tumor milieu. In luminal breast tumors, such interactions could be taking place mainly with two arms of the tumor microenvironment: hormones that are key regulators of the malignant process and growth-supporting factors that promote tumor cell proliferation. Indeed, the hormone estrogen is a key player in luminal breast tumors, where it enhances the proliferation of breast tumor cells, induces EMT, and consequently increases the migratory and invasive abilities of these cells [29–32]. Although the lack of ER is usually associated with worse prognosis [32, 33], the hormone by itself has definite potent tumor-promoting functions and thus is a major therapeutic target in breast cancer treatment. In parallel, growth-supporting factors like epidermal growth factor (EGF) are of large relevance. Luminal breast cancer cells usually do not exhibit amplification of the EGF-signaling HER2 receptor or show only low overexpression of this receptor; nevertheless, they bind EGF and respond to its tumor-promoting stimuli [34–37]. EGF enhances tumor cell proliferation, migration, invasion, and EMT [36, 38–40], and thus it should be taken into account when we consider joint activities of microenvironmental factors on breast cancer metastasis.

In view of the multi-factorial nature of the tumor microenvironment, in this study we determined the combined impact of the three arms—inflammatory (TNFα) + hormonal (estrogen) + growth-supporting (EGF)—on malignancy-promoting characteristics and functions of luminal breast tumor cells. This "combined stimulation" by TNFα + Estrogen + EGF provides a more relevant representation of the multifaceted nature of the tumor microenvironment in luminal breast tumors than the reductionist approach of testing the activity of each element alone. The "combined stimulation" approach is supported by published findings demonstrating coregulatory intracellular interactions existing between TNFα-, estrogen-, and/or EGF-mediated pathways in breast cancer and in other malignancies [34, 41, 42]. Accordingly, in this study we determined the impact of the TNFα + Estrogen + EGF stimulus and compared it to the effect of each factor on its own. Using the joint powers of the TNFα + Estrogen + EGF stimulation, we found that MCF-7 luminal breast tumor cells have acquired very high metastasis-related functions. Already at the initial phases of the study we found that the combined stimulation had a much higher influence than TNFα alone, estrogen alone, or EGF alone on the tumor-promoting aspects that were studied. Therefore, in more advanced stages of the research we focused on the effects of the joint stimulation by TNFα + Estrogen + EGF on functional tumor-promoting readouts, including tumor growth and metastasis formation.

Overall, our findings indicate that TNFα induces many metastasis-related functions in luminal breast tumor cells and that its activities are largely amplified by cooperativity with estrogen and EGF. The TNFα + Estrogen + EGF stimulation has endowed the cancer cells with high spreading and EMT characteristics and with tumor- and metastasis-promoting functions. Moreover, although TNFα was cytotoxic to some of the tumor cells, its cooperativity with estrogen and EGF has led to selection of tumors cells that have gained high metastasizing abilities *in vivo*, in an animal model system.

These observations suggest that a paradigm shift is required in the treatment of luminal breast cancer patients, in which therapies against TNFα should be introduced to the clinical regimen rather than the use of TNFα as a cytotoxic agent. Inhibitors of TNFα are already in clinical use for other indications (autoimmune diseases), and our findings suggest that they should be combined with antihormonal approaches and modalities targeting the EGF-HER2 pathway. We propose that such integrative therapies targeting multiple tumor-promoting factors may achieve a high therapeutic impact in luminal breast cancer patients.

2. Materials and Methods

2.1. Cell Cultures. MCF-7 cells are luminal breast tumor cells that express high levels of ER and PR and show low levels of expression of HER2 and of EGF receptors (EGFR) [43–45]. These cells were found to provide the unique setup of luminal breast tumor cells which is required for this study by (1) responding to TNFα [22, 46, 47]; (2) expressing estrogen receptor α (ERα) and responding to estrogen [34, 48, 49]; (3) responding to EGF despite relatively low expression of HER2 and EGFR [34–37]. The cells were kindly provided by Professor Kaye (Weizmann Institute of Science, Rehovot, Israel). In line with published MCF-7 characteristics [43–45], the cells were authenticated on the basis of expression and activity of ERα; *in vitro* estrogen responsiveness; tumor formation requiring estrogen and matrigel; and low expression of HER2. The cells were maintained in growth media containing DMEM supplemented by 10% fetal calf serum (FCS), 2 mM L-glutamine, 100 Units/mL penicillin, 100 μg/mL streptomycin, and 250 ng/mL amphotericin (all from Biological Industries, Beit Haemek, Israel).

2.2. Cell Stimulation. MCF-7 cells were plated over-night in complete media, washed in PBS, and stimulated for three days with TNFα, estrogen, and/or EGF. The concentrations of the three stimulants were selected based on extensive titration and kinetics analyses (data not shown), and they agree with the conventional dose range used in other research systems: TNFα at 50 ng/mL (cat. no. 300-01A; PeproTech, Rocky Hill, NJ, USA), estrogen at 10^{-8} M (cat. no. E8875; Sigma, Saint Louis, MO, USA) and EGF at 30 ng/mL (cat. no. 236-EG; R&D systems, Minneapolis, MN, USA). In all procedures, control non-stimulated cells were grown in the presence of the diluents of the above stimulators. Stimulation was performed in phenol red-free and serum-free DMEM. Media, including the stimulators, were changed daily.

When indicated, the pharmacological inhibitor of Src, PP2 (cat. no. 529573; Calbiochem, EMD Millipore, San Diego, CA, USA) was used in a conventional concentration of 2.5–5 μM. The inhibitor was added to cell cultures simultaneously with the stimulation of the cells by TNFα + Estrogen + EGF or to control non-stimulated cells and was present in culture throughout the duration of stimulation (three days). Control cells were treated with the solubilizer of the drug at similar dilutions (DMSO; Sigma).

2.3. Confocal Microscopy Analyses. Stimulated and non-stimulated MCF-7 cells were fixed with 8% paraformaldehyde (PFA; cat. no. 1.04005; Merck KGaA, Darmstadt, Germany), permeabilized by 0.2% Triton (cat. no. X-100; Sigma), and blocked with 2% BSA (cat. no. 0332-TAM; Amresco, Solon, OH, USA). Nuclei were visualized by DAPI (4′,6-diamidino-2-phenylindole; cat. no. 9564; Sigma) and actin fibers by FITC-conjugated phalloidin (cat. no. P-5282; Sigma). The following antibodies (Abs) were used: rabbit IgG against focal adhesion kinase (FAK; cat. no. sc-558; Santa Cruz biotechnology, Santa Cruz, CA, USA) and mouse IgG1 against paxillin (cat. no. 624001; Biolegend, San Diego, CA, USA). Then, the cells were incubated with the secondary Abs: Dylight-549-conjugated against rabbit IgG (cat. no. 111-505-144; Jackson Immunoresearch Laboratories, West Grove, PA, USA) or Alexa-647-conjugated against mouse IgG (cat. no. 115-606-146; Jackson Immunoresearch Laboratories). Baseline staining was obtained by nonrelevant isotype matched controls. Coverslips were mounted using fluorescent mounting medium (cat. no. E18-18; Golden Bridge International, Mukilteo, WA, USA) and read by Zeiss LSM 510-META confocal microscope (Carl Zeiss, Jena, Germany) at ×63 magnification.

2.4. Flow Cytometry. Expression levels of cell surface molecules were determined by flow cytometry (FACS) in stimulated and non-stimulated MCF-7 cells, using a Becton Dickinson FACSort (Mountain View, CA, USA). The following Abs were used: PE-conjugated mouse IgG1 against integrin β1 (CD29; cat. no. 303004; Biolegend), Alexa 488 conjugated-Rat IgG2a against integrin α6 (CD49f; cat. no. 313607; Biolegend), Alexa 488-conjugated Rat IgG2b against CD44 (cat. no. 103015; Biolegend) and mouse IgG1 against E-cadherin (Figure 7—cat. no. sc-21791; Santa Cruz biotechnology; Figure S2—cat. no. 324101; Biolegend). The Abs against E-cadherin were followed by FITC-conjugated Abs against mouse IgG (cat. no. 115-095-003; Jackson Immunoresearch Laboratories). Baseline staining was obtained by nonrelevant isotype matched controls. Staining patterns were determined using the win MDI software.

2.5. Quantitative Real-Time Polymerase Chain Reaction. Total RNA was isolated from stimulated and non-stimulated MCF-7 cells using the EZ-RNA kit (cat. no. 20-400-100; Biological Industries). RNA samples were used for generation of first-strand complementary DNA synthesis using the M-MLV reverse transcriptase (cat. no. AM2044; Ambion, Austin, TX, USA). Quantification of cDNA targets by quantitative real-time polymerase chain reaction (qPCR) was performed on Rotor Gene 6000 (Corbett Life Science, Concorde, NSW, Australia), using Rotor Gene 6000 series software. Transcripts were detected using Absolute Blue qPCR SYBR Green ROX mix (cat. no. AB-4163/A; Thermo Fisher Scientific, Waltham, MA, USA) according to the manufacturer's instructions. In each reaction, two pairs of specific primers were used, designed for different exons. The sequences of the primers as follows: for Zeb1-forward 5′-TGCAGCTGACTGTGAAGGTGT-3′, reverse 5′-CTTGCCCTTCCTTTCTGTCATC-3′; for Snail-forward 5′-CTAATCCAGAGTTTACCTTCCAGCA-3′, reverse 5′-AGTCCCAGATGAGCATTGGC-3′; for Slug-forward 5′-CCTGGTCAAGAAGCATTTCAA-3′, reverse 5′-CAGGCATGGAGTAACTCTCA-3′; for the normalizing gene rS9-forward 5′-TTACATCCTGGGCCTGAAGAT-3′ and reverse 5′-GGGATGTTCACCACCTGCTT-3′. PCR amplification of the genes rS9 and Slug was performed over 40 cycles (95°C for 15 sec, 59°C for 20 sec, 72°C for 15 sec), while amplification of Zeb1 was performed over 40 cycles (95°C for 15 sec, 59°C for 20 sec, 80°C for 15 sec), and of Snail over 45 cycles (95°C for 15 sec, 59°C for 20 sec, 84.5°C for 15 sec). Dissociation curves for each primer set indicated a single product, and no-template controls were negative after 40/45 cycles. Quantification was performed by standard curves, on the linear range of quantification.

2.6. Cell Viability. Stimulated and non-stimulated MCF-7 cells were recultured in 96-well plates in growth medium containing the stimulants. After 8 hr, media were removed and the cells were exposed to combined stimulation by TNFα + Estrogen + EGF, in the absence or presence of 1 μM doxorubicin (Teva Pharmaceutical, Netanya, Israel; kindly provided by Professor Peer, Tel Aviv University). The concentration of doxorubicin was selected following titration analyses (data not shown). After additional three days, media were removed, cells were washed, and XTT reagent (cat. no. 20-300-1000; Biological Industries) was added to the wells according to the manufacturer's instructions for 2 hr. Absorbance was measured at 450 nm and 630 nm. For each group (non-stimulated and stimulated cells) the percentage of cell survival was calculated compared to cells that were not exposed to doxorubicin. In other cases, cell viability was determined by trypan blue exclusion (cat. no. 03-102-1B; Biological industries), in two replicates. Viable cells were

counted using a hemocytometer, and total cell number was calculated.

2.7. ELISA Assays. Stimulated and non-stimulated MCF-7 cells were grown as described above. Conditioned medium (CM) was removed from the last 24 hr of cultures, and CXCL8 and CCL2 levels were determined by ELISA using standard curves with rhCXCL8 or rhCCL2 (cat. no. 200-08, 300-04, resp.; PeproTech), at the linear range of absorbance. The following Abs were used (all from PeproTech): For CXCL8: coating polyclonal Abs (cat. no. 500-P28), detecting biotinylated rabbit polyclonal Abs (cat. no. 500-P28Bt); For CCL2: coating monoclonal Abs (cat. no. 500-M71), detecting biotinylated rabbit polyclonal Abs (cat. no. 500-P34Bt). After the addition of streptavidin-horseradish peroxidase (cat. no. 016-030-084; Jackson Immunoresearch Laboratories), the substrate TMB/E solution (cat. no. ES001; Millipore, Temecula, CA, USA) was added. The reaction was stopped by the addition of 0.18 M H_2SO_4 and was measured at 450 nm. In parallel, cells were removed by trypsinization and counted by trypan blue exclusion (see above), and the results were normalized to cell numbers.

2.8. Gelatin Substrate Zymography. MCF-7 cells were plated in 24-well plates in growth medium. Following overnight incubation, the growth medium was removed and cells were stimulated for three days with TNFα + Estrogen + EGF as indicated above. CM of the last 24 hr were collected and separated on 7.5% SDS-polyacrylamide gels containing 0.1% gelatin substrate. After electrophoresis, gels were washed three times in 50 mM Tris/HCl pH 7.5, containing 2.5% Triton X-100. The gels were then washed three times in 50 mM Tris/HCl pH 7.4 buffer, followed by incubation in buffer containing 50 mM Tris/HCl pH 7.4, 0.02% NaN_3, and 10 mM $CaCl_2$ for 48 hr at 37°C. Following three washes in double distilled H_2O, the gels were stained with 0.1% coomassie blue and distained in 20% methanol and 10% glacial acetic acid until clear bands of protein degradation were visualized. In parallel, cells that were removed by trypsinization were counted by trypan blue exclusion (see above). The obtained bands were subjected to densitometry performed using Scion image software, and their density was normalized to cell number.

2.9. Assays of Tumor-Spheroids. 6-well plates were incubated overnight on a rocker with 1.2% Poly(2-hydroxyethyl methacrylate) (cat. no. P3932; Sigma) in methanol. MCF-7 cells were plated in phenol-red free DMEM/F12 medium supplemented with 2 mM L-glutamine, 100 Units/mL penicillin, 100 μg/mL streptomycin, 250 ng/mL amphotericin (all from Biological Industries), 0.4% BSA (cat. no. 0332-TAM; Amresco), B-27 serum-free supplement (cat. no. 17504; Gibco, Life Technologies, Grand Island, NY, USA), 20 ng/mL basic FGF (cat. no. 100-18B; Peprotech), 20 ng/mL EGF (cat. no. 236-EG; R&D systems), and 5 μg/mL insulin (cat. no. I9278; Sigma). After three days, tumor-spheroids were formed, and cells were stimulated with TNFα + Estrogen + EGF in the above-indicated concentrations or with the diluents of the above stimulators, for additional 24–96 hr. Cells were photographed daily using a light microscope at ×10 magnification.

For flow cytometry analyses that followed tumor-spheroid formation, cells were passed through a 40 μm nylon mesh cell strainer, in order to separate single cells from tumor-spheroids. Tumor-spheroids were later dissociated by trypsinization and the cells that were obtained by this procedure were compared to single cells that migrated out of tumor-spheroids formed by stimulated cells. Cell viability of all groups was determined by trypan blue exclusion (see above) and cells were stained using Abs against E-cadherin (see above).

2.10. Tumor Growth and Metastasis. MCF-7 cells were infected to stably express mCherry (by pQCXI-mCherry retroviral vector). The cells were either non-stimulated or stimulated by TNFα + Estrogen + EGF at the above-mentioned concentrations for three days. Then, the cells were washed and 4×10^6 cells/mouse were inoculated to the mammary fat pad of female athymic nude mice (Harlan Laboratories, Jerusalem, Israel). Prior to injection to mice, the cells were mixed 1 : 1 with matrigel (cat. no. 356234; BD Biosciences, Franklin Lakes, NJ, USA). One week prior to tumor cell inoculation, all mice were implanted subcutaneously with slow-release estrogen pellets (1.7 mg/pellet, 60 days release, cat. no. SE-121; Innovative Research of America, Sarasota, FL, USA) which are essential for the growth of MCF-7 cells in mice.

The CRi Maestro noninvasive intravital imaging system was used to monitor intact mice, at four different time points along the time course of up to 37 days (depending on the experiment). The Maestro device has provided two readouts: (1) size of primary tumors along the growth process of tumors in the intact mice; (2) absence or presence of metastases in the intact mice. When the experiments were terminated, organs were excised and metastasis formation was compared to the readouts obtained by the Maestro device. This analysis has indicated that in intact mice, the Maestro device detected macro-metastases in a reliable manner, but could not detect micrometastases that may have been formed. Accordingly, the data retrieved by the Maestro device at the different time points in intact mice actually provided information on the formation of macrometastases in different organs.

The regulations of Tel Aviv University Animal Care Committee did not allow continuation of the experiments to the stage of survival analysis. All procedures involving experimental animals were performed in compliance with local animal welfare laws, guidelines, and policies.

2.11. Statistical Analyses. Statistical analyses of *in vitro* experiments were done using Student's *t*-tests. Values of $P < 0.05$ were considered statistically significant, and all *in vitro* data were presented as mean ± standard deviation (SD). In the *in vivo* studies of primary tumors, data are presented as mean ± standard error of mean (SEM), and statistical analyses of tumor sizes were done using Student's *t*-tests, where values of $P < 0.05$ were considered statistically significant.

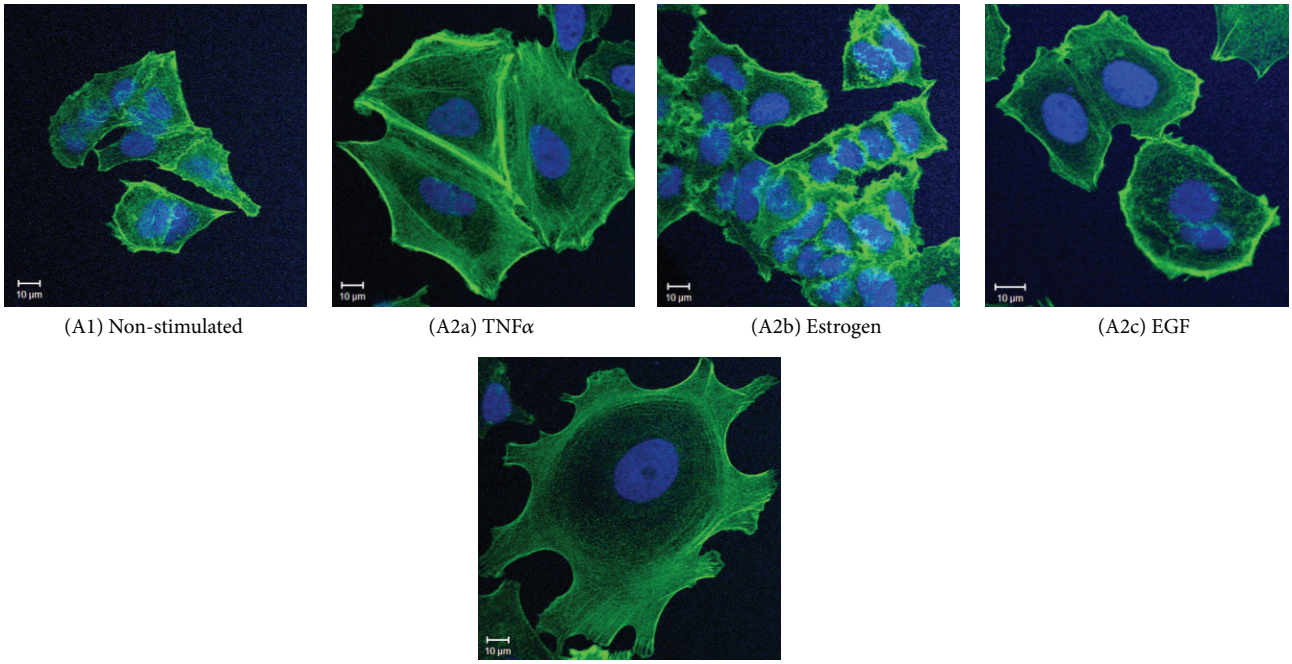

(A1) Non-stimulated (A2a) TNFα (A2b) Estrogen (A2c) EGF

(B) TNFα + Estrogen+ EGF

Figure 1: Combined stimulation by TNFα + Estrogen + EGF induces extensive morphological changes and spreading in breast tumor cells. Breast tumor cells were either (A1) not stimulated (cells grown in the presence of diluents) or stimulated by (A2a) TNFα (50 ng/mL), (A2b) estrogen (10^{-8} M), (A2c) EGF (30 ng/mL), or (B) TNFα + Estrogen + EGF (concentrations as above) for three days. The stimulatory conditions were selected following titration and kinetics analyses (data not shown). Actin filaments were detected by phalloidin staining (green) and cell nuclei by DAPI staining (blue). The cells were analyzed by confocal microscopy. In all panels, the results are from a representative experiment of $n \geq 3$.

3. Results

3.1. Combined Stimulation by TNFα + Estrogen + EGF Amplifies Tumor Cell Remodeling and Leads to Increased Cell Spreading and High Expression of Metastasis-Related Adhesion Molecules. TNFα, estrogen, and EGF were each shown to have the potential to promote metastasis-related properties in breast tumor cells, as described above; however, different research systems were used for the study of each of these factors. In our study, we have compared side by side the ability of TNFα, estrogen, and/or EGF to affect spreading and EMT properties, using the MCF-7 luminal breast tumor cells. These cells express receptors for all the three above-mentioned factors (references provided above), and represent a nonadvanced stage of breast malignancy that can be pushed forward towards a more aggressive/invasive phenotype in terms of acquisition of EMT properties [22, 26, 27].

First, we determined the effects of TNFα, estrogen, EGF, or all three factors together on tumor cell morphology, spreading and expression of adhesion molecules which promote tumor cell invasion and metastasis [50–53]. Stimulating the tumor cells for three days by TNFα has induced the formation of actin-rich cellular protrusions, accompanied by definite concentration of actin fibers at the cell cortex (Figure 1(A2a)). In contrast, estrogen alone had no effect on tumor cell morphology (Figure 1(A2b)), and EGF induced cell spreading but to lower extent than TNFα (Figure 1(A2c)). However, the most robust change in cell morphology, exemplified by extensive spreading and reorganization of stress fibers, was noted when estrogen and EGF were added to TNFα (Figure 1(B)). The cells that were exposed to the combined stimulation by TNFα + Estrogen + EGF have formed definite and large cellular protrusions, with actin stress fibers clearly apparent, which were minimally visible previously in the control non-stimulated cells (Figure 1(B) versus Figure 1(A1)). Additional analyses indicated also that the triple stimulation of TNFα + Estrogen + EGF was more effective in inducing spreading and cell remodeling than dual stimulations by Estrogen +TNFα or Estrogen + EGF (Figure S1 in Supplementary Material available online at http://dx.doi.org/10.1155/2013/720536) (the dual stimulations focused on combinations including estrogen because it is the most relevant factor to the luminal tumor cells we were using, characterized by ER expression). Together, these results provide evidence to strong impact of the combined stimulation by TNFα + Estrogen + EGF over other combinations, indicating that the joint activity of all three arms of the tumor microenvironment together is advantageous in inducing spreading and adhesion-related functions in luminal breast tumor cells.

Additional analyses indicated that the morphological changes induced by TNFα + Estrogen + EGF in the tumor cells were accompanied by redistribution of focal adhesion kinase (FAK) and paxillin, two key regulators of cell adhesion

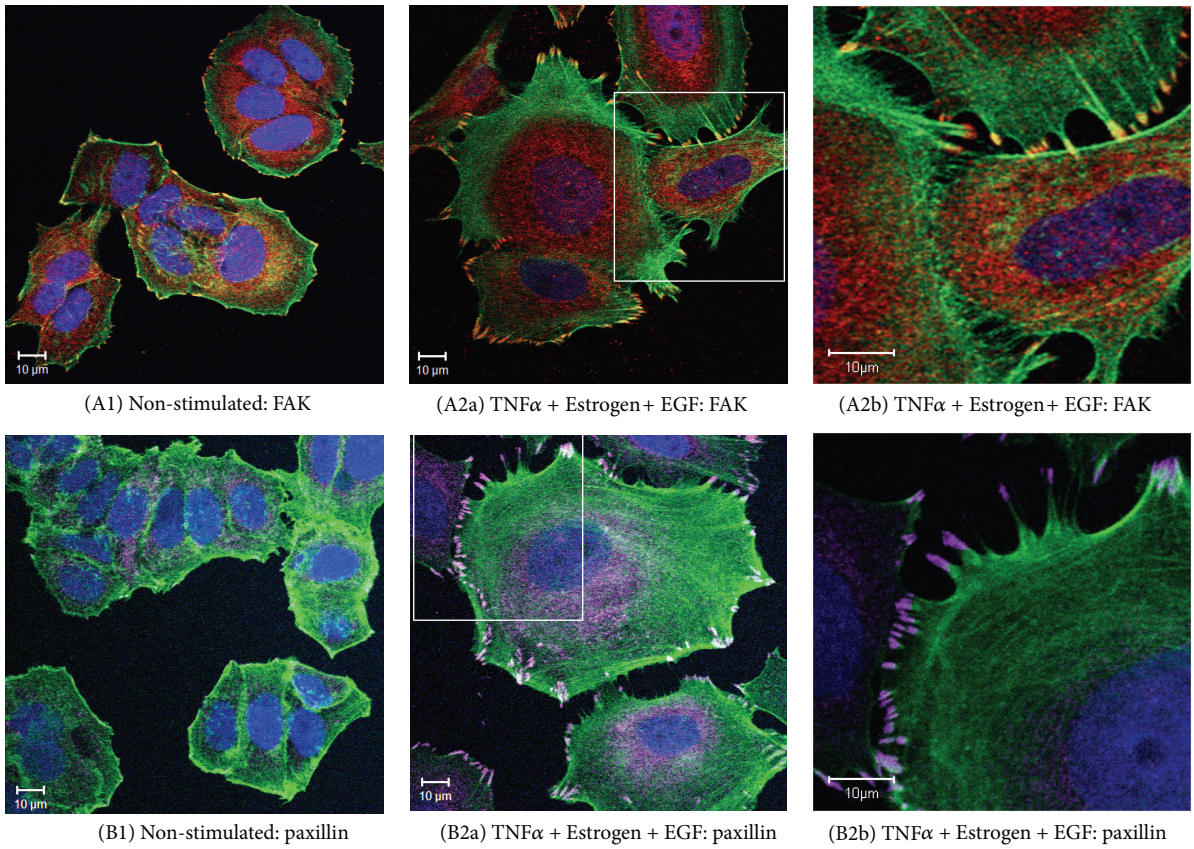

(A1) Non-stimulated: FAK (A2a) TNFα + Estrogen+ EGF: FAK (A2b) TNFα + Estrogen+ EGF: FAK

(B1) Non-stimulated: paxillin (B2a) TNFα + Estrogen + EGF: paxillin (B2b) TNFα + Estrogen + EGF: paxillin

Figure 2: Combined stimulation of breast tumor cells by TNFα + Estrogen + EGF induces the localization of FAK and paxillin in cell protrusions and formation of intertumor connecting tubes. Breast tumor cells were stimulated by TNFα + Estrogen + EGF (concentrations as in Figure 1) for three days. Non-stimulated: cells grown with the diluents of the above factors. (A) The expression of FAK. (A1) Non-stimulated cells. ((A2a), (A2b)) Cells stimulated by TNFα + Estrogen + EGF, where part (A2b) demonstrates the formation of tubes connecting between different tumor cells. FAK expression was detected by specific Abs (red), actin filaments by phalloidin staining (green), and cell nuclei by DAPI staining (blue). In all panels, the results are from a representative experiment of $n \geq 3$. (B) The expression of paxillin. (B1) Non-stimulated cells. ((B2a), (B2b)) Cells stimulated by TNFα + Estrogen + EGF, where part (B2b) demonstrates the formation of tubes connecting between different tumor cells. Paxillin expression was detected by specific Abs (purple), actin filaments by phalloidin staining (green), and cell nuclei by DAPI staining (blue). In all panels, the results are from a representative experiment of $n \geq 3$.

and spreading [50–53] (Figure 2). Moreover, we noticed that the cancer cells that were exposed to the combined stimulation by TNFα + Estrogen + EGF have detached from each other, and have formed connecting tubes (Figures 2(A2b) and 2(B2b)). Based on published reports [54, 55], such tubes may support exchange of intracellular components between the cancer cells. The activation of FAK and paxillin and their contribution to formation of cellular protrusions were found to be Src-mediated processes. This was indicated by potent inhibition of cell spreading and FAK/paxillin localization at cellular extremities by the specific Src inhibitor PP2 (Figure 3).

The powerful spreading induced by TNFα + Estrogen + EGF has led us to monitor the expression of the β1 integrin, known to be strongly involved in processes of tumor cell adhesion, spreading, and metastasis formation [56–60]. As shown in Figure 4, of the three factors mainly TNFα induced detectable upregulation in β1 expression although to a very limited extent; however, when TNFα activities were joined by estrogen and EGF, the resulting TNFα + Estrogen + EGF stimulation has led to much more substantial integrin β1 upregulation, in an extent that was stronger than the minimal effects induced by each of the factors alone (Figures 4(a1)–4(a3) versus Figure 4(B)).

The β1 integrin has been shown in many studies to stand in the basis of increased adhesion and invasion of tumor cells, including of breast origin [56–60]. Since integrins are acting as $\alpha\beta$ heterodimers, we searched for the α chain counterpart that would accompany the increased expression of β1. A thorough search through many different α subunits has identified increases in α6 in response to TNFα + Estrogen + EGF stimulation (Figure 4(c)). Accordingly, the combined stimulation has led to increase in a subpopulation of tumor cells expressing high levels of $\alpha 6\beta 1$. The $\alpha 6\beta 1$ heterodimer, otherwise known as VLA6, is a laminin receptor that has been identified in the past as invasion-supporting complex that promotes breast cancer progression [61, 62].

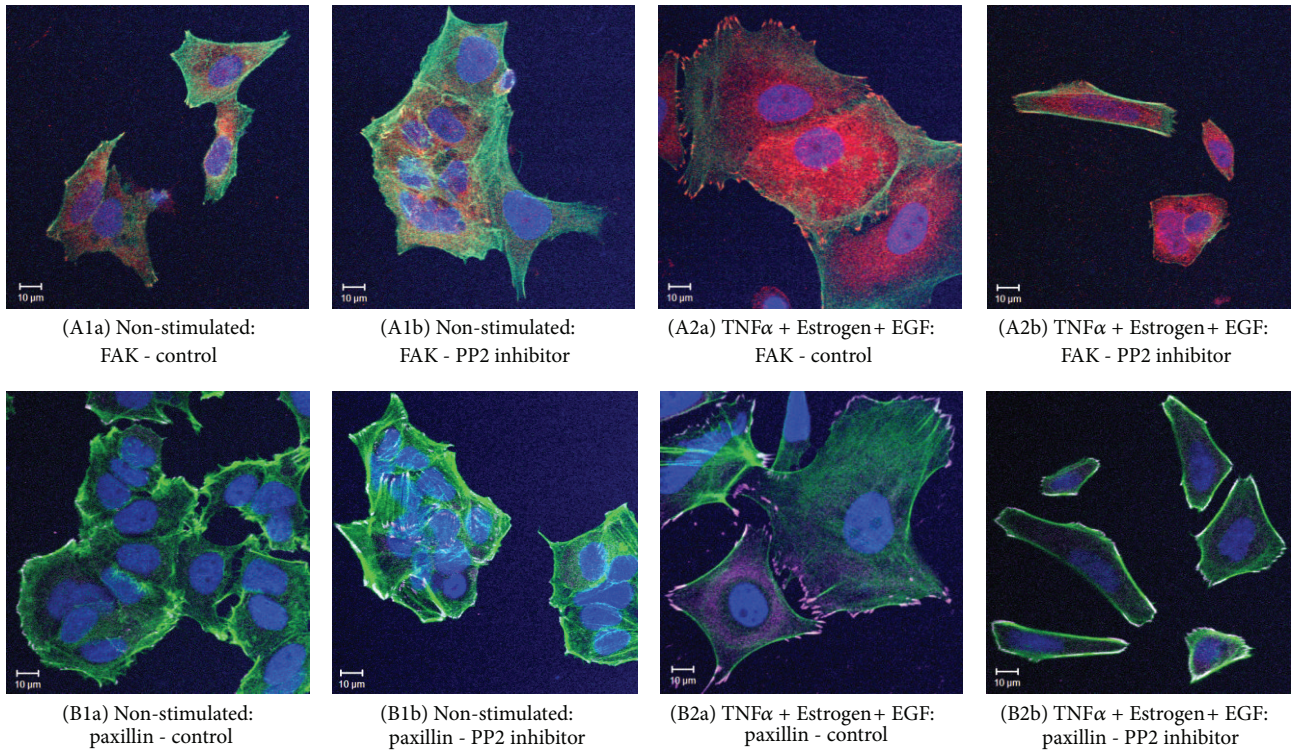

Figure 3: Cell-remodeling of breast tumor cells, induced by TNFα + Estrogen + EGF, depends on Src-induced mechanisms. Breast tumor cells were stimulated by TNFα + Estrogen + EGF (concentrations as in Figure 1) for three days. Non-stimulated: cells grown with the diluents of the above factors. The cells were either not exposed or exposed to the Src inhibitor PP2 (used at the range of 2.5–5 μM). (A) The expression of FAK, determined in the absence ((A1a), (A2a)) or in the presence ((A1b), (A2b)) of PP2 (2.5 μM in this specific experiment) in non-stimulated cells ((A1a), (A1b)) or in cells stimulated by TNFα + Estrogen + EGF ((A2a), (A2b)). FAK expression was detected by specific Abs (red), actin filaments by phalloidin staining (green), and cell nuclei by DAPI staining (blue). In all panels, the results are from a representative experiment of $n \geq 3$. (B) The expression of paxillin, determined in the absence ((B1a), (B2a)) or in the presence ((B1b), (B2b)) of PP2 (2.5 μM in this specific experiment) in non-stimulated cells ((B1a), (B1b)) or in cells stimulated by TNFα + Estrogen + EGF ((B2a), (B2b)). Paxillin expression was detected by specific Abs (purple), actin filaments by phalloidin (green), and cell nuclei by DAPI staining (blue). In all panels, the results are from a representative experiment of $n = 3$.

In parallel, we found that the combined stimulation by TNFα + Estrogen + EGF has induced strong upregulation in another adhesion molecule that is highly implicated in breast metastasis, CD44 (Figure 5) [6, 7, 63, 64]. As previously demonstrated for all other functions, the impact of the combined stimulation on CD44 elevation was definitely more powerful than each of the stimulators—TNFα, estrogen, or EGF—alone (Figure 5). Of interest was the fact that due to stimulation by TNFα + Estrogen + EGF, over 50% of the tumor cells acquired high expression levels of both β1 and CD44 together (Figure 5(c)).

Overall, the above results indicate that of all three factors TNFα was the strongest inducer, of spreading and expression of metastasis-related adhesion molecules by the luminal MCF-7 breast tumor cells and that its activities were strongly amplified by the cooperativity with the other two representatives of the tumor microenvironment, estrogen (hormonal) and EGF (growth-supporting).

3.2. Combined Stimulation by TNFα + Estrogen + EGF Is Advantageous over Each Factor Alone in Inducing EMT in Breast Tumor Cells. To follow on the above findings, we determined the abilities of TNFα, estrogen, and EGF—each alone or together—to induce EMT properties in the tumor cells. In cells undergoing EMT, reduced expression of E-cadherin facilitates detachment of cancer cells from each other [9, 10]. Accordingly, following three days of stimulation by TNFα, EGF, and estrogen, each separately, downregulation of cell surface expression of E-cadherin was noted to some extent, with TNFα inducing the most prominent effects of all three factors; however, very clearly, the most potent EMT phenotype was obtained upon joint stimulation by all three factors together, given in the form of TNFα + Estrogen + EGF (Figure 6). Also, in response to the combined stimulation, the cells have gained typical morphology of cells undergoing EMT, detaching from each other and expressing definite cellular protrusions (Figure 7(a)). Further supporting the ability of TNFα + Estrogen + EGF stimulation to induce EMT was the prominent increase in the expression of the known EMT activators Zeb1, Snail, and Slug [65–70] in the tumor cells (Figure 7(b); the EMT regulator twist was down-regulated; data not shown).

3.3. Combined Stimulation of Breast Tumor Cells by TNFα + Estrogen + EGF Leads to Functional Tumor-Promoting Consequences. Above, we have shown that the combined

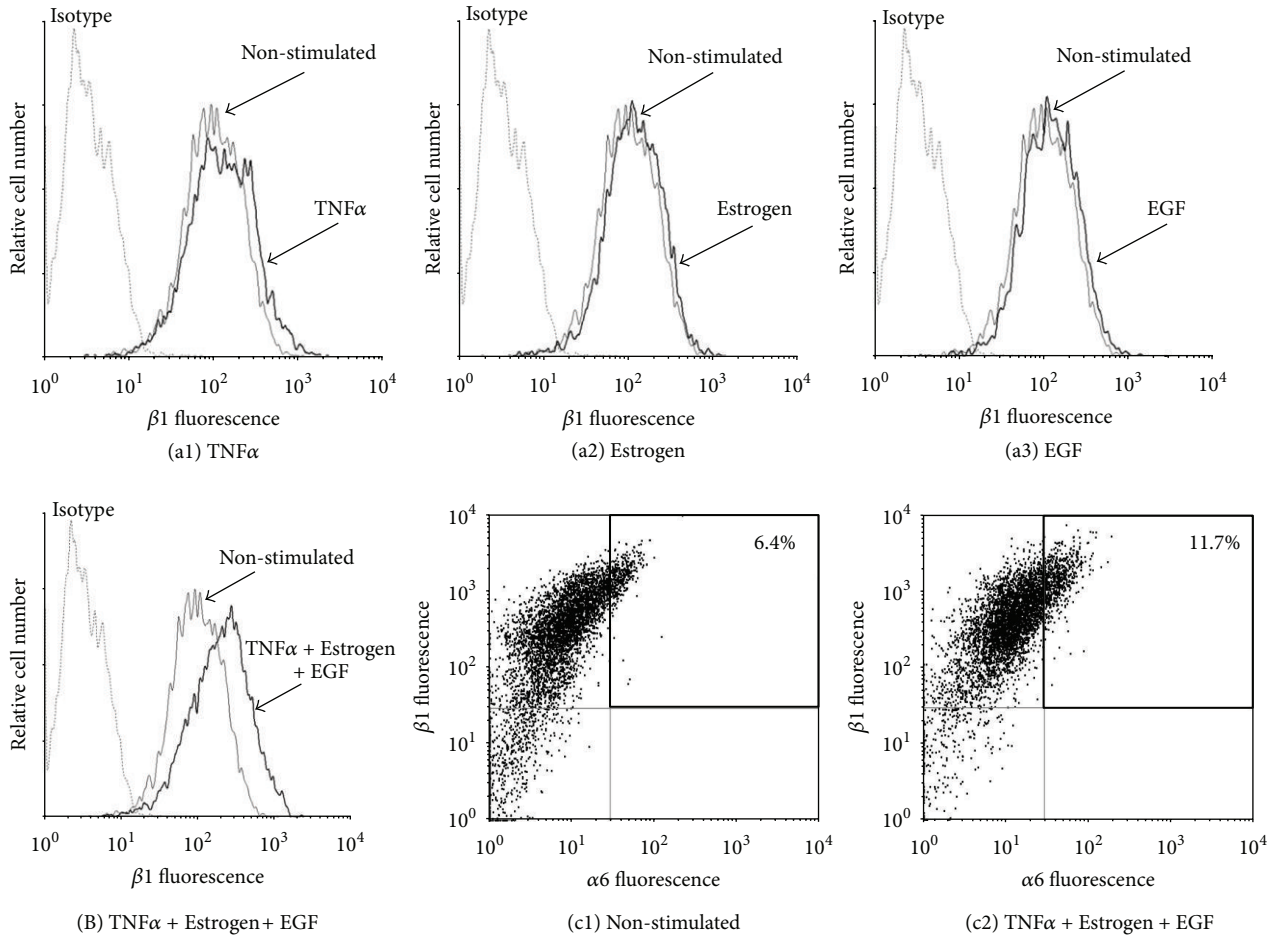

Figure 4: Combined stimulation of breast tumor cells by TNFα + Estrogen + EGF leads to increased expression of the β1 integrin and to emergence of high-VLA6 cell population ($\alpha 6\beta 1^{high}$). ((a), (B)) Determination of β1 expression. Breast tumor cells were stimulated by (a1) TNFα, (a2) estrogen, (a3) EGF, or (B) TNFα + Estrogen + EGF (concentrations as in Figure 1) for three days. Non-stimulated: cells grown with the diluents of the above factors. The expression of β1 on the surface of the cells was determined by FACS analyses, using specific Abs. Isotype: isotype matched Abs used as control in the FACS analyses. In all panels, the results are from a representative experiment of $n \geq 3$. (c) Coexpression of the β1 and α6 integrin subunits. (c1) Non-stimulated: cells grown with the diluents of the above factors. (c2) Cells stimulated by TNFα + Estrogen + EGF (concentrations as in Figure 1). The expression of β1 and of α6 on the surface of the cells was determined by FACS analyses using specific Abs, with axes set based on staining with isotype matched control Abs. In all panels, the results are from a representative experiment of $n \geq 3$.

stimulation by TNFα + Estrogen + EGF has strongly induced spreading and EMT properties in luminal breast tumor cells. To follow on the above findings, we determined the impact of the combined stimulation on tumor cell functions that are involved in increased tumor growth and progression. Because of its high clinical relevance to tumor progression, first we asked what is the effect of the combined stimulation on resistance of tumor cells to doxorubicin (adriamycin), which is a chemotherapy commonly used in the treatment of breast cancer patients [71, 72]. When doing this analysis, we were aware of the fact that MCF-7 cells are sensitive to TNFα cytotoxicity [73–75], and accordingly our routine procedure of TNFα + Estrogen + EGF stimulation for three days has led to death of approximately 40% of the tumor cells (Figure S2). Nevertheless, despite their apparent sensitivity to TNFα-induced cytotoxicity, tumor cells that were exposed to the combined stimulation were endowed with higher resistance to doxorubicin (Figure 8(a)). These results indicate that those tumor cells that have survived the TNFα-induced cytotoxicity were selected for high resistance to chemotherapy-induced death.

In parallel to the above, we determined the effects of the combined stimulation by TNFα + Estrogen + EGF on the ability of the tumor cells to acquire additional promalignancy functions. Doing a "per cell" analysis, we found that the stimulation of the tumor cells by TNFα + Estrogen + EGF has given rise to potent elevation in the release of the inflammatory chemokines CXCL8 (Figure 8(b1)) and CCL2 (Figure 8(b2)), which have been well characterized as strong tumor-promoting factors by virtue of their potent angiogenic activities and recruitment of tumor-supporting leukocytes to the tumors [76–81]. In addition, in response to

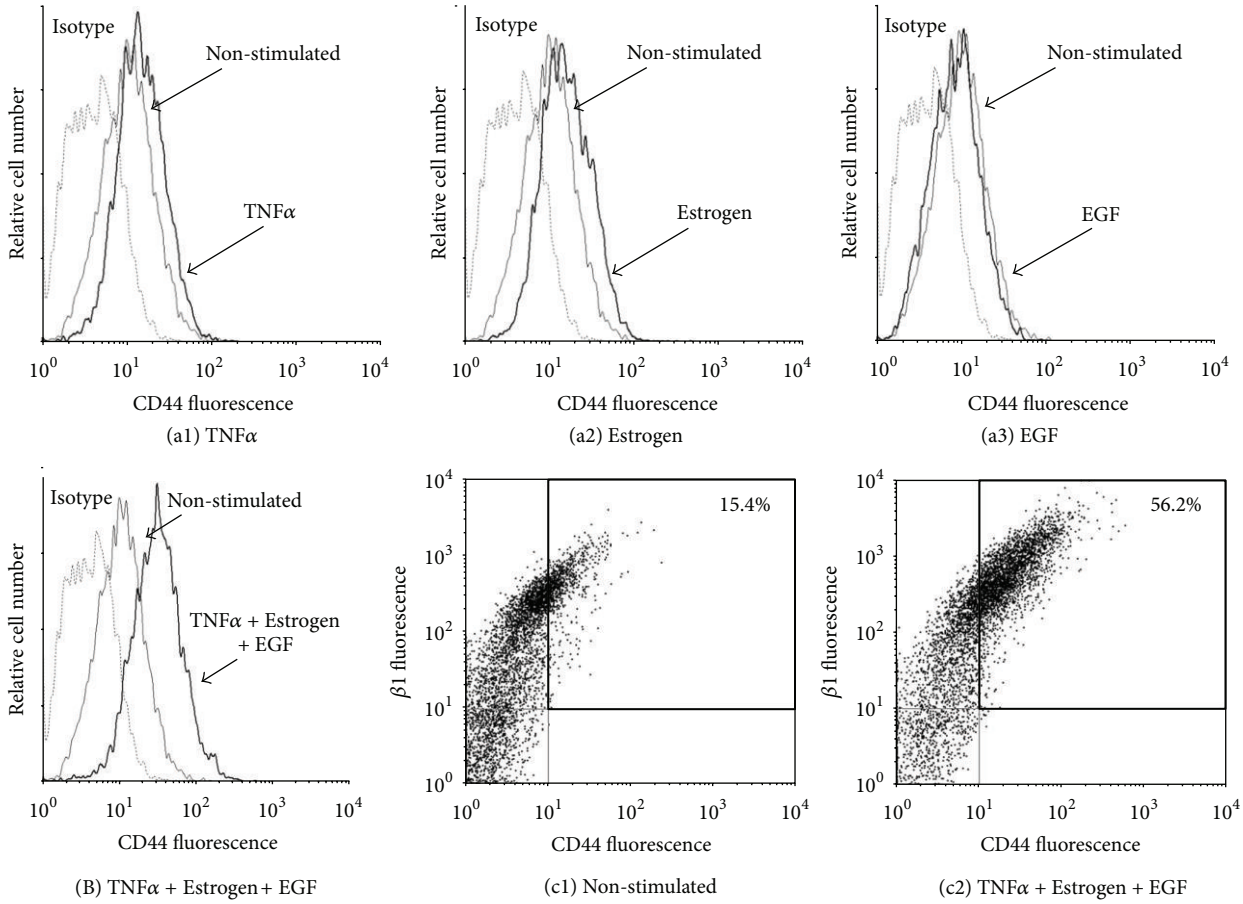

Figure 5: Combined stimulation of breast tumor cells by TNFα + Estrogen + EGF leads to potent induction in expression of CD44 and to emergence of a $CD44^{high}/\beta1^{high}$ cell population. ((a), (B)) Determination of CD44 expression. Breast tumor cells were stimulated by (a1) TNFα, (a2) estrogen, (a3) EGF, or (B) TNFα + Estrogen + EGF (concentrations as in Figure 1) for three days. Non-stimulated: cells grown with the diluents of the above factors. The expression of CD44 on the surface of the cells was determined by FACS analyses, using specific Abs to CD44. Isotype: isotype matched Abs used as control in the FACS analyses. In all panels, the results are from a representative experiment of $n \geq 3$. (c) Coexpression of CD44 and $\beta1$. (c1) Non-stimulated: cells grown with the diluents of the above factors. (c2) Cells stimulated by TNFα + Estrogen + EGF (concentrations as in Figure 1). The expression of CD44 and $\beta1$ on the surface of the cells was determined by FACS analyses using specific Abs, with axes set based on staining with isotype matched control Abs. In all panels, the results are from a representative experiment of $n \geq 3$.

the combined stimulation by TNFα + Estrogen + EGF, the tumor cells have acquired the ability to produce high levels of functional matrix metalloproteinase 9 (MMP9; Figure 8(c)), a key enzyme in degradation of the extracellular matrix (ECM) during local invasion end extravasation of the tumor cells [82].

Moreover, to follow on the cell-remodeling, EMT, and metastatic/invasive properties acquired by tumor cells that were exposed to the combined stimulation by TNFα + Estrogen + EGF, we determined the migratory functions of the cells. We took advantage of the high ability of MCF-7 cells to form tumor-spheroids and analyzed the ability of cancer cells to detach from the spheroids and move away from them. To this end, we have formed tumor-spheroids and then introduced the combined stimulation for additional 24–96 hr. These tests have shown that control, non-stimulated cells, kept the organized spherical structure throughout the 96 hr time course (Figure 9(a)). In contrast, cancer cells that were exposed to the combined stimulation have migrated out of the tumor-spheroids already after 48 hr of stimulation (Figure 9(b)). At the 96 hr time point, extensive outward migration was observed in the TNFα + Estrogen + EGF-stimulated cells, and a large proportion of single cells was detected (cell viability tests indicated that these single cells were alive) (Figure 9(b)). Here, it is interesting to note that the single cells that migrated out of tumor-spheroids formed in the presence of TNFα + Estrogen + EGF stimulation expressed lower levels of E-cadherin compared to the cells that remained in the spheroids (Table 1 and Figure S3). These results provide a direct connection between the processes of elevated EMT and migratory events that were induced by the combined stimulation of TNFα + Estrogen + EGF.

3.4. In Vivo Animal Studies Indicate That Tumor Cells Stimulated by TNFα + Estrogen + EGF Acquire High Metastatic Capacity. The results presented so far in this

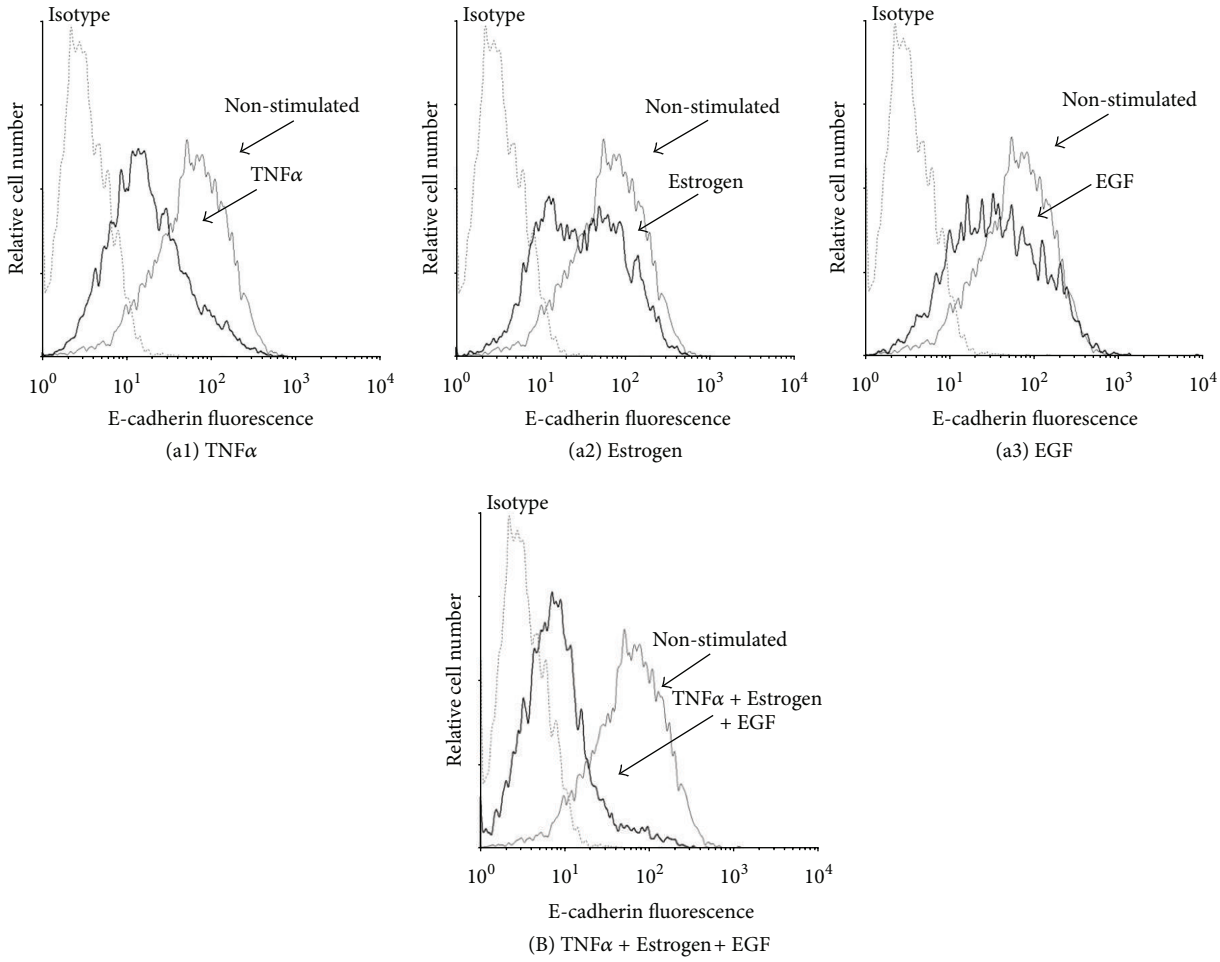

Figure 6: Combined stimulation by TNFα + Estrogen + EGF leads to potent downregulation of E-cadherin expression by breast tumor cells. ((a), (B)) Determination of E-cadherin expression. Breast tumor cells were stimulated by (a1) TNFα, (a2) estrogen, (a3) EGF, or (B) TNFα + Estrogen + EGF (concentrations as in Figure 1) for three days. Non-stimulated: cells grown with the diluents of the above factors. The expression of E-cadherin on the surface of the cells was determined by FACS analyses, using specific Abs to E-cadherin. Isotype: isotype matched Abs, used as control in the FACS analyses. In all panels, the results are from a representative experiment of $n > 3$.

Table 1: Breast tumor cells that migrated out of tumor-spheroids following TNFα + Estrogen + EGF stimulation express reduced levels of E-cadherin.

E-cadherin expression	Cells dissociated mechanically from tumor-spheroids formed by non-stimulated cells	Cells dissociated mechanically from tumor-spheroids formed in the presence of TNFα + Estrogen + EGF stimulation	Single cells that have detached spontaneously from tumor-spheroids formed in the presence of TNFα + Estrogen + EGF stimulation
Mean fluorescence (MFI)	15.8	15.4	11.5
% Positive cells	18.0	20.9	5.7
Score (MFI × %)	284.4	321.9	65.5
Normalized values	1.00	1.13	0.23

The table summarizes the analyses performed for E-cadherin expression in tumor-spheroid assays. The formation of tumor-spheroids and the ability of TNFα + Estrogen + EGF-stimulated cells to migrate out of the tumor-spheroids were shown in Figure 9. Then, tumor-spheroids and single cells were separated by a 40 μm nylon mesh. Cells from tumor-spheroids formed in the absence or in the presence of TNFα + Estrogen + EGF stimulation were dissociated mechanically by trypsinization and were stained for E-cadherin in comparison to cells that have detached spontaneously from the tumor-spheroids formed in the presence of TNFα + Estrogen + EGF stimulation. The three cell types were analyzed for surface expression of E-cadherin by flow cytometry analyses. The results are from a representative experiment of $n \geq 3$.

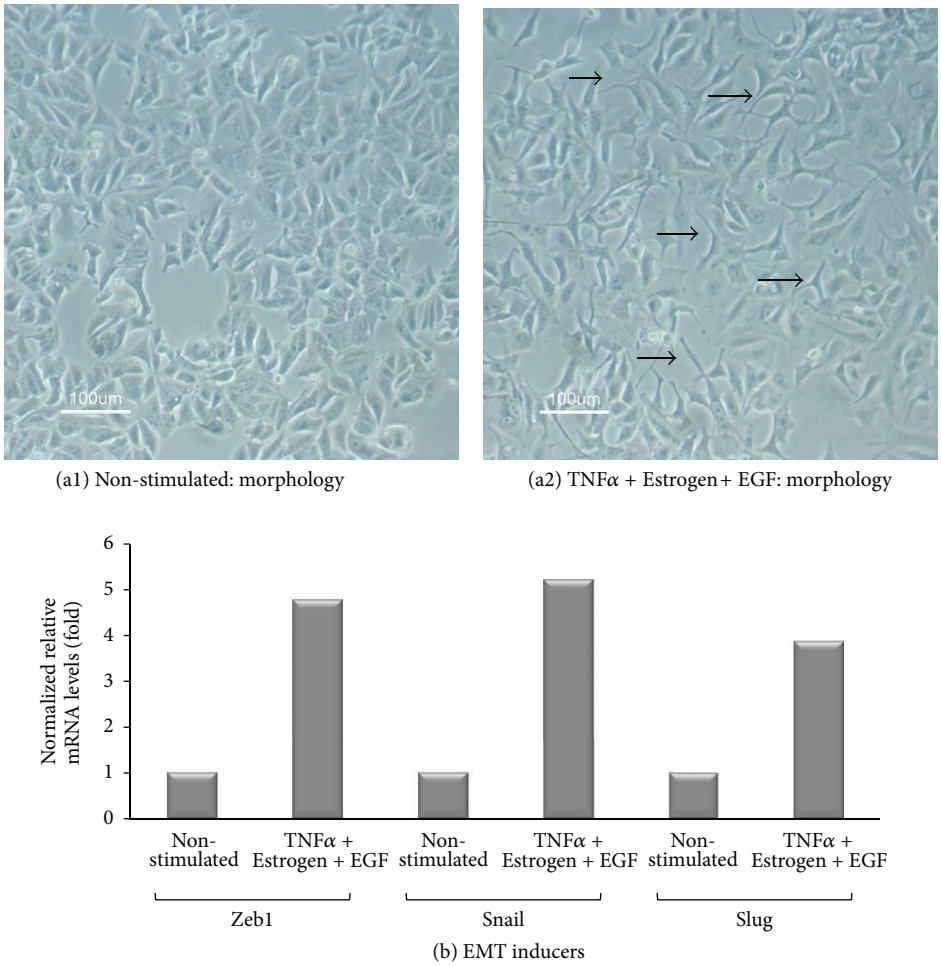

Figure 7: Combined stimulation by TNFα + Estrogen + EGF leads to acquisition of mesenchymal phenotype by the tumor cells, and to upregulation of EMT inducers. Breast tumor cells were stimulated by TNFα + Estrogen + EGF (concentrations as in Figure 1) for three days. Non-stimulated: cells grown with the diluents of the above factors. (a) Cell morphology was determined by light microscopy at ×20 magnification. (a1) Non-stimulated cells. (a2) Cells stimulated by TNFα + Estrogen + EGF. Arrows point to some of the cells that have undergone remodeling in response to TNFα + Estrogen + EGF stimulation. In all panels, the results are from a representative experiment of $n \geq 3$. (b) Expression of the EMT inducers Zeb1, Snail, and Slug in cells stimulated by TNFα + Estrogen + EGF and in non-stimulated cells (grown with the diluents of the factors), determined by qPCR analysis. In all panels, the results are from a representative experiment of $n \geq 3$.

study indicate that tumor cells exposed to the combined stimulation have acquired properties that may contribute to tumor growth and metastasis. These results have motivated us to determine the effects of the TNFα + Estrogen + EGF stimulation on formation of primary tumors at the mammary fat pad and on dissemination of metastasis. To enable detection of the tumor cells in *intact* animals, MCF-7 cells were infected to express the fluorescent protein mCherry. The tumor cells were stimulated for three days by TNFα + Estrogen + EGF *in vitro* then washed to remove the stimulators and inoculated to the mammary fat pad of mice. Because MCF-7 cells are sensitive to TNFα-induced cytotoxicity (Figure S2) [73–75], following the three days of stimulation by TNFα + Estrogen + EGF, we assured that equal numbers of live stimulated and non-stimulated cells were inoculated to the mice. Following tumor cell inoculation, the Maestro device has provided data on the size of primary tumors and appearance of macro-metastases in intact mice, in analyses that were performed at four time points along the course of the experiments (up to 37 days).

The findings of Figure 10(a1) show that cells exposed to the combined stimulation of TNFα + Estrogen + EGF have given rise to smaller tumors than control non-stimulated cells, due to possible reasons described further on (Section 4). However, a totally different picture was revealed when metastasis formation was addressed. Taking into account the fact that MCF-7 cells are well-characterized as non-metastatic cells [45, 83], it was exciting to see that the combined stimulation by TNFα + Estrogen + EGF for three days in culture has given rise to cells with high metastasizing ability *in vivo*. As expected, the control cells did not form macro-metastases at all, but in contrast the tumor cells that have been exposed to TNFα + Estrogen + EGF stimulation have given rise to macro-metastases in

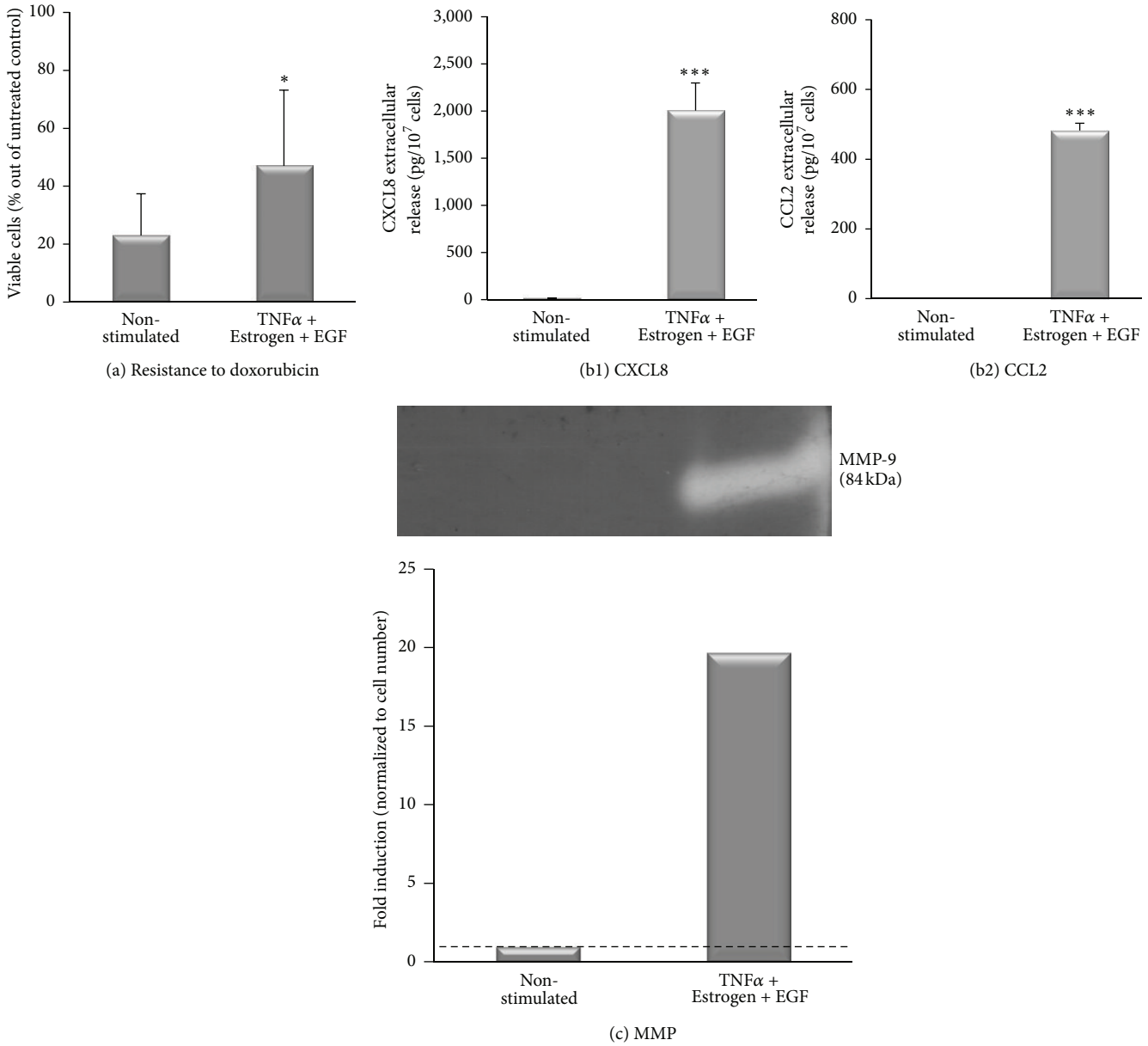

Figure 8: In response to combined stimulation by TNFα + Estrogen + EGF, breast tumor cells acquire functional promalignancy properties. Breast tumor cells were stimulated by TNFα + Estrogen + EGF (concentrations as in Figure 1) for three days. Non-stimulated: cells grown with the diluents of the above factors. (a) Resistance to doxorubicin. Following their stimulation with the above-mentioned factors, the cells were replated with the aforementioned stimulation in the presence or absence of 1 μM doxorubicin for additional three days. Cell viability was determined by XTT assay. $^{*}P < 0.05$ for the difference between stimulated and non-stimulated cells. The results are from a representative experiment of $n \geq 3$. (b) Release of promalignancy factors by the tumor cells, calculated per cell number. The expression of CXCL8 (b1) and CCL2 (b2) was determined in the CM of the cells by ELISA, at the linear range of absorbance. $^{***}P < 0.001$ for the differences between stimulated and non-stimulated cells. The results are from a representative experiment of $n = 3$. (c) Release of functional MMPs, determined by zymography assays performed on cell CM. The bar graph shows the quantitative expression of MMPs, calculated per cell number. The results are from a representative experiment of $n \geq 3$.

38% of the animals (Figures 10(a2), 10(b), and 10(c)), as determined in 2 independent experimental repeats showing similar results. Macro-metastases were also detected in 2/3 mice in another experiment in which non-stimulated cells were not included. The macro-metastases formed by TNFα + Estrogen + EGF-stimulated cells were detected in the liver, colon, and abdomen (Figure 10(d) shows metastases in the liver and in the colon).

Actually, the impact of the combined stimulation on the metastatic potential of the MCF-7 was dramatic: the tumor cells were exposed to this stimulus for only three days in culture, and based on our *in vitro* results only

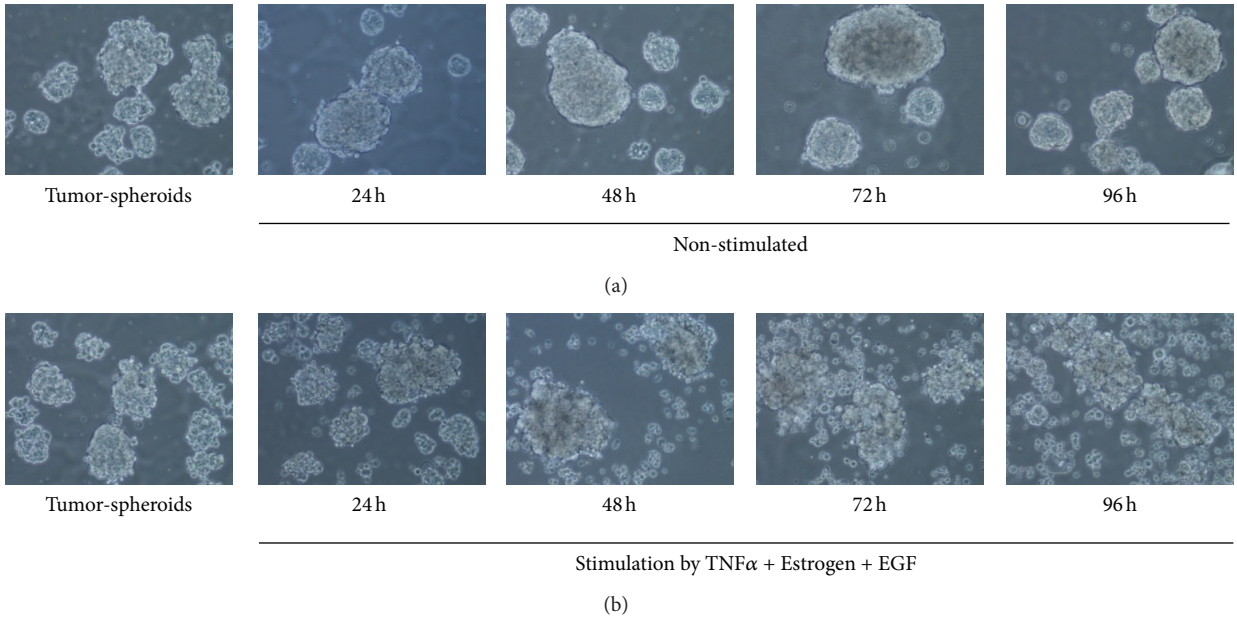

Figure 9: In response to combined stimulation by TNFα + Estrogen + EGF, breast tumor cells migrate out of tumor-spheroids. Non-stimulated breast tumor cells were plated in nonadherent conditions, and tumor-spheroids were allowed to form for 72 hr. Then, the cells were either non-stimulated (a), or stimulated by TNFα + Estrogen + EGF (concentrations as in Figure 1) (b) for additional 24–96 hr. Non-stimulated cells: cells grown with the diluents of the above factors. Cells were photographed daily using light microscopy at ×10 magnification. Cell viability tests indicated that single cells migrating out of tumor-spheroids formed in the presence of TNFα + Estrogen + EGF stimulation were alive. In all panels, the results are from a representative experiment of $n \geq 3$. The surface expression of E-cadherin by the cells that were included in this analysis is shown in Table 1 and in Figure S3.

a subpopulation (based on Figure 5, up to ~50% of the cells) has gained tumor and metastasizing abilities in culture (Figures 4–6). Also, in other *in vivo* studies that we have performed with oncogene-expressing MCF-7 cells that were stimulated by TNFα (in which mice were also injected twice-weekly with CM of such cells) suggest that the metastatic load of cells stimulated by TNFα + Estrogen + EGF is higher than the one induced by TNFα (data not shown). Taken together, the influence of the TNFα + Estrogen + EGF stimulation on the metastasizing capabilities of these cells *in vivo* is of major importance and of high clinical relevance.

4. Discussion

In this study, we demonstrated that the combination between promalignancy factors has a dramatic impact on the ability of luminal tumor cells to acquire metastasis-related properties and to disseminate to remote organs. When used singly, TNFα was more effective than the other two representatives of the tumor microenvironment—estrogen and EGF—and its activities were potently increased by cooperating with these two factors. Thus, it was the joint activities of all three arms together—inflammatory, hormonal, and growth-supporting—that led in a prominent efficacy to the devastating processes of tumor cell spreading, EMT, and metastasis.

Our findings have shown that as a result of the combined stimulation by TNFα + Estrogen + EGF, luminal breast tumor cells have gained an extensive spreading phenotype in which Src activation has given rise to tumor cell spreading and to localization of FAK and paxillin in tumor cell protrusions. In parallel, the cancer cells have detached from each other and underwent the metastasis-relevant process of EMT and migration. As a result of TNFα + Estrogen + EGF stimulation, new cell subtypes have dominated the tumor cell population, expressing high levels of VLA6 and of the metastasis-related adhesion molecules CD44 and β1, accompanied by high levels of CXCL8, CCL2, and MMPs that were released by the cells. Based on published findings [84–87], the elevation in β1, CD44, and CXCL8 may very much stand in the basis of the high resistance to doxorubicin gained by the TNFα + Estrogen + EGF-stimulated cells.

The above characteristics that were gained by the tumor cells following exposure to TNFα + Estrogen + EGF have led to an intriguing *in vivo* phenotype, in which the stimulated cells have produced smaller local tumors but expressed very high metastatic phenotype compared to control non-stimulated cells. Based on the *in vitro* results described previously, two nonexclusive mechanisms could lead to such results: (1) out of the three stimulators of the tumor cells, TNFα is the only one that is cytotoxic while estrogen and EGF are known to stimulate tumor cell growth. The tumor cells used in this study (MCF-7 cells) are known to be sensitive to TNFα-induced cytotoxicity [73–75]; accordingly, approximately 40% of the tumor cells were killed *in vitro* by their exposure to the combined stimulation of TNFα + Estrogen + EGF (Figure S2). Although after this stimulation only live cells were injected (in equal numbers to control cells)

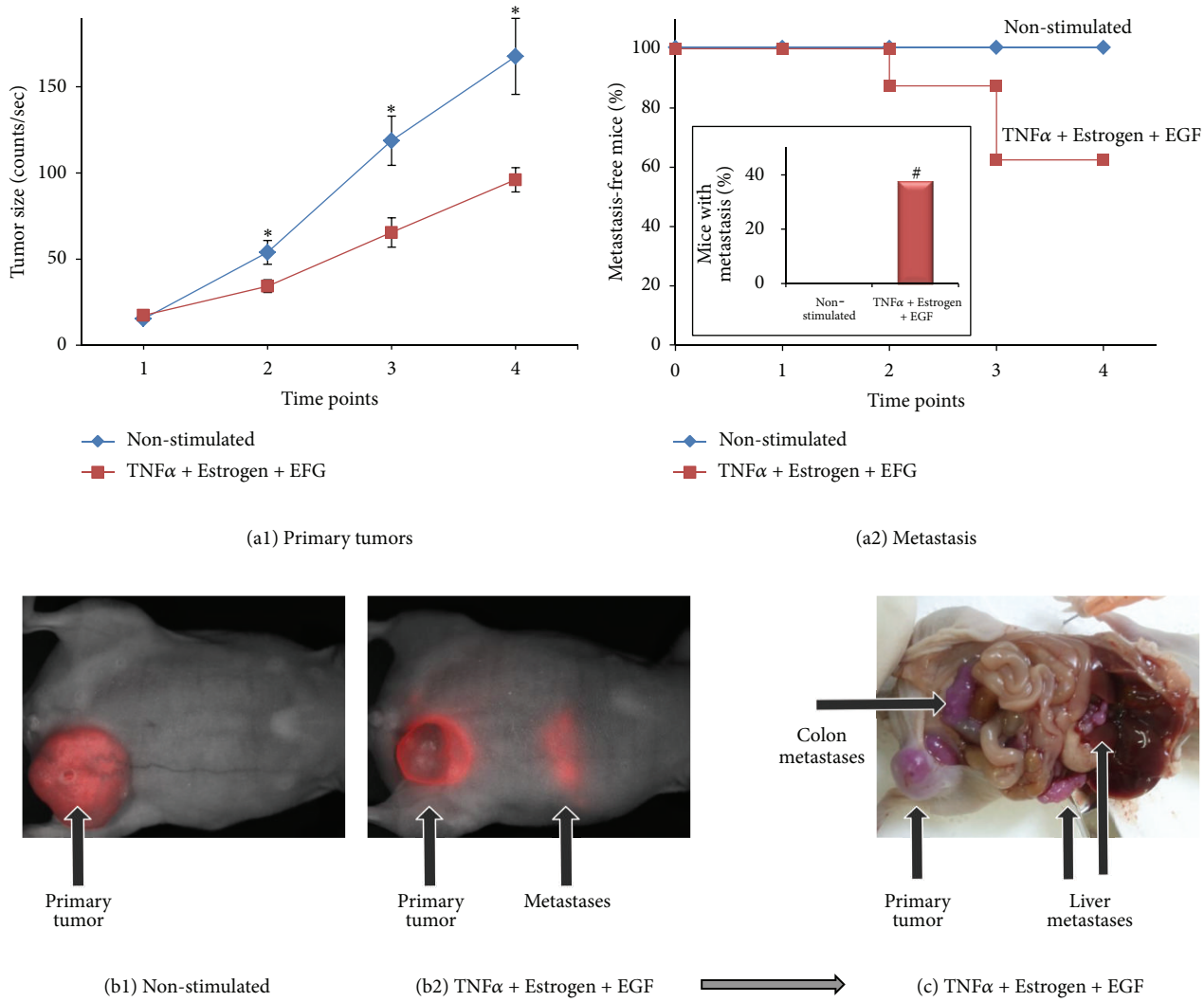

FIGURE 10: In response to combined stimulation by TNFα + Estrogen + EGF, breast tumor cells acquire high metastasizing abilities. mCherry-expressing breast tumor cells were stimulated by TNFα + Estrogen + EGF (concentrations as in Figure 1) for three days. Non-stimulated: cells grown with the diluents of the above factors. Following washing, equal numbers of live cells (4×10^6) were inoculated to the mammary fat pad of mice. Using the CRi Maestro intravital imaging system, tumors and metastases were followed in intact mice at four different time points along the experiments, up to 37 days. (a) Followup of primary tumors in the mammary fat pad and formation of macrometastases. (a1) Sizes of tumors at the mammary fat pads are presented as counts/sec of fluorescence emission, divided by 1,000, obtained at each time point by analyses with the CRi Maestro intravital imaging system. $^*P < 0.05$ for differences between the two groups of mice. The figure sums up the results obtained in two experimental repeats showing similar results, with a total $n = 6$ mice in the control group $n = 8$ mice in the group of mice inoculated with cells stimulated with TNFα + Estrogen + EGF. (a2) Kaplan-Meier analyses of metastasis-free mice, showing incidence of macrometastases detected by the Maestro device in intact animals in four time points along the experiments, up to 37 days. The figure sums up the results obtained in two experimental repeats showing similar results, with a total of $n = 6$ mice in the control group and $n = 8$ mice in the group of mice inoculated with cells stimulated with TNFα + Estrogen + EGF. *Inset*: the incidence of mice with macrometastases at the end-point of the experiments, determined in intact mice by the Maestro device (38% in the TNFα + Estrogen + EGF-stimulated tumor cells versus 0% in the control group, in two independent experiments providing similar results). $^{\#}$*Macrometastases were also observed in 2/3 mice in another experiment of TNFα + Estrogen + EGF cells* (in which control mice were not included). (b) Representative pictures obtained by the Maestro device in intact mice, showing tumor cells (red, mCherry) in both groups of mice. Non-stimulated tumor cells (b1) developed bigger tumors than tumor cells stimulated with TNFα + Estrogen + EGF (b2); however, macrometastases were detected only in the group of mice administered with tumor cells stimulated by TNFα + Estrogen + EGF (the image was obtained following prolonged excitation of mCherry in the CRi Maestro, in order to visualize the metastases). (c) A representative picture of the macrometastases that have developed in mice inoculated with tumor cells stimulated by TNFα + Estrogen + EGF, at the end of the experiment. The image shows the same mouse demonstrated in part (b2). Because of the expression of mCherry, the tumor cells carried a purple color. In this representative mouse, metastases were detected in the liver, colon, and above the kidney.

to the mice and the stimulus was removed beforehand, it is possible that some of the tumor cells were destined to die later on, after they have been introduced into the mouse. These cytotoxic effects of TNFα may have given rise to reduced growth of primary tumors. (2) the high spreading, EMT, and migration phenotypes endowed on the cancer cells by TNFα + Estrogen + EGF stimulation may have led to migration of tumor cells out of the primary focus soon after their inoculation to the mammary fat pad (as has been illustrated *in vitro* in Figure 9); thus, the cell inoculum from which the tumor developed was smaller after stimulation and gave rise to a smaller primary tumor than control non-stimulated cells. Such a mechanism is in good agreement with the high metastatic yield of the TNFα + Estrogen + EGF-stimulated cells (Figure 10). Obviously, such mechanisms suggest that it would be interesting to determine the EMT properties in primary tumors established by non-stimulated control cells compared to cells stimulated by TNFα + Estrogen + EGF.

Overall, our results suggest that some of the cancer cells that were stimulated by TNFα + Estrogen + EGF partly succumbed to the cytotoxic effects of TNFα and others migrated out of the initial tumor inoculum, giving rise to smaller primary tumors than those generated by control cells. But at the same time, these cells have gained many metastasis-promoting properties and became aggressive *in vivo*. Therefore, the small tumor growth endowed following TNFα + Estrogen + EGF stimulation provided a false benefit, because it has led to selection of cells expressing a higher metastasizing potential. Here, it is important to note that in the heterogeneous population of tumor cells, only some have acquired the high "spreading-EMT-metastasis"-related functions, and this can explain why metastases were not formed in all mice. Nevertheless, we would like to emphasize that the acquisition of a metastatic ability by MCF-7 cells is by itself extremely unique and important, even if not observed in all mice. MCF-7 cells are considered completely nonmetastatic, and even following over-expression of powerful proto-oncogenes such as H-Ras, they did not acquire the ability to form metastases *in vivo*, despite increased invasiveness *in vitro* [83].

Therefore, our findings indicate that under certain conditions—endowed by combined stimulation by three arms of the tumor microenvironment—MCF-7 cells became metastatic. In our *in vitro* analyses, TNFα was the most effective of all three elements, but its activities were potentiated by estrogen and EGF. Based on these studies, we propose that TNFα is the factor that dominated the high protumoral phenotypes and responses, leading to its most extreme impact on tumor cell spreading to remote organs.

Overall, while TNFα had the ability to exert cytotoxic effects that may reduce tumor growth, it cooperated with the two other arms of the tumor microenvironment and eventually turned into a metastasis-promoting entity. Here, it is important to note that all three factors—TNFα, estrogen, and EGF—are often expressed in luminal breast tumors in breast cancer patients. Past findings from our laboratory indicated that TNFα is expressed in approximately 90% of patients with recurrent disease, and many of these patients also express ER, and are therefore estrogen-responsive [22]. Other studies denoted that about 70% of breast tumors express the ligand EGF [88]. Taken together, these observations suggest that a relatively high subpopulation of luminal breast cancer patients may experience coexposure to TNFα + Estrogen + EGF and may thus acquire increased metastatic rate. Moreover, based on our results with doxorubicin resistance, the joint powers of all three factors together may further increase the resistance to chemotherapy in breast cancer patients, demonstrating another level at which the combined exposure to TNFα + Estrogen + EGF may be devastating to the patients.

5. Conclusions

The findings presented in this study have very high clinical relevance. Until a decade ago, many researchers suggested introducing TNFα as a therapeutic agent in cancer because of its cytotoxic activities. However, an increasing body of evidence puts TNFα on the stake as a key tumor-promoting factor that has harmful impacts on the malignancy cascade. Our findings pinpoint the devastating TNFα activities to be the life-threatening stage of metastasis formation, and these findings have a profound importance for breast cancer therapy. TNFα inhibitors, such as infliximab and etanercept have been FDA-approved and are being successfully used in the clinic for treatment of several autoimmune disorders [89–92]. Therefore, we suggest considering the addition of these established TNFα inhibitors to the treatment protocols of luminal breast cancer patients.

Specifically, we suggest taking the results of this study one step further, towards personalized cancer therapy. Knowing that antihormone therapies and inhibitors of EGFR/HER2 are already used for therapy of breast cancer [93, 94], we propose that patients diagnosed with high TNFα, estrogen, and EGF levels would benefit from targeting all three arms simultaneously and that clinicians should consider the possibility of treating such patients with a cocktail of all three modalities: TNFα inhibitors + antihormonal therapies + inhibitors of EGFR/HER2.

Obviously, extensive research is needed in order to assess the impact of TNFα inhibitors on breast tumor cells both *in vitro* and *in vivo*, and to design the proper clinical administration mode. However, we believe that the paradigm shift presented in this study on the roles of TNFα in metastasis may have a strong impact on therapeutic choices in the future. The feasibility of blocking several arms of the tumor microenvironment together should not be ignored, and reducing the cancer-related inflammation might also attenuate the tumor-promoting effects imposed by the other arms of the tumor microenvironment and thus inhibit tumor cells migration and invasion and their devastating outcome, metastasis formation.

Abbreviations

Abs: Antibodies
CM: Conditioned medium
DMSO: Dimethyl sulfoxide
EGF: Epidermal growth factor

EGFR: Epidermal growth factor receptor
EMT: Epithelial-to-mesenchymal transition
ER: Estrogen receptors
FACS: Fluorescence-activated cell sorting (flow cytometry)
FAK: Focal adhesion kinase
HRP: Horseradish peroxidase
MMPs: Matrix metalloproteinases
PR: Progesterone receptors
qRT-PCR: Quantitative real-time polymerase chain reaction
TNFα: Tumor necrosis factor α
PFA: Paraformaldehyde
DAPI: 4′,6-Diamidino-2-phenylindole.

Conflict of Interests

The authors disclose no potential conflict of interests.

Acknowledgment

The authors acknowledge the financial support provided to this study by The Israel Ministry of Health and Federico Foundation.

References

[1] P. Eroles, A. Bosch, J. Alejandro Pérez-Fidalgo, and A. Lluch, "Molecular biology in breast cancer: intrinsic subtypes and signaling pathways," *Cancer Treatment Reviews*, vol. 38, no. 6, pp. 698–707, 2012.

[2] S. Guiu, S. Michiels, F. Andre et al., "Molecular subclasses of breast cancer: how do we define them? The IMPAKT 2012 working group statement," *Annals of Oncology*, vol. 23, no. 12, pp. 2997–3006, 2012.

[3] S. C. Baumgarten and J. Frasor, "Minireview: inflammation: an instigator of more aggressive estrogen receptor (ER) positive breast cancers," *Molecular Endocrinology*, vol. 26, no. 3, pp. 360–371, 2012.

[4] H. Lahlou and W. J. Muller, "β1-integrins signaling and mammary tumor progression in transgenic mouse models: Implications for human breast cancer," *Breast Cancer Research*, vol. 13, no. 6, article 229, 2011.

[5] K. Raymond, M. M. Faraldo, M.-A. Deugnier, and M. A. Glukhova, "Integrins in mammary development," *Seminars in Cell and Developmental Biology*, vol. 23, no. 5, pp. 599–605, 2012.

[6] D. Naor, S. B. Wallach-Dayan, M. A. Zahalka, and R. V. Sionov, "Involvement of CD44, a molecule with a thousand faces, in cancer dissemination," *Seminars in Cancer Biology*, vol. 18, no. 4, pp. 260–267, 2008.

[7] S. Misra, P. Heldin, V. C. Hascall et al., "Hyaluronan-CD44 interactions as potential targets for cancer therapy," *FEBS Journal*, vol. 278, no. 9, pp. 1429–1443, 2011.

[8] D. S. Micalizzi, S. M. Farabaugh, and H. L. Ford, "Epithelial-mesenchymal transition in cancer: parallels between normal development and tumor progression," *Journal of Mammary Gland Biology and Neoplasia*, vol. 15, no. 2, pp. 117–134, 2010.

[9] A. Vincent-Salomon and J. P. Thiery, "Host microenvironment in breast cancer development: epithelia-mesenchymal transition in breast cancer development," *Breast Cancer Research*, vol. 5, no. 2, pp. 101–106, 2003.

[10] C. Scheel and R. A. Weinberg, "Phenotypic plasticity and epithelial-mesenchymal transitions in cancer and normal stem cells?" *International Journal of Cancer*, vol. 129, no. 10, pp. 2310–2314, 2011.

[11] C. D. Roskelley and M. J. Bissell, "The dominance of the microenvironment in breast and ovarian cancer," *Seminars in Cancer Biology*, vol. 12, no. 2, pp. 97–104, 2002.

[12] J. C. Tse and R. Kalluri, "Mechanisms of metastasis: epithelial-to-mesenchymal transition and contribution of tumor microenvironment," *Journal of Cellular Biochemistry*, vol. 101, no. 4, pp. 816–829, 2007.

[13] G. Lorusso and C. Rüegg, "The tumor microenvironment and its contribution to tumor evolution toward metastasis," *Histochemistry and Cell Biology*, vol. 130, no. 6, pp. 1091–1103, 2008.

[14] F. Balkwill, "Tumour necrosis factor and cancer," *Nature Reviews Cancer*, vol. 9, no. 5, pp. 361–371, 2009.

[15] F. Balkwill and A. Mantovani, "Cancer and inflammation: implications for pharmacology and therapeutics," *Clinical Pharmacology and Therapeutics*, vol. 87, no. 4, pp. 401–406, 2010.

[16] F. R. Balkwill and A. Mantovani, "Cancer-related inflammation: common themes and therapeutic opportunities," *Seminars in Cancer Biology*, vol. 22, no. 1, pp. 33–40, 2012.

[17] L. Bertazza and S. Mocellin, "The dual role of tumor necrosis factor (TNF) in cancer biology," *Current Medicinal Chemistry*, vol. 17, no. 29, pp. 3337–3352, 2010.

[18] S. Sangaletti, C. Tripodo, C. Ratti et al., "Oncogene-driven intrinsic inflammation induces leukocyte production of tumor necrosis factor that critically contributes to mammary carcinogenesis," *Cancer Research*, vol. 70, no. 20, pp. 7764–7775, 2010.

[19] M. A. Warren, S. F. Shoemaker, D. J. Shealy, W. Bshar, and M. M. Ip, "Tumor necrosis factor deficiency inhibits mammary tumorigenesis and a tumor necrosis factor neutralizing antibody decreases mammary tumor growth in neu/erbB2 transgenic mice," *Molecular Cancer Therapeutics*, vol. 8, no. 9, pp. 2655–2663, 2009.

[20] T. Hamaguchi, H. Wakabayashi, A. Matsumine, A. Sudo, and A. Uchida, "TNF inhibitor suppresses bone metastasis in a breast cancer cell line," *Biochemical and Biophysical Research Communications*, vol. 407, no. 3, pp. 525–530, 2011.

[21] M. A. Rivas, R. P. Carnevale, C. J. Proietti et al., "TNFα acting on TNFR1 promotes breast cancer growth via p42/P44 MAPK, JNK, Akt and NF-κB-dependent pathways," *Experimental Cell Research*, vol. 314, no. 3, pp. 509–529, 2008.

[22] G. Soria, M. Ofri-Shahak, I. Haas et al., "Inflammatory mediators in breast cancer: coordinated expression of TNFα & IL-1β with CCL2 & CCL5 and effects on epithelial-to-mesenchymal transition," *BMC Cancer*, vol. 11, article 130, 2011.

[23] D. W. Miles, L. C. Happerfield, M. S. Naylor, L. G. Bobrow, R. D. Rubens, and F. R. Balkwill, "Expression of tumour necrosis factor (TNFα) and its receptors in benign and malignant breast tissue," *International Journal of Cancer*, vol. 56, no. 6, pp. 777–782, 1994.

[24] L. F. Cui, X. J. Guo, J. Wei et al., "Overexpression of TNF-α and TNFRII in invasive micropapillary carcinoma of the breast: clinicopathological correlations," *Histopathology*, vol. 53, no. 4, pp. 381–388, 2008.

[25] I. García-Tuñón, M. Ricote, A. Ruiz, B. Fraile, R. Paniagua, and M. Royuela, "Role of tumor necrosis factor-α and its receptors in human benign breast lesions and tumors (in.situ and infiltrative)," *Cancer Science*, vol. 97, no. 10, pp. 1044–1049, 2006.

[26] C. Zhou, A. M. Nitschke, W. Xiong et al., "Proteomic analysis of tumor necrosis factor-α resistant human breast cancer cells reveals a MEK5/Erk5-mediated epithelial-mesenchymal transition phenotype," *Breast Cancer Research*, vol. 10, no. 6, article R105, 2008.

[27] Y. Ruike, Y. Imanaka, F. Sato, K. Shimizu, and G. Tsujimoto, "Genome-wide analysis of aberrant methylation in human breast cancer cells using methyl-DNA immunoprecipitation combined with high-throughput sequencing," *BMC Genomics*, vol. 11, no. 1, article 137, 2010.

[28] A. Ben-Baruch, "The tumor-promoting flow of cells into, within and out of the tumor site: regulation by the inflammatory axis of TNFα and chemokines," *Cancer Microenvironment*, vol. 5, no. 2, pp. 151–164, 2012.

[29] M. D. Planas-Silva and P. K. Waltz, "Estrogen promotes reversible epithelial-to-mesenchymal-like transition and collective motility in MCF-7 breast cancer cells," *Journal of Steroid Biochemistry and Molecular Biology*, vol. 104, no. 1-2, pp. 11–21, 2007.

[30] Y. Huang, S. V. Fernandez, S. Goodwin et al., "Epithelial to mesenchymal transition in human breast epithelial cells transformed by 17β-estradiol," *Cancer Research*, vol. 67, no. 23, pp. 11147–11157, 2007.

[31] P. Darbre, J. Yates, S. Curtis, and R. J. B. King, "Effect of estradiol on human breast cancer cells in culture," *Cancer Research*, vol. 43, no. 1, pp. 349–354, 1983.

[32] G. Deblois and V. Giguere, "Oestrogen-related receptors in breast cancer: control of cellular metabolism and beyond," *Nature Reviews Cancer*, vol. 13, pp. 27–36, 2012.

[33] E. W. Thompson, S. Paik, N. Brunner et al., "Association of increased basement membrane invasiveness with abscence of estrogen receptor and expression of vimentin in human breast cancer cell lines," *Journal of Cellular Physiology*, vol. 150, no. 3, pp. 534–544, 1992.

[34] K. Haim, P. Weitzenfeld, T. Meshel, and A. Ben-Baruch, "Epidermal growth factor and estrogen act by independent pathways to additively promote the release of the angiogenic chemokine CXCL8 by breast tumor cells," *Neoplasia*, vol. 13, no. 3, pp. 230–243, 2011.

[35] D. K. Biswas, A. P. Cruz, E. Gansberger, and A. B. Pardee, "Epidermal growth factor-induced nuclear factor κB activation: a major pathway of cell-cycle progression in estrogen-receptor negative breast cancer cells," *Proceedings of the National Academy of Sciences of the United States of America*, vol. 97, no. 15, pp. 8542–8547, 2000.

[36] R. Garcia, R. A. Franklin, and J. A. McCubrey, "EGF induces cell motility and multi-drug resistance gene expression in breast cancer cells," *Cell Cycle*, vol. 5, no. 23, pp. 2820–2826, 2006.

[37] F. Döll, J. Pfeilschifter, and A. Huwiler, "The epidermal growth factor stimulates sphingosine kinase-1 expression and activity in the human mammary carcinoma cell line MCF7," *Biochimica et Biophysica Acta*, vol. 1738, no. 1–3, pp. 72–81, 2005.

[38] T. Blick, E. Widodo, H. Hugo et al., "Epithelial mesenchymal transition traits in human breast cancer cell lines," *Clinical and Experimental Metastasis*, vol. 25, no. 6, pp. 629–642, 2008.

[39] C. K. Osborne, B. Hamilton, G. Titus, and R. B. Livingston, "Epidermal growth factor stimulation of human breast cancer cells in culture," *Cancer Research*, vol. 40, no. 7, pp. 2361–2366, 1980.

[40] J. R. Woodburn, "The epidermal growth factor receptor and its inhibition in cancer therapy," *Pharmacology and Therapeutics*, vol. 82, no. 2-3, pp. 241–250, 1999.

[41] M. A. Rivas, M. Tkach, W. Beguelin et al., "Transactivation of ErbB-2 induced by tumor necrosis factor α promotes NF-κB activation and breast cancer cell proliferation," *Breast Cancer Research and Treatment*, vol. 122, no. 1, pp. 111–124, 2010.

[42] H. B. Jijon, A. Buret, C. L. Hirota, M. D. Hollenberg, and P. L. Beck, "The EGF receptor and HER2 participate in TNF-alpha-dependent MAPK activation and IL-8 secretion in intestinal epithelial cells," *Mediators of Inflammation*, vol. 2012, Article ID 207398, 12 pages, 2012.

[43] T. Blick, H. Hugo, E. Widodo et al., "Epithelial mesenchymal transition traits in human breast cancer cell lines parallel the CD44HI/CD24lO/-stem cell phenotype in human breast cancer," *Journal of Mammary Gland Biology and Neoplasia*, vol. 15, no. 2, pp. 235–252, 2010.

[44] J. Kao, K. Salari, M. Bocanegra et al., "Molecular profiling of breast cancer cell lines defines relevant tumor models and provides a resource for cancer gene discovery," *PLoS ONE*, vol. 4, no. 7, Article ID e6146, 2009.

[45] M. Lacroix and G. Leclercq, "Relevance of breast cancer cell lines as models for breast tumours: an update," *Breast Cancer Research and Treatment*, vol. 83, no. 3, pp. 249–289, 2004.

[46] H. Seeger, D. Wallwiener, and A. O. Mueck, "Effects of estradiol and progestogens on tumor-necrosis factor-α-induced changes of biochemical markers for breast cancer growth and metastasis," *Gynecological Endocrinology*, vol. 24, no. 10, pp. 576–579, 2008.

[47] E. Azenshtein, G. Luboshits, S. Shina et al., "The CC chemokine RANTES in breast carcinoma progression: Regulation of expression and potential mechanisms of promalignant activity," *Cancer Research*, vol. 62, no. 4, pp. 1093–1102, 2002.

[48] S. C. Brooks, E. R. Locke, and H. D. Soule, "Estrogen receptor in a human cell line (MCF 7) from breast carcinoma," *Journal of Biological Chemistry*, vol. 248, no. 17, pp. 6251–6253, 1973.

[49] Z. Papoutsi, C. Zhao, M. Putnik, J.-Å. Gustafsson, and K. Dahlman-Wright, "Binding of estrogen receptor α/β heterodimers to chromatin in MCF-7 cells," *Journal of Molecular Endocrinology*, vol. 43, no. 2, pp. 65–72, 2009.

[50] L. C. Kim, L. Song, and E. B. Haura, "Src kinases as therapeutic targets for cancer," *Nature Reviews Clinical Oncology*, vol. 6, no. 10, pp. 587–595, 2009.

[51] N. A. Chatzizacharias, G. P. Kouraklis, and S. E. Theocharis, "Clinical significance of FAK expression in human neoplasia," *Histology and Histopathology*, vol. 23, no. 4-6, pp. 629–650, 2008.

[52] M. Luo and J.-L. Guan, "Focal adhesion kinase: a prominent determinant in breast cancer initiation, progression and metastasis," *Cancer Letters*, vol. 289, no. 2, pp. 127–139, 2010.

[53] S. K. Mitra and D. D. Schlaepfer, "Integrin-regulated FAK-Src signaling in normal and cancer cells," *Current Opinion in Cell Biology*, vol. 18, no. 5, pp. 516–523, 2006.

[54] J. Pasquier, B. S. Guerrouahen, H. Al Thawadi et al., "Preferential transfer of mitochondria from endothelial to cancer cells through tunneling nanotubes modulates chemoresistance," *Journal of Translational Medicine*, vol. 11, article 94, 2013.

[55] E. Lou, S. Fujisawa, A. Morozov et al., "Tunneling nanotubes provide a unique conduit for intercellular transfer of cellular

contents in human malignant pleural mesothelioma," *PLoS ONE*, vol. 7, no. 3, Article ID e33093, 2012.

[56] J. M. Nam, K. M. Ahmed, S. Costes et al., "Beta1-integrin via NF-kappaB signaling is essential for acquisition of invasiveness in a model of radiation treated in situ breast cancer," *Breast Cancer Research*, vol. 15, article R60, 2013.

[57] M. C. Schmid, C. J. Avraamides, P. Foubert et al., "Combined blockade of integrin-$\alpha 4\beta 1$ plus cytokines SDF-1α or IL-1β potently inhibits tumor inflammation and growth," *Cancer Research*, vol. 71, no. 22, pp. 6965–6975, 2011.

[58] G. Morozevich, N. Kozlova, I. Cheglakov, N. Ushakova, and A. Berman, "Integrin $\alpha 5\beta 1$ controls invasion of human breast carcinoma cells by direct and indirect modulation of MMP-2 collagenase activity," *Cell Cycle*, vol. 8, no. 14, pp. 2219–2225, 2009.

[59] N. Kusuma, D. Denoyer, J. A. Eble et al., "Integrin-dependent response to laminin-511 regulates breast tumor cell invasion and metastasis," *International Journal of Cancer*, vol. 130, no. 3, pp. 555–566, 2012.

[60] M. Sameni, J. Dosescu, K. M. Yamada, B. F. Sloane, and D. Cavallo-Medved, "Functional live-cell imaging demonstrates that $\beta 1$-integrin promotes type IV collagen degradation by breast and prostate cancer cells," *Molecular Imaging*, vol. 7, no. 5, pp. 199–213, 2008.

[61] X. H. Yang, A. L. Richardson, M. I. Torres-Arzayus et al., "CD151 accelerates breast cancer by regulating $\alpha 6$ integrin function, signaling, and molecular organization," *Cancer Research*, vol. 68, no. 9, pp. 3204–3213, 2008.

[62] I. A. Ivanova, J. F. Vermeulen, C. Ercan et al., "FER kinase promotes breast cancer metastasis by regulating alpha- and beta-integrin-dependent cell adhesion and anoikis resistance," *Oncogene*, 2013.

[63] M. Götte and G. W. Yip, "Heparanase, hyaluronan, and CD44 in cancers: a breast carcinoma perspective," *Cancer Research*, vol. 66, no. 21, pp. 10233–10237, 2006.

[64] N. Montgomery, A. Hill, S. McFarlane et al., "CD44 enhances invasion of basal-like breast cancer cells by upregulating serine protease and collagen-degrading enzymatic expression and activity," *Breast Cancer Research*, vol. 14, p. R84, 2012.

[65] S. Spaderna, O. Schmalhofer, M. Wahlbuhl et al., "The transcriptional repressor ZEB1 promotes metastasis and loss of cell polarity in cancer," *Cancer Research*, vol. 68, no. 2, pp. 537–544, 2008.

[66] A. Aghdassi, M. Sendler, A. Guenther et al., "Recruitment of histone deacetylases HDAC1 and HDAC2 by the transcriptional repressor ZEB1 downregulates E-cadherin expression in pancreatic cancer," *Gut*, vol. 61, no. 3, pp. 439–448, 2012.

[67] F. Fan, S. Samuel, K. W. Evans et al., "Overexpression of Snail induces epithelial-mesenchymal transition and a cancer stem cell-like phenotype in human colorectal cancer cells," *Cancer Medicine*, vol. 1, pp. 5–16, 2012.

[68] H. Siemens, R. Jackstadt, S. Hünten et al., "miR-34 and SNAIL form a double-negative feedback loop to regulate epithelial-mesenchymal transitions," *Cell Cycle*, vol. 10, no. 24, pp. 4256–4271, 2011.

[69] M. E. Baygi, Z.-S. Soheili, F. Essmann et al., "Slug/SNAI2 regulates cell proliferation and invasiveness of metastatic prostate cancer cell lines," *Tumor Biology*, vol. 31, no. 4, pp. 297–307, 2010.

[70] K. Zhang, D. Chen, X. Jiao et al., "Slug enhances invasion ability of pancreatic cancer cells through upregulation of matrix metalloproteinase-9 and actin cytoskeleton remodeling," *Laboratory Investigation*, vol. 91, no. 3, pp. 426–438, 2011.

[71] F. Stavridi and C. Palmieri, "Efficacy and toxicity of nonpegylated liposomal doxorubicin in breast cancer," *Expert Review of Anticancer Therapy*, vol. 8, no. 12, pp. 1859–1869, 2008.

[72] J. Prados, C. Melguizo, R. Ortiz et al., "Doxorubicin-loaded nanoparticles: new advances in breast cancer therapy," *Anti-Cancer Agents in Medicinal Chemistry*, vol. 12, no. 9, pp. 1058–1070, 2012.

[73] M. Egeblad and M. Jaattela, "Cell death induced by TNF or serum starvation is independent of ErbB receptor signaling in MCF-7 breast carcinoma cells," *International Journal of Cancer*, vol. 86, pp. 617–625, 2000.

[74] Z. Cai, A. Bettaieb, N. El Mahdani et al., "Alteration of the sphingomyelin/ceramide pathway is associated with resistance of human breast carcinoma MCF7 cells to tumor necrosis factor-α- mediated cytotoxicity," *Journal of Biological Chemistry*, vol. 272, no. 11, pp. 6918–6926, 1997.

[75] R. Simstein, M. Burow, A. Parker, C. Weldon, and B. Beckman, "Apoptosis, chemoresistance, and breast cancer: Insights from the MCF-7 cell model system," *Experimental Biology and Medicine*, vol. 228, no. 9, pp. 995–1003, 2003.

[76] T. Leibovich-Rivkin, Y. Lebel-Haziv, S. Lerrer, P. Weitzenfeld, and A. Ben-Baruch, "The versatile world of inflammatory chemokines in cancer," in *The Tumor Immunoenvironment*, M. R. Shurin, V. Umansky, and A. Malyguine, Eds., pp. 135–175, Springer, Amsterdam, The Netherlands, 2013.

[77] G. Soria and A. Ben-Baruch, "The inflammatory chemokines CCL2 and CCL5 in breast cancer," *Cancer Letters*, vol. 267, no. 2, pp. 271–285, 2008.

[78] N. Todorovic-Rakovic and J. Milovanovic, "Interleukin-8 in breast cancer progression," *Journal of Interferon & Cytokine Research* , vol. 22, no. 10, pp. 563–570, 2013.

[79] R. T. Abraham, "Chemokine to the rescue: interleukin-8 mediates resistance to PI3K-pathway-targeted therapy in breast cancer," *Cancer Cell*, vol. 22, pp. 703–705, 2012.

[80] A. Yadav, V. Saini, and S. Arora, "MCP-1: chemoattractant with a role beyond immunity: a review," *Clinica Chimica Acta*, vol. 411, no. 21-22, pp. 1570–1579, 2010.

[81] B.-Z. Qian, J. Li, H. Zhang et al., "CCL2 recruits inflammatory monocytes to facilitate breast-tumour metastasis," *Nature*, vol. 475, no. 7355, pp. 222–225, 2011.

[82] A. E. Place, S. Jin Huh, and K. Polyak, "The microenvironment in breast cancer progression: biology and implications for treatment," *Breast Cancer Research*, vol. 13, no. 6, article 227, 2011.

[83] E. P. Gelmann, E. W. Thompson, and C. L. Sommers, "Invasive and metastatic properties of MCF-7 cells and ras(H)-transfected MCF-7 cell lines," *International Journal of Cancer*, vol. 50, no. 4, pp. 665–669, 1992.

[84] F. Aoudjit and K. Vuori, "Integrin signaling inhibits paclitaxel-induced apoptosis in breast cancer cells," *Oncogene*, vol. 20, no. 36, pp. 4995–5004, 2001.

[85] A. Nista, C. Leonetti, G. Bernardini, M. Mattioni, and A. Santoni, "Functional role of alpha4beta1 and alpha5beta1 integrin fibronectin receptors expressed on adriamycin-resistant MCF-7 human mammary carcinoma cells," *International Journal of Cancer*, vol. 72, pp. 133–141, 1997.

[86] T. Ishimoto, O. Nagano, T. Yae et al., "CD44 variant regulates redox status in cancer cells by stabilizing the xCT subunit of system xc(-) and thereby promotes tumor growth," *Cancer Cell*, vol. 19, no. 3, pp. 387–400, 2011.

[87] Z. Shi, W. M. Yang, L. P. Chen et al., "Enhanced chemosensitization in multidrug-resistant human breast cancer cells by inhibition of IL-6 and IL-8 production," *Breast Cancer Research and Treatment*, vol. 135, no. 3, pp. 737–747, 2012.

[88] Z. Suo, B. Risberg, M. G. Karlsson, K. Villman, E. Skovlund, and J. M. Nesland, "The expression of EGFR family ligands in breast carcinomas," *International Journal of Surgical Pathology*, vol. 10, no. 2, pp. 91–99, 2002.

[89] J. S. Smolen and P. Emery, "Infliximab: 12 years of experience," *Arthritis Research and Therapy*, vol. 13, supplement 1, p. S2, 2011.

[90] T. A. Kerensky, A. B. Gottlieb, S. Yaniv, and S.-C. Au, "Etanercept: efficacy and safety for approved indications," *Expert Opinion on Drug Safety*, vol. 11, no. 1, pp. 121–139, 2012.

[91] L. C. R. Silva, L. C. M. Ortigosa, and G. Benard, "Anti-TNF-α agents in the treatment of immune-mediated inflammatory diseases: mechanisms of action and pitfalls," *Immunotherapy*, vol. 2, no. 6, pp. 817–833, 2010.

[92] P. P. Tak and J. R. Kalden, "Advances in rheumatology: new targeted therapeutics," *Arthritis Research and Therapy*, vol. 13, supplemet 1, p. S5, 2011.

[93] S. Dent, B. Oyan, A. Honig, M. Mano, and S. Howell, "HER2-targeted therapy in breast cancer: a systematic review of neoadjuvant trials," *Cancer Treatment Reviews*, vol. 39, no. 6, pp. 622–631, 2013.

[94] N. Patani, L. A. Martin, and M. Dowsett, "Biomarkers for the clinical management of breast cancer: international perspective," *International Journal of Cancer*, vol. 133, pp. 1–13, 2012.

Hindawi Publishing Corporation
Mediators of Inflammation
Volume 2013, Article ID 342351, 8 pages
http://dx.doi.org/10.1155/2013/342351

Clinical Study

Haplotype Analysis of Interleukin-8 Gene Polymorphisms in Chronic and Aggressive Periodontitis

Petra Borilova Linhartova,[1] Jan Vokurka,[2] Hana Poskerova,[2] Antonin Fassmann,[2] and Lydie Izakovicova Holla[1,2]

[1] *Department of Pathophysiology, Faculty of Medicine, Masaryk University, 625 00 Brno, Czech Republic*
[2] *Clinic of Stomatology, Institutions Shared with St. Anne's Faculty Hospital, Faculty of Medicine, Masaryk University, 656 91 Brno, Czech Republic*

Correspondence should be addressed to Lydie Izakovicova Holla; holla@med.muni.cz

Received 27 July 2013; Revised 9 October 2013; Accepted 4 November 2013

Academic Editor: Dennis Daniel Taub

Objectives. Periodontitis is an inflammatory disease characterized by connective tissue loss and alveolar bone destruction. Interleukin-8 (*IL8*) is important in the regulation of the immune response. The aim of this study was to analyze four polymorphisms in the *IL8* gene in relation to chronic (CP) and aggressive (AgP) periodontitis. *Methods*. A total of 492 unrelated subjects were included in this case-control association study. Genomic DNA of 278 patients with CP, 58 patients with AgP, and 156 controls were genotyped, using the 5′ nuclease TaqMan assay, for *IL8* (rs4073, rs2227307, rs2227306, and rs2227532) gene polymorphisms. Subgingival bacterial colonization was investigated by the DNA-microarray detection kit in a subgroup of subjects ($N = 247$). *Results*. Allele and genotype frequencies of all investigated *IL8* polymorphisms were not significantly different between the subjects with CP and/or AgP and controls ($P > 0.05$). Nevertheless, the A(−251)/T(+396)/T(+781) and T(−251)/G(+396)/C(+781) haplotypes were significantly less frequent in patients with CP (2.0% versus 5.1%, $P < 0.02$, OR = 0.34, 95% CI: 0.15–0.78, resp., 2.0% versus 4.5%, $P < 0.05$, OR = 0.41, 95% CI: 0.18–0.97) than in controls. *Conclusions*. Although none of the investigated SNPs in the *IL8* gene was individually associated with periodontitis, some haplotypes can be protective against CP in the Czech population.

1. Introduction

Periodontitis is an inflammatory disease which is initiated and maintained by the gram-negative bacteria of the subgingival biofilm [1]. Specific pathogen associated molecular patterns (PAMPs) and bacterial virulence factors stimulate an inflammatory host response that finally results in destruction of periodontal tissue and tooth loss [2]. Chronic periodontitis (CP) and generalized aggressive forms of periodontitis (AgP) appear to be associated with certain pathogens, including *Porphyromonas gingivalis*, *Campylobacter rectus*, *Tannerella forsythia*, *Peptostreptococcus micro*, and *Treponema* species [3, 4]. *Treponema denticola*, *P. gingivalis*, and *T. forsythia*, characterized as the "red complex," were strongly associated with the clinical progression of chronic periodontitis [1–5]. In contrast, AgP was more often diagnosed in patients positive for *Aggregatibacter actinomycetemcomitans*, but there were many individuals with AgP who did not harbor this microorganism [6].

In addition to the microbial challenge, other factors, such as genetics, environment, and host factors, play a role in the pathogenesis of these diseases [7–9]. Various compounds, such as cytokines, representing an important pathway of connective tissue destruction in periodontitis, have been detected in gingival crevicular fluid (GCF). IL-8, a member of the CXC chemokine family, was originally described by Matsushima and Oppenheim [10]. It is the most important chemoattractant and activator of human neutrophils and an important mediator for granulocyte accumulation [11]. IL-8 is involved in the initiation and amplification of acute inflammatory reactions and chronic inflammatory processes. Functions of IL-8 are mediated through two receptors (CXCR1 and CXCR2); the expression was detected on numerous cell lineages, including neutrophils and epithelial cells [12].

Gingival epithelial cells (GEC) are capable of upregulating *IL8* expression rapidly in response to *A. actinomycetemcomitans* challenge, facilitating thus the recruitment of neutrophils as a host defense mechanism [13, 14]. *IL8* expression in GEC is induced by *P. gingivalis* [15] and *T. forsythia* [16]; IL-8 production by gingival fibroblast cultures is also affected by lipopolysaccharides of *P. gingivalis* and *P. intermedia* [17]. The IL-8 levels in gingival crevicular fluid (GCF) are valuable in detecting the inflammation of periodontal tissue [18–20], and periodontal therapy reduces the IL-8 levels in GCF [21].

IL-8 is encoded by the *IL8* gene located on chromosome 4q13-21 (GenBank accession number M28130.1), consisting of four exons, three introns, and the proximal promoter region [22]. Several polymorphisms have been reported in the *IL8* gene [23–26] and some of them can regulate the IL-8 production. Some of SNPs in the *IL8* gene such as −845T/C (rs2227532), −738T/C, −251A/T (rs4073, previously referred to as −353A/T), +396T/G (rs2227307), and +781C/T (rs2227306) have been studied in patients with AgP or CP in the Brazilian population [27–32]. In addition, *IL8* −251T allele, which was associated with higher production of IL-8, increased the risk of developing acute suppurative form of apical periodontitis (AP), whereas *IL8* −251A "low-producing" allele was associated with chronic nonsuppurative form of AP in the Colombian population [33]. In the Chinese population, *IL8* −251A allele has been associated with decreased susceptibility to CP [34]. The cross-sectional study in Iran has also focused on the study of polymorphisms in the *IL8* gene but did not specify whether it was for patients with CP or AgP [35]. To date, no study analyzing allele, genotype, or haplotype frequencies of *IL8* gene polymorphisms in patients with periodontitis has been performed in Caucasians.

The aim of this study was to associate four SNPs in the *IL8* gene (rs4073, rs2227307, rs2227306, and rs2227532) and their haplotypes to CP and AgP and subgingival bacterial colonization in the Czech population.

2. Material and Methods

The study was performed with the approval of the Committees for Ethics of the Medical Faculty, Masaryk University Brno and St. Anne's Faculty Hospital. Written informed consent was obtained from all participants before inclusion in the study, in line with the Helsinki Declaration.

2.1. Study Population. All patients were recruited from the patient pool of the Periodontology Department, Clinic of Stomatology, St. Anne's Faculty Hospital, Brno, from 2005 to 2011. They had at least 20 remaining teeth and were in good general health. Exclusion criteria included history of cardiovascular disorders (such as coronary artery diseases or hypertension), diabetes mellitus, malignant diseases, immunodeficiency, current pregnancy, or lactation. Controls were selected from subjects referring to the Clinic of Stomatology for reasons other than periodontal disease (such as dental caries, orthodontic consultations, preventive dental checkups, etc.) during the same period as patients and matched for age, gender, and smoking status. Similarly as patients, all controls had at least 20 remaining teeth and were in good general health. Exclusion criteria were the same as those applied for patients with periodontitis.

2.2. Case-Control Association Study. A total of 492 unrelated Caucasian subjects of exclusively Czech ethnicity from the region of South Moravia were included in this case-control association study. Diagnosis of nonperiodontitis/periodontitis was based on the detailed clinical examination, medical and dental history, tooth mobility, and radiographic assessment. Probing depth (PD) and attachment loss (CAL) were collected with a UNC-15 periodontal probe from six sites on every tooth present. The loss of the alveolar bone was determined radiographically. We used the index of Mühlemann to evaluate decreases in alveolar bone levels.

(1) Generalized CP group ($N = 278$): all patients with chronic periodontitis (CP) fulfilled the diagnostic criteria defined according to CAL levels by the International Workshop for a Classification of Periodontal Diseases and Conditions for Chronic Periodontitis [36]. Inclusion criteria for patients suffering from generalized chronic periodontitis were as follows: ≥30% of the teeth were affected, PD was ≥4 mm, and the amount of CAL was consistent with the presence of dental plaque.

(2) Generalized AgP group ($N = 58$): patients with aggressive periodontitis with age at disease onset <35 years, attachment loss of 4 mm or more in at least 30% of the teeth (at least three of the affected teeth were not first molars and incisors), and the severity of attachment loss being inconsistent with the amount of dental plaque were included in this study.

(3) Control group (healthy/nonperiodontitis) ($N = 156$): controls were screened using a WHO probe and the CPITN (Community Periodontal Index of Treatment Needs) was assessed [37]; values of the CPITN index in controls were less than 3.

In order to adjust for the effect of smoking history on periodontal disease, the subjects (patients and controls) were classified into the following groups: subjects who never smoked (referred to as nonsmokers) and subjects who were former smokers for ≥5 pack years or current smokers (referred to as smokers). The pack years were calculated by multiplying the number of years of smoking by the average number of cigarette packs smoked per day.

2.3. Genetic Analysis

2.3.1. Isolation of Genomic DNA. DNA for genetic analysis was extracted from the peripheral blood leukocytes using standard phenol/chloroform procedures with proteinase K according to Sambrook et al. [38]. Isolation and storage of DNA (working samples at concentrations of 50 ng μL^{-1} at 4°C) as well as the genotyping of samples were conducted in the laboratory of the Department of Pathophysiology, Faculty of Medicine, Masaryk University, Brno, Czech Republic.

2.3.2. SNPs Genotyping TaqMan Assay. Four SNPs (−845C/T rs2227532, −251A/T rs4073, +396G/T rs2227307, and +781C/T rs2227306) in the *IL8* gene were genotyped using the 5′ nuclease TaqMan assay for allelic discrimination. Individual fluorogenic TaqMan probes, consisting of an oligonucleotide labelled with both a fluorescent reporter dye, FAM, and a quencher dye, VIC, were obtained from Life Technologies (Grand Island, NY, USA). Each reaction mixture was prepared using TaqMan Genotyping Master Mix (12.5 μL), TaqMan SNP Genotyping Assay (1.25 μL), and 50 ng of genomic DNA in 17.5 μL of dH_2O to make a 25.0 μL reaction volume. Genotyping was carried out simultaneously with 88 samples on 96-well plate (+8 negative controls). Details on SNPs detection are summarized in Table 1. The PCR thermocycling protocol consisted of 10 min at 95°C, followed by 40 cycles of 15 s at 92°C and 1 min at 60°C. Each genotyping plate contained eight wells without any DNA template (negative controls) and randomly selected duplicate samples (10% of plate samples). Allele genotyping from fluorescence measurements was then obtained using the ABI PRISM 7000 Sequence Detection System. SDS version 1.2.3 software was used to analyze real-time and endpoint fluorescence data. Genotyping was performed by one investigator (P. B. L.) unaware of the phenotype.

2.3.3. DNA Microarray Analysis of Oral Pathogens. Subgingival bacterial colonization (*Aggregatibacter actinomycetemcomitans*, *Porphyromonas gingivalis*, *Prevotella intermedia*, *Tannerella forsythia*, *Treponema denticola*, *Peptostreptococcus micros*, *and Fusobacterium nucleatum*) in subgingival pockets was investigated by the DNA microarray based on a periodontal pathogen detection kit (Protean Ltd., Ceske Budejovice, CR) in a subgroup of randomly selected subjects ($N = 151$ for CP, $N = 21$ for AgP, and $N = 75$ for controls) before subgingival scaling. Microbial samples were collected from the deepest pocket in periodontitis patients (and from the deepest sulcus in healthy subjects) of each quadrant by inserting a sterile paper point into a base of the pocket for 20 seconds. Bacterial plaque samples from each individual were pooled in one tube. This test determined the individual pathogens semiquantitatively as follows: (–) undetected, which corresponds to the number of bacteria less than 10^3, (+) slightly positive corresponding to the number of bacteria 10^3 to 10^4, (++) positive corresponding to the number of bacteria 10^4 to 10^5, and (+++) strongly positive, with the number of bacteria higher than 10^5.

2.4. Statistical Analysis. Comparisons were made between allelic and genotype frequencies in the patients with chronic or aggressive form of periodontitis and control population. The allele frequencies were calculated from the observed numbers of genotypes. The significance of differences in the allele frequencies among groups was determined by Fisher's exact test. χ^2 analysis was used to test for deviation of genotype distribution from Hardy-Weinberg equilibrium and comparison of differences in genotype combinations among groups.

To examine the linkage disequilibrium (LD) between all SNPs, pairwise LD coefficients (D′) and haplotype frequencies were calculated using the SNP Analyzer 2 program (http://snp.istech.info/istech/board/login_form.jsp). Variations in the quantity of subgingival bacteria corresponding to the particular genotypes/alleles were tested by χ^2 and Fisher's exact tests. Differences were considered significant at $P < 0.05$.

Power analysis was performed with respect to the case-control design of the study taking the incidence rate of markers and estimate of the odds ratio (OR) as end-point statistical measures. ORs with corresponding 95% confidence intervals (CI) were estimated using logistic regression models, adopting age, sex, and smoking as adjusting covariates. All calculations were performed using Statistica ver. 10.0 (StatSoft Inc., Tulsa, OK, USA) and SPSS software (SPSS 20.0.1, IBM Corporation, 2011).

3. Results

3.1. Case-Control Study. The mean ages for AgP patients (37.0 ± 8.2; years ± SD) and healthy subjects (41.0 ± 12.3) did not differ between the two groups. However, subjects with CP were significantly older (47.9 ± 8.7) than the patients with AgP ($P < 0.05$). Nearly, 27% of the periodontitis patients (28.0% of CP and 26.0% of AgP) and 28.0% of healthy subjects were smokers. There were no significant differences between the subjects with periodontitis and controls regarding the mean percentage of smokers and ratio of males/females (77/79 in controls, 136/142 in patients with CP, and 25/33 in patients with AgP).

Sample size of the study was planned in standard power calculation for case-control design of the study with the null and alternative hypotheses expressed on the basis of OR. The design was prospectively optimized assuming the prevalence of examined attribute among controls to be 0.5. The recruited sample (278 cases, 156 controls) allowed a statistically significant detection of OR out of the range of 0.55–1.80 (alpha = 0.05, power = 0.80). In case of the AgP group (58 cases, 156 controls), the statistically significantly detectable ORs estimates were out of the range of 0.39–2.59.

3.2. Single Nucleotide Polymorphism Analysis. All studied polymorphisms were in the Hardy-Weinberg equilibrium in the control group. Allele and genotype frequencies of all investigated *IL8* polymorphisms were not significantly different between the subjects with CP and/or AgP and controls ($P > 0.05$; Table 2). Considering that in the Czech population, SNP *IL8* −845TT genotype occurred in 98.4% of CP patients and even 100% of controls and AgP patients, we analyzed this polymorphism only in the subgroup of subjects ($N = 193$).

3.3. Haplotype Analysis. Based on the previous study [29] the haplotype analysis of these selected SNPs was performed in the *IL8* gene (−251T/A rs4073, +396T/G rs2227307, and +781C/T rs2227306). All variants in the *IL8* gene were in tight

Table 1: Details of SNPs in *IL8* detection.

SNPs	TaqMan SNP genotyping assay ID	Context sequence [VIC/FAM]
IL8 −845T/C (rs2227532)	C_1842904_10	GCTCTTATGCCTCCACTGGAATTAA[C/T] GTCTTAGTACCACTTGTCTATTCTG
IL8 −251A/T (rs4073)	C_11748116_10	TTATCTAGAAATAAAAAAGCATACA[A/T] TTGATAATTCACCAAATTGTGGAGC
IL8 +396T/G (rs222730732)	C_11748168_10	TATTCTGCTTTTATAATTTATACCA[G/T] GTAGCATGCATATATTTAACGTAAA
IL8 +781C/T (rs2227306)	C_11748169_10	AACTCTAACTCTTTATATAGGAAGT[C/T] GTTCAATGTTGTCAGTTATGACTGT

Table 2: Genotype and allele frequencies of *IL8* polymorphisms in control and periodontitis subgroups.

SNP	Genotype	Controls $N = 156$ (%)	CP $N = 278$ (%)	P value*	OR (95% CI)	AgP $N = 58$ (%)	P value*	OR (95% CI)
IL8 −251T/A (rs4073)	TT	49 (31.4)	95 (34.2)	—	1.00	18 (31.0)	—	1.00
	TA	78 (50.0)	120 (43.2)	0.37	0.76 (0.47–1.23)	27 (46.6)	0.76	1.08 (0.49–2.37)
	AA	29 (18.6)	63 (22.7)	0.78	1.22 (0.67–2.21)	13 (22.4)	0.67	1.27 (0.47–3.38)
	Allele							
	T	176 (56.4)	310 (55.8)	0.60	1.00	62 (53.4)	0.33	1.00
	A	136 (43.6)	246 (44.2)		0.93 (0.69–1.25)	54 (46.6)		0.89 (0.55–1.44)
IL8 +396T/G (rs2227307)	TT	54 (34.6)	100 (36.0)	—	1.00	20 (34.5)	—	1.00
	TG	74 (47.4)	118 (42.4)	0.58	0.86 (0.54–1.39)	27 (46.6)	0.74	1.15 (0.54–2.45)
	GG	28 (17.9)	60 (21.6)	0.67	1.28 (0.71–2.31)	11 (19.0)	0.92	1.00 (0.36–2.82)
	Allele							
	T	182 (58.3)	318 (57.2)	0.83	1.00	67 (57.8)	0.89	1.00
	G	130 (41.7)	238 (42.8)		0.91 (0.68–1.23)	49 (42.2)		0.99 (0.61–1.62)
IL8 +781C/T (rs2227306)	CC	55 (35.3)	103 (37.1)	—	1.00	20 (34.5)	—	1.00
	CT	76 (48.7)	121 (43.5)	0.51	0.82 (0.52–1.31)	27 (46.6)	0.84	1.10 (0.52–2.34)
	TT	25 (16.0)	54 (19.4)	0.66	1.24 (0.67–2.31)	11 (19.0)	0.66	1.07 (0.38–3.02)
	Allele							
	T	186 (59.6)	327 (58.8)	0.44	1.00	67 (57.8)	0.68	1.00
	C	126 (40.4)	229 (41.2)		1.06 (0.78–1.43)	49 (42.2)		1.05 (0.64–1.70)
IL8 −845T/C (rs2227532)	TT	52 (100.0)	120 (98.4)	—	1.00	19 (100.0)	—	1.00
	TC	0 (0.0)	2 (1.6)	0.49	#	0 (0.0)	1.00	#
	CC	0 (0.0)	0 (0.0)	1.00	#	0 (0.0)	1.00	#
	Allele							
	T	104 (100.0)	242 (99.2)	0.49	1.00	38 (100.0)	1.00	1.00
	C	0 (0.0)	2 (0.8)		#	0 (0.0)		#

*Differences between individual haplotypes (between controls and CP or controls and AgP) were analyzed using the Fisher exact test.
OR: odds ratio adjusted for age, sex, and smoking in logistic regression, reference categories designated with an OR of 1.0; CI: confidence interval, #nonapplicable (small numbers); #OR not calculated because of the presence of zero values.

linkage disequilibrium with each other to various degrees ($D' = 0.793$–1.000 in controls, $D' = 0.889$–0.951 in patients with CP, and $D' = 0.891$–1.000 in patients with AgP). The complex analysis revealed differences in *IL8* haplotype frequencies. Specifically, the A(−251)/T(+396)/T(+781) and T(−251)/G(+396)/C(+781) haplotypes were significantly less frequent in patients with CP (2.0% versus 5.1%, resp., 4.5%, $P < 0.05$) (Table 3). The decreased frequency of the TGC haplotype alleles in patients with CP was confirmed by the observation that TGC/TTC haplotype (arranged as genotypes) was less frequent in patients with CP (0.4% versus 2.6%, $P < 0.05$, OR = 0.09, 95% CI = 0.01–0.96). Moreover, an uncommon ATT/ATT haplotype (1.15% of the studied population) was found more, but nonsignificantly, in non-periodontitis controls (2.6% versus 0.4%, $P = 0.07$). There was also a nonsignificant trend in the ATC/TTC haplotype association with CP (2.2% versus 0.0%, $P = 0.08$, Table 4).

3.4. Microbiological Analysis. *F. nucleatum* occurred less frequently in nonperiodontitis subjects ($N = 75$) positive for T allele of *IL8* +396G/T variant (49.2% versus 77.8%, $P < 0.02$; OR = 0.28, 95% CI = 0.09–0.89) or TT genotype

Table 3: Distribution of *IL8* haplotypes in the studied groups.

Haplotypes (alleles of *IL8* SNPs)			Controls	CP			AgP		
IL8 −251T/A (rs4073)	*IL8*+396T/G (rs2227307)	*IL8* +781C/T (rs2227306)	$N = 312$ (%)	$N = 556$ (%)	P^a	OR (95% CI)	$N = 116$ (%)	P^a	OR (95% CI)
T	T	C	162 (51.9)	293 (52.7)	NS	0.99 (0.73–1.32)	62 (53.4)	NS	1.02 (0.63–1.65)
A	G	T	110 (35.3)	212 (38.1)	NS	1.17 (0.86–1.59)	46 (39.7)	NS	1.14 (0.70–1.87)
A	T	T	16 (5.1)	11 (2.0)	**0.018**	**0.34 (0.15–0.78)**	3 (2.6)	NS	0.62 (0.18–2.20)
T	G	C	14 (4.5)	11 (2.0)	**0.048**	**0.41 (0.18–0.97)**	2 (1.7)	NS	0.51 (0.11–2.30)
A	G	C	6 (1.9)	12 (2.2)	NS	1.40 (0.47–4.12)	2 (1.7)	NS	1.22 (0.23–6.35)
A	T	C	4 (1.3)	11 (2.0)	NS	1.79 (0.54–5.90)	1 (0.9)	NS	1.01 (0.11–9.29)
T	T	T	0 (0.0)	3 (0.5)	NS	*	0 (0.0)	NS	*
T	G	T	0 (0.0)	3 (0.5)	NS	*	0 (0.0)	NS	*
					P = NS			P = NS	

OR: odds ratio adjusted for age, sex, and smoking in logistic regression CI: confidence intervals.
[a]Differences between individual haplotypes (between controls and CP or controls and AgP) were analyzed using the Fisher exact test.
*OR not calculated because of the presence of zero values.
Bold: significant result.

Table 4: Distribution of *IL8* haplotypes (arranged as genotypes) in the studied groups.

Haplotypes (genotypes of *IL8* SNPs) −251T/A, +396T/G, +781C/T/251T/A, +396T/G, and +781C/T	Controls $N = 156$ (%)	CP $N = 278$ (%)	P^a	OR (95% CI)	AgP $N = 58$ (%)	P^a	OR (95% CI)
TTC/TTC	42 (26.9)	86 (30.9)	NS	1.18 (0.74–1.87)	17 (29.3)	NS	0.98 (0.46–2.09)
AGT/TTC	63 (40.4)	101 (36.3)	NS	0.80 (0.52–1.23)	24 (41.4)	NS	1.13 (0.57–2.24)
ATT/TTC	6 (3.8)	3 (1.1)	0.08	0.22 (0.05–1.06)	2 (3.4)	NS	1.03 (0.19–5.49)
TGC/TTC	**4 (2.6)**	**1 (0.4)**	**0.046**	**0.09 (0.01–0.96)**	0 (0.0)	NS	*
AGC/TTC	5 (3.2)	6 (2.2)	NS	0.90 (0.24–3.36)	1 (1.7)	NS	0.64 (0.07–6.00)
ATC/TTC	0 (0.0)	6 (2.2)	0.08	*	1 (1.7)	*	*
TTT/TTC	0 (0.0)	3 (1.1)	NS	*	0 (0.0)	*	*
TGT/TTC	0 (0.0)	1 (0.4)	*	*	0 (0.0)	*	*
AGT/AGT	20 (12.8)	47 (16.9)	NS	1.60 (0.87–2.93)	10 (17.2)	NS	1.12 (0.42–3.04)
ATT/AGT	1 (0.6)	5 (1.8)	NS	2.12 (0.20–22.08)	1 (1.7)	*	3.36 (0.20–55.97)
AGT/TGC	4 (2.6)	3 (1.1)	NS	0.31 (0.06–1.52)	0 (0.0)	NS	*
AGT/AGC	1 (0.6)	5 (1.8)	NS	3.28 (0.35–30.98)	1 (1.7)	*	5.06 (0.29–87.00)
AGT/ATC	1 (0.6)	4 (1.4)	NS	2.52 (0.27–23.83)	0 (0.0)	*	*
ATT/ATT	4 (2.6)	1 (0.4)	0.07	0.17 (0.02–1.59)	0 (0.0)	NS	*
TGC/TGC	3 (1.9)	3 (1.1)	NS	0.71 (0.13–3.82)	1 (1.7)	NS	1.21 (0.12–12.26)
ATT/ATC	1 (0.6)	0 (0.0)	*	*	0 (0.0)	*	*
ATC/ATC	1 (0.6)	0 (0.0)	*	*	0 (0.0)	*	*
TGT/TGT	0 (0.0)	1 (0.4)	*	*	0 (0.0)	*	*
AGC/TGC	0 (0.0)	1 (0.4)	*	*	0 (0.0)	*	*
			$P^b = 0.067$			P^b = NS	

OR: odds ratio adjusted for age, sex, and smoking in logistic regression; CI: confidence intervals.
[a]Differences between individual haplotypes (between controls and CP or controls and AgP) were analyzed using the Fisher exact test.
[b]Differences between individual haplotypes (between controls and CP or controls and AgP) were analyzed using the χ^2 test.
*OR not calculated because of the presence of zero values.
Bold: significant result.

(21.2% versus 55.6%, $P < 0.05$; OR = 0.22, 95% CI = 0.05–0.91). In contrast, *IL8* −251T allele carriers had an increased OR for individual presence of *A. actinomycetemcomitans* in AgP ($N = 21$) patients (91.7% versus 40.0%, $P < 0.01$; OR = 16.5, 95% CI = 1.88–145.0) and also TT genotype was more often found in *A. actinomycetemcomitans* presence (83.0% versus 13.3%, $P < 0.01$; OR = 32.5, 95% CI = 2.38–443.2). Patients with CP ($N = 151$) carrying CC genotype of *IL8* +781T/C variant had less frequent presence of *T. forsythia* in their subgingival microflora than subjects without this genotype (21.6% versus 35.1%, $P < 0.05$; OR = 0.51, 95% CI = 0.25–1.05). However, the relationship between periodontal bacteria and *IL8* gene polymorphisms must be assessed very carefully regarding small numbers of subjects in the respective subgroups.

4. Discussion

Cytokines involved in the inflammatory process, such as *IL8* and their genes, are important potential modifiers of individual susceptibility to AgP or CP. Although none of the investigated SNPs in the *IL8* gene was individually associated with aggressive or chronic periodontitis, the patients with CP showed lower A(−251)/T(+396)/T(+781) and T(−251)/G(+396)/C(+781) haplotype frequencies than the controls. The association of TGC haplotype with CP was confirmed by the relationship between TGC/TTC haplotype (arranged as genotypes) and CP. These results confirm the hypothesis that haplotypes are more powerful for detecting susceptibility alleles than individual polymorphisms. Our results differ from those obtained by Scarel-Caminaga et al. [29] who associated ATC/TTC and AGT/TGC haplotypes with chronic periodontitis in the Brazilian population. These contradictory findings may be due to variability of the examined populations. For example, the frequency of the ATC haplotype in the Czech population was less than 3.4%, compared to 23.7% in the Brazilians [29]. In the Brazilian population, some haplotypes of *IL8* −845(T/C)/−738(T/A)/−353(A/T) variants showed significant association to, or protection against, CP [28]. Of the three *IL8* SNPs, only one polymorphism was the same as in our study (i.e., SNP −251 (rs4073) referred to as −353 in Brazilian study). Polymorphism −845T/C (rs2227532) was also investigated in this study, but regarding a very low frequency of C allele, it was analyzed only in several individuals and therefore it was not included for any further haplotype assessment.

To date, eight studies evaluating the association of *IL8* SNPs (−251, +396, and +781) and CP or AgP in different populations (mostly in Brazilian but none in the Caucasian population) have been performed, with contradictory results [27–32, 34, 35]. Most of these studies analyzed only the individual SNP and were focused on examining of CP; only Andia et al. [32] studied the relationship between *IL8* −251 variant and AgP; however, no association was found. Similarly, Kim et al. [27] failed to find any association between CP and allele or genotype distribution of *IL8* −251 SNP. In contrast, another study discovered a significant association between *IL8* −251 SNP and CP in nonsmokers. The *IL8* −251TA heterozygote genotype was associated with increased levels of *IL8* mRNA transcripts and A allele had an increased risk for developing periodontitis [30]. This is consistent with the observation that the A allele of SNP *IL8* −251 tended to be associated with higher IL-8 production in lipopolysaccharide- (LPS-) stimulated human whole blood [25]. Very recently, Li et al. [34] found that A allele of *IL8* −251 variant was associated with decreased susceptibility to CP in Chinese population. Houshmand et al. [35] found a significant difference in the genotype frequencies of *IL8* −251A/T and +396G/T SNPs between subjects with periodontitis and a control group in Hamedan, Iran, but did not specify whether it was for patients with CP or AgP. Conversely, Corbi et al. [31] showed that the genetic susceptibility to CP in the *IL8* gene was not associated with worse periodontal clinical parameters and increased IL-8 concentration. With the exception of Scarel-Caminaga et al. [29] who associated the +396TT genotype with CP, no association between SNP at position +396 or +781 and CP in the Brazilian population was discovered.

Several studies have examined polymorphisms in interleukins in connection with a subgingival bacterial colonization in patients with periodontitis. In this study, SNPs in the gene encoding IL-8 were associated with the presence of pathogenic bacteria in subgingival dental plaque. The results showed that *IL8* −251T allele carriers had an increased OR for the individual presence of *A. actinomycetemcomitans* in AgP patients ($P < 0.01$) and an increased OR was also found for the presence of *T. forsythia* for T allele of *IL8* +781 in CP patients ($P < 0.05$). These data are in agreement with the notion that individual genetic susceptibility may influence the host response to infection [39]. Nibali et al. [40] found association between *IL6* SNPs and *A. actinomycetemcomitans*, which they confirmed by the haplotype analysis. Specifically, *IL6* −174GG genotype was associated with high (above median) counts of *A. actinomycetemcomitans* (both in all subjects and periodontally healthy subjects only) in Indians [41]. But Nibali et al. [42] also suggested that only a detection of known periodontopathogenic bacteria could not discriminate different forms of periodontitis. In contrast, Schulz et al. [43] found no evidence that SNPs in *IL1* gene cluster could be associated with subgingival colonization with *A. actinomycetemcomitans* and could thus be an independent risk indicator of AgP. In addition, Finoti et al. [44] observed that periodontal destruction may occur in patients who are considered to be genetically susceptible to CP with a lower microbial challenge because of the presence of the *IL8* ATC/TTC haplotype than in patients without this haplotype.

There are some limitations to this study that need to be considered. First, the major complicating factor in the study of isolated locus (such as *IL8*) is the nature of periodontitis as a multifactorial disease in which interaction between multiple genes plays a role and each genetic polymorphism has generally only a small effect. In addition, the interaction of gene variants with environmental factors (such as bacterial pathogens), socioeconomic factors, BMI, and others not analyzed in this study, potentially affect the observed phenotype. Second, the case-control approach used is generally quite vulnerable to the population stratification, for example, due to different ethnic origin. The present sample, however,

is exclusively of the Czech Caucasian origin, restricted to the limited geographical area populated by quite homogeneous population with low admixture. Finally, we did not measure RNA expression or protein levels of IL-8, therefore, we do not know the functional consequences of these polymorphisms in our subjects.

In conclusion, although none of the investigated SNPs in the *IL8* gene were individually associated with periodontitis, some haplotypes can be protective against CP in the Czech population. Clinical significance of these findings is low due to a very low frequency of the "protective" haplotypes. The individual *IL8* variants were associated with subgingival colonization with *A. actinomycetemcomitans* in AgP and with *T. forsythia* in CP in the Czech population. However, these relationships must be assessed very carefully regarding small numbers of subjects in the respective subgroups. Further studies are needed to clarify the association of these polymorphisms with periodontal diseases in other populations.

Conflict of Interests

The authors declare that they have no conflict of interests associated with this work.

Acknowledgments

This study was supported by the Internal Grant Agency (IGA NT11405-6) of the Czech Republic Ministry of Health and by project MUNI/A/0888/2012.

References

[1] S. S. Socransky, A. D. Haffajee, M. A. Cugini, C. Smith, and R. L. Kent Jr., "Microbial complexes in subgingival plaque," *Journal of Clinical Periodontology*, vol. 25, no. 2, pp. 134–144, 1998.

[2] G. C. Armitage, "Clinical evaluation of periodontal diseases," *Periodontology 2000*, vol. 7, pp. 39–53, 1995.

[3] R. Genco, K. S. Kornman, R. Williams et al., "Consensus report periodontal diseases: pathogenesis and microbial factors," *Annals of Periodontology*, vol. 1, pp. 926–932, 1996.

[4] G. C. Armitage, "Comparison of the microbiological features of chronic and aggressive periodontitis," *Periodontology 2000*, vol. 53, no. 1, pp. 70–88, 2010.

[5] B. Riep, L. Edesi-Neuß, F. Claessen et al., "Are putative periodontal pathogens reliable diagnostic markers?" *Journal of Clinical Microbiology*, vol. 47, no. 6, pp. 1705–1711, 2009.

[6] A. Mombelli, F. Casagni, and P. N. Madianos, "Can presence or absence of periodontal pathogens distinguish between subjects with chronic and aggressive periodontitis? A systematic review," *Journal of Clinical Periodontology*, vol. 29, no. 3, pp. 10–21, 2002.

[7] B. S. Michalowicz, D. Aeppli, J. G. Virag et al., "Periodontal findings in adult twins," *Journal of Periodontology*, vol. 62, no. 5, pp. 293–299, 1991.

[8] B. S. Michalowicz, "Genetic and heritable risk factors in periodontal disease," *Journal of Periodontology*, vol. 65, no. 5, pp. 479–488, 1994.

[9] R. C. Page and K. S. Kornman, "The pathogenesis of human periodontitis: an introduction," *Periodontology 2000*, vol. 14, pp. 9–11, 1997.

[10] K. Matsushima and J. J. Oppenheim, "Interleukin 8 and MCAF: novel inflammatory cytokines inducible by IL 1 and TNF," *Cytokine*, vol. 1, no. 1, pp. 2–13, 1989.

[11] C. Gronhoj Larsen, A. O. Anderson, E. Appella, J. J. Oppenheim, and K. Matsushima, "The neutrophil-activating protein (NAP-1) is also chemotactic for T lymphocytes," *Science*, vol. 243, no. 4897, pp. 1464–1466, 1989.

[12] G. Godaly, L. Hang, B. Frendeus, and C. Svanborg, "Transepithelial neutrophil migration is CXCR1 dependent in vitro and is defective in IL-8 receptor knockout mice," *Journal of Immunology*, vol. 165, no. 9, pp. 5287–5294, 2000.

[13] G. T.-J. Huang, S. K. Haake, and N.-H. Park, "Gingival epithelial cells increase interleukin-8 secretion in response to *Actinobacillus actinomycetemcomitans* challenge," *Journal of Periodontology*, vol. 69, no. 10, pp. 1105–1110, 1998.

[14] A. Sfakianakis, C. E. Barr, and D. Kreutzer, "Mechanisms of Actinobacillus actinomycetemcomitans-induced expression of interleukin-8 in gingival epithelial cells," *Journal of Periodontology*, vol. 72, no. 10, pp. 1413–1419, 2001.

[15] Y. Kusumoto, H. Hirano, K. Saitoh et al., "Human gingival epithelial cells produce chemotactic factors interleukin-8 and monocyte chemoattractant protein-1 after stimulation with *Porphyromonas gingivalis* via Toll-like receptor 2," *Journal of Periodontology*, vol. 75, no. 3, pp. 370–379, 2004.

[16] K. H. Shinsuke Onishi, S. Liang, P. Stathopoulou, D. Kinane, G. Hajishengallis, and A. Sharma, "Toll-like receptor 2-mediated interleukin-8 expression in gingival epithelial cells by the *Tannerella forsythia* leucine-rich repeat protein BspA," *Infection and Immunity*, vol. 76, no. 1, pp. 198–205, 2008.

[17] M. Tamura, M. Tokuda, S. Nagaoka, and H. Takada, "Lipopolysaccharides of Bacteroides intermedius (*Prevotella intermedia*) and *Bacteroides* (*Porphyromonas*) gingivalis induce interleukin-8 gene expression in human gingival fibroblast cultures," *Infection and Immunity*, vol. 60, no. 11, pp. 4932–4937, 1992.

[18] C. C. Tsai, Y. P. Ho, and C. C. Chen, "Levels of interleukin-1 beta and interleukin-8 in gingival crevicular fluids in adult periodontitis," *Journal of periodontology*, vol. 66, no. 10, pp. 852–859, 1995.

[19] A. I. Dongari-Bagtzoglou and J. L. Ebersole, "Increased presence of interleukin-6 (IL-6) and IL-8 secreting fibroblast subpopulations in adult periodontitis," *Journal of Periodontology*, vol. 69, no. 8, pp. 899–910, 1998.

[20] C. Giannopoulou, J. J. Kamma, and A. Mombelli, "Effect of inflammation, smoking and stress on gingival crevicular fluid cytokine level," *Journal of Clinical Periodontology*, vol. 30, no. 2, pp. 145–153, 2003.

[21] P. Goutoudi, E. Diza, and M. Arvanitidou, "Effect of periodontal therapy on crevicular fluid interleukin-6 and interleukin-8 levels in chronic periodontitis," *International Journal of Dentistry*, vol. 2012, Article ID 362905, 8 pages, 2012.

[22] N. Mukaida, M. Shiroo, and K. Matsushima, "Genomic structure of the human monocyte-derived neutrophil chemotactic factor IL-8," *Journal of Immunology*, vol. 143, no. 4, pp. 1366–1371, 1989.

[23] M. F. Fey and A. Tobler, "An interleukin-8 (IL-8) cDNA clone identifies a frequent HindIII polymorphism," *Human Genetics*, vol. 91, no. 3, p. 298, 1993.

[24] E. Renzoni, P. Lympany, P. Sestini et al., "Distribution of novel polymorphisms of the interleukin-8 and CXC receptor 1 and 2 genes in systemic sclerosis and cryptogenic fibrosing alveolitis," *Arthritis and Rheumatism*, vol. 43, no. 7, pp. 1633–1640, 2000.

[25] J. Hull, A. Thomson, and D. Kwiatkowski, "Association of respiratory syncytial virus bronchiolitis with the interleukin 8 gene region in UK families," *Thorax*, vol. 55, no. 12, pp. 1023–1027, 2000.

[26] B. H. Rovin, L. Lu, and X. Zhang, "A novel interleukin-8 polymorphism is associated with severe systemic lupus erythematosus nephritis," *Kidney International*, vol. 62, no. 1, pp. 261–265, 2002.

[27] Y. J. Kim, A. C. Viana, K. M. C. Curtis, S. R. P. Orrico, J. A. Cirelli, and R. M. Scarel-Caminaga, "Lack of association of a functional polymorphism in the interleukin 8 gene with susceptibility to periodontitis," *DNA and Cell Biology*, vol. 28, no. 4, pp. 185–190, 2009.

[28] Y. J. Kim, A. C. Viana, K. M. C. Curtis et al., "Association of haplotypes in the *IL8* gene with susceptibility to chronic periodontitis in a Brazilian population," *Clinica Chimica Acta*, vol. 411, no. 17-18, pp. 1264–1268, 2010.

[29] R. M. Scarel-Caminaga, Y. J. Kim, A. C. Viana et al., "Haplotypes in the Interleukin 8 gene and their association with chronic periodontitis susceptibility," *Biochemical Genetics*, vol. 49, no. 5-6, pp. 292–302, 2011.

[30] D. C. Andia, N. F. P. De Oliveira, A. M. Letra, F. H. Nociti Jr., S. R. P. Line, and A. P. De Souza, "Interleukin-8 gene promoter polymorphism (rs4073) may contribute to chronic periodontitis," *Journal of Periodontology*, vol. 82, no. 6, pp. 893–899, 2011.

[31] S. C. T. Corbi, G. Anovazzi, L. S. Finoti et al., "Haplotypes of susceptibility to chronic periodontitis in the Interleukin 8 gene do not influence protein level in the gingival crevicular fluid," *Archives of Oral Biology*, vol. 57, no. 10, pp. 1355–1361, 2012.

[32] D. C. Andia, A. Letra, R. C. Casarin, M. Z. Casati, S. R. Line, and A. P. de Souza, "Genetic analysis of the *IL8* gene polymorphism (rs4073) in generalized aggressive periodontitis," *Archives of Oral Biology*, vol. 58, no. 2, pp. 211–217, 2013.

[33] M. P. Amaya, L. Criado, B. Blanco et al., "Polymorphisms of proinflammatory cytokine genes and the risk for acute suppurative or chronic nonsuppurative apical periodontitis in a Colombian population," *International Endodontic Journal*, vol. 46, no. 1, pp. 71–78, 2013.

[34] G. Li, Y. Yue, Y. Tian et al., "Association of matrix metalloproteinase (MMP)-1, 3, 9, interleukin (IL)-2, 8 and cyclooxygenase (COX)-2 gene polymorphisms with chronic periodontitis in a Chinese population," *Cytokine*, vol. 60, no. 2, pp. 552–560, 2012.

[35] B. Houshmand, M. Hajilooi, A. Rafiei, M. Bidgoli, and S. Soheilifar, "Evaluation of IL-8 gene polymorphisms in patients with periodontitis in Hamedan, Iran," *Dental Research Journal*, vol. 9, no. 4, pp. 427–432, 2012.

[36] G. C. Armitage, "Development of a classification system for periodontal diseases and conditions," *Annals of Periodontology*, vol. 4, no. 1, pp. 1–6, 1999.

[37] World Health Organisation, *Oral Health Surveys: Basic Methods*, WHO, Geneva, Switzerland, 4th ed edition, 1997.

[38] J. J. Sambrook, E. F. Fritsch, and T. Maniatis, *Molecular Cloning: a Laboratory Manual*, Cold Spring Harbor Laboratory Press, Cold Spring Harbor, NY, USA, 1989.

[39] G. S. Cooke and A. V. S. Hill, "Genetics of susceptibility to human infectious disease," *Nature Reviews Genetics*, vol. 2, no. 12, pp. 967–977, 2001.

[40] L. Nibali, M. S. Tonetti, D. Ready et al., "Interleukin-6 polymorphisms are associated with pathogenic bacteria in subjects with periodontitis," *Journal of Periodontology*, vol. 79, no. 4, pp. 677–683, 2008.

[41] L. Nibali, I. Madden, F. Franch Chillida, L. J. A. Heitz-Mayfield, P. M. Brett, and N. Donos, "IL6 -174 Genotype Associated with *Aggregatibacter actinomycetemcomitans* in Indians," *Oral Diseases*, vol. 17, no. 2, pp. 232–237, 2011.

[42] L. Nibali, F. D'Aiuto, D. Ready, M. Parkar, R. Yahaya, and D. Donos, "No association between *A. actinomycetemcomitans* or *P. gingivalis* and chronic or aggressive periodontitis diagnosis," *Quintessence International*, vol. 43, no. 3, pp. 247–254, 2012.

[43] S. Schulz, J. M. Stein, W. Altermann et al., "Single nucleotide polymorphisms in interleukin-1gene cluster and subgingival colonization with *Aggregatibacter actinomycetemcomitans* in patients with aggressive periodontitis," *Human Immunology*, vol. 72, no. 10, pp. 940–946, 2011.

[44] L. S. Finoti, S. C. Corbi, G. Anovazzi et al., "Association between *IL8* haplotypes and pathogen levels in chronic periodontitis," *European Journal of Clinical Microbiology and Infectious Diseases*, vol. 32, no. 10, pp. 1333–1340, 2013.

Hindawi Publishing Corporation
Mediators of Inflammation
Volume 2013, Article ID 378971, 9 pages
http://dx.doi.org/10.1155/2013/378971

Research Article

Intricacies for Posttranslational Tumor-Targeted Cytokine Gene Therapy

Jeffry Cutrera,[1,2] Denada Dibra,[2] Arun Satelli,[2] Xuexing Xia,[2] and Shulin Li[2]

[1] *Department of Musculoskeletal Oncology, Shanghai Tenth People's Hospital, Tongji University School of Medicine, Shanghai 200072, China*
[2] *Department of Pediatrics, UT Graduate School of Biomedical Sciences, The University of Texas MD Anderson Cancer Center, Unit 853, 1515 Holcombe Boulevard, Houston, TX 77030, USA*

Correspondence should be addressed to Shulin Li; sli4@mdanderson.org

Received 30 August 2013; Accepted 30 October 2013

Academic Editor: Mohammad Athar

The safest and most effective cytokine therapies require the favorable accumulation of the cytokine in the tumor environment. While direct treatment into the neoplasm is ideal, systemic tumor-targeted therapies will be more feasible. Electroporation-mediated transfection of cytokine plasmid DNA including a tumor-targeting peptide-encoding sequence is one method for obtaining a tumor-targeted cytokine produced by the tumor-bearing patient's tissues. Here, the impact on efficacy of the location of targeting peptide, choice of targeting peptide, tumor histotype, and cytokine utilization are studied in multiple syngeneic murine tumor models. Within the same tumor model, the location of the targeting peptide could either improve or reduce the antitumor effect of interleukin (IL)12 gene treatments, yet in other tumor models the tumor-targeted IL12 plasmid DNAs were equally effective regardless of the peptide location. Similarly, the same targeting peptide that enhances IL12 therapies in one model fails to improve the effect of either IL15 or PF4 for inhibiting tumor growth in the same model. These interesting and sometimes contrasting results highlight both the efficacy and personalization of tumor-targeted cytokine gene therapies while exposing important aspects of these same therapies which must be considered before progressing into approved treatment options.

1. Introduction

Immunotherapy is one of the most promising treatment strategies for cancer and other diseases; however, several obstacles need to be overcome before immunotherapies are widely accepted in the clinics. Several cytokines and chemokines, such as interleukin (IL) 2 [1, 2], interferon (IFN) α [3], IL12 [4–8], IL15 [9–12], and chemokine platelet factor 4 (PF4) [13–15], are very effective for inhibiting tumor growth via immunomodulatory mechanisms in mouse models, and dozens of either active or completed clinical trials utilize cytokines alone or as an adjuvant for treating cancer [16]. However, only IL-2 and IFNα have been approved by the FDA for the treatment of a small subset of cancers, and these therapies are only administered systemically in recombinant protein form [17]. One strategy that may soon help improve these therapies is gene therapy, the administration of DNA which encodes for a therapeutic protein. Although not ideal for producing all types of therapeutic proteins, the increase in safety and efficacy while reducing costs makes immune gene therapies feasible [18–20].

For most immune gene therapies the gene product must be located in the tumor microenvironment to be most effective; therefore, gene products not directly produced in the tumor need to be targeted to the tumor environment. For instance, targeting IL12 to the tumor microenvironment is critical for inducing tumor-specific T cell immune responses [5, 7, 21], and using antibodies specific for the tumor antigen L19 can increase the antitumor efficacy of IL15 [22]. Indeed, hundreds of targeting motifs have been created ranging from small peptides to large multifunctional antibodies with the intentions of improving the efficacy of multiple cancer therapies; however, the success of these targeted therapies may not only rely on the expression of the targeted ligand [3, 5, 23–26].

A previous report from our lab demonstrated the strong antitumor effects of a distantly administered tumor-targeted

IL12 (ttIL12) gene therapy in multiple syngeneic cancer models [5]. This strategy utilized the tumor-targeting peptide VNTANST which targets tumor-specific ectopic expression of vimentin [27]. While further investigating the antitumor potential of the ttIL12 and the diverse potential of the VNTANST peptide, several important intricacies for successfully choosing both an appropriate targeting motif and immune payload became evident. This report will expand on the critical factors which determine the efficacy of tumor-targeted immune therapies using posttranslational delivery mechanisms.

2. Materials and Methods

2.1. In Vitro Experiments. The 4T1, SCCVII, EMT6, B16F10, RM1, and CT26 cell lines were purchased from American Type Culture Collection (ATCC, Manassas, VA, USA), and the LLC and K7M3 cells were donated by Augusto C. Ochoa (LSU School of Medicine, New Orleans, LA, USA) and Genie Kleinerman (MD Anderson Cancer Center, Houston, TX, USA), respectively. All cells were maintained in DMEM with 10% FBS and 1% Penn/Strep (Life Technologies, Carlsbad, CA, USA) at 37°C and 5% CO2.

The IL-12, IL-15, and PF4 plasmid DNA (pDNA) were constructed as previously described [5] using the EndoFree Plasmid Preparation Kit (Qiagen, Alameda, CA, USA). *In vitro* transfections of pDNA, IFNγ induction assay, and IL12/IFNγ ELISAs were performed as previously described [5].

2.2. In Vivo Tumor Models and Treatments. All animals and procedures performed on animals followed National Institute of Health (NIH) guidelines and were approved by the Institutional Animal Care and Use Committee at the University of Texas MD Anderson Cancer Center. Six- to eight-week-old female Balb/C, C3H, and C57/Bl6 mice were purchased from the NIH (Bethesda, MD, USA). Orthotopic tumor models were created via mammary fat pad (EMT6 and 4T1), subcutaneous (B16F10 and SCCVII), or intraosseous (K7M3) inoculations. Subcutaneous injections were used to establish ectopic tumors for CT26, RM1, and LLC models. These inoculations were performed as previously described [28]. For the K7M3 orthotopic model, the primary tumor site, right tibia, was amputated prior to the first treatment to prevent tumor-burden-mandated euthanasia. The lower limb was removed at the knee joint and the wound was closed with one or two wound clips as previously described [28].

All IL12 and IL15 pDNA were delivered via intramuscular injection of 5 μg in 30 μL half-strength saline in the right and left rear tibialis muscles followed by percutaneous electroporation (two 20 msec, 450 V/cm pulses with a 100 msec interval) via caliper electrodes. The PF4 treatments were performed via hydrodynamic injection into the tail vein with 10 μg pDNA in 1.2 mL saline delivered in 5 to 7 s. All treatments were repeated once in all experiments, and black arrows in the figures represent treatments.

2.3. In Vivo Therapeutic Analyses. The volumes, V, of primary tumors for all models except K7M3 were measured via calipers measuring the longest diameter, a, and the diameter, b, perpendicular to a, and applying the following formula: $V = (\pi/8) * (a * b^2)$. To analyze lung metastasis in the 4T1, EMT6, and K7M3 models, lungs were inflated with 15% India ink and then placed into Fekete's solution for 24 h. The next day, white nodules were counted [5]. The vessel density in 4T1 tumors as portrayed in Supplementary Figure 3 available online at http://dx.doi.org/10.1155/2013/378971 was measured via immunohistochemistry with an α-CD31 antibody (Cat. no. 01951A, BD Biosciences, San Jose, CA, USA) using a standard frozen section staining protocol and then counting the number of CD31-positive vessels per section.

2.4. Statistics. A one-way ANOVA with Tukey's post hoc test was used for ELISA and lung metastases (except for Figure 3(d)), and a two-way ANOVA with Tukey's post hoc test was used to analyze tumor volume growth rates. Mantel-Cox tests were used to analyze survival. Student's t-tests were used to determine significance for lung metastases in Figure 3(d), vessel density in Supplementary Figure 3, and side-by-side analyses of tumor growth or metastatic development. All analyses were performed and graphs were created with GraphPad Prism for Windows (GraphPad Software, San Diego, CA, USA).

3. Results

3.1. Location of the Peptide-Coding Sequence in the IL12-Encoding Gene Plasmid Affects the Therapeutic Efficacy of ttIL12 Treatments. For our original experiments with ttIL12, the tumor-targeting peptide sequences were inserted directly prior to the stop codon in the p40 subunit coding region of an IL12 pDNA (Figure 1(a)). Placing the sequence in this location did not affect the expression or activity of the IL12 product [5], so the heterodimeric quaternary structure of the IL12 protein offers another potential location, the p35 subunit. Thus, two more ttIL12 plasmids were created, one with the VNTANST-coding sequence inserted prior to the stop codon in the p35 subunit (ttIL12-p35; Figure 1(b)) and the other with VNTANST-coding sequence in both subunits (ttIL12-p35/p40; Figure 1(c)). The new plasmids were capable of expressing equivalent amounts of IL12 (Figure 1(d)), and the IL12 was equally as effective for inducing IFNg from splenocytes, a hallmark of IL12 function (Figure 1(e)).

Since the 4T1 tumor model previously responded well to ttIL12-p40 and is spontaneously metastatic, this breast adenocarcinoma model was chosen to test the efficacy of the new ttIL12 pDNAs via intratumoral injections with electroporation (EP) for treating distantly located tumors (see Section 2). Surprisingly, only treatments with ttIL12-p40 pDNA significantly inhibited primary tumor growth, reduced metastatic tumor development, and extended survival time compared to wtIL12 and other ttIL12 pDNAs, while the ttIL12-p35, ttIL12-p35/p40, and wtIL12 treatments were all effective compared to the control-treated groups (Figures 2(a)–2(c)). Differently, both the ttIL12-p40 and the ttIL12-p35/p40 significantly inhibited primary tumor growth in the colon carcinoma model CT26 (Supplementary Figure 1(a)).

Similar results were seen in the mouse melanoma model B16F10. Since no benefits were seen from the ttIL12-p35/p40

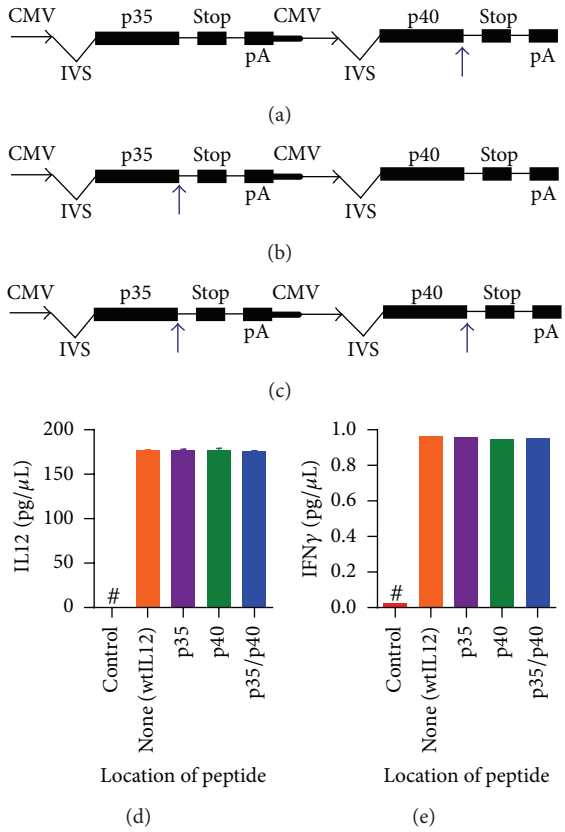

Figure 1: Expression and activity of IL12 is not affected by insertion of tumor-targeting sequence in either subunit. Multiple VNTANST-IL12 plasmids were created with the VNTANST sequence inserted directly prior to the stop codon in the p40 subunit (a), p35 subunit (b), or both subunits (c). The blue arrows represent the VNTANST-coding sequence insertion site in the plasmid DNA. CMV: cytomegalovirus promoter; IVS: intron; pA: bovine growth hormone polyadenylation signal; STOP: stop codon. (d) Transfection of these plasmids and wild-type IL12 and a control plasmid into cells resulted in equivalent amounts of expressed IL12 in the medium of transfected cells. (e) The peptide IL12 products induced equivalent levels of IFNγ from harvested murine splenocytes. # represents $P < 0.05$ compared to all other groups.

dual targeting, this group was not included in this experiment. Again, the ttIL12-p35 did not show any benefit compared to wtIL12 while the ttIL12-p40 clearly slowed the tumor progression (Figures 2(d) and 2(e)). Surprisingly, the SCCVII model produced different results. The ttIL12-p40 treatments reduced tumor volume (Supplementary Figure 1(b)) and significantly extended survival; however, there was no significant extension of survival compared to ttIL12-p35 or ttIL12-p35/p40 (Figure 2(f)).

3.2. The Efficacy of IL15 Gene Treatments Can Also Be Improved with the Addition of the Tumor-Targeting Peptide Sequence. Many other cytokines that have been employed for anticancer treatments should also benefit from targeting the cytokine to the tumor environment; therefore, a tumor-targeted IL15 (ttIL15) pDNA was constructed by inserting the VNTANST-coding sequence directly prior to the stop codon in the IL15 coding region (Figure 3(a)). First, this ttIL15 was tested in an orthotopic osteosarcoma model, K7M3. Due to the fast growing nature of the primary bone tumor in this model, the primary tumor site, the right tibia, was amputated and, therefore, only spontaneously metastatic tumors were present at the onset of treatments. Different from treatments in all other tumor models, the left and front rear tibialis muscles were the treatment sites since the right tibia was amputated. Surprisingly, the wtIL15 and ttIL15 gene treatments equally inhibited metastatic tumor growth (Figure 3(b)). Contrastingly, the tumor-targeting strategy did lead to slight inhibition of primary tumor growth in the 4T1 model. The primary 4T1 tumors in ttIL15 treated mice were significantly smaller than both wtIL15 and control-treated groups on day 15 after the first treatment (Figure 3(c)); however, the tumor growth rates were much faster than those seen with ttIL12 or wtIL12 gene treatments (Figure 2(a)). The inhibition of metastatic tumor development also increased with the ttIL15 gene treatments in the 4T1 model (Figure 3(d)), but, again, the inhibition was not as strong as seen with ttIL12 treatments (Figure 2(b)). In a separate breast cancer model, EMT6, neither wtIL15 nor ttIL15 inhibited primary tumor growth or metastatic tumor development (Supplementary Figure 2).

3.3. Tumor Targeting Does Not Improve Antitumor Efficacy of PF4 Treatments. Another cytokine which has shown promise for anticancer therapy is PF4. PF4 has antiangiogenic effects that can inhibit tumor growth [13]; therefore, a tumor-targeted PF4 (ttPF4) pDNA was constructed to test whether the VNTANST sequence can improve the efficacy of this antiangiogenic therapy. An *in vitro* expression assay via PF4 ELISA showed that equivalent levels of PF4 were produced from both wild-type PF4 and tt-PF4 pDNAs (data not shown). The wtPF4 treatments did show minor inhibition of primary 4T1 tumor growth, but the ttPF4 did not inhibit primary tumor growth compared to the control treatments (Figure 4(a)). Typically, PF4 and other antiangiogenic treatments can decrease the vessel density in tumors, but the vessel densities in the primary tumors were nearly identical after wtIL12 or ttIL12 treatments (Supplementary Figure 3). Interestingly, both ttPF4 and wtPF4 inhibited metastatic tumor development, but the ttPF4 treatments did not provide any further benefit for reducing the development of metastatic tumor growth (Figure 4(b)).

3.4. Not All Tumor-Targeting Peptides Work with this Delivery Method. The preceding data along with data published previously [5] has shown that the targeting peptide VNTANST can be used to increase the efficacy of IL12 and IL15 gene therapy in several tumors models. However, the efficacy of VNTANST has not been compared to other well-known tumor-targeting peptides, such as RGD4C [29] and CNGRC [30, 31]. To this end, several new tumor-targeted IL12 plasmids were constructed by inserting the coding sequences for well-documented tumor-targeting peptides prior to the stop codon on the p40-coding region (Figure 1(a)), and their antitumor efficacy was tested in the 4T1 tumor model. In

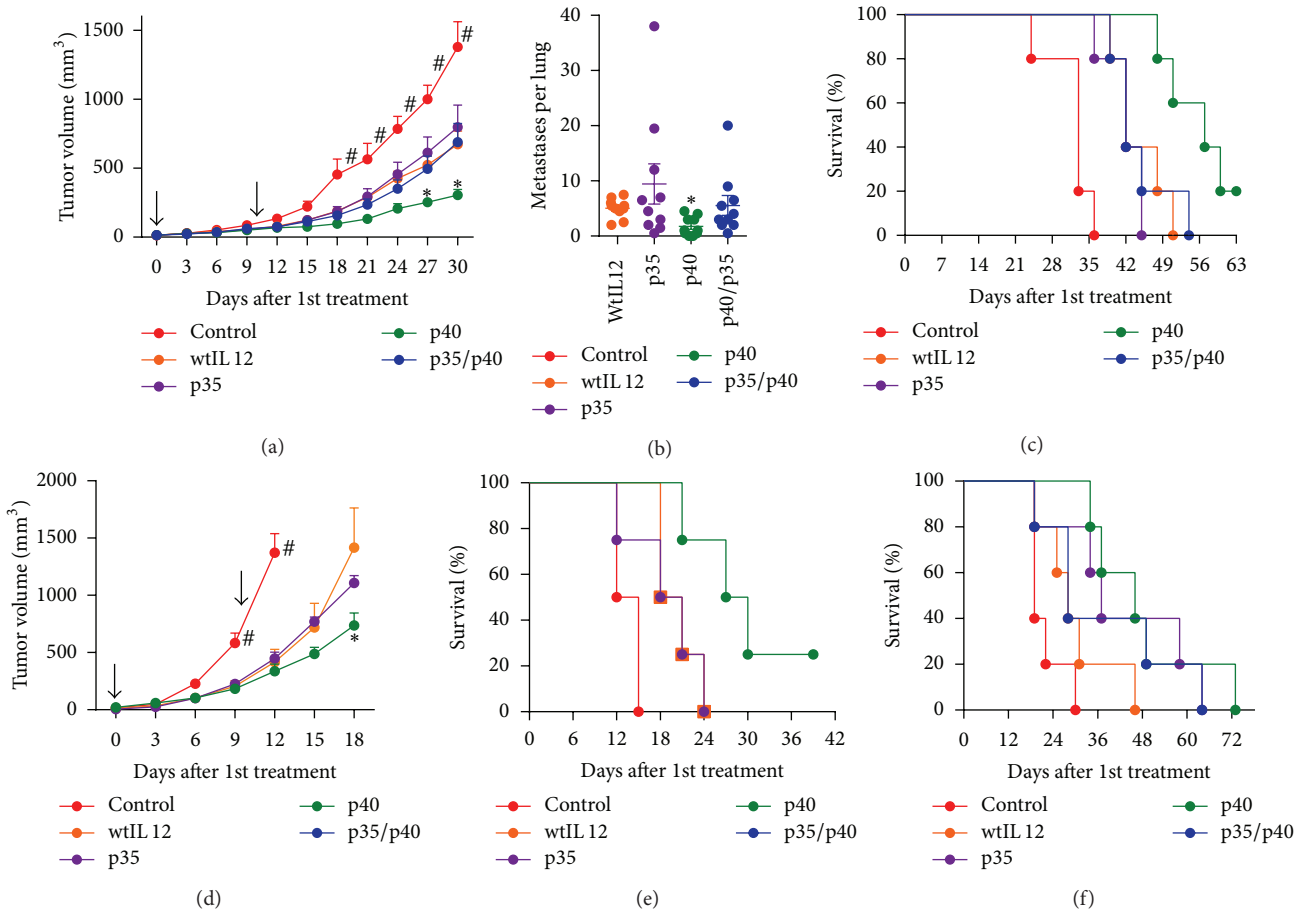

Figure 2: Location of the tumor-targeting sequence affects the induced antitumor response in a tumor histotype-specific manner. The ttIL12-p40 pDNA treatments increased the antitumor activity compared to the wtIL12 pDNA treatments in the 4T1 ((a) primary tumor growth; (b) lung metastases; (c) survival) and B16F10 ((d) primary tumor growth, (e) survival) tumor models. (f) In the SCCVII model, all ttIL12-peptide pDNA treatments significantly extend survival. Black arrows represent treatment dates. # represents $P < 0.05$ compared to all other groups. ∗ represents $P < 0.05$ compared to all other IL12 treatment groups.

this aggressive tumor model, only the targeted plasmids with VNTANST and CDGRC peptides and wtIL12 gene treatments were capable of inhibiting primary tumor growth compared to all other peptide-targeting plasmids, and only VNTANST-IL12-treated tumors were significantly smaller than wtIL12 tumors on day 18 when compared side-by-side (Figure 5(a)). Similar results were seen in an orthotopic squamous cell carcinoma model (Supplementary Figure 4). Yet, again the inhibition of metastatic tumors differs from the primary inhibition. Here, all IL12 treatments except for RGD4C-IL12 were capable of significantly inhibiting the spontaneous development of 4T1 lung metastases, and only VNTANST-IL12 treatments resulted in fewer lung tumors than wtIL12 (Figure 5(b)). Surprisingly, the RGD4C peptide, which is renowned for its tumor-targeting capabilities, did not inhibit primary or metastatic tumor growth in this strategy, but the shorter peptide CDGRC, which utilizes the same RGD targeting sequence, was able to significantly inhibit primary and metastatic tumor growth.

3.5. Optimal Dose of Tumor-Targeted pDNA Is Required to Achieve Successful Tumor Inhibition. In an attempt to increase the efficacy of ttIL12 treatments, 4T1 tumor-bearing mice were given a higher dose, and the amount of ttIl12 pDNA administered to the mice was increased 3-fold to 15 μg pDNA per rear tibialis per treatment (total of 30 μg per treatment). Unexpectedly, the higher dose of ttIL12 ablated the antitumor efficacy of the ttIL12 treatments and failed to increase the efficacy of wtIL12 treatments (Figure 6).

4. Discussion

As cancer continues to be one of the main causes of death with little to no reduction in incidence rates, immunotherapy is on the cusp of becoming an accepted and widespread treatment option that could significantly improve the quality of life and extend survival of cancer patients [20, 21, 32–34]. However, the pleiotropic nature of cytokines and the potential for side effects necessitate that these treatments be tailored not only to the specific tumor type but also to the heterotrophic idiosyncrasies seen within each patient. The data presented in this report further displays the efficacy of the VNTANST peptide in posttranslationally tumor-targeted gene therapy while also exposing the importance of choosing the exact

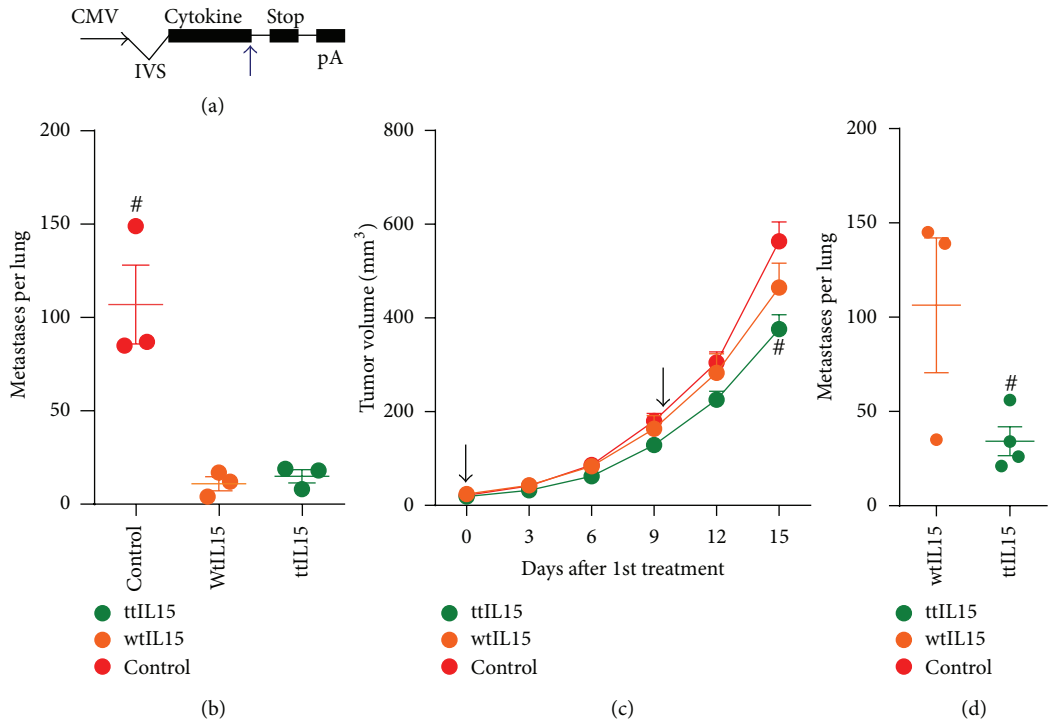

FIGURE 3: Tumor-targeting-mediated improvement of IL15-induced antitumor efficacy depends on the tumor histotype. (a) Diagrammatic representation of the IL15 plasmid with the IL15-coding region in the "Cytokine" region. The blue arrows represent the VNTANST-coding sequence insertion site in the plasmid DNA. CMV: cytomegalovirus promoter; IVS: intron; pA: bovine growth hormone polyadenylation signal; STOP: stop codon. (b) Equivalent inhibition of K7M3 lung metastases from wtIL15 and ttIL15 pDNA treatments (treatments on days 0 and 7). Inhibition of primary tumor growth (c) and metastatic lung tumor development (d) by ttIL15 pDNA compared to wtIL15 pDNA. Black arrows represent treatments. # represents $P < 0.05$ compared to all other groups.

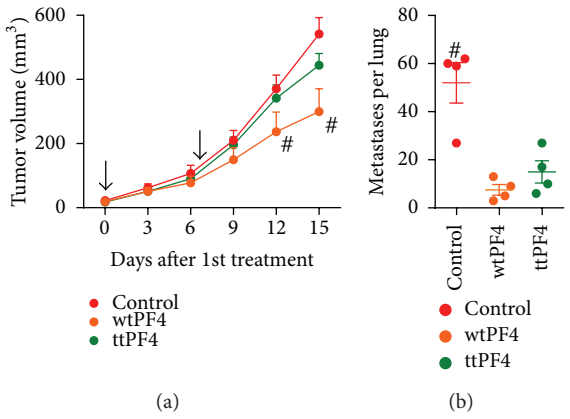

FIGURE 4: Tumor-targeting PF4 gene therapy with the VNTANST sequence does not improve anticancer efficacy. Black arrows represent treatments. # represents $P < 0.05$ compared to all other groups. (a) Only wtPF4 was capable of inhibiting primary tumor growth, but both wtPF4 and ttPF4 equally inhibited the development of lung metastases (b). Black arrows represent treatments. # represents $P < 0.05$ compared to all other groups.

configuration of cytokine, targeting motif, and dose for each specific patient.

A previous publication demonstrated that the peptide VNTANST homes to tumor-specific cell-surface vimentin in breast adenocarcinoma (4T1), colon carcinoma (CT26), and squamous cell carcinoma (SCCVII) [5]. Furthermore, ttIL12 pDNA with the VNTANST-coding sequence inserted in the IL12 plasmid was more effective for inhibiting primary tumor growth, inhibiting metastatic tumor development, and extending survival in these syngeneic models. Four more tumor models were tested to determine if the ttIL12 would be effective in treating more tumor varieties. The ttIL12 only increased the antitumor efficacy of IL12 gene treatments in the melanoma model B16F10 (Figures 2(d) and 2(e)) while there were no increases in efficacy in the RM1 and EMT6 models (Supplementary Figures 5(a) and 5(b)) and a loss of any efficacy in the LLC model (Supplementary Figure 5(c)). The lack of efficacy in these models is surprising as the level of cell-surface vimentin in the LLC model is equivalent to SCCVII and CT26 models and expression in RM1 and EMT6 is 3–5-fold higher than expression in the 4T1 model (Supplementary Figure 6). These results highlight the fact that not every immune therapy will be effective for all tumor histotypes, even if the targeted motif is expressed in the tumor. So, the effects of these immunomodulatory treatments, especially those that rely on tumor-specific ligands, need to be thoroughly studied.

The different strategies for targeting immune agents to the tumor environment are continuously being tweaked and modified to improve the efficacy of the targeting. The peptide sequences RGD and NGR target to $\alpha_v\beta_3$ and aminopeptidase

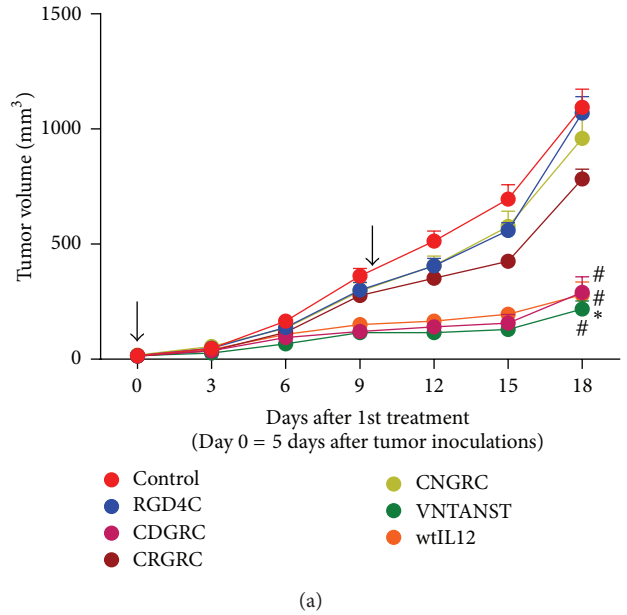

(a)

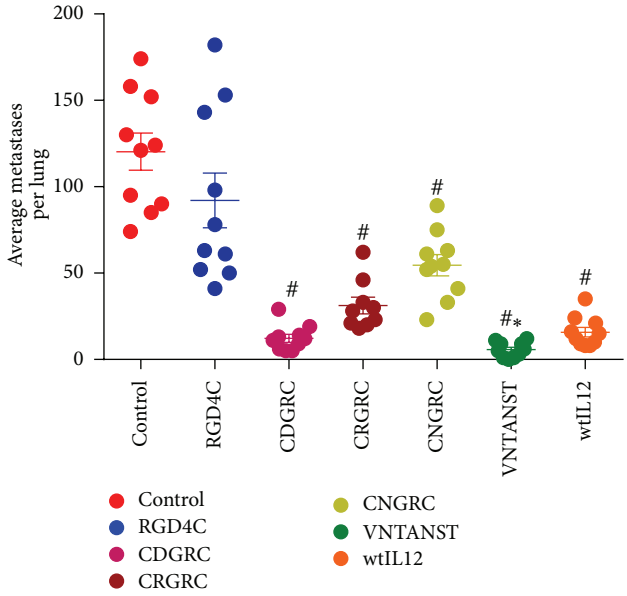

(b)

Figure 5: Not all tumor-targeting peptides can be successfully utilized in this gene delivery method. (a) Multiple tumor-targeting IL12 pDNAs were created by inserting the tumor-targeting peptide-coding sequences into the p40 subunit of the IL12 pDNA as in Figure 1(a). Only the wtIL12, VNTANST-IL12, and CDGRC-IL12 pDNA treatments inhibited primary tumor growth compared to the control pDNA treatments in the 4T1 tumor model. In side-by-side statistical analyses, the inhibition of primary tumor growth with VNTANST-IL12 was significantly inhibited compared to the wtIL12 and CDGRC-IL12 data on day 18 only. (b) Similar results were seen in the development of metastatic tumors in the same mice with only RGD4C not reducing development compared to control. Again, VNTANST-IL12 was significantly different from all groups in side-by-side analyses. Black arrows represent treatments. # represents $P < 0.05$ compared to control. ∗ represents $P < 0.05$ compared to all other groups.

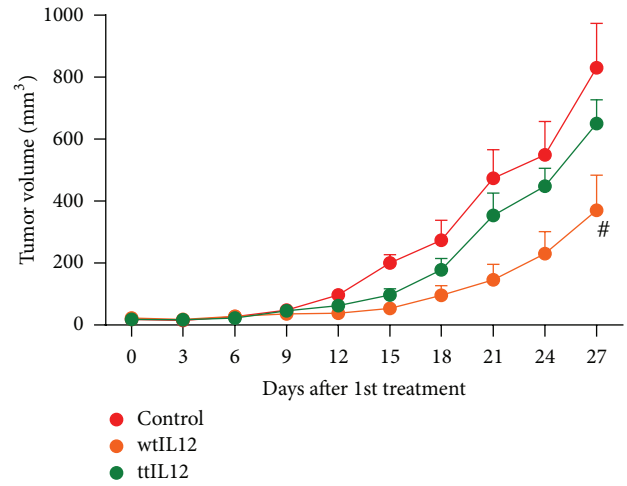

Figure 6: Increasing the dose of ttIL12 pDNA abrogates its therapeutic benefits. Increasing the dose by 3-fold to 30 μg pDNA per treatment resulted in a loss of inhibition by ttIL12 pDNA treatments, while the wtDNA treatments retained the ability to inhibit primary tumor growth in 4T1 primary tumor growth. Black arrows represent treatments. # represents $P < 0.05$ compared to all other groups.

n [23, 29–31, 35], respectively; however, these and other peptide sequences are rarely used in their bare form [35–42]. For instance, RGD and NGR peptides are more effective when capped on each side with cysteine residues to form a cyclic secondary structure. The VNTANST targeting sequence does not contain innate self-binding cysteine residues, and modifying the sequence to include capping cysteine residues does not significantly affect the targeting abilities of the peptide (data not shown). Other studies show that adding 4 more peptides to form the RGD4C peptide (ACDCRGDCFCG) improves by 20–30-fold the affinity for its $\alpha_v\beta_3$ ligand [23, 31, 35]. Furthermore, a tetrameric RGD4C "raft" has been successfully used for imaging tumors using positron emission tomography and other imaging techniques. This and other multimeric formulations have greater affinity for the $\alpha_v\beta_3$ integrin which makes it an ideal choice for these specific imaging studies [43, 44].

On the other hand, the CDGRC-IL12 pDNA, and other peptide-IL12 pDNA, greatly surpassed the efficacy of RGD4C-IL12 gene treatments for inhibiting tumor growth in this specific gene delivery method (Figure 5(a)). In concert with these results, previously published data demonstrated that CDGRC was capable of improving the therapeutic efficacy of another therapeutic cytokine gene, IFNα. Structural analysis of the CDGRC peptide found that it binds not only the $\alpha_v\beta_3$ but also aminopeptidase n, the target for the NGR peptides [3]. To our knowledge, no published evidence shows that RGD4C is capable of also binding to aminopeptidase n, suggesting that the improved therapeutic efficacy of CDGRC-IL12 may be due to binding to dual targets. An alternative possibility is that the larger size of the RGD4C (1149.34 Da) peptide elicited an efficacy-depleting immune response from the host compared to the shorter

CDGRC (552.64 Da) or VNTANST (705.72 Da) peptides [45]. Although the RGD4C peptide and its multimeric derivatives are undoubtedly capable of targeting payloads to tumor environments, the smaller peptides seem to be more suited to this posttranslationally targeted gene therapy strategy.

As shown previously, inserting the tumor-targeting peptide sequence prior to the stop codon in the subunit coding regions of the IL12 pDNA does not affect the expression or activity of the resulting IL12 protein. Since IL12 has 2 subunits, there may be more optimal configurations for placing the peptide sequence instead of just the p40 subunit as used for all previous experiments [5], so two other ttIL12 pDNAs were created (Figures 1(a)–1(c)). Interestingly, the effect of the peptide location appeared to be tumor-specific. In the 4T1 model, only the ttIL12-p40 pDNA was able to improve efficacy over the wtIL12 pDNA (Figures 2(a)–2(c)). Similar results were seen in the B16F10 models (Figures 2(d)-2(e)). In the less aggressive CT26 colon carcinoma model both the ttIL12-p40 and ttIL12-p40/p35 pDNAs equally improved the inhibition of primary tumors, while the ttIL12-p35 failed to improve upon the wtIL12 pDNA treatments (Supplementary Figure 1(a)). Notably, treatment with any ttIL12 pDNA extended survival in the SCCVII model (Figure 2(f)); however, only the ttIL12-p40 significantly increased primary tumor growth inhibition (Supplementary Figure 1(b)). These opposing results further advocate for the power of personalizing the targeting strategy in these therapies depending on the tumor histotype as the same targeting motif had different results based on location in different tumor models.

In addition to modifying the peptide or other targeting motif, selecting the proper immune modulatory element is critical for successful treatment of cancer. Using the VNTANST peptide to target IL15 in the 4T1 model produced interesting results. First, there was a slight yet significant inhibition in tumor growth (Figure 3(c)) and a 3-fold decrease in lung metastases compared to the wtIL15 (Figure 3(d)). However, both the primary and metastatic growth was much higher than seen with the tt- and wtIL12 pDNA treatments (Figures 2(a) and 2(b)). Contrastingly, both wtIL15 and ttIL15 equally inhibited metastatic tumor growth in the K7M3 osteosarcoma model (Figure 3(a)). Once more, the tumor histotype is an important factor to consider when choosing the targeting motif.

Additionally, the reduced effect of the IL15 could be explained by recent elucidation of IL15 in cancer therapy. Reports have shown that IL15 is in its most active form when bound to IL15rα, a soluble portion of the IL15 receptor [22]. So, after treatment with ttIL15 or wtIL15, the accumulated IL15 protein in the tumor environment is limited by the lack of available IL15rα. Although IL15 itself can upregulate the expression of IL15rα, a pDNA encoding for the ttIL15 with the IL15rα may increase the efficacy.

Targeting PF4, another cytokine which has shown some promise in anticancer therapies, was also attempted in the 4T1 tumor model; however, only the wtPF4 was able to inhibit primary tumor growth, although only slightly (Figure 4(a)). Also, both wtPF and ttPF4 were capable of inhibiting metastatic tumor growth though no differences were seen between wtPF4 and ttPF4 treatments (Figure 4(b)). Several studies have shown that PF4 can inhibit tumor growth through its antiangiogenic and immune stimulatory properties [13–15], and the slight regression from wtPF4 treatments is in agreement with other antiangiogenic treatments. However, it is surprising to see that there was no further benefit in the 4T1 metastatic tumors since the VNTANST targeting should have increased the intratumoral level of PF4, yet thettPF4 did not reduce vessel density in the primary tumors (Supplementary Figure 3).

Similarly, administering an increased amount of ttIL12 pDNA did not increase the efficacy of ttIL12. Instead, ttIL12 lost efficacy when the dose was elevated to 30 μg per treatment (3-fold higher than the dose used in all other studies) in the 4T1 model, yet the wtIL12 efficacy remained the same (Figure 6). Since there were no gross signs of IL12-induced toxicity, the best dose is not necessarily the maximum tolerated dose. These results further demonstrate the importance of understanding the intricate nature of immune modulatory therapies so they can safely and effectively induce an antitumor immune response.

5. Conclusions

The data presented here further confirm that the VNTANST peptide is effective for delivering cytokines to both primary and metastatic tumor sites in multiple tumor models to enhance the antitumor efficacy; contrariwise, this peptide or the targeting of its payload did not improve treatment outcomes in RM1, LLC, or EMT6 models. Furthermore, this posttranslational tumor-targeting strategy can work with other tumor-targeting peptides and other cytokine payloads; however, several intricate details about these treatments must first be clearly identified. These details include the proper target in the tumor environment, the suitable targeting motif, ideal location of the motif on the payload, appropriate immune payload, and the optimal dose level, among many others. Although it may appear that these details may hinder the impact of immune gene therapies for cancer treatments, it is truly only through understanding the effects of these intricate facets of the therapy that we can develop safer, cheaper, and more effective cancer therapies.

Conflict of Interests

The authors have no conflict of interests to report.

Acknowledgments

This research was supported in part by the National Institutes of Health through MD Anderson's Cancer Center Support Grant CA016672 and NIH Grant RO1CA120895 as well as through the Chinese National Science Foundation Research Fellowship for International Young Scientists (Fellowship no. 813111042). The funding sources did not have any roles in designing, implementing, or preparing these studies or this paper.

References

[1] Y.-J. Ko, G. J. Bubley, R. Weber et al., "Safety, pharmacokinetics, and biological pharmacodynamics of the immunocytokine EMD 273066 (huKS-IL2): results of a phase I trial in patients with prostate cancer," *Journal of Immunotherapy*, vol. 27, no. 3, pp. 232–239, 2004.

[2] S. K. Seung, B. Curti, M. Crittenden, and W. Urba, "Radiation and immunotherapy: renewed allies in the war on cancer," *Oncoimmunology*, vol. 1, no. 9, pp. 1645–1647, 2012.

[3] R. Craig, J. Cutrera, S. Zhu, X. Xia, Y.-H. Lee, and S. Li, "Administering plasmid DNA encoding tumor vessel-anchored IFN-α for localizing gene product within or into tumors," *Molecular Therapy*, vol. 16, no. 5, pp. 901–906, 2008.

[4] M. B. Atkins, M. J. Robertson, M. Gordon et al., "Phase I evaluation of intravenous recombinant human interleukin 12 in patients with advanced malignancies," *Clinical Cancer Research*, vol. 3, no. 3, pp. 409–417, 1997.

[5] J. Cutrera, D. Dibra, X. Xia, A. Hasan, S. Reed, and S. Li, "Discovery of a linear peptide for improving tumor targeting of gene products and treatment of distal tumors by IL-12 gene therapy," *Molecular Therapy*, vol. 19, no. 8, pp. 1468–1477, 2011.

[6] S. D. Reed, A. Fulmer, J. Buckholz et al., "Bleomycin/interleukin-12 electrochemogene therapy for treating naturally occurring spontaneous neoplasms in dogs," *Cancer Gene Therapy*, vol. 17, no. 7, pp. 457–464, 2010.

[7] M. J. Robertson, C. Cameron, M. B. Atkins et al., "Immunological effects of interleukin 12 administered by bolus intravenous injection to patients with cancer," *Clinical Cancer Research*, vol. 5, no. 1, pp. 9–16, 1999.

[8] M. N. Torrero, X. Xia, W. Henk, S. Yu, and S. Li, "Stat1 deficiency in the host enhances interleukin-12-mediated tumor regression," *Cancer Research*, vol. 66, no. 8, pp. 4461–4467, 2006.

[9] E. Chertova, C. Bergamaschi, O. Chertov et al., "Characterization and favorable in vivo properties of heterodimeric soluble IL-15.IL-15 Ralpha cytokine compared to IL-15 monomer," *Journal of Biological Chemistry*, vol. 288, no. 25, pp. 18093–18103, 2013.

[10] M. Kaspar, E. Trachsel, and D. Neri, "The antibody-mediated targeted delivery of interleukin-15 and GM-CSF to the tumor neovasculature inhibits tumor growth and metastasis," *Cancer Research*, vol. 67, no. 10, pp. 4940–4948, 2007.

[11] R. M. Teague, B. D. Sather, J. A. Sacks et al., "Interleukin-15 rescues tolerant CD8+ T cells for use in adoptive immunotherapy of established tumors," *Nature Medicine*, vol. 12, no. 3, pp. 335–341, 2006.

[12] W. Xu, M. Jones, B. Liu et al., "Efficacy and mechanism-of-action of a novel superagonist interleukin-15: interleukin-15 receptor alphaSu/Fc fusion complex in syngeneic murine models of multiple myeloma," *Cancer Research*, vol. 73, no. 10, pp. 3075–3086, 2013.

[13] G. Lippi and E. J. Favaloro, "Recombinant platelet factor 4: a therapeutic, anti-neoplastic chimera?" *Seminars in Thrombosis and Hemostasis*, vol. 36, no. 5, pp. 558–569, 2010.

[14] Z. Wang and H. Huang, "Platelet factor-4 (CXCL4/PF-4): an angiostatic chemokine for cancer therapy," *Cancer Letters*, vol. 331, no. 2, pp. 147–153, 2013.

[15] L. Yang, J. Du, J. Hou, H. Jiang, and J. Zou, "Platelet factor-4 and its p17-70 peptide inhibit myeloma proliferation and angiogenesis in vivo," *BMC Cancer*, vol. 11, article 261, 2011.

[16] "ClinicalTrials.gov," 2012, www.ClinicalTrials.gov.

[17] National Cancer Institute, "Biological Therapies for Cancer," Cancer Fact Sheets, 2013, http://www.cancer.gov/cancertopics/factsheet/Therapy/biological.

[18] A. J. Mellott, M. L. Forrest, and M. S. Detamore, "Physical non-viral gene delivery methods for tissue engineering," *Annals of Biomedical Engineering*, vol. 41, no. 3, pp. 446–468, 2013.

[19] J. L. Santos, D. Pandita, J. Rodrigues, A. P. Pêgo, P. L. Granja, and H. Tomás, "Non-viral gene delivery to mesenchymal stem cells: methods, strategies and application in bone tissue engineering and regeneration," *Current Gene Therapy*, vol. 11, no. 1, pp. 46–57, 2011.

[20] W. Wang, W. Li, N. Ma, and G. Steinhoff, "Non-viral gene delivery methods," *Current Pharmaceutical Biotechnology*, vol. 14, no. 1, pp. 46–60, 2013.

[21] A. I. Daud, R. C. DeConti, S. Andrews et al., "Phase I trial of interleukin-12 plasmid electroporation in patients with metastatic melanoma," *Journal of Clinical Oncology*, vol. 26, no. 36, pp. 5896–5903, 2008.

[22] M. Jakobisiak, J. Golab, and W. Lasek, "Interleukin 15 as a promising candidate for tumor immunotherapy," *Cytokine and Growth Factor Reviews*, vol. 22, no. 2, pp. 99–108, 2011.

[23] R. Craig and S. Li, "Function and molecular mechanism of tumor-targeted peptides for delivering therapeutic genes and chemical drugs," *Mini-Reviews in Medicinal Chemistry*, vol. 6, no. 7, pp. 757–764, 2006.

[24] M. Croft, C. A. Benedict, and C. F. Ware, "Clinical targeting of the TNF and TNFR superfamilies," *Nature Reviews Drug Discovery*, vol. 12, no. 2, pp. 147–168, 2013.

[25] J. Cutrera and S. Li, "Passive and active tumor homing cytokine therapy," in *Targeted Cancer Immune Therapy*, J. Lustgarten, Y. Cui, and S. Li, Eds., pp. 97–113, Springer, New York, NY, USA, 2009.

[26] P. Fournier and V. Schirrmacher, "Bispecific antibodies and trispecific immunocytokines for targeting the immune system against cancer: preparing for the future," *BioDrugs*, vol. 27, no. 1, pp. 35–53, 2013.

[27] A. Satelli and S. Li, "Vimentin in cancer and its potential as a molecular target for cancer therapy," *Cellular and Molecular Life Sciences*, vol. 68, no. 18, pp. 3033–3046, 2011.

[28] J. Cutrera, B. Johnson, L. Ellis, and S. Li, "Intraosseous inoculation of tumor cells into bone marrow promotes distant metastatic tumor development: a novel tool for mechanistic and therapeutic studies," *Cancer Letters*, vol. 329, no. 1, pp. 68–73, 2013.

[29] F. Curnis, A. Gasparri, A. Sacchi, R. Longhi, and A. Corti, "Coupling tumor necrosis factor-α with αV integrin ligands improves its antineoplastic activity," *Cancer Research*, vol. 64, no. 2, pp. 565–571, 2004.

[30] G. Colombo, F. Curnis, G. M. S. De Mori et al., "Structure-activity relationships of linear and cyclic peptides containing the NGR tumor-homing motif," *Journal of Biological Chemistry*, vol. 277, no. 49, pp. 47891–47897, 2002.

[31] A. Corti, F. Curnis, W. Arap, and R. Pasqualini, "The neovasculature homing motif NGR: more than meets the eye," *Blood*, vol. 112, no. 7, pp. 2628–2635, 2008.

[32] S. Bhatia, M. E. Menezes, S. K. Das et al., "Innovative approaches for enhancing cancer gene therapy," *Discovery Medicine*, vol. 15, no. 84, pp. 309–317, 2013.

[33] E. Cha and A. Daud, "Plasmid IL-12 electroporation in melanoma," *Human Vaccines and Immunotherapeutics*, vol. 8, no. 11, pp. 1734–1738, 2012.

[34] L. Heller, K. Merkler, J. Westover et al., "Evaluation of toxicity following electrically mediated interleukin-12 gene delivery in a B16 mouse melanoma model," *Clinical Cancer Research*, vol. 12, no. 10, pp. 3177–3183, 2006.

[35] J. Park, K. Singha, S. Son et al., "A review of RGD-functionalized nonviral gene delivery vectors for cancer therapy," *Cancer Gene Therapy*, vol. 19, no. 11, pp. 741–748, 2012.

[36] W. Chen, P. A. Jarzyna, G. A. F. van Tilborg et al., "RGD peptide functionalized and reconstituted high-density lipoprotein nanoparticles as a versatile and multimodal tumor targeting molecular imaging probe," *FASEB Journal*, vol. 24, no. 6, pp. 1689–1699, 2010.

[37] H. Dehari, Y. Ito, T. Nakamura et al., "Enhanced antitumor effect of RGD fiber-modified adenovirus for gene therapy of oral cancer," *Cancer Gene Therapy*, vol. 10, no. 1, pp. 75–85, 2003.

[38] D. Ma, Y. Chen, L. Fang et al., "Purification and characterization of RGD tumor-homing peptide conjugated human tumor necrosis factor α over-expressed in Escherichia coli," *Journal of Chromatography B*, vol. 857, no. 2, pp. 231–239, 2007.

[39] Y. Okada, N. Okada, H. Mizuguchi et al., "Optimization of antitumor efficacy and safety of in vivo cytokine gene therapy using RGD fiber-mutant adenovirus vector for preexisting murine melanoma," *Biochimica et Biophysica Acta*, vol. 1670, no. 3, pp. 172–180, 2004.

[40] Y. Okada, N. Okada, S. Nakagawa et al., "Tumor necrosis factor α-gene therapy for an established murine melanoma using RGD (Arg-Gly-Asp) fiber-mutant adenovirus vectors," *Japanese Journal of Cancer Research*, vol. 93, no. 4, pp. 436–444, 2002.

[41] K. Temming, R. M. Schiffelers, G. Molema, and R. J. Kok, "RGD-based strategies for selective delivery of therapeutics and imaging agents to the tumour vasculature," *Drug Resistance Updates*, vol. 8, no. 6, pp. 381–402, 2005.

[42] H. Wang, K. Chen, W. Cai et al., "Integrin-targeted imaging and therapy with RGD4C-TNF fusion protein," *Molecular Cancer Therapeutics*, vol. 7, no. 5, pp. 1044–1053, 2008.

[43] A. Briat, C. H. F. Wenk, M. Ahmadi et al., "Reduction of renal uptake of 111In-DOTA-labeled and A700-labeled RAFT-RGD during integrin $\alpha v\beta 3$ targeting using single positron emission computed tomography and optical imaging," *Cancer Science*, vol. 103, no. 6, pp. 1105–1110, 2012.

[44] L. Sancey, E. Garanger, S. Foillard et al., "Clustering and internalization of integrin $\alpha v\beta 3$ with a tetrameric RGD-synthetic peptide," *Molecular Therapy*, vol. 17, no. 5, pp. 837–843, 2009.

[45] L. Diao and B. Meibohm, "Pharmacokinetics and pharmacokinetic-pharmacodynamic correlations of therapeutic peptides," *Clinical Pharmacokinetics*, vol. 52, no. 10, pp. 855–868, 2013.

Hindawi Publishing Corporation
Mediators of Inflammation
Volume 2013, Article ID 764290, 5 pages
http://dx.doi.org/10.1155/2013/764290

Research Article

A Possible Role for CD8+ T Lymphocytes in the Cell-Mediated Pathogenesis of Pemphigus Vulgaris

Federica Giurdanella,[1] Luca Fania,[1] Maria Gnarra,[1] Paola Toto,[2] Daniela Di Rollo,[3] Daniel N. Sauder,[4,5] and Claudio Feliciani[1]

[1] *Department of Dermatology, Policlinico A. Gemelli Hospital, Catholic University of the Sacred Heart, Largo Agostino Gemelli 8, 00168 Rome, Italy*
[2] *Department of Dermatology, University G. D'Annunzio of Chieti-Pescara, Via dei Vestini 5, 66013 Chieti, Italy*
[3] *Department of Medicine and Aging Science, University G. D'Annunzio of Chieti-Pescara, Via dei Vestini 31, 66013 Chieti, Italy*
[4] *Department of Dermatology, Princeton University Hospital, 253 Witherspoon Street, Princeton, NJ 08540, USA*
[5] *Faculty of Medicine, University of Ottawa, 451 Smyth Rd., Ottawa, ON, Canada K1H8M5*

Correspondence should be addressed to Claudio Feliciani; feliciani@rm.unicatt.it

Received 29 July 2013; Accepted 11 October 2013

Academic Editor: Dennis Daniel Taub

Pemphigus vulgaris (PV) is an autoimmune blistering disease whose pathogenesis involves both humoral and cell-mediated immune response. Though the pathogenetic role of autoantibodies directed against desmoglein 3 is certain, a number of other factors have been suggested to determine acantholysis in PV. In this study we examined the possible role of CD8+ T cells in the development of acantholysis by a passive transfer of PV autoantibodies using CD8 deficient mice, and we also studied the inflammatory infiltrate of PV skin lesions by immunohistochemical staining. The results of the immunohistochemical staining to study the expression of CD3, CD4, and CD8 in PV skin lesions showed that CD4+ are more expressed than CD8+ in the inflammatory infiltrate of PV lesions, confirming the data of the previous literature. The passive transfer study showed a lower incidence of pemphigus in the group of CD8 deficient mice compared to the control one of wild-type mice. These results suggest that CD8+ T cells may play a role in the pathogenesis of PV, perhaps through the Fas/FasL pathway.

1. Introduction

Pemphigus vulgaris (PV) is a life-threatening autoimmune blistering disease mediated by autoantibodies (autoAbs) directed against desmogleins (Dsg) located on the surface of keratinocyte cells (KC). This leads to an intraepithelial loss of adhesion called acantholysis, and clinically it presents with vescicles and blisters [1]. AutoAbs in PV are directed mainly against desmoglein 3 (Dsg 3), a desmosomal glycoprotein situated in the skin predominantly in the suprabasilar epidermal layer, and less frequently against desmoglein 1 [2]. Though the pathogenetic role of antidesmoglein autoAbs is certain, the exact mechanism through which they lead to acantholysis is still incompletely understood. Complement [3], plasminogen-plasmin [4], cytokines [5], cell-mediated immunity, and other autoantibodies such as anticholinergic receptor antibodies have been suggested in determining acantholysis in PV [6]. Studies conducted so far regarding the role of T cells involved mainly CD4+ lymphocytes for their cooperation with B cells and subsequently for the induction and regulation of autoAbs production [7]. The function of CD8+ T cells has not been explored yet, but some authors hypothesize their role in cell-mediated pathogenesis of PV [8]. Other studies suggested a possible role of natural killer (NK) cells [9] as well as Fas and caspase 8 in PV [10]. These molecules' function in the apoptosis mechanism is well known. In PV these molecules result in a shrinking of keratinocytes that leads to detachment inducing acantholysis [11]. Fas is a member of the tumor necrosis factor (TNF) receptor family that is bound by Fas ligand, expressed on T CD8+ cells. In this study we sought to evaluate the role of CD8+ cells performing a passive transfer of PV autoAbs using CD8 deficient mice ($CD8^{-}/^{-}$). The results of these studies suggest a role for CD8 in the pathogenesis of PV.

2. Materials and Methods

2.1. Immunohistochemistry. Immunohistochemical staining was performed using the alkaline phosphatase-antialkaline phosphatase (APAAP) method on 7 μm skin sections of 7 PV patients [12]. Monoclonal antibodies against CD3 (1 : 20; DAKO, Glostrup, Denmark), CD4 (1 : 20; DAKO), and CD8 (1 : 20; DAKO) were used. For the quantitative study, stained cells were first counted in three consecutive microscopic fields (250x), both in the dermis and in the epidermis, and then summed; the average value was then calculated.

2.2. Preparation of Pemphigus IgG. Plasma was obtained from the plasmapheresis of one patient with clinical, histologic, and immunologic features consisting of the diagnosis of PV, during the acute phase of the disease. Total IgG concentration was measured by nephelometry using monospecific goat anti-human IgG (Beckman Instruments, Missasauga, ON, Canada). Pemphigus Ab titers were measured by indirect immunofluorescence (IIF) using monkey esophagus epithelium as the tissue substrate [13]. As a negative control, IgG fractions were isolated and removed from PV plasma using protein A (PA). Isolation of IgG fractions from PV plasma was achieved by standardized technique using staphylococcal protein A coupled to Sepharose 4B [14] (Pharmacia Biotech, Uppsala, Sweden). PA was washed four times in cold PBS and finally incubated with PV plasma overnight at 4°C. The supernatant was collected and used as negative control. Absence of IgG fractions in the control plasma was assessed by IIF staining on a monkey esophagus epithelium substrate and confirmed by nephelometry. PV plasma and control plasma were filter sterilized with Millex (pore size 0.22 mm; Millipore, Bedford, MA) and stored at −20°C.

2.3. Mice. The following strains were used: $CD8^{-}/^{-}$ and C57BL/6 ($CD8^{-}/^{-}$ control). All mice were housed and bred under specific pathogen-free conditions in the animal facility of the Sunnybrook Health Science Centre. Neonates (<24 h of age) were used. An average of 15 mice within each experimental group was used, and each experiment was repeated at least three times. All animal procedures were approved by the Sunnybrook Health Science Centre animal care committee.

$CD8^{-}/^{-}$ Mice. The generation of mice homozygous for CD8 gene mutations ($CD8^{-}/^{-}$) was obtained by disruption of the Lyt-2 gene through homologous recombination, and the mutation was interbred into the C57BL/6 background before generating CD8-deficient ($CD8^{-}/^{-}$) mice. Mice homozygous for the defect were used as the knockout (KO) mice, with the wild-type (WT) animals serving as the nondeficient controls.

2.4. Passive Transfer Model. To induce PV in mice, we utilized the model of Anhalt et al. [15] with minor modifications. Briefly, plasma was injected intradermally, in the dorsal area, into neonatal mice through a 30-gauge needle. The total dose administered ranged from 30 to 50 μL/g of body weight in a single administration. We chose a dose of 30 μL/g because this was the minimum dose inducing the disease in WT mice. $CD8^{-}/^{-}$ mice and C57BL/6 mice were injected with the same dose of PV plasma. As a negative control, gene targeted mutant mice and WT mice were injected with plasma depleted of IgG by treatment with protein A. Mice were examined 24 h after the injections. Cutaneous lesions consisting of intact blisters or erosions were enumerated.

2.5. Tissue Specimens Staining. Lesional and perilesional skin were obtained for light microscopy and direct immunofluorescence (DIF) 24 h after injection with PV IgG. At the time of biopsies, serum was also obtained and assayed for IIF on a monkey esophagus epithelium to detect the IgG titer.

2.6. Direct Immunofluorescence. Perilesional skin was biopsied and specimens were snap frozen in liquid nitrogen until use. Cryostat sections (5 μm) were used, and DIF studies were performed according to standard techniques [16]. Briefly, specimens were washed in PBS for 10 minutes, incubated for 30 minutes with FITC-conjugated $F(ab')_2$ fragment of rabbit anti-human IgG, specific for γ-chains (1 : 25; Dako, Glostrup, Denmark), and washed in PBS for 15 minutes. Slides were covered with buffered glycerol, and results were read in a Nikon Optiphot immunofluorescence microscope (Nikon, Melville, NY).

2.7. Indirect Immunofluorescence. Sera were collected 24 h after PV IgG treatment or PA treatment (IgG depleted), and IIF studies were performed according to standard techniques [16]. Cryostat sections (5 μm) of monkey esophagus were used as substrate, washed for 10 min in PBS, incubated for 30 min with different concentrations of sera (1 : 1-1 : 600), washed in PBS for 15 min, labeled with FITC-conjugated $F(ab')_2$ fragment of rabbit anti-human IgG (DAKO, Glostrup, Denmark) for 30 min, and then washed again in PBS for 10 min. Slides were covered with buffered glycerol, and results were examined using a Nikon Optiphot immunofluorescence microscope (Nikon, Melville, NY).

2.8. Histologic Technique. Skin biopsies from mice were fixed in 10% formalin and stained with hematoxylin and eosin.

2.9. Statistical Analysis. Data regarding the incidence of the disease in KO and control mice were analyzed using the χ^2 test; a P value <0.05 was considered to be significant.

3. Results

3.1. Immunohistochemistry CD3-CD4-CD8. CD3+ T cells were detected both in the dermis (32.8 ± 1.6 cells counted as mentioned in Section 2), with a perivascular distribution, and in the epidermis (7.9 ± 2.8) of all patients. CD4+ T cells were found in the superficial and papillary dermis (33.6 ± 4.8) with scattered and perivascular distribution, and a fewer number of them were detected in the basal and suprabasal layers near the dermal-epidermal junction (4.2±1.2). A number of CD8+ T cells (14.2 ± 1.6) were observed in perivascular areas of dermal lesional skin (CD4/CD8 = 2.7) (Table 1).

Table 1: T cellular markers identified in human skin lesions of PV patients by immunohistochemistry. The calculated average number of stained cells in three consecutive microscopic fields (250x) is reported.

	Dermis	Epidermis
CD3	32.8 ± 1.6	7.9 ± 2.8
CD4	33.6 ± 4.8	4.2 ± 1.2
CD8	14.2 ± 1.6	2.9 ± 1.3

3.2. Pemphigus Vulgaris IgG. Pemphigus plasma was obtained as described in Section 2. IIF for PV IgG using monkey esophagus as substrate demonstrated a titer of 1 : 2460, and an IgG concentration of 5.9 mg/mL was measured by nephelometry. PA-treated plasma showed absence of intercellular staining on monkey esophagus, and IgG levels were below the level of detection using the nephelometric analysis.

3.3. Passive Transfer of PV. The passive transfer of PV IgG demonstrated a direct correlation between the amount of PV IgG injected and the incidence of the disease. Acantholysis and inflammatory infiltrate were evident in mice given plasma containing PV IgG and absent in mice injected with IgG-depleted plasma. The epidermis of mice injected with PV IgG who developed PV lesions showed human IgG bound to the intercellular cell surface by DIF. No staining was found in mice injected with PA-treated plasma. No difference was observed in the intensity of fluorescence in different strains of mice treated with an equal dose of PV IgG. The IgG titer in all PV plasma injected mice detected by IIF ranged between 1 : 100 in mice treated with 30 μL/g PV plasma and 1 : 200 in mice injected with 50 μL/g. No circulating PV IgG were detected in mice injected with PA-treated plasma. In all of the WT mice, IgG deposits were observed with a minimal dose of 30 μL/g PV plasma (177 μg/g PV IgG). At this dose, about 10% of mice displayed clinical evidence of disease. With an administered dose of 50 μL/g PV plasma (295 μg/g PV IgG), 75% of the WT mice developed blisters.

When a dose-response study was performed on $CD8^{-}/^{-}$ mice, a lower incidence of pemphigus was observed. In particular, with a dose of 30 μL/g PV plasma, 0% (0/5) of the $CD8^{-}/^{-}$ mice injected showed evidence of disease as compared with 9.5% (4/42) of C57BL/6 mice (difference statistically not significant). With an injected dose of 50 μL/g, 44% (13/29) of the $CD8^{-}/^{-}$ mice developed PV lesions, compared with 72% (26/36) of the control group (difference statistically significant) (Figure 2).

4. Discussion and Conclusions

The immunopathogenesis of PV involves both humoral and cell-mediated response. While antibodies to desmoglein are pathogenic, CD4+, CD8+, and NK cells are also implicated. The function of CD4+ cells has previously been examined. It is known that CD4+ Th1 cells promote the IgG1 production by means of B cells, while IgG4, IgA, and IgE autoAbs are induced by the cooperation of CD4+ Th2 with B cells [9]. The function of CD8+ cells in the pathogenesis of PV is

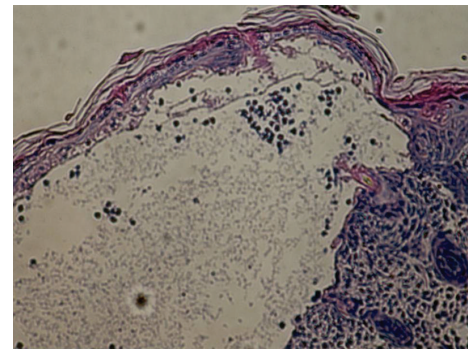

(a)

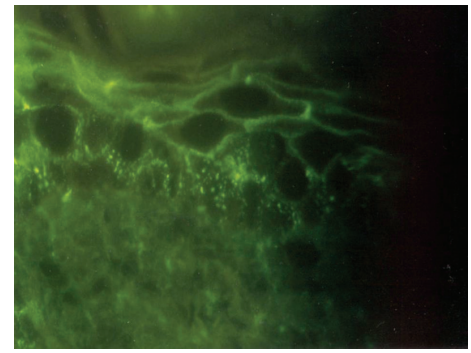

(b)

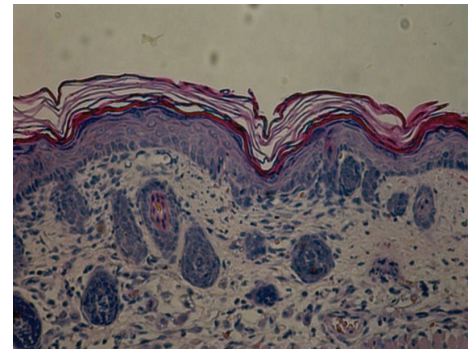

(c)

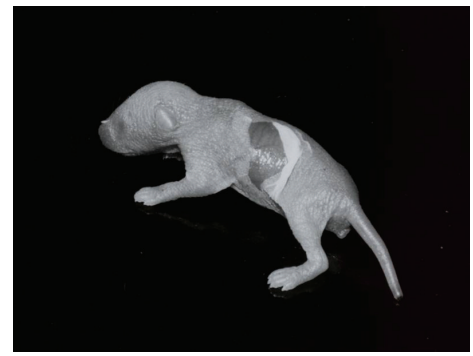

(d)

Figure 1: (a) Histology of a PV lesion from a wild-type mice injected with PV IgG. (b) Direct immunofluorescence in wild-type mice injected with PV IgG showing IgG bounded to the intercellular cell surface (100x). (c) Histology of mice treated with IgG deprived plasma, no acantholysis is observed. Immunofluorescence studies were also negative (data not shown). (d) A large erosion on the back of a mice treated with PV IgG.

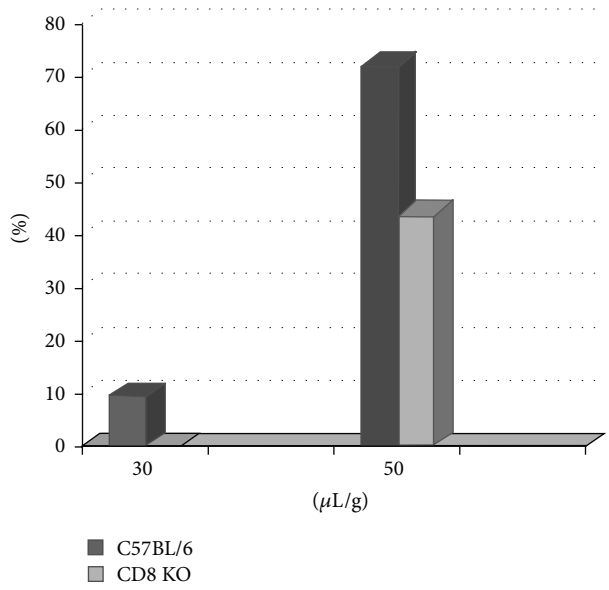

Figure 2: Incidence of disease in KO mice and control-C57BL/6 mice in passive transfer model of IgG PV. With a dose of 30 μL/g PV plasma, 0% (0/5) of the $CD8^{-}/^{-}$ mice developed PV, compared with 9.5% (4/42) of C57BL/6 mice. With an injected dose of 50 μL/g, 44% (13/29) of the $CD8^{-}/^{-}$ mice showed PV lesions, compared with 72% (26/36) of the control group.

still unclear, but their role has been hypothesized by some authors. They occasionally observed that CD8+ T cells from patients with active PV were responsive to in vitro stimulation with Dsg 3. Specifically they secreted IL-2 and INF-γ but not IL-4 or IL-5, being the first cytokines implicated in the cell-mediated immune response and the latters in the humoral one. This suggests a role for CD8+ T cells in the cell-mediated pathogenesis of PV [9].

The characterization of the infiltrate of PV human skin lesions showed mostly CD4+ T-cells and less commonly, about 10%, CD8+ cells [17]. In our study we analyzed the T cell infiltrate of skin lesions in patients affected by PV by means of immunohistochemistry for the expression of CD3, CD4, and CD8. The results confirm the data of the literature because CD4+ are more expressed in PV human skin lesions than CD8+ with a ratio of 2.7. Control mice (WT) developed PV lesions (9.5% with 30 μL/g and 72% with 50 μL/g), whereas CD8 knockout group was relatively resistant (0% with 30 μL/g and 44% with 50 μL/g). As expected, mice that received 50 μL/g PV plasma developed more PV lesions than those injected with 30 μL/g. Histological analyses and DIF and IIF tests confirmed the diagnosis of PV in mice that presented cutaneous lesions after the injection of PV plasma, while in the totality of mice treated with IgG deprived plasma, all tests were negative (Figure 1). These results suggest that CD8+ T cells may play a role in the pathogenesis of PV. CD8+ T cells mediate immunity in part through granzymes or inducing apoptosis by the Fas/Fas ligand (FasL) system. This death cell pathway depends mainly on Fas/FasL interaction through the activation of the caspases system. Some reports showed that, in keratinocytes treated with pemphigus sera, the activation of caspases was observed. Other reports demonstrated that inhibitors of caspases provoke the blockade of acantholysis [11]. An in vitro study showed that the addiction of anti-FasL Abs has partially inhibited the IgG-PV induced apoptosis in cultures of keratinocytes [11].

We thus suggest a role of CD8+ T lymphocytes in the pathogenesis of PV which in part may be mediated through perhaps Fas-FasL signaling.

References

[1] J. R. Stanley, M. Yaar, P. Hawley-Nelson, and S. I. Katz, "Pemphigus antibodies identify a cell surface glycoprotein synthesized by human and mouse keratinocytes," *Journal of Clinical Investigation*, vol. 70, no. 2, pp. 281–288, 1982.

[2] M. Amagai, "Pemphigus: autoimmunity to epidermal cell adhesion molecules," *Advances in Dermatology*, vol. 11, pp. 319–353, 1996.

[3] S. Kawana, W. D. Geoghegan, R. E. Jordon, and S. Nishiyama, "Deposition of the membrane attack complex of complement in pemphigus vulgaris and pemphigus foliaceus skin," *Journal of Investigative Dermatology*, vol. 92, no. 4, pp. 588–592, 1989.

[4] P. Fabbri, T. Lotti, and E. Panconesi, "Pathogenesis of pemphigus. The role of epidermal plasminogen activators in acantholysis," *International Journal of Dermatology*, vol. 24, no. 7, pp. 422–425, 1985.

[5] S. A. Grando, B. T. Glukhenky, G. N. Drannik, E. V. Epshtein, A. P. Kostromin, and T. A. Korostash, "Mediators of inflammation in blister fluids from patients with pemphigus vulgaris and bullous pemphigoid," *Archives of Dermatology*, vol. 125, no. 7, pp. 925–930, 1989.

[6] R. S. Kalish, "Pemphigus vulgaris: the other half of the story," *Journal of Clinical Investigation*, vol. 106, no. 12, pp. 1433–1435, 2000.

[7] K. Nishifuji, M. Amagai, M. Kuwana, T. Iwasaki, and T. Nishikawa, "Detection of antigen-specific B cells in patients with pemphigus vulgaris by enzyme-linked immunospot assay: requirement of T cell collaboration for autoantibody production," *Journal of Investigative Dermatology*, vol. 114, no. 1, pp. 88–94, 2000.

[8] M. Hertl and C. Veldman, "T-cellular autoimmunity against desmogleins in pemphigus, an autoantibody-mediated bullous disorder of the skin," *Autoimmunity Reviews*, vol. 2, no. 5, pp. 278–283, 2003.

[9] H. Takahashi, M. Amagai, A. Tanikawa et al., "T helper type 2-biased natural killer cell phenotype in patients with pemphigus vulgaris," *Journal of Investigative Dermatology*, vol. 127, no. 2, pp. 324–330, 2007.

[10] M. Puviani, A. Marconi, E. Cozzani, and C. Pincelli, "Fas ligand in pemphigus sera induces keratinocyte apoptosis through the activation of caspase-8," *Journal of Investigative Dermatology*, vol. 120, no. 1, pp. 164–167, 2003.

[11] S. A. Grando, J.-C. Bystryn, A. I. Chernyavsky et al., "Apoptolysis: a novel mechanism of skin blistering in pemphigus vulgaris linking the apoptotic pathways to basal cell shrinkage and suprabasal acantholysis," *Experimental Dermatology*, vol. 18, no. 9, pp. 764–770, 2009.

[12] J. L. cordell, B. Falini, and W. N. Erber, "Immunoenzymatic labeling of monoclonal antibodies using immune complexes of alkaline phosphatase and monoclonal anti-alkaline phosphatase (APAAP complexes)," *Journal of Histochemistry and Cytochemistry*, vol. 32, no. 2, pp. 219–229, 1984.

[13] C. Feibelman, G. Stolzner, and T. T. Provost, "Pemphigus vulgaris. Superior sensitivity of monkey esophagus in the determination of pemphigus antibody," *Archives of Dermatology*, vol. 117, no. 9, pp. 561–562, 1981.

[14] T. J. Miller and H. O. Stone, "The rapid isolation of ribonuclease-free immunoglobulin G by protein A-sepharose affinity chromatography," *Journal of Immunological Methods*, vol. 24, no. 1-2, pp. 111–125, 1978.

[15] G. J. Anhalt, R. S. Labib, and J. J. Voorhees, "Induction of pemphigus in neonatal mice by passive transfer of IgG from patients with the disease," *The New England Journal of Medicine*, vol. 306, no. 20, pp. 1189–1196, 1982.

[16] G. Pohla-Gubo and H. Hintner, "Direct and indirect immunofluorescence for the diagnosis of bullous autoimmune diseases," *Dermatologic Clinics*, vol. 29, no. 3, pp. 365–372, 2011.

[17] J. Schaller, H. W. Niedecken, E. Biwer, J. A. Stefan, H. W. Kreysel, and U. F. Haustein, "Characterization of lymphocytic infiltrate cells in bullous pemphigoid and pemphigus vulgaris," *Dermatologische Monatsschrift*, vol. 176, no. 11, pp. 661–668, 1990.

Hindawi Publishing Corporation
Mediators of Inflammation
Volume 2013, Article ID 457189, 12 pages
http://dx.doi.org/10.1155/2013/457189

Research Article

Hyperoxia Exacerbates Postnatal Inflammation-Induced Lung Injury in Neonatal BRP-39 Null Mutant Mice Promoting the M1 Macrophage Phenotype

Mansoor A. Syed and Vineet Bhandari

Division of Perinatal Medicine, Department of Pediatrics, Yale University School of Medicine, 333 Cedar Street, New Haven, CT 06520-8064, USA

Correspondence should be addressed to Mansoor A. Syed; mansoor.syed@yale.edu

Received 8 August 2013; Revised 2 October 2013; Accepted 3 October 2013

Academic Editor: Salahuddin Ahmed

Rationale. Hyperoxia exposure to developing lungs—critical in the pathogenesis of bronchopulmonary dysplasia—may augment lung inflammation by inhibiting anti-inflammatory mediators in alveolar macrophages. *Objective*. We sought to determine the O_2-induced effects on the polarization of macrophages and the role of anti-inflammatory BRP-39 in macrophage phenotype and neonatal lung injury. *Methods*. We used RAW264.7, peritoneal, and bone marrow derived macrophages for polarization (M1/M2) studies. For *in vivo* studies, wild-type (WT) and BRP-39$^{-/-}$ mice received continuous exposure to 21% O_2 (control mice) or 100% O_2 from postnatal (PN) 1 to PN7 days, along with intranasal lipopolysaccharide (LPS) administered on alternate days (PN2, -4, and -6). Lung histology, bronchoalveolar lavage (BAL) cell counts, BAL protein, and cytokines measurements were performed. *Measurements and Main Results*. Hyperoxia differentially contributed to macrophage polarization by enhancing LPS induced M1 and inhibiting interleukin-4 induced M2 phenotype. BRP-39 absence led to further enhancement of the hyperoxia and LPS induced M1 phenotype. In addition, BRP-39$^{-/-}$ mice were significantly more sensitive to LPS plus hyperoxia induced lung injury and mortality compared to WT mice. *Conclusions*. These findings collectively indicate that BRP-39 is involved in repressing the M1 proinflammatory phenotype in hyperoxia, thereby deactivating inflammatory responses in macrophages and preventing neonatal lung injury.

1. Introduction

Development of respiratory distress syndrome (RDS) adversely affects patient populations in neonatal intensive care units, which increases the risk of developing the chronic lung disease, bronchopulmonary dysplasia (BPD) [1]. This occurs primarily in preterm infants as a consequence of severe lung injury resulting from mechanical ventilation and oxygen exposure and is characterized by inflammation and epithelial cell death. Premature infants are also more likely to be exposed to infection; prenatal or postnatal inflammation accelerates the development of BPD by itself or combined with a variety of postnatal injuries, resulting in disruption of lung alveolar and vascular development [2–6].

Mouse breast regression protein-39 (BRP-39; Chi3l1) and its human homologue YKL-40 are chitinase-like proteins present in a variety of cells, including monocytes and macrophages, and have been shown to play a role in various macrophage mediated inflammatory diseases [7]. In our previous work, we demonstrated that the levels of tracheal YKL-40 are lower in premature babies that develop BPD or die compared with those without these complications [8].

M1 macrophage polarization is associated with inflammation and tissue destruction [9, 10], whereas the M2 macrophage has an anti-inflammatory phenotype that is associated with wound repair and angiogenesis [11, 12]. Macrophages are polarized to the M1 state by lipopolysaccharide (LPS), interferon gamma (IFNγ), and other stimulants which upregulate proinflammatory cytokines including interleukin- (IL-) 1β, IL-6, and IL-12 and increase the production of reactive oxygen species and nitrogen intermediates [13]. In contrast, macrophages are polarized to the M2 state

by IL-4 [14], which upregulates scavenger receptors, mannose receptor, and IL-1 receptor antagonist [13]. M2 cells also secrete the anti-inflammatory cytokine IL-10 and downregulate the production of proinflammatory cytokines [14]. These cells also upregulate arginase-1 (Arg1), which metabolizes arginine to ornithine and polyamines, and thereby diminish the inducible nitric-oxide synthase (iNOS) reaction [9, 10].

M1 polarization supports resistance to intracellular bacteria and controls the acute phase of inflammation. However, an excessive or sustained M1 activated state is deleterious for the host, as demonstrated in acute infections and sepsis [10, 15].

Given the critical interaction of hyperoxia with inflammation in the pathogenesis of neonatal lung injury resulting in BPD, we hypothesized that hyperoxia exposure would exacerbate inflammation-induced M1 and suppress the M2 phenotype in macrophages. Our aims were to study the impact of hyperoxia exposure on LPS induced effects on the M1/M2 phenotype in *in vitro* systems. Furthermore, this study was designed to evaluate the role of macrophage polarization and BRP-39 in LPS and hyperoxia plus LPS induced injury in *in vitro* and developmentally appropriate *in vivo* lung injury models.

We show that hyperoxia in the presence of LPS promotes M1 and inhibits the M2 phenotype in macrophages. Hyperoxia and/or LPS decreases BRP-39 expression, and its deletion promotes the M1 phenotype in macrophages. Neonatal BRP-39 null mutant (BRP-$39^{-/-}$) mice have significantly increased mortality on concomitant LPS and hyperoxia exposure. In addition, in the surviving BRP-$39^{-/-}$ mice lungs, there are significant alveolar simplification and inflammation.

2. Materials and Methods

2.1. Cell Culture. Primary murine peritoneal macrophages, bone marrow derived macrophages (BMDMs), and the murine macrophage cell line RAW264.7 were isolated or cultured as previously described [16, 17]. LPS-EB Ultrapure (100 ng/mL; Invitrogen) and IL-4 (10 ng/mL; Cell Signaling Technology, Inc.) were used as indicated.

2.2. Neonatal Mice Lung Injury Model. We used C57BL6/J mice in our experimental studies. All animal work was approved by the Institutional Animal Care and Use Committee at the Yale University School of Medicine. BRP-$39^{-/-}$ mice were generated and characterized as described earlier [8] and were a kind gift from Jack Elias, MD. Mice pups delivered on postnatal day 1 (PN1) were randomly divided into four groups: the control group, receiving saline and room air exposure, the LPS group, receiving an intranasal dose (3 μg/3 μL) of LPS on alternate days (PN2, -4, and -6) in room air (RA), and the LPS and hyperoxia groups, receiving an intranasal LPS dose (PN2, -4 and -6) and 100% oxygen exposure from PN1-7. After exposure to hyperoxia for 1 week, pups were killed immediately.

2.3. Oxygen Exposure. For the exposure to hyperoxia (100% O_2), newborn (NB) mice (along with their mothers) were placed in cages in an airtight Plexiglas chamber ($55 \times 40 \times 50$ cm), as described previously [18–20]. Exposure to oxygen was initiated on PN1 of life. Two lactating dams were used. Mothers were alternated in hyperoxia and RA every 24 h. The litter size was kept limited to 12 pups to control for the effects of litter size on nutrition and growth. Throughout the experiment, they were given free access to food and water. Oxygen levels were constantly monitored by an oxygen sensor that was connected to a relay switch incorporated into the oxygen supply circuit. The inside of the chamber was kept at atmospheric pressure, and mice were exposed to a 12 h light-dark cycle.

2.4. Real-Time PCR. Total RNA was reverse-transcribed by the iScript cDNA synthesis kit (Bio-Rad), amplified using SYBR Green PCR Master Mix (Bio-Rad), and detected by the opticon 2 real-time machine (MJ Research).

2.5. ELISA. Supernatants and tissue homogenates were analyzed by sandwich ELISA for IL-1β, IL-6, and IL-10, as per manufacturer's (R&D Systems) instructions [8, 20–23].

2.6. Immunoblot Analysis. Detection of Arg1 (BD Biosciences), Ym1 (Chi3l3) (STEMCELL Technologies), iNOS, and β-actin (Santa Cruz Biotechnology Inc.) was done using appropriate antibodies by Western analysis, as described previously [18, 20, 24]. Proteins were visualized with the pico ECL Western blotting kit (Pierce), and blots were exposed to HyBlot autoradiography films (Denville Scientific Inc.).

2.7. Histology. Lung tissues obtained from the NB mice from the LPS and hyperoxia experiments at PN7 were subjected to a standard protocol for lung inflation and fixed overnight in 10% buffered formalin. After washing in fresh PBS, fixed tissues were dehydrated, cleared, and embedded in paraffin by routine methods. Sections (5 μm) were collected on Superfrost Plus positively charged microscope slides (Fisher Scientific Co., Houston, TX, USA), deparaffinized, and stained with hematoxylin and eosin, as described previously [8, 18, 20, 25, 26].

2.8. Lung Morphometry. Alveolar size was estimated from the mean chord length of the airspace, as described previously [18–20]. Chord length increases with alveolar enlargement. Septal thickness was measured, as described previously [27].

2.9. Statistics. For the *in vitro* and animal studies, values were expressed as means ± SEM. As appropriate, groups were compared with the two-way ANOVA and corrected for multiple comparisons by the Tukey test and the logrank test (for the survival analysis), using GraphPad Prism 3.0 (GraphPad Software, Inc., San Diego, CA, USA). In all analyses, a $P < 0.05$ was considered statistically significant.

3. Results

3.1. Hyperoxia Differentially Regulates M1/M2 Phenotype in Macrophages. To determine whether hyperoxia is critical to macrophage polarization, we first performed quantitative real-time PCR (qPCR) analysis in RAW or peritoneal

macrophages after stimulation with well-established M1 (LPS) or M2 (IL-4) polarizing agents [15]. To determine whether hyperoxia affects LPS induced M1 markers, cells were stimulated with LPS in presence or absence of hyperoxia for 16 h and then iNOS and IL-6 mRNA expression were evaluated. LPS treatment led to the activation of iNOS and IL-6, as expected; however, concomitant hyperoxia augmented LPS induced iNOS and IL-6 mRNA expression (Figures 1(a) and 1(b)). These differential effects on iNOS were confirmed at the protein level by Western blot analyses (Figure 1(c)). Furthermore, hyperoxia augmented LPS induced the proinflammatory cytokine IL-1β and attenuated anti-inflammatory IL-10 concentrations in cell culture supernatants (Figures 1(d) and 1(e)).

Macrophages are highly heterogeneous cells that can quickly change their phenotype and function in response to different stimuli, and studies have documented the flexibility of macrophage activation [15]. We next investigated whether hyperoxia affects IL-4 induced M2 phenotype. Hyperoxia potently inhibited IL-4 induced M2 markers Arg1 and Fizz1 mRNA expression (Figures 2(a) and 2(b)). Western blot of Arg1 also confirmed the results of the mRNA expression (Figure 2(c)). KLF4, a novel regulator of macrophage polarization and essential for IL-4 mediated macrophage M2 phenotype [28], was also attenuated by hyperoxia (Figure 2(d)).

Taken together, our data would suggest that hyperoxia-exposure further polarizes LPS induced macrophages towards the M1 phenotype, with significant inhibition of the M2 phenotype.

3.2. BRP-39 Decreases with Hyperoxia and Acts as a Marker for the M2 Phenotype in Macrophages. Mouse breast regression protein-39 and its human homologue YKL-40 are chitinase-like proteins that have been shown to play a role in various macrophages mediated inflammatory events [29, 30]. To determine if BRP-39 gene is critical in macrophage polarization, we first performed qPCR analysis of LPS and IL-4 induced BRP-39 in RAW macrophages. These two stimuli differentially regulated the BRP-39 mRNA expression and were particularly noteworthy, as it was greatly decreased by LPS, hyperoxia, and LPS plus hyperoxia exposure (Figure 3(a)). On the other hand, BRP-39 mRNA expression was strongly enhanced by IL-4 but diminished by addition of hyperoxia (Figure 3(b)), assaying the pattern followed by other M2 phenotype markers.

3.3. BRP-39 Regulates M1/M2 Macrophage Polarization. To study the function of BRP-39 in the process of macrophage polarization, we utilized a loss of function approach. As noted earlier, LPS activated the M1 phenotype signaling, which was augmented by hyperoxia (Figure 1). Here, we show that upon stimulation with LPS and hyperoxia, peritoneal macrophages from BRP-39$^{-/-}$ mice produced a higher level of iNOS and IL-6 mRNA expression than wild-type (WT) macrophages in LPS alone and LPS with hyperoxia treated groups (Figure 4(a)). These findings were further confirmed at the protein level by Western blot of iNOS (Figure 4(b)) and ELISA measurement of IL-6 (Figure 4(c)).

To elucidate whether the differential response of BRP-39 mRNA in IL-4 and IL-4 plus hyperoxia groups (Figure 3) was due to change in macrophage polarization, we stimulated WT and BRP-39$^{-/-}$ peritoneal macrophages and found equally robust induction of the M2 markers Arg1 and Fizz1 in the IL-4 stimulated group, which was diminished by concomitant exposure to hyperoxia in WT macrophages (Figures 5(a) and 5(b)). Similarly, IL-4 stimulated BRP-39$^{-/-}$ macrophages also expressed high levels of Arg1 and Fizz1, which was significantly decreased compared to the WT IL-4 group (Figures 5(a) and 5(b)). However, BRP-39$^{-/-}$ macrophages had a further significant decreased expression of Arg1 mRNA, as compared to WT, on hyperoxia plus IL-4 exposure (Figures 5(a) and 5(b)). We confirmed the results of the decrease in Arg1 expression at the protein level and noted the same pattern with the additional M2 marker, Ym1, utilizing BMDMs (Figure 5(c)).

Taken together, our data would suggest that BRP-39 is a critical regulator of the macrophage phenotype upon LPS and concomitant hyperoxia-exposure, polarizing them towards the M2 phenotype.

3.4. BRP-39 Protects against LPS with Concomitant Hyperoxia Induced Mortality. In survival studies, WT and BRP-39$^{-/-}$ neonatal mice underwent 100% oxygen or RA exposure for 7 days along with intranasal instillation with LPS (3 μg/3 μL) on alternate days (PN2, -4, and -6). Mortality was 20% at 7 days after LPS alone or with hyperoxia exposure in WT mice (Figure 6). In BRP-39$^{-/-}$ neonatal mice, the mortality was also 20% at 7 days after LPS alone. However, it significantly increased to almost 60% in animals which received exposure of LPS combined with hyperoxia, by PN7 (Figure 6).

3.5. BRP-39 Modulates Oxygen-Induced Augmentation of Neonatal Lung Injury. To begin assessing BRP-39 mediated differences in alveolar inflammation, we measured lung bronchoalveolar lavage (BAL) protein levels and inflammatory cell counts and assessed lung histology. Lung injury at PN7 was significantly increased in LPS plus oxygen-exposed BRP-39$^{-/-}$ mice compared with similarly treated WT mice and all other treatment groups (Figure 7). In this group, we observed a significant increase in histologic damage (Figure 7(a)), chord length (Figure 7(b)), septal thickness (Figure 7(c)), BAL total cell counts (Figure 7(d)), and BAL protein (Figure 7(e)) compared with all other groups.

In BRP-39$^{-/-}$ neonatal mice, LPS plus oxygen augmented lung injury, so we sought to determine whether M1 macrophages were responsible for this proinflammatory state. Therefore, we measured proinflammatory M1 cytokine markers IL-6 and IL-1β in lung homogenates. IL-6 and IL-1β were significantly increased in BRP-39$^{-/-}$ neonatal mice lungs exposed to LPS plus oxygen compared with WT mice exposed to LPS plus oxygen and other experimental groups (Figures 8(a) and 8(b)).

To summarize, our data would suggest that LPS with concomitant hyperoxia exposure-induced mortality and lung injury in neonatal mice is regulated, in part, by BRP-39. The mechanism of these effects appears to be mediated, at least in

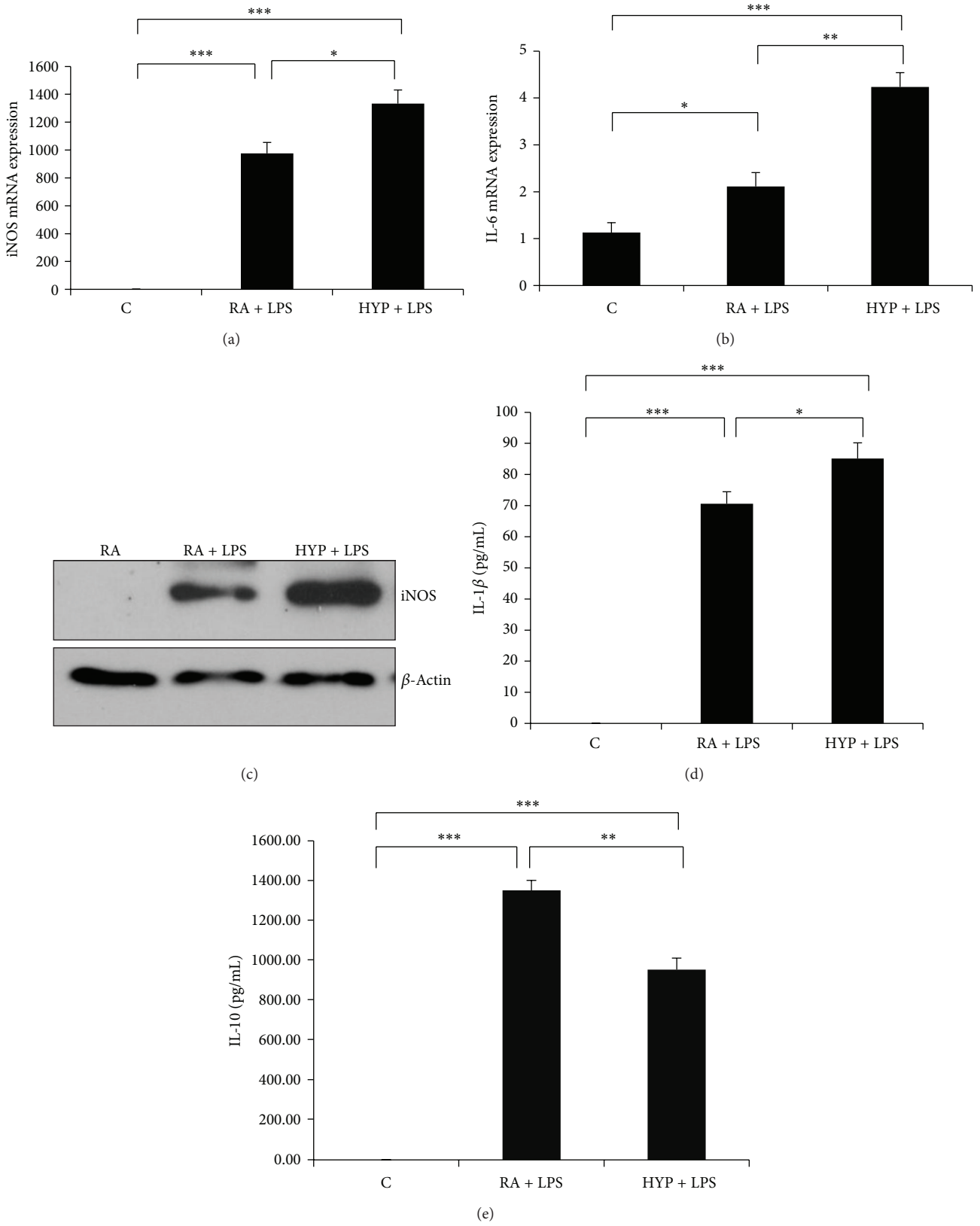

Figure 1: Hyperoxia promotes the M1 phenotype in macrophages. Inducible nitric oxide synthase (iNOS) and interleukin-6 (IL-6) mRNA expression were measured by real-time PCR in the RAW264.7 macrophages after stimulation with lipopolysaccharide (LPS; 100 ng/mL) for 16 h in room air (RA) or 95% hyperoxia (HYP) ((a) and (b)). Representative Western blot showing 24 h LPS mediated protein induction of iNOS in RA and HYP groups (c). IL-1β and IL-10 were measured by ELISA in the supernatants of macrophages after stimulation for 24 h with LPS ((d)-(e)). Results expressed as the mean ± SEM of data obtained from three independent experiments. C: control (RA). $^{*}P < 0.05$, $^{**}P < 0.01$, and $^{***}P < 0.001$.

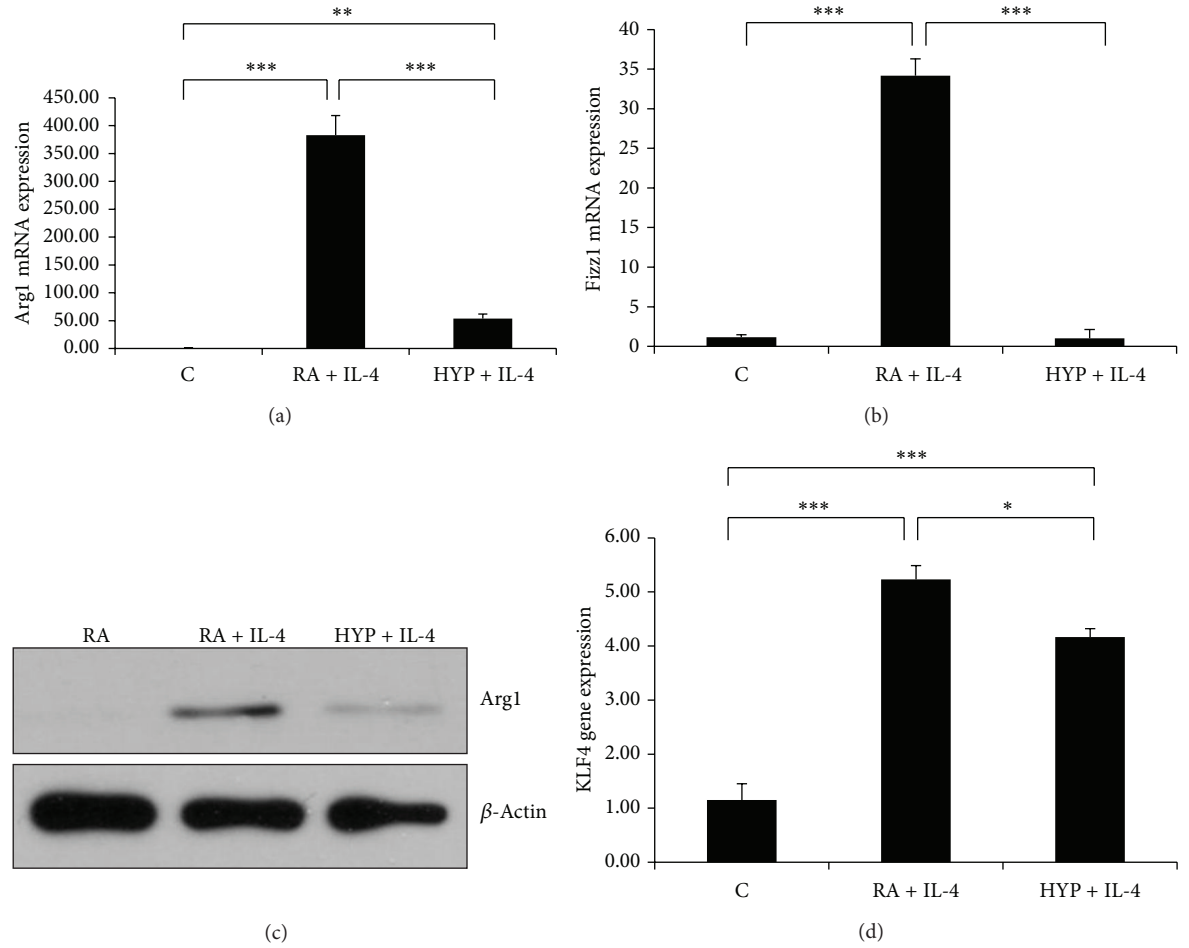

Figure 2: Hyperoxia inhibits the M2 phenotype in macrophages. Arg1 and Fizz1 mRNA were measured by real-time PCR in the RAW macrophages after stimulation with interleukin-4 (IL-4; 10 ng/mL) for 16 h in room air (RA) or 95% hyperoxia (HYP)((a) and (b)). Western blot showing IL-4 mediated protein induction of Arg1 in RA and HYP groups (c). KLF4 mRNA expression level was assessed by qPCR in macrophages stimulated with IL-4 in RA and HYP (d). Results expressed as the mean ± SEM of data obtained from three independent experiments. C: control (RA). $^{*}P < 0.05$, $^{***}P < 0.001$.

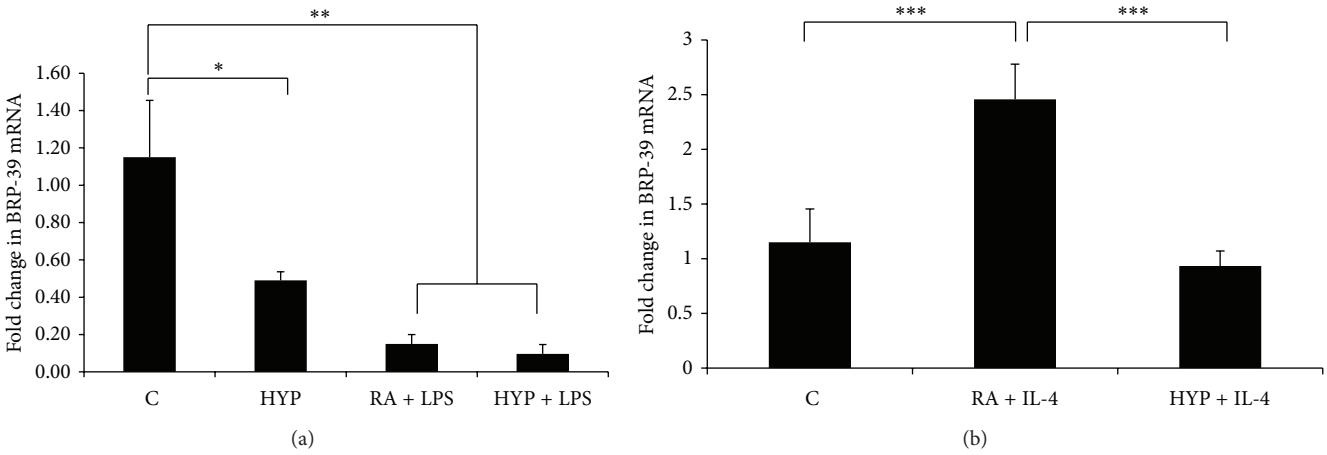

Figure 3: BRP-39 decreases with hyperoxia and acts as a marker for the M2 phenotype in macrophages. BRP-39 mRNA levels in mouse RAW macrophages after 16 h of stimulation with lipopolysaccharide (LPS; 100 ng/mL) (a) or interleukin-4 (IL-4; 10 ng/mL) (b). Results expressed as the mean ± SEM of data obtained from three independent experiments. C: control (RA); HYP: hyperoxia. $^{**}P < 0.01$, $^{***}P < 0.001$.

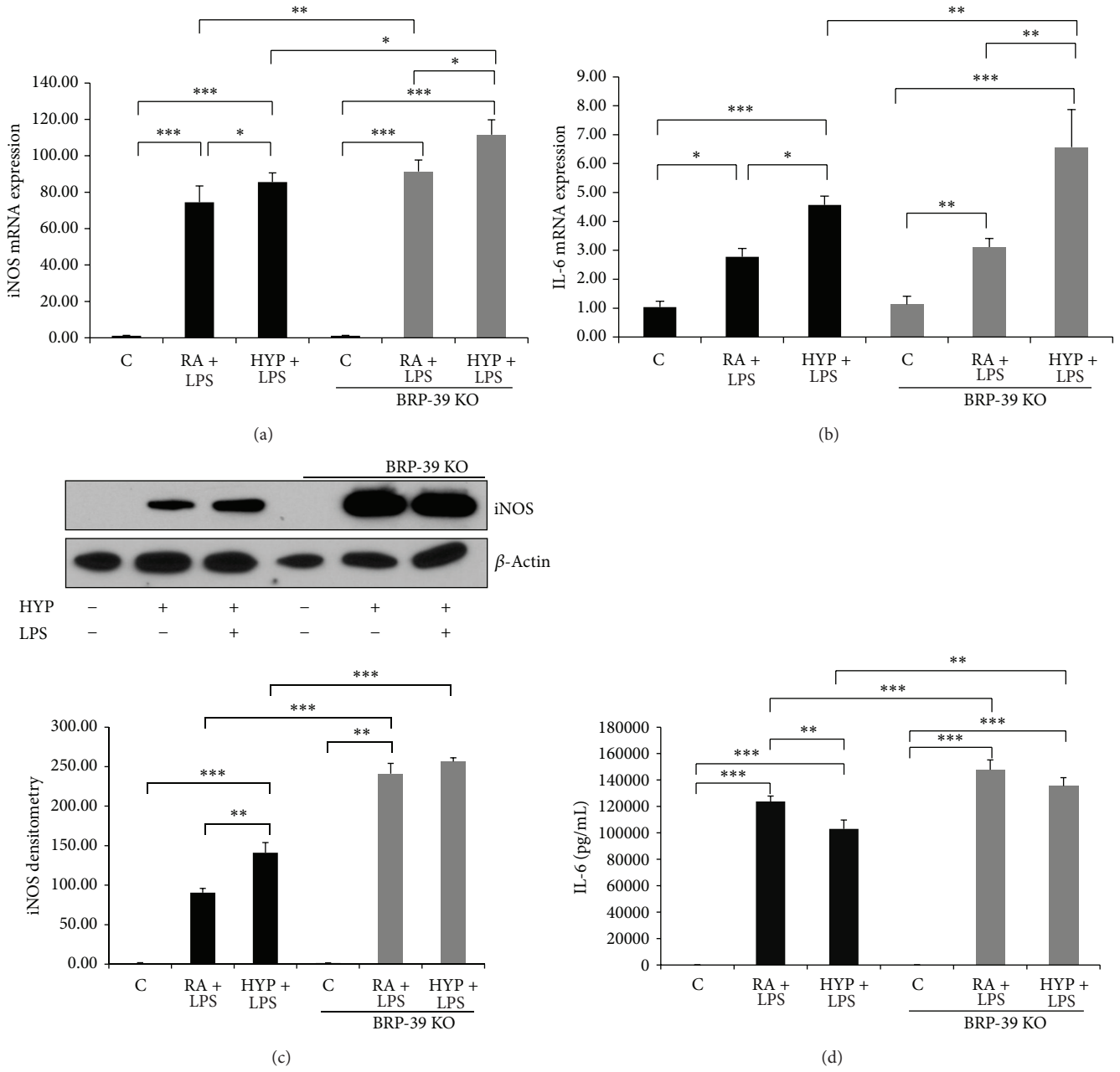

Figure 4: BRP-39 deletion promotes the M1 phenotype in macrophages. Enhanced expression of M1 marker genes, inducible nitric oxide synthase (iNOS), and interleukin-6 (IL-6) mRNA expression in BRP-39$^{-/-}$ peritoneal macrophages stimulated by lipopolysaccharide (LPS; 100 ng/mL) for 16 h ((a) and (b)). Western blot and densitometry showing increased iNOS protein expression in BRP-39$^{-/-}$ bone marrow derived macrophages (BMDMs) stimulated by LPS (100 ng/mL) or LPS plus hyperoxia for 24 h (c). BRP-39$^{-/-}$ BMDMs generate increased IL-6 after LPS (100 ng/mL) stimulation for 16 h as compared to wild type (WT) (d). Results expressed as the mean ± SEM; $n = 3$, in each group. C: control (RA); HYP: hyperoxia; BRP39 KO: BRP39 knock out or BRP-39$^{-/-}$. $^{*}P < 0.05$, $^{**}P < 0.01$, and $^{***}P < 0.001$.

part, by enhancement of the proinflammatory state, including increased M1 markers, noted in the absence of BRP-39.

4. Discussion

We have identified a novel role for the BRP-39 protein in the regulation of macrophage polarization *in vitro* and *in vivo*. A lack of BRP-39 in macrophages promotes a heightened responsiveness to LPS and LPS plus hyperoxia with respect to expression of genes that characterize M1 classically activated macrophages. Furthermore, *in vivo* studies utilizing a LPS and hyperoxia induced lung injury in neonatal mice reveal that BRP-39 absence in myeloid cells promotes exacerbation of disease, which is associated with an increased expression of M1 cytokines, as well as aberrant lung structure. Collectively, these findings identify BRP-39 as a modulator of macrophage

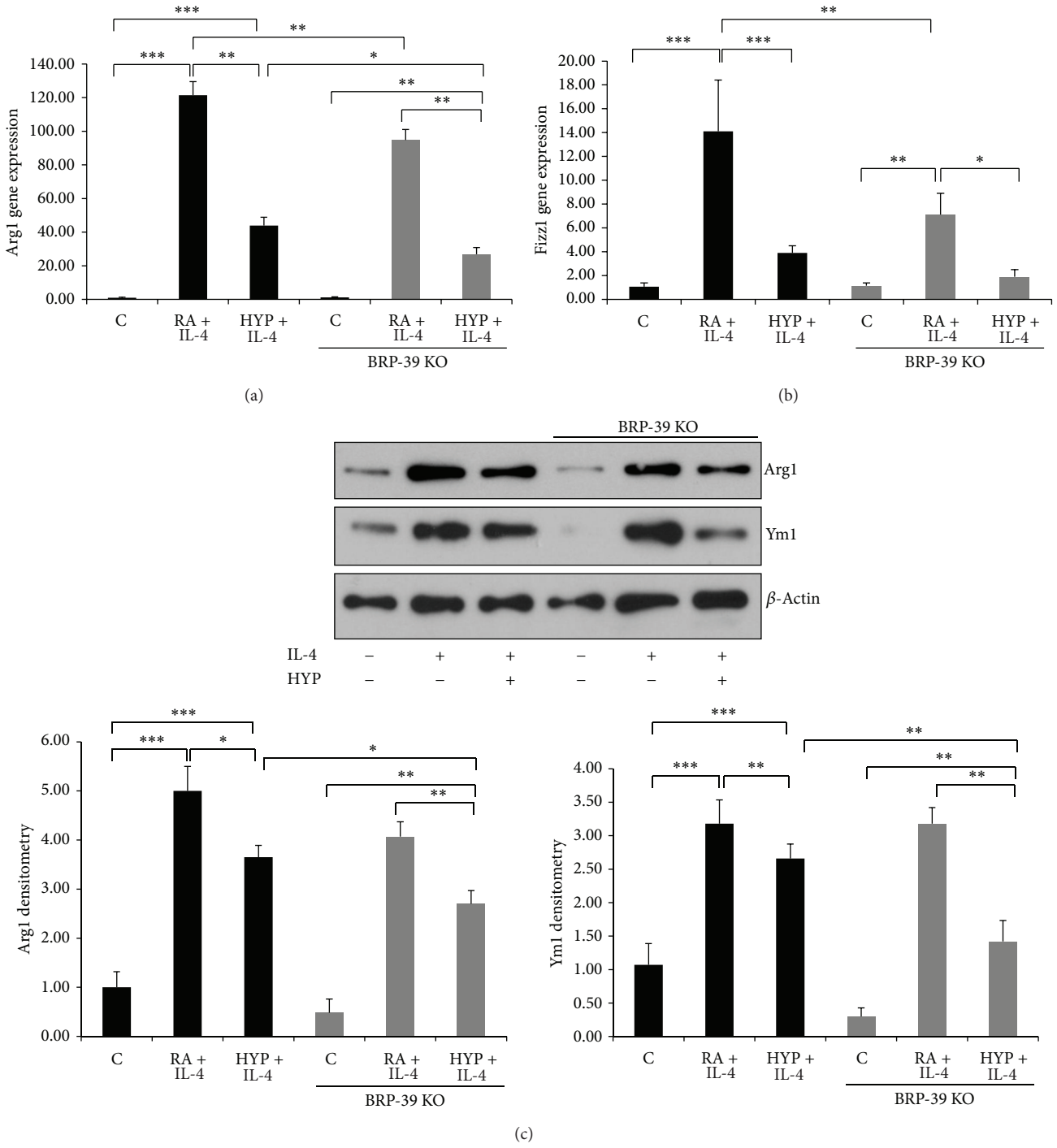

Figure 5: BRP-39 deletion inhibits M2 phenotype in macrophages. Attenuated expression of M2 marker genes Arg1 and Fizz1 in BRP-39$^{-/-}$ peritoneal macrophages stimulated with interleukin-4 (IL-4; 10 ng/mL) for 16 h ((a) and (b)). Protein levels (Western blot and densitometry) of M2 markers Arg1 and Ym1 in bone marrow derived macrophages (BMDMs) (c). Results expressed as the mean ± SEM of data obtained from three independent experiments stimulated with IL-4 (10 ng/mL) for 24 h. C: control (RA); HYP: hyperoxia; BRP39 KO: BRP39 knock out or BRP-39$^{-/-}$. $^{*}P < 0.05$, $^{**}P < 0.01$, and $^{***}P < 0.001$.

activation and M1/M2 polarization, which has an impact on mortality and lung injury upon LPS and hyperoxia exposure in neonatal mice.

Macrophages are central mediators of the inflammatory response, contributing both to the initiation and the resolution of inflammation [10, 31, 32]. Activated macrophages can be M1 or M2 polarized. The importance of the macrophage inflammatory state in animal models of lung injury has been increasingly recognized [32–34]. The present studies were undertaken to first define the role of hyperoxia

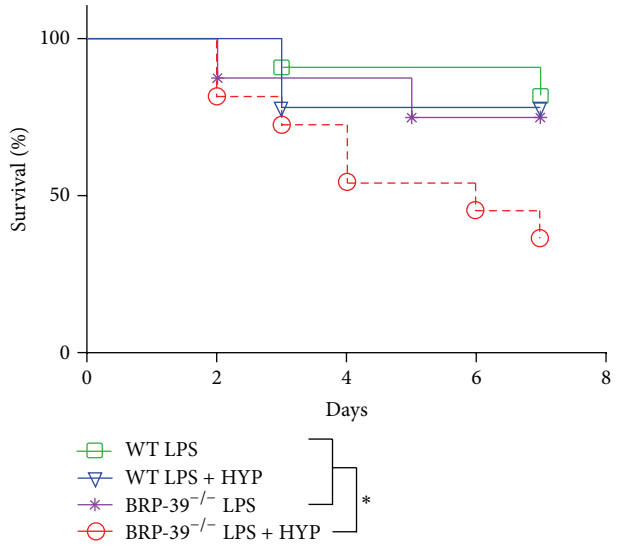

Figure 6: BRP-39 deletion enhances mortality in neonatal mice exposed to LPS combined with hyperoxia. Newborn (NB) BRP-39$^{-/-}$ or wild-type (WT) mice were exposed to 100% O_2 from postnatal (PN) PN1-7 and survival was assessed. The groups were as follows: WT mice pups treated with lipopolysaccharide (LPS; $n = 7$), WT mice pups treated with LPS plus hyperoxia (HYP) ($n = 3$), BRP-39$^{-/-}$ mice pups treated with LPS ($n = 11$), and BRP-39$^{-/-}$ mice pups treated with LPS plus HYP ($n = 8$). LPS treatment consisted of intranasal administration on alternate days (PN2, -4, and -6) with 3 μg/3 μL in presence or absence of 100% oxygen. $^{*}P < 0.05$.

in M1/M2 polarization and its effect on acute lung injury. Secondly, we wanted to demonstrate the role of BRP-39 in M1/M2 macrophage polarization in postnatal inflammatory and hyperoxia induced acute lung injury conditions, both factors being responsible, at least in part, for development of the neonatal disease BPD [1, 5]. We used the LPS and LPS plus hyperoxia-exposed WT and BRP-39$^{-/-}$ primary macrophages and lung injury models to test our hypotheses.

We showed that the hyperoxia augmented LPS induced proinflammatory M1 macrophage phenotype and attenuated IL-4 induced anti-inflammatory phenotype. M1 polarized macrophages showed higher levels of iNOS and IL-6 mRNA expression and protein concentration, which was augmented by hyperoxia exposure (Figure 1). A recently published study also showed hyperoxia augmented LPS induced inflammation in macrophages [35]. We have also recently reported that hyperoxia itself induces IFNγ in neonatal lungs [18, 23] and IFNγ-overexpressing transgenic mice lungs have a BPD-like phenotype in RA [18, 23]. We speculate that such a BPD phenotype may be secondary to enhanced M1 macrophage recruitment in lungs upon IFNγ stimulation. The importance of classically activated M1 macrophages in the pathogenesis of lung injury is also supported by several other reports that suggest that direct activation of these cells can augment tissue damage [34, 36, 37].

M2 polarized macrophages, characterized by various markers including Arg1 and Fizz1 and induced by TH2 cytokines IL-4 and IL-13, play an important role during alveolar development [33]. This has important potential clinical implications, not only for understanding normal developmental processes but also for addressing neonatal lung injury and inflammation [33]. The present study demonstrated that hyperoxia attenuated IL-4 induced M2 phenotype markers Arg1 and Fizz1, which suggests that hyperoxia inhibited M2 polarization in macrophages. Several studies have linked M2 macrophage activation state to tissue repair and regeneration [33, 38, 39] and a recent study identifies M2 macrophages localizing to sites of branching morphogenesis and increasing in number during the alveolarization stage, suggesting an important role during postnatal lung development [33].

Hyperoxia exposure and inflammation are the leading causes of lung injury of neonates with RDS leading to BPD [4, 5, 33, 40, 41]. In keeping with its importance, the cellular and molecular events that are involved in lung injury have been extensively investigated. The studies have highlighted a number of important events, including production of IL-1β and IL-6 [8, 22, 42, 43].

An interesting observation provided by our study is that BRP-39 was differentially expressed with M1 and M2 stimulants, showing a similar behavior as a M2 marker, even after exposure to hyperoxia; these data support BRP-39 being involved in macrophage function. Several previous studies have demonstrated that BRP-39 is a critical regulator of myeloid cell biology [8, 29, 44], but our novel observations introduce the role of BRP-39 in modulation of M1/M2 macrophage polarization for the first time, to the best of our knowledge.

Our initial evaluation revealed a significant decrease in BRP-39 expression in macrophages upon LPS, hyperoxia, and LPS plus hyperoxia groups exposure as compared to control groups. In accord with these findings, our group has already reported that the levels of tracheal aspirate YKL-40 (the human homolog of BRP-39) were lower in premature infants treated with hyperoxia for respiratory failure who subsequently developed BPD or died compared with those that did not experience these complications [8]. The decreased levels of BRP-39 upon LPS or/and hyperoxia exposure in macrophages further support our hypothesis that BRP-39 is essential for protection from lung injury by modulating macrophage polarization and is involved in the pathogenesis of BPD.

Macrophages in the postnatal lung displayed a M2 phenotype which is characteristic of macrophages involved in tissue remodeling functions [33]. In the present report, we noted that ablation of BRP-39 gives rise to an enhanced inflammatory M1 phenotype as compared to wild type upon exposure to LPS and hyperoxia. We believe that it is due to the hyperresponsiveness of macrophages to LPS signals in the presence of hyperoxia. *In vivo* and *in vitro* data presented in this report revealed that the ablation of BRP-39 resulted in enhanced M1 polarization as they expressed elevated iNOS, IL-6, and IL-1β levels.

Modulating the M1/M2 polarization status of macrophages can affect the severity of acute inflammatory conditions of the lung [38, 45]. Data presented in this report show that the lack of BRP-39 increases severity of lung injury and mortality in neonatal mice after LPS and hyperoxia exposure compared to WT mice, enhancing damage and inflammation,

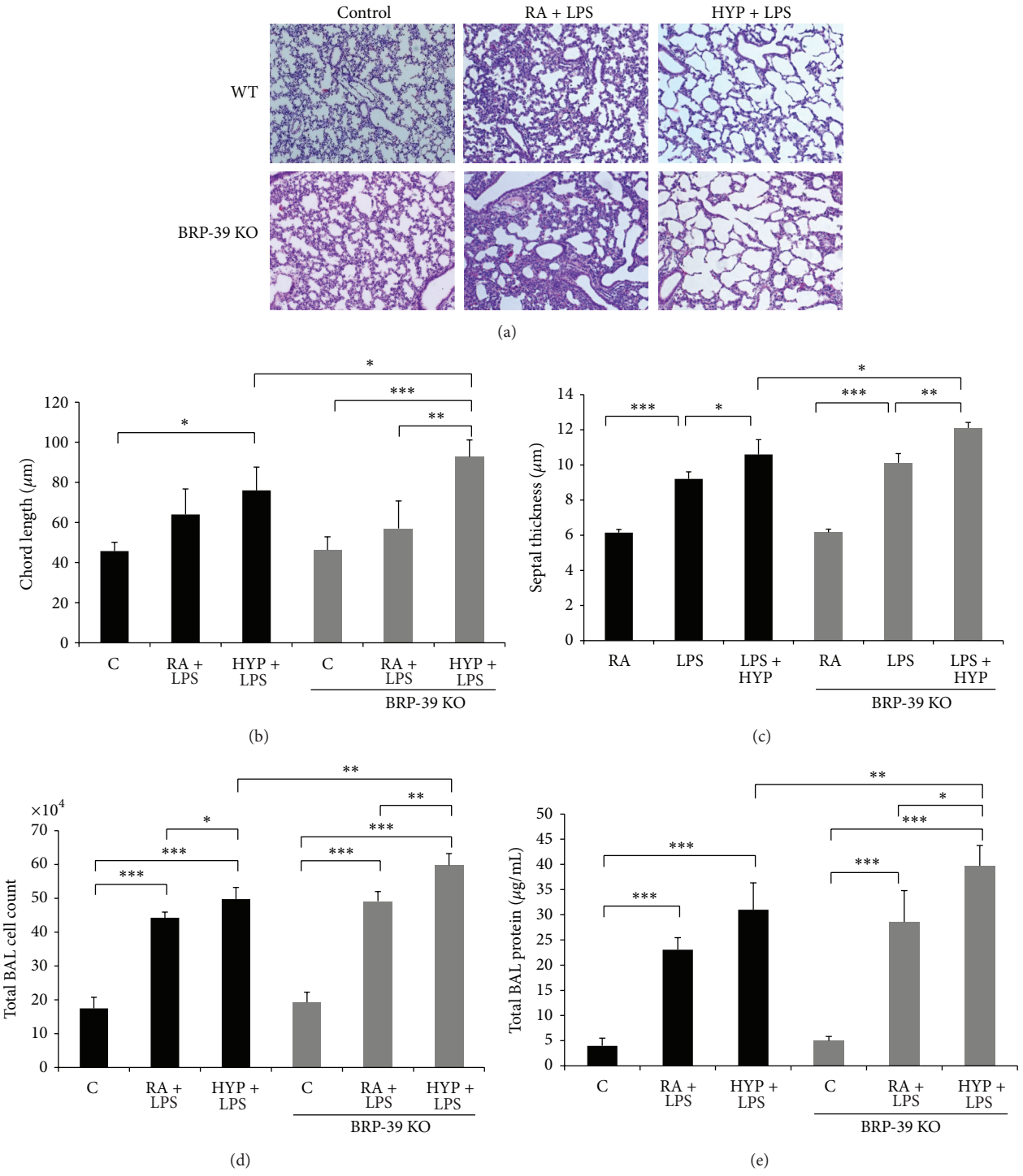

FIGURE 7: BRP-39 modulates LPS induced hyperoxia augmentation of neonatal lung injury. Newborn (NB) BRP-39$^{-/-}$ or wild-type (WT) mice were treated with LPS intranasal administration (3 μg/3 μL) on alternate days (postnatal or PN2, -4, -6) in presence or absence of 100% O_2 from PN1–7. Representative photomicrographs of lung histology (H&E stain, 10x) of NB BRP-39$^{-/-}$ or WT mice exposed to room air (RA) or hyperoxia (HYP) or LPS as noted above are shown at PN7 (a). The figures are illustrative of a minimum of 3 animals in each group. Alveolar size, as measured by chord length and septal thickness, confirmed features noted on lung histology ((b) and (c)). Each bar represents the mean ± SEM of a minimum of three animals. Bronchoalveolar lavage (BAL) total cell counts (d) and protein levels (e) of NB BRP-39$^{-/-}$ or WT mice exposed to RA or HYP model, or given treatment as noted above, at PN7. Each bar represents the mean ± SEM of a minimum of three animals. C: control (RA); HYP: hyperoxia; BRP39 KO: BRP39 knock out or BRP-39$^{-/-}$. $^{*}P < 0.05$, $^{**}P < 0.01$, and $^{***}P < 0.001$.

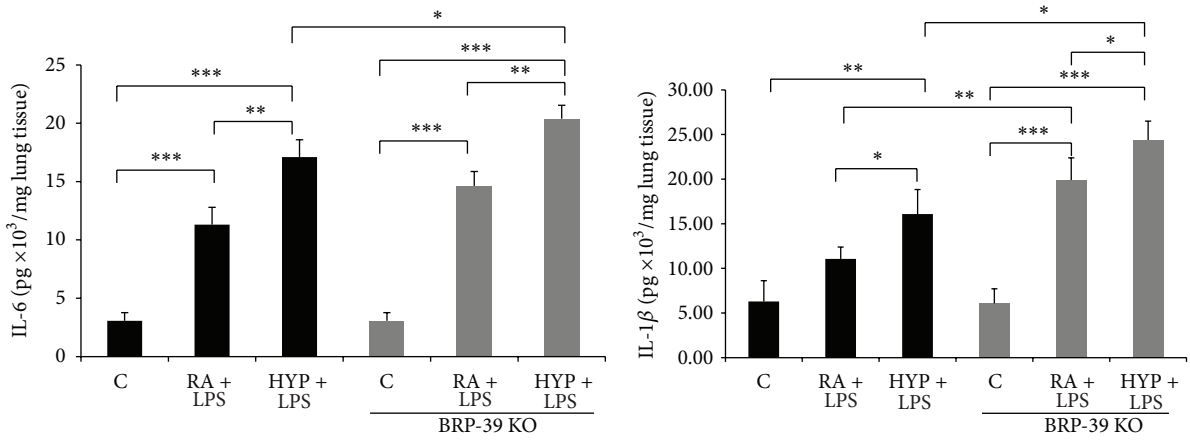

FIGURE 8: BRP-39 deletion promotes proinflammatory cytokines in neonatal mice exposed to LPS combined with hyperoxia. Newborn (NB) BRP-39$^{-/-}$ or wild-type (WT) mice were treated with LPS intranasal administration (3 μg/3 μL) on alternate days (postnatal or PN2, -4, -6) in presence or absence of 100% O_2 from PN1–7. Interleukin-6 (IL-6) and IL-1β levels were measured in lung tissue homogenates of indicated treatment groups of WT and BRP-39$^{-/-}$ mice ((a) and (b)). Each bar represents the mean ± SEM of a minimum of five animals. Results represent three independent experiments. C: control (RA); HYP: hyperoxia; BRP39 KO: BRP39 knock out or BRP-39$^{-/-}$. $^{*}P < 0.05$, $^{**}P < 0.01$, and $^{***}P < 0.001$.

as evidenced by increased lung inflammatory cytokines, morphometry, and inflammatory cells. Our results are further supported by earlier studies showing that deletion of BRP-39 renders mice more susceptible to lung injury [8, 29].

These findings support the role of macrophage polarization in the development of LPS and hyperoxia plus LPS induced lung injury and suggests that BRP-39 plays an important role in the control of macrophage responsiveness and inflammation. Akt activation in macrophages has been described to determe the M1 and M2 phenotypes, specifically macrophage M2 differentiation that was associated with enhanced PI3 K/Akt signaling [46, 47]. A previous study from our group has reported that BRP-39 signaling activates Akt-ERK and p38 MAPK pathways [8]. So, it is possible that BRP-39 can affect the macrophage phenotype by modulating Akt signaling. Further studies would be required to define this relationship.

Thus, macrophage BRP-39 is a critical modifier of the oxygen-induced augmentation of inflammation and lung injury after intranasal LPS. In the absence of BRP-39, mice exposed to LPS plus oxygen exhibit more severe lung injury, and alveolar macrophages from these mice demonstrate an augmented proinflammatory M1 phenotype, known to be associated with poor outcomes. Furthermore, supplemental oxygen delivery along with LPS augments the macrophage proinflammatory state even in WT mice, at least in part, by attenuating BRP-39 after LPS and hyperoxia induction. Therefore, strategies to regulate BRP-39 expression in myeloid cells can be exploited to restrict the duration of M1 polarization and subsequent effects on inflammation and lung injury. However, additional studies are necessary to establish the (patho) physiological significance of our novel findings in the clinical setting.

5. Conclusion

In summary, we noted that a lack of BRP-39 in the developing lung led to both alveolar simplification and inflammatory pulmonary phenotype upon LPS administration, which was further worsened by hyperoxia exposure. These effects were associated with alterations in the macrophage polarization state from M2 to M1. We speculate that the M1/M2 polarization mediates the pulmonary effects of LPS or LPS plus hyperoxia in the developing lung. Our study has improved the understanding of the role of macrophage polarization in injury to developing lungs. Our findings have potential clinical relevance for addressing neonatal inflammatory disturbances of pulmonary development and highlight macrophage modulation as a potential intervention to cure BPD.

Authors' Contribution

M. A. Syed, V. Bhandari contributed to the concept and design of the paper. M. A. Syed contributed to the acquisition of data. M. A. Syed, V. Bhandari contributed to the data analysis and interpretation. M. A. Syed, V. Bhandari contributed to the drafting and/or critical revision for intellectual content. All authors have approved the version of the submitted manuscript.

Acknowledgment

This paper is supported in part by Grant HL85103 (V. Bhandari) from the NHLBI of the National Institutes of Health, USA.

References

[1] A. Bhandari and V. Bhandari, "Pitfalls, problems, and progress in bronchopulmonary dysplasia," *Pediatrics*, vol. 123, no. 6, pp. 1562–1573, 2009.

[2] A. N. Husain, N. H. Siddiqui, and J. T. Stocker, "Pathology of arrested acinar development in postsurfactant bronchopulmonary dysplasia," *Human Pathology*, vol. 29, no. 7, pp. 710–717, 1998.

[3] A. H. Jobe and M. Ikegami, "Antenatal infection/inflammation and postnatal lung maturation and injury," *Respiratory Research*, vol. 2, no. 1, pp. 27–32, 2001.

[4] A. Bhandari and V. Bhandari, "Pathogenesis, pathology and pathophysiology of pulmonary sequelae of bronchopulmonary dysplasia in premature infants," *Frontiers in Bioscience*, vol. 8, pp. e370–e380, 2003.

[5] V. Bhandari, "Hyperoxia-derived lung damage in preterm infants," *Seminars in Fetal and Neonatal Medicine*, vol. 15, no. 4, pp. 223–229, 2010.

[6] R. M. Viscardi, "Perinatal inflammation and lung injury," *Seminars in Fetal and Neonatal Medicine*, vol. 17, no. 1, pp. 30–35, 2012.

[7] E. Gwyer-Findlay and T. Hussell, "Macrophage-mediated inflammation and disease: a focus on the lung," *Mediators Inflammation*, vol. 2012, Article ID 140937, 6 pages, 2012.

[8] M. H. Sohn, M. J. Kang, H. Matsuura et al., "The chitinase-like proteins breast regression protein-39 and YKL-40 regulate hyperoxia-induced acute lung injury," *American Journal of Respiratory and Critical Care Medicine*, vol. 182, no. 7, pp. 918–928, 2010.

[9] A. Sica and A. Mantovani, "Macrophage plasticity and polarization: *in vivo* veritas," *The Journal of Clinical Investigation*, vol. 122, no. 3, pp. 787–795, 2012.

[10] S. Gordon and F. O. Martinez, "Alternative activation of macrophages: mechanism and functions," *Immunity*, vol. 32, no. 5, pp. 593–604, 2010.

[11] H. He, J. Xu, C. M. Warren et al., "Endothelial cells provide an instructive niche for the differentiation and functional polarization of M2-like macrophages," *Blood*, vol. 120, no. 15, pp. 3152–3162, 2012.

[12] A. Mantovani and M. Locati, "Orchestration of macrophage polarization," *Blood*, vol. 114, no. 15, pp. 3135–3136, 2009.

[13] Y. Schwartz and A. V. Svistelnik, "Functional phenotypes of macrophages and the M1-M2 polarization concept. Part I. pro-inflammatory phenotype," *Biochemistry*, vol. 77, no. 3, pp. 246–260, 2012.

[14] S. J. Van Dyken and R. M. Locksley, "Interleukin-4- and interleukin-13-mediated alternatively activated macrophages: roles in homeostasis and disease," *Annual Review of Immunology*, vol. 31, pp. 317–343, 2013.

[15] S. K. Biswas, M. Chittezhath, I. N. Shalova, and J. Y. Lim, "Macrophage polarization and plasticity in health and disease," *Immunologic Research*, vol. 53, no. 1–3, pp. 11–24, 2012.

[16] M. A. Syed, M. Joo, Z. Abbas et al., "Expression of TREM-1 is inhibited by PGD2 and PGJ2 in macrophages," *Experimental Cell Research*, vol. 316, no. 19, pp. 3140–3149, 2010.

[17] X. Zhang, R. Goncalves, and D. M. Mosser, "The isolation and characterization of murine macrophages," *Current Protocols in Immunology*, Chapter 14: p. Unit 14. 1, 2008.

[18] A. Harijith, R. Choo-Wing, S. Cataltepe et al., "A role for matrix metalloproteinase 9 in IFNγ-mediated injury in developing lungs: relevance to bronchopulmonary dysplasia," *American Journal of Respiratory Cell and Molecular Biology*, vol. 44, no. 5, pp. 621–630, 2011.

[19] V. Bhandari, R. Choo-Wing, C. G. Lee et al., "Developmental regulation of NO-mediated VEGF-induced effects in the lung," *American Journal of Respiratory Cell and Molecular Biology*, vol. 39, no. 4, pp. 420–430, 2008.

[20] R. Choo-Wing, J. H. Nedrelow, R. J. Homer, J. A. Elias, and V. Bhandari, "Developmental differences in the responses of IL-6 and IL-13 transgenic mice exposed to hyperoxia," *American Journal of Physiology*, vol. 293, no. 1, pp. 142–150, 2007.

[21] L. Johnson-Varghese, N. Brodsky, and V. Bhandari, "Effect of antioxidants on apoptosis and cytokine release in fetal rat type II pneumocytes exposed to hyperoxia and nitric oxide," *Cytokine*, vol. 28, no. 1, pp. 10–16, 2004.

[22] R. Gavino, L. Johnson, and V. Bhandari, "Release of cytokines and apoptosis in fetal rat type II pneumocytes exposed to hyperoxia and nitric oxide: modulatory effects of dexamethasone and pentoxifylline," *Cytokine*, vol. 20, no. 6, pp. 247–255, 2002.

[23] R. Choo-Wing, M. A. Syed, A. Harijith et al., "Hyperoxia and interferon-γ—induced injury in developing lungs occur via cyclooxygenase-2 and the endoplasmic reticulum stress-dependent pathway," *American Journal of Respiratory Cell and Molecular Biology*, vol. 48, no. 6, pp. 749–757, 2013.

[24] Z. H. Aghai, J. Camacho, J. G. Saslow et al., "Impact of histological chorioamnionitis on tracheal aspirate cytokines in premature infants," *American Journal of Perinatology*, vol. 29, no. 7, pp. 567–572, 2012.

[25] V. Bhandari, R. Choo-Wing, C. G. Lee et al., "Hyperoxia causes angiopoietin 2-mediated acute lung injury and necrotic cell death," *Nature Medicine*, vol. 12, no. 11, pp. 1286–1293, 2006.

[26] V. Bhandari, R. Choo-Wing, A. Harijith et al., "Increased hyperoxia-induced lung injury in nitric oxide synthase 2 null mice is mediated via angiopoietin 2," *American Journal of Respiratory Cell and Molecular Biology*, vol. 46, no. 5, pp. 668–676, 2012.

[27] H. Sun, R. Choo-Wing, J. Fan et al., "Small molecular modulation of macrophage migration inhibitory factor in the hyperoxia-induced mouse model of bronchopulmonary dysplasia," *Respiratory Research*, vol. 14, article 27, 2013.

[28] X. Liao, N. Sharma, F. Kapadia et al., "Krüppel-like factor 4 regulates macrophage polarization," *The Journal of Clinical Investigation*, vol. 121, no. 7, pp. 2736–2749, 2011.

[29] C. S. Dela Cruz, W. Liu, C. H. He et al., "Chitinase 3-like-1 promotes Streptococcus pneumoniae killing and augments host tolerance to lung antibacterial responses," *Cell Host & Microbe*, vol. 12, no. 1, pp. 34–46, 2012.

[30] H. Matsuura, D. Hartl, M. J. Kang et al., "Role of breast regression protein-39 in the pathogenesis of cigarette smoke-induced inflammation and emphysema," *American Journal of Respiratory Cell and Molecular Biology*, vol. 44, no. 6, pp. 777–786, 2011.

[31] Z. Yuan, M. A. Syed, D. Panchal, D. Rogers, M. Joo, and R. T. Sadikot, "Curcumin mediated epigenetic modulation inhibits TREM-1 expression in response to lipopolysaccharide," *The International Journal of Biochemistry & Cell Biology*, vol. 44, no. 11, pp. 2032–2043, 2012.

[32] S. Herold, K. Mayer, and J. Lohmeyer, "Acute lung injury: how macrophages orchestrate resolution of inflammation and tissue repair," *Frontiers in Immunology*, vol. 2, article 65, 2011.

[33] C. V. Jones, T. M. Williams, K. A. Walker et al., "M2 macrophage polarisation is associated with alveolar formation during postnatal lung development," *Respiratory Research*, vol. 14, article 41, 2013.

[34] L. K. Johnston, C. R. Rims, S. E. Gill, J. K. McGuire, and A. M. Manicone, "Pulmonary macrophage subpopulations in the induction and resolution of acute lung injury," *American Journal of Respiratory Cell and Molecular Biology*, vol. 47, no. 4, pp. 417–426, 2012.

[35] N. R. Aggarwal, F. R. D'Alessio, Y. Eto et al., "Macrophage A2A adenosinergic receptor modulates oxygen-induced augmentation of murine lung injury," *American Journal of Respiratory Cell and Molecular Biology*, vol. 48, no. 5, pp. 635–646, 2013.

[36] Z. H. Aghai, J. G. Saslow, K. Mody et al., "IFN-γ and IP-10 in tracheal aspirates from premature infants: relationship with bronchopulmonary dysplasia," *Pediatric Pulmonology*, vol. 48, no. 1, pp. 8–13, 2013.

[37] H. Qin, A. T. Holdbrooks, Y. Liu, S. L. Reynolds, L. L. Yanagisawa, and E. N. Benveniste, "SOCS3 deficiency promotes M1 macrophage polarization and inflammation," *Journal of Immunology*, vol. 189, no. 7, pp. 3439–3448, 2012.

[38] P. J. Murray and T. A. Wynn, "Protective and pathogenic functions of macrophage subsets," *Nature Reviews Immunology*, vol. 11, no. 11, pp. 723–737, 2011.

[39] M. A. Alikhan, C. V. Jones, T. M. Williams et al., "Colony-stimulating factor-1 promotes kidney growth and repair via alteration of macrophage responses," *American Journal of Pathology*, vol. 179, no. 3, pp. 1243–1256, 2011.

[40] M. A. O'Reilly, S. H. Marr, M. Yee, S. A. McGrath-Morrow, and B. P. Lawrence, "Neonatal hyperoxia enhances the inflammatory response in adult mice infected with influenza A virus," *American Journal of Respiratory and Critical Care Medicine*, vol. 177, no. 10, pp. 1103–1110, 2008.

[41] V. Bhandari, N. Hussain, T. Rosenkrantz, and M. Kresch, "Respiratory tract colonization with mycoplasma species increases the severity of bronchopulmonary dysplasia," *Journal of Perinatal Medicine*, vol. 26, no. 1, pp. 37–42, 1998.

[42] P. Fu, V. Mohan, S. Mansoor, C. Tiruppathi, R. T. Sadikot, and V. Natarajan, "Role of nicotinamide adenine dinucleotide phosphate-reduced oxidase proteins in *Pseudomonas aeruginosa*-induced lung inflammation and permeability," *American Journal of Respiratory Cell and Molecular Biology*, vol. 48, no. 4, pp. 477–488, 2013.

[43] Z. Yuan, D. Panchal, M. A. Syed et al., "Induction of cyclooxygenase-2 signaling by *Stomatococcus mucilaginosus* highlights the pathogenic potential of an oral commensal," *Journal of Immunology*, vol. 191, no. 7, pp. 3810–3817, 2013.

[44] K. Otsuka, H. Matsumoto, A. Niimi et al., "Sputum YKL-40 levels and pathophysiology of asthma and chronic obstructive pulmonary disease," *Respiration*, vol. 83, no. 6, pp. 507–519, 2012.

[45] J. L. Tan, S. T. Chan, E. M. Wallace, and R. Lim, "Human amnion epithelial cells mediate lung repair by directly modulating macrophage recruitment and polarization," *Cell Transplant*, 2013.

[46] A. Arranz, C. Doxaki, E. Vergadi et al., "Akt1 and Akt2 protein kinases differentially contribute to macrophage polarization," *Proceedings of the National Academy of Sciences of the United States of America*, vol. 109, no. 24, pp. 9517–9522, 2012.

[47] W. Zhang, W. Xu, and S. Xiong, "Macrophage differentiation and polarization via phosphatidylinositol 3-kinase/Akt-ERK signaling pathway conferred by serum amyloid P component," *Journal of Immunology*, vol. 187, no. 4, pp. 1764–1777, 2011.

Hindawi Publishing Corporation
Mediators of Inflammation
Volume 2013, Article ID 727189, 9 pages
http://dx.doi.org/10.1155/2013/727189

Research Article

Chemokines and Neurodegeneration in the Early Stage of Experimental Ischemic Stroke

Pawel Wolinski[1] and Andrzej Glabinski[1,2]

[1] *Department of Propedeutics of Neurology, Medical University of Lodz, ul. Pabianicka 62, Lodz, Poland*
[2] *Department of Neurology, Epileptology and Stroke, Medical University of Lodz, ul Zeromskiego 113, Lodz, Poland*

Correspondence should be addressed to Andrzej Glabinski; aglabinski@gmail.com

Received 25 July 2013; Revised 15 September 2013; Accepted 11 October 2013

Academic Editor: Alisa E. Koch

Neurodegeneration is a hallmark of most of the central nervous system (CNS) disorders including stroke. Recently inflammation has been implicated in pathogenesis of neurodegeneration and neurodegenerative diseases. The aim of this study was analysis of expression of several inflammatory markers and its correlation with development of neurodegeneration during the early stage of experimental stroke. Ischemic stroke model was induced by stereotaxic intracerebral injection of vasoconstricting agent endothelin-1 (ET-1). It was observed that neurodegeneration appears very early in that model and correlates well with migration of inflammatory lymphocytes and macrophages to the brain. Although the expression of several studied chemotactic cytokines (chemokines) was significantly increased at the early phase of ET-1 induced stroke model, no clear correlation of this expression with neurodegeneration was observed. These data may indicate that chemokines do not induce neurodegeneration directly. Upregulated in the ischemic brain chemokines may be a potential target for future therapies reducing inflammatory cell migration to the brain in early stroke. Inhibition of inflammatory cell accumulation in the brain at the early stage of stroke may lead to amelioration of ischemic neurodegeneration.

1. Introduction

Stroke is still a major cause of death and long-term disability worldwide and it is associated with significant clinical and socioeconomical problems. Despite the continuous efforts to develop the new pharmacological strategies, there is no effective neuroprotective therapy so far for ischemic stroke. Novel approaches are needed to improve the recovery and quality of life of stroke patients. Development of tissue damage after ischemic insult is dependent not only on duration and intensity of the blood flow reduction, but also on flow independent mechanisms, especially in the peri-infarct brain area. The blood flow dependent mechanisms of tissue damage develop in brain ischemic focus in the short time after onset of blood flow reduction. At that time cell death is a consequence of the acute energy failure and permanent anoxic cells depolarization is induced by loss of ionic gradients. A few hours later, the infarct expands into the adjacent penumbra, and cellular damage is mainly triggered by excitotoxicity, mitochondrial disturbances, reactive oxygen species production, and programmed cell death [1, 2].

Excitotoxicity is a pathologic process based on massive activation of AMPA and NMDA receptors in the brain. Inappropriate activation of AMPA and NMDA receptors is a trigger for subsequent dysregulation of calcium ions homeostasis in the neurons and finally results in neuronal loss. Massive activation of those receptors is observed in many CNS disorders including stroke, epilepsy, multiple sclerosis, amyotrophic lateral sclerosis, Parkinson, Alzheimer, and Huntington diseases. The most important factor leading to AMPA and NMDA upregulation is glutamate. Glutamate is an important neurotransmitter in physiological concentration, but in pathologically high concentration it is neurotoxic [3–5].

Lately, it is suggested that stroke triggers immune responses leading to inflammatory cell activation and infiltration of cerebral parenchyma. In the stroke brain upregulation of a variety of cytotoxic agents like cytokines, matrix metalloproteinases (MMPs), nitric oxide (NO), and more ROS can be detected [6–8]. There is also upregulation of expression of some chemokines like CCL2 in the CSF [9, 10] and serum of patients with stroke [11]. Studies in experimental stroke (middle cerebral artery occlusion model (MCAo)) confirmed involvement of chemokine CCL2 and its receptors CCR2 in stroke development [12]. Upregulated expression of CCL5 in serum of ischemic stroke patients is controversial. Zaremba et al. reported no difference in the level of CCL5 [13] but Montecucco and colleagues detected increased expression of plasma CCL5 in symptomatic as compared with asymptomatic patients [14]. Moreover, Canouï-Poitrine confirmed that, higher systemic levels of CCL5 and CXCL10 in asymptomatic men are independent predictors of ischemic stroke [15]. There is also a recent report from Tokami et al. supporting the concept that CCL5 may be neuroprotective during stroke development [16]. They showed upregulation of CCL5 but not CCL2, CCL3, and CCL4 on day 0 in stroke patients. This upregulation correlated with plasma concentrations of neuroprotective factors BDNF, EGF, and VEGF [16]. Other data from MCAo model also showed upregulation of several chemokines and their receptors including CCL7 [17], CXCL10 [18], CCL20 [19], and chemokine receptors CXCR4 [20] and CCR6 [19].

ET-1 induced model of stroke has been previously described by Anthony et al. who induced the acute rat cerebral blood volume changes after intravenous and intracranial injections of this vasoconstrictor [21, 22]. After microinjection of ET-1 into selected brain regions they observed using magnetic resonance imaging (MRI) an acute reduction of local perfusion in the injected hemisphere, loss of neurons in the grey matter and a macrophage/microglia and astrocyte response. After injection of ET-1 into the cortical white matter, those authors observed amyloid precursor protein-positive immunostaining (indicative of axonal disruption) and an increase in tau-1 immunostaining in oligodendrocytes. Similar to the grey matter lesions, no neutrophils were present and macrophage/microglia response did not occur. Additionally, no breakdown in the blood-brain barrier was detected in the white and grey matter [22].

In this study expression of several chemokines including: CCL2, CCL3, CCL5, and CXCL2 as well as expression of markers of neuroinflammation like CD3, F4/80, and IL-1 beta was studied. Correlation of this expression with intensity of early neurodegeneration detected in the brain during the ET-1 induced model of stroke was also analyzed.

2. Material and Methods

2.1. Animals. In all experiments, 8- to 12-week-old female SJL/J mice (n = five for each time point) were used. All animals were housed at the animal facility of The Medical University of Lodz, Lodz, Poland, under standard conditions. All animals were used in accordance with the Institutional Animal Care and Use Guidelines. All experiments in this study have been approved by the Local Ethics Committee for Affairs Experiments on Animals.

2.2. Induction of Endothelin-1 Induced Stroke Model. Animal stroke model was induced by stereotactic, intracerebral injection of endothelin-1 (ET-1, Sigma-Aldrich, Poznan, Poland,) (20 pmol in 1 μL of PBS per mouse) into the left hemisphere of the brain. ET-1 is a potent vasoconstrictor agent of small and large vessels. Prior injection mice were anaesthetized with mixture of ketamine (1,15 mg, Biowet, Pulawy, Poland) and ksylazine (0,1 mg, Biowet, Pulawy, Poland) per mouse. After complete anaesthetization mice were placed in stereotactic frame (David Kopf Instruments, CA, USA), skin on the head was cut, and a small hole in the skull was made using surgical drill. ET-1 was administered with a Hamilton syringe (32G needle) (Hamilton Company, Bonaduz, GR, Switzerland). Site of injection (A-2 mm, L-1, 2 mm, D-2, 5 mm) was selected using the stereotactic atlas "*The Mouse Brain in Stereotaxic Coordinates*" *Second Edition*, George Paxinos and Keith B.J. Franklin. Tissue samples were collected 24 and 72 hours after the model induction. As a controls, brains from uninjected mice and from mice injected in the same way with PBS were used.

2.3. Extraction of RNA and Proteins. To obtain RNA animals, were perfused with a saline solution. Tissues were weighed and then homogenized using a mechanical homogenizer Ultra Turrax (IKA, Staufen, Germany). Tissues were homogenized in a volume of 1ml of TRIzol LS Reagent (Gibco BRL, Invitrogen, Carlsbad, CA, USA). Homogenates were stored at −80°C until use. RNA was isolated from the homogenates with TRIzol LS Reagent using phenol-chloroform method described by Chomczynski and Sacchi (Chomczynski and Sacchi, 1987). After RNA isolation, its concentration was estimated using the photometric method (BioPhotometr Plus, Eppendorf Company, Wien, Austria). To obtain the proteins for the ELISA assay, the animals were perfused with a saline solution. Harvested organs were weighed using a laboratory balance (Radwag Radom, Poland) and homogenized using a mechanical homogenizer Ultra Turrax (IKA). Homogenisation was performed in a volume of 1 mL HEPES buffer pH 7.4 containing: HEPES −20 mM; EDTA −1.5 mM; benzamidynę −0.5 mM; chicken egg owoinhibitor −10 ug/mL PMSF (phenylmetylsulfonyl fluoride) −0.1 mM (Sigma-Aldrich, Poznan, Poland). After homogenization homogenates were frozen and stored at −80°C. Supernatants were obtained after centrifugation (20 000 × g, time 30 minutes at 4°C MPW, Warsaw, Poland).

2.4. Analysis of Gene Expression at the RNA Level by Real-Time PCR. Analysis of the RNA expression was performed using the Corbett Real-Time PCR Machine Rotor Gene 3000 apparatus (Corbett Research, Sydney, Australia). The key enzyme used in this reaction was Taq polymerase with activity of 5 U/mL. Additional reaction components were buffer for polymerase, 25 mm MgCl2, 10 mM dNTPs, fluorescent dye EvaGreen (Biomibo, Warsaw, Poland), 10 μM primers

specific to the duplicated sequences, and RNase/DNase free water. For each reaction 2 μL of cDNA derived from the reverse transcription reaction was used and the total volume was 20 μL. As a control histone H3 gene and reference RNA (QPCR Mouse Reference Total cellular RNA, Stratagene, La Jolla, CA, USA) were used.

2.5. Analysis of Gene Expression at the Protein Level by ELISA. Quantitative analysis of gene expression at the protein level was performed using ELISA method with commercially available immunoenzymatic Quantikine Kits (R & D Systems, MN, USA). Each set consisted of 96 well plates coated by manufacturer, standard proteins used to prepare the calibration, secondary and tertiary antibodies combined with the horseradish peroxidase enzyme, and washing buffer and color substrate for peroxidase. The assay procedure was performed according to the protocol provided by the manufacturer. After stopping the color reaction protein concentration was evaluated using a photometric reader VICTOR2 Wallac 1420 (PerkinElmer, Waltham, MA, USA) with for 450 nm filters, corrected at 595 nm. All samples were analyzed in duplicates.

2.6. Quantitative Assessment of the Level of Neurodegeneration Using ELISA Method. Quantitative assessment of the intensity of neurodegeneration was performed using ELISA method with primary antibodies directed against phosphorylated neurofilaments. The first step was the coating of 96 well Maxisorb Microtitre plate (Nunc, Roskilde, Denmark) with monoclonal anti-NfH antibodies (SMI35R, Sternberger Monoclonals, Convance Princeton, NJ, USA) and overnight incubation at 4°C. Primary antibodies were diluted in carbonate buffer, pH 9.6. The next day tested samples and standard curve samples (neurofilament 200 kD, Progen, Heidelberg, Germany) were added. As a secondary antibody rabbit polyclonal antineurofilament 200 antibody (Sigma-Aldrich, Poznan, Poland) was used. As a tertiary antibody swine antibodies against rabbit immunoglobulin conjugated with horseradish peroxidase (Dako, Glostrup, Denmark) were used. The final step was the addition of color substrate for horseradish peroxidase, which was 3,3′5,5′-tetramethylbenzidine (Sigma-Aldrich, Poznan, Poland). Inhibition of the reaction was performed with 1 M HCl and finally color photometric assessment was done using VICTOR2 reader Wallac 1420 (PerkinElmer, Waltham, MA, USA). The analysis was performed using 450 nm filter with correction at 595 nm. All samples were analyzed in duplicates and the concentration of NfH was determined by referring to the standard curve.

2.7. Detection of Localization of Neurodegeneration Using Fluoro-Jade C Dye. Assessment of the localization and severity of neurodegeneration at the level of protein was performed using the fluorescent Fluoro-Jade C dye (Chemicon, Millipore, Warsaw, Poland). Animals were perfused with 4% buffered formalin solution and tissues samples were embedded in paraffin blocks. 10 μm thick sections were applied to a polished Super Frost slides (Menzel-Glaser Braunschweig, Germany). Before final staining paraffin was removed by one hour incubation at 60°C and two 10-minute incubations in xylenes. Tissue was rehydrated in a series of alcohols. Fluoro-Jade C staining was performed according to the protocol provided by the manufacturer (Chemicon). For staining of nuclei sections were counterstained using the blue fluorescent dye DAPI (Sigma-Aldrich, Poznan, Poland). Then the tissue was mounted and coverslipped using DPX (Sigma-Aldrich, Poznan, Poland).

2.8. Image Acquisition. For the analysis and acquisition of images an inverted microscope AxioObserver A1 (Carl Zeiss Inc., Goettingen, Germany) was used. The following lenses made by Carl Zeiss Inc. were used: Plan-Achromat: 4X/0.10, A- Plan 10X/0.25 Ph1; LD A-Plan 20X/0.3; LD Plan-Neofluar 40X/0.6, Ph2 Korr. The images were obtained with a digital camera, AxioCam MRc5 (Carl Zeiss Group, Goettingen, Germany) attached to the microscope. For image acquisition we used Axio-Vision Rel. 4.6 software (Carl Zeiss Group). After obtaining an image no further processing was necessary.

2.9. Statistical Analysis. For statistical analysis nonparametric Kruskal-Wallis and Mann-Whitney tests were used. For correlation analyses Kendal tau test was used. A value of $P < 0.05$ was considered statistically significant.

3. Results

3.1. Expression of Inflammatory Markers in the Brain during the Early Stage of Animal Model of Stroke. Significant upregulation of expression of T cell line marker - CD3 was observed in the ET-1-injected hemisphere at 72 h after injection ($P = 0.03$, Mann-Whitney test) (Figure 1(a)). At that time a significant difference in expression of CD3 was detected between ipsilateral and contralateral hemispheres ($P = 0.019$, Mann-Whitney test) (Figure 1(a)). Expression of CD3 in ipsilateral hemisphere was also increased when compared to PBS injected hemisphere ($P = 0.28$, Mann-Whitney test).

The expression of monocyte/macrophage lineage marker F4/80 was significantly elevated only in ET-1 injected hemisphere at 72 hours after injection. At that time significant difference was observed in expression of F4/80 between ET-1 injected hemisphere and untreated control group ($P = 0.022$; Mann-Whitney test) (Figure 1(b)). We detected also a significant difference in expression of F4/80 between ipsilateral and contralateral hemispheres of ET-1 injected mice at 72 hours after injection ($P = 0.035$, Mann-Whitney test) (Figure 1(b)).

Upregulation of cytokine IL-1β expression was observed in ET-1 injected hemispheres only at 24 h after injection. Significant difference in expression of IL-1β was observed between contralateral hemispheres and normal control group at 72 hours after injection ($P = 0.03$ and 0.019, resp.; Mann-Whitney test) (Figure 1(c)). We detected also a significant difference in expression of IL-1β between ipsilateral and contralateral hemispheres of ET-1 injected mice 72 hours after injection ($P = 0.019$, $P = 0.019$, resp.; Mann-Whitney test) (Figure 1(c)).

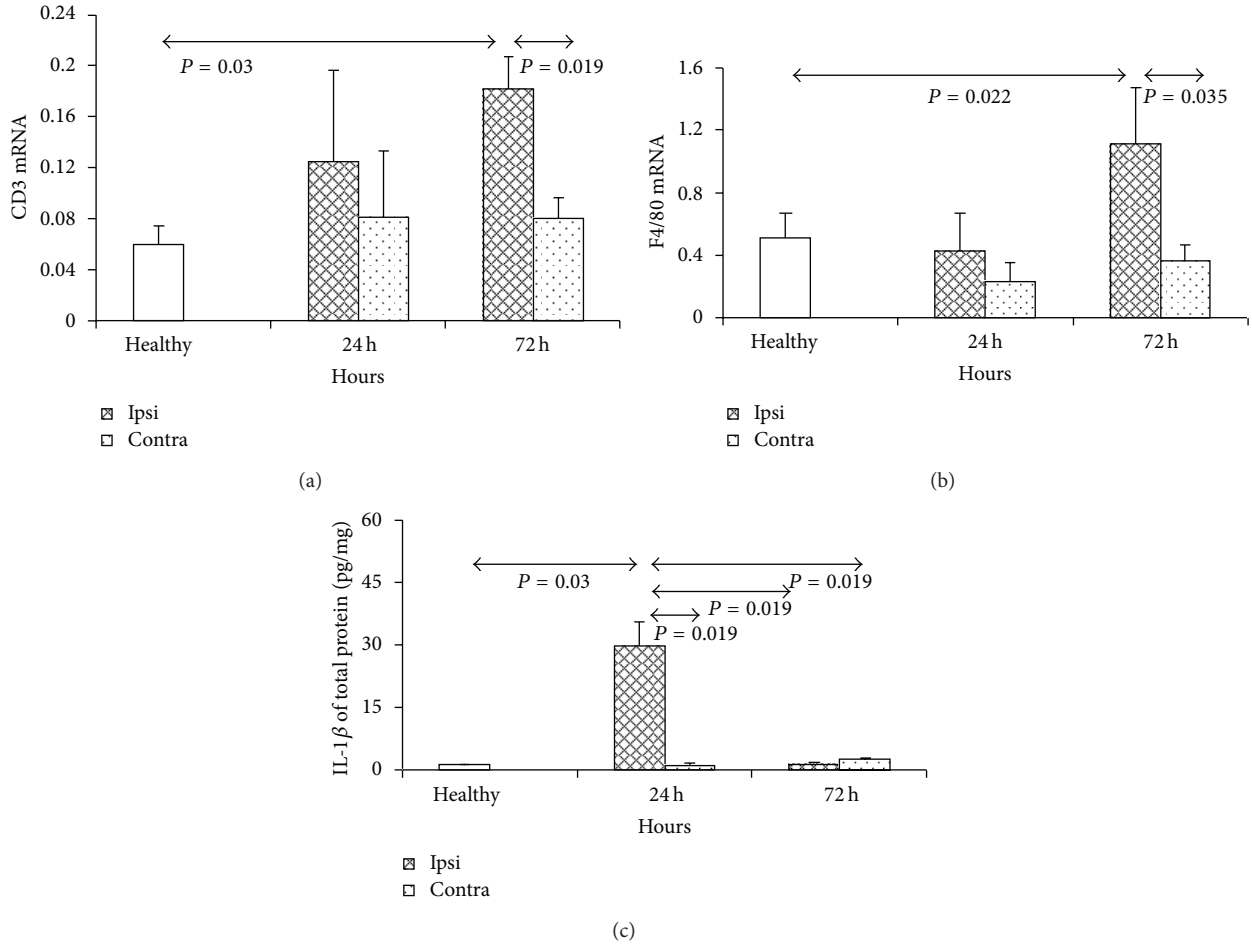

Figure 1: Expression of T cell line marker CD3 (a), macrophage cell line marker F4/80 (b), and inflammatory cytokine IL1 beta (c) in mouse brain during acute stroke model induced by ET-1. The model was induced as described in Materials and Methods. Each analysed group contained 5 mice. Bars represented mean ± SD. Ipsi hemisphere injected with ET-1, contra-contralateral hemisphere, healthy- normal uninjected control.

3.2. Expression of Chemokines in ET-1-Induced Stroke Model. Upregulation of chemokine CCL2 expression was observed in ipsilateral hemispheres at 24 and 72 h after injection of ET-1 ($P = 0.005$, $P = 0.005$, resp.; Mann-Whitney test) (Figure 2(a)). At 24 h CCL2 expression in ipsilateral hemisphere was significantly higher than at 72 h ($P = 0.019$; Mann-Whitney test). Significant difference in CCL2 expression after ET-1 injection was also observed between ipsilateral and contralateral hemispheres at 24 h and 72 h ($P = 0.012$ and 0.036, resp.; Mann-Whitney test) (Figure 2(a)).

We also showed that during early stage of ET-1-injection stroke model expression of CCL3 is significantly upregulated at 24 and 72 h after model induction (Figure 2(b)). There was significant upregulation of CCL3 expression in ipsilateral hemispheres of ET-1 injected mice in comparison to normal controls and contralateral hemispheres at 24 h after injection ($P = 0.008$ and 0.012, resp.; Mann-Whitney test). At 72 h after model induction we observed significant upregulation of CCL3 expression in ET-1-injected hemispheres in comparison to normal brains and contralateral hemispheres ($P = 0.014$ and 0.019, resp.; Mann-Whitney test) (Figure 2(b)).

Increased expression of the third analyzed inflammatory chemokine—CCL5 was observed in ET-1-injected hemispheres in comparison to uninjected animals at 24 and 72 h ($P = 0.008$, and 0.008 resp.; Mann-Whitney test) (Figure 2(c)). Significant difference was also observed in CCL5 expression between ipsilateral and contralateral hemispheres at 24 h and 72 h after injection of ET-1 ($P = 0.008$ and 0.012, resp.; Mann-Whitney test) (Figure 2(c)).

Initially increasing expression of CXCL2 in ET-1 injected hemispheres was detected with the peak at 24 h and subsequent decrease at 72 h but still significantly higher than in normal controls ($P = 0.036$, and 0.036, resp.; Mann-Whitney test) (Figure 2(d)). At 24 h CXCL2 expression in ipsilateral hemisphere was significantly higher than at 72 h ($P = 0.012$; Mann-Whitney test) and then at 24 h after ET-1 injection in contralateral hemispheres ($P = 0.012$; Mann-Whitney test) (Figure 2(d)).

The expression of CXCL12 in the ET-1 and PBS-injected brains and normal controls did not show a significant difference between analysed groups (data not shown).

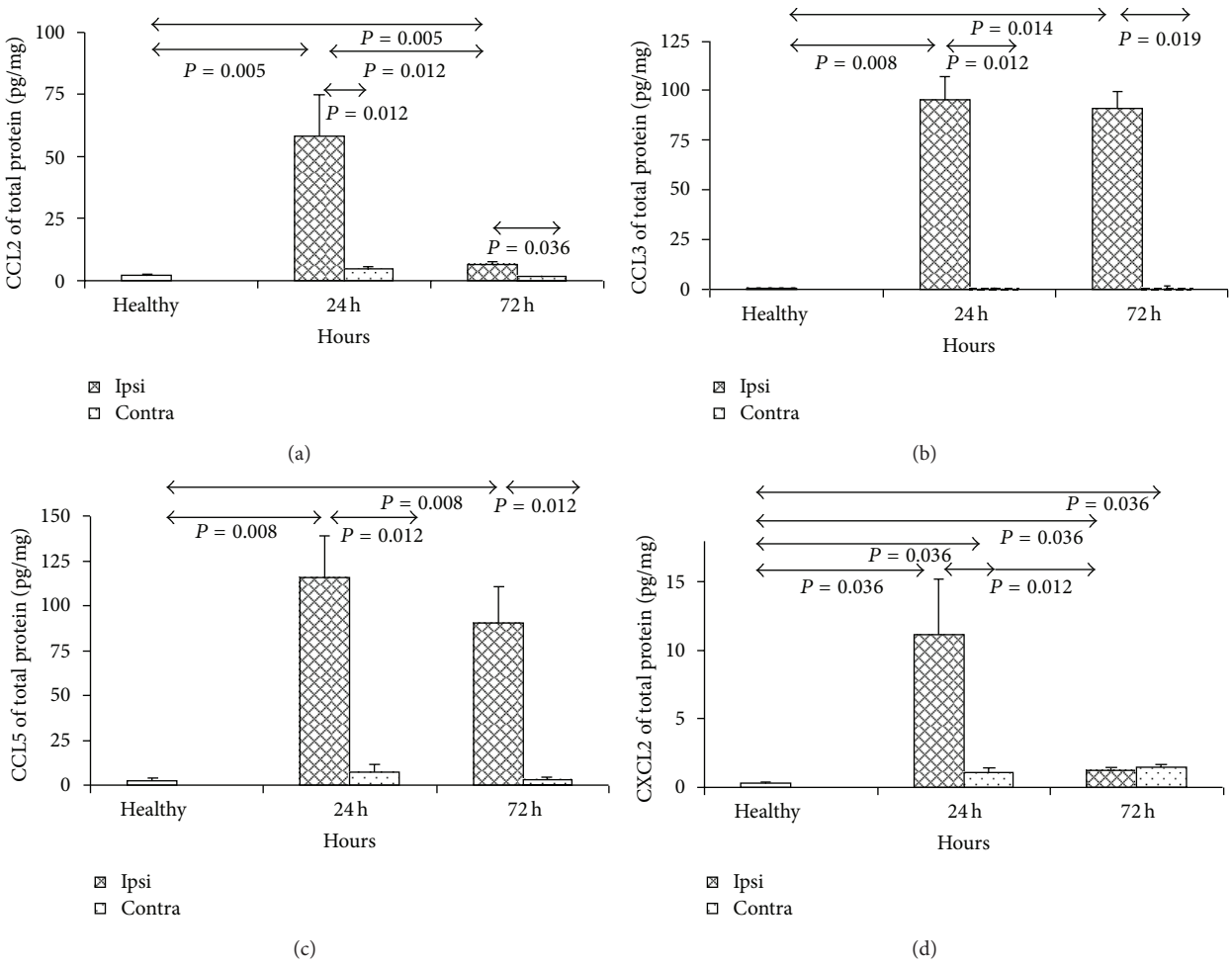

Figure 2: Expression of chemokines CCL2 (a), CCL3 (b), CCL5 (c), and CXCL2 (d) in mouse brain during acute stroke model induced by ET-1. The model was induced as described in Section 2. Each analysed group contained 5 mice. Bars represented mean and ±SD. Ipsi hemisphere injected with ET-1, contra-contralateral hemisphere, healthy- normal uninjected control.

3.3. Analysis of Intensity and Localization of Neurodegeneration in ET-1-Induced Stroke Model. The most severe neurodegeneration was observed in ET-1-injected hemispheres at 24 and 72 h after model induction ($P = 0.019$ and 0.029, resp.; Mann-Whitney test) (Figure 3(a)). There was also increased neurodegeneration in contralateral hemispheres of ET-1 injected mice at 24 and 72 h, but it was significantly lower than in ipsilateral hemispheres ($P = 0.03$, and 0.03, resp.; Mann-Whitney test) (Figure 3(a)).

The localization of ischemic lesion was detected in ET-1 injected ipsilateral hemispheres using cresyl violet staining (Figure 3(b), large box). Inside the ischemic focus injured neurons were abundant (detected by Fluoro-Jade and marked by arrows) cells nuclei counterstained with DAPI are marked on the picture by arrowheads (Figure 3(c)).

3.4. Correlation between Inflammatory Markers and Neurodegeneration in ET-1 Stroke Model. We observed the positive correlation between expression of lymphocyte lineage marker CD3 (Kendall Tau = −0,62; $P = 0.0004$) (Figure 4(a)) as well as monocyte/macrophage lineage marker F4/80 (Kendall Tau = −0,56; $P = 0.0007$) (Figure 4(b)) and the severity of neurodegeneration in ET-1 injected brain hemispheres.

Although the expression of several studied chemotactic inflammatory mediators (chemokines CCL2, CCL3, CCL5, and CXCL2) was significantly increased in the early stage of this stroke model, there was no clear correlation between this expression and intensity of neurodegeneration (data not shown).

4. Discussion

In this study we analyzed potential relationship between neuroinflammation and neurodegeneration in experimental model of ischemic stroke induced by intracerebral ET-1 injection. We focused on a group of proinflammatory chemokines, especially the classical representatives of CCL subfamily. The reason for selecting these chemokines was their confirmed participation in pathogenesis of many central nervous system diseases. During the first few days of the experimental brain ischemia we observed increasing neurodegeneration in ET-1 injected hemisphere. There are several studies showing

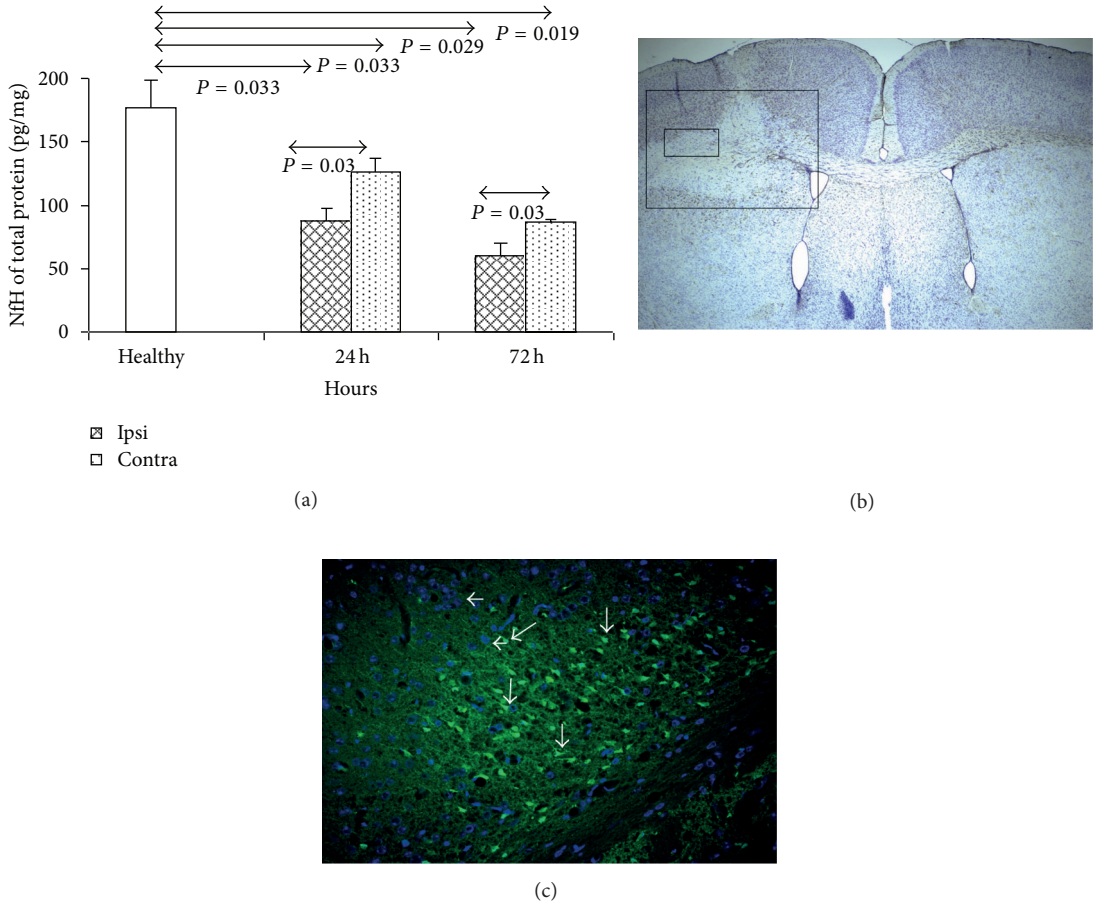

Figure 3: Neurodegeneration in stroke model induced by ET-1. (a) Quantitative analysis of neurodegeneration using ELISA for phosphorylated neurofilaments, (b) localization of neurodegeneration using Cresyl violet staining and GFAP-counterstaining. Large box-stroke area (72 h after ET-1 induction), small box-area showed in C. (c) Localization of neurodegeneration in a stroke model using Fluoro-Jade C staining. White arrows-degenerated neurons. The model was induced and staining performed as described in Materials and Methods. Each analysed group contained 5 mice. Bars represented mean ± SD. Ipsi hemisphere injected with ET-1, contra-contralateral hemisphere, healthy - normal uninjected control.

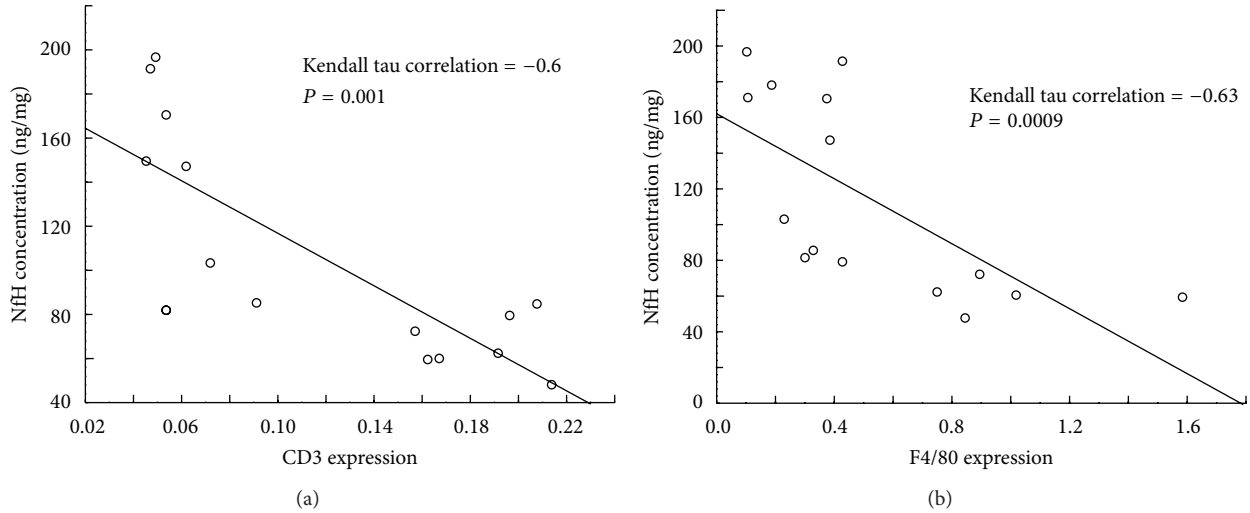

Figure 4: Positive correlation between development of inflammation measured by expression of T cell line marker CD3 (a) and macrophage marker F4/80 (b) with intensity of neurodegeneration measured by ELISA for phosphorylated neurofilaments in ET-1 injected ischemic hemisphere. ET-1 model of stroke was induced as described in Section 2.

that neurodegeneration occurs early during brain ischaemia [23, 24]. At that time also inflammatory changes appear in ischemic brain area [25]. The relationship between those two processes is complex and still requires further studies. To measure the intensity of neuroinflammation the expression of inflammatory cells markers (CD3 for T cells and F4/80 for monocytes/macrophages) has been measured at the same time. This analysis showed increased lymphocyte migration to ischemic brain hemisphere at 72 h after model induction. Similarly, infiltration of ipsilateral hemisphere by monocytes/macrophages was significantly increased at 72 h after initiation of brain ischemia. Comparable observation was reported by others who showed the presence of macrophages/activated microglia at 72 h after intracerebral injection of ET-1 to rat brain [22]. In another study using MCAo stroke model, the influx of mononuclear cells to the site of brain ischemia was recorded between 2 and 15 days after model induction [26].

The presence of neuroinflammation during early brain ischemia was also confirmed in our study by elevated expression of inflammatory mediator-cytokine IL-1β. Its presence was observed as early as 24 h after model induction. Expression of IL-1β during brain ischemia has been detected by Barone et al. in several cell types including astrocytes, microglia, neurons, and endothelium [27]. In another study increased production of IL-1β was reported even at 3–6 hours after induction of brain ischemia. The peak of this expression was observed at 12 h, and it returned to baseline level after 5 days. Other studies confirmed also that inflammatory mediators, such as IL-1β and TNFα, are important contributors to CNS neural tissue damage induced by ischemia [28, 29].

In our stroke model analysis of the relationship between the infiltration of ischemic hemisphere by mononuclear inflammatory cells and the intensity of neurodegeneration measured by the presence of phosphorylated neurofilaments showed positive correlation. This may suggest that there is close connection between neuroinflammation and neurodegeneration in ischemic stroke. Migration of inflammatory cells from the blood to the ischemic brain may be at least partially induced by chemotactic cytokines-chemokines. To study this concept we analyzed the expression of some chemokines in the brain. The highest expression of CCL2 was observed in our model at 24 h after initiation of brain ischemia. Increased expression of CCL2 was still observed at 72 h but was at that time significantly lower. Increased expression of CCL2 in MCAo model in the ipsilateral hemisphere was observed on neurons at 12 h and on astrocytes at 24 h after cardiac arrest, suggesting that these cells are the potential source of CCL2 during ischemic stroke [30]. Minami and Satoh using double *in situ* hybridization method pointed to microglia as the cellular source of CCL2 during MCAo [31]. It was shown in another MCAo study that CCL2 leads to infiltration of the CNS by monocytes and thus enhances brain damage induced by ischemia [30]. Also in human stroke patients elevated level of CCL2 was detected in cerebrospinal fluid and serum [9, 11].

The highest CCL3 expression was detected at 24 h after ET-1 injection. At 72 h this expression was still increased but it was much lower than at 24 h. Also at the protein level we observed significant increase in CCL3 production in the ischemic hemisphere. Our results are in line with the report by Gourmala et al. who observed an increase in CCL3 expression at mRNA level already at 1 h after MCAo in rats, with peak expression at 8–16 h [32]. In addition, they observed higher expression of CCL3 during temporary MCAo than in permanent MCAo, suggesting the impact of reperfusion on the neuroinflammation in the damaged tissue. Gourmala et al. using *in situ* hybridization localized the expression of CCL3 on microglial cells/macrophages during brain ischemia [32]. In addition, another studies have concluded that CCL3 application to the brain ventricles after complete MCAo enhances MCAo harmful effects [33].

We observed almost 46-fold and 30-fold increase in CCL5 expression at 24 h and 72 h, respectively, after induction of ET-1 induced stroke model. There are only a few reports concerning the role of CCL5 in the development of ischemic stroke [15]. Zaremba et al. showed no difference in the level of CCL5 in serum from stroke patients [13]. It was suggested that CCL5 mediates blood-brain-barrier (BBB) disruption and CNS tissue damage as well as inflammation after reperfusion during MCAo model. Terao et al. suggested that platelets are the potential source of CCL5 in rats with MCAo [34]. These data were not confirmed by Tokami and colleagues who observed neuroprotective effect of CCL5 in ischemic stroke suggesting that CCL5 is expressed during stroke mostly in neurons [16].

In ET-1 induced experimental stroke a significant increase in CXCL2 expression at 24 h after brain ischemia induction was also observed. This increase returned to the baseline level 48 h later. Rabuffetti et al. observed increased expression of CXCL2 in the brain of rats with the permanent MCAo [35] as well as in the brain and spleen during temporary MCAo in mice. In other study increased CXCL2 expression was observed at 6 h of reperfusion and decreased by almost half at 22 h after reperfusion [36]. Vikman et al. showed increased CXCL2 expression in the brain vessels in the model of subarachnoid haemorrhage and in organotypic cultures [37]. CXCL2 involvement in the inflammatory process in the CNS during MCAo was also confirmed in a SCID mice. MCAo induced in SCID mice led to development of significantly reduced area of brain damage and lower inflammatory infiltration in ipsilateral hemispheres. Reduced expression of many inflammatory mediators including CXCL2 was also observed in T- and B-cell-deficient mice MCAo study [38]. Unfortunately, therapy of ischemic stroke with CXCL2 receptor-CXCR2 antagonists SB225002 was not successful [39]. In report presented by Copin et al. the CXCL1/CXCL2 chemokine-binding protein Evasin-3 treatment was associated with reduction in neutrophilic inflammation in mice MCAo model. However, Evasin-3 administration after cerebral ischemia onset failed to improve poststroke outcomes [40].

Although in our study the expression of several studied chemokines was significantly increased at the early phase of ET-1 induced stroke model, no clear correlation of this expression with neurodegeneration was observed. These data indicates that chemokines do not induce neurodegeneration directly. Instead of that they suggest that inhibition of

inflammatory cell accumulation in the brain at the early stage of stroke may lead to amelioration of ischemic neurodegeneration. Upregulated in the ischemic brain chemokines may be a potential target for future therapies reducing inflammatory cell migration to the brain in early stroke.

Acknowledgments

This study was supported by the European Union FP6 (INNOCHEM, grant number LSHB-CT-2005-518167) and research grant N N401 1275 33 from the Polish Ministry of Science and Higher Education.

References

[1] U. Dirnagl, C. Iadecola, and M. A. Moskowitz, "Pathobiology of ischaemic stroke: an integrated view," *Trends in Neurosciences*, vol. 22, no. 9, pp. 391–397, 1999.

[2] K.-A. Hossmann, "Pathophysiology and therapy of experimental stroke," *Cellular and Molecular Neurobiology*, vol. 26, no. 7-8, pp. 1057–1083, 2006.

[3] T. Anzai, K. Tsuzuki, N. Yamada et al., "Overexpression of Ca^{2+}-permeable AMPA receptor promotes delayed cell death of hippocampal CA1 neurons following transient forebrain ischemia," *Neuroscience Research*, vol. 46, no. 1, pp. 41–51, 2003.

[4] S. Liu, L. Lau, J. Wei et al., "Expression of Ca^{2+}-permeable AMPA receptor channels primes cell death in transient forebrain ischemia," *Neuron*, vol. 43, no. 1, pp. 43–55, 2004.

[5] T.-H. Yeh, H.-M. Hwang, J.-J. Chen, T. Wu, A. H. Li, and H.-L. Wang, "Glutamate transporter function of rat hippocampal astrocytes is impaired following the global ischemia," *Neurobiology of Disease*, vol. 18, no. 3, pp. 476–483, 2005.

[6] P. Ludewig, J. Sedlacik, M. Gelderblom et al., "Carcinoembryonic antigen-related cell adhesion molecule 1 inhibits MMP-9-mediated blood-brain-barrier breakdown in a mouse model for ischemic stroke," *Circulation Research*, vol. 113, no. 8, pp. 1013–1022, 2013.

[7] A. Abdullah, V. Ssefer, U. Ertugrul et al., "Evaluation of serum oxidant/antioxidant balance in patients with acute stroke," *Journal of Pakistan Medical Association*, vol. 63, no. 5, pp. 590–593, 2013.

[8] H. Hyun, K. Lee, K. H. Min et al., "Ischemic brain imaging using fluorescent gold nanoprobes sensitive to reactive oxygen species," *Journal of Controlled Release*, vol. 170, no. 3, pp. 352–357, 2013.

[9] J. Losy and J. Zaremba, "Monocyte chemoattractant protein-1 is increased in the cerebrospinal fluid of patients with ischemic stroke," *Stroke*, vol. 32, no. 11, pp. 2695–2696, 2001.

[10] A. M. Stowe, B. K. Wacker, P. D. Cravens et al., "CCL2 upregulation triggers hypoxic preconditioning-induced protection from stroke," *Journal of Neuroinflammation*, vol. 9, article 33, 2012.

[11] A. Arakelyan, J. Petrkova, Z. Hermanova, A. Boyajyan, J. Lukl, and M. Petrek, "Serum levels of the MCP-1 chemokine in patients with ischemic stroke and myocardial infarction," *Mediators of Inflammation*, vol. 2005, no. 3, pp. 175–179, 2005.

[12] M. W. Sieber, R. A. Claus, O. W. Witte, and C. Frahm, "Attenuated inflammatory response in triggering receptor expressed on myeloid cells 2 (TREM2) knock-out mice following stroke," *PLoS ONE*, vol. 8, no. 1, Article ID e52982, 2013.

[13] J. Zaremba, J. Ilkowski, and J. Losy, "Serial measurements of levels of the chemokines CCL2, CCL3 and CCL5 in serum of patients with acute ischaemic stroke," *Folia Neuropathologica*, vol. 44, no. 4, pp. 282–289, 2006.

[14] F. Montecucco, S. Lenglet, A. Gayet-Ageron et al., "Systemic and intraplaque mediators of inflammation are increased in patients symptomatic for ischemic stroke," *Stroke*, vol. 41, no. 7, pp. 1394–1404, 2010.

[15] F. Canouï-Poitrine, G. Luc, Z. Mallat et al., "Systemic chemokine levels, coronary heart disease, and ischemic stroke events: the PRIME study," *Neurology*, vol. 77, no. 12, pp. 1165–1173, 2011.

[16] H. Tokami, T. Ago, H. Sugimori et al., "RANTES has a potential to play a neuroprotective role in an autocrine/paracrine manner after ischemic stroke," *Brain Research*, vol. 1517, pp. 122–132, 2013.

[17] X. Wang, X. Li, S. Yaish-Ohad, H. M. Sarau, F. C. Barone, and G. Z. Feuerstein, "Molecular cloning and expression of the rat monocyte chemotactic protein-3 gene: a possible role in stroke," *Molecular Brain Research*, vol. 71, no. 2, pp. 304–312, 1999.

[18] X. Wang, X. Li, D. B. Schmidt et al., "Identification and molecular characterization of rat CXCR3: receptor expression and interferon-inducible protein-10 binding are increased in focal stroke," *Molecular Pharmacology*, vol. 57, no. 6, pp. 1190–1198, 2000.

[19] Y. Terao, H. Ohta, A. Oda, Y. Nakagaito, Y. Kiyota, and Y. Shintani, "Macrophage inflammatory protein-3alpha plays a key role in the inflammatory cascade in rat focal cerebral ischemia," *Neuroscience Research*, vol. 64, no. 1, pp. 75–82, 2009.

[20] B. Schönemeier, S. Schulz, V. Hoellt, and R. Stumm, "Enhanced expression of the CXCl12/SDF-1 chemokine receptor CXCR7 after cerebral ischemia in the rat brain," *Journal of Neuroimmunology*, vol. 198, no. 1-2, pp. 39–45, 2008.

[21] N. R. Sibson, A. M. Blamire, V. H. Perry, J. Gauldie, P. Styles, and D. C. Anthony, "TNF-α reduces cerebral blood volume and disrupts tissue homeostasis via an endothelin- and TNFR2-dependent pathway," *Brain*, vol. 125, no. 11, pp. 2446–2459, 2002.

[22] P. M. Hughes, D. C. Anthony, M. Ruddin et al., "Focal lesions in the rat central nervous system induced by endothelin-1," *Journal of Neuropathology and Experimental Neurology*, vol. 62, no. 12, pp. 1276–1286, 2003.

[23] F. J. Northington, D. M. Ferriero, E. M. Graham, R. J. Traystman, and L. J. Martin, "Early neurodegeneration after hypoxia-ischemia in neonatal rat is necrosis while delayed neuronal death is apoptosis," *Neurobiology of Disease*, vol. 8, no. 2, pp. 207–219, 2001.

[24] K. C. Chan, K. X. Cai, H. X. Su et al., "Early detection of neurodegeneration in brain ischemia by manganese-enhanced MRI," in *Proceedings of the Annual International Conference of the IEEE Engineering in Medicine and Biology Society*, vol. 2008, pp. 3884–3887, 2008.

[25] B. Rodriguez-Grande, V. Blackabey, B. Gittens et al., "Loss of substance P and inflammation precede delayed neurodegeneration in the substantia nigra after cerebral ischemia," *Brain, Behavior, and Immunity*, vol. 29, pp. 51–61, 2013.

[26] P. M. Kochanek and J. M. Hallenbeck, "Polymorphonuclear leukocytes and monocytes/macrophages in the pathogenesis of cerebral ischemia and stroke," *Stroke*, vol. 23, no. 9, pp. 1367–1379, 1992.

[27] F. C. Barone, B. Arvin, R. F. White et al., "Tumor necrosis factor-α: a mediator of focal ischemic brain injury," *Stroke*, vol. 28, no. 6, pp. 1233–1244, 1997.

[28] G. Z. Feuerstein, X. Wang, and F. C. Barone, "The role of cytokines in the neuropathology of stroke and neurotrauma," *NeuroImmunoModulation*, vol. 5, no. 3-4, pp. 143–159, 1998.

[29] T. Chiba, T. Itoh, M. Tabuchi et al., "Interleukin-1beta accelerates the onset of stroke in stroke-prone spontaneously hypertensive rats," *Mediators of Inflammation*, vol. 2012, Article ID 701976, 2013.

[30] Y. Chen, J. M. Hallenbeck, C. Ruetzler et al., "Overexpression of monocyte chemoattractant protein 1 in the brain exacerbates ischemic brain injury and is associated with recruitment of inflammatory cells," *Journal of Cerebral Blood Flow and Metabolism*, vol. 23, no. 6, pp. 748–755, 2003.

[31] M. Minami and M. Satoh, "Chemokines and their receptors in the brain: pathophysiological roles in ischemic brain injury," *Life Sciences*, vol. 74, no. 2-3, pp. 321–327, 2003.

[32] N. G. Gourmala, S. Limonta, D. Bochelen, A. Sauter, and H. W. G. M. Boddeke, "Localization of macrophage inflammatory protein: macrophage inflammatory protein-1 expression in rat brain after peripheral administration of lipopolysaccharide and focal cerebral ischemia," *Neuroscience*, vol. 88, no. 4, pp. 1255–1266, 1999.

[33] S. Takami, M. Minami, I. Nagata, S. Namura, and M. Satoh, "Chemokine receptor antagonist peptide, viral MIP-II, protects the brain against focal cerebral ischemia in mice," *Journal of Cerebral Blood Flow and Metabolism*, vol. 21, no. 12, pp. 1430–1435, 2001.

[34] S. Terao, G. Yilmaz, K. Y. Stokes et al., "Blood cell-derived RANTES mediates cerebral microvascular dysfunction, inflammation, and tissue injury after focal ischemiareperfusion," *Stroke*, vol. 39, no. 9, pp. 2560–2570, 2008.

[35] M. Rabuffetti, C. Sciorati, G. Tarozzo, E. Clementi, A. A. Manfredi, and M. Beltramo, "Inhibition of caspase-1-like activity by Ac-Tyr-Val-Ala-Asp-chloromethyl ketone induces long-lasting neuroprotection in cerebral ischemia through apoptosis reduction and decrease of proinflammatory cytokines," *Journal of Neuroscience*, vol. 20, no. 12, pp. 4398–4404, 2000.

[36] H. Offner, S. Subramanian, S. M. Parker, M. E. Afentoulis, A. A. Vandenbark, and P. D. Hurn, "Experimental stroke induces massive, rapid activation of the peripheral immune system," *Journal of Cerebral Blood Flow and Metabolism*, vol. 26, no. 5, pp. 654–665, 2006.

[37] P. Vikman, S. Ansar, M. Henriksson, E. Stenman, and L. Edvinsson, "Cerebral ischemia induces transcription of inflammatory and extracellular-matrix-related genes in rat cerebral arteries," *Experimental Brain Research*, vol. 183, no. 4, pp. 499–510, 2007.

[38] P. D. Hurn, S. Subramanian, S. M. Parker et al., "T- and B-cell-deficient mice with experimental stroke have reduced lesion size and inflammation," *Journal of Cerebral Blood Flow and Metabolism*, vol. 27, no. 11, pp. 1798–1805, 2007.

[39] V. H. Brait, J. Rivera, B. R. S. Broughton, S. Lee, G. R. Drummond, and C. G. Sobey, "Chemokine-related gene expression in the brain following ischemic stroke: no role for CXCR2 in outcome," *Brain Research*, vol. 1372, pp. 169–179, 2011.

[40] J. C. Copin, R. F. da Silva, R. A. Fraga-Silva et al., "Treatment with Evasin-3 reduces atherosclerotic vulnerability for ischemic stroke, but not brain injury in mice," *Journal of Cerebral Blood Flow & Metabolism*, vol. 33, no. 4, pp. 490–498, 2013.

Hindawi Publishing Corporation
Mediators of Inflammation
Volume 2013, Article ID 540370, 10 pages
http://dx.doi.org/10.1155/2013/540370

Review Article

Cytokines and Chemokines as Regulators of Skeletal Muscle Inflammation: Presenting the Case of Duchenne Muscular Dystrophy

Boel De Paepe and Jan L. De Bleecker

Laboratory for Myopathology, Department of Neurology and Neuromuscular Reference Center, Ghent University Hospital, De Pintelaan 185, 9000 Ghent, Belgium

Correspondence should be addressed to Boel De Paepe; boel.depaepe@ugent.be

Received 12 July 2013; Accepted 9 September 2013

Academic Editor: Charles J. Malemud

Duchenne muscular dystrophy is a severe inherited muscle disease that affects 1 in 3500 boys worldwide. Infiltration of skeletal muscle by inflammatory cells is an important facet of disease pathophysiology and is strongly associated with disease severity in the individual patient. In the chronic inflammation that characterizes Duchenne muscle, cytokines and chemokines are considered essential activators and recruiters of inflammatory cells. In addition, they provide potential beneficiary effects on muscle fiber damage control and tissue regeneration. In this review, current knowledge of cytokine and chemokine expression in Duchenne muscular dystrophy and its relevant animal disease models is listed, and implications for future therapeutic avenues are discussed.

1. Introduction

Duchenne muscular dystrophy (DMD) is an X-linked muscle disease, with a prevalence of 1 in 3500 boys worldwide. Patients develop progressive weakness of skeletal and respiratory muscles and dilated cardiomyopathy. Clinical onset is usually between 2 and 5 years of age. Most patients loose independent ambulation in their teens, after which scoliosis develops. Death usually occurs before forty years of age and is most often the result of respiratory or cardiac failure. The biochemical cause of DMD is a severe deficiency of dystrophin, an essential component of the sarcolemmal dystrophin-associated glycoprotein complex. When complex assembly is disturbed, the linkage between the muscle cell's cytoskeleton and the extracellular matrix is compromised, leading to sarcolemmal instability and increased vulnerability to mechanical stress [1]. Fibers undergo necrosis by excessive Ca^{2+} influx [2] and are progressively replaced by connective and adipose tissue.

The immune system plays a pivotal role in the pathogenesis of DMD. Contraction of dystrophin deficient myofibers produces severe damage and generates cycles of muscle fiber necrosis and regeneration. Necrotizing myofibers are attacked by macrophages; inflammatory cells are present throughout the endomysial, perimysial, and perivascular areas. Macrophages are the most abundant immune cells observed in DMD muscle and both proinflammatory M1 phenotype macrophages and regeneration-focussed M2 phenotype macrophages are present. Within the inflammatory areas, few T cells, B cells, and dendritic cells are also present. Infiltrating T cells are predominantly CD4+, and smaller numbers of CD8+ T cells can be found [3]. The T cell receptor repertoire of CD4+ and CD8+ T cells does not display dominant Vα or Vβ rearrangements, which points toward a nonspecific cell recruitment to sites of muscle fiber destruction [4]. In addition to their involvement in muscle damage, T cells also play an important role in the fibrotic processes present in dystrophic muscle. T cell deficiency significantly

reduces collagen matrix accumulation in the murine disease model [5]. The underlying mechanisms are complex and rely on the interplay of immune cells and cytokines [6].

The build up of the inflammatory response is complexly regulated through interactions between adhesion molecules, receptors, and soluble factors, recruiting immune cells from the blood stream to the muscle tissue [7].

2. Animal Models of DMD

In the last decade, improved genetic testing has made diagnostic muscle biopsies redundant in most cases, which means that nowadays DMD muscle samples only rarely become available for pathological research. It is therefore even more imperative to investigate animal models to gain insight into human disease. This is a feasible approach, as the dystrophin-associated protein complex is evolutionary ancient and highly conserved among species. By far the most studied model for DMD is the murine mdx model. Mdx mice have a premature stop codon in the dystrophin gene, which leads to the loss of functional protein. One should however remain cautious when extrapolating data obtained in the mdx model to human disease. The clinical phenotype of mdx mice is less severe and follows a different time course than human disease. Also, of importance in the context of this review, there are notable differences in the cytokine system of mouse compared to man. Dystrophin-deficient dogs seem to more closely mimic human disease, for example, the severe myopathy in golden retriever muscular dystrophy (GRMD) [8]. Dystrophin-deficient hypertrophic feline muscular dystrophy (HFMD) is characterized by early disease onset and continuous muscle fiber regeneration in the absence of significant inflammatory infiltration or proliferation of connective or adipose tissue. Some HFMD-affected cats develop cardiomyopathy [9]. Recently, zebrafish with mutations in the sapje locus containing the dystrophin gene have become available. Zebrafish embryos represent a convenient model to study disease [10] and are extremely suited to first-line drug screening [11]. It is to be expected that studies in DMD disease models, addressing the underlying disease mechanisms as well as therapeutic efficiencies, will continue to proliferate in the near future.

3. Cytokines

Initially, no distinct pattern of cytokine expression could be shown for DMD [12], but since then several inflammatory factors have been reported to preferentially associate with the disease [13].

3.1. TNF Family of Cytokines. The proinflammatory members of the tumor necrosis factor (TNF) family are important regulators of chronic inflammation. TNF-α (TNFSF2), the prototypic catabolic cytokine and most studied member of the TNF-family, is associated with helper T cell type-1-(Th1-) mediated cellular immunity. TNF-α is upregulated in DMD sera [14] with levels increased 1000 times in comparison to levels in healthy subjects [15]. TNF-α mRNA expression is significantly higher in circulating lymphocytes of DMD patients compared to controls [16]. In DMD skeletal muscle tissues, a proportion of muscle fibers are TNF-α immunoreactive [17] most of which are regenerating muscle fibers [18]. However, the primary source of TNF-α in DMD muscle is the inflammatory cells (Figure 1(a)) that, by doing so, further perpetuate the inflammatory response. Diaphragm of mdx mice contains significantly higher TNF-α mRNA levels than controls [19], and TNF-α protein strongly colocalizes with tissue infiltrating macrophages [20]. In contrast to what was expected, TNF-α knockout mdx mice do not exhibit an amelioration of muscle pathology [21], adding nuance to the considered destructive role of TNF-α in muscle dystrophy. Lymphotoxin-β (LT-β; TNFSF3) is a key factor in lymphoneogenesis and, through the expression of adhesion molecules, cytokines and chemokines, it regulates innate and adaptive immune responses. LT-β protein levels are significantly upregulated in muscular dystrophies, compared to normal skeletal muscle. Blood vessels and the sarcolemma of DMD fibers are LT-β positive, and staining is further enhanced in the regenerating fibers, sometimes accompanied with sarcoplasmic staining [22]. LT-β expressed by muscle fibers could serve as an anchor point to attract inflammatory cells to the tissue sites.

Muscle fiber necrosis, an accidental form of cell death triggered by physical tissue damage, is an abundant phenomenon in DMD. However, regulated forms of cell death could alternatively be involved in muscle damage development. Recently, a regulated form of necrosis, which can be initiated by TNF-α-induced receptor-interacting protein kinase activity, has been recognized [23]. In addition, the well-characterized process of apoptosis follows a series of programmed events, relying upon regulated expression of specific proteins that signal cells to their death. DNA fragmentation and changes in cell structure characteristic to apoptotic processes can be observed in soleus muscle from mdx mice [24]. Also, the percentage of apoptotic nuclei is higher in DMD muscle than in controls [25]. Several TNF cytokine family members are actively involved in apoptosis. FasL (TNFSF6) has been shown to induce muscle cell apoptosis *in vitro* [26]. FasL mRNA expression is significantly higher in peripheral blood lymphocytes of DMD patients compared to controls [16]. A small proportion of DMD muscle fibers express the corresponding receptor Fas [27]. Induction of both ligand and receptor could, unlike in idiopathic inflammatory myopathies [28], indicate an involvement of Fas/FasL—mediated apoptosis in DMD muscle atrophy and degeneration. TNF-like weak inducer of apoptosis (TWEAK; TNFSF12) is a major inducer of muscle wasting [29] and preventer of muscle regeneration [30]. To our knowledge, no data is available at this moment regarding TWEAK expression in DMD.

3.2. Interleukins. Interleukins (IL), of which 36 different forms have been identified so far, play a major role in the immune system. Most important data available at this moment will be discussed under this heading, except for IL-8 which will be discussed in the chemokine section.

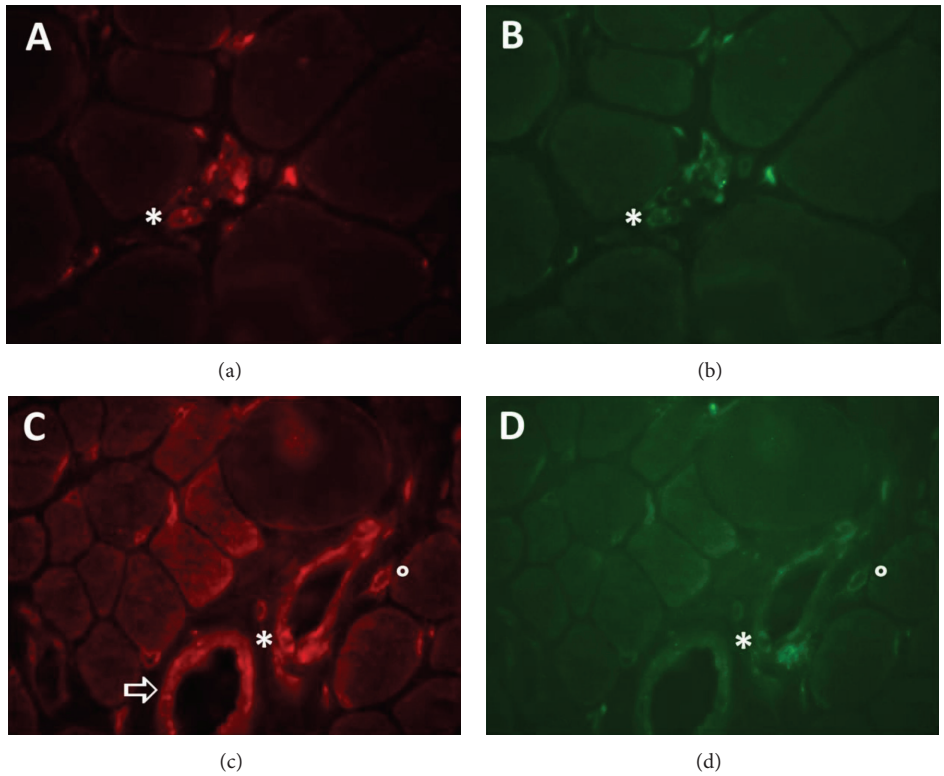

Figure 1: Immunofluorescent detection of TNF-α and IFN-γ in Duchenne muscular dystrophy. (a)-(b) Muscle biopsy taken from an 8-year-old patient with Duchenne muscular dystrophy caused by duplication of dystrophin exon 2, resulting in severe muscle damage, few groups of revertant fibers, and strong utrophin staining. TNF-α (red in (a)) is detected in a small cluster of inflammatory cells and colocalizes with CD3 (green in (b)). The asterisk is an indicative that helps to identify an individual TNF-α+ T cell. (c)-(d) Muscle biopsy taken from a 2-year-old patient with Duchenne muscular dystrophy caused by c.5299-5302dupATTT in dystrophin exon 37. Myopathological evaluation of the biopsy described definite muscle damage, few groups of revertant fibers, and strong utrophin staining. IFN-γ (red in (c)) is strongly expressed on the blood vessel endothelium (arrow) and on perivascular CD3+ T cells (green in (d)). Highlighted are an IFN-γ+ CD3+ T cell attached to the luminal side of the blood vessel (asterisk) and an interstitial IFN-γ+ CD3+ T cell (circle).

The involvement of proinflammatory IL-1 in muscular dystrophy remains a topic of debate. Neither IL-1α nor IL-1β immunoreactivity could be shown in a study investigating 8 DMD muscle samples [17], and the IL-1 family has been reported downregulated in DMD serum [31]. However, another study describes IL-1β as being increased in DMD muscle [32]. Also, diaphragm of mdx mice contains significantly higher IL-1β mRNA levels than control mice [19], and IL-1β protein colocalizes with the infiltrating macrophages [20].

IL-6 is a cytokine with both proinflammatory and anti-inflammatory properties. It is a helper T cell type 2 (Th2) cytokine, meaning that it promotes IgE and eosinophilic responses in atropy and counteracts Th1-driven proinflammatory responses. On the other hand, IL-6 exhibits proinflammatory activity through activation of the transcription factor nuclear factor κB. IL-6 concentrations are significantly higher in serum of DMD patients (3.77 $\pm$ 2.71 pg/mL) compared to healthy age-matched controls (1.93 $\pm$ 1.38 pg/mL) [31] and follow the disease time-course [32]. In DMD muscle, IL-6 mRNA levels display a significant increase compared to controls. The level increases with age: from 26-fold at age 4 years to 148-fold between 5 and 9 years [33]. Blocking IL-6 through injection with a monoclonal antibody causes an increase of muscle inflammation in the mdx mouse model, further suggesting an anti-inflammatory effect, possibly by mediating muscle repair [34].

IL-10 functions as a suppressor of inflammation through its differential effect on the different macrophage subtypes: deactivating M1 macrophages and activating the M2 phenotype. M1 macrophages function within the Th1 response and produce copious amounts of proinflammatory cytokines, while M2 macrophages promote angiogenesis and tissue repair and remodeling [35], a phenomenon also present in muscle [36]. IL-10 prevents the production of Th1-associated cytokines such as TNF-α and IFN-γ [37]. Its expression is 8 to 15-fold increased in mdx quadriceps compared with wild type muscle, possibly as a protective reflex of the tissue. IL-10 null mutation causes severe reduction of muscle strength due to an imbalance between M1 and M2 macrophages [38].

IL-15 has proinflammatory characteristics as a stimulator of T cell proliferation and NK-activity but can also be of benefit to tissue recovery by increasing myogenic differentiation [39]. Mdx diaphragm contains some IL-15 reactivity

especially in proximity of inflammatory cells. Treatment with recombinant IL-15 has a mild anabolic effect on diaphragm function [40].

IL-17 is a potent amplifier of ongoing inflammation and plays an important role in the progression of chronic inflammation and autoimmunity. IL-17 induces TNF-α, IL-1β, and IL-6 expression and stimulates the production of chemokines such as CXCL1, CXCL5, IL-8, CCL2, and CCL7 [41]. In DMD quadriceps muscle IL-17 mRNA is induced while being undetectable in control muscle, and expression is associated with functional outcome at 6 years of age [42].

3.3. Interferons. The interferon (IFN) family members are divided among three classes. Type I IFN (in humans IFN-α, IFN-β, and IFN-ω) are associated with innate immunity. The sole human IFN type II is the proinflammatory Th1 cytokine IFN-γ. IFN-γ expression is elevated in mdx muscle in the early disease stage when many M1 macrophages are present [43]. In the regenerating stage of disease, IFN-γ ablation causes a significant reduction in muscle fiber injury, an effect probably mediated through the observed shift in favor of M2 phenotype macrophages [44]. In DMD muscle, the strongest IFN-γ expression is observed in the blood vessel endothelial cells and in interstitial T cells (Figure 1(c)).

3.4. Transforming Growth Factors. Transforming growth factors (TGF) are a large group of cytokines that include TGF-β 1 to 3 and myostatin. Several members of the TGF family play important roles as regulators of skeletal muscle homeostasis and have been implicated in inherited and acquired muscle disorders.

TGF-β is a pleiotropic cytokine with important roles in inflammation, cell growth, and tissue repair [45]. TGF-β is a fibrogenic cytokine that induces synthesis and accumulation of extracellular matrix components. In adult muscle, TGF-β negatively affects skeletal muscle regeneration by inhibiting satellite cell proliferation and myofiber fusion. TGF-β1 mRNA levels are significantly higher in 30-day-old GRMD than in healthy dogs. TGF-β immunoreactivity is mostly confined to the connective tissue and varies between individual animals. Interestingly, in adult GRMD dogs TGF-β mRNA levels decrease to levels lower than those in normal dogs [46]. TGF-β1 activation appears to be associated with muscle wasting in DMD. TGF-β1 expression, mostly originating from muscle resident fibroblasts, is most pronounced in the early stages of muscle fibrosis and peaks between 2 and 6 years of age [47]. Fibroblasts from DMD muscle biopsies differ from control fibroblasts, displaying higher rates of proliferation. In addition, DMD muscle-derived fibroblasts contain significantly higher TGF-β protein levels, though similar levels of TGF-β1 mRNA are present as in controls [48]. Of special interest to determine patient prognosis is that a haplotype of the latent TGF-β binding protein 4 gene has been shown to correlate with prolonged ambulation of DMD patients [49].

Skeletal muscle specific myostatin (TGF-β8) is an inhibitor of muscle growth. Mdx mice lacking myostatin display less fibrosis in the diaphragm and are stronger and more muscular than their normal mdx counterparts [50]. Another study found that myostatin is downregulated in muscle from DMD infants as well as symptomatic patients [51] indicating that this pathway may contribute less to muscle wasting in human disease. Myofibroblasts prepared from DMD biopsies, however, have been shown to express significantly higher myostatin mRNA levels than controls [48].

4. Chemokines

Chemotactic cytokines or chemokines are subdivided into families according to their primary structure (most belong to the alpha (CXCL) or beta (CCL) families) and exert their biological functions by binding to G protein-coupled receptors [52]. Chemokines interact with other cytokines and adhesion molecules and their activities go way further than the attraction of leukocytes to inflammatory sites. CCL17, for instance, has been shown to enhance tissue fibrosis [53]. While the chemokine expression profile in healthy skeletal muscle is fairly limited, many chemokines are induced or upregulated in dystrophic muscle (Tables 1 and 2) [54–58]. The individual muscle tissue distribution of some chemokines has been determined and shows that they can differentially be allocated to inflammatory cells, blood vessel endothelium, and/or the muscle fibers themselves (Figure 2). Three chemokines, being CXCL8 (IL-8), CCL2, and CCL5, come forward as possible effectors of the cytotoxic activities of M1 macrophages in DMD. CCL2 upregulation in particular seems an early event in muscle dystrophy, present in DMD before the age of 2 years [55] and detectable in 14-day old mdx mice [57].

5. Comparison with Myositis of Other Origins

Muscular dystrophies are a clinically, biochemically, and genetically heterogeneous group of disorders [59]. Dystrophin mutations are not just responsible for DMD but also cause a spectrum of other X-linked conditions, such as the milder Becker muscular dystrophy (BMD), cardiomyopathies, and mental retardation. Also, defects in other dystrophin-associated proteins cause disease, including autosomal recessive inherited limb-girdle muscular dystrophies. In many subtypes, muscle inflammation and muscle wasting contribute to disease progression, potentially implicating cytokines and chemokines in their pathogenesis. For instance, the presence of endomysial and perivascular inflammation is an established hallmark of dysferlinopathy [60].

In contrast to the relatively limited amount of published DMD data, a multitude of reports is available on the expression of cytokines in the different idiopathic inflammatory myopathies (IIM), which include dermatomyositis (DM), polymyositis (PM) and sporadic inclusion body myositis (IBM) [61]. This allows for some comparison between primary muscle inflammation in IIM and dystrophy-associated muscle inflammation. In a single BMD patient included in a multiplex cytokine immunoassay study, CCL2 levels are 11 pg/mg muscle protein, while those in 6 patients per IIM group were 45 ± 51 (DM), 15 ± 9 (PM) and 13 ± 9 (IBM),

Table 1: Alpha-chemokine expression in Duchenne muscular dystrophy and its mouse model.

Systematic name	Common name	Tissue	mRNA quantity	Protein quantity	Protein localization	Reference
CXCL1	GRO-alpha	DMD quadriceps muscles			BV, MF, Mφ, T, DC	[54]
CXCL2	GRO-beta	DMD quadriceps muscles			BV, MF, Mφ	[54]
CXCL3	GRO-gamma	DMD quadriceps muscles			BV, MF, Mφ, DC	[54]
CXCL8	IL-8	DMD quadriceps muscles			BV, MF, Mφ	[54]
CXCL10	IP-10	DMD quadriceps muscles			BV, (MF), Mφ, T	[54]
CXCL11	ITAC	DMD quadriceps muscles			BV, (MF), Mφ	[54]
CXCL12	SDF-1	DMD quadriceps muscles	Increased 2.3x			[55]
		DMD quadriceps muscles			BV, MF	[54]
		DMD serum		Increased 1.2x		[56]
CXCL14	BRAK	mdx hindlimb muscles	Increased 1.7x			[57]

Breast and kidney derived (BRAK); blood vessel (BV), alpha-chemokine (CXCL), dendritic cell (DC), Duchenne mouse model (mdx), growth related oncogene (GRO), interleukin 8 (IL-8), interferon-inducible protein of 10 kd (IP-10), interferon-inducible T cell alpha chemo-attractant (ITAC), muscle fiber (MF), macrophage (Mφ), stromal cell-derived factor (SDF), T cell (T). Rare observations are indicated between brackets.

Table 2: Beta-chemokine expression in Duchenne muscular dystrophy and its mouse model.

Systematic name	Common name	Tissue	mRNA quantity	Protein quantity	Protein localization	Reference
CCL2	MCP-1	mdx hindlimb muscles	Increased 62.7x	Increased 4.1x	MF, Mφ	[57]
		DMD quadriceps muscles	Increased 1.4x			[55]
					BV, Mφ	[54]
CCL3	MIP-1 alpha	mdx diaphragm	Increased			[58]
CCL5	RANTES	mdx hindlimb muscles		Increased 2.3x		[57]
		mdx diaphragm	Increased	Increased		[58]
		DMD quadriceps muscles			Mφ	[54]
CCL7	MCP-3	mdx hindlimb muscles	Increased 14.7x			[57]
		DMD quadriceps muscles			Mφ	[54]
CCL8	MCP-2	mdx hindlimb muscles	Increased 28.9x			[57]
CCL9	MIP-1 gamma	mdx hindlimb muscles	Increased 7.9x	Increased 2.4x		[57]
CCL11	eotaxin	mdx hindlimb muscles		Increased 2.0x		[57]
CCL17	TARC	DMD quadriceps muscles			(Mφ)	[54]

Blood vessel (BV), beta-chemokine (CCL), Duchenne muscular dystrophy (DMD), monocyte chemoattractant protein (MCP), Duchenne mouse model (mdx), muscle fiber (MF), macrophage (Mφ), macrophage inflammatory protein (MIP), regulated upon activation, normal T cell expressed and secreted (RANTES), thymus and activation-regulated chemokine (TARC). Rare observations are indicated between brackets.

respectively [62]. In DMD quadriceps muscle, TNF-α, IL-6, and CCL2 mRNA levels are lower than in juvenile DM [42]. The observed more moderate expression levels could be indicative to the secondary nature of muscle inflammation as opposed to the primary inflammatory origin of the IIM. Although there unmistakably are universal inflammatory processes at hand, data also point to specific roles for cytokines and chemokines in DMD. The expression profiles of M1 macrophages are peculiar when DMD and IIM are compared. Also, in IIM strong expression of CXCR3 is observed on the muscle infiltrating T cells, indicating their involvement in Th1 immune responses. Such polarization of T cells is less obvious in DMD muscle. In fact, the muscle infiltrating T cells in DMD express a strikingly limited repertoire of chemokines in comparison to their IIM counterparts [54].

6. Relevance to DMD Disease Management

The medical community still awaits the coming of age of molecular dystrophin salvaging therapies [63]. In this respect, exon skipping [64] and suppression of stop codons [65] are considered strategies of increasing functional dystrophin expression. However, surfacing results of clinical trials, more particular those using AAV-mediated delivery of mini-dystrophin, are suggestive of important acquisition of T cell immunity targeting the dystrophin protein [66]. Earlier, it had been postulated that such priming was unlikely, due to the presence of revertant fibers in many patients which would theoretically safeguard dystrophin replacement from the immune system. Nonetheless, it is becoming more and more obvious that monitoring of cellular immune responses will

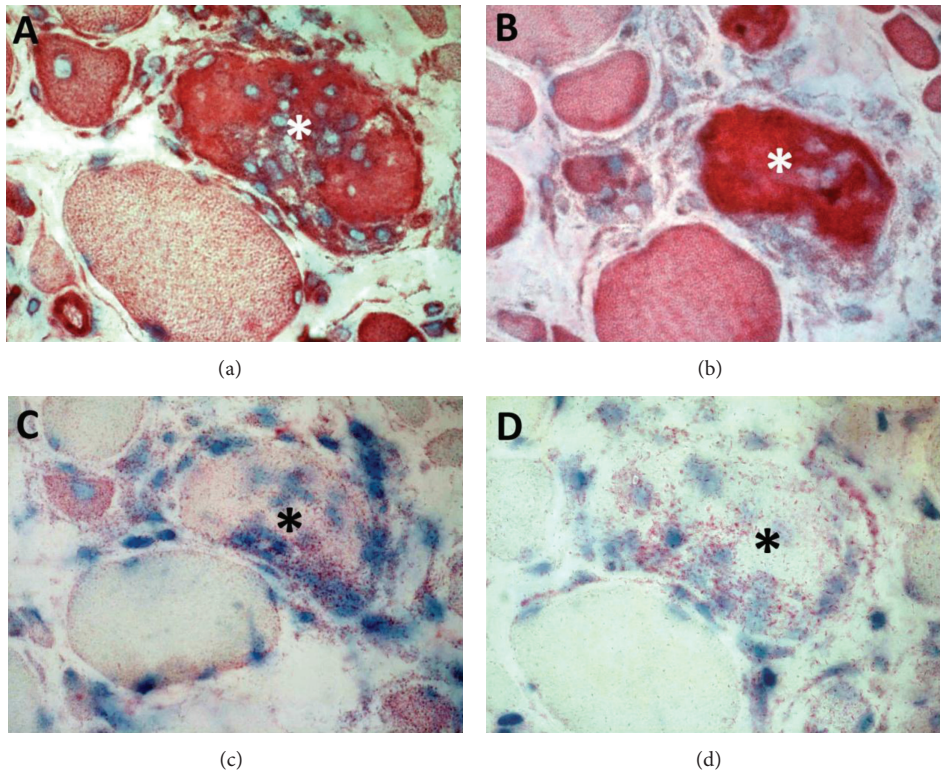

Figure 2: Chemokine staining in Duchenne muscular dystrophy. Nonconsecutive sections showing the same microscopic field containing a necrotic muscle fiber invaded by macrophages (asterisk). The muscle biopsy was taken from an 8-year-old patient with Duchenne muscular dystrophy caused by duplication of dystrophin exon 2. Upon diagnostic myopathological evaluation, the biopsy displayed severe muscle damage, few groups of revertant fibers, and strong utrophin staining. Chemokines were immunostained and visualized with a secondary antibody using the streptavidin-biotin labeling system and 3-amino-9-ethylcarbazole chromogen (Dako, Glostrup, Denmark). Cell nuclei were counterstained with hematoxylin (blue). The sarcoplasm of a necrotic fiber is strongly positive for CXCL8 (red in (a)) and CXCL11 (red in (b)). The cytoplasm of the necrotic fiber and its invading inflammatory cells are moderately positive for CCL5 (red in (c)) and faintly positive for CCL17 (red in (d)). Small regenerating fibers stain for all four chemokines with varying intensities.

be a priority in all ongoing and future experimental therapies aimed at increasing the number of dystrophin positive muscle fibers. A recent study demonstrated that circulating dystrophin primed T cells are frequently encountered in DMD, increased with age, and reduced by glucocorticoid therapy [67].

Immunosuppression, administering glucocorticoids in particular, remains standard treatment for DMD today. Although anti-inflammatory therapy may add years to DMD patient ambulation, steroids are associated with important adverse effects [68]. The characterization of the factors that drive inflammation and guide specific subsets of leukocytes to the tissues raises hopes of attempting more selective immunomodulatory intervention. Strategies aimed at neutralizing individual cytokines or chemokines could be an amenable approach to reduce side effects.

6.1. Targeting the Culprits While Sparing the Protectors. Specifically targeting cytokines and chemokines with predominant proinflammatory activities, such as TNF-α, is under exploration. The TNF-α neutralizing antibody infliximab delays and reduces muscle damage in mdx mice [69]. Soluble TNF-receptor etanercept, a dimeric fusion protein composed of an extracellular ligand-binding portion of the human p75 TNF-receptor linked to the Fc portion of human IgG, reduces muscle fibrosis [70] and necrosis [71]. The disruption of chemokine-mediated signaling also seems, at first glance, an attractive therapeutic possibility. An approach could be to selectively block a chemokine receptor with a key catabolic role by either a small-molecule antagonist, antibody, binding protein, or protein agonist [72]. Several chemokine-receptor antibodies are entering the clinic, including an anti-CCR2 monoclonal antibody named MLN1202 (Millenium Pharmaceuticals, Cambridge, MA, USA) currently being tried for various inflammatory diseases. However, strategies targeting the chemokine system present with certain inherent difficulties. Firstly, several chemokines are up-regulated in DMD. The redundancy of function of part of them makes it difficult to design effective therapeutic interventions. Secondly, there could be considerable inter-patient variability, as well as differences between the stages of the disease. More research is necessary to address these issues. Thirdly, chemokines can have benefits for tissue recovery, by activating muscle fiber regeneration and recruiting non-cytotoxic macrophage subpopulations that stimulate muscle tissue rebuilding [73]. For instance, when considering the anti-CCR2 avenue, its ligand

CCL2 has the potential to drive forward chronic inflammation, but the importance of CCL2 in muscle regeneration has also been recognized [74, 75].

In addition, strategies aimed at neutralizing fibrogenic cytokines or cytokines associated with muscle wasting are under exploration for treating DMD. For instance, the TGF-β1 antagonist pirfenidone improves cardiac function in mdx mice [76]. The TGF-β blocker suramin decreases fibrosis and offers benefit in grip strength in mdx mice [77]. A TGF-β neutralizing antibody decreases fibrosis and improves regeneration in mdx mice [78]. Inhibition of myostatin with a neutralizing antibody [79], soluble decoy receptor [80], or myostatin binding propeptide [81] has also been put forward. An *in vitro* model, using nodules of DMD muscle-derived fibroblasts grown onto a solid substrate, has been developed which allows convenient screening of potential antifibrotic agents [82].

6.2. Reprogramming the Immune Response. While M1 macrophages have a destructive cytokine repertoire, the M2 phenotype promotes angiogenesis, tissue repair, and remodeling. In mdx muscle, M1 macrophages predominate during the early, acute stage. The balance tips over to the M2 phenotype in the regenerative and progressive phase of the disease. In other words, the M1/M2 balance evolves beneficially with M1 macrophages undergoing deactivation as the disease progresses from the acute necrotic to the regenerative phase. M1 density significantly reduces with age in mdx soleus (4 versus 12 weeks) [43]. This could account for the milder disease phenotype of mdx mice compared to human disease, as in contrast percentages of M1 and M2 phenotype macrophages seem strikingly constant in DMD muscle taken at different disease stages [54]. Therapeutic agents regulating the M1/M2 balance in favor of the M2 phenotype, such as cannabinoid CB2 receptor agonists, could be of benefit to patients [83]. Interestingly, glucocorticoids as such have also been shown to favor a shift of macrophage phenotype, reducing the numbers of M1 macrophages by half in patients treated with prednisone (0.75 mg/kg/day) during 6 months [84].

7. Conclusions

In dystrophic skeletal muscle, part of the accumulating muscle damage is caused by ongoing activation of inflammatory cells rather than by direct mechanical damage. Current knowledge, of which a large part is summarized in this review, supports an important and diversified role for cytokines and chemokines in the DMD-associated muscle inflammation. The fact that a number of chemokines are expressed directly by the muscle fibers suggests that the tissue itself contributes to the chemotaxic process, actively perpetuating the chronic inflammation.

Abbreviations

BMD: Becker muscular dystrophy
CCL: Beta-chemokine
CXCL: Alpha-chemokine
DMD: Duchenne muscular dystrophy
GRMD: Golden retriever muscular dystrophy
HFMD: Hypertrophic feline muscular dystrophy
IIM: Idiopathic inflammatory myopathies
IFN: Interferon
IL: Interleukin
TGF: Transforming growth factor
TNF: Tumor necrosis factor.

Acknowledgments

The authors thank Professor Dr. Jean-Jacques Martin of the Department of Ultrastructural Neuropathology, Born-Bunge Institute, University of Antwerp and Antwerp University Hospital, Belgium, for providing patient biopsies and expert opinion.

References

[1] N. Deconinck and B. Dan, "Pathophysiology of Duchenne muscular dystrophy: current hypotheses," *Pediatric Neurology*, vol. 36, no. 1, pp. 1–7, 2007.

[2] B. J. Petrof, "Molecular pathophysiology of myofiber injury in deficiencies of the dystrophin-glycoprotein complex," *American Journal of Physical Medicine and Rehabilitation*, vol. 81, no. 11, pp. S162–S174, 2002.

[3] R. M. McDouall, M. J. Dunn, and V. Dubowitz, "Nature of the mononuclear infiltrate and the mechanism of muscle damage in juvenile dermatomyositis and Duchenne muscular dystrophy," *Journal of the Neurological Sciences*, vol. 99, no. 2-3, pp. 199–217, 1990.

[4] R. Mantegazza, F. Andreetta, P. Bernasconi et al., "Analysis of T cell receptor repertoire of muscle-infiltrating T lymphocytes in polymyositis. Restricted Vα/β rearrangements may indicate antigen-driven selection," *Journal of Clinical Investigation*, vol. 91, no. 6, pp. 2880–2886, 1993.

[5] J. Morrison, Q. L. Lu, C. Pastoret, T. Partridge, and G. Bou-Gharios, "T-cell-dependent fibrosis in the mdx dystrophic mouse," *Laboratory Investigation*, vol. 80, no. 6, pp. 881–891, 2000.

[6] J. Morrison, D. B. Palmer, S. Cobbold, T. Partridge, and G. Bou-Gharios, "Effects of T-lymphocyte depletion on muscle fibrosis in the mdx mouse," *American Journal of Pathology*, vol. 166, no. 6, pp. 1701–1710, 2005.

[7] J. Middleton, A. M. Patterson, L. Gardner, C. Schmutz, and B. A. Ashton, "Leukocyte extravasation: chemokine transport and presentation by the endothelium," *Blood*, vol. 100, no. 12, pp. 3853–3860, 2002.

[8] N. J. H. Sharp, J. N. Kornegay, S. D. Van Camp et al., "An error in dystrophin mRNA processing in golden retriever muscular dystrophy, an animal homologue of Duchenne muscular dystrophy," *Genomics*, vol. 13, no. 1, pp. 115–121, 1992.

[9] F. Gaschen and J.-M. Burgunder, "Changes of skeletal muscle in young dystrophin-deficient cats: a morphological and morphometric study," *Acta Neuropathologica*, vol. 101, no. 6, pp. 591–600, 2001.

[10] D. I. Bassett and P. D. Currie, "The zebrafish as a model for muscular dystrophy and congenital myopathy," *Human Molecular Genetics*, vol. 12, no. 2, pp. R265–R270, 2003.

[11] G. Kawahara, J. A. Karpf, J. A. Myers, M. S. Alexander, J. R. Guyone, and L. M. Kunkel, "Drug screening in a zebrafish

model of Duchenne muscular dystrophy," *Proceedings of the National Academy of Sciences of the United States of America*, vol. 108, no. 13, pp. 5331–5336, 2011.

[12] I. Lundberg, J. M. Brengman, and A. G. Engel, "Analysis of cytokine expression in muscle in inflammatory myopathies, Duchenne dystrophy, and non-weak controls," *Journal of Neuroimmunology*, vol. 63, no. 1, pp. 9–16, 1995.

[13] J. G. Tidball and M. Wehling-Henricks, "Damage and inflammation in muscular dystrophy: potential implications and relationships with autoimmune myositis," *Current Opinion in Rheumatology*, vol. 17, no. 6, pp. 707–713, 2005.

[14] E. Porreca, M. D. Guglielmi, A. Uncini et al., "Haemostatic abnormalities, cardiac involvement and serum tumor necrosis factor levels in X-linked dystrophic patients," *Thrombosis and Haemostasis*, vol. 81, no. 4, pp. 543–546, 1999.

[15] K. Saito, D. Kobayashi, M. Komatsu et al., "A sensitive assay of tumor necrosis factor α in sera from Duchenne muscular dystrophy patients," *Clinical Chemistry*, vol. 46, no. 10, pp. 1703–1704, 2000.

[16] E. Abdel-Salam, I. Abdel-Meguid, and S. S. Korraa, "Markers of degeneration and regeneration in Duchenne muscular dystrophy," *Acta Myologica*, vol. 28, no. 3, pp. 94–100, 2009.

[17] D. S. Tews and H. H. Goebel, "Cytokine expression profile in idiopathic inflammatory myopathies," *Journal of Neuropathology and Experimental Neurology*, vol. 55, no. 3, pp. 342–347, 1996.

[18] S. Kuru, A. Inukai, T. Kato, Y. Liang, S. Kimura, and G. Sobue, "Expression of tumor necrosis factor-α in regenerating muscle fibers in inflammatory and non-inflammatory myopathies," *Acta Neuropathologica*, vol. 105, no. 3, pp. 217–224, 2003.

[19] A. Kumar and A. M. Boriek, "Mechanical stress activates the nuclear factor-kappaB pathway in skeletal muscle fibers: a possible role in Duchenne muscular dystrophy," *FASEB Journal*, vol. 17, no. 3, pp. 386–396, 2003.

[20] K. Hnia, J. Gayraud, G. Hugon et al., "L-arginine decreases inflammation and modulates the nuclear factor-κB/matrix metalloproteinase cascade in mdx muscle fibers," *American Journal of Pathology*, vol. 172, no. 6, pp. 1509–1519, 2008.

[21] M. J. Spencer, M. W. Marino, and W. M. Winckler, "Altered pathological progression of diaphragm and quadriceps muscle in TNF-deficient, dystrophin-deficient mice," *Neuromuscular Disorders*, vol. 10, no. 8, pp. 612–619, 2000.

[22] K. K. Creus, B. De Paepe, J. Weis, and J. L. De Bleecker, "The multifaceted character of lymphotoxin β in inflammatory myopathies and muscular dystrophies," *Neuromuscular Disorders*, vol. 22, no. 8, pp. 712–719, 2012.

[23] P. Vandenabeele, L. Galluzzi, T. Vanden Berghe, and G. Kroemer, "Molecular mechanisms of necroptosis: an ordered cellular explosion," *Nature Reviews Molecular Cell Biology*, vol. 11, no. 10, pp. 700–714, 2010.

[24] J. G. Tidball, D. E. Albrecht, B. E. Lokensgard, and M. J. Spencer, "Apoptosis precedes necrosis of dystrophin-deficient muscle," *Journal of Cell Science*, vol. 108, no. 6, pp. 2197–2204, 1995.

[25] A. Serdaroğlu, K. Gücüyener, S. Erdem, G. Köse, E. Tan, and Ç. Okuyaz, "Role of apoptosis in Duchenne's muscular dystrophy," *Journal of Child Neurology*, vol. 17, no. 1, pp. 66–68, 2002.

[26] M. Kondo, Y. Murakawa, N. Harashima, S. Kobayashi, S. Yamaguchi, and M. Harada, "Roles of proinflammatory cytokines and the Fas/Fas ligand interaction in the pathogenesis of inflammatory myopathies," *Immunology*, vol. 128, no. 1, pp. e589–e599, 2009.

[27] L. Behrens, A. Bender, M. A. Johnson, and R. Hohlfeld, "Cytotoxic mechanisms in inflammatory myopathies. Co-expression of Fas and protective Bcl-2 in muscle fibres and inflammatory cells," *Brain*, vol. 120, no. 6, pp. 929–938, 1997.

[28] J. L. De Bleecker, V. I. Meire, I. E. Van Walleghem, I. M. Groessens, and J. M. Schröder, "Immunolocalization of Fas and Fas ligand in inflammatory myopathies," *Acta Neuropathologica*, vol. 101, no. 6, pp. 572–578, 2001.

[29] C. Dogra, H. Changotra, S. Mohan, and A. Kumar, "Tumor necrosis factor-like weak inducer of apoptosis inhibits skeletal myogenesis through sustained activation of nuclear factor-κB and degradation of MyoD protein," *Journal of Biological Chemistry*, vol. 281, no. 15, pp. 10327–10336, 2006.

[30] A. Mittal, S. Bhatnagar, A. Kumar, P. K. Paul, S. Kuang, and A. Kumar, "Genetic ablation of TWEAK augments regeneration and post-injury growth of skeletal muscle in mice," *American Journal of Pathology*, vol. 177, no. 4, pp. 1732–1742, 2010.

[31] A. Rufo, A. Del Fattore, M. Capulli et al., "Mechanisms inducing low bone density in Duchenne muscular dystrophy in mice and humans," *Journal of Bone and Mineral Research*, vol. 26, no. 8, pp. 1891–1903, 2011.

[32] N. P. Evans, S. A. Misyak, J. L. Robertson, J. Bassaganya-Riera, and R. W. Grange, "Immune-mediated mechanisms potentially regulate the disease time-course of Duchenne muscular dystrophy and provide targets for therapeutic intervention," *Physical Medicine and Rehabilitation*, vol. 1, no. 8, pp. 755–768, 2009.

[33] S. Messina, G. L. Vita, M. Aguennouz et al., "Activation of NF-κB pathway in Duchenne muscular dystrophy: relation to age," *Acta Myologica*, vol. 30, pp. 16–23, 2011.

[34] M. C. Kostek, K. Nagaraju, E. Pistilli et al., "IL-6 signaling blockade increases inflammation but does not affect muscle function in the mdx mouse," *BMC Musculoskeletal Disorders*, vol. 13, p. 106, 2012.

[35] A. Mantovani, A. Sica, S. Sozzani, P. Allavena, A. Vecchi, and M. Locati, "The chemokine system in diverse forms of macrophage activation and polarization," *Trends in Immunology*, vol. 25, no. 12, pp. 677–686, 2004.

[36] L. Arnold, A. Henry, F. Poron et al., "Inflammatory monocytes recruited after skeletal muscle injury switch into antiinflammatory macrophages to support myogenesis," *Journal of Experimental Medicine*, vol. 204, no. 5, pp. 1057–1069, 2007.

[37] D. F. Fiorentino, A. Zlotnik, T. R. Mosmann, M. Howard, and A. O'Garra, "IL-10 inhibits cytokine production by activated macrophages," *Journal of Immunology*, vol. 147, no. 11, pp. 3815–3822, 1991.

[38] S. A. Villalta, C. Rinaldi, B. Deng, G. Liu, B. Fedor, and J. G. Tidball, "Interleukin-10 reduces the pathology of mdx muscular dystrophy by deactivating M1 macrophages and modulating macrophage phenotype," *Human Molecular Genetics*, vol. 20, no. 4, pp. 790–805, 2011.

[39] P. S. Furmanczyk and L. S. Quinn, "Interleukin-15 increases myosin accretion in human skeletal myogenic cultures," *Cell Biology International*, vol. 27, no. 10, pp. 845–851, 2003.

[40] L. J. Harcourt, A. G. Holmes, P. Gregorevic, J. D. Schertzer, N. Stupka, and G. S. Lynch, "Interleukin-15 administration improves diaphragm muscle pathology and function in dystrophic mdx mice," *American Journal of Pathology*, vol. 166, no. 4, pp. 1131–1141, 2005.

[41] J. C. Waite and D. Skokos, "Th17 response and inflammatory autoimmune diseases," *International Journal of Inflammation*, vol. 2012, Article ID 819467, 10 pages, 2012.

[42] L. De Pasquale, A. D'Amico, M. Verardo, S. Petrini, E. Bertini, and F. De Benedetti, "Increased muscle expression of interleukin-17 in Duchenne muscular dystrophy," *Neurology*, vol. 78, no. 17, pp. 1309–1314, 2012.

[43] S. A. Villalta, H. X. Nguyen, B. Deng, T. Gotoh, and J. G. Tidbal, "Shifts in macrophage phenotypes and macrophage competition for arginine metabolism affect the severity of muscle pathology in muscular dystrophy," *Human Molecular Genetics*, vol. 18, no. 3, pp. 482–496, 2009.

[44] S. A. Villalta, B. Deng, C. Rinaldi, M. Wehling-Henricks, and J. G. Tidball, "IFN-γ promotes muscle damage in the mdx mouse model of Duchenne muscular dystrophy by suppressing M2 macrophage activation and inhibiting muscle cell proliferation," *Journal of Immunology*, vol. 187, no. 10, pp. 5419–5428, 2011.

[45] G. C. Blobe, W. P. Schiemann, and H. F. Lodish, "Role of transforming growth factor β in human disease," *The New England Journal of Medicine*, vol. 342, no. 18, pp. 1350–1358, 2000.

[46] L. Passerini, P. Bernasconi, F. Baggi et al., "Fibrogenic cytokines and extent of fibrosis in muscle of dogs with X-linked golden retriever muscular dystrophy," *Neuromuscular Disorders*, vol. 12, no. 9, pp. 828–835, 2002.

[47] P. Bernasconi, E. Torchiana, P. Confalonieri et al., "Expression of transforming growth factor-β1 in dystrophic patient muscles correlates with fibrosis. Pathogenetic role of a fibrogenic cytokine," *Journal of Clinical Investigation*, vol. 96, no. 2, pp. 1137–1144, 1995.

[48] S. Zanotti, S. Gibertini, and M. Mora, "Altered production of extra-cellular matrix components by muscle-derived Duchenne muscular dystrophy fibroblasts before and after TGF-β1 treatment," *Cell and Tissue Research*, vol. 339, no. 2, pp. 397–410, 2010.

[49] K. M. Flanigan, E. Ceco, K. M. Lamar et al., "LTBP4 genotype predicts age of ambulatory loss in Duchenne muscular dystrophy," *Annals of Neurology*, vol. 73, no. 4, pp. 481–488, 2013.

[50] K. R. Wagner, A. C. McPherron, N. Winik, and S.-J. Lee, "Loss of myostatin attenuates severity of muscular dystrophy in mdx mice," *Annals of Neurology*, vol. 52, no. 6, pp. 832–836, 2002.

[51] Y.-W. Chen, K. Nagaraju, M. Bakay et al., "Early onset of inflammation and later involvement of TGFβ in Duchenne muscular dystrophy," *Neurology*, vol. 65, no. 6, pp. 826–834, 2005.

[52] M. Locati and P. M. Murphy, "Chemokines and chemokine receptors: biology and clinical relevance in inflammation and AIDS," *Annual Review of Medicine*, vol. 50, pp. 425–440, 1999.

[53] Y. Yogo, S. Fujishima, T. Inoue et al., "Macrophage derived chemokine (CCL22), thymus and activation-regulated chemokine (CCL17), and CCR4 in idiopathic pulmonary fibrosis," *Respiratory Research*, vol. 10, article no. 80, 2009.

[54] B. De Paepe, K. K. Creus, J. J. Martin, and J. L. De Bleecker, "Upregulation of chemokines and their receptors in Duchenne muscular dystrophy: potential for attenuation of myofiber necrosis," *Muscle & Nerve*, vol. 46, no. 6, pp. 917–925, 2012.

[55] M. Pescatori, A. Broccolini, C. Minetti et al., "Gene expression profiling in the early phases of DMD: a constant molecular signature characterizes DMD muscle from early postnatal life throughout disease progression," *FASEB Journal*, vol. 21, no. 4, pp. 1210–1226, 2007.

[56] E. Abdel-Salam, I. Ehsan Abdel-Meguid, R. Shatla, and S. S. Korraa, "Stromal cell-derived factors in Duchenne muscular dystrophy," *Acta Myologica*, vol. 29, no. 3, pp. 398–403, 2010.

[57] J. D. Porter, W. Guo, A. P. Merriam et al., "Persistent overexpression of specific CC class chemokines correlates with macrophage and T-cell recruitment in mdx skeletal muscle," *Neuromuscular Disorders*, vol. 13, no. 3, pp. 223–235, 2003.

[58] A. Demoule, M. Divangahi, G. Danialou et al., "Expression and regulation of CC class chemokines in the dystrophic (mdx) diaphragm," *American Journal of Respiratory Cell and Molecular Biology*, vol. 33, no. 2, pp. 178–185, 2005.

[59] E. Mercuri and F. Muntoni, "Muscular dystrophies," *The Lancet*, vol. 381, no. 9869, pp. 845–860, 2013.

[60] E. Gallardo, R. Rojas-García, N. De Luna, A. Pou, R. H. Brown Jr., and I. Illa, "Inflammation in dysferlin myopathy: immunohistochemical characterization of 13 patients," *Neurology*, vol. 57, no. 11, pp. 2136–2138, 2001.

[61] B. De Paepe, K. K. Creus, and J. L. De Bleecker, "Chemokines in idiopathic inflammatory myopathies," *Frontiers in Bioscience*, vol. 13, no. 7, pp. 2548–2577, 2008.

[62] G. S. Baird and T. J. Montine, "Multiplex immunoassay analysis of cytokines in idiopathic inflammatory myopathy," *Archives of Pathology & Laboratory Medicine*, vol. 132, no. 2, pp. 232–238, 2008.

[63] M. Van Putten and A. Aartsma-Rus, "Opportunities and challenges for the development of antisense treatment in neuromuscular disorders," *Expert Opinion on Biological Therapy*, vol. 11, no. 8, pp. 1025–1037, 2011.

[64] J. C. Van Deutekom, A. A. Janson, I. B. Ginjaar et al., "Local dystrophin restoration with antisense oligonucleotide PRO051," *The New England Journal of Medicine*, vol. 357, no. 26, pp. 2677–2686, 2007.

[65] F. Muntoni and D. Wells, "Genetic treatments in muscular dystrophies," *Current Opinion in Neurology*, vol. 20, no. 5, pp. 590–594, 2007.

[66] J. R. Mendell, K. Campbell, L. Rodino-Klapac et al., "Dystrophin immunity in Duchenne's muscular dystrophy," *The New England Journal of Medicine*, vol. 363, no. 15, pp. 1429–1437, 2010.

[67] K. M. Flanigan, K. Campbell, L. Viollet et al., "Anti-dystrophin T-cell responses in Duchenne muscular dystrophy: prevalence and a glucocorticoid treatment effect," *Human Gene Therapy Methods*, 2013.

[68] B. L. Y. Wong and C. Christopher, "Corticosteroids in Duchenne muscular dystrophy: a reappraisal," *Journal of Child Neurology*, vol. 17, no. 3, pp. 183–190, 2002.

[69] M. D. Grounds and J. Torrisi, "Anti-TNFα (Remicade) therapy protects dystrophic skeletal muscle from necrosis," *FASEB Journal*, vol. 18, no. 6, pp. 676–682, 2004.

[70] L. E. Gosselin and D. A. Martinez, "Impact of TNF-α blockade on TGF-β1 and type I collagen mRNA expression in dystrophic muscle," *Muscle and Nerve*, vol. 30, no. 2, pp. 244–246, 2004.

[71] S. Hodgetts, H. Radley, M. Davies, and M. D. Grounds, "Reduced necrosis of dystrophic muscle by depletion of host neutrophils, or blocking TNFα function with Etanercept in mdx mice," *Neuromuscular Disorders*, vol. 16, no. 9-10, pp. 591–602, 2006.

[72] T. N. C. Wells, C. A. Power, J. P. Shaw, and A. E. I. Proudfoot, "Chemokine blockers—therapeutics in the making?" *Trends in Pharmacological Sciences*, vol. 27, no. 1, pp. 41–47, 2006.

[73] J. G. Tidball and M. Wehling-Henricks, "Macrophages promote muscle membrane repair and muscle fibre growth and regeneration during modified muscle loading in mice in vivo," *Journal of Physiology*, vol. 578, no. 1, pp. 327–336, 2007.

[74] L. Yahiaoui, D. Gvozdic, G. Danialou, M. Mack, and B. J. Petrof, "CC family chemokines directly regulate myoblast responses to skeletal muscle injury," *Journal of Physiology*, vol. 586, no. 16, pp. 3991–4004, 2008.

[75] G. L. Warren, T. Hulderman, D. Mishra et al., "Chemokine receptor CCR2 involvement in skeletal muscle regeneration," *FASEB Journal*, vol. 19, no. 3, pp. 413–415, 2005.

[76] C. Van Erp, N. G. Irwin, and A. J. Hoey, "Long-term administration of pirfenidone improves cardiac function in mdx mice," *Muscle & Nerve*, vol. 34, no. 3, pp. 327–334, 2006.

[77] A. P. T. Taniguti, A. Pertille, C. Y. Matsumura, H. S. Neto, and M. J. Marques, "Prevention of muscle fibrosis and myonecrosis in mdx mice by suramin, a TGF-β1 blocker," *Muscle & Nerve*, vol. 43, no. 1, pp. 82–87, 2011.

[78] F. Andreetta, P. Bernasconi, F. Baggi et al., "Immunomodulation of TGF-beta1 in mdx mouse inhibits connective tissue proliferation in diaphragm but increases inflammatory response: implications for antifibrotic therapy," *Journal of Neuroimmunology*, vol. 175, no. 1-2, pp. 77–86, 2006.

[79] S. Bogdanovich, T. O. B. Krag, E. R. Barton et al., "Functional improvement of dystrophic muscle by myostatin blockade," *Nature*, vol. 420, no. 6914, pp. 418–421, 2002.

[80] K. J. Morine, L. T. Bish, J. T. Selsby et al., "Activin IIB receptor blockade attenuates dystrophic pathology in a mouse model of Duchenne muscular dystrophy," *Muscle & Nerve*, vol. 42, no. 5, pp. 722–730, 2010.

[81] C. Qiao, J. Li, J. Jiang et al., "Myostatin propeptide gene delivery by adeno-associated virus serotype 8 vectors enhances muscle growth and ameliorates dystrophic phenotypes in mdx mice," *Human Gene Therapy*, vol. 19, no. 3, pp. 241–253, 2008.

[82] S. Zanotti, S. Gilbertini, P. Salvadori, R. Mantegazza, and M. Mora, "Duchenne muscular dystrophy fibroblast nodules: a cell-based assay for screening anti-fibrotic agents," *Cell and Tissue Research*, vol. 353, no. 3, pp. 659–670, 2013.

[83] A. Louvet, F. Teixeira-Clerc, M.-N. Chobert et al., "Cannabinoid CB2 receptors protect against alcoholic liver disease by regulating Kupffer cell polarization in mice," *Hepatology*, vol. 54, no. 4, pp. 1217–1226, 2011.

[84] M. R. Hussein, S. A. Hamed, M. G. Mostafa, E. E. Abu-Dief, N. F. Kamel, and M. R. Kandil, "The effects of glucocorticoid therapy on the inflammatory and dendritic cells in muscular dystrophies," *International Journal of Experimental Pathology*, vol. 87, no. 6, pp. 451–461, 2006.

Hindawi Publishing Corporation
Mediators of Inflammation
Volume 2013, Article ID 539156, 7 pages
http://dx.doi.org/10.1155/2013/539156

Research Article

Strength Training and Testosterone Treatment Have Opposing Effects on Migration Inhibitor Factor Levels in Ageing Men

D. Glintborg,[1] L. L. Christensen,[1] T. Kvorning,[2] R. Larsen,[3] K. Brixen,[1] D. M. Hougaard,[4] B. Richelsen,[5] J. M. Bruun,[5,6] and M. Andersen[1]

[1] *Department of Endocrinology, Odense University Hospital, 5000 Odense C, Denmark*
[2] *Institute of Sport Science and Clinical Biomechanics, University of Southern Denmark, 5000 Odense, Denmark*
[3] *Department of Informatics and Mathematical Modelling, Technical University of Denmark, 2800 kongens Lyngby, Denmark*
[4] *Department of Clinical Biochemistry and Immunology, Statens Serum Institut, 2300 Copenhagen S, Denmark*
[5] *Department of Internal Medicine and Endocrinology (MEA), Aarhus University Hospital, 8000 Aarhus, Denmark*
[6] *Medical Department, Regional Hospital Randers, 8900 Randers, Denmark*

Correspondence should be addressed to D. Glintborg; dorte.glintborg@rsyd.dk

Received 1 April 2013; Revised 24 July 2013; Accepted 2 August 2013

Academic Editor: Salahuddin Ahmed

Background. The beneficial effects of testosterone treatment (TT) are debated. *Methods.* Double-blinded, placebo-controlled study of six months TT (gel) in 54 men aged 60–78 with bioavailable testosterone (BioT) <7.3 nmol/L and waist >94 cm randomized to TT (50–100 mg/day, $n = 20$), placebo ($n = 18$), or strength training (ST) ($n = 16$) for 24 weeks. Moreover, the ST group was randomized to TT ($n = 7$) or placebo ($n = 9$) after 12 weeks. *Outcomes*. Chemokines (MIF, MCP-1, and MIP-1α) and lean body mass (LBM), total, central, extremity, visceral, and subcutaneous (SAT) fat mass established by DXA and MRI. *Results*. From 0 to 24 weeks, MIF and SAT decreased during ST + placebo versus placebo, whereas BioT and LBM were unchanged. TT decreased fat mass (total, central, extremity, and SAT) and increased BioT and LBM versus placebo. MIF levels increased during TT versus ST + placebo. ST + TT decreased fat mass (total, central, and extremity) and increased BioT and LBM versus placebo. From 12 to 24 weeks, MCP-1 levels increased during TT versus placebo and MCP-1 levels decreased during ST + placebo versus placebo. *Conclusion*. ST + placebo was associated with decreased MIF levels suggesting decreased inflammatory activity. TT may be associated with increased inflammatory activity. This trial is registered with ClinicalTrials.gov NCT00700024.

1. Introduction

Testosterone replacement therapy is indicated in severe hypogonadism, whereas the indication for testosterone therapy (TT) in aging hypogonadal men without hypothalamic, pituitary, or testicular disease is debated [1, 2]. In particular, the effects of TT on metabolic and cardiovascular outcomes are undetermined [3]. Recently, we reported that TT increased lean body mass (LBM) and lipid oxidation [1], whereas lower extremity fat mass (LEFM) and abdominal subcutaneous adipose tissue (SAT) decreased, but visceral adipose tissue (VAT) was unchanged [4]. In addition to these testosterone-induced changes in body composition and lipid metabolism, we observed decreased levels of high density lipoprotein, adiponectin, and osteoprotegerin [5], whereas the cardiovascular risk markers, LDL, c-reactive protein, and insulin sensitivity measured by clamp were unchanged [1, 4]. Recent meta-analyses found no effect of TT on cardiovascular outcomes, but the duration of the included studies was limited and cardiovascular outcomes were not reported in all trials [6]. The overall interpretation of the combined effects of TT on metabolic and cardiovascular risk factors remains undetermined, and additional studies are needed.

Adiposity is a major component of the metabolic syndrome and an independent risk factor for the development of type 2 diabetes and cardiovascular disease [7]. Human adipose tissue produces and releases a number of bioactive proteins, collectively referred to as adipokines [8]. Adipokines are primarily secreted by adipose tissue-resident

macrophages [9]. In obesity, the number of adipose tissue-resident macrophages is increased in both SAT and VAT [10, 11], and circulating mononuclear cells are in a more inflammatory state [12]. Chemokines are an important subgroup of adipokines, which activate (chemoattract) mononuclear cells during the process of inflammation. Increasing adiposity is associated with influx of monocytes to the AT with concomitant differentiation of AT-resident macrophages from a primarily anti-inflammatory to a proinflammatory state [10]. Interestingly, the influx of monocytes may be orchestrated by several chemokines. Monocyte chemoattractant protein-1 (MCP-1) and migration inhibitor factor (MIF) are positively associated with obesity [13–15]; these chemokines have the ability to induce insulin resistance [16] and are predictors for type 2 diabetes [17]. Obesity is inversely associated with testosterone levels [18], but the effect of TT on chemokine levels remains to be established.

Aging men with low normal testosterone levels are often characterized by decreased LBM, decreased muscle strength, and relative inactivity [19]. Physical exercise is associated with decreased chemokine levels [13, 31]. We are not aware of previous studies evaluating the effect of combined testosterone and strength exercise on chemokine levels in ageing men.

In the present study, we investigated the effects of TT on chemokine levels in aging men with low normal testosterone levels [18] and increased waist circumference. We hypothesized that decreased SAT during TT could be associated with decreased chemokine levels. We furthermore examined if strength exercise with and without TT was associated with decreased chemokine levels.

2. Methods

The study was a single center, randomized, placebo-controlled, six-month study to assess the effect of testosterone gel and strength training (ST) on body composition, components of the metabolic syndrome, and quality of life in men with low normal bioavailable testosterone (BioT) levels and increased body fat. The inclusion criteria for participation in the study were age 60–78 years, BioT <7.3 nmol/L, and waist circumference >94 cm. The exclusion criteria were hematocrit >50%, prostate cancer or a prostate specific antigen >3 ng/dL, previous or ongoing malignant disease, severe ischemic heart or respiratory disease, disability, diabetes mellitus, alcohol or drug abuse, abnormal routine blood samples (TSH, ionized calcium, hemoglobin, and liver and kidney functions), and treatment with 5α reductase inhibitors, morphine, or oral glucocorticoid steroids.

The sample size of the study was determined by the effect of TT on LBM and has been described previously [1]. LBM was chosen as the primary study outcome based on a meta-analysis on testosterone therapy in ageing men by Isidori et al. [20]. Chemokine levels were secondary study outcomes.

Subjects were randomly assigned to receive testosterone (TT, $n = 20$), placebo ($n = 18$), or engage in strength training ($n = 16$) as previously described [1]. After 12 weeks, the ST group was randomized into two groups receiving testosterone or placebo (ST + TT, $n = 7$, and ST + placebo, $n = 9$) (Figure 1). Treatment with testosterone and placebo was double blinded. Randomization numbers were assigned to the participants in order of enrollment into the study. The study was approved by the local Ethics Committee and declared in http://www.clinicaltrials.gov/ (NCT00700024). All participants gave written informed consent. Exclusion criteria were hematocrit >50%, prostate cancer or a prostate specific antigen (PSA) >3 ng/dL, previous or ongoing malignant disease, severe ischemic heart or respiratory disease, disability, diabetes mellitus, alcohol or drug abuse, abnormal routine blood samples (TSH, ionized calcium, hemoglobin, and liver and kidney functions), and treatment with 5α reductase inhibitors, morphine, or oral glucocorticoid steroids. Four patients had previous apoplexia cerebri, and three patients had ischemic heart disease. None of the study participants were restricted during daily living activities. A total of 42% of participants were on antihypertensive drugs, 29% were on cholesterol-lowering drugs, 10% were on inhalation steroids, 6% were on antidepressants, and 4% were treated for enlarged prostate. The distribution of concomitant medication in the treatment arms was equal. No cholesterol-lowering drugs or other medications were introduced during the study. Participants received 5–10 g gel/50–100 mg testosterone (Testim, Ipsen, France) or 5–10 g gel/placebo. The randomization list, medicine labeling, and randomization and code break envelopes were generated by Ipsen Scandinavia (Kista, Sweden) to ensure double blinding. Compliance was monitored by participant self-reporting at each visit. The study outcomes were evaluated at baseline and after three and six months' intervention.

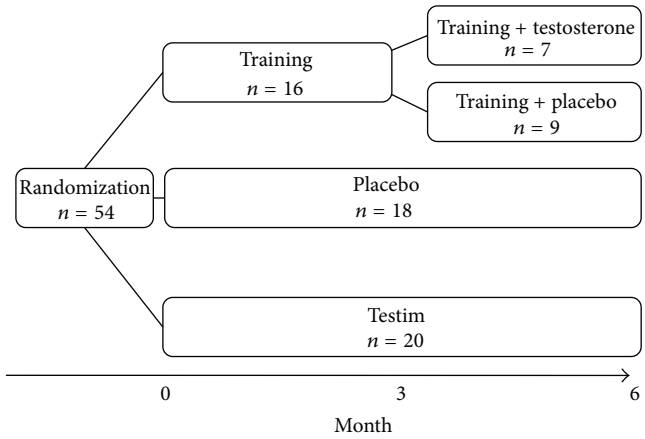

Figure 1: Study design.

2.1. Training Protocol. The training protocol has been described recently [21]. In brief, participants performed 5 min bicycling for warm up (approximately 100 W) followed by a progressive heavy strength training program including exercises for the entire body and gradually increased training loads [21]. All training sessions were supervised, and patients and supervisors were blinded for placebo/testosterone treatment. All subjects participated in minimum 2 out of 3 weekly training sessions (mean training adherence 75 ± 8%).

Subjects were advised to refrain from self-initiated resistance exercise training and intense endurance training but were allowed to continue on other habitual activities throughout the study. All subjects received 0.2 liter of skimmed chocolate milk (containing 7 g protein, 20 g carbohydrate, and 1 g fat) after each strength training session, but in addition, subjects were informed not to change their diet.

2.2. Biochemical Analyses

2.2.1. Chemokines. Plasma levels of the investigated chemokines were assessed using a specific human enzyme-linked immunosorbent assay (ELISA) method (DuoSet, R&D Systems Europe Ltd., UK). MCP-1, macrophage inflammatory protein- (MIP-) 1α, and MIF assays had intra-assay coefficient of variation (CV) of 8.1% ($n = 12$), 7.1% ($n = 12$), and 4.6% ($n = 12$), respectively. The samples used for the chemokine analyses had not previously been thawed.

2.2.2. Testosterone and SHBG. Testosterone was measured after an overnight fast between 8 and 9 AM. Serum total testosterone was measured by liquid chromatography tandem mass spectrometry after ether extraction. For testosterone measurements, the intra-assay coefficient of variation was 10% for total testosterone >0.2 nmol/L and 30% in the range between 0.1 and 0.2 nmol/L. SHBG was measured by autoDELFIA assay, and BioT was calculated according to the formulas of Vermeulen et al. [22], http://www.issam.ch/freetesto.htm. During calculations, we used the assumption that albumin concentration in participants was 4.3 g/L. A single measurement of testosterone was performed to determine eligibility. BioT levels were all below 7.3 nmol/L at reevaluation after three weeks on placebo treatment ($n = 18$). The normal range and 95% confidence interval for BioT were 7.3 nmol/L (7.0–7.5 nmol/L) [18].

2.3. Body Composition Measures

2.3.1. Dual X-Ray Absorptiometry (DXA). TFM, central fat mass (CFM), lower extremity fat mass (LEFM), and LBM were measured by DXA using a Hologic Discovery device (Waltham, MA, USA). The CV was 0.8% for TFM and 0.6% for LBM, respectively.

2.3.2. Magnetic Resonance Imaging. Magnetic resonance imaging was performed as previously reported [4]. In brief, a 3.0 Tesla High field MR Unit was used (Philips Achieva, Phillips Healthcare, Best, The Netherlands). One abdominal slice (10 mm thick, intervertebral space of L4/L5, perpendicular to subcutaneous fat) was recorded. Computer software was used to trace the different compartments of fat on the abdomen and for assessment of the areas of SAT and VAT. The thigh fat area was determined on one femoral slice (15 cm from the major trochanter and perpendicular to subcutaneous fat) using a T1-weighted gradient-echo sequence (repetition time 400 ms, echo time 18 ms, acquisition matrix 376 × 335, field of view 230 × 230 mm). Computer software was used to trace fat and muscle compartments on the thigh to assess subcutaneous and intramuscular fat and thigh muscle area [23]. Due to various reasons (claustrophobia, did not attend, and did not want examination), complete MRI data were only available for 54 patients. The number of patients not attending first MRI was placebo: 2, TT: 1, ST + placebo: 1, and ST + TT: 2. The number of patients not attending the MRI at study termination was placebo: 2, TT: 1, ST + placebo: 2, and ST + TT: 1. Patients without MRI were included in the data analyses that did not include MRI data.

2.4. Statistical Analysis. Pretreatment differences between patients in the testosterone and placebo group were tested using the Mann-Whitney U tests. The effect of placebo, TT, ST + placebo, and ST + TT was analyzed by comparing delta (Δ) values of hormonal and metabolic variables using the Mann-Whitney U tests. Δ-values were calculated as post treatment level minus pretreatment level of each analyzed variable. In this way, Δ-values were positive if the measured variable increased during intervention. Δchemokine levels were correlated with Δ-values of hormonal and metabolic variables using the Spearman nonparametric correlation tests.

All statistics were performed using SPSS 17.0 (SPSS Inc., Chicago, USA) for calculations and P values < 0.05. were considered significant. Data are given as median and interquartile range.

3. Results

3.1. Study Population ($n = 54$). Baseline data are shown in Table 1. There were no significant differences at baseline regarding age, chemokine levels, and body composition. Baseline data on testosterone and body composition in the testosterone and placebo groups have been presented previously [1, 4].

3.2. Intervention. Changes in chemokines, BioT, and body composition during 3 and 6 months' intervention are shown in Table 2 (effects of TT and ST on BioT and body composition have recently been discussed) [4, 21]. MIP-1α levels and VAT were unchanged during all interventions at 3 and 6 months, VAT data not shown.

TT alone had no significant effects on muscle strength, whereas ST significantly increased muscle strength independent of the addition of testosterone (data not shown, discussed in [21]).

3.3. Six-Month Effects (6–0). Circulating MIF levels decreased during ST + placebo and were significantly different from changes in MIF during placebo and changes during TT, but not from changes in MIF during ST + TT (Table 2).

TT increased BioT and LBM versus placebo, and fat mass (TFM, CFM, LEFM, and SAT) decreased.

ST + placebo decreased fat mass (TFM, LEFM, and SAT) versus placebo without significantly affecting BioT and LBM.

ST + TT was followed by similar BioT and LBM compared to TT alone. The beneficial effects of ST + TT on fat mass measures were comparable to ST + placebo.

Table 1: Baseline data.

	Placebo ($n = 18$)	TT ($n = 20$)	ST ($n = 16$)
Age (years)	67 (65–70)	68 (62–72)	68 (62–73)
MIF (pg/mL)	203 (128–378)	182 (117–453)	259 (199–498)
MCP-1 (pg/mL)	71 (59–86)	72 (63–105)	87 (64–101)
MIP-1α (pg/mL)	27 (13–1981)	17 (9–1257)	29 (11–1764)
BioT (nmol/L)	4.4 (3.3–6.0)	5.1 (4.3–6.1)	5.3 (2.2–6.2)
LBM (kg)	64.7 (58.5–73.3)	64.6 (57.2–71.3)	65.4 (60.2–72.0)
Waist (cm)	105 (98–118)	107 (103–115)	107 (104–115)
Fat mass (kg)	23.9 (18.2–33.1)	24.3 (21.4–31.8)	25.2 (22.5–28.7)
Central fat mass (kg)	13.1 (9.0–18.4)	14.0 (12.5–18.2)	14.7 (12.3–17.4)
SAT	24.2 (21.5–34.9)	29.3 (24.5–40.7)	27.9 (24.6–33.1)
VAT	15.6 (11.5–20.0)	15.1 (12.4–19.3)	16.5 (12.3–19.3)

Data presented as median (interquartile range).
Baseline data from the subgroups ST + placebo and ST + TT can be seen in Table 2.
No significant differences, Mann-Whitney test between groups.
BioT: bioavailable testosterone.
LBM: lean body mass.
SAT: subcutaneous adipose tissue.
VAT: visceral adipose tissue.

3.4. Three-Month Effects (3–0). Chemokine levels were unchanged during the first three months of intervention (Table 2).

3.5. Three-Month Effects (6–3). ST + placebo versus placebo and versus ST + TT was followed by decreased MCP-1 levels (Table 2).

3.6. Bivariate Associations between ΔChemokines and ΔBody Composition Measures ST + TT (6–0). ΔMIF was significantly associated with Δfat ($r = -0.83$, $P < 0.05$) and ΔLEfat ($r = -0.86$, $P < 0.05$). ΔMIP was significantly associated with Δfat ($r = -0.93$, $P < 0.001$), ΔCFM ($r = -0.75$, $P < 0.05$), and ΔLEfat ($r = -0.96$, $P < 0.001$).

3.7. TT and ST + Placebo (6–0). No significant associations were found between Δchemokine levels and Δfat mass measures during TT or during ST + placebo.

4. Discussion

In the present study, MIF levels increased during TT, whereas ST + placebo was associated with decreased MIF and MCP-1 levels in ageing men with low normal BioT and increased waist circumference. Our findings suggest opposing effects of TT and ST on inflammatory status.

Given the on-going debate on testosterone therapy in aging hypogonadal men without pituitary or testicular disease, it is important to clarify possible favorable or unfavorable effects of testosterone therapy [24]. Our findings of positive associations between testosterone and chemokine levels support previous observations of higher circulating MIF in males compared to females [17, 25] and findings from cross-sectional studies [25]. Patients with polycystic ovary syndrome and hyperandrogenemia showed a BMI and SHBG independent correlation between chemokine levels and testosterone, further supporting that high testosterone levels may increase inflammation markers [26]. In the present study, ΔBioT and Δchemokine levels were not associated, and these data do not support a direct effect of testosterone on inflammatory status. Instead, the effects of TT on chemokine secretion could be indirectly affected by other (inflammatory) pathways or by factors such as fat mass or LBM as discussed below.

We are not aware of previous studies that evaluated the long-term effect of randomized TT on chemokine levels in ageing male study populations. Six-month DHEAS treatment in women with adrenal insufficiency did not affect MCP-1 levels despite increased LBM [27], but fat distribution was unchanged and MIF data were not available in the study. Interestingly, animal studies showed that rats express MIF in Leydig cells, but whether MIF affects human reproduction is undetermined [25, 28]. Exogenous testosterone could increase MIF levels through a decreased testicular LH stimulation, but future studies are needed to test this hypothesis. The present data along with previous studies therefore support that increased testosterone levels are associated with increased chemokine levels. Increased circulating levels of MCP-1 and MIF are positively associated with the development of various metabolic diseases such as type 2 diabetes, atherosclerosis, and cardiovascular disease [29, 30]. The impact of increased chemokine levels during testosterone treatment on long-term cardiovascular risk awaits long-term studies.

In the present study, ST was associated with reduced MIF and MCP-1 levels suggesting decreased inflammatory activity. These findings support previous reports in which lifestyle intervention with diet and/or increased physical activity decreased circulating chemokine levels, reduced infiltration of macrophages into the AT, and improved whole-body inflammation [31]. We found that MCP-1 levels decreased during the last three months of the intervention period. This could suggest that longer time of exercise is needed to improve inflammatory status perhaps mediated by improved body composition during physical exercise. Chemokine secretion is higher in VAT than in SAT [11, 32] and inflammation is unchanged when the SAT depot is selectively reduced by abdominal liposuction [33]. Our study supports these findings as SAT decreased along with adiponectin during TT [4]. In the present study, however, VAT was unchanged during TT and ST, and the highest decrease in SAT was observed during TT. We found that ΔMIF and ΔMIP were strongly inversely associated with ΔLEFM supporting that a "pear-shape" is associated with decreased inflammatory activity [34, 35] as well as higher adiponectin levels [35].

Table 2: Clinical and biochemical characteristics in patients during testosterone, placebo, and strength training.

			Placebo $n = 18$	TT $n = 20$	ST ST + placebo $n = 9$	ST ST + TT $n = 7$
MIF (pg/mL)	$t = 0$	(3–0)	203 (128–378)	182 (117–453)	266 (118–660)	253 (228–394)
	$t = 3$	(6–3)	205 (136–411)	282 (183–582)	207 (119–704)	277 (239–376)
	$t = 6$	(6–0)*	227 (141–649)	412 (170–777)	129 (101–471)$^{¤\#}$	235 (169–301)
MCP-1 (pg/mL)	$t = 0$	(3–0)	71 (59–85)	72 (63–105)	98 (62–109)	85 (59–87)
	$t = 3$	(6–3)*	74 (56–101)	84 (67–107)$^{\#}$	93 (70–117)$^{\#}$	76 (58–93)$^{¤\S}$
	$t = 6$	(6–0)	82 (62–101)	80 (64–100)	72 (58–93)	79 (59–105)
MIP-1α (pg/mL)	$t = 0$	(3–0)	27 (13–1981)	17 (8–1257)	13 (8–827)	200 (18–2884)
	$t = 3$	(6–3)	26 (13–1855)	17 (11–1318)	14 (9–798)	263 (18–2390)
	$t = 6$	(6–0)	31 (13–1800)	16 (10–1059)	13 (8–856)	347 (18–2152)
BioT (nmol/L)	$t = 0$	(3–0)*	4.4 (3.3–6.0)	5.1 (4.3–6.1)$^{\#\#}$	5.1 (5.0–6.2)$^{¤}$	5.7 (4.8–6.2)$^{\#\#\S\S}$
	$t = 3$	(6–3)	4.3 (3.3–4.8)	8.1 (5.6–12.3)	4.5 (4.2–5.0)	4.5 (4.1–5.1)
	$t = 6$	(6–0)**	3.9 (3.4–4.8)	9.7 (6.5–13.8)$^{\#}$	4.3 (3.7–4.4)$^{¤}$	12.8 (7.3–16.3)$^{\#\#\S}$
LBM (kg)	$t = 0$	(3–0)**	64.7 (58.5–73.2)	64.7 (57.2–71.2)$^{\#}$	63.2 (59.8–68.7)	70.9 (65.1–78.2)$^{\#\#\S}$
	$t = 3$	(6–3)	65.2 (58.9–73.3)	66.1 (59.9–72.2)	63.2 (57.5–68.9)	73.1 (63.3–78.2)
	$t = 6$	(6–0)*	64.3 (58.8–74.7)	65.8 (59.3–72.6)$^{\#}$	63.8 (5.9–6.9)	75.4 (66.0–78.7)$^{\#}$
Fat mass (kg)	$t = 0$	(3–0)	23.9 (18.2–33.1)	24.4 (21.4–31.8)	25.0 (20.9–28.9)	25.4 (24.0–27.1)
	$t = 3$	(6–3)	24.3 (18.0–32.1)	23.8 (21.4–31.3)	25.9 (21.5–28.0)	25.9 (22.9–26.3)
	$t = 6$	(6–0)*	25.1 (19.2–31.3)	23.0 (20.3–30.2)$^{\#}$	24.2 (21.5–27.8)$^{\#}$	24.7 (21.5–25.9)$^{\#}$
CFM (kg)	$t = 0$	(3–0)	13.1 (9.0–18.4)	14.0 (12.5–18.2)	13.9 (11.8–17.6)	15.0 (13.7–16.9)
	$t = 3$	(6–3)	13.1 (8.5–18.4)	13.6 (12.2–18.2)	14.5 (12.2–16.5)	14.6 (13.6–15.7)
	$t = 6$	(6–0)*	13.5 (9.2–17.6)	13.9 (11.2–17.4)$^{\#}$	12.4 (12.1–15.6)	13.5 (13.1–15.9)$^{\#}$
LEfat (kg)	$t = 0$	(3–0)	6.9 (5.6–9.5)	6.5 (5.6–7.9)	7.2 (5.7–8.6)	7.4 (6.4–8.1)
	$t = 3$	(6–3)	7.2 (5.3–9.8)	6.4 (5.5–8.2)	7.2 (5.7–8.4)	6.8 (6.6–7.5)
	$t = 6$	(6–0)*	7.2 (5.8–9.7)	6.1 (5.2–8.0)$^{\#}$	6.8 (5.3–8.2)$^{\#}$	6.6 (6.5–7.2)$^{\#}$
SAT	$t = 0$	(3–0)	24.2 (21.5–34.9)	29.2 (24.5–40.7)	29.6 (24.9–39.7)	27.9 (23.2–28.3)
	$t = 3$	(6–3)*	23.7 (20.8–35.3)	29.7 (24.2–40.1)$^{\#\#}$	30.3 (25.2–39.9)$^{\#}$	26.7 (23.4–28.7)$^{¤\S}$
	$t = 6$	(6–0)**	25.7 (20.2–36.5)	25.6 (21.7–37.2)$^{\#}$	29.7 (24.0–37.4)$^{\#}$	26.6 (23.5–31.1)$^{¤\S}$

Data presented as median (interquartile range).
Kruskall-Wallis tests followed by Mann-Whitney test performed on delta values.
$^{*}P < 0.05$ between groups, $^{**}P < 0.001$ between groups (delta values).
$^{\#}P < 0.05$ versus placebo, $^{\#\#}P < 0.001$ versus placebo.
$^{¤}P < 0.05$ versus testosterone.
$^{\S}P < 0.05$ versus training + placebo.
ST: strength training.
TT: testosterone treatment.
LBM: lean body mass.
SAT: subcutaneous adipose tissue.
Visceral adipose tissue was unchanged during all interventions, and these results are omitted from the table.

The strong inverse association between ΔMIF and ΔMIP and central and total fat mass during ST + TT treatment was an unexpected finding in the present study. ΔVAT and ΔSAT were unassociated with Δchemokine levels suggesting that changed fat mass was not the only predictor of chemokine levels.

In the present study, resistance training and not aerobic training was included in the intervention. A recent study in patients with type 2 diabetes found that aerobic training was associated with similar weight loss but had more beneficial effects on inflammatory markers than ST [36]. Future studies are needed to evaluate possible effects of various exercise interventions on inflammatory status in men during TT.

Change in LBM was our main study outcome [20]. We found that LBM was unaffected by ST alone, whereas TT alone or in combination with ST significantly increased LBM with no additional effect of the addition of testosterone. Our findings of increased LBM independent of muscle strength are in agreement with previous studies and have recently been discussed [21]. We found no significant association between changes in chemokine levels and changes in LBM, suggesting that muscle tissue is not the main regulator of chemokine

secretion. Indeed, muscle tissue expresses and releases very low levels of chemokines even in relation to exercise [31].

In conclusion, the findings of the present study support that TT and ST have similar and positive effects on fat mass; however, ST is superior to TT regarding chemokine levels, inflammatory status, and body strength. Further studies on cardiovascular end points are needed to determine the long-term effects of TT alone and in combination with lifestyle intervention in ageing men with low normal BioT.

Authors' Contribution

D. Glintborg and L. L. Christensen contributed equally to the paper.

Acknowledgments

The authors thank the Novo Nordisk Foundation, Ipsen Scandinavia, for kindly providing Testim and placebo, and the Institute of Clinical Research-University of Southern Denmark.

References

[1] L. Frederiksen, K. Højlund, D. M. Hougaard, K. Brixen, and M. Andersen, "Testosterone therapy increased muscle mass and lipid oxidation in aging men," *Age*, vol. 34, no. 1, pp. 145–156, 2012.

[2] P. Dandona and S. Dhindsa, "Update: hypogonadotropic hypogonadism in type 2 diabetes and obesity," *Journal of Clinical Endocrinology and Metabolism*, vol. 96, no. 9, pp. 2643–2651, 2011.

[3] S. Basaria, A. D. Coviello, T. G. Travison et al., "Adverse events associated with testosterone administration," *The New England Journal of Medicine*, vol. 363, no. 2, pp. 109–122, 2010.

[4] L. Frederiksen, K. Højlund, D. M. Hougaard et al., "Testosterone therapy decreases subcutaneous fat and adiponectin in aging men," *European Journal of Endocrinology*, vol. 166, no. 3, pp. 469–476, 2012.

[5] L. Frederiksen, D. Glintborg, K. Hojlund et al., "Osteoprotegerin levels decrease during testosterone therapy in aging men and are associated with changed distribution of regional fat," *Hormone and Metabolic Research*, vol. 45, no. 4, pp. 308–313, 2013.

[6] M. M. Fernández-Balsells, M. H. Murad, M. Lane et al., "Adverse effects of testosterone therapy in adult men: a systematic review and meta-analysis," *Journal of Clinical Endocrinology and Metabolism*, vol. 95, no. 6, pp. 2560–2575, 2010.

[7] R. H. Eckel, S. M. Grundy, and P. Z. Zimmet, "The metabolic syndrome," *Lancet*, vol. 365, no. 9468, pp. 1415–1428, 2005.

[8] M. Fasshauer and R. Paschke, "Regulation of adipocytokines and insulin resistance," *Diabetologia*, vol. 46, no. 12, pp. 1594–1603, 2003.

[9] J. N. Fain, D. S. Tichansky, and A. K. Madan, "Most of the interleukin 1 receptor antagonist, cathepsin S, macrophage migration inhibitory factor, nerve growth factor, and interleukin 18 release by explants of human adipose tissue is by the non-fat cells, not by the adipocytes," *Metabolism*, vol. 55, no. 8, pp. 1113–1121, 2006.

[10] S. P. Weisberg, D. McCann, M. Desai, M. Rosenbaum, R. L. Leibel, and A. W. Ferrante Jr., "Obesity is associated with macrophage accumulation in adipose tissue," *Journal of Clinical Investigation*, vol. 112, no. 12, pp. 1796–1808, 2003.

[11] J. M. Bruun, A. S. Lihn, S. B. Pedersen, and B. Richelsen, "Monocyte chemoattractant protein-1 release is higher in visceral than subcutaneous human adipose tissue (AT): implication of macrophages resident in the AT," *Journal of Clinical Endocrinology and Metabolism*, vol. 90, no. 4, pp. 2282–2289, 2005.

[12] P. Dandona, A. Aljada, H. Ghanim et al., "Increased plasma concentration of macrophage Migration Inhibitory Factor (MIF) and MIF mRNA in mononuclear cells in the obese and the suppressive action of metformin," *Journal of Clinical Endocrinology and Metabolism*, vol. 89, no. 10, pp. 5043–5047, 2004.

[13] T. S. Church, M. S. Willis, E. L. Priest et al., "Obesity, macrophage migration inhibitory factor, and weight loss," *International Journal of Obesity*, vol. 29, no. 6, pp. 675–681, 2005.

[14] T. Christiansen, B. Richelsen, and J. M. Bruun, "Monocyte chemoattractant protein-1 is produced in isolated adipocytes, associated with adiposity and reduced after weight loss in morbid obese subjects," *International Journal of Obesity*, vol. 29, no. 1, pp. 146–150, 2005.

[15] J. Westerbacka, M. Kolak, T. Kiviluoto et al., "Genes involved in fatty acid partitioning and binding, lipolysis, monocyte/macrophage recruitment, and inflammation are overexpressed in the human fatty liver of insulin-resistant subjects," *Diabetes*, vol. 56, no. 11, pp. 2759–2765, 2007.

[16] H. Sell and J. Eckel, "Monocyte chemotactic protein-1 and its role in insulin resistance," *Current Opinion in Lipidology*, vol. 18, no. 3, pp. 258–262, 2007.

[17] C. Herder, N. Klopp, J. Baumert et al., "Effect of macrophage migration inhibitory factor (MIF) gene variants and MIF serum concentrations on the risk of type 2 diabetes: results from the MONICA/KORA Augsburg Case-Cohort Study, 1984–2002," *Diabetologia*, vol. 51, no. 2, pp. 276–284, 2008.

[18] T. L. Nielsen, C. Hagen, K. Wraae et al., "Visceral and subcutaneous adipose tissue assessed by magnetic resonance imaging in relation to circulating androgens, sex hormone-binding globulin, and luteinizing hormone in young men," *Journal of Clinical Endocrinology and Metabolism*, vol. 92, no. 7, pp. 2696–2705, 2007.

[19] C. Cooper, W. Dere, W. Evans et al., "Frailty and sarcopenia: definitions and outcome parameters," *Osteoporosis International*, vol. 7, pp. 1839–1848, 2012.

[20] A. M. Isidori, E. Giannetta, E. A. Greco et al., "Effects of testosterone on body composition, bone metabolism and serum lipid profile in middle-aged men: a meta-analysis," *Clinical Endocrinology*, vol. 63, no. 3, pp. 280–293, 2005.

[21] T. Kvorning, L. L. Christensen, K. Madsen et al., "Mechanical muscle function and lean body mass during supervised strength training and testosterone therapy in aging men with low normal testosterone levels—a placebo-controlled, randomized, double-blind study," *Journal of the American Geriatrics Society*, vol. 61, no. 6, pp. 957–962, 2013.

[22] A. Vermeulen, L. Verdonck, and J. M. Kaufman, "A critical evaluation of simple methods for the estimation of free testosterone in serum," *Journal of Clinical Endocrinology and Metabolism*, vol. 84, no. 10, pp. 3666–3672, 1999.

[23] T. H. Mosbech, K. Pilgaard, A. Vaag, and R. Larsen, "Automatic segmentation of abdominal adipose tissue in MRI," *Lecture Notes in Computer Science*, vol. 6688, pp. 501–511, 2011.

[24] G. Corona, G. Rastrelli, L. Vignozzi, E. Mannucci, and M. Maggi, "Testosterone, cardiovascular disease and the metabolic syndrome," *Best Practice and Research*, vol. 25, no. 2, pp. 337–353, 2011.

[25] A. M. Aloisi, G. Pari, I. Ceccarelli et al., "Gender-related effects of chronic non-malignant pain and opioid therapy on plasma levels of macrophage migration inhibitory factor (MIF)," *Pain*, vol. 115, no. 1-2, pp. 142–151, 2005.

[26] D. Glintborg, M. Andersen, B. Richelsen, and J. M. Bruun, "Plasma monocyte chemoattractant protein-1 (MCP-1) and macrophage inflammatory protein-1α are increased in patients with polycystic ovary syndrome (PCOS) and associated with adiposity, but unaffected by pioglitazone treatment," *Clinical Endocrinology*, vol. 71, no. 5, pp. 652–658, 2009.

[27] J. J. Christiansen, J. M. Bruun, J. S. Christiansen, J. O. Jørgensen, and C. H. Gravholt, "Long-term DHEA substitution in female adrenocortical failure, body composition, muscle function, and bone metabolism: a randomized trial," *European Journal of Endocrinology*, vol. 165, no. 2, pp. 293–300, 2011.

[28] A. Meinhardt, M. Bacher, G. Wennemuth, R. Eickhoff, and M. Hedger, "Macrophage migration inhibitory factor (MIF) as a paracrine mediator in the interaction of testicular somatic cells," *Andrologia*, vol. 32, no. 1, pp. 46–48, 2000.

[29] I. F. Charo and R. M. Ransohoff, "Mechanisms of disease: the many roles of chemokines and chemokine receptors in inflammation," *The New England Journal of Medicine*, vol. 354, no. 6, pp. 610–621, 2006.

[30] R. Kleemann and R. Bucala, "Macrophage migration inhibitory factor: critical role in obesity, insulin resistance, and associated comorbidities," *Mediators of Inflammation*, vol. 2010, Article ID 610479, 7 pages, 2010.

[31] J. M. Bruun, J. W. Helge, B. Richelsen, and B. Stallknecht, "Diet and exercise reduce low-grade inflammation and macrophage infiltration in adipose tissue but not in skeletal muscle in severely obese subjects," *American Journal of Physiology. Endocrinology and Metabolism*, vol. 290, no. 5, pp. E961–E967, 2006.

[32] I. Harman-Boehm, M. Blüher, H. Redel et al., "Macrophage infiltration into omental versus subcutaneous fat across different populations: effect of regional adiposity and the comorbidities of obesity," *Journal of Clinical Endocrinology and Metabolism*, vol. 92, no. 6, pp. 2240–2247, 2007.

[33] S. Klein, L. Fontana, L. Young et al., "Absence of an effect of liposuction on insulin action and risk factors for coronary heart disease," *The New England Journal of Medicine*, vol. 350, no. 25, pp. 2549–2557, 2004.

[34] K. Karastergiou, S. R. Smith, A. S. Greenberg, and S. K. Fried, "Sex differences in human adipose tissues—the biology of pear shape," *Biology of Sex Differences*, vol. 1, article 13, 2012.

[35] L. Frederiksen, T. L. Nielsen, K. Wraae et al., "Subcutaneous rather than visceral adipose tissue is associated with adiponectin levels and insulin resistance in young men," *Journal of Clinical Endocrinology and Metabolism*, vol. 94, no. 10, pp. 4010–4015, 2009.

[36] P. Lucotti, L. D. Monti, E. Setola et al., "Aerobic and resistance training effects compared to aerobic training alone in obese type 2 diabetic patients on diet treatment," *Diabetes Research and Clinical Practice*, vol. 94, no. 3, pp. 395–403, 2011.

Hindawi Publishing Corporation
Mediators of Inflammation
Volume 2013, Article ID 530429, 11 pages
http://dx.doi.org/10.1155/2013/530429

Research Article

Palmitic Acid Induces Production of Proinflammatory Cytokines Interleukin-6, Interleukin-1β, and Tumor Necrosis Factor-α via a NF-κB-Dependent Mechanism in HaCaT Keratinocytes

Bing-rong Zhou, Jia-an Zhang, Qian Zhang, Felicia Permatasari, Yang Xu, Di Wu, Zhi-qiang Yin, and Dan Luo

Department of Dermatology, The First Affiliated Hospital of Nanjing Medical University, Nanjing 210029, China

Correspondence should be addressed to Dan Luo; daniluo2013@njmu.edu.cn

Received 9 May 2013; Revised 23 July 2013; Accepted 24 July 2013

Academic Editor: Salahuddin Ahmed

To investigate whether palmitic acid can be responsible for the induction of inflammatory processes, HaCaT keratinocytes were treated with palmitic acid at pathophysiologically relevant concentrations. Secretion levels of interleukin-6 (IL-6), tumor necrosis factor-α (TNF-α), interleukin-1β (IL-1β), NF-κB nuclear translocation, NF-κB activation, Stat3 phosphorylation, and peroxisome proliferator-activated receptor alpha (PPARα) mRNA and protein levels, as well as the cell proliferation ability were measured at the end of the treatment and after 24 hours of recovery. Pyrrolidine dithiocarbamate (PDTC, a selective chemical inhibitor of NF-κB) and goat anti-human IL-6 polyclonal neutralizing antibody were used to inhibit NF-κB activation and IL-6 production, respectively. Our results showed that palmitic acid induced an upregulation of IL-6, TNF-α, IL-1β secretions, accompanied by NF-κB nuclear translocation and activation. Moreover, the effect of palmitic acid was accompanied by PPARα activation and Stat3 phosphorylation. Palmitic acid-induced IL-6, TNF-α, IL-1β productions were attenuated by NF-κB inhibitor PDTC. Palmitic acid was administered in amounts able to elicit significant hyperproliferation and can be attenuated by IL-6 blockage. These data demonstrate for the first time that palmitic acid can stimulate IL-6, TNF-α, IL-1β productions in HaCaT keratinocytes and cell proliferation, thereby potentially contributing to acne inflammation and pilosebaceous duct hyperkeratinization.

1. Introduction

Acne is a chronic inflammation of the pilosebaceous units in certain area, including face and trunk, that mainly occurs in adolescence. Its pathogenesis is complex and is dependent on the interplay of multiple factors such as genetic predisposition, excess of sebum production, abnormal follicular proliferation, and development of inflammation [1]. Inflammation is indicated as a key component of the pathogenesis of acne [2]. An immunological reaction to the gram-positive microbe Propionibacterium acnes may play a major role in the initiation of the inflammatory reaction [3]. However, some published studies also indicate that in addition to Propionibacterium acnes, some components such as free fatty acid (FFA), arachidonic acid, linoleic acid, and some proinflammatory cytokines are associated with acne inflammation, and inflammation-inducing effects may not depend on the presence of Propionibacterium acnes. In addition, peroxisome proliferator-activated receptor (PPAR)α and neural factors are also related to acne inflammation [4–7].

Human sebaceous glands secrete a lipid mixture containing squalene and wax esters, as well as cholesterolesters, triglycerides, and possibly some free cholesterol [8–10]. Sebaceous lipids are responsible for the three-dimensional organization of skin surface lipids and the integrity of the skin barrier [11]. Besides, sebaceous lipids and its products were detected to express proinflammatory and anti-inflammatory properties [6, 12]. The early study found that FFA induces skin inflammation and stimulates sebaceous duct hyperkeratosis in animal models. Zouboulis evaluated the experimental results of patients with inflammatory lesions successfully

treated with a new anti-inflammatory agent that specifically blocks the formation of leukotriene (LT) B4, demonstrating a significant reduction of FFA in sebum [12]. The decrease in FFA directly correlated with the improvement of inflammatory lesions. It is known that bacterial hydrolases convert some of the triglycerides to FFA on the skin surface [13]; however, there is also evidence indicating that sebaceous glands can also synthesize considerable amounts of FFA [12]. The main ingredients of FFA secreted by sebaceous glands are linoleic acid (LA), palmitic acid (PA), and oleic acid (OA). The composition of comedonal free fatty acids has been studied, demonstrating that the proportion of LA is markedly decreased in acne comedones, while PA is significantly increased [14, 15]. Akamatsu et al. have found that the decreased levels of LA in acne comedones contribute, in part, to the worsening of acne inflammation by the failure of low level of LA to inhibit neutrophil ROS generation and phagocytosis [16]. Further studies have indicated that PA can reduce the neutrophils to produce hydrogen peroxide; by their role in oxidative stress and damage to the epidermal barrier function, the proinflammatory mediators thereby more easily pass through the hair follicles into the dermis and aggravate acne inflammation [17]. However, the mechanisms of FFA in inducing acne inflammation have not been thoroughly studied.

A number of proinflammatory cytokines, including interleukin-6 (IL-6), tumor necrosis factor-α (TNF-α), and interleukin-1β (IL-1β), have been implicated in the inflammatory process of acne [18, 19]. IL-6 has been shown to be a key player in acute and chronic inflammation [20]. Serum IL-6 levels were significantly higher in acne patients than that in normal population, suggesting a role for IL-6 in the pathogenesis of acne [21]. TNF-α and IL-1β can be induced by NF-κB activation [22]. These two cytokines (TNF-α and IL-1β) propagate the acne inflammatory response by acting on endothelial cells to elaborate adhesion molecules to facilitate recruitment of inflammatory cells into the skin [23, 24].

The aim of this study was to investigate the possible role of PA in the initiation and development of inflammatory events using human HaCaT keratinocytes as model. We evaluated the effect of PA on IL-6, TNF-α, and IL-1β secretion in HaCaT cells. We also focused on the activation of NF-κB, which coordinates the expression of different proinflammatory genes, secretion of the cytokine IL-6, TNF-α, and IL-1β, and induction of PPARα. The latter inhibits the synthesis of proinflammatory molecules via a decreased activity of the NF-κB signaling pathway [25].

2. Materials and Methods

2.1. Materials. Palmitic acid (PA) powder was bought from Sigma Co. Ltd. PA powder was added to a 10% solution of fatty acid free BSA and dissolved by shaking gently overnight at 37°C to yield an 200 mmol/L solution of PA complexed to BSA. Antibodies for PPAR-α, p-Stat3, and total-Stat3 were bought from Cell Signaling Technology, California, USA; antibody for LaminB was bought from Santa Cruz Biotechnology, CA, USA; antibodies for NF-κB p65, IKKα, IκBα, β-Actin, Cy3-conjugated mouse anti-rabbit immunoglobulins, pyrrolidine dithiocarbamate (PDTC, a selective chemical inhibitor of NF-κB), cell culture supplies, CCK-8 Kit, and BCA Protein Assay Kit were all bought from Beyotime Institute of Biotechnology; Trizol was bought from Invitrogen, Carlsbad, CA; real-time PCR Assay Kits were bought from Nanjing KGI Bioteknologi Development Co, Ltd. IL-6 Sandwich ELISA Kit was bought from JingMei Bioengineer Company, Shenzhen. Helenalin was bought from Merlin Standard Chemicals, Singapore. Goat anti-human IL-6 polyclonal neutralizing antibody was obtained from R&D Systems, Minneapolis, MN, USA.

2.2. Method

2.2.1. Cell Culture. Keratinocyte line HaCaT cells were cultured in a cell incubator at 37°C, 5% CO_2, in DMEM medium containing 10% fetal bovine serum and 1% penicillin and streptomycin. After cells became polygon arranging as a single layer, they were vaccinated at the density of 1×10^9/L with 0.25% trypsin solution. The cultured cells were used for experiment when they adhered to the culture plate and the confluence reached 70%~80%.

2.2.2. Experiment Grouping and Treatment of Cells. HaCaT keratinocytes were either without or with pretreatment for 1 hour with 10 μM PDTC and then treated in serum-free conditions for 24 hours with PA at concentrations of 75, 100, 125, and 150 μmol/L. For certain experiments, goat anti-human IL-6 polyclonal neutralizing antibody was added into cell culture system at a concentration of 10 μg/mL. At the end of the treatment, fresh medium was added. Cells were collected at the end of the treatment or after 24 hours from the addition of fresh medium. As for IL-6, IL-1β, and TNF-α release detection, at the end of the treatment, supernatants were collected, fresh medium was added, and free cell supernatants were collected after 24 hours.

2.2.3. Immunofluorescence and Confocal Microscopy Detection of NF-κB p65 in HaCaT Cells. The cells were washed with 0.01 M phosphate-buffered saline (PBS) and fixed in 4% formaldehyde for 30 min at room temperature. After being permeabilized with 1% Triton X-100 for 10 min, the cells were blocked with PBS containing 5% bovine serum albumin for 30 min at room temperature and immunofluorescent staining was performed using a specific mouse polyclonal antibody against NF-κB p65 (dilution, 1 : 500) followed by Cy3-conjugated mouse anti-rabbit immunoglobulins (red). The slides were counterstained with Hoechst 33258 (blue). Finally, the cover slips were mounted on the slides and fluorescence was visualized using a confocal laser fluorescence microscope (Carl Zesis Zen 2008, Carl Zeiss Inc., Germany). Photographic images were taken from five random fields. Substitution of the primary antibody with a normal mouse IgG was used as control.

2.2.4. Preparation of Cytoplasmic and Nuclear Extracts. Briefly, cells were scraped from dishes in PBS, pelleted,

washed in hypotonic buffer (10 mM HEPES buffer, pH 7.9, 1.5 mM $MgCl_2$, 5 mM KCl, 1 mM PMSF, 1 mM dithiothreitol, 1 mM Na_3VO_4, 1 mM NaF), and lysed by resuspension in the same buffer with 0.1% Nonidet P-40. Cytoplasmic extracts were isolated by centrifugation at 10,000 rpm for 10 min. Nuclear pellets were washed in hypotonic buffer and resuspended in cold extraction buffer (20 mM HEPES, 25% glycerol, 450 mM KCl, 1 mM EDTA, 1 mM PMSF, 1 mM Na_3VO_4, 1 mM NaF), gently agitated at 4°C for 45 min, and spun at 13,000 rpm for 30 min at 4°C. Supernatants were collected, and protein concentrations were determined with BCA Protein Assay Kit.

2.2.5. Western Blotting Tests for the Protein Expression of NF-κB p65, IKKα, IκBα, p-Stat3, and PPAR-α in HaCaT Cells. An aliquot of protein extracted from cytoplasmic or nuclear extracts was subjected to 10% SDS-PAGE by electrophoresis under reducing conditions and transferred to PVDF membrane. The blotted membrane was then blocked with 5% nonfat dry milk in 1 × TBS (0.1% Tween 20) for 1 h at room temperature and incubated overnight at 4°C with primary antibodies to NF-κB p65 (dilution, 1 : 500), to IKKα (dilution, 1 : 250), to IκBα (dilution, 1 : 250), to PPAR-α (dilution, 1 : 500), to p-Stat3 (dilution, 1 : 500), to total-Stat3 (dilution, 1 : 500), to β-actin (dilution, 1 : 2,000), and to LaminB (dilution, 1 : 1,000). Following the incubation with horseradish peroxidase-conjugated sheep anti-mouse secondary antibodies (dilution, 1 : 2,000) for 1 h at room temperature, the blotted membrane was detected by Pierce ECL reagents (Thermo Fisher Scientific) and captured on X-ray film. Quantification of protein bands was established by Band-Scan software (PROZYME, San Leandro, California, USA) and expressed as a value relative to the density of the internal control (β-actin or LaminB).

2.2.6. Real-Time PCR Detection of the Expression of PPAR-α mRNA in HaCaT Cells. Trizol was added to break down the cells, followed by extraction of total RNA, measurement of concentration, and then measurement of purity. After ensuring that the quality met the requirements of the experiment, cDNA was obtained by reverse transcription. It was diluted 10 times and amplified according to a 20 μL reaction system. Primers were synthesized by Nanjing Kaiji Bio-tech Co., Ltd. (Table 1). Amplification conditions are as follows: pre-degeneration at 95°C for 5 min, entering reaction circles, degeneration at 95°C for 15 min, annealing for 30 s at 60°C, extending for 30 s at 72°C, keeping at 72°C for 10 min after 40 cycles.

2.2.7. ELISA Analysis of the Expression of IL-6, IL-1β, and TNF-α in Cell Supernatants. Measurement of IL-6, IL-1β, and TNF-α were performed using commerical ELISA kits. This assay uses the quantitative sandwich immunoassay technique. The standard curve demonstrated a direct relationship between OD and secreted cytokine levels.

2.2.8. Cell Proliferation Assay. Cell proliferation was assayed using a CCK-8 Kit. In brief, 100 μL of cells (2×10^3 cells/well) was transferred into 96-well plates after digestion with trypsin, and five parallel wells were used for each treatment. After attachment, the cells were subjected to the different treatments and then cultured for 24 h in a 5% CO_2 incubator at 37°C. Subsequently, 10 μL of CCK-8 was added to each well, and the cells were cultured for another 3 h. Cell density was determined by measuring the absorbance at 450 nm using a Varioskan Flash (Thermo Scientific, USA).

Table 1: Primers used in the real-time RT-PCR amplification of the human PPAR-α gene and GAPDH mRNAs.

Gene name		primer sequences
PPARα	Forward primer	5′-TTCGCAATCCATCGGCGAG-3′
	Reverse primer	5′-CCACAGGATAAGTCACCGAGG-3′
GAPDH	Forward primer	5′-TGTTGCCATCAATGACCCCTT-3′
	Reverse primer	5′-CTCCACGACGTACTCAGCG-3′

2.3. Statistical Analysis. SPSS13.0 software was used for data analysis, and the form of average ± standard deviation was used to indicate measurement data. ANOVA was used for intergroup comparison, $P < 0.05$ was considered statistically significant.

3. Results

3.1. Induction of IL-6, IL-1β, and TNF-α Secretion in HaCaT Keratinocytes by PA. We observed, by means of ELISA analysis, an increase in a dose-dependent manner in the release of IL-6, IL-1β, and TNF-α in HaCaT keratinocyte supernatant treated with PA at a concentration of 75, 100, 125, and 150 μmol/L 24 hours after PA removal (Figures 1(a), 1(b) and 1(c)). The obtained results demonstrate that PA is able to induce an inflammatory stimulus in HaCaT keratinocytes by increasing IL-6, IL-1β, and TNF-α secretion.

3.2. Induction of NF-κB Nuclear Translocation in HaCaT Keratinocytes by PA. We used immunofluorescence staining to examine the localization of NF-κB p65 in HaCaT keratinocytes. NF-κB p65 was stained with Cy3-conjugated mouse anti-rabbit immunoglobulins (red) and nuclei were stained with Hoechst 33342 (blue). We found that NF-κB p65 positive staining was predominantly localized in control cytoplasm (Figure 2). Interestingly, NF-κB p65 staining significantly shifted to the nuclei with PA stimulation immediately after the treatment (Figure 2(a)) and 24 hours after the PA depletion (Figure 2(b)). The nuclear translocation of NF-κB p65 subunit was further confirmed by the results derived from the western blotting studies. Upregulation of nuclear NF-κB p65 protein levels in a dose-dependent manner was observed in cells treated with PA at 75, 100, 125, and 150 μmol/L compared to control, immediately after the treatment (Figure 3(a)). The level of nuclear NF-κB

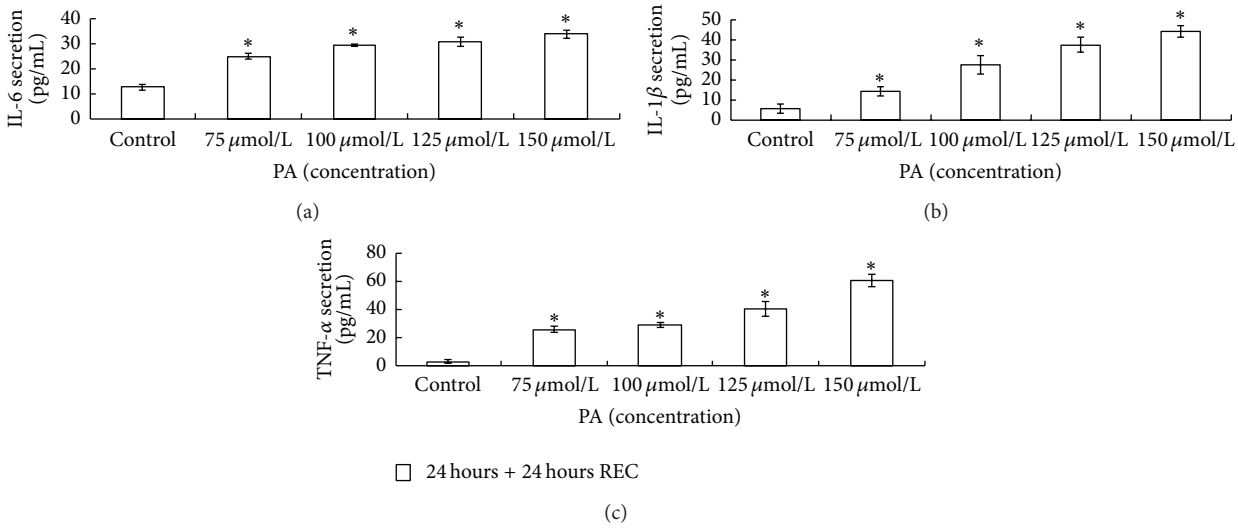

Figure 1: PA induces an upregulation of IL-6, IL-1β, and TNF-α secretion in HaCaT keratinocytes. HaCaT keratinocytes were untreated or treated with PA (75, 100, 125, and 150 μmol/L) for 24 hours under serum-free conditions, and collected 24 hours after PA depletion. IL-6 (a), IL-1β (b), and TNF-α (c) releases were determined by ELISA kits. Results are expressed as average mean of protein concentration (pg/mL) ± SD and represent the mean of three experiments in duplicate. Asterisks (*) indicate significant differences of $P < 0.05$, respectively, between the PA-treated groups and nontreated group.

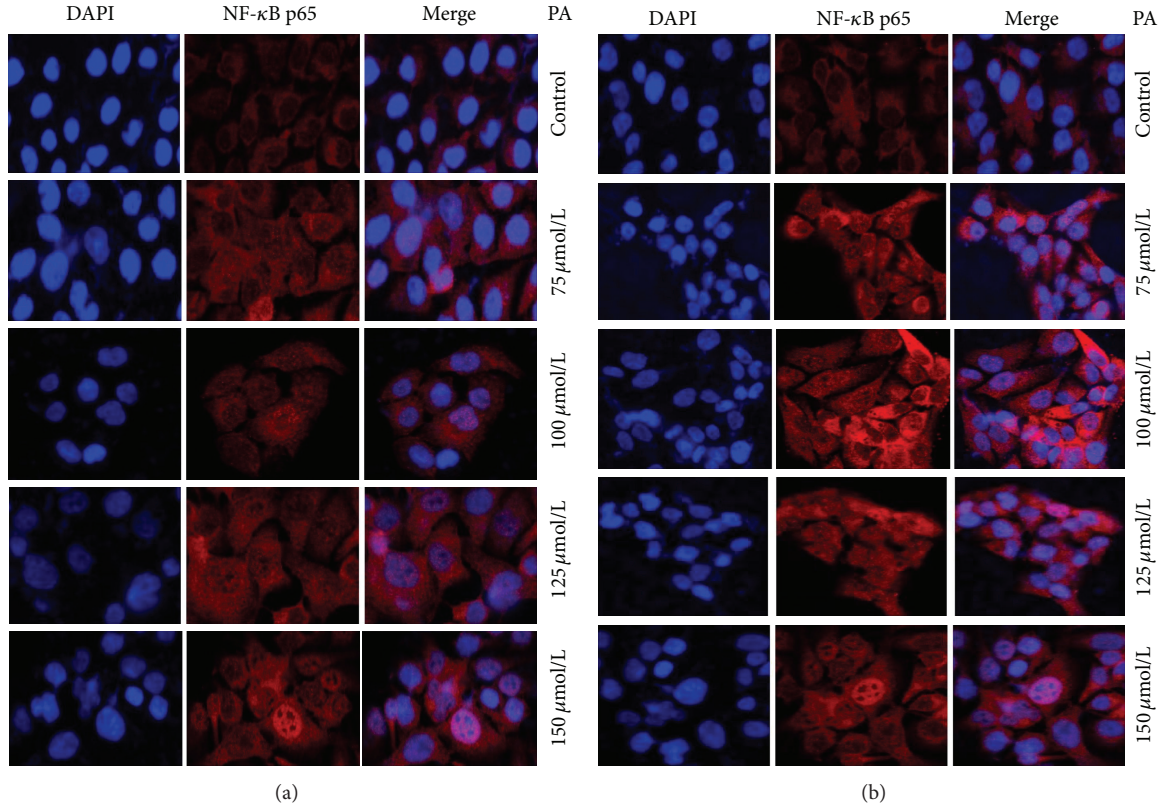

Figure 2: PA-induced nuclear translocation of NF-κB p65 subunit in HaCaT cells immediately after the treatment and 24 hours after the PA depletion. Keratinocytes were untreated or treated with PA (75, 100, 125, and 150 μmol/L) for 24 hours under serum-free conditions. Immunostaining was performed with specific mouse anti-p65 antibody followed by Cy3-conjugated mouse anti-rabbit immunoglobulins (red) immediately after the treatment (a) and 24 hours after the PA depletion (b). Images are representative of three independent experiments.

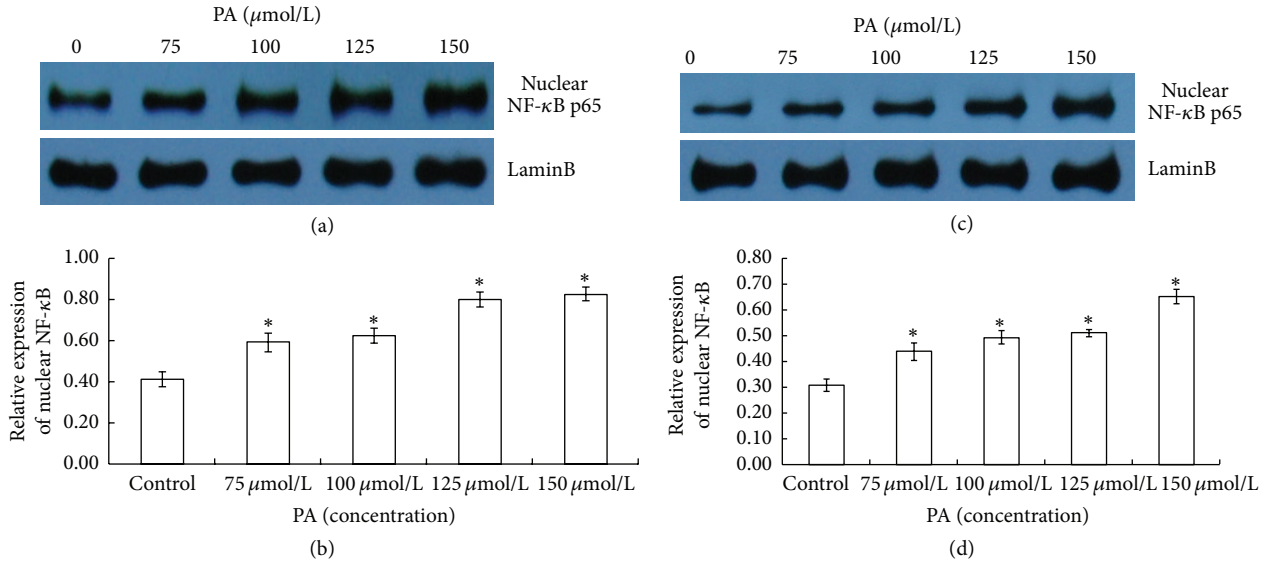

Figure 3: PA induces nuclear translocation of NF-κB p65 subunit in HaCaT cells measured by western blotting. Keratinocytes were untreated or treated with PA (75, 100, 125, and 150 μmol/L) for 24 hours under serum-free conditions. The cells were harvested, and nuclear extracts were analyzed with NF-κB p65 by western blot immediately after the treatment (a) and 24 hours after the PA depletion (c). The densitometry values are means ± SD of three independent experiments ((b) and (d)). Asterisks (*) indicate significant differences of $P < 0.05$, respectively, between the PA-treated groups and nontreated group.

p65 protein expression in treated cells also increased dose dependently 24 hours after PA removal (Figure 3). The results obtained in these results demonstrate that PA is able to induce NF-κB nuclear translocation in HaCaT keratinocytes.

3.3. Induction of IKKα Activation and IκBα Degradation in HaCaT Keratinocytes by PA. Upregulation of IKKα protein levels in a dose dependent manner were observed in cells treated with PA at 100, 125, and 150 μmol/L compared to control, immediately after the treatment and 24 hours after the PA depletion (Figures 4(a) and 4(b)). The level of IκBα protein expression in 75, 100, 125, and 150 μmol/L PA treated cells decreased dose dependently immediately after the treatment and 24 hours after the PA depletion (Figures 4(d) and 4(e)). The results obtained in these results demonstrate that PA is able to induce NF-κB activation in HaCaT keratinocytes.

3.4. Induction of PPARα Expression and Phospho-Stat3 in HaCaT Keratinocytes by PA. Immediately after treatment, PA at 75, 100, 125, and 150 μmol/L caused an upregulation of PPARα mRNA levels compared to controls (Figure 5(a)). Afterwards, the level of PPARα gene expression in the treated cells decreased during the following 24 hours (Figure 5(a)). Significant upregulation of PPARα protein levels was observed by means of western blot analysis in cells treated with PA at 100, 125, and 150 μmol/L compared to controls, immediately and 24 hours after PA removal (Figures 5(b) and 5(c)). On the contrary, the treatment of HaCaT keratinocytes with PA at 75 μmol/L did not exert any effect on the expression pattern of PPARα, compared to untreated controls (Figures 5(b) and 5(c)). The PPARα upregulation supports the data mentioned above, which highlighted the possible induction of inflammatory response in HaCaT keratinocytes after the treatment with PA. Significant upregulation of levels of p-Stat3 was also observed by means of western blot analysis in cells treated with PA at 100, 125, and 150 μmol/L compared to total Stat3, immediately and 24 hours after PA removal (Figures 6(a) and 6(b)).

3.5. PA-Induced IL-6, IL-1β, and TNF-α Production Is Attenuated by Inhibitor of NF-κB. We examined the effect of inhibition of NF-κB on IL-6, IL-1β, and TNF-α expression in response to PA. As shown by CCK-8 detection, pretreatment for 1 hour with 10 μM PDTC, a selective chemical inhibitor of NF-κB, had no obvious toxicity to HaCaT cell viability. Moreover, 10 μM PDTC was proved to inhibit PA-induced IKKα activation and IκBα degradation (see supplementary Figure S1 in Supplementary Material available online at http://dx.doi.org/10.1155/2013/530429). The solvent dimethylsulfoxide (0.1%) was used as a vehicle and control. PA-stimulated IL-6, IL-1β, and TNF-α productions were significantly attenuated by PDTC, showing that these PA-induced proinflammatory cytokine expressions involve activation of NF-κB activation (Figure 7). Dimethylsulfoxide had no effect on PA-induced IL-6, IL-1β, and TNF-α production.

3.6. Induction of Cell Proliferation by PA Is Dependent of IL-6 Production. In order to evaluate the possible role of PA in the hyperkeratinization of the pilosebaceous duct, we focused on the proliferative response of HaCaT keratinocytes after treatment with PA in a concentration range of 75 to 150 μmol/L by means of CCK-8 test. We observed that PA concentrations between 75 and 150 μmol/L induced a significant proliferative stimulus (Figure 8(a)). These data suggest that PA may be involved in the induction of the

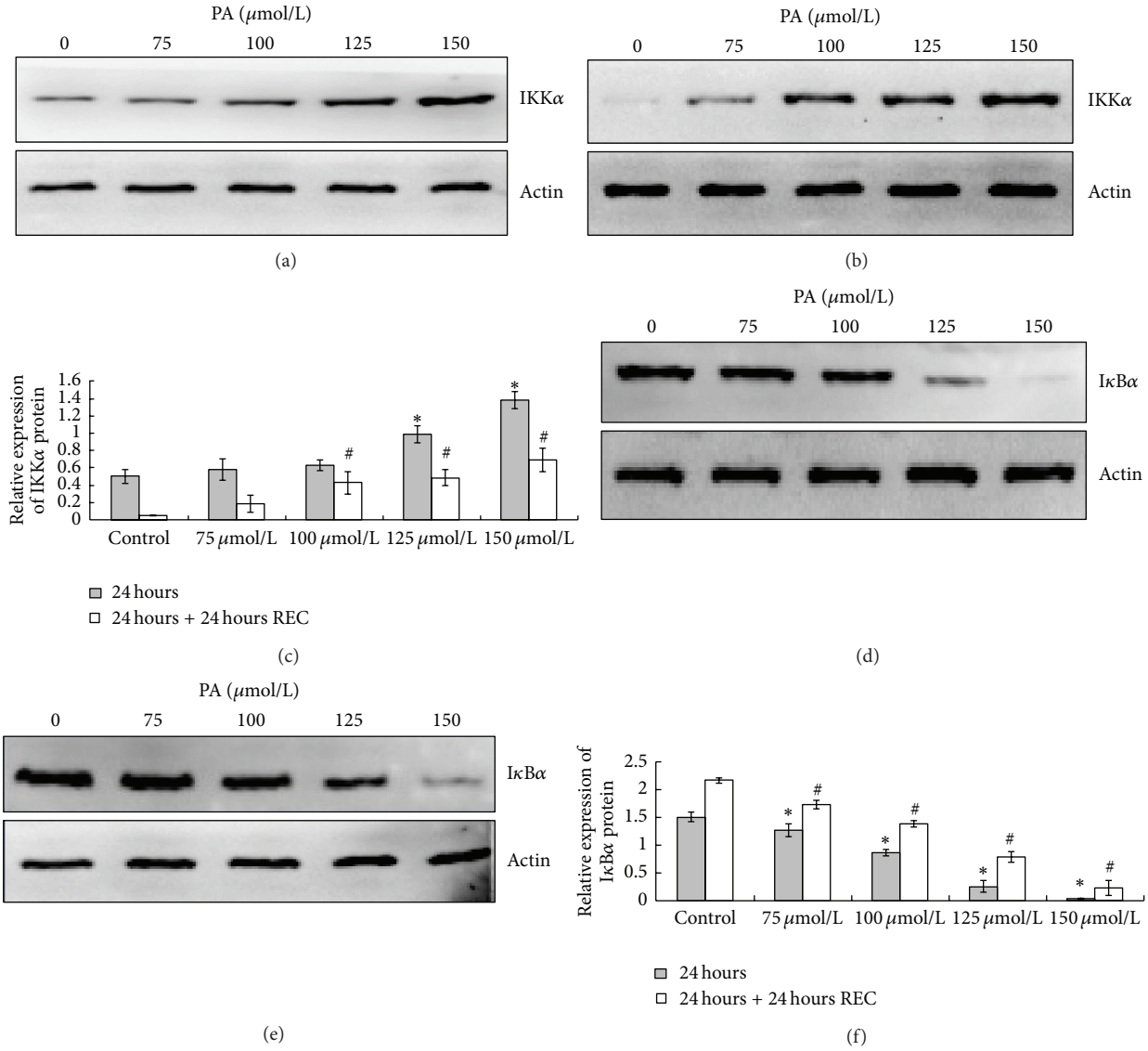

Figure 4: PA induces activation of IKKα and degradation of IκBα in HaCaT cells measured by western blotting. Keratinocytes were untreated or treated with PA (75, 100, 125, and 150 μmol/L) for 24 hours under serum-free conditions. The cells were harvested, and nuclear extracts were analyzed with IKKα by western blot immediately after the treatment (a) and 24 hours after the PA depletion (b). The densitometry values are means ± SD of three independent experiments (c). The protein expression of IκBα immediately after the treatment (d) and 24 hours after the PA depletion (e) were also determined by western blot. The densitometry values are means ± SD of three independent experiments (f). *indicate significant differences of $P < 0.05$, respectively, between the PA-treated groups and nontreated group immediately after the treatment groups (24 hours); $^\#$indicate significant differences of $P < 0.05$, respectively, between the PA-treated groups and nontreated group in 24 hours after the PA depletion groups (24 hours + 24 hours REC).

hyperkeratosis of the pilosebaceous duct. Interestingly, PA-induced cell proliferative effect was significantly attenuated by the addition of 10 μg/mL goat anti-human IL-6 polyclonal neutralizing antibody in cell culture system (Figure 8(b)). These data demonstrate that autocrine IL-6 production is causally linked to cell proliferation in this in vitro model.

4. Discussion

In this study, we supplemented HaCaT cells with PA to mimic the influx of excess FFAs into keratinocytes. For experiments, we used the human keratinocyte cell line HaCaT, which retains biochemical and morphological properties characteristic of keratinocytes, and has proven useful for studying the possible roles of inflammatory mediators in acne vulgaris [25].

Our data demonstrate that exposure of keratinocytes (HaCaT cells) to pathophysiologically relevant concentrations of PA results in increased IL-6, IL-1β, and TNF-α secretion. This is in agreement with several studies that suggest a link between these three proinflammatory cytokines and PA-induced inflammation [26, 27]. For example, Staiger et al. reported palmitate-induced interleukin-6 expression in

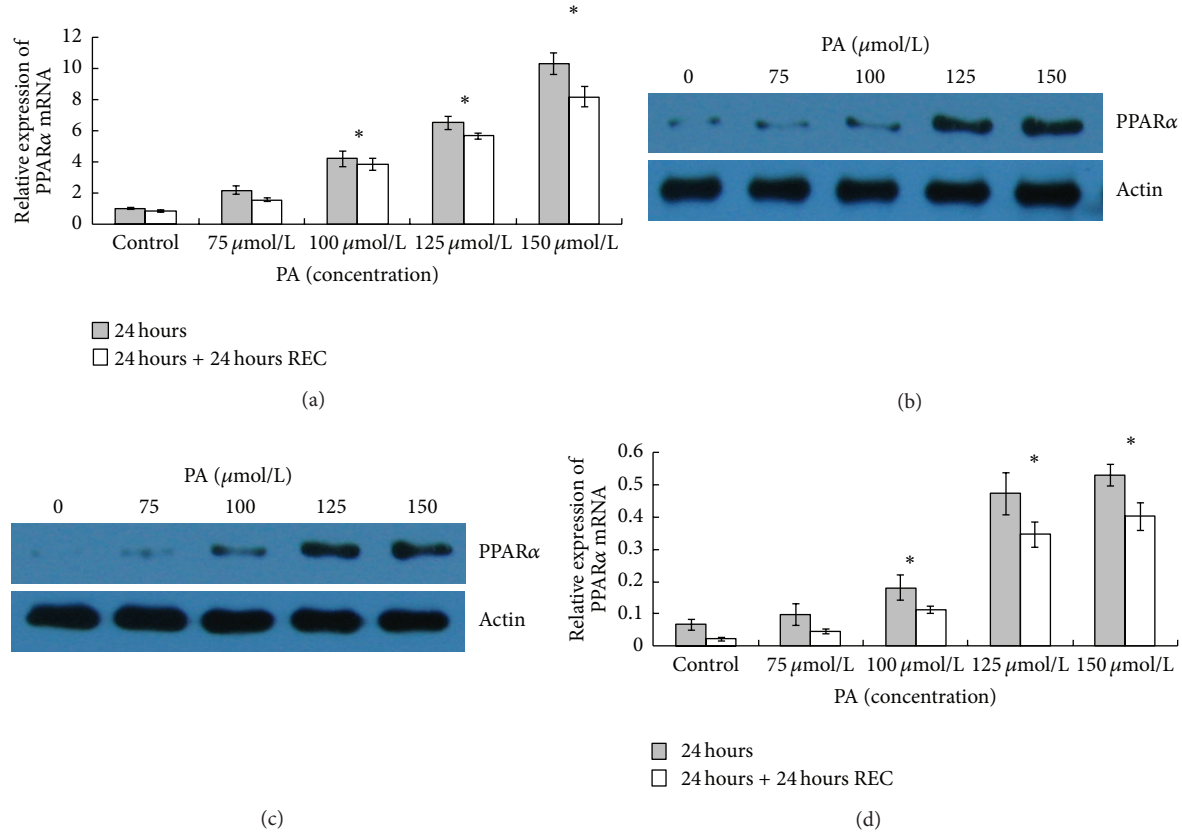

Figure 5: PA induces an upregulation of PPARα mRNA and protein levels in HaCaT keratinocytes. HaCaT keratinocytes were untreated or treated with PA (75, 100, 125, and 150 μmol/L) for 24 hours in serum-free conditions, and collected immediately and 24 hours after PA depletion. (a) PPAR-α mRNA levels were determined by real-time RT-PCR. The values shown represent mean ± SD of three experiments. Expression of PPARα after treated or untreated with PA immediately (b) and 24 hours (c) were detected by western blotting. The band intensities were evaluated by densitometric analysis (d). The values shown represent the mean ± SD of three experiments. Asterisks (*) indicate significant differences of $P < 0.05$, respectively, between the PA-treated groups and nontreated group.

human coronary artery endothelial cells and suggested a potential contribution of palmitate to vascular inflammation [27]. Importantly, evidence from previous publications shows that IL-6 is elevated in patients with acne, suggesting that this inflammatory cytokine also may contribute to the development of acne [21]. It was reported that PA significantly decreased H_2O_2 generation both by neutrophils and in the xanthine-xanthine oxidase system, while neutrophil chemotaxis and phagocytosis as well as O_2^- and $OH^\bullet$ generation by both systems were not markedly affected in the presence of PA [17]. The authors suggested that PA may be involved in the pathogenesis of acne inflammation from a standpoint of oxidative tissue injury [17]. Besides, it is well documented that IL-6 phosphorylates transcription factor Stat3 at Tyr705 residue and has a role in inflammation [28–30]. Our present data showed that the p-Stat3 level was significantly induced following PA treatment. In this context, we suggested that PA may also contribute to acne inflammation via increasing IL-6 secretion.

Besides IL-6, we also found that TNF-α and IL-1β were increased following PA treatment, which are also critically important in acne inflammation. These two proinflammatory cytokines not only amplify the NF-κB signaling pathways that originally led to their production through cell surface receptor activation (an autocrine loop), but also will stimulate nearby cells in a paracrine manner. For example, TNF-α and IL-1β are known to upregulate adhesion molecules, such as ICAM-1 and VCAM-1 on endothelial cells [31, 32]. Thus, the observation that ICAM-1, E-selectin, and VCAM-1 expression levels on the luminal surface of endothelial cells are increased in inflammatory acne papules may be a consequence of TNF-α and IL-1β induction in the milieu [33]. The elaboration of adhesion molecules is necessary to slow the flow of circulating inflammatory cells for their eventual diapedesis into the inflamed tissue [31, 32].

NF-κB is known to be an important transcription factor for proinflammatory gene expression, and appears to regulate IL-6, IL-1β, and TNF-α secretions in a cell type-specific and stimulus-specific manner [34, 35]. Activation of NF-κB is mediated through the action of a family of serine/threonine kinases known as IκB kinase (IKK). The IKK (IKKα and/or IKKβ) phosphorylates IκB proteins and the members of the NF-κB family. In our current study, we observed that NF-κB p65 is activated in a dose-dependent manner in

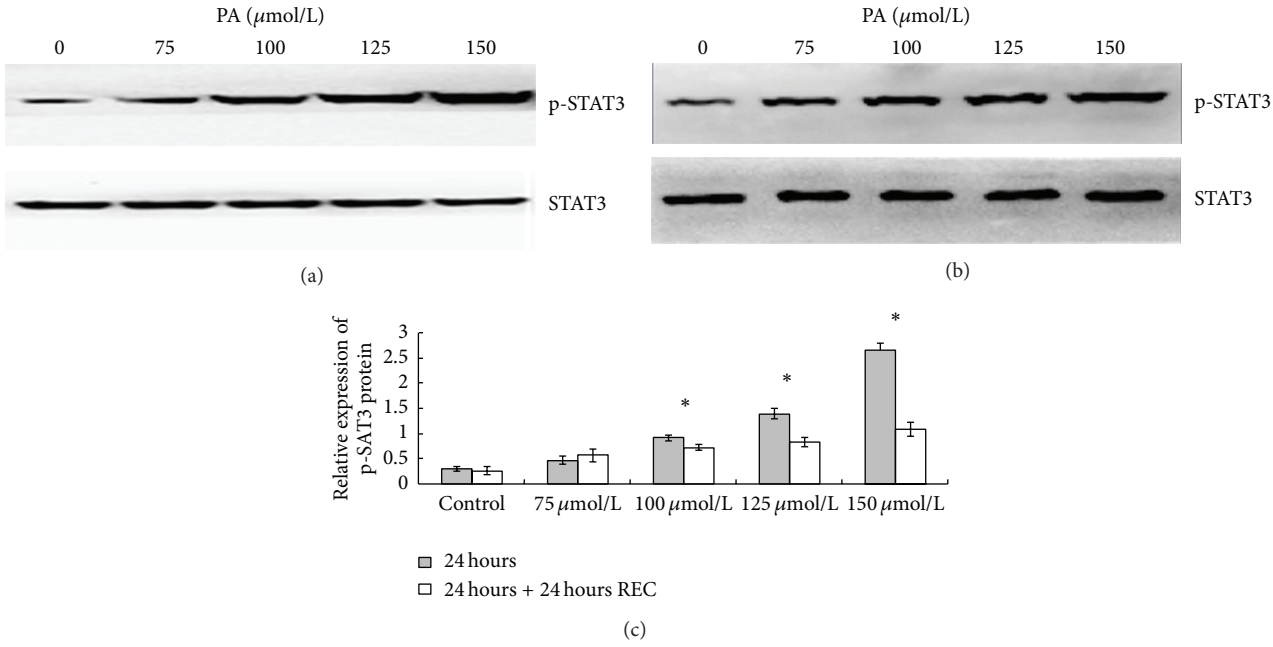

Figure 6: PA induces activation of p-Stat3 (Tyr705) in HaCaT cells measured by western blotting. Keratinocytes were untreated or treated with PA (75, 100, 125, and 150 μmol/L) for 24 hours under serum-free conditions. The cells were harvested, and nuclear extracts were analyzed with p-Stat3 and total Stat3 by western blot immediately after the treatment (a) and 24 hours after the PA depletion (b). The densitometry values are means ± SD of three independent experiments (c). Asterisks (*) indicate significant differences of $P < 0.05$, respectively, between the PA-treated groups and nontreated group.

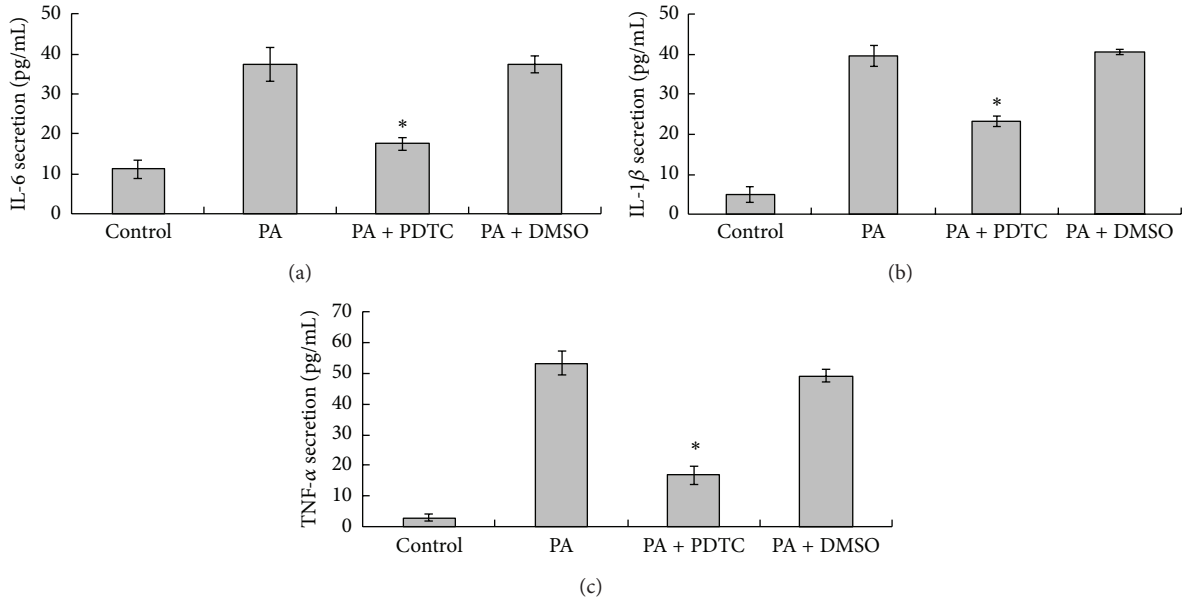

Figure 7: Effect of NF-κB inhibitor PDTC on PA-induced IL-6, IL-1β, and TNF-α production. HaCaT cells were untreated or exposed to 0.15 mM PA for 24 hours, either without or with pretreatment for 1 hour with 10 μmol/L PDTC or 0.1% dimethylsulfoxide (DMSO, as vehicle control). IL-6 (a), IL-1β (b), and TNF-α (c) productions were measured by ELISA. Each experiment was done in triplicate. Data are mean ± standard deviation. $^*P < 0.05$ compared with PA.

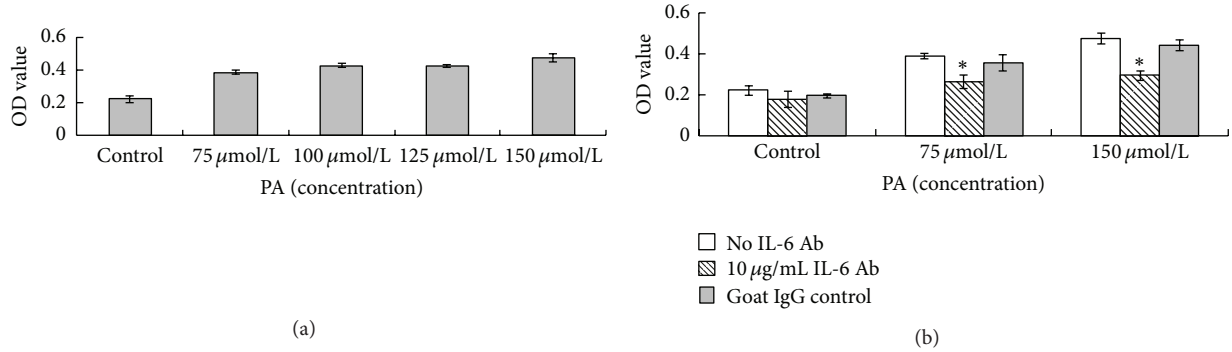

Figure 8: Induction of cell proliferation by palmitic acid is dependent of IL-6. (a) Cells were untreated or treated with PA (75, 100, 125, and 150 μmol/L) for 24 hours. Cell viability was measured by a CCK-8 assay kit. Data are expressed as mean ± standard deviation ($n = 5$). $^*P < 0.05$ compared with control. (b) Cells were untreated or treated with PA (75 and 150 μmol/L) for 24 hours, with or without the presence of 10 μg/mL goat anti-human IL-6 polyclonal neutralizing antibody (IL-6 Ab) or control goat IgG in cell culture system. Cell viability was measured by a CCK-8 assay kit. Data are expressed as mean ± standard deviation ($n = 5$). $^*P < 0.05$ compared with treatments without IL-6 Ab.

human HaCaT cells following PA exposure and subsequently translocated to the nucleus. PA exposure also resulted in an increased degradation of IκBα protein. This suggests that the activation of NF-κB p65 in HaCaT cells is mediated through the inhibition of IκBα protein proteolysis. It is well documented that IκBα is bound to NF-κB p65 through a protein-protein interaction and thus prevents migration of NF-κB p65 into the nucleus [36]. Additionally, the IKK complex is an important site for integrative signals that regulate the NF-κB pathway. We observed that PA exposure resulted in an increase in IKKα protein expression in HaCaT cells. These data suggest that PA-induced NF-κB activation and nuclear translocation of NF-κB p65 through greater activation of IKKα and degradation of IκBα proteins. Besides, PA-induced IL-6, IL-1β, and TNF-α expressions were attenuated by a NF-κB inhibitor, strongly implicating this transcription factor in the regulation of PA-induced IL-6, IL-1β, and TNF-α expressions. PPARα exerts a modulatory role in the control of the inflammatory response by antagonizing NF-κB signaling pathway. After the treatment with PA, HaCaT keratinocytes exhibited higher levels of PPARα transcripts probably as a feedback in anti-inflammatory response to the stimulus.

Our study clearly demonstrates that exposure to excess PA induces HaCaT keratinocyte proliferation and IL-6 production in HaCaT keratinocytes. IL-6 is reported to stimulate keratinocyte proliferation and is therefore studied in diseases associated with epidermal hyperplasia and in wound healing [37–39]. Sebaceous duct keratinocytes from comedones exhibit a hyperproliferative response compared to normal keratinocytes [40, 41]. The hyperproliferative behavior of HaCaT keratinocytes induced by PA could support the idea that FFA may be involved in comedone formation and, in particular, that PA may be responsible for this event. However, whether IL-6 is responsible for the PA-induced HaCaT keratinocyte proliferation is not yet clear. Our data suggested that the PA-induced HaCaT cell proliferation was attenuated by adding IL-6 polyclonal neutralizing antibody into cell culture system, strongly indicating that autocrine of IL-6 is primarily responsible for regulation of PA-induced keratinocytes proliferation. Hence, the interrelation between PA-induced keratinocyte proliferation and IL-6 production may be an important factor in comedone formation.

In conclusion, we show for the first time that one major type of FFA, palmitic acid, stimulates human HaCaT keratinocytes to produce proinflammatory cytokines IL-6, IL-1β, and TNF-α in a dose-dependent manner, via activation of NF-κB. Besides, the elevated level of IL-6 may also contribute to PA-induced keratinocyte proliferation.

Conflict of Interests

The authors declare that they have no conflict of interest.

Authors' Contribution

Bing-rong Zhou and Jia-an Zhang contributed equally to the paper.

Acknowledgments

This work was supported by Grant from the China National Natural Science Foundation (81000700 and 81171518), science project from traditional Chinese medicine Bureau of Jiangsu Province (LZ11084), and Jiangsu National Natural Science Foundation (BK2012877).

References

[1] C. C. Zouboulis, A. Eady, M. Philpott et al., "What is the pathogenesis of acne?" *Experimental Dermatology*, vol. 14, no. 2, pp. 143–152, 2005.

[2] A. B. Fleischer Jr., "Inflammation in rosacea and acne: implications for patient care," *Journal of Drugs in Dermatology*, vol. 10, no. 6, pp. 614–620, 2011.

[3] U. Jappe, E. Ingham, J. Henwood, and K. T. Holland, "Propionibacterium acnes and inflammation in acne; P. acnes has T-cell mitogenic activity," *British Journal of Dermatology*, vol. 146, no. 2, pp. 202–209, 2002.

[4] W. J. Lee, H. D. Jung, H. J. Lee, B. S. Kim, S.-J. Lee, and D. W. Kim, "Influence of substance-P on cultured sebocytes," *Archives of Dermatological Research*, vol. 300, no. 6, pp. 311–316, 2008.

[5] M. Toyoda, M. Nakamura, T. Makino, M. Kagoura, and M. Morohashi, "Sebaceous glands in acne patients express high levels of neutral endopeptidase," *Experimental Dermatology*, vol. 11, no. 3, pp. 241–247, 2002.

[6] M. Toyoda and M. Morohashi, "New aspects in acne inflammation," *Dermatology*, vol. 206, no. 1, pp. 17–23, 2003.

[7] P. Sertznig and J. Reichrath, "Peroxisome proliferator-activated receptors (PPARs) in dermatology: challenge and promise," *Dermato-Endocrinology*, vol. 3, no. 3, pp. 130–135, 2011.

[8] T. Nikkari, "Comparative chemistry of sebum," *Journal of Investigative Dermatology*, vol. 62, no. 3, pp. 257–267, 1974.

[9] P. Ramasastry, D. T. Downing, P. E. Pochi, and J. S. Strauss, "Chemical composition of human skin surface lipids from birth to puberty," *Journal of Investigative Dermatology*, vol. 54, no. 2, pp. 139–144, 1970.

[10] A. J. Thody and S. Shuster, "Control and function of sebaceous glands," *Physiological Reviews*, vol. 69, no. 2, pp. 383–416, 1989.

[11] G. S. K. Pilgram, J. van der Meulen, G. S. Gooris, H. K. Koerten, and J. A. Bouwstra, "The influence of two azones and sebaceous lipids on the lateral organization of lipids isolated from human stratum corneum," *Biochimica et Biophysica Acta*, vol. 1511, no. 2, pp. 244–254, 2001.

[12] C. C. Zouboulis, "Is acne vulgaris a genuine inflammatory disease?" *Dermatology*, vol. 203, no. 4, pp. 277–279, 2001.

[13] A. R. Shalita, "Genesis of free fatty acids," *Journal of Investigative Dermatology*, vol. 62, no. 3, pp. 332–335, 1974.

[14] K. Perisho, P. W. Wertz, K. C. Madison, M. E. Stewart, and D. T. Downing, "Fatty acids of acylceramides from comedones and from the skin surface of acne patients and control subjects," *Journal of Investigative Dermatology*, vol. 90, no. 3, pp. 350–353, 1988.

[15] P. W. Wertz, M. C. Miethke, S. A. Long, J. S. Strauss, and D. T. Downing, "The composition of the ceramides from human stratum corneum and from comedones," *Journal of Investigative Dermatology*, vol. 84, no. 5, pp. 410–412, 1985.

[16] H. Akamatsu, J. Komura, Y. Miyachi, Y. Asada, and Y. Niwa, "Suppressive effects of linoleic acid on neutrophil oxygen metabolism and phagocytosis," *Journal of Investigative Dermatology*, vol. 95, no. 3, pp. 271–274, 1990.

[17] H. Akamatsu, Y. Niwa, and K. Matsunaga, "Effect of palmitic acid on neutrophil functions in vitro," *International Journal of Dermatology*, vol. 40, no. 10, pp. 640–643, 2001.

[18] G. M. Graham, M. D. Farrar, J. E. Cruse-Sawyer, K. T. Holland, and E. Ingham, "Proinflammatory cytokine production by human keratinocytes stimulated with Propionibacterium acnes and P. acnes GroEL," *British Journal of Dermatology*, vol. 150, no. 3, pp. 421–428, 2004.

[19] J. Kim, "Review of the innate immune response in acne vulgaris: activation of toll-like receptor 2 in acne triggers inflammatory cytokine responses," *Dermatology*, vol. 211, no. 3, pp. 193–198, 2005.

[20] C. Gabay, "Interleukin-6 and chronic inflammation," *Arthritis Research and Therapy*, vol. 8, supplement 2, p. S3, 2006.

[21] M. Salamon, A. Sysa-Jedrzejowska, J. Lukamowicz, M. Lukamowicz, E. Swiatkowska, and A. Wozniacka, "Concentration of selected cytokines in serum of patients with acne rosacea," *Przeglad Lekarski*, vol. 65, no. 9, pp. 371–374, 2008.

[22] B. H. Kim, E. Roh, H. Y. Lee et al., "Benzoxathiole derivative blocks lipopolysaccharide-induced nuclear factor-κB activation and nuclear factor-κB-regulated gene transcription through inactivating inhibitory κB kinase β," *Molecular Pharmacology*, vol. 73, no. 4, pp. 1309–1318, 2008.

[23] B. R. Vowels, S. Yang, and J. J. Leyden, "Induction of proinflammatory cytokines by a soluble factor of Propionibacterium acnes: implications for chronic inflammatory acne," *Infection and Immunity*, vol. 63, no. 8, pp. 3158–3165, 1995.

[24] S. Kang, S. Cho, J. H. Chung, C. Hammerberg, G. J. Fisher, and J. J. Voorhees, "Inflammation and extracellular matrix degradation mediated by activated transcription factors nuclear factor-κB and activator protein-1 in inflammatory acne lesions in vivo," *American Journal of Pathology*, vol. 166, no. 6, pp. 1691–1699, 2005.

[25] M. Ottaviani, T. Alestas, E. Flori, A. Mastrofrancesco, C. C. Zouboulis, and M. Picardo, "Peroxidated squalene induces the production of inflammatory mediators in HaCaT keratinocytes: a possible role in acne vulgaris," *Journal of Investigative Dermatology*, vol. 126, no. 11, pp. 2430–2437, 2006.

[26] D. Tian, Y. Qiu, Y. Zhan et al., "Overexpression of steroidogenic acute regulatory protein in rat aortic endothelial cells attenuates palmitic acid-induced inflammation and reduction in nitric oxide bioavailability," *Cardiovascular Diabetology*, vol. 11, article 144, 2012.

[27] H. Staiger, K. Staiger, N. Stefan et al., "Palmitate-induced interleukin-6 expression in human coronary artery endothelial cells," *Diabetes*, vol. 53, no. 12, pp. 3209–3216, 2004.

[28] I. Stoian, B. Manolescu, V. Atanasiu, O. Lupescu, and C. Buşu, "IL-6—STAT-3—hepcidin: linking inflammation to the iron metabolism," *Romanian Journal of Internal Medicine*, vol. 45, no. 3, pp. 305–309, 2007.

[29] R. Atreya and M. F. Neurath, "Signaling molecules: the pathogenic role of the IL-6/STAT-3 trans signaling pathway in intestinal inflammation and in colonic cancer," *Current Drug Targets*, vol. 9, no. 5, pp. 369–374, 2008.

[30] M. F. Neurath and S. Finotto, "IL-6 signaling in autoimmunity, chronic inflammation and inflammation-associated cancer," *Cytokine and Growth Factor Reviews*, vol. 22, no. 2, pp. 83–89, 2011.

[31] H. C. Ledebur and T. P. Parks, "Transcriptional regulation of the intercellular adhesion molecule-1 gene by inflammatory cytokines in human endothelial cells. Essential roles of a variant NF-κb site and p65 homodimers," *Journal of Biological Chemistry*, vol. 270, no. 2, pp. 933–943, 1995.

[32] C. C. Chen and A. M. Manning, "Transcriptional regulation of endothelial cell adhesion molecules: a dominant role for NF-κB," *Agents and Actions Supplements*, vol. 47, pp. 135–141, 1995.

[33] A. H. T. Jeremy, D. B. Holland, S. G. Roberts, K. F. Thomson, and W. J. Cunliffe, "Inflammatory events are involved in acne lesion initiation," *Journal of Investigative Dermatology*, vol. 121, no. 1, pp. 20–27, 2003.

[34] J. F. Ndisang, "Role of heme oxygenase in inflammation, insulin-signalling, diabetes and obesity," *Mediators of Inflammation*, vol. 2010, Article ID 359732, 2010.

[35] T. Olszowski, I. Baranowska-Bosiacka, I. Gutowska, and D. Chlubek, "Pro-inflammatory properties of cadmium," *Acta Biochimica Polonica*, vol. 59, no. 4, pp. 475–482, 2012.

[36] P. A. Baeuerle and D. Baltimore, "Nf-κB: ten years after," *Cell*, vol. 87, no. 1, pp. 13–20, 1996.

[37] M. Sato, D. Sawamura, I. Shinsuke, T. Yaguchi, K. Hanada, and I. Hashimoto, "In vivo introduction of the interleukin 6 gene

into human keratinocytes: induction of epidermal proliferation by the fully spliced form of interleukin 6, but not by the alternatively spliced form," *Archives of Dermatological Research*, vol. 291, no. 7-8, pp. 400–404, 1999.

[38] J. T. Elder, C. I. Sartor, D. K. Boman, S. Benrazavi, G. J. Fisher, and M. R. Pittelkow, "Interleukin-6 in psoriasis: expression and mitogenicity studies," *Archives of Dermatological Research*, vol. 284, no. 6, pp. 324–332, 1992.

[39] R. M. Grossman, J. Krueger, D. Yourish et al., "Interleukin 6 is expressed in high levels of psoriatic skin and stimulates proliferation of cultured human keratinocytes," *Proceedings of the National Academy of Sciences of the United States of America*, vol. 86, no. 16, pp. 6367–6371, 1989.

[40] H. E. Knaggs, D. B. Holland, C. Morris, E. J. Wood, and W. J. Cunliffe, "Quantification of cellular proliferation in acne using the monoclonal antibody Ki-67," *Journal of Investigative Dermatology*, vol. 102, no. 1, pp. 89–92, 1994.

[41] B. R. Hughes, C. Morris, W. J. Cunliffe, and I. M. Leigh, "Keratin expression in pilosebaceous epithelia in truncal skin of acne patients," *British Journal of Dermatology*, vol. 134, no. 2, pp. 247–256, 1996.